

# Biology of C-reactive protein

**Edited by**

Alok Agrawal and Yi Wu

**Published in**

Frontiers in Immunology



## FRONTIERS EBOOK COPYRIGHT STATEMENT

The copyright in the text of individual articles in this ebook is the property of their respective authors or their respective institutions or funders. The copyright in graphics and images within each article may be subject to copyright of other parties. In both cases this is subject to a license granted to Frontiers.

The compilation of articles constituting this ebook is the property of Frontiers.

Each article within this ebook, and the ebook itself, are published under the most recent version of the Creative Commons CC-BY licence. The version current at the date of publication of this ebook is CC-BY 4.0. If the CC-BY licence is updated, the licence granted by Frontiers is automatically updated to the new version.

When exercising any right under the CC-BY licence, Frontiers must be attributed as the original publisher of the article or ebook, as applicable.

Authors have the responsibility of ensuring that any graphics or other materials which are the property of others may be included in the CC-BY licence, but this should be checked before relying on the CC-BY licence to reproduce those materials. Any copyright notices relating to those materials must be complied with.

Copyright and source acknowledgement notices may not be removed and must be displayed in any copy, derivative work or partial copy which includes the elements in question.

All copyright, and all rights therein, are protected by national and international copyright laws. The above represents a summary only. For further information please read Frontiers' Conditions for Website Use and Copyright Statement, and the applicable CC-BY licence.

ISSN 1664-8714  
ISBN 978-2-8325-5090-8  
DOI 10.3389/978-2-8325-5090-8

## About Frontiers

Frontiers is more than just an open access publisher of scholarly articles: it is a pioneering approach to the world of academia, radically improving the way scholarly research is managed. The grand vision of Frontiers is a world where all people have an equal opportunity to seek, share and generate knowledge. Frontiers provides immediate and permanent online open access to all its publications, but this alone is not enough to realize our grand goals.

## Frontiers journal series

The Frontiers journal series is a multi-tier and interdisciplinary set of open-access, online journals, promising a paradigm shift from the current review, selection and dissemination processes in academic publishing. All Frontiers journals are driven by researchers for researchers; therefore, they constitute a service to the scholarly community. At the same time, the *Frontiers journal series* operates on a revolutionary invention, the tiered publishing system, initially addressing specific communities of scholars, and gradually climbing up to broader public understanding, thus serving the interests of the lay society, too.

## Dedication to quality

Each Frontiers article is a landmark of the highest quality, thanks to genuinely collaborative interactions between authors and review editors, who include some of the world's best academicians. Research must be certified by peers before entering a stream of knowledge that may eventually reach the public - and shape society; therefore, Frontiers only applies the most rigorous and unbiased reviews. Frontiers revolutionizes research publishing by freely delivering the most outstanding research, evaluated with no bias from both the academic and social point of view. By applying the most advanced information technologies, Frontiers is catapulting scholarly publishing into a new generation.

## What are Frontiers Research Topics?

Frontiers Research Topics are very popular trademarks of the *Frontiers journals series*: they are collections of at least ten articles, all centered on a particular subject. With their unique mix of varied contributions from Original Research to Review Articles, Frontiers Research Topics unify the most influential researchers, the latest key findings and historical advances in a hot research area.

Find out more on how to host your own Frontiers Research Topic or contribute to one as an author by contacting the Frontiers editorial office: [frontiersin.org/about/contact](https://frontiersin.org/about/contact)



# Biology of C-reactive protein

## Topic editors

Alok Agrawal – East Tennessee State University, United States

Yi Wu – Xi'an Jiaotong University, China

## Citation

Agrawal, A., Wu, Y., eds. (2024). *Biology of C-reactive protein*.

Lausanne: Frontiers Media SA. doi: 10.3389/978-2-8325-5090-8

# Table of contents

05	<b>Editorial: Biology of C-reactive protein</b> Alok Agrawal and Yi Wu
08	<b>C-reactive protein isoforms as prognostic markers of COVID-19 severity</b> Blanca Molins, Marc Figueras-Roca, Oliver Valero, Víctor Llorenç, Sara Romero-Vázquez, Oriol Sibila, Alfredo Adán, Carolina García-Vidal and Alex Soriano
16	<b>C-reactive protein – My perspective on its first half century, 1930-1982</b> Irving Kushner
21	<b>Fueling the flames of colon cancer – does CRP play a direct pro-inflammatory role?</b> Anne Helene Køstner, Anniken Jørlo Fuglestad, Jeanette Baehr Georgsen, Patricia Switten Nielsen, Kristina Bang Christensen, Helle Zibrandtsen, Erik Thorlund Parner, Ibraheem M. Rajab, Lawrence A. Potempa, Torben Steiniche and Christian Kersten
33	<b>Combination of anti-C1qA08 and anti-mCRP a.a.35-47 antibodies is associated with renal prognosis of patients with lupus nephritis</b> Xiao-Ling Liu, Ying Tan, Feng Yu, Shang-Rong Ji and Ming-Hui Zhao
44	<b>C-reactive protein as the biomarker of choice to monitor the effects of exercise on inflammation in Parkinson's disease</b> Niyati Mehta, Nijee S. Luthra, Daniel M. Corcos and Giamila Fantuzzi
49	<b>Comparison of C-reactive protein with distinct hyperinflammatory biomarkers in association with COVID-19 severity, mortality and SARS-CoV-2 variants</b> Tudorita Gabriela Paranga, Mariana Pavel-Tanasa, Daniela Constantinescu, Claudia Elena Plesca, Cristina Petrovici, Ionela-Larisa Miftode, Mihaela Moscalu, Petru Cianga and Egidia Gabriela Miftode
71	<b>C-reactive protein: a target for therapy to reduce inflammation</b> Salma A. Rizo-Téllez, Meriem Sekheri and János G. Filep
81	<b>C-reactive protein binds to short phosphoglycan repeats of <i>Leishmania</i> secreted proteophosphoglycans and activates complement</b> Eu Shen Seow, Eve C. Doran, Jan-Hendrik Schroeder, Matthew E. Rogers and John G. Raynes
94	<b>Pentameric C-reactive protein is a better prognostic biomarker and remains elevated for longer than monomeric CRP in hospitalized patients with COVID-19</b> Francis R. Hopkins, Johan Nordgren, Rafael Fernandez-Botran, Helena Enocsson, Melissa Govender, Cecilia Svanberg, Lennart Svensson, Marie Hagbom, Åsa Nilsson-Augustinsson, Sofia Nyström, Christopher Sjöwall, Johanna Sjöwall and Marie Larsson

- 101 **C-reactive protein deficiency ameliorates experimental abdominal aortic aneurysms**  
Yu Fu, Haole Liu, Kexin Li, Panpan Wei, Naqash Alam, Jie Deng, Meng Li, Haibin Wu, Xue He, Haiwen Hou, Congcong Xia, Rong Wang, Weirong Wang, Liang Bai, Baohui Xu, Yankui Li, Yi Wu, Enqi Liu and Sihai Zhao
- 111 **Mutations on a conserved distal enhancer in the porcine C-reactive protein gene impair its expression in liver**  
Carles Hernández-Banqué, Teodor Jové-Juncà, Daniel Crespo-Piazuelo, Olga González-Rodríguez, Yulixais Ramayo-Caldas, Anna Esteve-Codina, Marie-José Mercat, Marco C. A. M. Bink, Raquel Quintanilla and Maria Ballester
- 122 **A biofunctional review of C-reactive protein (CRP) as a mediator of inflammatory and immune responses: differentiating pentameric and modified CRP isoform effects**  
Margaret E. Olson, Mary G. Hornick, Ashley Stefanski, Haya R. Albanna, Alesia Gjoni, Griffin D. Hall, Peter C. Hart, Ibraheem M. Rajab and Lawrence A. Potempa
- 133 **Biological significance of C-reactive protein, the ancient acute phase functionary**  
Shelley Bhattacharya and Chayan Munshi
- 140 **Structural insights into the biological functions of the long pentraxin PTX3**  
Anna Margherita Massimino, Filippo Emanuele Colella, Barbara Bottazzi and Antonio Inforzato
- 150 **Serum CRP interacts with SPARC and regulate immune response in severe cases of COVID-19 infection**  
Chengyang Liu, Chenyang Zheng, Xipeng Shen, Ling Liang and Qiuyu Li
- 159 **C-reactive protein lowers the serum level of IL-17, but not TNF- $\alpha$ , and decreases the incidence of collagen-induced arthritis in mice**  
Sanjay K. Singh, Amanda Prislovsky, Donald N. Ngwa, Undral Munkhsaikhan, Ammaar H. Abidi, David D. Brand and Alok Agrawal



## OPEN ACCESS

EDITED AND REVIEWED BY

Francesca Granucci,  
University of Milano-Bicocca, Milan, Italy

\*CORRESPONDENCE

Alok Agrawal

✉ agrawal@etsu.edu

Yi Wu

✉ wuyi\_med@xjtu.edu.cn

RECEIVED 06 June 2024

ACCEPTED 11 June 2024

PUBLISHED 19 June 2024

## CITATION

Agrawal A and Wu Y (2024) Editorial:  
Biology of C-reactive protein.  
*Front. Immunol.* 15:1445001.  
doi: 10.3389/fimmu.2024.1445001

## COPYRIGHT

© 2024 Agrawal and Wu. This is an open-access article distributed under the terms of the [Creative Commons Attribution License \(CC BY\)](#). The use, distribution or reproduction in other forums is permitted, provided the original author(s) and the copyright owner(s) are credited and that the original publication in this journal is cited, in accordance with accepted academic practice. No use, distribution or reproduction is permitted which does not comply with these terms.

# Editorial: Biology of C-reactive protein

Alok Agrawal<sup>1\*</sup> and Yi Wu<sup>2\*</sup>

<sup>1</sup>Department of Biomedical Sciences, James H. Quillen College of Medicine, East Tennessee State University, Johnson City, TN, United States, <sup>2</sup>MOE Key Laboratory of Environment and Genes Related to Diseases, School of Basic Medical Sciences, Xi'an Jiaotong University, Xi'an, China

## KEYWORDS

C-reactive protein, COVID-19, inflammation, pentraxin, PTX3

## Editorial on the Research Topic

## Biology of C-reactive protein

C-reactive protein (CRP) was discovered almost 100 years ago in the sera of patients suffering of pneumococcal pneumonia [ (1), reviewed in (2)]. Since then, there has been two major questions about CRP: how does CRP appear in the blood within hours of acute inflammation and what does CRP do in inflammatory states? The goal of this Research Topic was to cover the latest developments on the mechanisms of expression of the CRP gene and on the structure-function relationships of CRP.

The history of research on the biology of CRP since its discovery in 1930 till 1982 is summarized in a personal perspective article by [Kushner](#). It was only during the first 50 years when three fundamental discoveries about CRP were made. One, the primary ligand-binding specificity of CRP was for phosphocholine-containing substances (3). Two, ligand-complexed CRP activated the classical pathway of the complement system [reviewed in (4)]. Three, CRP bound to Fc receptors even if CRP was not complexed with its ligand or even if there was no conformational change in the structure of CRP [reviewed in (5)].

CRP is an acute phase protein produced by the liver [reviewed in (6)]. The expression of the CRP gene in hepatocytes and the subsequent biosynthesis of the protein increase dramatically in response to pro-inflammatory cytokines produced during acute inflammation. The mechanism of CRP gene expression in acute phase is not fully understood. Recently, it has been reported that an enhancer located upstream of the proximal promoter of the CRP gene is critical for the acute phase expression of CRP (7). An original research article by [Hernández-Banqué et al.](#) reports the mechanism of expression of the porcine CRP gene. The authors show that the porcine and human CRP proximal promoter regions have been conserved, sharing binding sites for transcription factors. Like in the human CRP gene, there is a highly conserved putative enhancer on the porcine CRP gene. The enhancer-promoter interaction was found to be necessary for the acute phase induction of CRP expression in liver.

Since the serum level of CRP rises in inflammatory states, serum CRP is used as a non-specific biomarker for inflammation before and during the treatment of inflammatory diseases (6). In a perspective article by [Mehta et al.](#), the authors make a case for CRP to be used as a primary biomarker of inflammation and therefore disease progression and severity of Parkinson's disease, particularly in studies examining the impact of an intervention on the signs and symptoms of the disease.

CRP has been related to COVID-19 caused by severe acute respiratory syndrome coronavirus-2 (SARS-CoV-2) [reviewed in (8)]. Three original research articles are presented here showing the usefulness of CRP as a biomarker of COVID-19. Hopkins et al. report that the levels of CRP are significantly raised and associated with disease severity in patients with severe COVID-19, suggesting that the serum CRP level is a useful biomarker for predicting disease severity. Their data also indicated that there was a low level of inflammation which lasted for at least six weeks following COVID-19. Molins et al. investigated the potential of monomeric CRP (mCRP, a dissociated subunit of pentameric CRP) in serum as a biomarker of disease severity in COVID-19 patients. They found that the patients with severe disease had higher levels of both pentameric CRP and mCRP. However, mCRP but not pentameric CRP was independently associated to disease severity, indicating the potential of serum mCRP levels as a biomarker of clinical severity in COVID-19. Paranga et al. show that the patients with severe COVID-19 have higher serum levels of CRP compared to the moderate cases. The data also identified CRP as the best discriminate between severe and non-severe forms of COVID-19.

Native CRP is composed of five identical subunits arranged in a cyclic pentameric symmetry (9). CRP has been shown to exist and function as a pattern recognition molecule in three different structural conformations: native pentameric CRP, non-native pentameric CRP (a transitional conformation where the pentamer is structurally altered) and mCRP. Olson et al. reviews the published literature on the functions of these three forms of CRP and conclude that pentameric CRP is anti-inflammatory while mCRP is pro-inflammatory. This review provides a revised understanding of the structure-function relationships of CRP as related to innate immunity and inflammation.

*In vitro*, CRP exhibits two functions: a recognition function and an effector function. The recognition function involves the binding of CRP to a ligand. The effector function of CRP involves complement activation by liganded CRP. Combined, these two functions of CRP have been shown to provide innate immunity against pneumococcal infection [reviewed in (10)]. In this Research Topic, there are six original research reports focusing on the functions of CRP in abdominal aortic aneurysms, inflammatory autoimmune arthritis, cancer, COVID-19, *Leishmania* parasite infection and nephritis. Fu et al. investigated the functions of CRP in abdominal aortic aneurysms employing a mouse model of the disease. They report that the serum CRP levels are higher in aneurysmal than that in non-aneurysmal aortas. CRP contributed to the pathogenesis of the disease since the deficiency of CRP was found to suppress aneurysmal aortic dilation and CRP did so by attenuating aneurysmal elastin destruction, macrophage accumulation and matrix metalloproteinase-2 expression. Singh et al. investigated the functions of CRP in inflammatory arthritis employing a mouse model of collagen-induced arthritis. They report that CRP lowers the serum level of IL-17, but not TNF- $\alpha$ , and decreases the incidence of collagen-induced arthritis in mice. Kostner et al. investigated the functions of CRP in cancer and within the tumor microenvironment in a colon cancer cohort. They show that mCRP is abundantly present within tumors from patients with high serum CRP levels. mCRP was detected exclusively within tumors. Some tumor cells were also found to colocalize with mCRP, suggesting a direct interaction or mCRP

expression by the tumor itself. Liu et al. investigated the relationship between serum CRP levels and circulating megakaryocyte proportion in COVID-19 patients. They found that serum CRP levels correlated with megakaryocyte marker genes, and megakaryocytes were significantly accumulated in severe cases. The authors propose a model of how CRP regulates immune responses in COVID-19 infection. Seow et al. investigated the interactions between CRP and the parasite *Leishmania mexicana*. They show that CRP binds to short phosphoglycan repeats of proteophosphoglycans secreted by the parasite and subsequently activates the complement system. Liu et al. investigated the functions of CRP in lupus nephritis. They show that the majority of nephritis patients have autoantibodies to both C1q and mCRP. They also show that mCRP interacts with C1q and that this interaction inhibits the classical pathway of complement activation.

CRP is a member of the pentraxin family of proteins. The other major pentraxins are serum amyloid P component (SAP) and long pentraxin 3 (PTX3). PTX3 is the prototype of long pentraxins while CRP and SAP are short pentraxins [reviewed in (11)]. Both SAP and PTX3 have also been implicated in inflammatory diseases. A review article by Massimino et al. summarizes the current state of knowledge on PTX3. They review the biosynthesis and structure-function relationships of PTX3 in light of the most recent advances in its structural biology, with a focus on the interplay with complement and the emerging roles as a component of the extracellular matrix.

CRP is also a target for developing therapeutics. Rizo-Téllez et al. review recent advances in the strategies to therapeutically lower the serum CRP levels and the development of CRP antagonists specially an inhibitor that could change the conformation of CRP. The authors also discuss the therapeutic potential in mitigating the deleterious actions attributed to CRP under various pathologies, including cardiovascular, pulmonary and autoimmune diseases and cancer.

CRP has been conserved from arthropods to humans [reviewed in (12, 13)]. However, it remains unclear how CRP confers immunity to invertebrates against pathogens. Bhattacharya and Munshi review the published literature on the significance of the presence of CRP in invertebrates. They review the site of synthesis of CRP, the constitutive and induced levels of CRP in the plasma of invertebrates, and the primary structure of CRP from various invertebrate species. Since invertebrates lack an acquired immune response, the authors propose that the invertebrates are dependent on the multifunctional roles of CRP leading to evolutionary success of the invertebrate phyla.

In conclusion, this Research Topic contains perspective articles, review article and original research articles on the following aspects of CRP: mechanisms of expression of the CRP gene, use of CRP as a biomarker of inflammation, structure-function relationships of CRP, functions of the CRP homologs in inflammatory states, CRP in relation to COVID-19 and on the evolution of CRP across the animal kingdom.

## Author contributions

AA: Writing – original draft, Writing – review & editing. YW: Writing – original draft, Writing – review & editing.



## Conflict of interest

The authors declare that the research was conducted in the absence of any commercial or financial relationships that could be construed as a potential conflict of interest.

The author(s) declared that they were an editorial board member of Frontiers, at the time of submission. This had no impact on the peer review process and the final decision.

## Publisher's note

All claims expressed in this article are solely those of the authors and do not necessarily represent those of their affiliated organizations, or those of the publisher, the editors and the reviewers. Any product that may be evaluated in this article, or claim that may be made by its manufacturer, is not guaranteed or endorsed by the publisher.

## References

1. Tillett WS, Francis T Jr. Serological reactions in pneumonia with a non-protein somatic fraction of pneumococcus. *J Exp Med.* (1930) 52:561–71. doi: 10.1084/jem.52.4.561
2. Ji S-R, Zhang S-H, Chang Y, Li H-Y, Wang M-Y, Lv J-M, et al. C-reactive protein: The most familiar stranger. *J Immunol.* (2023) 210:699–707. doi: 10.4049/jimmunol.2200831
3. Volanakis JE, Kaplan MH. Specificity of C-reactive protein for choline phosphate residues of pneumococcal C-polysaccharide. *Proc Soc Exp Biol Med.* (1971) 136:612–4. doi: 10.3181/00379727-136-35323
4. Volanakis JE. Complement activation by C-reactive protein complexes. *Ann N Y Acad Sci.* (1982) 389:235–50. doi: 10.1111/j.1749-6632.1982.tb22140.x
5. Lu J, Mold C, Du Clos TW, Sun PD. Pentraxins and Fc receptor-mediated immune responses. *Front Immunol.* (2018) 9:2607. doi: 10.3389/fimmu.2018.02607
6. Gabay C, Kushner I. Acute-phase proteins and other systemic responses to inflammation. *N Engl J Med.* (1999) 340:448–54. doi: 10.1056/NEJM199902113400607
7. Wang M-Y, Zhang C-M, Zhou H-H, Ge Z-B, Su C-C, Lou Z-H, et al. Identification of a distal enhancer that determines the expression pattern of acute phase marker C-reactive protein. *J Biol Chem.* (2022) 298:102160. doi: 10.1016/j.jbc.2022.102160
8. Pepys MB. C-reactive protein predicts outcome in COVID-19: is it also a therapeutic target? *Eur Heart J.* (2021) 42:2280–3. doi: 10.1093/eurheartj/ehab169
9. Shrive AK, Cheetham GMT, Holden D, Myles DAA, Turnell WG, Volanakis JE, et al. Three-dimensional structure of human C-reactive protein. *Nat Struct Biol.* (1996) 3:346–54. doi: 10.1038/nsb0496-346
10. Ngwa DN, Agrawal A. Structure-function relationships of C-reactive protein in bacterial infection. *Front Immunol.* (2019) 10:166. doi: 10.3389/fimmu.2019.00166
11. Bottazzi B, Inforzato A, Messa M, Barbagallo M, Magrini E, Garlanda C, et al. The pentraxins PTX3 and SAP in innate immunity, regulation of inflammation and tissue remodelling. *J Hepatol.* (2016) 64:1416–27. doi: 10.1016/j.jhep.2016.02.029
12. Torzewski M. C-reactive protein: friend or foe? Phylogeny from heavy metals to modified lipoproteins and SARS-CoV-2. *Front Cardiovasc Med.* (2022) 9:797116. doi: 10.3389/fcvm.2022.797116
13. Pathak A, Agrawal A. Evolution of C-reactive protein. *Front Immunol.* (2019) 10:943. doi: 10.3389/fimmu.2019.00943



## OPEN ACCESS

## EDITED BY

Yi Wu,  
Xi'an Jiaotong University, China

## REVIEWED BY

Karlheinz Peter,  
Baker Heart and Diabetes Institute,  
Australia  
Christopher Sjöwall,  
Linköping University, Sweden  
Lawrence Albert Potempa,  
Roosevelt University, United States

## \*CORRESPONDENCE

Blanca Molins  
✉ bmolins@recerca.clinic.cat

## SPECIALTY SECTION

This article was submitted to  
Molecular Innate Immunity,  
a section of the journal  
Frontiers in Immunology

RECEIVED 22 November 2022

ACCEPTED 26 December 2022

PUBLISHED 18 January 2023

## CITATION

Molins B, Figueras-Roca M, Valero O,  
Llorenç V, Romero-Vázquez S,  
Sibila O, Adán A, García-Vidal C and  
Soriano A (2023) C-reactive protein  
isoforms as prognostic markers  
of COVID-19 severity.  
*Front. Immunol.* 13:1105343.  
doi: 10.3389/fimmu.2022.1105343

## COPYRIGHT

© 2023 Molins, Figueras-Roca, Valero,  
Llorenç, Romero-Vázquez, Sibila, Adán,  
García-Vidal and Soriano. This is an  
open-access article distributed under  
the terms of the [Creative Commons  
Attribution License \(CC BY\)](https://creativecommons.org/licenses/by/4.0/). The use,  
distribution or reproduction in other  
forums is permitted, provided the  
original author(s) and the copyright  
owner(s) are credited and that the  
original publication in this journal is  
cited, in accordance with accepted  
academic practice. No use,  
distribution or reproduction is  
permitted which does not comply with  
these terms.

# C-reactive protein isoforms as prognostic markers of COVID-19 severity

Blanca Molins<sup>1\*</sup>, Marc Figueras-Roca<sup>1,2</sup>, Oliver Valero<sup>3</sup>,  
Víctor Llorenç<sup>1,2</sup>, Sara Romero-Vázquez<sup>1</sup>, Oriol Sibila<sup>4</sup>,  
Alfredo Adán<sup>1,2</sup>, Carolina García-Vidal<sup>5</sup> and Alex Soriano<sup>5,6</sup>

<sup>1</sup>Group of Ocular Inflammation: Clinical and Experimental Studies, Institut d'Investigacions Biomèdiques Agustí Pi i Sunyer (IDIBAPS), Barcelona, Spain, <sup>2</sup>Institut Clínic d'Oftalmologia (ICOF), Hospital Clínic, Barcelona, Spain, <sup>3</sup>Statistical Department, Universitat Autònoma de Barcelona, Barcelona, Spain, <sup>4</sup>Respiratory Department, Hospital Clínic of Barcelona-IDIBAPS, CIBERES, University of Barcelona, Barcelona, Spain, <sup>5</sup>Department of Infectious Diseases, Hospital Clínic of Barcelona-IDIBAPS, University of Barcelona, Barcelona, Spain, <sup>6</sup>CIBERINF, Barcelona, Spain

C-reactive protein (CRP), an active regulator of the innate immune system, has been related to COVID-19 severity. CRP is a dynamic protein undergoing conformational changes upon activation in inflammatory microenvironments between pentameric and monomeric isoforms. Although pentameric CRP is the circulating isoform routinely tested for clinical purposes, monomeric CRP shows more proinflammatory properties. Therefore, we aimed to determine the potential of monomeric CRP in serum as a biomarker of disease severity in COVID-19 patients (admission to intensive care unit [ICU] and/or in-hospital mortality). We retrospectively determined clinical and biological features as well as pentameric and monomeric CRP levels in a cohort of 97 COVID-19 patients within 72h of hospital admission. Patients with severe disease had higher levels of both pentameric and monomeric CRP. However, multivariate analysis showed increased mCRP but not pCRP to be independently associated to disease severity. Notably, mCRP levels higher than 4000 ng/mL (OR: 4.551, 95% CI: 1.329–15.58), together with number of co-morbidities, low lymphocyte count, and procalcitonin levels were independent predictors of disease severity in the multivariate model. Our results show the potential of mCRP levels as a marker of clinical severity in COVID-19 disease.

## KEYWORDS

C-reactive protein, COVID-19, isoforms, inflammation, prognosis

## 1 Introduction

Coronavirus disease 2019 (COVID-19), caused by severe acute respiratory syndrome coronavirus 2 (SARS-CoV-2) infection was declared in March 2020 a global pandemic by the World Health Organization with more than 4 million related deaths since then (1). COVID-19 is asymptomatic or mild in most cases. Yet, 10% of patients present severe

disease due to pneumonia, acute respiratory distress syndrome (ARDS), systemic inflammation, thrombosis, and multiorgan failure, causing death in 1–3% of patients. Indeed, some patients with mild symptoms may present a sudden progression to severe disease (2).

Noteworthy, although hospitalization for COVID-19 is needed only in a minority of patients and disease management has majorly improved since the first outbreak in March 2020, the highly infectious nature of SARS-CoV-2 driving to high incidence spikes in short periods of time is still posing a threat to health care systems worldwide. Thus, predicting individual prognosis is crucial to provide a personalized treatment to reduce mortality. Age, male sex, hypertension, the presence of certain co-morbidities, and several blood biomarkers have been consistently associated with worse prognosis (3, 4).

C-reactive protein (CRP), an acute phase reactant and an active regulator of the innate immune system, is increased in COVID-19 patients and has been associated to disease severity (5, 6). Among its multiple functions, CRP activates the classical pathway and inactivates the alternative pathway of the complement system (7). CRP is mainly synthesized in the liver upon interleukin- (IL-) 6 induction and its levels can increase up to 100-fold in response to several forms of tissue damage, infection and inflammation. In plasma, CRP circulates as a disk-shaped pentamer (also known as pentameric CRP, pCRP) composed of five 23 kDa non-covalently bound subunits (8). Nevertheless, low pH, oxidative stress and bioactive lipids from activated cells can dissociate pCRP into its monomeric subunits (9, 10) by means of phospholipase A<sub>2</sub> activation and subsequent lysophosphatidylcholine cell surface exposure (11). This conformation of CRP, named monomeric CRP (mCRP), shows different biological functions and antigenicity-expressing neopeptides than pCRP representing the tissue-associated insoluble form of CRP. Although there is no standardized method, circulating levels of mCRP in serum can be measured by means of customized ELISA (12). Unlike pCRP, mCRP presents a prothrombotic and proinflammatory phenotype (13–16). Given that most reports on the role of CRP in systemic diseases are based on the pentameric conformation, additional research on the specific implications of mCRP over pCRP should be addressed.

Considering the hyperinflammatory nature of COVID-19 complications and the fact that mCRP dissociates from pCRP in proinflammatory microenvironments and it is also the main active proinflammatory isoform of CRP, we hypothesized that mCRP could be considered as a more specific prognostic marker of inflammatory progression and severity than pCRP in COVID-19. Thus, we aimed to evaluate mCRP and pCRP levels in COVID-19 patients at hospital admission to determine their prognostic value to progression to more severe disease forms.

## 2 Methods

### 2.1 Study design, patients, and data collection

We performed an observational retrospective study of 97 patients admitted to the hospital (Hospital Clinic of Barcelona, Spain) for > 48h with confirmed acute SARS-CoV-2 infection by rRT-PCR performed on nasopharyngeal and throat swabs between March 1st and September 30th 2020. Included patients had serum samples preserved in the COVIDBANK within 72h of admission for further determination of circulating levels of mCRP. The COVIDBANK is a biorepository of biological samples from SARS-CoV-2 patients treated in Hospital Clinic of Barcelona with the aim of providing samples of quality for SARS-CoV-2-related scientific research. The Institutional Ethics Committee of Hospital Clinic of Barcelona approved the study (HCB/2020/0874) and patients gave their informed consent to the COVIDBANK.

Data were retrospectively obtained for all patients included in the study from the electronic health records. Variables included were age, sex, and co-morbidities (chronic heart disease, diabetes mellitus, chronic kidney disease, hypertension, solid malignant neoplasm, chronic respiratory disease, haematologic disease, hepatopathy, solid organ transplant, HIV). Biochemical variables included blood cell count (eosinophils, basophils, lymphocytes), creatinine, D-dimer, ferritin, lactate dehydrogenase (LDH), procalcitonin, troponin, and pCRP at admission. The composite outcome variable included the need of intensive care unit (ICU) admission and/or in-hospital mortality at any time during in-hospital stay. In addition, mCRP levels were determined from preserved serum samples of the COVIDBANK.

### 2.2 Serum mCRP determination

Serum mCRP was detected with the ELISA protocol described by Zhang et al. with some modifications (12, 17). Briefly, mouse anti-human CRP mAb CRP-8 (Sigma-Aldrich, C1688) was immobilized as capture antibody at 1:1000 in coating buffer (10 mM sodium carbonate/bicarbonate, pH 9.6) for 18h at 4°C. This commercially available monoclonal antibody has been reported to specifically recognize mCRP, but not pCRP (18). After washing three times for 2 min each with TBS, non-specific binding was blocked with filtered 1% BSA-TBS for 1 hour at 37°C. Samples were diluted 1:100 in blocking buffer and added into wells for 1h at 37°C. Then, washing step was repeated and samples were incubated with sheep anti-human CRP polyclonal antibody (MBS223280, MyBioSource) at 1:5000 in blocking buffer for 1h at room

temperature (RT), before incubation with a HRP-labelled donkey anti-sheep IgG (Abcam) at 1:10000 in blocking buffer for 30 min at RT. Signalling was detected with VersaMax Microplate Reader and the OD value of each sample was calculated as  $OD_{450} - OD_{570}$  nm. A standard curve was prepared by serial dilutions of mCRP (0–50 ng/mL) obtained by urea-chelation of pCRP (Calbiochem) (16) in blocking buffer (1% BSA-TBS) in the presence of reference diluted sera (1:100). The concentration of mCRP in the reference sera was below detection level and therefore undetectable following 1:100 dilution. Controls using purified pCRP at a concentration of 100 ng/mL, which would be equivalent to 10 µg/mL after 1:100 dilution, only generated background signal, showing specificity for mCRP.

## 2.3 Statistical analysis

Categorical variables were described as absolute (N) and relative (%) frequencies and Chi square or Fisher's test was used for comparisons. Quantitative variables following a normal distribution were represented as mean  $\pm$  standard deviation and differences between groups were determined with Student's t-test. Variables with a non-normal distribution were expressed as median and minimum and maximum value and the Mann-Whitney test was employed to determine significant differences. Linear relationships were analysed by determination of Spearman correlation coefficient. Statistical assumptions were made based on significance level below 0.05.

To determine the variables associated with disease severity (need for ICU admission and/or in-hospital mortality), a multivariable logistic regression model was performed adding the variables with a P value lower than 0.2 in the bivariate analysis. Variables with more than 10% of missing values were excluded. Quantitative variables added to the multivariate analysis were dichotomized as follows: age ( $>70$ ), pCRP ( $>10$  µg/mL), mCRP ( $>4000$  ng/mL), creatinine ( $>1.1$  mg/dL in women and  $>1.3$  mg/dL in men), D-dimer ( $>500$  ng/mL), lymphocytes ( $<0.004 \times 10^9/L$ ), procalcitonin ( $>0.5$  ng/mL), ferritin ( $>306$  ng/mL in women and  $>336$  ng/mL in men), troponin ( $>50$  ng/mL). Cut-off values of pCRP, creatinine, D-dimer, lymphocyte count, procalcitonin, and ferritin were chosen based on their abnormal levels associated to pathology. The final model was reached through backward stepwise removal of variables with p-value higher than 0.1 and using Wald tests to demonstrate that each model was better than its previous iteration. Odds ratio (OR) with 95% confidence interval (CI) were calculated. To assess the predictive ability of each model, we calculated the area under the receiver operating characteristic (ROC) curve with its respective 95% confidence interval (95% CI) and determined the cut-off value to maximize sensitivity and specificity. Statistical analyses were performed using SAS v9.4 software (SAS Institute Inc., Cary, NC, USA).

## 3 Results

Study population consisted of 97 patients admitted to Hospital Clínic of Barcelona between March and September 2020 for  $>48$ h with confirmed acute SARS-CoV-2 infection. The mean age was  $60 \pm 17$  years and 59 (61%) were males. The most common co-morbidities were hypertension (50.5%), diabetes mellitus (28.9%), chronic heart disease (23.7%), chronic respiratory disease (21.6%), solid malignant neoplasm (15.5%), and chronic kidney disease (15.5%). Other minor co-morbidities included chronic liver disease, hematologic disease, solid organ transplant, and HIV infection. A total of 27 (27.8%) patients were admitted to the ICU and the in-hospital mortality rate was 25.8% (Table 1). Although the majority of patients that died were previously admitted to ICU (15/25, 60%), some died in normal ward (10/25, 40%). Severe disease was defined as ICU admission and/or in-hospital mortality.

Patients with severe disease (37/97) were older ( $68.76 \pm 14.8$  vs.  $55.02 \pm 16.1$  years,  $P<0.001$ ) and had more co-morbidities ( $2.43$  [0.00–5.00] vs.  $1.20$  [0.00–5.00],  $P<0.001$ ). Patients with higher levels at admission of creatinine ( $1.17$  [0.24–6.49] vs.  $0.85$  [0.50–4.05] mg/dL,  $P=0.012$ ), D-dimer ( $1200$  [400–28400] vs.  $450$  [200–6000] ng/mL,  $P<0.001$ ), procalcitonin ( $0.18$  [0.03–15.03] vs.  $0.08$  [0.00–1.58] ng/mL,  $P<0.001$ ), troponin ( $11.65$  [0.00–304] vs.  $3.25$  [0–803] ng/L,  $P<0.001$ ), pCRP ( $11.61$  [1.65–33.50] vs.  $5.63$  [0.00–33.34] µg/mL,  $P=0.013$ ), and mCRP ( $3551.3$  [30–9806] vs.  $206$  [30–8086], ng/mL  $P<0.001$ ) and lower lymphocyte count ( $0.60$  [0.10–2.90] vs.  $1.15$  [0.30–2.20]  $10^9/L$ ,  $P<0.001$ ) were also more likely to develop severe disease. Chronic kidney and heart disease, hypertension, and solid malignant neoplasm were also associated to disease severity (Table 1). As shown in Figure 1, patients that required ICU admission and/or died had higher levels of both monomeric ( $*P<0.001$ ) and pentameric CRP ( $*P=0.013$ ). mCRP significantly correlated with pCRP ( $r=0.377$ ,  $P<0.001$ ), although the correlation coefficient was only intermediate (Figure 1C). When analysing the ratio  $\log\_mCRP/pCRP$  no association with disease severity was found. In fact, when determining the correlation of  $\log\_mCRP/pCRP$  with established severity markers only a statistically significant correlation was observed for creatinine ( $r=0.241$ ,  $P=0.019$ ) and troponin ( $r=0.264$ ,  $P=0.015$ ), but not for procalcitonin ( $r=-0.007$ ,  $P=0.94$ ), lymphocyte count ( $r=-0.173$ ,  $P=0.096$ ), ferritin ( $r=-0.157$ ,  $P=0.139$ ), and D-dimer ( $r=0.133$ ,  $P=0.208$ ). Instead, mCRP significantly correlated with more markers of severity including procalcitonin ( $r=0.278$ ,  $P=0.007$ ), lymphocyte count ( $r=-0.335$ ,  $P=0.001$ ), creatinine ( $r=0.205$ ,  $P=0.044$ ), troponin ( $r=0.275$ ,  $P=0.01$ ), and D-dimer ( $r=0.329$ ,  $P=0.001$ ) but not with ferritin ( $r=0.087$ ,  $P=0.410$ ). Nevertheless, in most cases correlation coefficient was weak ( $r<0.3$ ).

Quantitative variables were then dichotomized and added to the multivariate analysis: number of pathologies, high levels of

**TABLE 1** Clinical and analytical features of COVID-19 patients upon admission and significant risk factors for disease severity (ICU admission and/or in-hospital mortality) on bivariate analysis.

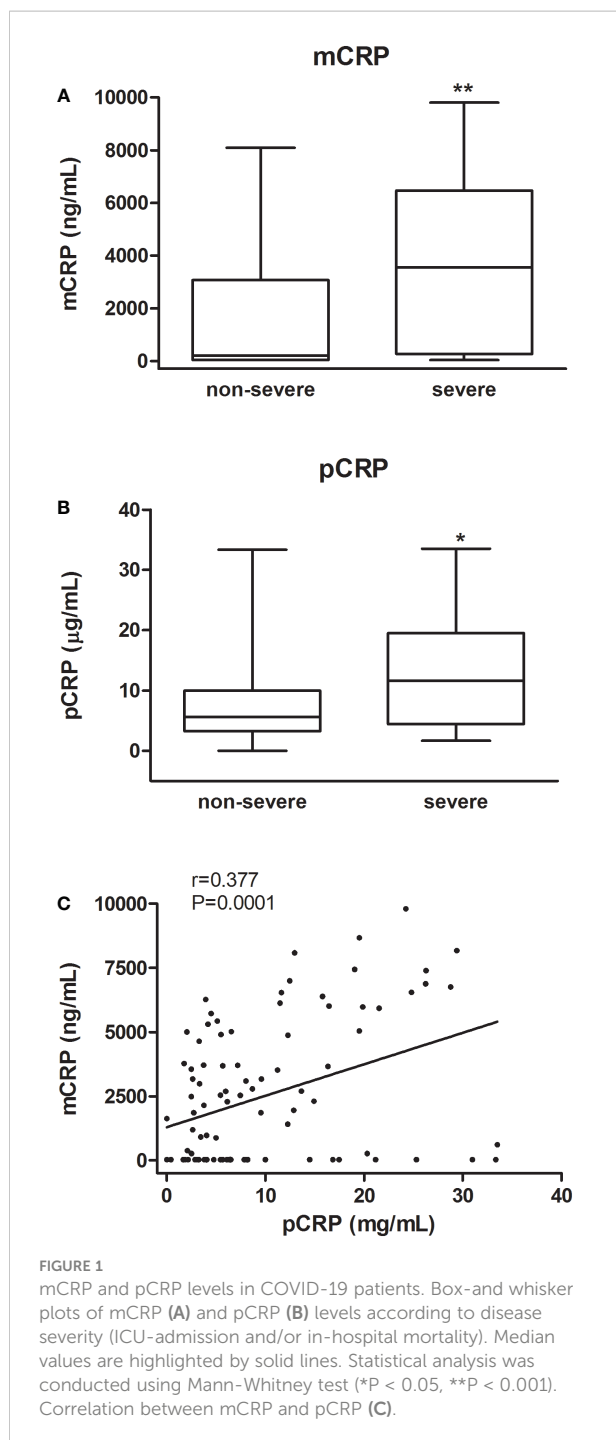
Variable	Total N=97	Non-severe disease N=60	Severe disease N=37	P-value
Age, mean (SD), years	60.3 (16.9)	55.02 (16.1)	68.76 (14.8)	*<0.001
Male, N (%)	59 (60.2)	36 (61.0)	23 (39.0)	0.911
<b>Pre-existing comorbidities, N (%)</b>				
Chronic heart disease	23 (23.7)	7 (30.4)	16 (69.6)	*<0.001
Diabetes mellitus	28 (28.9)	15 (53.6)	13 (46.4)	0.285
Chronic kidney disease	15 (15.5)	3 (20.0)	12 (80.0)	*<0.001
Hypertension	49 (50.5)	24 (49.0)	25 (51.0)	*0.008
Solid malignant neoplasm	15 (15.5)	5 (33.3)	10 (66.7)	*0.013
Chronic respiratory disease	21 (21.6)	15 (71.4)	6 (28.6)	0.308
Other pathologies		3 (33.3)	6 (66.7)	0.064
Haematologic disease	2 (2.1)	1 (50.0)	1 (50.0)	1.000
Chronic liver disease	3 (3.1)	0 (0)	3 (100)	0.053
Solid organ transplant	3 (3.1)	1 (33.3)	2 (66.7)	0.556
HIV	3 (3.1)	1 (33.3)	2 (66.7)	0.556
Number of pathologies, median (min-max)	1.67 (0.00-5.00)	1.20 (0.00-5.00)	2.43 (0.00-5.00)	*<0.001
<b>Analytical variables, median (min-max)</b>				
Basophils, 10 <sup>9</sup> /L	0.00 (0.00-0.10)	0.00 (0.00-0.10)	0.00 (0.00-0.10)	0.838
Eosinophils, 10 <sup>9</sup> /L	0.00 (0.00-0.50)	0.00 (0.00-0.40)	0.00 (0.00-0.50)	0.150
Lymphocytes, 10 <sup>9</sup> /L	1.00 (0.10-2.90)	1.15 (0.30-2.20)	0.60 (0.10-2.90)	*<0.001
Creatinine, mg/dL	0.87 (0.24-6.49)	0.85 (0.50-4.05)	1.17 (0.24-6.49)	*0.012
D-dimer, ng/mL	650 (200-28400)	450 (200-6000)	1200 (400-28400)	*<0.001
Ferritin, ng/mL	596 (12-6126)	487 (12-4309)	740 (21-6126)	0.127
LDH, U/L	302 (148-971)	298 (148-675)	332 (168-971)	0.178
Procalcitonin, ng/mL	0.12 (0.00-15.03)	0.08 (0.00-1.58)	0.18 (0.03-15.03)	*<0.001
Troponin, ng/L	7.20 (0.00-803)	3.25 (0.00-803)	11.65 (0.00-304)	*<0.001
pCRP, µg/mL	6.43 (0.00-33.50)	5.63 (0.00-33.34)	11.61 (1.65-33.50)	*0.013
mCRP, ng/mL	1860 (30-9805)	206.0 (30-8086)	3551.3 (30-9806)	*<0.001
Log, mCRP/pCRP	5.44 (-0.11-7.82)	4.75 (-0.11-7.82)	5.64 (0.54-7.27)	0.216
*Statistically significant.				

mCRP (>4000 ng/mL) and procalcitonin (>0.5 ng/mL), and low lymphocyte count (<0.004 x10<sup>9</sup>/L) were independently associated to disease severity. Lymphocyte count (OR: 4.615, 95% CI: 1.493–14.26), procalcitonin (OR: 18.199, 95% CI: 2.235–148.17), and mCRP (OR: 4.551, 95% CI: 1.329–15.58) were retained in the model as independent predictors of severity (Table 2). The area under the ROC curve (AUC) was 0.869 (95% CI: 0.794–0.945, and the best cut-off had a 86.1% sensitivity and 75.0% specificity) showing a good ability to predict in-hospital mortality (Figure 2).

## 4 Discussion

Since the first outbreak in early 2020 huge labour has been devoted to understand COVID-19 pathophysiology and to identify prognosis factors for disease severity worldwide. The wide range of signs, symptoms and clinic severity urge to a personalized approach for disease management. In this regard, certain blood biomarkers such as IL-6, ferritin, D-dimer, and CRP may be able to anticipate the development of the cytokine





storm leading to COVID-19 complications (19, 20). Here, we provide insights on the potential of the conformational isoforms of CRP to predict disease severity, defined as ICU admission and/or in-hospital mortality. Our results show that high levels of circulating mCRP in COVID-19 patients at hospital admission are independently associated to disease severity.

CRP is a dynamic protein subjected to conformational changes upon activation in inflammatory microenvironments

between circulating (pCRP) and monomeric (mCRP) tissue-based isoforms. Notably, mCRP manifests potent proinflammatory effects and activates platelets (16), leukocytes (15), and endothelial cells (21). Moreover, mCRP deposition has been localized in inflamed tissues, thus suggesting an active role in the progression of several inflammatory disorders including Alzheimer's disease (22), cardiovascular disease (23), and age-related macular degeneration (24). Although mCRP could represent a more accurate marker of inflammation, pentameric pCRP is the CRP isoform determined for clinical purposes.

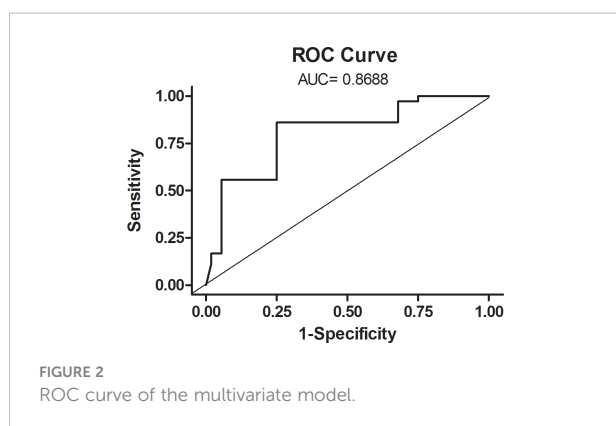
Currently, there are no commercially available assays to determine serum or plasma levels of mCRP, likely due to the insoluble nature of the monomeric subunit. However, several reports have developed customized ELISA assays to determine circulating mCRP using specific antibodies against mCRP. Some authors have generated their own antibodies against mCRP (25–27), others have used mCRP antibodies (clone 8C10) developed by Potempa et al. (28), while others have used the commercially available clone CRP-8 that has been described to specifically recognize mCRP (12, 29). In our study, we followed the protocol described by Zhang et al., and used the monoclonal antibody CRP-8 to quantify circulating mCRP in our cohort as this protocol avoided cross-reactivity with pCRP. Alternatively, flow cytometry has also been used by some authors to determine circulating mCRP (30, 31).

The precise nature of the mCRP detected by ELISA is unclear as both highly denaturated or globular mCRP forms may be present in serum samples. Given the reduced solubility of mCRP it is conceivable that detected mCRP can be also bound to microparticles. Alternatively, circulating mCRP can be found in a globular form with binding properties similar to the pentameric form as recently described by Williams et al. (29). Indeed, further research regarding the structure and function of physiological circulating mCRP is warranted.

No standardized method for circulating mCRP determination has been established yet and different techniques and protocols may result in different mCRP values, which currently limit the translational application of mCRP in the clinical setting. Yet, few

**TABLE 2** Significant risk factors for disease severity (ICU admission and/or in-hospital mortality) on multivariate regression analysis.

Variable	OR	95% CI	P-value
Number of pathologies			*0.036
1 vs. 0	10.660	1.448–78.48	
2 vs. 0	12.135	1.787–82.41	
2 vs. 1	1.138	0.344–3.77	
mCRP >4000 ng/mL	4.551	1.329–15.58	*0.016
Lymphocytes $<0.004 \times 10^9/L$	4.615	1.493–14.26	*0.008
Procalcitonin >0.5 ng/mL	18.199	2.235–148.17	*0.007
*Statistically significant.			



studies have determined circulating mCRP levels in several diseases including skin related autoimmune disorders (0–120 ng/mL) (12), Adult-Onset Still's disease (0–1000 ng/mL) (25), systemic lupus erythematosus (1–7 ng/mL), antineutrophil cytoplasmic antibody-associated vasculitis (5–20 ng/mL) (28), atherosclerosis (0–50 ng/mL) (27), and chronic pulmonary obstructive disease (600–1000 ng/mL) (26). In these studies, mCRP levels were lower than those for hospitalized COVID-19 patients from our study. As a matter of fact, the study of Karlsson et al. also included a control group of healthy subjects with a mean level of mCRP below 10 ng/mL (28). Although differences may be attributed to the method used to determine mCRP it is conceivable that COVID-19 patients at hospital admission may present increased levels of mCRP compared to other pathologies. Because mCRP dissociates from pCRP, it is also conceivable that high levels of pCRP, as the ones of our cohort, lead to higher levels of mCRP. Indeed, mCRP significantly correlated with pCRP although the correlation coefficient was not particularly strong.

Given the wide range of COVID-19 clinical presentation, severe disease was considered on either ICU admission and/or in-hospital death in order to search for high external validity findings. Accordingly, our results showed that both mCRP and pCRP were significantly associated to disease severity in the bivariate analysis. Interestingly, mCRP, but not pCRP, was independently associated to disease severity in the multivariate analysis. Because mCRP represents the proinflammatory conformation of CRP we also aimed to determine whether the ratio mCRP/pCRP was associated to disease severity. Nevertheless, unlike mCRP, this variable was not associated to disease severity. Notably, the multivariate model including mCRP, number of pathologies, low lymphocyte count, and procalcitonin had an AUC of 0.869, with a 86.1% sensitivity and 75.0% specificity in the best cut-off showing a good ability to predict in-hospital mortality. Although our results suggest that mCRP could serve as a prognostic factor of disease severity in COVID-19, a standardized method for determining circulating mCRP should be established before its clinical application.

Whether mCRP plays a role in the progression of COVID-19 or is merely a marker remains unclear. A recent study showed that mCRP can bind to the SARS-CoV-2 spike receptor binding-domain (RBD) and competes with the binding of the spike RBD to angiotensin-converting enzyme 2 (ACE2) receptor (32). Increased levels of CRP induced by SARS-CoV-2 infection may eventually lead to unrestrained inflammation. Indeed, CRP apheresis can reduce the immune response in COVID-19 patients, as showed in a case series report of seven patients (33). Targeting mCRP in COVID-19 patients could represent a novel therapeutic target. Besides CRP apheresis, approaches aimed at inhibiting either CRP dissociation into mCRP (34, 35) or antibodies against mCRP (36) could represent attractive alternatives to prevent the cytokine storm and hyperinflammatory status associated to COVID-19. Yet, caution should be taken when targeting CRP as the effects of CRP isoforms may differ depending on the infection stage; in early phases of infection CRP acts as a soluble pattern recognition receptor targeting necrotic or damaged tissue, while in late phases of infection, unrestrained levels of CRP may cause hyperinflammation with its subsequent complications. mCRP is mainly generated within inflamed tissues and has a short circulating half-life (21), thus suggesting that circulating mCRP might not play a direct role in autoimmune induction. Yet, it may act as an indicator of local mCRP accumulation and subsequent inflammation. Immunostaining of mCRP in damaged infected tissue could shed light on the role of mCRP in COVID-19 pathophysiology.

In summary, despite certain intrinsic limitations including retrospective and single centre nature together with limited sample size, our study shows for the first time the role of circulating mCRP as a prognostic factor of disease severity in COVID-19 which should be confirmed in prospective multicentric studies. It should be also pointed that our patient cohort was recruited during the first outbreak of the pandemic, before proper treatments and vaccines were available, which may differ with the phenotype of current COVID-19 patients as disease is now better understood and treated. Determination of mCRP levels in vaccinated COVID-19 patients would help to better understand the role of mCRP in COVID-19. Further studies are warranted to elucidate the role of mCRP in the different stages of SARS-COV-2 infection in order to identify novel targets to prevent the eventual progression to cytokine storm.

## Data availability statement

The raw data supporting the conclusions of this article will be made available by the authors, without undue reservation.

## Ethics statement

The studies involving human participants were reviewed and approved by The Institutional Ethics Committee of Hospital Clinic of Barcelona. The patients/participants provided their written informed consent to participate in this study.

## Author contributions

BM, MF-R, CG-V, and AS contributed to the design of the study and experiments. BM, OV, SR-V, MF-R, and VL performed the experiments, data capture, and analysis. BM, MF-R, OS, AA, CG-V, and AS performed the data interpretation. All authors contributed to the article and approved the submitted version.

## Funding

This study has been funded by Instituto de Salud Carlos III (ISCIII) through the project PI19/00265 and co-funded by the European Union. We are indebted to the Fundació Glòria Soler for its contribution and support to the COVIDBANK of HCB-IDIBAPS. This work was financed by *ad hoc* patronage funds for

research on COVID-19 from donations from citizens and organizations to the Hospital Clínic de Barcelona-Fundació Clínic per a la Recerca Biomèdica.

## Conflict of interest

AS has received honoraria for talks on behalf of Merck Sharp and Dohme, Pfizer, Novartis, Gilead, Menarini and Angelini, as well as grant support from Pfizer and Gilead.

The remaining authors declare that the research was conducted in the absence of any commercial or financial relationships that could be construed as a potential conflict of interest.

## Publisher's note

All claims expressed in this article are solely those of the authors and do not necessarily represent those of their affiliated organizations, or those of the publisher, the editors and the reviewers. Any product that may be evaluated in this article, or claim that may be made by its manufacturer, is not guaranteed or endorsed by the publisher.

## References

1. COVID-19 map - Johns Hopkins coronavirus resource center. Available at: <https://coronavirus.jhu.edu/map.html> (Accessed August 16, 2022).
2. Wu C, Chen X, Cai Y, Xia J, Zhou X, Xu S, et al. Risk factors associated with acute respiratory distress syndrome and death in patients with coronavirus disease 2019 pneumonia in Wuhan, China. *JAMA Intern Med* (2020) 180:934–43. doi: 10.1001/JAMAINTERNMED.2020.0994
3. Tian W, Jiang W, Yao J, Nicholson CJ, Li RH, Sigurslid HH, et al. Predictors of mortality in hospitalized COVID-19 patients: A systematic review and meta-analysis. *J Med Virol* (2020) 92:1875–83. doi: 10.1002/JMV.26050
4. Grasselli G, Zangrillo A, Zanella A, Antonelli M, Cabrini L, Castelli A, et al. Baseline characteristics and outcomes of 1591 patients infected with SARS-CoV-2 admitted to ICUs of the Lombardy region, Italy. *JAMA* (2020) 323:1574–81. doi: 10.1001/JAMA.2020.5394
5. Knight SR, Ho A, Pius R, Buchan I, Carson G, Drake TM, et al. Risk stratification of patients admitted to hospital with covid-19 using the ISARIC WHO clinical characterisation protocol: development and validation of the 4C mortality score. *BMJ* (2020) 370:m3339. doi: 10.1136/BMJ.M3339
6. Liu F, Li L, Da X, Wu J, Luo D, Zhu YS, et al. Prognostic value of interleukin-6, c-reactive protein, and procalcitonin in patients with COVID-19. *J Clin Virol* (2020) 127:104370. doi: 10.1016/j.jcv.2020.104370
7. Black S, Kushner I, Samols D. C-reactive protein. *J Biol Chem* (2004) 279:48487–90. doi: 10.1074/jbc.R400025200
8. Volanakis JE. Human c-reactive protein: Expression, structure, and function. *Mol Immunol* (2001) 38:189–97. doi: 10.1016/S0161-5890(01)00042-6
9. Lauer N, Mihlan M, Hartmann A, Schlötzer-Schrehardt U, Keilhauer C, Scholl HPN, et al. Complement regulation at necrotic cell lesions is impaired by the age-related macular degeneration-associated factor-his 402 risk variant. *J Immunol* (2011) 187:4374–83. doi: 10.4049/jimmunol.1002488
10. Eisenhardt SU, Habersberger J, Murphy A, Chen Y, Woollard KJ, Bassler N, et al. Dissociation of pentameric to monomeric c-reactive protein on activated platelets localizes inflammation to atherosclerotic plaques. *Circ Res* (2009) 105:128–37. doi: 10.1161/CIRCRESAHA.108.190611
11. Thiele JR, Habersberger J, Braig D, Schmidt Y, Goerendt K, Maurer V, et al. Dissociation of pentameric to monomeric c-reactive protein localizes and aggravates inflammation: *In vivo* proof of a powerful proinflammatory mechanism and a new anti-inflammatory strategy. *Circulation* (2014) 130:35–50. doi: 10.1161/CIRCULATIONAHA.113.007124
12. Zhang L, Li HY, Li W, Shen ZY, Di WY, SR Ji, et al. An ELISA assay for quantifying monomeric c-reactive protein in plasma. *Front Immunol* (2018) 9:511. doi: 10.3389/FIMMU.2018.00511
13. Molins B, Pascual A, Llorenç V, Zarranz-Ventura J, Mesquida M, Adán A, et al. C-reactive protein isoforms differentially affect outer blood-retinal barrier integrity and function. *Am J Physiol - Cell Physiol* (2017) 312:C244–53. doi: 10.1152/ajpcell.00057.2016
14. Khreiss T, József L, Hossain S, Chan JSD, Potempa LA, Filep JG. Loss of pentameric symmetry of c-reactive protein is associated with delayed apoptosis of human neutrophils. *J Biol Chem* (2002) 277:40775–81. doi: 10.1074/jbc.M205378200
15. Khreiss T, József L, Potempa LA, Filep JG. Conformational rearrangement in c-reactive protein is required for proinflammatory actions on human endothelial cells. *Circulation* (2004) 109:2016–22. doi: 10.1161/01.CIR.0000125527.41598.68
16. Molins B, Peña E, Vilahur G, Mendieta C, Slevin M, Badimon L. C-reactive protein isoforms differ in their effects on thrombus growth. *Arterioscler Thromb Vasc Biol* (2008) 28:2239–46. doi: 10.1161/ATVBAHA.108.174359
17. Romero-Vázquez S, Adán A, Figueras-Roca M, Llorenç V, Slevin M, Vilahur G, et al. Activation of c-reactive protein proinflammatory phenotype in the blood retinal barrier *in vitro*: Implications for age-related macular degeneration. *Aging (Albany NY)* (2020) 12:13905–23. doi: 10.18632/aging.103655
18. Schwedler SB, Guderian F, Dämmrich J, Potempa LA, Wanner C. Tubular staining of modified c-reactive protein in diabetic chronic kidney disease. *Nephrol Dial Transplant* (2003) 18:2300–7. doi: 10.1093/NDT/GFG407

19. Galván-Román JM, Rodríguez-García SC, Roy-Vallejo E, Marcos-Jiménez A, Sánchez-Alonso S, Fernández-Díaz C, et al. IL-6 serum levels predict severity and response to tocilizumab in COVID-19: An observational study. *J Allergy Clin Immunol* (2021) 147:72–80.e8. doi: 10.1016/j.jaci.2020.09.018
20. Zhou F, Yu T, Du R, Fan G, Liu Y, Liu Z, et al. Clinical course and risk factors for mortality of adult inpatients with COVID-19 in wuhan, China: a retrospective cohort study. *Lancet (London England)* (2020) 395:1054–62. doi: 10.1016/S0140-6736(20)30566-3
21. Li HY, Wang J, Wu YX, Zhang L, Liu ZP, Filep JG, et al. Topological localization of monomeric c-reactive protein determines proinflammatory endothelial cell responses. *J Biol Chem* (2014) 289:14283–90. doi: 10.1074/JBC.M114.555318
22. Gan Q, Wong A, Zhang Z, Na H, Tian H, Tao Q, et al. Monomeric c-reactive protein induces the cellular pathology of alzheimer's disease. *Alzheimer's Dement (New York N Y)* (2022) 8(1):e12319. doi: 10.1002/TRC2.12319
23. Slevin M, Matou-Nasri S, Turu M, Luque A, Rovira N, Badimon L, et al. Modified c-reactive protein is expressed by stroke neovessels and is a potent activator of angiogenesis *in vitro*. *Brain Pathol* (2010) 20:151–65. doi: 10.1111/J.1750-3639.2008.00256.X
24. Chirco KR, Whitmore SS, Wang K, Potempa LA, Halder JA, Stone EM, et al. Monomeric c-reactive protein and inflammation in age-related macular degeneration. *J Pathol* (2016) 240:173–83. doi: 10.1002/path.4766
25. Fujita C, Sakurai Y, Yasuda Y, Homma R, Huang C-L, Fujita M. mCRP as a biomarker of adult-onset still's disease: Quantification of mCRP by ELISA. *Front Immunol* (2022) 0:938173. doi: 10.3389/FIMMU.2022.938173
26. Munuswamy R, De Brandt J, Burtin C, Derave W, Aumann J, Spruit MA, et al. Monomeric CRP is elevated in patients with COPD compared to non-COPD control persons. *J Inflammation Res* (2021) 14:4503–7. doi: 10.2147/JIR.S320659
27. Wang J, Tang B, Liu X, Wu X, Wang H, Xu D, et al. Increased monomeric CRP levels in acute myocardial infarction: a possible new and specific biomarker for diagnosis and severity assessment of disease. *Atherosclerosis* (2015) 239:343–9. doi: 10.1016/j.atherosclerosis.2015.01.024
28. Karlsson J, Wetterö J, Weiner M, Rönnelid J, Fernandez-Botran R, Sjöwall C. Associations of c-reactive protein isoforms with systemic lupus erythematosus phenotypes and disease activity. *Arthritis Res Ther* (2022) 24:139. doi: 10.1186/S13075-022-02831-9
29. Williams RD, Moran JA, Fryer AA, Littlejohn JR, Williams HM, Greenhough TJ, et al. Monomeric c-reactive protein in serum with markedly elevated CRP levels shares common calcium-dependent ligand binding properties with an *in vitro* dissociated form of c-reactive protein. *Front Immunol* (2020) 11:115. doi: 10.3389/FIMMU.2020.00115
30. Melnikov I, Kozlov S, Pogorelova O, Tripoten M, Khamchieva L, Saburova O, et al. The monomeric c-reactive protein level is associated with the increase in carotid plaque number in patients with subclinical carotid atherosclerosis. *Front Cardiovasc Med* (2022) 9:968267. doi: 10.3389/FCVM.2022.968267
31. Crawford JR, Trial JA, Nambi V, Hoogeveen RC, Taffet GE, Entman ML. Plasma levels of endothelial microparticles bearing monomeric c-reactive protein are increased in peripheral artery disease. *J Cardiovasc Transl Res* (2016) 9:184–93. doi: 10.1007/S12265-016-9678-0
32. Li H, Gao N, Liu C, Liu X, Wu F, Dai N, et al. The cholesterol-binding sequence in monomeric c-reactive protein binds to the SARS-CoV-2 spike receptor-binding domain and blocks interaction with angiotensin-converting enzyme 2. *Front Immunol* (2022) 13:918731. doi: 10.3389/FIMMU.2022.918731
33. Schumann C, Heigl F, Rohrbach JJ, Sheriff A, Wagner L, Wagner F, et al. A report on the first 7 sequential patients treated within the c-reactive protein apheresis in COVID (CACOV) registry. *Am J Case Rep* (2022) 23:e935263. doi: 10.12659/AJCR.935263
34. Zeller J, Cheung Tung Shing KS, Nero TL, McFadyen JD, Krippner G, Bogner B, et al. A novel phosphocholine-mimetic inhibits a pro-inflammatory conformational change in c-reactive protein. *EMBO Mol Med* (2022) e16236. doi: 10.15252/EMMM.202216236
35. Zeller J, Bogner B, McFadyen JD, Kiefer J, Braig D, Pietersz G, et al. Transitional changes in the structure of c-reactive protein create highly pro-inflammatory molecules: Therapeutic implications for cardiovascular diseases. *Pharmacol Ther* (2022) 235:108165. doi: 10.1016/j.pharmthera.2022.108165
36. Fujita C, Sakurai Y, Yasuda Y, Takada Y, Huang C-L, Fujita M. Anti-monomeric c-reactive protein antibody ameliorates arthritis and nephritis in mice. *J Immunol* (2021) 207:1755–62. doi: 10.4049/JIMMUNOL.2100349



## OPEN ACCESS

## EDITED BY

Alok Agrawal,  
East Tennessee State University,  
United States

## REVIEWED BY

Robert Munford,  
National Institutes of Health (NIH),  
United States  
Annette Karen Shrive,  
Keele University, United Kingdom

## \*CORRESPONDENCE

Irving Kushner  
✉ [ixk2@case.edu](mailto:ixk2@case.edu)

## SPECIALTY SECTION

This article was submitted to  
Molecular Innate Immunity,  
a section of the journal  
Frontiers in Immunology

RECEIVED 23 January 2023

ACCEPTED 10 February 2023

PUBLISHED 02 March 2023

## CITATION

Kushner I (2023) C-reactive protein –  
My perspective on its first half  
century, 1930-1982.  
*Front. Immunol.* 14:1150103.  
doi: 10.3389/fimmu.2023.1150103

## COPYRIGHT

© 2023 Kushner. This is an open-access  
article distributed under the terms of the  
[Creative Commons Attribution License](#)  
(CC BY). The use, distribution or  
reproduction in other forums is permitted,  
provided the original author(s) and the  
copyright owner(s) are credited and that  
the original publication in this journal is  
cited, in accordance with accepted  
academic practice. No use, distribution or  
reproduction is permitted which does not  
comply with these terms.

# C-reactive protein – My perspective on its first half century, 1930-1982

Irving Kushner\*

Department of Medicine, Case Western Reserve University at MetroHealth Medical Center, Cleveland, OH, United States

C-reactive protein (CRP) was discovered in 1930 in the sera of patients during the acute phase of pneumococcal pneumonia and was so named because it bound to the C-polysaccharide of the pneumococcal cell wall. During the next half century many questions raised by this discovery were answered. Phosphorylcholine was found to be the moiety of the C-polysaccharide to which CRP bound. The molecular structure of CRP was elucidated: five identical subunits arranged in cyclic symmetry, giving rise to the term pentraxin. Initially felt to be not normally present in the blood, CRP was found to be a component of normal serum in trace amounts. Its site of origin was determined to be the hepatocyte. It became clear that the presumed humoral mediator responsible for CRP induction was of leukocytic origin. Binding of CRP to its ligand activated the complement system, one of the important effector mechanisms of innate immunity. CRP was found to stimulate phagocytosis of some bacterial species *via* binding to Fc receptors and was found to be protective *in vivo* against the pneumococcus in mice. It appeared likely that a related function of CRP was clearance of necrotic tissue. CRP was recognized as being a highly evolutionary conserved molecule. Its discovery during the acute phase of pneumococcal pneumonia led to its being dubbed an acute phase protein. What we today call “the acute phase response”, refers to the large number of behavioral, physiologic, biochemical, and nutritional changes that occur during inflammatory states.

## KEYWORDS

C-reactive protein, acute phase response, complement, phagocytosis, Rockefeller Institute

**Abbreviations:** CRP, C-reactive protein.



## Introduction

In 1958, I started my career as a research fellow at what was then called Metropolitan General Hospital, a major teaching hospital of the Case Western Reserve University School of Medicine in Cleveland. Working under Melvin Kaplan, co-developer of the fluorescent antibody technique, I was assigned the task, employing that technique, of determining the site of production of Cx-reactive protein, as rabbit C-reactive protein (CRP) was known at the time. (We failed.) Over the ensuing years I observed the gradual accretion of knowledge about CRP, culminating in the landmark meeting under the auspices of the New York Academy of Sciences in June 1982 described below. I will focus here on what I regard as the high points of our understanding, as they evolved. This personal review does not attempt to be comprehensive or all-inclusive. I apologize to those colleagues whose work, often seminal, I have omitted.

## The discovery of C-reactive protein at The Rockefeller Institute

The Rockefeller Institute for Medical Research was established in 1906, in an era when pneumonia was a leading cause of death in the United States. When the bacteriologist Oswald Avery joined the Institute in 1913, a considerable effort in his lab was directed to understanding pneumonia, and of its most common etiologic agent, *Streptococcus pneumoniae*, generally referred to at the time as the pneumococcus. (I remind you that it was Avery's lab which discovered in 1944 that genes were made of DNA.) (1). CRP was discovered in the course of these studies, one might rather say blundered into.

Avery and his collaborators had found that a polysaccharide (different for each pneumococcal type) made up the pneumococcal capsule, and that it was the capsule that renders the organism virulent - resistant to phagocytosis. This finding led to the use of type-specific serum therapy, the only way to treat pneumonia until the introduction of anti-microbial drugs in the late 1930s.

Then, in 1930, as recounted by Maclyn McCarty (2), William Tillett, in the Avery lab, prepared a different polysaccharide fraction, not from the capsule but rather from the cell wall, designated the "C" fraction because it appeared to be analogous to the C polysaccharide of the hemolytic streptococcus studied by Rebecca Lancefield a few years previously. Tillett and Thomas Francis set up precipitin tests against sera from serial bleedings of pneumonia patients, presuming they would detect antibodies to the "C" fraction. But the results were completely the opposite of what they had expected. A precipitate formed when the "C" substance was mixed with sera obtained at the time of admission to the hospital and throughout the febrile period (the acute phase), then diminished in the patients who recovered, and ultimately disappeared. These findings were published in 1930 (3).

This was not how antibodies behaved. It was clear that the C-precipitation phenomenon differed from immune reactions. It took the investigators a while to digest this finding. Ultimately, they realized that they were dealing with something new, different from an antibody response. It appeared that there was a substance of some kind in acute phase sera that was C-reactive.

## The molecule itself

It wasn't until a decade later, in 1941, that a series of papers from the Avery lab reported that the C-reactive substance was a protein; thus, a *C-reactive protein* (4–6). It is of interest that these authors stated that CRP was "not normally present in the blood".

In the early years, the Rockefeller institute largely carried the ball on CRP studies. In 1965, Emil Gotschlich and Gerald Edelman, of the Institute, reported that CRP was composed of probably identical subunits with a molecular weight of about 21,500 Da (7). The primary structure of CRP was reported in a pair of papers from Gotschlich's lab about a decade later (8, 9). They found that CRP had a unique sequence containing 187 amino acids in a single polypeptide chain, and a minimal molecular weight of 20,946 Da. And in 1977, Alex Osmand et al, working in Henry Gewurz's lab at the Rush Medical College in Chicago, reported that CRP was composed of five subunits arranged in cyclic symmetry, and suggested the term *pentraxin* for such a structure (10).

## Is CRP really "not normally present in the blood"?

For several decades, it was held that CRP was not normally present in the blood. Finally, in 1972, C.O. Kindmark, of the University of Lund in Sweden, employing a more sensitive assay than had previously been employed, reported that CRP was indeed a component of normal serum (11), a finding confirmed in 1976 by David Claus in the Gewurz lab (12), and again in 1981 in Mark Pepys' lab at the Royal Postgraduate Medical School in London (13). In the latter study, serum CRP concentrations in the healthy adults they studied were under 3 mg/L in 90% of healthy adults and under 10 mg/L in almost all.

## Where is it made?

In 1966, J. Hurlimann, working in the Jeanette Thorbecke lab at New York University, found that C (14)-amino acid incorporation *in vitro* into CRP could be demonstrated in culture fluids from liver tissue, and no other organ, in inflamed rabbits and monkeys (14). A dozen years later, the specific liver cell type responsible for CRP production in rabbits was identified as the hepatocyte by Irving Kushner employing immunoenzymatic techniques, working in Gerard Feldmann's lab at the Hôpital Beaujon in Clichy, France (15).

## How do hepatocytes know that they should produce it?

Following acute myocardial infarction, CRP concentrations were found to rise exponentially, with a mean doubling time of 8.2 h. Levels continued to rise for nearly two days in individuals with mild infarction and over three days in those with extensive infarction (16). Studies in isolated perfused rabbit livers revealed that secretion rates of CRP from livers from inflamed animals did not increase exponentially after removal of the liver from the rabbit. Rather they continued to secrete

CRP at the rate achieved at the time of removal from the living animal (17), indicating that acceleration of CRP synthesis required continuing exposure to an *in vivo* mediator, as had been presumed.

By 1982, inflammation-associated cytokines just were beginning to be identified. There was considerable interest at the time in endogenous pyrogens, soluble factors from leukocytes capable of inducing fever in rabbits (18). Ralph Kampschmidt's lab at the Samuel Roberts Noble Foundation in Ardmore, OK found that such preparations could induce a broad array of acute phase changes, including CRP, in experimental animals, as did Don Bornstein's lab at the SUNY Upstate Medical University in Syracuse, NY (19–22), indicating that the presumed humoral mediator responsible for CRP induction was of leukocytic origin.

## Are there other acute phase proteins?

Avery's lab referred to CRP as "the acute phase protein". But was CRP unique, or were there other acute phase proteins? The development of immunochemical methods in the 1960s permitted quantitation of the concentrations of individual plasma proteins. It was soon learned that the concentrations of a number of plasma proteins rose (positive acute phase proteins), while concentrations of others fell (negative acute phase proteins) following inflammatory stimuli such as surgical procedures. Noteworthy positive acute phase proteins identified at the time included  $\alpha_1$ -antitrypsin,  $\alpha_1$ -acid glycoprotein, haptoglobin and ceruloplasmin, while concentrations of albumin, transferrin,  $\alpha_1$ - and  $\beta$ -lipoprotein decreased (23, 24). A few years later, Keith McAdam and Jean Sipe at the National Cancer Center in Bethesda found that the newly discovered amyloid precursor Serum Amyloid A (SAA) was also a major acute phase protein, comparable to CRP in the magnitude of increase following stimulus (25).

## Why does CRP bind to the C polysaccharide?

John Volanakis, working in Melvin Kaplan's lab in Cleveland and Emil Gotschlich's lab at the Rockefeller Institute independently demonstrated that phosphorylcholine was the moiety of the C polysaccharide that CRP bound to (26, 27). While CRP was found to bind to a variety of other molecules (28), phosphorylcholine was of greatest interest. Phosphorylcholine is displayed by a variety of microorganisms, raising the possibility that CRP might protect against some infections. And it is widely distributed throughout nature as a constituent of cell membranes.

## What does CRP do?

### Promotion of inflammation by complement activation

Two laboratories, those of Volanakis and Kaplan in Cleveland, and J. Siegal and R. Rent in the Gewurz lab, in the mid-1970s

reported that binding of CRP to its ligand activated the complement system *via* the classical pathway (29–32). Activation of complement, one of the important effector mechanisms of innate immunity, leads to opsonization of pathogens as well as to generation of the classical inflammatory response.

## Phagocytosis of bacteria

CRP was found to bind to some pathogenic bacteria, raising the possibility that it facilitated phagocytosis; that it might be an opsonin (33, 34) CRP was found to stimulate phagocytosis of some bacterial species (35–37). But phagocytosis requires phagocytes. Richard Mortenson and Jo Ann Duszkievicz at Ohio State University and Karen James and B. Hansen in the Gewurz laboratory reported that CRP binds to macrophages and lymphocytes via Fc receptors (38, 39). Indeed, CRP was found to be protective *in vivo* against the pneumococcus by Carolyn Mold, Terry Du Clos and their collaborators, and workers in the Volanakis lab (40, 41).

## Clearance of necrotic tissue

In experimental animals in which tissue injury was induced by intramuscular injection of croton oil, Kushner and Kaplan, employing immunofluorescent methods, found that CRP localized to necrotic myofibers and no other tissue (42). Comparable CRP localization to necrotic cardiac muscle fibers was seen when myocardial infarction was induced by cardiac artery ligation (43).

These findings raised the possibility that a function of CRP might be to target necrotic tissue for removal of necrotic debris, facilitating phagocytosis of damaged cells. Phosphorylcholine is a constituent of all cell membranes, and this possibility was supported by the finding in John Volanakis' lab that CRP bound to artificial phosphatidylcholine bilayers (44) but that alteration of the normal organization of phosphatidylcholine bilayers was required for binding of CRP to occur (45). Necrotic cells are cleared by phagocytic cells, and the role of CRP in their clearance is undoubtedly comparable to its role in phagocytosis of bacteria – necrotic cells are targeted by CRP, which in turn binds to Fc receptors on phagocytes. In addition, the activation of complement would lead to initiation of innate immunity, and generation of the classical inflammatory response locally.

## Phylogeny

CRP is a highly conserved molecule (46). Early studies from the Rockefeller lab identified CRP in sera from rabbits and monkeys (47). Before long it was also identified in several land-based vertebrate species (48) and then in the fish species Plaice (49). It turned out that CRP appeared very early in the course of evolution; a protein from the hemolymph of *Limulus polyphemus* – the Horseshoe Crab (nearly half a billion years on this planet) – was found which resembles human CRP (50).

## Clinical considerations

The original discoverers of CRP felt that it was elicited by infection with Gram positive organisms. But as early as 1933, Rachel Ash, of the Children's Hospital in Philadelphia, employing a precipitation test with the C polysaccharide, found that infection with Gram negative organisms also gave positive tests (51). The first clinical use for determination of CRP in the blood, developed at the Rockefeller Institute by H. C. Anderson and Maclyn McCarty, employed antibodies to CRP in a capillary precipitin test as a marker of disease activity in acute rheumatic fever (52). Subsequently, hundreds of papers were published reporting the use of CRP determination to indicate the presence of an inflammatory process, estimate its severity, and monitor the course of illness in a great variety of medical conditions.

## The acute phase response

Oswald Avery had been fascinated by the appearance of CRP during the acute phase of infectious diseases. He was quoted by Rene Dubos: "Avery never discussed the C-reactive protein without turning the conversation to what he was wont to call 'the chemistry of the host'. Although he never spelled out what he meant by that expression, he clearly had in mind all the unidentified body substances and mechanisms of a nonimmunological nature, both protective and destructive, that come into play in the course of infectious processes" (53). It soon became apparent that the acute phase response was not limited to infectious processes, but also occurred after tissue injury, such as occurs in surgical procedures and myocardial infarction. And although CRP is an "acute phase" protein, it was clear from the beginning that the acute phase response occurs in chronic diseases as well as in acute diseases, and often persists for extended periods. What Avery termed the "chemistry of the host" is today termed "the acute phase response" - the large number of behavioral, physiologic, biochemical, and nutritional changes that occur during inflammatory states (54).

## Taking stock after half a century

In 1981, Mark Pepys brought CRP to the attention of the broad biomedical community with an essay published in the *Lancet*, classified by them as an "Occasional Survey", with a thorough, scholarly summary of what was known about CRP at the time (28).

## References

1. Kushner I, Samols D. Oswald Avery And the pneumococcus. *Pharos Alpha Omega Alpha Honor Med Soc* (2011) 74:14–8.
2. McCarty M. Historical perspective on c-reactive protein. *Ann N Y Acad Sci* (1982) 389:1–10. doi: 10.1111/j.1749-6632.1982.tb22121.x
3. Tillet WS, Francis T Jr. Serological reactions in pneumonia with a non-protein somatic fraction of pneumococcus. *J Exp Med* (1930) 52:561–71. doi: 10.1084/jem.52.4.561
4. Abernethy TJ, Avery OT. The occurrence during acute infections of a protein not normally present in the blood: I. distribution of the reactive protein in patients' sera and the effect of calcium on the flocculation reaction with c polysaccharide of pneumococcus. *J Exp Med* (1941) 73:173–82. doi: 10.1084/jem.73.2.173
5. MacLeod CM, Avery OT. The occurrence during acute infections of a protein not normally present in the blood. II. isolation and properties of the reactive protein. *J Exp Med* (1941) 73:183–90. doi: 10.1084/jem.73.2.183

The late John Volanakis, Henry Gewurz and I ran into one another at a meeting of The Central Society for Clinical Research at the Drake Hotel in Chicago in November 1979. We were aware that the late 1970s had seen increasing interest in CRP and the acute phase response and concluded that the time had come to organize an international meeting about CRP, SAA and the acute phase response in general. Under the auspices of the New York Academy of Sciences, that meeting, entitled "C-Reactive Protein and the Plasma Protein Response to Tissue Injury", was held at the Barbizon-Plaza Hotel in New York City on September 21–23, 1981 (55). (The original projected title, "C-Reactive Protein and the Acute Phase Response", was rejected because it was felt that very few scientists were familiar with the term "Acute Phase Response", and inflammation was generally defined at the time as the response to tissue injury.) Thirty-six papers were presented at this meeting, and there were 26 posters.

The field has taken off since then.

## Author contributions

The author confirms being the sole contributor of this work and has approved it for publication.

## Acknowledgments

I gratefully acknowledge the helpful suggestions of Nate Berger, David Samols, Stanley Ballou and Maria Antonelli.

## Conflict of interest

The author declares that the research was conducted in the absence of any commercial or financial relationships that could be construed as a potential conflict of interest.

## Publisher's note

All claims expressed in this article are solely those of the authors and do not necessarily represent those of their affiliated organizations, or those of the publisher, the editors and the reviewers. Any product that may be evaluated in this article, or claim that may be made by its manufacturer, is not guaranteed or endorsed by the publisher.

6. MacLeod CM, Avery OT. The occurrence during acute infections of a protein not normally present in the blood. III. immunological properties of the c-reactive protein and its differentiation from normal blood proteins. *J Exp Med* (1941) 73:191–200. doi: 10.1084/jem.73.2.191
7. Gotschlich EC, Edelman GM. C-reactive protein: A molecule composed of subunits. *Proc Natl Acad Sci USA* (1965) 54:558–66. doi: 10.1073/pnas.54.2.558
8. Oliveira EB, Gotschlich EC, Liu TY. Primary structure of human c-reactive protein. *Proc Natl Acad Sci USA* (1977) 74:3148–51. doi: 10.1073/pnas.74.8.3148
9. Oliveira EB, Gotschlich EC, Liu TY. Primary structure of human c-reactive protein. *J Biol Chem* (1979) 254:489–502. doi: 10.1016/S0021-9258(17)37943-7
10. Osmand AP, Friedenson B, Gewurz H, Painter RH, Hofmann T, Shelton E. Characterization of c-reactive protein and the complement subcomponent C1t as homologous proteins displaying cyclic pentameric symmetry (pentraxins). *Proc Natl Acad Sci USA* (1977) 74:739–43. doi: 10.1073/pnas.74.2.739
11. Kindmark CO. The concentration of c-reactive protein in sera from healthy individuals. *Scand J Clin Lab Invest* (1977) 29:407–11. doi: 10.3109/00365517209080258
12. Claus DR, Osmand AP, Gewurz H. Radioimmunoassay of human c-reactive protein and levels in normal sera. *J Lab Clin Med* (1976) 87:120–8.
13. Shine B, de Beer FC, Pepys MB. Solid phase radioimmunoassays for human c-reactive protein. *Clin Chim Acta* (1981) 117:13–23. doi: 10.1016/0009-8981(81)90005-X
14. Hurlimann J, Thorbecke GJ, Hochwald GM. The liver as the site of c-reactive protein formation. *J Exp Med* (1966) 123:365–78. doi: 10.1084/jem.123.2.365
15. Kushner I, Feldmann G. Control of the acute phase response: Demonstration of c-reactive protein synthesis and secretion by hepatocytes during acute inflammation in the rabbit. *J Exp Med* (1978) 148:466–77. doi: 10.1084/jem.148.2.466
16. Kushner I, Broder ML, Karp D. Control of the acute phase response. serum c-reactive protein kinetics after acute myocardial infarction. *J Clin Invest* (1978) 61:235–42. doi: 10.1172/JCI108932
17. Kushner I, Ribich WN, Blair JB. Control of the acute-phase response. c-reactive protein synthesis by isolated perfused rabbit livers. *J Lab Clin Med* (1980) 96:1037–45.
18. Dinarello CA. The history of fever, leukocytic pyrogen and interleukin-1. *Temperature (Austin)* (2015) 2:8–16. doi: 10.1080/23328940.2015.1017086
19. Merriman CR, Pulliam LA, Kampschmidt RF. Effect of leukocytic endogenous mediator on c-reactive protein in rabbits. *Proc Soc Exp Biol Med* (1975) 149:782–4. doi: 10.3181/00379727-149-38898
20. Bornstein DL, Walsh EC. Endogenous mediators of the acute-phase reaction. i. rabbit granulocytic pyrogen and its chromatographic subfractions. *J Lab Clin Med* (1978) 91:236–45.
21. Bornstein DL. Leukocytic pyrogen: A major mediator of the acute phase reaction. *Ann N Y Acad Sci* (1982) 389:323–37. doi: 10.1111/j.1749-6632.1982.tb22147.x
22. Kampschmidt RF, Upchurch HF, Pulliam LA. Characterization of a leukocyte-derived endogenous mediator responsible for increased plasma fibrinogen. *Ann N Y Acad Sci* (1982) 389:338–53. doi: 10.1111/j.1749-6632.1982.tb22148.x
23. Crockson RA, Payne CJ, Ratcliff AP, Sothill JF. Time sequence of acute phase reactive proteins following surgical trauma. *Clin Chim Acta* (1966) 14:435–41. doi: 10.1016/0009-8981(66)90030-1
24. Aronsen KF, Ekelund G, Kindmark CO, Laurell CB. Sequential changes of plasma proteins after surgical trauma. *Scand J Clin Lab Invest (Suppl)* (1972) 124:127–36. doi: 10.3109/00365517209102760
25. McAdam KP, Sipe JD. Murine model for human secondary amyloidosis: Genetic variability of the acute-phase serum protein SAA response to endotoxins and casein. *J Exp Med* (1976) 144:1121–7. doi: 10.1084/jem.144.4.1121
26. Volanakis JE, Kaplan MH. Specificity of c-reactive protein for choline phosphate residues of pneumococcal c-polysaccharide. *Proc Soc Exp Biol Med* (1971) 136:612–4. doi: 10.3181/00379727-136-35323
27. Heidelberger M, Gotschlich EC, Higginbotham JD. Inhibition experiments with pneumococcal c and dehydrated type-IV polysaccharides. *Carbohydr Res* (1972) 22:1–4. doi: 10.1016/S0008-6215(00)85719-5
28. Pepys MB. C-reactive protein fifty years on. *Lancet* (1981) 1:653–7. doi: 10.1016/S0140-6736(81)91565-8
29. Kaplan MH, Volanakis JE. Interaction of c-reactive protein complexes with the complement system. i. consumption of human complement associated with the reaction of c-reactive protein with pneumococcal c-polysaccharide and with the choline phosphatides, lecithin, and sphingomyelin. *J Immunol* (1974) 112:2135–47. doi: 10.4049/jimmunol.112.6.2135
30. Volanakis JE, Kaplan MH. Interaction of c-reactive protein complexes with the complement system. II. consumption of guinea pig complement by CRP complexes: Requirement for human C1q. *J Immunol* (1974) 113:9–17. doi: 10.4049/jimmunol.113.1.9
31. Siegel J, Rent R, Gewurz H. Interactions of c-reactive protein with the complement system. i. protamine-induced consumption of complement in acute phase sera. *J Exp Med* (1974) 140:631–47. doi: 10.1084/jem.140.3.631
32. Volanakis JE. Complement activation by c-reactive protein complexes. *Ann N Y Acad Sci* (1982) 389:235–50. doi: 10.1111/j.1749-6632.1982.tb22140.x
33. Kindmark CO. *In vitro* binding of human c-reactive protein by some pathogenic bacteria and zymosan. *Clin Exp Immunol* (1972) 11:283–9.
34. Mold C, Rodgers CP, Kaplan RL, Gewurz H. Binding of human c-reactive protein to bacteria. *Infect Immun* (1982) 38:392–5. doi: 10.1128/iai.38.1.392-395.1982
35. Kindmark CO. Stimulating effect of c-reactive protein on phagocytosis of various species of pathogenic bacteria. *Clin Exp Immunol* (1971) 8:941–8.
36. Mortensen RF, Osmand AP, Lint TF, Gewurz H. Interaction of c-reactive protein with lymphocytes and monocytes: complement-dependent adherence and phagocytosis. *J Immunol* (1976) 117:774–81. doi: 10.4049/jimmunol.117.3.774
37. Nakayama S, Mold C, Gewurz H, Du Clos TW. Opsonic properties of c-reactive protein *in vivo*. *J Immunol* (1982) 128:2435–8. doi: 10.4049/jimmunol.128.6.2435
38. Mortensen RF, Duszkievicz JA. Mediation of CRP-dependent phagocytosis through mouse macrophage fc-receptors. *J Immunol* (1977) 119:1611–6. doi: 10.4049/jimmunol.119.5.1611
39. James K, Hansen B, Gewurz H. Binding of c-reactive protein to human lymphocytes. II. interaction with a subset of cells bearing the fc receptor. *J Immunol* (1981) 127:2545–50. doi: 10.4049/jimmunol.127.6.2545
40. Mold C, Nakayama S, Holzer TJ, Gewurz H, Du Clos TW. C-reactive protein is protective against *Streptococcus pneumoniae* infection in mice. *J Exp Med* (1981) 154:1703–8. doi: 10.1084/jem.154.5.1703
41. Yother J, Volanakis JE, Briles DE. Human c-reactive protein is protective against fatal *Streptococcus pneumoniae* infection in mice. *J Immunol* (1982) 128:2374–6. doi: 10.4049/jimmunol.128.5.2374
42. Kushner I, Kaplan MH. Studies of acute phase protein. i. An immunohistochemical method for the localization of cx-reactive protein in rabbits: association with necrosis in local inflammatory lesions. *J Exp Med* (1961) 114:961–73. doi: 10.1084/jem.114.6.961
43. Kushner I, Rakita L, Kaplan MH. Studies of acute-phase protein. II. localization of cx-reactive protein in heart in induced myocardial infarction in rabbits. *J Clin Invest* (1963) 42:286–92. doi: 10.1172/JCI104715
44. Volanakis JE, Wirtz KWA. Interaction of c-reactive protein with artificial phosphatidylcholine bilayers. *Nature* (1971) 281:155–7. doi: 10.1038/281155a0
45. Volanakis JE, Narkates AJ. Interaction of c-reactive protein with artificial phosphatidylcholine bilayers and complement. *J Immunol* (1981) 126:1820–5. doi: 10.4049/jimmunol.126.5.1820
46. Baltz ML, de Beer FC, Feinstein A, Munn EA, Milstein CP, Fletcher TC, et al. Phylogenetic aspects of c-reactive protein and related proteins. *Ann N Y Acad Sci* (1982) 389:49–75. doi: 10.1111/j.1749-6632.1982.tb22125.x
47. Gotschlich E, Stetson CA Jr. Immunologic cross-reactions among mammalian acute phase proteins. *J Exp Med* (1960) 111:441–51. doi: 10.1084/jem.111.4.441
48. Patterson LT, Mora EC. Occurrence of a substance analogous to c-reactive protein in the blood of the domestic fowl. *Tex Rep Biol Med* (1964) 22:716–21.
49. Baldo EA, Fletcher TC. C-reactive protein-like precipitins in plaice. *Nature* (1973) 246:145–6. doi: 10.1038/246145a0
50. Robey FA, Liu TY. Limulin: A c-reactive protein from *Limulus polyphemus*. *J Biol Chem* (1981) 256:969–75. doi: 10.1016/S0021-9258(19)70074-X
51. Ash R. Nonspecific precipitins for pneumococci fraction c in acute infections. *J Infect Dis* (1933) 53:89–97. doi: 10.1093/infdis/53.1.89
52. Anderson HC, McCarty M. Determination of c-reactive protein in the blood as a measure of the activity of the disease process in acute rheumatic fever. *Am J Med* (1950) 8:445–55. doi: 10.1016/0002-9343(50)90226-9
53. Dubos RJ. The professor, the institute, and DNA. In: Oswald T, editor. *Avery, His life and scientific achievements*. New York: Rockefeller University Press (1976). p. 238.
54. Kushner I. The phenomenon of the acute phase response. *Ann N Y Acad Sci* (1982) 389:39–48. doi: 10.1111/j.1749-6632.1982.tb22124.x
55. Kushner I, Volanakis JE, Gewurz H. C-reactive protein and the plasma protein response to tissue injury. *Ann N Y Acad Sci* (1982) 389:482.





## OPEN ACCESS

## EDITED BY

Yi Wu,  
Xi'an Jiaotong University, China

## REVIEWED BY

Ming-Yu Wang,  
Lanzhou University, China  
James David McFadyen,  
Baker Heart and Diabetes Institute,  
Australia

## \*CORRESPONDENCE

Anne Helene Køstner  
✉ ankoesh@sshf.no

## SPECIALTY SECTION

This article was submitted to  
Molecular Innate Immunity,  
a section of the journal  
Frontiers in Immunology

RECEIVED 20 February 2023

ACCEPTED 07 March 2023

PUBLISHED 17 March 2023

## CITATION

Køstner AH, Fuglestad AJ, Georgsen JB,  
Nielsen PS, Christensen KB, Zibrandtsen H,  
Parner ET, Rajab IM, Potempa LA,  
Steiniche T and Kersten C (2023) Fueling  
the flames of colon cancer – does CRP  
play a direct pro-inflammatory role?  
*Front. Immunol.* 14:1170443.  
doi: 10.3389/fimmu.2023.1170443

## COPYRIGHT

© 2023 Køstner, Fuglestad, Georgsen,  
Nielsen, Christensen, Zibrandtsen, Parner,  
Rajab, Potempa, Steiniche and Kersten. This  
is an open-access article distributed under  
the terms of the [Creative Commons  
Attribution License \(CC BY\)](#). The use,  
distribution or reproduction in other  
forums is permitted, provided the original  
author(s) and the copyright owner(s) are  
credited and that the original publication in  
this journal is cited, in accordance with  
accepted academic practice. No use,  
distribution or reproduction is permitted  
which does not comply with these terms.

# Fueling the flames of colon cancer – does CRP play a direct pro-inflammatory role?

Anne Helene Køstner<sup>1,2\*</sup>, Anniken Jørlo Fuglestad<sup>1,3</sup>,  
Jeanette Baehr Georgsen<sup>4</sup>, Patricia Switten Nielsen<sup>4,5</sup>,  
Kristina Bang Christensen<sup>4</sup>, Helle Zibrandtsen<sup>5</sup>,  
Erik Thorlund Parner<sup>6</sup>, Ibraheem M. Rajab<sup>7</sup>,  
Lawrence A. Potempa<sup>7</sup>, Torben Steiniche<sup>4</sup>  
and Christian Kersten<sup>1,3</sup>

<sup>1</sup>Center for Cancer Treatment, Sorlandet Hospital, Kristiansand, Norway, <sup>2</sup>Department of Clinical Science, University of Bergen, Bergen, Norway, <sup>3</sup>Department of Oncology, Akershus University Hospital, Nordbyhagen, Norway, <sup>4</sup>Department of Pathology, Aarhus University Hospital, Aarhus, Denmark, <sup>5</sup>Department of Clinical Medicine, Aarhus University, Aarhus, Denmark, <sup>6</sup>Section for Biostatistics, Department of Public Health, Aarhus University, Aarhus, Denmark, <sup>7</sup>College of Science, Health and Pharmacy, Roosevelt University Schaumburg, Schaumburg, IL, United States

**Background:** Systemic inflammation, diagnostically ascribed by measuring serum levels of the acute phase reactant C-reactive protein (CRP), has consistently been correlated with poor outcomes across cancer types. CRP exists in two structurally and functionally distinct isoforms, circulating pentameric CRP (pCRP) and the highly pro-inflammatory monomeric isoform (mCRP). The aim of this pilot study was to map the pattern of mCRP distribution in a previously immunologically well-defined colon cancer (CC) cohort and explore possible functional roles of mCRP within the tumor microenvironment (TME).

**Methods:** Formalin-fixed, paraffin-embedded (FFPE) tissue samples from 43 stage II and III CC patients, including 20 patients with serum CRP 0-1 mg/L and 23 patients with serum CRP >30 mg/L were immunohistochemically (IHC) stained with a conformation-specific mCRP antibody and selected immune and stromal markers. A digital analysis algorithm was developed for evaluating mCRP distribution within the primary tumors and adjacent normal colon mucosa.

**Results:** mCRP was abundantly present within tumors from patients with high serum CRP (>30 mg/L) diagnostically interpreted as being systemically inflamed, whereas patients with CRP 0-1 mg/L exhibited only modest mCRP positivity (median mCRP per area 5.07% (95%CI:1.32-6.85) vs. 0.02% (95%CI:0.01-0.04),  $p<0.001$ ). Similarly, tissue-expressed mCRP correlated strongly with circulating pCRP (Spearman correlation 0.81,  $p<0.001$ ). Importantly, mCRP was detected exclusively within tumors, whereas adjacent normal colon mucosa showed no mCRP expression. Double IHC staining revealed colocalization of mCRP with endothelial cells and neutrophils. Intriguingly, some tumor cells also colocalized with mCRP, suggesting a direct interaction or mCRP expression by the tumor itself.

**Conclusion:** Our data show that the pro-inflammatory mCRP isoform is expressed in the TME of CC, primarily in patients with high systemic pCRP values. This strengthens the hypothesis that CRP might not only be an inflammatory marker but also an active mediator within tumors.

#### KEYWORDS

systemic inflammation, C-reactive protein (CRP), CRP isoforms, monomeric CRP, colon cancer, immunohistochemistry (IHC), biomarkers, tumor microenvironment

## Background

Systemic inflammation, diagnostically ascribed by measuring levels of the acute phase protein CRP in serum, has consistently been correlated with poor outcomes across cancer types (1–3). However, the biological relationship between CRP and inflammation remained unresolved and controversial for decades. Recently, evidence has been advanced showing that CRP exists in different structural isoforms with distinct biological activities (4). The circulating CRP isoform is a highly soluble pentameric molecule (pCRP) composed of 5 identical globular subunits arranged in a ring-shaped structure (5). Each subunit contains a calcium dependent binding site enabling interaction with phosphocholine (PC), a major component of plasma membranes, defined as the primary ligand for pCRP. However, for the PC ligand to become accessible for CRP binding, structural remodeling of the membrane lipid is required. This may occur when cells become activated, either by an infectious or non-infectious inflammatory stimulus or following cell damage or apoptosis and may involve the activity of the enzyme phospholipase A2 (6). Upon interaction with the exposed PC groups, pCRP begins to change structure first into an intermediate swollen pentameric form designated pCRP\* (or mCRP<sub>m</sub>), then into the fully dissociated, less soluble and antigenically distinct monomeric, modified form, referred to as mCRP (7, 8). Experimental studies have shown that the biological effects of CRP are dependent on its structural conformation, demonstrating strong pro-inflammatory properties of mCRP, whereas pCRP appears to exhibit mainly weak anti-inflammatory activities (9, 10). *In vitro* studies directly comparing the biological effects of the two isoforms, have shown that mCRP has approximately 10–100-fold more potent inflammatory capacity than its precursor molecule pCRP (11).

Notably, once formed, mCRP deposits within tissues due to its low aqueous solubility where it may interact directly with various cells and components of the microenvironment (3, 11). Specifically, it has been shown that mCRP can engage with both epithelial and endothelial cells, platelets, and various immune cells such as macrophages and neutrophils (9, 12, 13). Additionally, mCRP can interact directly with components of the extracellular matrix as well as fibroblasts, which are major constituents of the tumor stroma (3). At the molecular level, data have shown that mCRP preferentially binds to cholesterol rich lipid rafts that are important microdomains of plasma membranes involved in a wide range of cellular processes including signal transduction (9, 14). Following membrane insertion,

mCRP can stimulate intracellular signaling including activation of pro-inflammatory pathways such as those involving the pivotal transcription factor NF- $\kappa$ B and its downstream mediators (3).

While most research on the different isoforms of CRP has been carried out in cardiovascular and neurodegenerative disorders, as well as some autoimmune diseases, little is known about their role in cancer (11, 13, 15–18). In line with our previous work (19), focusing on why cancer patients with elevated blood CRP levels have inferior outcomes, the hypothesis evolved that the potent monomeric/modified form of CRP may play a direct pro-inflammatory role within the TME of systemically inflamed cancer patients. First, by localizing the inflammatory response as circulating pCRP binds to exposed PC molecules expressed by cells that have been activated due to the inflammatory TME, leading to *in-situ* dissociation of pCRP into the pro-inflammatory monomeric isoform. Secondly, as mCRP accumulates within the tumor, a process which is considered perpetual and non-resolving, owing to the chronic nature of systemic inflammation, mCRP may play a direct and active role through the recruitment and activation of inflammatory cells and components of the TME, potentially fueling and shaping the local inflammatory response, and ultimately promote tumor progression.

In order to explore whether there is a role for mCRP in systemically inflamed cancer patients, the aim of this proof-of-concept study was to identify and map the pattern of mCRP distribution in a previously immunologically well-defined cohort of colon cancer (CC) patients. Using complementary strategies including immunohistochemistry (IHC)-based colocalization imaging techniques, we were able to elucidate potential functional roles of mCRP in the microenvironment of CC tissue.

## Materials and methods

### Patients and tissue samples

Formalin-fixed, paraffin-embedded (FFPE) tissue samples were retrospectively obtained from 43 stage II and III CC patients, including 20 patients with circulating CRP of 0–1 mg/L (CRP-low patients) and 23 patients with CRP >30 mg/L (CRP-high patients), undergoing resection for their primary tumors at Sørlandet Hospital, Norway, between 2005 and 2015. Clinical information and follow-up data were obtained from a local colorectal cancer



database as described previously (19). Characteristics of CRP-high and CRP-low patients are detailed in Table 1.

Serum CRP values were determined using a standardized immunoturbidimetric assay, which previously has shown specificity for pCRP without interference with mCRP (20), performed on blood samples taken within 14 days (at the day closest to the resection) prior to the operation in order to reflect a state of chronic inflammation. Exclusion criteria were clinical evidence of infection, use of antibiotics or immunosuppressive drugs within 4 weeks prior to the operation or a history of chronic inflammatory disease including autoimmune disorders.

The study was approved by the Norwegian Regional Ethics Committee.

## Immunohistochemistry and double immunofluorescence

Whole slides from FFPE tumor blocks were immunohistochemically stained with a conformation-specific mCRP monoclonal antibody

(mCRP-mAb 9C9), which has been fully characterized previously demonstrating specificity for mCRP and not pCRP (21, 22). FFPE sections were cut at 3 µm, mounted on Superfrost Plus slides (Thermo Fisher Scientific, Waltham, MA), dried for 1 hour at 60°C, and prepared for IHC staining using standard kits from Benchmark Ultra (Ventana, Roche Diagnostics International AG, Basel, Switzerland) for deparaffinization, rehydration, antigen retrieval, and endogenous peroxidase blocking. Next, sections were incubated with the primary antibody (mCRP mAb 9C9 at dilution 1:100) for 30 minutes followed by DAB (3, 3'-diaminobenzidine) substrate chromogen solution for antigen visualization. Negative controls were performed by replacing the primary antibody with antibody diluent (Agilent S2022; DAKO), but otherwise prepared similarly. All sections were counterstained with hematoxylin and mounted before they were scanned at ×20 magnification using NanoZoomer 2.0 HT (Hamamatsu Phototonics KK, Hamamatsu City, Japan).

To map the pattern of mCRP distribution and explore possible colocalization with immune, endothelial and tumor markers, double stainings with chromogenic IHC and IF were performed on tumor slides from selected patients with elevated circulating CRP and

TABLE 1 Clinical characteristics of colon cancer patients according to the level of circulating CRP.

Characteristic	CRP 0-1, N = 20 <sup>1</sup>	CRP ≥30, N = 23 <sup>1</sup>	p-value <sup>2</sup>
Age	67 (60, 71)	78 (71,86)	0.003
Sex			0.70
Female	11 (55%)	14 (61%)	
Male	9 (45%)	9 (39%)	
Stage			<0.001
II	0 (0%)	10 (43%)	
III	20 (100%)	13 (57%)	
Tumor site			0.77
Left	4 (20%)	3 (13%)	
Right	10 (50%)	14 (61%)	
Sigmoid	6 (30%)	6 (26%)	
Adjuvant chemotherapy			<0.001
None	3 (15%)	19 (83%)	
Only 5-FU based	6 (30%)	3 (13%)	
Platinum doublet	11 (55%)	1 (4.3%)	
MMR-Status			0.002
MSS	20 (100%)	14 (61%)	
MSI	0 (0%)	9 (39%)	
Survival status			0.010
Alive	15 (75%)	7 (30%)	
Dead	4 (20%)	9 (39%)	
Recurrence	1 (5.0%)	7 (30%)	
Follow-up (years)	9.3 (8.7, 10.9)	8.8 (5.2, 11.3)	0.58

<sup>1</sup>Median (IQR); n (%).

<sup>2</sup>Wilcoxon rank sum test; Pearson's Chi-squared test; Fisher's exact test.

pronounced mCRP expression as evaluated by the mCRP single staining. Antibodies against the following markers were applied in addition to anti-mCRP: CD34 for endothelial cells, CD68 for macrophages, CD66b for neutrophils and pan-cytokeratin (pan-CK) as tumor marker. All antibodies were commercially available except for mCRP-mAb 9C9. Origin and incubation times for the applied antibodies are listed in [Supplementary Table S1](#).

All double stainings were performed after antigen retrieval as described above. For double IHC, FFPE sections were incubated sequentially, first, with mCRP-mAb at dilution 1:100 for 30 minutes followed by chromogenic DAB staining. The slides were then incubated with the appropriate second primary antibody as listed above at the time indicated for each antibody applying Ultra-view fast red as chromogenic dye. Finally, slides were counterstained with hematoxylin, mounted and scanned at  $\times 20$  magnification using NanoZoomer 2.0 HT (Hamamatsu, Japan).

Double IF was performed, using the tyramide signal amplification strategy on the Discovery Ultra Autostainer (Ventana Medical systems) applying two different fluorophores in a sequential manner for visualization of the respective antigens. First, tissue sections were incubated with mCRP-mAb (dilution 1:10) for 30 min, using rhodamine as fluorescent dye, followed by incubation with the appropriate second primary antibody (as listed above) using DCC (N'-dicyclohexylcarbodiimide) as the selected fluorophore. Stained slides were mounted with Vectashield Antifade Mounting Medium, which included DAPI as nuclear counterstain, whereafter they were stored overnight at 4°C, protected from light. Mounted slides were scanned at  $\times 20$  using NanoZoomer S60 (Hamamatsu, Japan).

## Digital image analysis

Image analysis was performed using Visiopharm Integrator System software version 2019.02 (VIS; Visiopharm A/S, Hørsholm, Denmark).

Regions of interest (ROIs) were defined by a trained pathologist. The tumor was outlined as one region encompassing the invasive margin and tumor center. On slides where normal colon mucosa was present (11 out of 43), this was annotated as a separate ROI. Two AI-based algorithms were utilized for the segmentation and annotation of either tumor epithelium or normal colon mucosa in addition to their surrounding stromal tissue, as outlined in [Figure 1](#). Training of the algorithms included a representative set of whole slide images (WSI) where stromal tissue, unstained background, and either tumor epithelium or normal colon mucosa were manually annotated at pixel-level. Using input images of 512  $\times$  512 pixels, U-nets as presented by Ronneberger et al. were trained in VIS's Author AI ([23](#)). Learning rates based on Adam Optimization were set at  $1 \times 10^{-5}$ , and data augmentation was utilized ([24](#)).

In the designated regions outlined by the AI applications, mCRP was identified by thresholding of the brown staining color (DAB), which was highlighted by a color deconvolution step. Post-processing algorithms included morphological operations and changes by area or surrounding. All results of the image analyses were manually reviewed to ensure that areas with mucin, tissue folds, and other technical artefacts were excluded from the analysis.

mCRP was quantified as area proportions defined as: area of positive mCRP staining divided by the total area of the given ROI. Since the area of mCRP was small compared to the total area of the tumor, proportions were multiplied with 1000 and given per mile instead of percentages. Area proportions of mCRP were calculated both as a combined score of total mCRP within the whole tumor as well as separately for the tumor epithelium and tumor stroma, respectively. Finally, mCRP was evaluated within the region of normal colon mucosa, scoring epithelium and stroma combined, on applicable slides.

Double IHC and IF stainings were evaluated and interpreted manually by visual examination only, using NDP. View 2.0 (Hamamatsu).

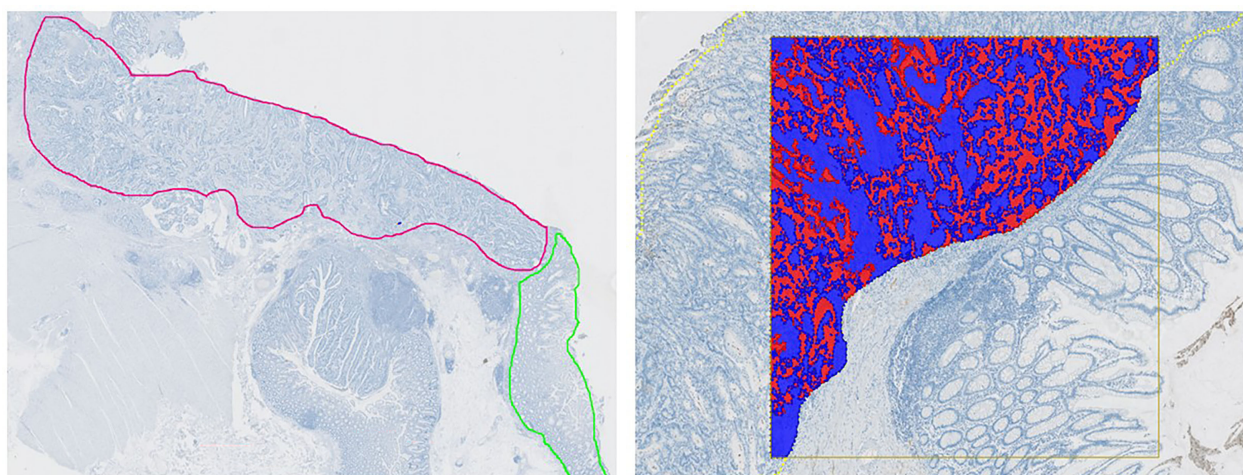


FIGURE 1

Automated Image Analysis Workflow. Left: Whole slide image with annotated tumor regions. Tumor in red and adjacent normal colon mucosa in green. Right: An AI-based algorithm was developed for analyzing the pattern of mCRP distribution and accurately segment tumor epithelium (red) and tumor stroma (blue).

## Immune phenotypes and microsatellite instability analysis

Immune cell densities (CD8+ T-cells, CD4+ T-cells, Foxp3+ T-cells, CD20+ B-cells, CD66b+ neutrophils, CD68+ macrophages) assessed within the same tumor regions were captured from a series of multiplexed IHC (mIHC) performed in a previous study (19). However, due to technical issues with the mIHC, 7 patients did not have corresponding immunological profiles and had to be excluded from the mCRP-immune cell correlation analyses.

Mismatch repair (MMR) status was determined by an experienced pathologist through IHC evaluation of the DNA mismatch repair proteins MHL1, MSH2, MSH6, and PMS2. Tumors that were negative in one or more of the four stainings, or inconsistent with IHC, were verified with the Idylla MSI test (Biocartis) as described previously (25). Accordingly, patients were classified as either microsatellite stable (MSS) or unstable (MSI).

## Statistical analysis

The distribution of mCRP was assessed as mCRP proportions, as specified above. The median mCRP proportion within groups were calculated and compared using the median test. Differences in patient characteristics were evaluated using Fisher's exact test and the two-sample t-test with unequal variance. The correlation between mCRP and circulating CRP was assessed using Spearman correlation analysis. Associations between mCRP and the immune markers obtained from mIHC were analyzed using Spearman correlations and heatmaps were generated. The Aalen-Johansen method was applied to estimate the risk of CC death or recurrence and compared between CRP-high and CRP-low patients using the log-rank test. For identification of the most optimal threshold/cutoff value for tumor mCRP expression used in the analysis of the prognostic impact of mCRP, a receiver operating characteristics (ROC) curve was computed. Due to competing risks (death of colon cancer and death of other causes) varying at different time points, the ROC-curve was calculated at the time of median follow-up using the quantified level of mCRP tumor expression for all patients. The optimal mCRP cutoff value was defined as the point on the ROC curve with sensitivity and specificity closest to 100%, which corresponded graphically to the point on the curve with the minimum distance to the upper left corner. The cumulative risk curves for CC death or recurrence are shown for patients with mCRP tumor expression below and above the optimal cutoff value.  $P < 0.05$  was considered statistically significant for all analyses. R software version 4.2 was used for statistical calculations.

## Results

### mCRP is expressed predominantly by tumors from systemically inflamed patients and is exclusively present within tumor tissue and not adjacent normal colon mucosa

As depicted in Figure 2, mCRP was abundantly present in tumors from systemically inflamed CC patients whereas non-

inflamed patients exhibited only modest mCRP positivity (median mCRP per area 5.07‰ (95%CI, 1.32-6.85) vs. 0.02‰ (95%CI, 0.01-0.04)  $p < 0.001$ ). Correspondingly, tissue-expressed mCRP correlated strongly with circulating CRP (Spearman correlation 0.81 (95%CI, 0.67-0.89),  $p < 0.001$ ). Further analysis of the pattern of mCRP expression demonstrated that MSI positive tumors exhibited significantly more mCRP compared with CRP-high MSS and CRP-low MSS patients, respectively (data shown in Table 2). Furthermore, AI-based image analysis discriminating between tumor epithelium and tumor stroma, showed significantly more mCRP expression in the stromal compartment as compared to the tumor epithelium. Notably, mCRP was detected exclusively within the tumor area whereas adjacent normal colon mucosa showed no mCRP expression (representative image shown in Figure 2C).

## Prognostic impact of the CRP isoforms

Given the known prognostic role of systemic inflammation and the strong correlation between tissue-bound mCRP and circulating serum CRP, we sought to evaluate whether mCRP had an independent impact on survival outcomes within our cohort. As shown in Figure 3, patients with tumors exhibiting mCRP density above the ROC-curve identified cutoff value of tumor mCRP expression tended to perform poorer in terms of increased risk of CC death or recurrence compared with patients that had tumors with mCRP density below the optimal mCRP cutoff value, although this did not reach statistical significance. Nonetheless, elevated serum CRP was confirmed to be predictive of compromised survival and increased risk of recurrence within our cohort (Figure 3C).

### mCRP colocalizes with neutrophils and endothelial cells in the TME

To elucidate potential functional roles of mCRP in the TME, we took a stepwise approach. First, by performing a correlation analysis of the quantified mCRP IHC results with the immune profiles obtained previously on the same patients and tumor areas, followed by double IHC and IF for mCRP and selected immune and endothelial markers. As shown in Figure 4 the most evident association was with the neutrophils, showing a highly significant correlation between mCRP and cd66b+ neutrophils (Spearman correlation 0.57,  $p < 0.001$ ). This was supported by double IHC demonstrating strong colocalization of mCRP and areas of neutrophil infiltration (Figure 5A). At the sub-cellular level, however, immunofluorescent labeling showed only occasional direct cellular overlap, but confirmed the pattern of close proximity, indicative of an interaction, and to a lesser extent, intracellular uptake of mCRP into the neutrophils.

Moreover, mCRP seemed to coincide with areas of necrosis, with or without neutrophil infiltration, where non-specificity could be ruled out by negative control staining (Figure 5B).

Less evident, but still present, was colocalization of mCRP and CD68+ macrophages (Figure 5C). However, mCRP-positive macrophages seemed primarily to coincide with highly immune



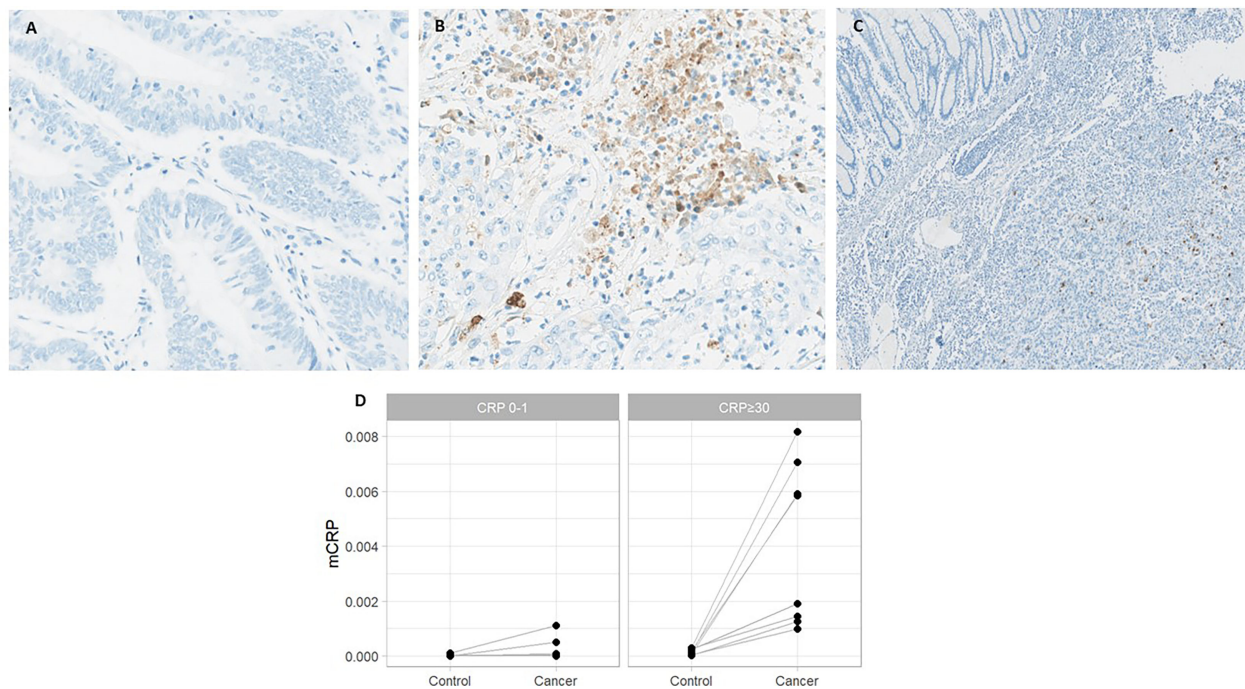


**FIGURE 2** mCRP expression in systemically inflamed and non-inflamed colon cancer patients and adjacent normal colon mucosa. Representative images from patients with (A) normal and (B) elevated circulating CRP. (C) Normal colon mucosa adjacent to the tumor with no mCRP expression. (D) Quantified mCRP (proportion of area with positive mCRP staining) assessed within the tumor and adjacent normal colon mucosa (control) in CRP-high and CRP-low patients.

infiltrated areas in general, as the majority of macrophages present more globally dispersed within the tumor tissue showed less mCRP positivity, suggesting that mCRP might be an amplifier of the local inflammatory response.

Based on data from previous studies in cardio- and cerebrovascular diseases, demonstrating a direct interaction between mCRP and endothelial cells, we performed double immune stainings with mCRP and the specific endothelial marker CD34. Notably, mCRP co-localized with endothelial cells lining intratumoral vessels and was present within the lumen of some vessels, suggesting a systemic origin of the monomeric isoform (Figure 5D). Additionally, mCRP could be detected within the vessel wall of some mCRP/CD34-positive intratumoral vessels.

Interestingly, in some tumors, mCRP appeared rather scattered around in the tumor stroma, occasionally forming aggregates, but more often globally dispersed as small granules within the connective tissue, suggesting a potential interaction between

mCRP and components of the ECM, although this was not directly evaluated by IHC (Figure 5E).

### Positive colocalization of mCRP and tumor cells

Serendipitously, when examining the pattern of mCRP distribution, it became evident that some tumor cells were closely surrounded by mCRP, forming a halo-like coating around individual tumor cell nuclei (Figure 5F). To further elucidate this observation, we performed double immune stainings with mCRP and the gastrointestinal specific cytoplasmatic tumor marker pan-cytokeratin. Using double IHC and IF we were able to demonstrate colocalization and evidence of direct overlap of mCRP and tumor cells, indicating close interaction and/or intracellular uptake of mCRP, or potentially, mCRP expression by the tumor itself (representative images shown in Figure 6).

**TABLE 2** mCRP distribution in colon cancer patients stratified for serum CRP and MSI-status.

	n	mCRP stroma	mCRP tumor	P-value
All (per mille), Median (CI)	43	0.70 (0.08-4.33)	0.08 (0.01-0.48)	<0.001
CRP 0-1 (per mille), Median (CI)	20	0.02 (0.01-0.07)	0.00 (0.00-0.01)	<0.001
CRP ≥30, MSS (per mille), Median (CI)	14	5.45 (1.79-8.01)	0.33 (0.12-2.87)	<0.001
CRP ≥30, MSI (per mille), Median (CI)	9	(3.45-131.76)	2.52 (0.80-13.53)	0.027

Quantification of tissue-associated mCRP expression estimated by IHC.

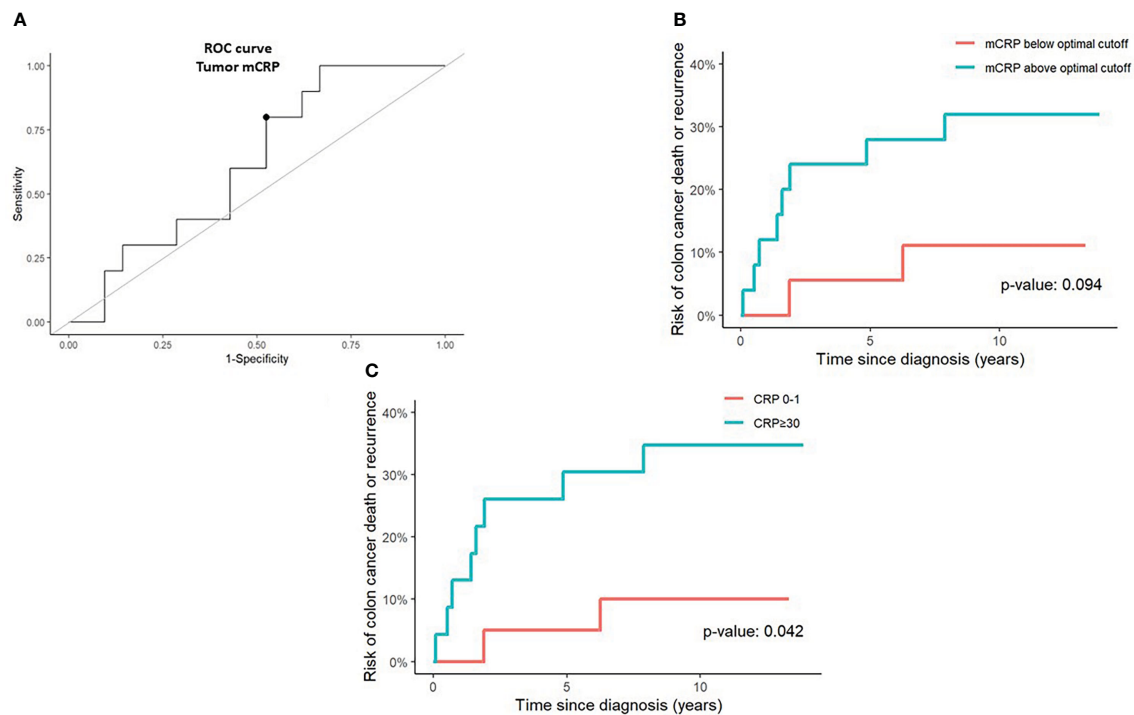


FIGURE 3

Prognostic value of tumor mCRP expression and serum CRP in colon cancer patients. (A) A receiver operating characteristics (ROC) curve was calculated to determine the optimal tumor mCRP cutoff value (marked by a bullet) defined as the point on the curve with sensitivity and specificity closest to 100%, corresponding graphically to the point with the minimum distance to the upper left corner (B) Risk of colon cancer death or recurrence above and below the optimal tumor mCRP cutoff value identified from the ROC curve. (C) Risk of colon cancer death or recurrence in CRP-high (serum CRP >30 mg/L) and CRP-low (serum CRP 0–1 mg/L) patients. The optimal mCRP cutoff value was defined.

## Discussion

In this study we explore the presence of the mCRP isoform and its correlation with innate and adaptive immune cells and serum levels of pCRP in a cohort of stage II and III CC patients. We report that the monomeric form of CRP (mCRP) is present within tumors and that the level of expression correlates strongly with the level of circulating pCRP. Additionally, mCRP expression is associated significantly with tumor infiltrating neutrophils. Importantly, mCRP was expressed exclusively within tumors whereas adjacent normal colon mucosa showed no mCRP positivity.

Persistent elevation of blood CRP levels alongside malignancies is increasingly recognized as an independent predictor of adverse outcomes, both in terms of compromised survival and treatment responses (1, 3, 26). Despite mounting evidence, generated primarily in cardiovascular and neurodegenerative disorders (12, 13, 15, 27, 28), for the existence of different isoforms of CRP with distinct biological properties and direct effects within tissue, this study is the first to apply this emerging concept into the clinical setting of cancer patients. The focus of our previous research has primarily been to understand the biology behind CRP as a biomarker, investigating whether elevated CRP might be a readout of a particular immunological phenotype of the TME. Hence, the idea that CRP itself, in its monomeric, modified form, is present within tumors and might act as a participant in the pathological process has added a new and intriguing layer to this

hypothesis and may profoundly change the view on how the local inflammatory response in cancer potentially can be targeted.

Circulating CRP is a pentameric molecule with weak and primarily anti-inflammatory effects through its ability to activate the classical complement pathway, induce phagocytosis and delay apoptosis (10). The much more potent effector function of CRP, however, becomes evident first when pCRP dissociates into the monomeric form exhibiting strong pro-inflammatory properties (12). In cardiovascular disease, it has been shown that activated platelets and endothelial cells, particularly under ischemic conditions, play a pivotal role in the pCRP dissociation process and for the build-up of atherosclerotic plaques (29, 30). Specifically, mCRP and not pCRP, has been detected within atherosclerotic plaques and infarcted myocardium where it co-localizes with oxidized lipoprotein, macrophages and complement factors and is capable of inducing leucocyte migration and adhesion to the endothelium enhancing thrombus formation, excessive inflammation, and ultimately aggravate tissue injury (12, 29). Once formed, *in vitro* studies have shown that mCRP can be inserted into the cell membrane of endothelial cells and activate signaling pathways associated with both angiogenesis and inflammation (14, 29). In line with these findings, we found that mCRP colocalized with endothelial cells lining intratumoral vessels, supporting the hypothesis that endothelial cells, presumably activated by the tumor or the inflammatory microenvironment, is involved in the pCRP-mCRP dissociation process and may contribute to localizing the inflammatory response. Conceivably, newly formed mCRP can then

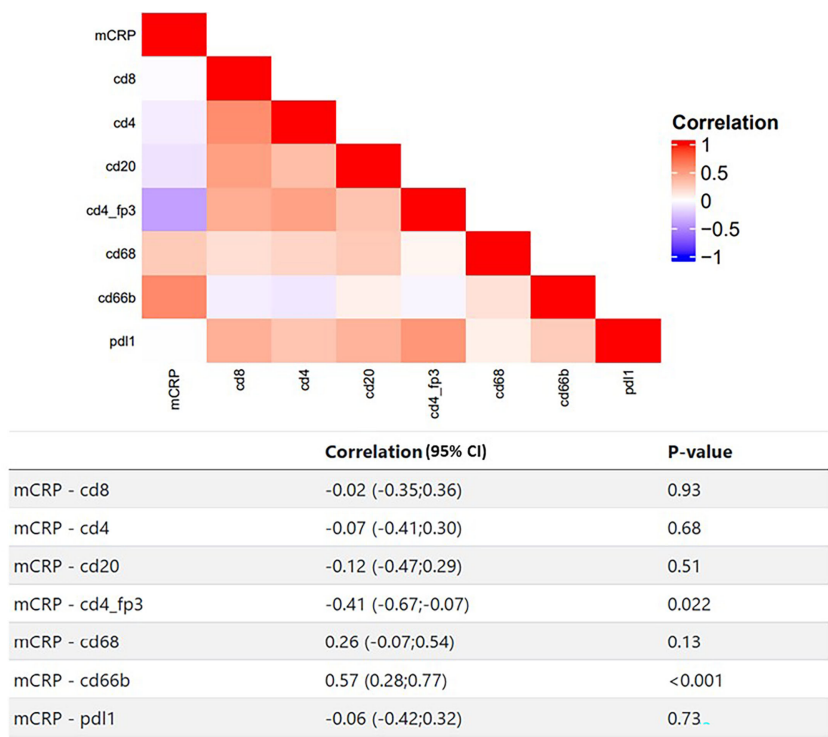


**FIGURE 4**  
Correlating mCRP and selected adaptive and innate immune markers in colon cancer patients. Heatmap and corresponding table of Spearman correlations between mCRP and individual immune markers. Red color indicates positive correlation, blue indicates negative correlation, white indicates no correlation.

either directly activate the endothelial cells resulting in enhanced leucocyte migration to the tumor, and/or as we demonstrate here, accumulate within the tumor tissue. This occurs particularly in systemically inflamed patients where mCRP may exert its pro-inflammatory effects through direct interaction with different cell types and components of the TME.

To elucidate possible functional roles of mCRP in the microenvironment of our colon tumors, we performed double immune stainings demonstrating prominent colocalization of mCRP and CD66b+ neutrophils. At the sub-cellular level, IF revealed occasional direct cellular overlap, indicating possible uptake of mCRP into the neutrophils, although the predominant pattern was that mCRP coincided with highly neutrophil infiltrated areas, suggesting a close relationship between the two. Given the fundamental role of neutrophil function in acute as well as chronic inflammatory conditions, possible direct effects of CRP on these cells have been of particular interest. Hence, *in vitro* studies have shown that mCRP can delay neutrophil apoptosis and enhance neutrophil adhesion to endothelial cells, which is critical for extravasation of neutrophils into inflamed tissue (31, 32). Additionally, following mCRP stimulation, Kreiss et al. found that neutrophils increased both gene expression and secretion of the pro-inflammatory cytokine IL-8 (33). Intriguingly, growing evidence indicates that IL-8 plays a pivotal role in the TME through the ability to stimulate tumor cell proliferation and promote epithelial-to-mesenchymal transition (EMT), thus facilitating tumor progression and metastasis (34).

We have previously shown that elevated circulating CRP associates with a neutrophil enriched and immunosuppressive TME (19). Together with these findings suggesting direct crosstalk between mCRP and neutrophils, this does not only reinforce a profound role for neutrophils in the microenvironment of tumors but adds new information on why neutrophils, particularly during a chronic inflammatory state, seem to be such potent players favoring a detrimental inflammatory response and subsequently how this potentially can be targeted.

Of note, we also observed that mCRP seemed to coincide with areas of necrosis, with or without neutrophil infiltration, showing a pattern of high mCRP expression within and in the vicinity of necrotic areas. This phenomenon could be related to the notion that mCRP can induce aberrant angiogenesis, which has been shown in infarcted brain tissue, resulting in leaky vessels that compromise sufficient blood supply to the tumor leading to necrosis (35). In cancer biology, necrosis is associated with poor prognosis and treatment resistance and has been linked to an immunosuppressive microenvironment, possibly through the release of damage-associated molecular patterns (DAMPs) from dying cells, which triggers an inflammatory response (36). Hence, the ability of mCRP to induce tumor necrosis could potentially contribute to a hostile and predominant immunosuppressive microenvironment supporting a more aggressive tumor phenotype.

Within this context it should be mentioned that a series of older studies conducted in various experimental, primarily murine, cancer models, using CRP, either in its pentameric form or



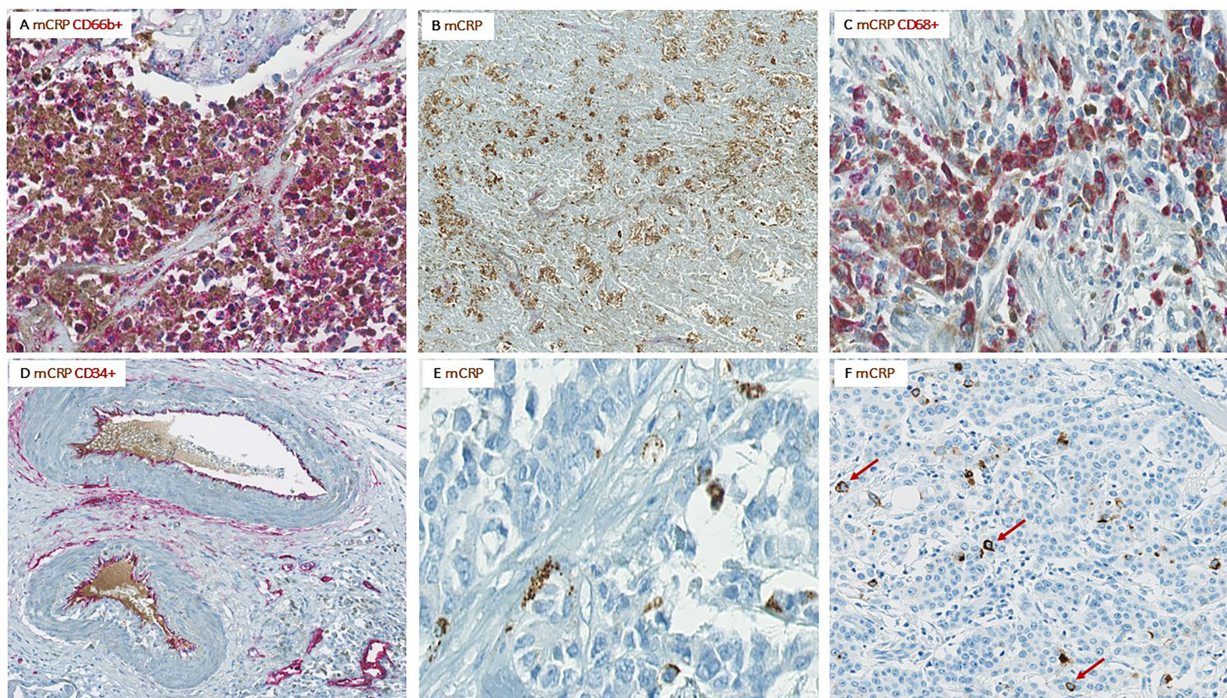


FIGURE 5

Colocalization of mCRP with various components of the TME. Representative images from CC patients with elevated serum CRP and pronounced mCRP tumor expression. (A) Highly neutrophil infiltrated tumor area with strong mCRP expression. (B) Necrotic area within a tumor with high mCRP expression. (C) Colocalization of mCRP and macrophages. (D) Colocalization of mCRP and endothelial cells lining intratumoral vessels as well as some mCRP within the vessel lumen. (E) mCRP scattered diffusely as small granules within the connective tissue of the tumor stroma. (F) Tumor cell nuclei surrounded by mCRP (marked by arrows).

injecting mCRP directly, found similar correlation with necrosis as demonstrated in the present study (11). Contrary to our hypothesis, though, the addition of CRP to the experimental models associated with tumor regression and anti-metastatic effects. However, within all these experimental set-ups CRP was applied only for a short period of time (weeks) and primarily as boosts with CRP injection on selected days. Hence, such system models would mimic an acute inflammatory response and not the situation during chronic

systemic inflammation, which was the case for the patients within our cohort. In cancer patients with persistent elevation of blood CRP levels, the inflammation is proposed to be sustained due to the ongoing inflammatory stimulus from the evolving tumor that potentiates hepatic and potentially, tumor intrinsic CRP production, leading to the “wound that never heals”. Considering the pro-inflammatory effects of mCRP together with the capacity of activated cells to induce pCRP dissociation, persistent pCRP

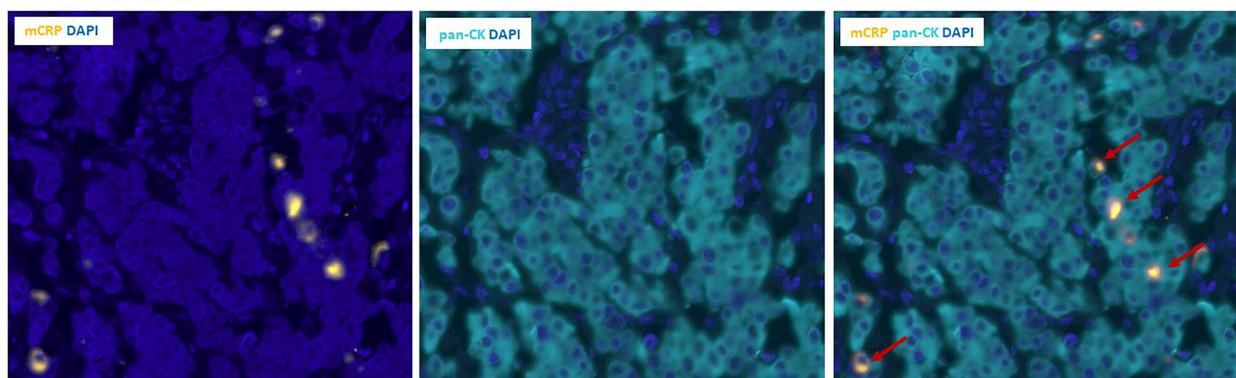


FIGURE 6

Double immunofluorescence labeling of mCRP and tumor cells in colon cancer tissue. Left and middle panels: Unmixed images showing individual stains of mCRP (yellow) to the left and pan-CK positive tumor cells (teal) in the middle. Right panel: Composite image showing double positive mCRP+/pan-CK+ tumor cells (marked by arrows). DAPI (blue) was used for visualization of nuclei. Pan-CK, Pan-cytokeratin.

exposure may then result in excessive tumor inflammation and tissue damage ultimately facilitating tumor growth and exacerbation of the disease.

Previous studies have demonstrated that mCRP can interact with components of the ECM, such as collagen, fibronectin and laminin, which are integral parts of connective tissues playing a crucial role for tissue maintenance and homeostasis (11, 37, 38). In tumors, however, this highly dynamic network becomes dysregulated, and together with other components of the tumor stroma, contributes to a tumor permissive microenvironment. Importantly, low tumor-stroma ratio associates with poor survival and treatment outcome in multiple cancer types (39, 40). In our cohort, we found that mCRP, in addition to the above-described distribution pattern, often was scattered diffusely as small granules embedded within the stroma, unrelated to any particular cell type. Consistent with previous studies delineating the precise ligands for mCRP (5), this morphological pattern could indicate possible crosstalk between mCRP and components of the ECM. Given the putative pro-inflammatory properties of mCRP, such direct interactions could potentially contribute to excessive stromal formation. Apart from enlargement of the tumor, abundant ECM deposition has been linked to increased stromal stiffness, which subsequently can contribute to treatment resistance and favor tumor aggressiveness (40).

Serendipitously, when examining the pattern of mCRP distribution, it became apparent that some tumor cells were decorated by mCRP. Using double immune stainings with pan-cytokeratin as a tumor marker, we found evidence of direct overlap indicating close interaction and/or mCRP expression by tumor cells. Whether the positive mCRP/tumor staining depicts direct uptake of mCRP into tumor cells or represents an intrinsic feature that the evolving tumor acquires to support its own growth and formation of a tumor permissive microenvironment, remains elusive and should be expanded on in further studies.

Indeed, studies have shown that although the liver is the main source of CRP, extrahepatic production do exist (10, 41, 42). Specifically, macrophages, endothelial cells, smooth muscle cells as well as adipocytes and lymphocytes have been reported to synthesize CRP (10). Hence, we cannot rule out that the observed intratumoral mCRP is produced locally by inflammatory and/or tumor cells. The strong correlation with circulating serum CRP, however, indicates that the primary source of tissue-associated mCRP in our tumors was from systemic pCRP. Nonetheless, regardless of origin, given the evidence described above, persistent presence of mCRP within the tumor, which is considered an ongoing, non-resolving state due to the chronic nature of tumor-associated systemic inflammation, may potentially play a direct and active role in aggravating the localized inflammatory response. Notably, the versatile binding capacity of mCRP to a number of different cellular and non-cellular ligands, may potentially translate into multiple effects within the TME through its direct interaction with diverse targets that most likely will impact the evolving tumor.

This study has several limitations. Above all, it is a proof-of-concept study primarily performed for testing hypotheses and exploring a rather new and, in our opinion, underappreciated concept in clinical oncology, thus limiting the sample size. Hence, our findings need to be verified and further explored in larger

studies, which we are currently conducting. Next, we used FFPE tissue and IHC to elucidate possible functional roles of mCRP within tumors. While this methodological strategy provides high morphological precision regarding localization of the applied markers, the ability to evaluate direct functionality is, however, limited. This aspect should therefore be addressed in other kind of experiments, preferentially using fresh tissue. Finally, our tumor samples, although whole slides, only represent a snapshot of the immunological process, and do not mirror the long-term conditions and temporal dynamics. Hence, serial biopsies will be valuable to further dissect and evaluate how mCRP affects the immune response over time and impacts tumor evolution.

Taken together, we provide evidence for the existence of the monomeric form of CRP in CC being expressed exclusively within tumor tissue, primarily in systemically inflamed patients. mCRP expression colocalized with neutrophils and endothelial cells as well as areas of necrosis indicating a direct role in the microenvironment of tumors. In line with findings from studies conducted in other diseases, we suggest mCRP as a potential tissue-associated player with capability of actively shaping and fueling the local tumor immune response, presumably by creating a more tumor permissive environment and negatively affect patient outcome. These findings, if verified in further studies, puts CRP in a new perspective, acting not only as a biomarker of unfavorable prognosis and outcomes in cancer, but also as an active mediator with direct effects within tumors, and opens a new and intriguing approach for targeting the TME.

## Data availability statement

The original contributions presented in the study are included in the article/[Supplementary Material](#). Further inquiries can be directed to the corresponding author.

## Ethics statement

The studies involving human participants were reviewed and approved by Norwegian Regional Ethics Committee. Written informed consent for participation was not required for this study in accordance with the national legislation and the institutional requirements.

## Author contributions

AK contributed to data collection, analysis, and interpretation, and drafted the manuscript. JG, KC, and HZ prepared human tissue and performed lab work. PN performed digital image analysis and data interpretation. AF, IR, and LP provided materials, contributed to data interpretation and discussion of content. ET conducted statistical analyses and data curation. TS contributed to data interpretation, methods and discussion of content. CK participated in data interpretation, discussion of content and conceptual framework. All authors contributed to the article and approved the submitted version.



## Acknowledgments

We would like to thank research nurse Bente Mirjam Christensen at Sørlandet Hospital for excellent support with the clinical colorectal cancer database. The fluorescence work within this study benefited from resources supported by Toyota-Fonden, Denmark.

## Conflict of interest

The authors declare that the research was conducted in the absence of any commercial or financial relationships that could be construed as a potential conflict of interest.

## References

- Shrotriya S, Walsh D, Nowacki AS, Lorton C, Aktas A, Hullihen B, et al. Serum c-reactive protein is an important and powerful prognostic biomarker in most adult solid tumors. *PLoS One* (2018) 13(8):e0202555. doi: 10.1371/journal.pone.0202555
- Bruserud Ø, Aarstad HH, Tvedt THA. Combined c-reactive protein and novel inflammatory parameters as a predictor in cancer—what can we learn from the hematological experience? *Cancers* (2020) 12(7):1966. doi: 10.3390/cancers12071966
- Hart PC, Rajab IM, Alebraheem M, Potempa LA. C-reactive protein and cancer—diagnostic and therapeutic insights. *Front Immunol* (2020) 11:595835. doi: 10.3389/fimmu.2020.595835
- Rajab IM, Hart PC, Potempa LA. How c-reactive protein structural isoforms with distinctive bioactivities affect disease progression. *Front Immunol* (2020) 11:2126. doi: 10.3389/fimmu.2020.02126
- Potempa LA, Qiu WQ, Stefanski A, Rajab IM. Relevance of lipoproteins, membranes, and extracellular vesicles in understanding c-reactive protein biochemical structure and biological activities. *Front Cardiovasc Med* (2022) 9:979461. doi: 10.3389/fcvm.2022.979461
- Thiele JR, Habersberger J, Braig D, Schmidt Y, Goerendt K, Maurer V, et al. Dissociation of pentameric to monomeric c-reactive protein localizes and aggravates inflammation. *Circulation* (2014) 130(1):35–50. doi: 10.1161/CIRCULATIONAHA.113.007124
- Ji SR, Wu Y, Zhu L, Potempa LA, Sheng FL, Lu W, et al. Cell membranes and liposomes dissociate c-reactive protein (CRP) to form a new, biologically active structural intermediate: mCRP(m). *FASEB J* (2007) 21(1):284–94. doi: 10.1096/fj.06-6722com
- Braig D, Nero TL, Koch HG, Kaiser B, Wang X, Thiele JR, et al. Transitional changes in the CRP structure lead to the exposure of proinflammatory binding sites. *Nat Commun* (2017) 8:14188. doi: 10.1038/ncomms14188
- Wu Y, Potempa LA, El Kebir D, Filep JG. C-reactive protein and inflammation: Conformational changes affect function. *Biol Chem* (2015) 396(11):1181–97. doi: 10.1515/hsz-2015-0149
- Sproston FR, Ashworth JJ. Role of c-reactive protein at sites of inflammation and infection. *Front Immunol* (2018) 9:754. doi: 10.3389/fimmu.2018.00754
- Potempa LA, Rajab IM, Olson ME, Hart PC. C-reactive protein and cancer: Interpreting the differential bioactivities of its pentameric and monomeric, modified isoforms. *Front Immunol* (2021) 12:744129. doi: 10.3389/fimmu.2021.744129
- McFadyen JD, Kiefer J, Braig D, Loseff-Silver J, Potempa LA, Eisenhardt SU, et al. Dissociation of c-reactive protein localizes and amplifies inflammation: Evidence for a direct biological role of c-reactive protein and its conformational changes. *Front Immunol* (2018) 9:1351. doi: 10.3389/fimmu.2018.01351
- Slevin M, Krupinski J. A role for monomeric c-reactive protein in regulation of angiogenesis, endothelial cell inflammation and thrombus formation in cardiovascular/cerebrovascular disease? *Histol Histopathol* (2009) 24(11):1473–8. doi: 10.14670/hh-24.1473
- Ji SR, Ma L, Bai CJ, Shi JM, Li HY, Potempa LA, et al. Monomeric c-reactive protein activates endothelial cells via interaction with lipid raft microdomains. *FASEB J* (2009) 23(6):1806–16. doi: 10.1096/fj.08-116962
- Luan Y-y, Yao Y-m. The clinical significance and potential role of c-reactive protein in chronic inflammatory and neurodegenerative diseases. *Front Immunol* (2018) 9:1302. doi: 10.3389/fimmu.2018.01302
- Slevin M, Heidari N, Azamfiroi L. Monomeric c-reactive protein: Current perspectives for utilization and inclusion as a prognostic indicator and therapeutic target. *Front Immunol* (2022) 13:866379. doi: 10.3389/fimmu.2022.866379

## Publisher's note

All claims expressed in this article are solely those of the authors and do not necessarily represent those of their affiliated organizations, or those of the publisher, the editors and the reviewers. Any product that may be evaluated in this article, or claim that may be made by its manufacturer, is not guaranteed or endorsed by the publisher.

## Supplementary material

The Supplementary Material for this article can be found online at: <https://www.frontiersin.org/articles/10.3389/fimmu.2023.1170443/full#supplementary-material>

- Strang F, Scheichl A, Chen Y-C, Wang X, Htun N-M, Bassler N, et al. Amyloid plaques dissociate pentameric to monomeric c-reactive protein: A novel pathomechanism driving cortical inflammation in alzheimer's disease? *Brain Pathol* (2012) 22(3):337–46. doi: 10.1111/j.1750-3639.2011.00539.x
- Al-Baradie RS, Pu S, Liu D, Zeinolabediny Y, Ferris G, Sanfeli C, et al. Monomeric c-reactive protein localized in the cerebral tissue of damaged vascular brain regions is associated with neuro-inflammation and neurodegeneration—an immunohistochemical study. *Front Immunol* (2021) 12:644213. doi: 10.3389/fimmu.2021.644213
- Køstner AH, Nielsen PS, Georgsen JB, Parner ET, Nielsen MB, Kersten C, et al. Systemic inflammation associates with a myeloid inflamed tumor microenvironment in primary resected colon cancer—may cold tumors simply be too hot? *Front Immunol* (2021) 12:716342. doi: 10.3389/fimmu.2021.716342
- Crawford JR, Trial J, Nambi V, Hoogveen RC, Taffet GE, Entman ML. Plasma levels of endothelial microparticles bearing monomeric c-reactive protein are increased in peripheral artery disease. *J Cardiovasc Transl Res* (2016) 9(3):184–93. doi: 10.1007/s12265-016-9678-0
- Ying SC, Gewurz H, Kinoshita CM, Potempa LA, Siegel JN. Identification and partial characterization of multiple native and neoantigenic epitopes of human c-reactive protein by using monoclonal antibodies. *J Immunol* (1989) 143(1):221–8. doi: 10.4049/jimmunol.143.1.221
- Ying SC, Shephard E, de Beer FC, Siegel JN, Harris D, Gewurz BE, et al. Localization of sequence-determined neopeptides and neutrophil digestion fragments of c-reactive protein utilizing monoclonal antibodies and synthetic peptides. *Mol Immunol* (1992) 29(5):677–87. doi: 10.1016/0161-5890(92)90205-c
- Ronneberger O, Fischer P, Brox T. *U-Net: Convolutional networks for biomedical image segmentation. medical image computing and computer-assisted intervention – MICCAI 2015*. Cham: Springer International Publishing (2015).
- Kingma DP, Ba JA. A method for stochastic optimization. *arXiv* (2017) 1412.6980. doi: 10.48550/arXiv.1412.6980
- Craene BD, Jvd V, Rondelez E, Vandenbroeck L, Peeters K, Vanhoey T, et al. Detection of microsatellite instability (MSI) in colorectal cancer samples with a novel set of highly sensitive markers by means of the idylla MSI test prototype. *J Clin Oncol* (2018) 36(15\_suppl):e15639–e. doi: 10.1200/JCO.2018.36.15\_suppl.e15639
- Han CL, Meng GX, Ding ZN, Dong ZR, Chen ZQ, Hong JG, et al. The predictive potential of the baseline c-reactive protein levels for the efficiency of immune checkpoint inhibitors in cancer patients: A systematic review and meta-analysis. *Front Immunol* (2022) 13:827788. doi: 10.3389/fimmu.2022.827788
- Slevin M, García-Lara E, Capitanescu B, Sanfeliu C, Zeinolabediny Y, AlBaradie R, et al. Monomeric c-reactive protein aggravates secondary degeneration after intracerebral haemorrhagic stroke and may function as a sensor for systemic inflammation. *J Clin Med* (2020) 9(9):3053. doi: 10.3390/jcm9093053
- Slevin M, Matou-Nasri S, Turu M, Luque A, Rovira N, Badimon L, et al. Modified c-reactive protein is expressed by stroke neovessels and is a potent activator of angiogenesis in vitro. *Brain Pathol* (2010) 20(1):151–65. doi: 10.1111/j.1750-3639.2008.00256.x
- Badimon L, Peña E, Arderiu G, Padró T, Slevin M, Vilahur G, et al. C-reactive protein in atherothrombosis and angiogenesis. *Front Immunol* (2018) 9:430. doi: 10.3389/fimmu.2018.00430
- Sheriff A, Kayser S, Brunner P, Vogt B. C-reactive protein triggers cell death in ischemic cells. *Front Immunol* (2021) 12:630430. doi: 10.3389/fimmu.2021.630430
- Kheiss T, József L, Hossain S, Chan JSD, Potempa LA, Filep JG. Loss of pentameric symmetry of c-reactive protein is associated with delayed apoptosis of

- human neutrophils\*. *J Biol Chem* (2002) 277(43):40775–81. doi: 10.1074/jbc.M205378200
32. Heuertz RM, Schneider GP, Potempa LA, Webster RO. Native and modified c-reactive protein bind different receptors on human neutrophils. *Int J Biochem Cell Biol* (2005) 37(2):320–35. doi: 10.1016/j.biocel.2004.07.002
33. Khreiss T, József L, Potempa LA, Filep JG. Loss of pentameric symmetry in c-reactive protein induces interleukin-8 secretion through peroxynitrite signaling in human neutrophils. *Circ Res* (2005) 97(7):690–7. doi: 10.1161/01.Res.0000183881.11739.Cb
34. Xiong X, Liao X, Qiu S, Xu H, Zhang S, Wang S, et al. CXCL8 in tumor biology and its implications for clinical translation. *Front Mol Biosciences*. (2022) 9:723846. doi: 10.3389/fmolb.2022.723846
35. Di Napoli M, Slevin M, Popa-Wagner A, Singh P, Lattanzi S, Divani AA. Monomeric c-reactive protein and cerebral hemorrhage: From bench to bedside. *Front Immunol* (2018) 9:1921. doi: 10.3389/fimmu.2018.01921
36. Lee SY, Ju MK, Jeon HM, Jeong EK, Lee YJ, Kim CH, et al. Regulation of tumor progression by programmed necrosis. *Oxid Med Cell Longev* (2018) 2018:3537471. doi: 10.1155/2018/3537471
37. Ullah N, Ma F-R, Han J, Liu X-L, Fu Y, Liu Y-T, et al. Monomeric c-reactive protein regulates fibronectin mediated monocyte adhesion. *Mol Immunol* (2020) 117:122–30. doi: 10.1016/j.molimm.2019.10.013
38. Li HY, Wang J, Meng F, Jia ZK, Su Y, Bai QF, et al. An intrinsically disordered motif mediates diverse actions of monomeric c-reactive protein. *J Biol Chem* (2016) 291(16):8795–804. doi: 10.1074/jbc.M115.695023
39. Xu M, Zhang T, Xia R, Wei Y, Wei X. Targeting the tumor stroma for cancer therapy. *Mol Cancer* (2022) 21(1):208. doi: 10.1186/s12943-022-01670-1
40. Kozlova N, Grossman JE, Iwanicki MP, Muranen T. The interplay of the extracellular matrix and stromal cells as a drug target in stroma-rich cancers. *Trends Pharmacol Sci* (2020) 41(3):183–98. doi: 10.1016/j.tips.2020.01.001
41. Minamiya Y, Miura M, Hinai Y, Saito H, Ito M, Imai K, et al. The CRP 1846T/T genotype is associated with a poor prognosis in patients with non-small cell lung cancer. *Tumor Biol* (2010) 31(6):673–9. doi: 10.1007/s13277-010-0086-9
42. Salazar J, Martínez MS, Chávez-Castillo M, Núñez V, Añez R, Torres Y, et al. C-reactive protein: An in-depth look into structure, function, and regulation. *Int Sch Res Notices* (2014) 2014:653045. doi: 10.1155/2014/653045



## OPEN ACCESS

## EDITED BY

Yi Wu,  
Xi'an Jiaotong University, China

## REVIEWED BY

Hong Lei,  
The Affiliated Children's Hospital of Xi'an  
Jiaotong University, China  
Christopher Sjöwall,  
Linköping University, Sweden

## \*CORRESPONDENCE

Ying Tan  
✉ tanying@bjmu.edu.cn

## SPECIALTY SECTION

This article was submitted to  
Molecular Innate Immunity,  
a section of the journal  
Frontiers in Immunology

RECEIVED 07 March 2023

ACCEPTED 31 March 2023

PUBLISHED 17 April 2023

## CITATION

Liu XL, Tan Y, Yu F, Ji SR and Zhao MH  
(2023) Combination of anti-C1qA08 and  
anti-mCRP a.a.35-47 antibodies  
is associated with renal prognosis  
of patients with lupus nephritis.  
*Front. Immunol.* 14:1181561.  
doi: 10.3389/fimmu.2023.1181561

## COPYRIGHT

© 2023 Liu, Tan, Yu, Ji and Zhao. This is an  
open-access article distributed under the  
terms of the [Creative Commons Attribution  
License \(CC BY\)](#). The use, distribution or  
reproduction in other forums is permitted,  
provided the original author(s) and the  
copyright owner(s) are credited and that  
the original publication in this journal is  
cited, in accordance with accepted  
academic practice. No use, distribution or  
reproduction is permitted which does not  
comply with these terms.

# Combination of anti-C1qA08 and anti-mCRP a.a.35-47 antibodies is associated with renal prognosis of patients with lupus nephritis

Xiao-Ling Liu<sup>1,2,3,4,5,6</sup>, Ying Tan<sup>2,3,4,5,6\*</sup>, Feng Yu<sup>7</sup>, Shang-Rong Ji<sup>1</sup>  
and Ming-Hui Zhao<sup>2,3,4,5,6</sup>

<sup>1</sup>Ministry of Education (MOE) Key Laboratory of Cell Activities and Stress Adaptations, School of Life Sciences, Lanzhou University, Lanzhou, China, <sup>2</sup>Renal Division, Peking University First Hospital, Beijing, China, <sup>3</sup>Institute of Nephrology, Peking University, Beijing, China, <sup>4</sup>Key Laboratory of Renal Disease, Ministry of Health of China, Beijing, China, <sup>5</sup>Key Laboratory of Chronic Kidney Disease (CKD) Prevention and Treatment, Ministry of Education of China, Beijing, China, <sup>6</sup>Research Units of Diagnosis and Treatment of Immune-Mediated Kidney Diseases, Chinese Academy of Medical Sciences, Beijing, China, <sup>7</sup>Department of Nephrology, Peking University International Hospital, Beijing, China

**Objective:** The aim of this study is to explore the prevalence and clinicopathological associations between anti-C1qA08 antibodies and anti-monomeric CRP (mCRP) a.a.35-47 antibodies and to explore the interaction between C1q and mCRP.

**Methods:** Ninety patients with biopsy-proven lupus nephritis were included from a Chinese cohort. Plasma samples collected on the day of renal biopsy were tested for anti-C1qA08 antibodies and anti-mCRP a.a.35-47 antibodies. The associations between these two autoantibodies and clinicopathologic features and long-term prognosis were analyzed. The interaction between C1q and mCRP was further investigated by ELISA, and the key linear epitopes of the combination of cholesterol binding sequence (CBS; a.a.35-47) and C1qA08 were tested by competitive inhibition assays. The surface plasmon resonance (SPR) was used to further verify the results.

**Results:** The prevalence of anti-C1qA08 antibodies and anti-mCRP a.a.35-47 antibodies were 50/90 (61.1%) and 45/90 (50.0%), respectively. Levels of anti-C1qA08 antibodies and anti-mCRP a.a.35-47 antibodies were negatively correlated with serum C3 concentrations ((0.5(0.22-1.19) g/L vs. 0.39(0.15-1.38) g/L,  $P=0.002$ ) and (0.48(0.44-0.88) g/L vs. 0.41(0.15-1.38) g/L,  $P=0.028$ ), respectively. Levels of anti-C1qA08 antibodies were correlated with the score of fibrous crescents and tubular atrophy ( $r=-0.256$ ,  $P=0.014$  and  $r=-0.25$ ,  $P=0.016$ , respectively). The patients with double positive antibodies showed worse renal prognosis than that of the double negative group (HR 0.899 (95% CI: 0.739-1.059),  $P=0.0336$ ). The binding of mCRP to C1q was confirmed by ELISA. The key linear epitopes of the combination were a.a.35-47 and C1qA08, which were confirmed by competitive inhibition experiments and SPR.

**Conclusion:** The combination of anti-C1qA08 and anti-mCRP a.a.35-47 autoantibodies could predict a poor renal outcome. The key linear epitopes of the combination of C1q and mCRP were C1qA08 and a.a.35-47. A08 was an important epitope for the classical pathway complement activation and a.a.35-47 could inhibit this process.

#### KEYWORDS

anti-C1qA08 autoantibody, anti-mCRP a.a.35-47 autoantibody, autoantibodies, renal prognosis, lupus nephritis

## Introduction

Systemic lupus erythematosus (SLE) is a systemic autoimmune disease with multiple autoantibodies. Lupus nephritis (LN) is the most prevalent secondary glomerulonephritis in China. LN is the one of the principal causes of morbidity and mortality among various major organ manifestations of lupus (1). The development of glomerulonephritis in SLE was associated with the presence of some specific nephritogenic autoantibodies, such as anti-double-stranded DNA (anti-dsDNA) antibodies (2–4), anti-Sm antibodies, anti-C1q antibodies (5–8), and anti-C-reactive protein (CRP) antibodies (9, 10), whereas more than 150 autoantibodies were reported in SLE. It is still controversial that which autoantibodies are associated with renal clinical and pathological activity and the renal outcome. At present, the exact immunological pathogenesis of SLE and LN is still unclear. It may be caused by apoptotic cell clearance encountering an immune complex in the kidney, which in turn causes complement activation to result in kidney damage.

C1q is the classical pathway promoter of complement activation and is the largest complement protein. C1q is composed of six subunits, each of which consists of three chains A, B, and C, and is divided into three parts: a head region, a collagen region, and a tail portion. C1q is the most positively charged protein in serum, and its ligands are diverse (11). The head region of C1 can be combined with antigen-antibody complex, apoptotic cells, CRP, and pentraxin-3 (PTX3), and the collagen region can be combined with C1r, C1s, and mCRP. The main physiological function of C1q is to clear immune complexes and apoptotic bodies and to exert different biological functions in combination with different ligands (12–15). Vanhecke D et al. confirmed that the linear epitope A08 located on the A chain is an important antigen recognition site for anti-C1q autoantibodies (16). Long-term follow-up studies using large cohorts in some studies have shown that anti-C1qA08 antibodies were associated with disease activity and prognosis in Chinese patients with LN (17). H. Jiang et al. demonstrated for the first time that CRP binds to C1q and that CRP mainly binds to peptides 14-26 of the C1q A-chain collagen region, which is basically identical to the amino acid sequence of the linear epitope of A08 mentioned above (18).

CRP has two opposite structural faces, the ligand binding surface, and the effective surface. When CRP binds to a ligand, its effect surface can bind to complement C1q, thereby activating the

classical pathway (19). The pentameric CRP, which is expressed during body infection and systemic inflammation, is involved in the process of apoptotic cell clearance (12). With the dissociation of the pentameric structure, the conformation of the CRP subunit changes and exhibits an mCRP epitope (20). Studies have reported that damaged cell membranes can induce CRP dissociation (21). In the inflammatory microenvironment, mCRP is likely to exert pro-inflammatory effects in a “functional state”. As an acute-phase plasma protein, CRP can rapidly increase its concentration by 1000 times in inflammation (22, 23). SLE is a classic immunoinflammatory disease, but the concentration of CRP as a marker of inflammation is only slightly elevated or maintains normal levels during disease activity in SLE patients (24, 25). A previous report found that anti-mCRP antibodies were not only associated with disease activity but also with renal prognosis in LN (26), and a.a.35-47 seemed to be the most important epitope of mCRP (27).

This study investigated the associations of clinical, laboratory and pathological features and prognosis of LN with a panel of autoantibodies, including anti-C1qA08 and anti-mCRP a.a.35-47 antibodies in a large cohort of Chinese patients with LN. The combination of anti-C1qA08 and anti-mCRP a.a.35-47 antibodies could indicate higher renal disease activity and predict renal outcome. Studies on the interactions between C1q and mCRP were further explored to show their role in the development of LN.

## Material and methods

### Patients

Between January 2000 and July 2010, 90 patients with LN were diagnosed by renal biopsy and pathological examination at the First Hospital of Peking University and had complete clinical pathology and follow-up data. All patients were fulfilled the 1997 American College of Rheumatology (ACR) revised criteria for SLE (28). The SLEDAI score was used to evaluate the patient's systemic disease activity (29, 30).

Informed consent was obtained from all the patients. The research was in compliance with the Declaration of Helsinki. The design of this work was approved by the local ethical committees. The composite endpoints were defined as death, end-stage renal



disease (ESRD),  $\geq 30\%$  reduction from baseline estimated glomerular filtration rate (eGFR) or LN flares.

The serum of the patient was obtained on the day of the renal biopsy prior to the initiation of immunosuppressive therapy. At the same time, 60 healthy blood donors matched with the age and sex of the patients were selected as normal controls. Serum was stored in a refrigerator at  $-80^{\circ}\text{C}$  after being packed to avoid repeated freezing and thawing. Kidney biopsy specimens were examined by immunofluorescence and electron microscopy. Pathological parameters, including activity indices (AI) and chronicity indices (CI), were determined by renal pathologists (31, 32).

The research was in compliance with the Declaration of Helsinki. It was approved by the ethics committee of Peking University First Hospital (No. 20161163).

## Peptides synthesis

Biotinylated and nonbiotinylated peptides ( $>95\%$  purity) were synthesized by GenScript. Peptides A08 (GRPGRGRPGLKG) and B78 (PGKVGPKGPMGPK) were derived from the collagen like region (CLR) sequences of the C1q-A chain and the C1q-B chain, respectively. Peptide A08-C (GAPGKDGYDGLPG) was derived from the C1q-C chain and located at the N-terminal region homologous to peptide A08. It was used as a negative control peptide. Peptides 35-47 (VCLHIFYTELSSTR) and 199-206 (FTKPQLWP), which were derived from the mCRP. The purified peptides were then confirmed by high-performance liquid chromatography for purity and by mass spectrometry to verify the correct sequence.

## Detection of anti-C1qA08 and anti-mCRP a.a.35-47 antibodies by ELISA

The final concentration of avidin was  $5\mu\text{g/ml}$  in a 96-well microtiter plate, and overnight at  $4^{\circ}\text{C}$ , and the avidin-free well was used as a non-antigen control. It was washed with PBST and then blocked with  $0.1\%$  collagen at  $37^{\circ}\text{C}$  for 1 hour. The biotin-labelled peptide A08/a.a.35-47 to  $5\mu\text{g/ml}$  was diluted with PBS, added to the plate, and incubated at  $37^{\circ}\text{C}$  for 2 hours. Avidin specifically binds to biotin to immobilize the peptide on the plate. The plasma sample (1:200) was added and diluted and incubated at  $37^{\circ}\text{C}$  for 1 hour. Alkaline phosphatase (AP)-labelled goat anti-human IgG (1:5000) was added and incubated for 1 hour at  $37^{\circ}\text{C}$ . Finally, after an alkaline phosphatase substrate solution added, the absorbance at 405 nm was measured with a microplate reader. The cut-off value was set as the mean  $+2\text{SD}$  of the 60 healthy blood donors.

## C1q binding assays

The final concentration of C1q was diluted  $5\mu\text{g/ml}$  with carbonate buffer, and  $100\mu\text{l}$  of the coated 96-well microtiter plate

was taken and incubated overnight at  $4^{\circ}\text{C}$ . Wells were washed with Phosphate Buffered Solution containing  $0.1\%$  TWEEN-20 (PBST) and blocked with  $1\%$  BSA/PBS for 1 hour. Different concentrations of mCRP were added at  $37^{\circ}\text{C}$  for 1 hour. In the competition assay, mCRP was incubated with different concentrations of the relevant peptides a.a.35-47 and a.a.199-206 at  $37^{\circ}\text{C}$  for 30 minutes in each well. Binding was detected with mCRP antibody and alkaline phosphatase (AP)-labelled goat anti-mouse IgG antibody (1:5000). The absorbance at 405 nm was measured. At the same time, mCRP  $4\mu\text{g/ml}$  was diluted with carbonate buffer, fixed in a 96-well microtiter plate, and incubated overnight at  $4^{\circ}\text{C}$ . Wells were washed with PBST containing  $0.1\%$  TWEEN-20 and blocked with  $1\%$  BSA/PBS at  $37^{\circ}\text{C}$  for 1 hour, and C1q was incubated with different concentrations of related peptides A08, B78, and A08-C for 37 minutes at  $37^{\circ}\text{C}$  to each well. Binding was detected using a C1q antibody and an alkaline phosphatase (AP)-labelled goat anti-rabbit IgG antibody (1:10000), and the absorbance at 405 nm was measured.

The interaction of C1q with mCRP and peptides a.a.35-47, a.a.199-206 was detected using the Biacore T200 direct assay. Next, the interaction of mCRP with C1q and peptides A08, B78, and A08-C were examined. CRP was immobilized on a CM5 chip, followed by a 200 s denaturing agent (8 M urea and 5 mM EDTA) at a flow rate of  $30\mu\text{l/min}$  to denature CRP to mCRP, then at a flow rate of  $30\mu\text{l/min}$  in a  $0.05\%$  P-20. The analyte was injected into the PBS and only the injection buffer was used as a negative control in the other channel.

## Anti-C1qA08 antibody inhibited the binding of C1q to mCRP

The human complement component C1q ( $4\mu\text{g/ml}$ ) was first diluted with carbonate buffer and was coated on the wells of polystyrene microtiter plates. After blocking with  $0.1\%$  collagen at  $37^{\circ}\text{C}$  for 1 hour, each well was washed with PBS containing  $0.1\%$  TWEEN-20 (PBST). The mCRP ( $2\mu\text{g/ml}$ ) was added with different concentrations of C1qA08 mAb (17-9), preincubated for 30 min at  $37^{\circ}\text{C}$ , and then added to a 96-well microtiter plate. After washing, A08-specific antibody 3H12 (1:200) was diluted and added to the plate for 1 hour at  $37^{\circ}\text{C}$ . Alkaline phosphatase (AP)-labelled goat anti-mouse IgG was added and incubated for 1 hour at  $37^{\circ}\text{C}$ . The P-nitrophenyl phosphate (1 mg/ml; Sigma-Aldrich) was diluted in substrate buffer (1.0 M diethanolamine and 0.5 mM  $\text{MgCl}_2$  (pH 9.8). Then optical density was measured at 405 nm.

## C3 deposition assay

C3 deposition assay was performed as previously described by Roumenina LT et al. (33). The recombinant  $\alpha 3(\text{IV})\text{NC1}$  ( $2\mu\text{g/ml}$ ) was first diluted with carbonate buffer and coated on the wells of polystyrene microtiter plates. After blocking with  $0.1\%$  collagen at  $37^{\circ}\text{C}$  for 1 hour, each well was washed with PBS containing  $0.1\%$  TWEEN-20 (PBST). Total IgG from patients with anti-glomerular

basement membrane disease and positive anti- $\alpha$ 3(IV)NC1 autoantibody were purified by a protein G column (34) and were diluted to 20  $\mu$ g/ml in PBST for the binding of anti- $\alpha$ 3(IV)NC1 autoantibody. The plate was washed with veronal buffered saline containing 0.1% TWEEN-20 (VBST), and then normal human serum was diluted 1:100 with VBST. The diluted serum was added with different concentrations of mCRP and a.a.35-47, preincubated for 30 min at 37°C, and then added to a 96-well microtiter plate. Incubate for 1 hour at 37°C. After washing, rabbit anti-human C3c antibody (1:10000) was diluted and added to the plate for 1 hour at 37°C. Alkaline phosphatase (AP)-labelled goat anti-rabbit IgG was added and incubated for 1 hour at 37°C. The P-nitrophenyl phosphate was used in the substrate buffer. Optical density was measured at 405 nm.

## Statistical analysis

The data were analysed using SPSS 21.0 statistical software (SPSS, Inc, Chicago, IL, USA). Quantitative data were expressed as mean  $\pm$  SD or median with a range minimum–maximum. For comparison of clinical features and pathologic data of patients, the 1-way analysis of variance. Spearman correlation was performed to analyse correlation. Kaplan-Meier curves were used to analyse prognosis. Univariate survival analysis was carried out with the log-rank test. Results were expressed as HR with a 95% CI. Statistical significance was considered  $P < 0.05$ .

## Results

### General patient data

Clinical data of 90 LN patients from the Peking University First Hospital were shown in Table 1. There were 15 (16.7%) male and 75 (83.3%) female patients with a median age of 29 (13 to 67) years. 20

patients were classified as class III (22.2%, including 8 as class III +V) and 70 as class IV (77.8%, including 16 as class IV +V). The demographic and clinical data were summarized in Table 1.

### The associations between anti-C1qA08 and anti-mCRP a.a. 35-47 autoantibodies and clinicopathologic features of LN patients

The cut-off values of the anti-C1qA08 antibodies and anti-mCRP a.a.35-47 antibodies were illustrated in Figure 1. In the discovery cohort, the anti-C1qA08 autoantibodies were detected in 55 of 90 (61.1%) patients, which was significantly higher than that in the normal healthy subjects (0/60, 0%,  $P < 0.0001$ ). Anti-mCRP a.a.35-47 antibodies were detected in 45 of 90 (50.0%) patients, which were significantly higher than that in the normal healthy subjects (4/60, 6.67%,  $P < 0.001$ ).

The associations between with anti-C1qA08 antibodies and anti-mCRP a.a.35-47 antibodies and clinicopathologic features were shown in Tables 2; 3. Levels of anti-C1qA08 antibodies and anti-mCRP a.a.35-47 antibodies were negatively correlated with serum C3 concentrations ((0.5(0.22-1.19) g/L vs. 0.39(0.15-1.38) g/L,  $P=0.002$ ) and (0.48(0.44-0.88) g/L vs. 0.41(0.15-1.38) g/L,  $P=0.028$ )). Levels of anti-C1qA08 antibodies were correlated with the score of fibrous crescents and tubular atrophy ( $r=-0.256$ ,  $P=0.014$  and  $r=-0.25$ ,  $P=0.016$ , respectively).

Further combined analysis of the two antibodies showed 36 cases of anti-C1qA08+/anti-mCRP a.a.35-47+ antibodies (double-positive antibody) and 26 cases of anti-C1qA08-/anti-mCRP a.a.35-47- (double-negative antibodies). The associations between double-positive and double-negative antibodies and clinicopathologic features were shown in Tables 4; 5. Serum concentrations of C3 and C4 in patients with double positive antibodies were significantly lower than that in the double negative group ((0.52(0.25-1.19) g/L vs. 0.39(0.15-0.98) g/L,  $P=0.004$ ) and (0.12(0.03-0.22) g/L vs. 0.05 (0.02-0.18) g/L,  $P<0.001$ ), respectively). And the double positive

TABLE 1 General clinical profiles of patients with lupus nephritis at renal biopsy.

Clinical Evaluation		Laboratory Assessment	
Number of patients	90	Leukocytopenia, no. (%)	20(22.2)
Age (median and range) (years)	32.51(14-67)	Thrombocytopenia, no. (%)	12(13.3)
Female, no. (%)	84.4%	Hematuria, no. (%)	72(80.0)
Hypertension (BP $\geq$ 140/90mmHg), no. (%)	47(52.2)	Leukocyturia, no. (%)	49(54.4)
Nephrotic syndrome, no. (%)	49(54.4)	Hemoglobin, mean $\pm$ s.d.(g/L)	108.4 $\pm$ 24.6
Acute kidney injury, no. (%)	18(20.0)	Urinary protein, median (range) (g/24h)	3.8(0.2-22.45)
Anemia, no. (%)	41(45.6)	Serum creatinine, median (range) (umol/L)	75.4(26.1-792.0)
Neurological disorder, no. (%)	5(5.6)	C3 level, median (range) (g/L)	0.5(0.15-1.38)
SLEDAI, mean $\pm$ s.d	17.4 $\pm$ 6.3	C4 level, median (range) (g/L)	0.11(0.00-1.01)
Follow-up time, m, median (range)	56.73(27-86)	ANA (+), no. (%)	87(96.7)
Duration from SLE onset to renal biopsy, (months), mean $\pm$ s.d	24.0 $\pm$ 3.9	Anti-dsDNA antibodies, no. (%)	69(76.7)

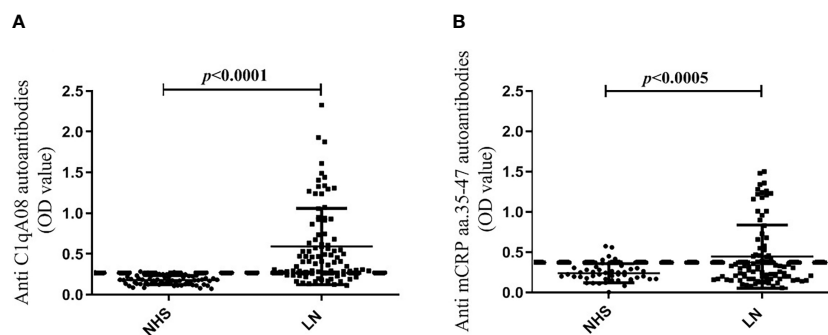


FIGURE 1

(A) Comparisons of levels of anti-A08 antibodies in LN and healthy blood donors. (B) Comparisons of levels of anti-mCRP a.a.35-47 antibodies in LN and healthy blood donors.

TABLE 2 Associations of anti-C1qA08 antibodies and anti-mCRP a.a.35-47 antibodies with clinical parameters.

	Anti-mCRP a.a.35-47 -/+ (P value)	Anti-C1qA08-/+ (P value)
SLEDAI scores	16.89 ± 5.87/18.36 ± 7.127(0.283)	18.60 ± 6.273/17.18 ± 6.679(0.331)
Acute kidney injury(-/+)	10(22.2%)/9(19.1%)(0.716)	6(20%)/13(21%)(0.914)
Hemoglobin(g/L)	110(47-177)/109(60-144)(0.656)	110(63-156)/109(47-177)(0.714)
Hematuria(-/+)	35(77.8%)/39(83%)(0.530)	25(83.3%)/49(79.0%)(0.626)
Leukocyturia(-/+)	24(53.3%)/25(53.2%)(0.585)	18(60%)/31(50.0%)(0.199)
Proteinuria(g/d)	4.43(0.48-22.45)/3.5(0.23-20.62)(0.182)	4.46(0.48-15.38)/3.57(0.23-22.45)(0.157)
Serum creatinine(μmol/L)	75.7(36.7-618)/77(26.1-792)(0.984)	76.35(36.7-618)/76.4(26.1-792)(0.825)
Serum C3(g/L)	0.5(0.22-1.19)/0.39(0.15-1.38)(0.002)	0.48(0.44-0.88)/0.41(0.15-1.38)(0.028)

TABLE 3 Associations of anti-C1qA08 antibodies and anti-mCRP a.a.35-47 antibodies with renal pathology scores.

Renal pathology score	Anti-mCRP a.a.35-47 antibodies		Anti-C1qA08 antibodies	
	r value	p value	r value	P value
Activity indices score	-0.082	0.514	0.042	0.737
Cellular fiber crescent	-0.136	0.196	-0.066	0.533
Neutrophil infiltration and/or nuclear fragmentation	0.000	0.997	0.088	0.406
Wire loop/transparent thrombus	0.076	0.471	0.065	0.538
Interstitial inflammatory	-0.017	0.872	-0.144	0.172
Chronicity indices score	-0.125	0.321	-0.072	0.568
Spherical sclerosis	0.036	0.732	0.037	0.726
Fibrous crescent	-0.134	0.201	-0.256	0.014
Tubular atrophy	-0.132	0.209	-0.250	0.016

TABLE 4 Comparisons of clinical manifestations of patients with and without double positive antibodies.

	Double negative antibodies	Double positive antibodies	<i>p</i> value
SLEDAI scores	18 ± 6	19 ± 6	0.463
Acute kidney injuries	19.2%	25.0%	0.592
Hemoglobin(g/L)	42.3%	55.6%	0.303
Hematuria	80.8%	83.3%	1.000
Leukocyturia	60.0%	63.9%	0.758
Proteinuria(g/d)	4.5(0.5-15.4)	3.1(0.2-22.5)	0.158
Serum creatinine(μmol/L)	74.6(36.7-273.7)	83.5(34.7-792.0)	0.185
Serum C3(g/L)	0.52(0.25-1.19)	0.39(0.15-0.98)	0.004
Serum C4(g/L)	0.12(0.03-0.22)	0.05(0.02-0.18)	<0.001
Anti-dsDNA antibody	73.1%	91.4%	0.118

antibodies in patients were negatively associated with fibrous crescent, tubular atrophy and IgG deposition ( $r=-0.210$ ,  $P=0.017$ ,  $r=-0.248$ ,  $P=0.022$ , and  $r=-0.365$ ,  $P=0.004$ , respectively).

Finally, we used Kaplan-Meier analysis to compare the renal survival between patients with and without anti-C1qA08 or anti-mCRP a.a.35-47 antibodies. We found that patients with anti-C1qA08 antibodies had significantly worse renal prognosis than those without ( $P=0.027$ , HR 0.143 (95% CI:0.502-17.003)) (Figure 2A); The survival rate of patients with anti-mCRP a.a.35-47 antibodies was worse than those without ( $P=0.059$ , HR 7.465 (95% CI:0.929-59.983)) (Figure 2B); Patients with double-positive antibodies had significantly worse renal prognosis than those with

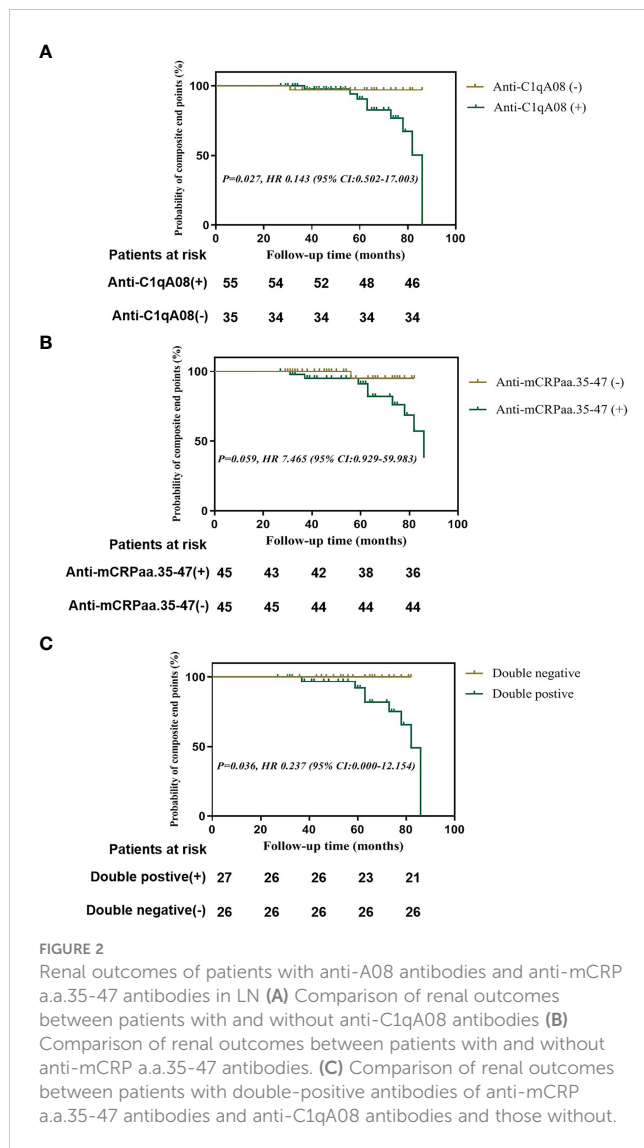
double-negative antibodies ( $P=0.036$ , HR 0.237 (95% CI:0.000-12.154)) (Figure 2C).

### Binding of mCRP to C1q by enzyme-linked immunosorbent assay and surface plasmon resonance

The ELISA method was performed to detect the binding of mCRP and C1q and the binding of their key epitopes, respectively. Firstly, the binding of C1q and mCRP was dose-dependent (Figure 3A).

TABLE 5 Comparisons of pathological manifestations of patients with and without double positive antibodies.

Renal pathology score	Double positive antibodies	
	<i>r</i> value	<i>P</i> value
Activity indices score	0.126	0.400
Cell/cell fiber crescent	0.008	0.953
Neutrophil infiltration and/or nuclear fragmentation	0.017	0.896
Interstitial inflammatory	0.143	0.267
Chronicity indices score	0.192	0.196
Global sclerosis	0.071	0.581
Fibrous crescent	-0.210	0.017
Tubular atrophy	-0.248	0.022
IgG deposition	-0.365	0.004
IgA deposition	-0.102	0.429
IgM deposition	-0.160	0.213
C3c deposition	0.129	0.316



To further clarify the key epitope of the combination of the two proteins, it was known that the key linear epitope of the C1q antibody is A08, and the anti-C1qA08 antibody was related to the poor prognosis of LN patients. It may be used as a non-invasive “biology marker” that can predict the long-term prognosis of patients with LN. mCRP was coated on a 96-well microtiter plate, then C1q and different concentrations of related peptides A08, B78, and A08-C mixture were added (Figure. 3B). As the concentration of related peptides increased, A08 significantly inhibited the binding of C1q and mCRP. When it reached 80  $\mu\text{g/ml}$ , it inhibited 80% of the binding. B78 also has a certain effect but was relatively weak, while A08-C had almost no influence. The key epitope of binding between mCRP and C1q was A08.

To further clarify the key epitopes on mCRP, C1q was coated on a 96-well plate, and then mCRP and different concentrations of related peptides as a.a.35-47 mixture and a.a.199-206 mixture were

added (Figure 3C). As the peptide concentration increased, a.a.35-47 significantly inhibited the binding of mCRP and C1q. When the concentration of a.a.35-47 up to 80  $\mu\text{g/ml}$ , the inhibition rate up to 90%, while a.a.199-206 had no effect. a.a.35-47 was the key epitope for mCRP and C1q binding.

We further used optical surface plasmon resonance (SPR) to verify the key epitopes of C1q-related peptides to which mCRP directly binded. Firstly, human C1q was coupled to the CM5 chip, and purified mCRP with a concentration gradient was injected, the combination of the C1q and mCRP was dose-dependent. (Figure 4A).

To further clarify the binding epitope, mCRP was immobilized on the CM5 chip. However, mCRP was precipitated in an acetate buffer. We then coated the pentameric CRP on the chip, injected a certain amount of high-concentration deforming agent urea, and the CRP was finally converted into mCRP. And then injected different concentrations of peptides A08, B78, and A08-C. mCRP was mainly combined with A08 by comparing the KD value (Figures 4B-D). Then C1q was coated on the chip, and different concentrations of peptides a.a.35-47 and a.a.199-206 were injected. The comparison of KD values showed that C1q was mainly bound to a.a.35-47 of mCRP ( $KD=2.937 \times 10^{-6}$ ) (Figures 4E, F).

## Anti-C1qA08 antibody inhibited the binding of C1q to mCRP

C1q A08 mAb (17-9) can bind to eight or 10 amino acids of the C-terminus of A08. C1q was first coated on ELISA plates. mCRP was co-incubated with the anti-C1qA08 antibody and competed with C1q for binding. The binding of mCRP to C1q was significantly inhibited as the concentration of A08 antibody increased (Figure 5). When the anti-C1qA08 antibody was added at 80  $\mu\text{g/ml}$ , the inhibition rate exceeded 50%. Thus, the anti-C1qA08 antibody could inhibit the binding of mCRP to C1q and also demonstrated that A08 was the two key binding epitopes.

## C3 deposition

Our results showed that a.a.35-47 was the key sequence on mCRP which mediated the binding of mCRP and C1q, while A08 was the key sequence on C1q which mediated the binding of C1q and mCRP. In LN, the classical pathway could be activated. We speculated that mCRP and a.a.35-47 might be involved in the activation of the classical complement pathway. *In vitro*,  $\alpha 3(\text{IV})\text{NC1}$  immune complex was immobilized onto microtiter wells, and 1% serum from healthy volunteers was added into wells. The complement can be activated by C1q binding to immune complexes and thus lead to the production of C3c. Different concentrations of mCRP were added to the serum in the subsequent experiments, and with the increase of the concentration of mCRP, the deposition of C3c decreased (Figure 6A). Similarly, different concentrations of a.a.35-47 were added to the serum, with the increase of concentration of a.a.35-47, the deposition of C3c decreased

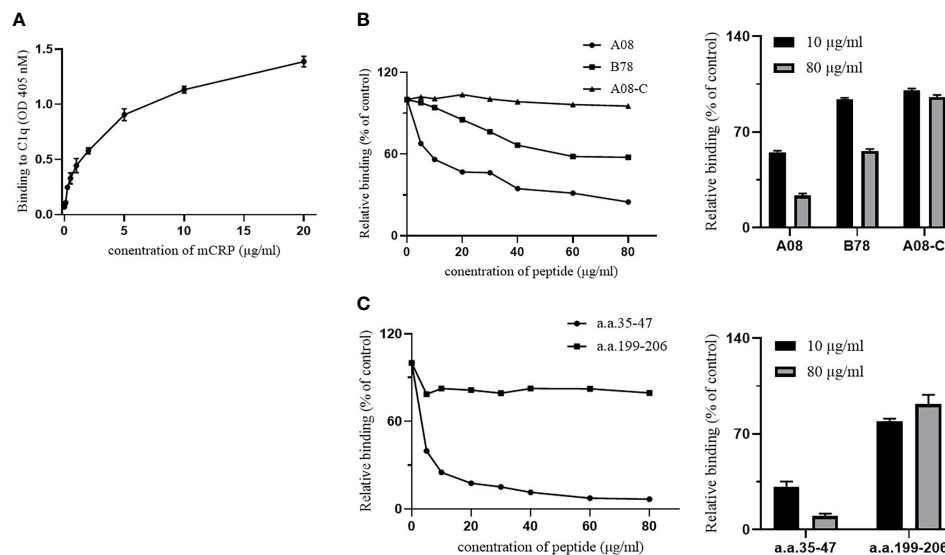


FIGURE 3

The binding epitopes of mCRP and C1q by ELISA. (A) C1q was immobilized on the ELISA plate, and then different concentrations of mCRP were added. The binding activity of mCRP to C1q was measured using mCRP-specific antibody 3H12. As the concentration of mCRP increased, the absorbance increased and was dose-dependent. (B) Fix the urea-denatured mCRP on the microplate, and different concentrations of peptides A08, B78, and A08-C were added to the plate. The inhibition of binding of C1q to mCRP was inhibited by 80% when 80 μg/ml of A08 was added. (C) Fix C1q on the microplate, then different concentrations of peptides a.a.35-47 and a.a.199-206 were added to the plate. We observed that a.a.35-47 significantly inhibited the binding of mCRP to C1q, and it inhibited by 90% when added to 80 μg/ml of a.a.35-47.

(Figure 6A). The above results demonstrated that mCRP could inhibit complement activation, and a.a.35-47 could also inhibit the complement activation. The inhibition rate could reach over 60% when 20 μg/ml mCRP was added to the serum. In addition, it elevated to more than 75% when 80 μg/ml mCRP was added to the serum (Figure 6B). The inhibition rate could reach over 40% when 20 μg/ml a.a.35-47 were added to the serum, while 40 μg/ml a.a.35-47 could inhibit 50% of activation (Figure 6C).

## Discussion

LN is one of the most serious complications of SLE, with over 50% of SLE patients developing LN in China (35, 36). The complement system is widely considered to be a 'double-edged sword' in LN (37, 38), with complement activation promoting pathogen clearance, but also causing tissue damage due to immune complex deposition. C1q is an important component of the classical pathway to complement and can bind to ligands such as mCRP, IgG, and fibronectin, et al. Both autoantibodies against C1qA08 and mCRP a.a.35-47 showed influence on prognosis. But the interaction between C1q and mCRP is still under discussion.

In our study, anti-C1qA08 antibodies and mCRP a.a.35-47 antibodies were prevalent in patients with LN, which was in accordance with previous studies. Moreover, the double-positive group showed more severe hypocomplementemia, which indicated that complement activation might exist in the double-positive group. We further found that levels of anti-C1qA08 and anti-mCRP a.a.35-47

antibodies correlated with the score of IgG deposition, fibrous crescents, and tubular atrophy, which suggested that these two autoantibodies were associated with renal pathological lesions and suggested the pathogenic role of these two autoantibodies (39). More importantly, patients with both anti-C1qA08 antibody and anti-mCRP a.a.35-47 antibodies had a worse prognosis. The clinicopathological analysis suggested that these two antibodies might not only be biomarkers but also of importance in the pathogenesis of LN.

Thus, we tested the combination of the C1q and mCRP and the key epitope of the binding activity. The combination of C1q and mCRP was proved by ELISA and SPR. Whether it was coated by C1q and then added mCRP, or coated mCRP and added C1q, the binding could be detected in a concentration-dependent manner. At the same time, the SPR method directly detected the combination of the two proteins, and the results showed that it was in the form of fast binding and slow dissociation, and the dissociation constant was very small, which proved that the binding force was super strong. The binding force of the two proteins was so strong that it was difficult to dissociate, so we speculated that mCRP might be involved in the pathogenesis of LN through binding to C1q. Both C1q and mCRP were macromolecular proteins, so it was necessary to further clarify the binding site of the two proteins. We first studied the important epitopes of C1q and mCRP reported in the literature, and then we used the competitive binding assays to verify the bound epitopes. The results suggested that A08 was an important epitope for the binding of C1q to mCRP, and a.a.35-47 was an important epitope for the binding of mCRP to C1q. After that, SPR was used tentatively to combine the two peptides. However, it was failed because the peptide



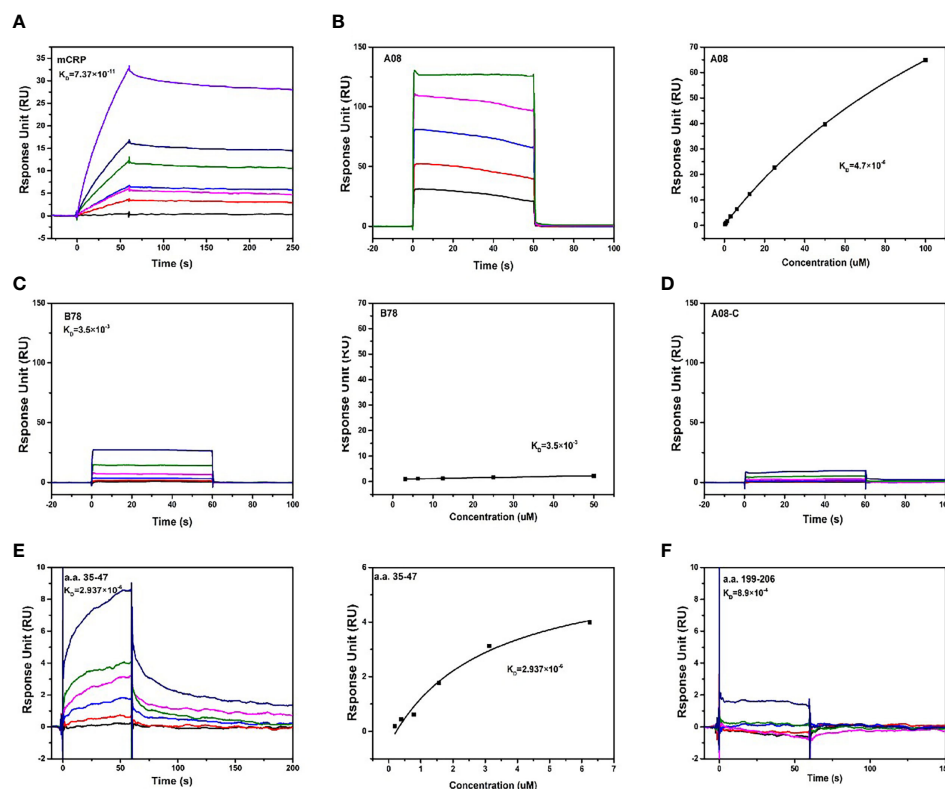


FIGURE 4

The binding epitopes of mCRP and C1q by SPR method. (A) Fix C1q on the CM5 chip and add different concentrations of mCRP, K<sub>D</sub>=0.0737 nM. (B) To clarify the key epitopes of binding, CRP was coupled to the CM5 chip, 200 s of the urea-deforming agent was injected, and CRP was depolymerized into mCRP. Recombined peptides of different concentrations A08, K<sub>D</sub>=4.7 μM. The curve was dose-dependent. (C) Based on B, change A08 to B78, K<sub>D</sub>=3.5 mM, the binding was very weak, and the steady-state curve showed that the response value changes a little as the concentration increases. (D) Similarly, different concentrations of A08-C were injected, K<sub>D</sub>=0. mCRP was hardly combined with A08-C. (E) C1q was immobilized on a CM5 chip, and different concentrations of a.a.35-47 were injected, which was characterized by slow binding and fast dissociation. The steady-state curve was used to determine the binding to dose-dependent, K<sub>D</sub>=2.937 μM. (F) C1q was fixed on the CM5 chip and different concentrations of a.a.199-206, K<sub>D</sub>=0.89 mM was injected. Therefore, C1q mainly bound to a.a.35-47 of mCRP, and mCRP mainly bound to the A08 epitope of C1q.

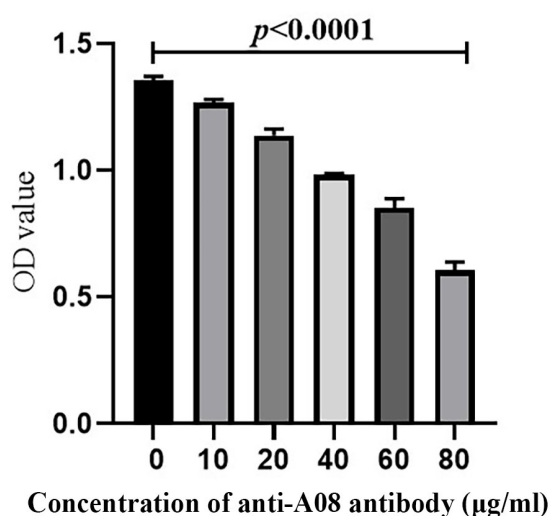


FIGURE 5

The anti-C1qA08 antibody inhibited the binding of C1q to mCRP. The addition of different concentrations of C1qA08 antibody, as shown by the graph could inhibit the binding of mCRP to C1q, and when 80 μg/ml anti-C1qA08 antibody was added, the inhibition rate exceeded 50%.

could be fixed. We then used the monoclonal antibody of A08 to further inhibit the binding of C1q and mCRP, which turned out that A08 was the main binding site of C1q and mCRP.

We used an A08-specific antibody 17-9 mAb inhibition assay to demonstrate that A08 was a key epitope for C1q binding to mCRP. The results showed that 17-9 mAb could significantly inhibit the binding of both, so A08 was the key epitope. The complement system exerted an important role in the clearance of immune complexes in different tissues, and it was an important pathogenesis involved in LN that the dysfunction for the clearance of immune complexes and apoptotic cells. The result from C3 deposition showed that mCRP and a.a.35-47 could inhibit the activation of complement classical pathway through binding to C1q, which might interfere with the clearance of immune complex or apoptotic cells afterwards.

The main limitation of the current study was that there was no antibody to a.a.35-47 and therefore no direct inhibition assays for binding of a.a.35-47 and C1q were performed. More work needs to be done to clarify the associations of mCRP and C1q in the pathogenesis of LN.

In conclusion, a combination of anti-C1qA08 and anti-mCRP a.a.35-47 antibodies could better predict the prognosis of LN. The key linear epitopes of the combination of C1q and mCRP were a.a.35-47

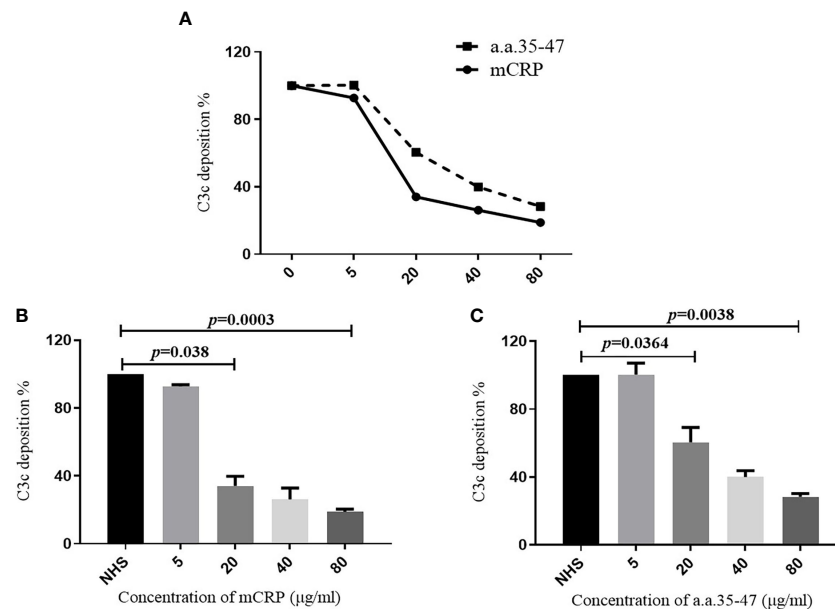


FIGURE 6

Detection of C3c deposition. To assess whether mCRP and a.a.35-47 can affect the ability of C1q to activate the classical pathway of complement. (A) Adding different concentrations of mCRP, a.a.35-47, C3c deposition decreases as the concentration increases. (B) Different concentrations of mCRP were added. As the concentration of C3c decreased, the complement was inhibited. When the concentration of mCRP reached 20 μg/ml, it could be inhibited to 30%. (C) When different concentrations of a.a.35-47 peptide were added, C3c deposition decreased with increasing concentration, and complement was inhibited. When the concentration of a.a.35-47 reached 80 μg/ml, it could be inhibited to 30%. Therefore, mCRP and a.a.35-47 in the liquid phase could inhibit complement activation.

and C1qA08. A08 was an important epitope for the classical pathway complement activation and a.a.35-47 could inhibit this process.

Foundation of China (No. 82000666), and the CAMS Innovation Fund for Medical Sciences (2019-I2M-5-046).

## Data availability statement

The original contributions presented in the study are included in the article/Supplementary Material. Further inquiries can be directed to the corresponding author.

## Ethics statement

The studies involving human participants were reviewed and approved by Renal Division, Peking University First Hospital, Beijing, China. The patients/participants provided their written informed consent to participate in this study.

## Author contributions

Writing—original draft: XL. Review and editing: YT and SJ. All authors have read and agreed to the published version of the manuscript. All authors contributed to the article and approved the submitted version.

## Funding

This work was supported by grants from the Beijing Natural Science Foundation (No. 7192207), the National Natural Science

## Conflict of interest

The authors declare that the research was conducted in the absence of any commercial or financial relationships that could be construed as a potential conflict of interest.

## Publisher's note

All claims expressed in this article are solely those of the authors and do not necessarily represent those of their affiliated organizations, or those of the publisher, the editors and the reviewers. Any product that may be evaluated in this article, or claim that may be made by its manufacturer, is not guaranteed or endorsed by the publisher.

## Supplementary material

The Supplementary Material for this article can be found online at: <https://www.frontiersin.org/articles/10.3389/fimmu.2023.1181561/full#supplementary-material>

### SUPPLEMENTARY FIGURE 1

The correlation analysis of levels of anti-C1qA08 antibodies and anti-mCRP a.a.35-47 antibodies.

## References

- Cervera R, Khamashta MA, Font J, Sebastiani GD, Gil A, Lavilla P, et al. Morbidity and mortality in systemic lupus erythematosus during a 10-year period: a comparison of early and late manifestations in a cohort of 1,000 patients. *Medicine* (2003) 82(5):299–308. doi: 10.1097/01.md.0000091181.93122.55
- Swaak T, Smeenk R. Clinical significance of antibodies to double stranded DNA (dsDNA) for systemic lupus erythematosus (SLE). *Clin Rheumatol* (1987) 6 Suppl 1:56–73. doi: 10.1007/BF02200721
- Okamura M, Kanayama Y, Amastu K, Negoro N, Kohda S, Takeda T, et al. Significance of enzyme linked immunosorbent assay (ELISA) for antibodies to double stranded and single stranded DNA in patients with lupus nephritis: correlation with severity of renal histology. *Ann Rheum Dis* (1993) 52(1):14–20. doi: 10.1136/ard.52.1.14
- Linnik MD, Hu JZ, Heilbrunn KR, Strand V, Hurley FL, Joh T, et al. Relationship between anti-double-stranded DNA antibodies and exacerbation of renal disease in patients with systemic lupus erythematosus. *Arthritis Rheum* (2005) 52(4):1129–37. doi: 10.1002/art.20980
- Sinico RA, Radice A, Ikehata M, Giammarresi G, Corace C, Arrigo G, et al. Anti-C1q autoantibodies in lupus nephritis: prevalence and clinical significance. *Ann N Y Acad Sci* (2005) 1050:193–200. doi: 10.1196/annals.1313.020
- Marto N, Bertolaccini ML, Calabuig E, Hughes GR, and Khamashta MA. Anti-C1q antibodies in nephritis: correlation between titres and renal disease activity and positive predictive value in systemic lupus erythematosus. *Ann Rheum Dis* (2005) 64(3):444–8. doi: 10.1136/ard.2004.024943
- Fang QY, Yu F, Tan Y, Xu LX, Wu LH, Liu G, et al. Anti-C1q antibodies and IgG subclass distribution in sera from Chinese patients with lupus nephritis. *Nephrol Dial Transplant* (2009) 24(1):172–8. doi: 10.1093/ndt/gfn453
- Trendelenburg M, Lopez-Trascasa M, Potlukova E, Moll S, Regenass S, Fremeaux-Bacchi V, et al. High prevalence of anti-C1q antibodies in biopsy-proven active lupus nephritis. *Nephrol Dial Transplant* (2006) 21(11):3115–21. doi: 10.1093/ndt/gfl436
- Tan Y, Yu F, Yang H, Chen M, Fang Q, Zhao MH. Autoantibodies against monomeric c-reactive protein in sera from patients with lupus nephritis are associated with disease activity and renal tubulointerstitial lesions. *Hum Immunol* (2008) 69(12):840–4. doi: 10.1016/j.humimm.2008.09.006
- Sjowall C, Zickert A, Skogh T, Wettero J, Gunnarsson I. Serum levels of autoantibodies against c-reactive protein correlate with renal disease activity and response to therapy in lupus nephritis. *Arthritis Res Ther* (2009) 11(6):R188. doi: 10.1186/ar2880
- Nayak A, Pednekar L, Reid KB, Kishore U. Complement and non-complement activating functions of C1q: a prototypal innate immune molecule. *Innate Immun* (2012) 18(2):350–63. doi: 10.1177/1753425910396252
- Nauta AJ, Daha MR, van Kooten C, Roos A. Recognition and clearance of apoptotic cells: a role for complement and pentraxins. *Trends Immunol* (2003) 24(3):148–54. doi: 10.1016/S1471-4906(03)00030-9
- Brenicova E, Diebold SS. Nucleic acids and endosomal pattern recognition: how to tell friend from foe? *Front Cell Infect Microbiol* (2013) 3:37. doi: 10.3389/fcimb.2013.00037
- Schumaker VN, Hanson DC, Kilchherr E, Phillips ML, Poon PH. A molecular mechanism for the activation of the first component of complement by immune complexes. *Mol Immunol* (1986) 23(5):557–65. doi: 10.1016/0161-5890(86)90119-7
- Korb LC, Ahearn JM. C1q binds directly and specifically to surface blebs of apoptotic human keratinocytes: complement deficiency and systemic lupus erythematosus revisited. *J Immunol* (1997) 158(10):4525–8. doi: 10.4049/jimmunol.158.10.4525
- Vanhecke D, Roumenina LT, Wan H, Osthoff M, Schaller M. Identification of a major linear C1q epitope allows detection of systemic lupus erythematosus anti-C1q antibodies by a specific peptide-based enzyme-linked immunosorbent assay. *Arthritis Rheum* (2012) 64(11):3706–14. doi: 10.1002/art.34605
- Pang Y, Tan Y, Li Y, Zhang J, Guo Y, Guo Z, et al. Serum A08 C1q antibodies are associated with disease activity and prognosis in Chinese patients with lupus nephritis. *Kidney Int* (2016) 90(6):1357–67. doi: 10.1016/j.kint.2016.08.010
- James LP, Lamps LW, McCullough S, Hinson JA. Interleukin 6 and hepatocyte regeneration in acetaminophen toxicity in the mouse. *Biochem Biophys Res Commun* (2003) 309(4):857–63. doi: 10.1016/j.bbrc.2003.08.085
- Biro A, Rovo Z, Papp D, Cervenak L, Varga L, Fust G, et al. Studies on the interactions between c-reactive protein and complement proteins. *Immunology* (2007) 121(1):40–50. doi: 10.1111/j.1365-2567.2007.02535.x
- Potempa LA, Siegel JN, Fiedel BA, Potempa RT, Gewurz H. Expression, detection and assay of a neoantigen (Neo-CRP) associated with a free, human c-reactive protein subunit. *Mol Immunol* (1987) 24(5):531–41. doi: 10.1016/0161-5890(87)90028-9
- Ji SR, Wu Y, Zhu L, Potempa LA, Sheng FL, Lu W, et al. Cell membranes and liposomes dissociate c-reactive protein (CRP) to form a new, biologically active structural intermediate: mCRP(m). *FASEB J* (2007) 21(1):284–94. doi: 10.1096/fj.06-6722com
- Ji SR, Zhang SH, Chang Y, Li HY, Wang MY, Lv JM, et al. C-reactive protein: The most familiar stranger. *J Immunol* (2023) 210(6):699–707. doi: 10.4049/jimmunol.2200831
- Ibraheem MR, Daniel M, Margaret EO, Jenna MBA, Mihee LC, Matthew SN, et al. C-reactive protein in gallbladder diseases: diagnostic and therapeutic insights. *Biophysics Rep* (2020) 6(2-3):49–67. doi: 10.1007/s41048-020-00108-9
- Becker GJ, Waldburger M, Hughes GR, Pepys MB. Value of serum c-reactive protein measurement in the investigation of fever in systemic lupus erythematosus. *Ann Rheum Dis* (1980) 39(1):50–2. doi: 10.1136/ard.39.1.50
- Honig S, Gorevic P, Weissmann G. C-reactive protein in systemic lupus erythematosus. *Arthritis Rheum* (1977) 20(5):1065–70. doi: 10.1002/art.1780200505
- Pesickova SS, Rysava R, Lenicek M, Vitek L, Potlukova E, Hruskova Z, et al. Prognostic value of anti-CRP antibodies in lupus nephritis in long-term follow-up. *Arthritis Res Ther* (2015) 17:371. doi: 10.1186/s13075-015-0879-8
- Li QY, Li HY, Fu G, Yu F, Wu Y, Zhao MH. Autoantibodies against c-reactive protein influence complement activation and clinical course in lupus nephritis. *J Am Soc Nephrol* (2017) 28(10):3044–54. doi: 10.1681/ASN.2016070735
- Hochberg MC. Updating the American college of rheumatology revised criteria for the classification of systemic lupus erythematosus. *Arthritis Rheum* (1997) 40(9):1725. doi: 10.1002/art.1780400928
- Bombardier C, Gladman DD, Urowitz MB, Caron D, Chang CH. Derivation of the SLEDAI. a disease activity index for lupus patients. the committee on prognosis studies in SLE. *Arthritis Rheum* (1992) 35(6):630–40. doi: 10.1002/art.1780350606
- Liang MH, Socher SA, Larson MG, Schur PH. Reliability and validity of six systems for the clinical assessment of disease activity in systemic lupus erythematosus. *Arthritis Rheum* (1989) 32(9):1107–18. doi: 10.1002/anr.1780320909
- Austin HA 3rd, Boumpas DT, Vaughan EM, Balow JE. Predicting renal outcomes in severe lupus nephritis: contributions of clinical and histologic data. *Kidney Int* (1994) 45(2):544–50. doi: 10.1038/ki.1994.70
- Austin HA 3rd, Muenz LR, Joyce KM, Antonovych TT, Balow JE. Diffuse proliferative lupus nephritis: identification of specific pathologic features affecting renal outcome. *Kidney Int* (1984) 25(4):689–95. doi: 10.1038/ki.1984.75
- Roumenina LT, Radanova M, Atanasov BP, Popov KT, Kaveri SV, Lacroix-Desmazes S, et al. Heme interacts with c1q and inhibits the classical complement pathway. *J Biol Chem* (2011) 286(18):16459–69. doi: 10.1074/jbc.M110.206136
- Zhao J, Cui Z, Yang R, Jia XY, Zhang Y, Zhao MH. Anti-glomerular basement membrane autoantibodies against different target antigens are associated with disease severity. *Kidney Int* (2009) 76(10):1108–15. doi: 10.1038/ki.2009.348
- Maningding E, Dall'Era M, Trupin L, Murphy LB, Yazdany J. Racial and ethnic differences in the prevalence and time to onset of manifestations of systemic lupus erythematosus: The California lupus surveillance project. *Arthritis Care Res* (2020) 72(5):622–9. doi: 10.1002/acr.23887
- Hernandez Cruz B, Alonso F, Calvo Alen J, Pego-Reigosa JM, Lopez-Longo FJ, Galindo-Izquierdo M, et al. Differences in clinical manifestations and increased severity of systemic lupus erythematosus between two groups of hispanics: European caucasians versus Latin American mestizos (data from the RELESSER registry). *Lupus* (2020) 29(1):27–36. doi: 10.1177/0961203319889667
- Bao L, Cunningham PN, Quigg RJ. Complement in lupus nephritis: New perspectives. *Kidney Dis* (2015) 1(2):91–9. doi: 10.1159/000431278
- Mizuno M, Suzuki Y, Ito Y. Complement regulation and kidney diseases: recent knowledge of the double-edged roles of complement activation in nephrology. *Clin Exp Nephrol* (2018) 22(1):3–14. doi: 10.1007/s10157-017-1405-x
- Sjowall C, Olin AI, Skogh T, Wettero J, Morgelin M, Nived O, et al. C-reactive protein, immunoglobulin G and complement co-localize in renal immune deposits of proliferative lupus nephritis. *Autoimmunity* (2013) 46(3):205–14. doi: 10.3109/08916934.2013.764992



## OPEN ACCESS

## EDITED BY

Alok Agrawal,  
East Tennessee State University,  
United States

## REVIEWED BY

Valentino Racki,  
University of Rijeka, Croatia

## \*CORRESPONDENCE

Niyati Mehta

✉ niyati.mehta@northwestern.edu

RECEIVED 02 March 2023

ACCEPTED 02 May 2023

PUBLISHED 12 May 2023

## CITATION

Mehta N, Luthra NS, Corcos DM and  
Fantuzzi G (2023) C-reactive protein  
as the biomarker of choice to  
monitor the effects of exercise on  
inflammation in Parkinson's disease.  
*Front. Immunol.* 14:1178448.  
doi: 10.3389/fimmu.2023.1178448

## COPYRIGHT

© 2023 Mehta, Luthra, Corcos and Fantuzzi.  
This is an open-access article distributed  
under the terms of the [Creative Commons  
Attribution License \(CC BY\)](#). The use,  
distribution or reproduction in other  
forums is permitted, provided the original  
author(s) and the copyright owner(s) are  
credited and that the original publication in  
this journal is cited, in accordance with  
accepted academic practice. No use,  
distribution or reproduction is permitted  
which does not comply with these terms.

# C-reactive protein as the biomarker of choice to monitor the effects of exercise on inflammation in Parkinson's disease

Niyati Mehta<sup>1\*</sup>, Nijee S. Luthra<sup>2</sup>, Daniel M. Corcos<sup>1</sup>  
and Giamila Fantuzzi<sup>3</sup>

<sup>1</sup>Department of Physical Therapy and Human Movement Sciences, Northwestern University, Chicago, IL, United States, <sup>2</sup>Movement Disorder and Neuromodulation Center, University of California, San Francisco, San Francisco, CA, United States, <sup>3</sup>Department of Kinesiology and Nutrition, College of Applied Health Science, University of Illinois at Chicago, Chicago, IL, United States

Parkinson's disease (PD), a heterogeneous disease with no disease-modifying treatments available, is the fastest growing neurological disease worldwide. Currently, physical exercise is the most promising treatment to slow disease progression, with evidence suggesting it is neuroprotective in animal models. The onset, progression, and symptom severity of PD are associated with low grade, chronic inflammation which can be quantified by measuring inflammatory biomarkers. In this perspective, we argue that C-reactive protein (CRP) should be used as the primary biomarker for monitoring inflammation and therefore disease progression and severity, particularly in studies examining the impact of an intervention on the signs and symptoms of PD. CRP is the most studied biomarker of inflammation, and it can be detected using relatively well-standardized assays with a wide range of detection, allowing for comparability across studies while generating robust data. An additional advantage of CRP is its ability to detect inflammation irrespective of its origin and specific pathways, an advantageous characteristic when the cause of inflammation remains unknown, such as PD and other chronic, heterogeneous diseases.

## KEYWORDS

C-reactive protein, Parkinson's disease, inflammation, exercise, biomarker

## Introduction

Physical exercise is a promising treatment to slow disease progression in various chronic, complex, heterogeneous diseases that share an inflammatory component, such as metabolic syndromes, type II diabetes, multiple sclerosis, Parkinson's Disease (PD) and many others. Several ongoing intervention studies are assessing the effectiveness of multiple

exercise modalities and intensities on disease progression (1–4). In this perspective, we will focus on PD.

PD is the fastest growing neurological disease worldwide and has no disease-modifying treatments. Despite the heterogeneity of its signs and symptoms, treatment of PD relies largely on dopaminergic medications to alleviate motor symptoms. However, over time, the effectiveness of these medications is challenged by continued disease progression and a rise in adverse effects (5, 6). A growing body of evidence supports the beneficial role of exercise in PD. In animal models of PD, exercise is neuroprotective (7) while in humans multiple exercise modalities reduce signs and symptoms of PD (8–10). However, the mechanisms by which exercise provides benefits in PD—as in many other diseases—remain unclear. Inflammation is an emerging component of PD pathogenesis that can be a target for neuroprotection and disease modification (11). Indeed, at least one study reports that chronic use of nonsteroidal anti-inflammatory drugs reduces the risk of PD by about 45%, suggesting that inflammation may play a pathogenic role in PD (12).

Several biomarkers, both individually and as multi-molecular panels, can be used to determine the presence of and quantify the severity of inflammation. Of these, the acute-phase protein C-reactive protein (CRP) is the most studied (13). Here, we elaborate on the reasons for selecting CRP as the biomarker of choice to monitor inflammation in response to exercise in PD and in studies examining the effect of exercise in other diseases with an inflammatory component (14).

## C-reactive protein

Circulating levels of CRP increase rapidly during the acute-phase response, which can be initiated by infection, inflammation, or trauma (15). Inflammatory mediators such as the cytokine IL-6 induce transcription and translation of the CRP gene in hepatocytes (16), with other mediators and cell types also contributing to the rise in circulating levels of CRP (17–19). The biology and regulation of production of CRP have been extensively reviewed and we refer the reader to this vast literature for details (16, 20–24).

The designation of CRP as an acute-phase protein is misleading because levels of CRP (and of other positive acute-phase proteins) increase in virtually all conditions characterized by inflammation, irrespective of whether the course is acute or chronic. In response to an acute infection, CRP levels in peripheral blood can reach concentrations >1 g/L, i.e., thousands of folds up from the ≤1 mg/L observed in non-infected individuals (21). However, CRP levels increase more modestly, yet significantly and consistently, in a wide range of chronic, non-infectious conditions, such as cardiovascular disease (CVD), accelerated vascular aging, autoimmune diseases, obesity, Type 2 Diabetes, Alzheimer's disease, and PD (14, 20, 25). In these conditions, CRP levels rarely reach the peak observed during acute infections, largely staying below 10 mg/L, but they signal the presence of low grade, chronic inflammation (26). Inflammaging, the presence of low-level chronic inflammation in older adults, is also associated with a modest but consistent elevation in CRP (27).

## CRP in Parkinson's Disease

Plasma and cerebrospinal fluid (CSF) CRP levels are associated with PD risk, prognosis, and symptom severity. A meta-analysis of 23 studies shows that individuals with PD have significantly higher CRP levels both in the peripheral circulation and in the CSF compared with matched healthy controls (13), indicating that either inflammation is a risk factor for PD or that PD leads to inflammation, and possibly both. Newly diagnosed PD patients have higher systemic CRP levels than people without PD, suggesting that inflammation is already present in the early stages of disease (28). Additionally, across the time course of the disease, patients with PD exhibit higher systemic and CSF CRP levels compared to healthy controls (13) and, independent of disease duration or symptom severity, baseline CRP levels in patients with PD are associated with risk of death and predicted life prognosis (29). CRP levels are also related to PD disease stage, as patients with higher Hoehn & Yahr scores, and therefore more severe motor symptoms, exhibit higher levels of systemic CRP (30, 31). One study found that CSF CRP concentrations correlate with motor symptom severity, measured using the Movement Disorders Society Unified Parkinson's Disease Rating Scale (MDS-UPDRS) motor examination score (Part III), in male PD patients and with measures of cognitive performance in female patients, suggesting a possible sex dimorphism in CRP as a marker of inflammation in PD and/or in the pathogenic mechanisms of motor versus non-motor symptoms (32). Moreover, CSF CRP levels are higher in patients with PD-related dementia as compared to PD patients without dementia (33) and are also associated with severity of depression, anxiety, and fatigue in PD (33). Thus, despite the heterogeneous nature of PD, CRP—and therefore inflammation—is associated with many of its manifestations in terms of risk, progression, and symptom severity.

## CRP: marker or maker?

There are many ways in which CRP may directly contribute to disease pathogenesis in PD, given its known role in the clearance of necrotic material, recruitment of the complement system, and more (34). However, epidemiological studies indicate that CRP is unlikely to play a major direct role in the pathogenesis of PD, similarly to what has been demonstrated in CVD. Genetic variants in the promoter of the CRP gene that modulate circulating levels of CRP have helped clarify the role of CRP in the pathogenesis of CVD. While elevated levels of CRP consistently predict adverse cardiovascular events, epidemiological studies demonstrated a lack of association between CRP genetic variants and CVD (30). That is, high CRP due to genetic variants without underlying inflammation does not increase the risk of CVD by itself, demonstrating that it is the underlying inflammation that contributes to disease risk, not CRP itself. Similarly, in PD, a large Genome-Wide Association Study failed to identify an association between CRP genetic variants and increased risk of PD (35). These studies indicate that while CRP predicts disease risk and progression, its participation in disease



pathogenesis is questionable, at best. Thus, in PD, we should consider CRP as a marker rather than a maker, i.e., as a biomarker that detects the presence of inflammation and quantifies its severity rather than as a direct participant in disease pathogenesis.

## CRP and physical exercise

In clinical studies, CRP is well established as a biomarker to monitor the effects of exercise on inflammation. Indeed, more than 400 randomized controlled trials in various populations and at least 80 systematic reviews or meta-analyses have evaluated the effect of different modalities and intensities of exercise on CRP levels. While there may be a short-lived increase in CRP levels after each exercise bout, since exercise can be an acute stressor, most studies indicate that over time physical exercise lowers CRP levels (7, 36), with aerobic exercise being the most beneficial, especially in older adults (36). Evidence suggests that physical exercise reduces CRP levels following a dose-response relationship, with higher intensity exercise causing a greater reduction in CRP over time compared to lower intensity exercise, and with longer interventions being more efficacious than those of shorter duration (37). Although no studies have yet examined the effect of exercise on CRP levels in PD, exercise, particularly aerobic interventions, counteract the increase in CRP that accompanies aging (27, 38). This is relevant to PD, as age is its primary risk factor (39–41), and can be described as a pre-PD state (39). Furthermore, exercise is a critical component in the prevention and management on Type 2 Diabetes, a condition that is associated with more severe symptoms and accelerated progression of PD and that shares inflammation as a pathogenic mechanism (14).

## Discussion

There are several ongoing trials examining the effects of exercise interventions on PD (2, 4), including the Study in Parkinson's disease of exercise phase 3 (SPARX3). SPARX3 is a Phase 3, multisite, randomized, two-arm (1:1 allocation), parallel group, evaluator-blinded, clinical trial to test the superiority hypothesis that high-intensity, endurance treadmill exercise slows the progression of the signs of PD compared to moderate-intensity endurance treadmill exercise (4). A change in the MDS-UPDRS Part III score is the primary outcome. Several biomarkers serve as secondary outcomes that might point to the mechanisms underlying the effects of exercise intensity in PD, including a potential reduction in inflammation (42).

In SPARX3, we could have chosen a variety of biomarkers to monitor inflammation in response to endurance exercise. Indeed, we plan to explore levels of cytokines and several other mediators in participants' systemic circulation. However, several reasons led us to select CRP as the sole inflammation-related pre-specified outcome.

The fact that CRP is by far the most studied biomarker of inflammation, both in exercise and in PD as well as in many other diseases, will permit comparison between the findings of SPARX3 and those of hundreds of other studies. Moreover, compared to

other mediators, CRP allows for better comparability across studies due to the higher standardization of the CRP assay compared to that of most cytokines and many other inflammatory mediators. Moreover, unlike most cytokines, levels of CRP can be reliably quantified even in the absence of inflammation, thus avoiding the clustering of values at the lower edge of the sensitivity curve that plagues most cytokine assays.

Lastly, and perhaps most importantly, CRP is nonspecific, meaning that it can detect the presence of inflammation, and quantify its changes, irrespective of the ultimate origin of the inflammatory response and of the mechanisms at play. This characteristic of CRP is very useful in PD, in which the cause and pathways of inflammation have not been identified. Similarly, because the mechanisms by which exercise reduces inflammation are also unidentified thus far, the lack of specificity of CRP becomes an asset. Studies that aim to investigate the location, triggers, and pathways of inflammation in PD, and the mechanisms by which exercise reduces inflammation, must quantify specific markers, such as individual cytokines. However, if the aim of a study is to determine whether inflammation is present and/or whether its severity can be altered through an intervention—as is the case in SPARX3—a nonspecific marker such as CRP is more appropriate, as its modulation is independent of the origin and characteristics of the inflammatory response. Thus, nonspecific is not always a dirty word, particularly when it comes to the interplay of PD, exercise, and inflammation. If SPARX3 demonstrates that endurance exercise is associated with reduced levels of CRP, as is our hypothesis, studies evaluating the mechanisms underlying this effect will be warranted.

For all the reasons outlined above, CRP should be utilized as the biomarker of choice for evaluating the response to exercise interventions in PD and other neurodegenerative diseases and chronic conditions. However, like any biomarker, there are limitations in the utility of CRP. First, CRP is sensitive to any form of inflammation, meaning that inflammation unrelated to PD, such as an infection, will increase CRP levels. This, however, is a challenge of nearly all inflammatory biomarkers, and not unique to CRP. Also, CRP levels are affected by genetics, and this will influence CRP levels irrespective of disease severity and exercise effectiveness. However, this can be overcome by averaging CRP levels across subjects to reduce the effect of genetic variations on CRP levels and/or by utilizing intra-subject longitudinal comparisons. Despite these limitations, we argue that CRP is the most effective biomarker for monitoring the effects of exercise interventions on the level of inflammation in PD and other conditions.

## Conclusion

Researchers investigating the effects of physical exercise in PD and many other diseases are faced with lack of knowledge about the specific pathways in which inflammation is implicated both in disease pathogenesis and in the beneficial effects of the intervention. Here we argued that the current situation should not hamper progress in the field, that evaluating the effectiveness of exercise in PD and other conditions does not need to wait for mechanistic studies to elucidate such pathways. Indeed, choosing

CRP as the biomarker of choice to monitor the state of inflammation during an intervention overcomes many of the limitations of current knowledge.

## Data availability statement

The original contributions presented in the study are included in the article/supplementary material. Further inquiries can be directed to the corresponding author.

## Author contributions

NM – execution, writing, and editing of the final version of the manuscript. NL – writing and editing of the final version of the manuscript. DC – writing and editing of the final version of the manuscript. GF – execution, writing, and editing of the final version of the manuscript. All authors contributed to the article and approved the submitted version.

## References

1. Corporation OHIR. *Exercise training in patients with persistent or permanent atrial fibrillation* (2019). Available at: <https://ClinicalTrials.gov/show/NCT03397602>.
2. Hospital SJs and Medical Center P. *Exercise in advanced parkinson's disease (PD) with deep brain stimulation (DBS)* (2022). Available at: <https://ClinicalTrials.gov/show/NCT05204680>.
3. University IM. *Comparison of the effects of green exercise programs on metabolic syndrome parameters in elderly individuals* (2022). Available at: <https://ClinicalTrials.gov/show/NCT05251597>.
4. University N, Pittsburgh Uo and Group TPS. *Study in Parkinson disease of exercise* (2021). Available at: <https://ClinicalTrials.gov/show/NCT04284436>.
5. Bartus RT, Emerich D, Snodgrass-Belt P, Fu K, Salzberg-Brenhouse H, Lafreniere D, et al. A pulmonary formulation of l-dopa enhances its effectiveness in a rat model of parkinson's disease. *J Pharmacol Exp Ther* (2004) 310(2):828–35. doi: 10.1124/jpet.103.064121
6. Connolly BS, Lang AE. Pharmacological treatment of Parkinson disease: a review. *JAMA* (2014) 311(16):1670–83. doi: 10.1001/jama.2014.3654
7. da Costa Daniele TM, de Bruin PFC, de Matos RS, de Bruin GS, Maia Chaves CJ, de Bruin VMS. Exercise effects on brain and behavior in healthy mice, alzheimer's disease and parkinson's disease model-a systematic review and meta-analysis. *Behav Brain Res* (2020) 383:112488. doi: 10.1016/j.bbr.2020.112488
8. Gamborg M, Hvid LG, Dalgas U, Langeskov-Christensen M. Parkinson's disease and intensive exercise therapy - an updated systematic review and meta-analysis. *Acta Neurol Scand* (2022) 145(5):504–28. doi: 10.1111/ane.13579
9. Gollan R, Ernst M, Lieker E, Caro-Valenzuela J, Monsef I, Dresen A, et al. Effects of resistance training on motor- and non-motor symptoms in patients with parkinson's disease: a systematic review and meta-analysis. *J Parkinsons Dis* (2022) 12(6):1783–806. doi: 10.3233/JPD-223252
10. Schenkman M, Moore CG, Kohrt WM, Hall DA, Delitto CA, Cornella CL, et al. Effect of high-intensity treadmill exercise on motor symptoms in patients with *De novo* Parkinson disease a phase 2 randomized clinical trial. *JAMA Neurol* (2017) 75(2):219–26. doi: 10.1186/s13063-022-06703-0
11. Hirsch EC, Vyas S, Hunot S. Neuroinflammation in parkinson's disease. *Parkinsonism Relat Disord* (2012) 18 Suppl 1:S210–2. doi: 10.1016/S1353-8020(11)70065-7
12. Chen H, Zhang S, Hernán MA, Schwarzschild MA, Willett WC, Colditz GA, et al. Nonsteroidal anti-inflammatory drugs and the risk of Parkinson disease. *Arch Neurol*. (2003) 60:1059–64. doi: 10.1001/archneur.60.8.1059
13. Qiu X, Xiao Y, Wu J, Gan L, Huang Y, Wang J. C-reactive protein and risk of parkinson's disease: a systematic review and meta-analysis. *Front Neurol* (2019) 10:384. doi: 10.3389/fneur.2019.00384
14. Cullinane PW, de Pablo Fernandez E, König A, Outeiro TF, Jaunmuktane Z, Warner TT. Type 2 diabetes and parkinson's disease: a focused review of current concepts. *Mov Disord* (2022) 2:162–77. doi: 10.1002/mds.29298
15. Black S, Kushner I, Samols D. C-reactive protein. *J Biol Chem* (2004) 279 (47):48487–90. doi: 10.1074/jbc.R400025200
16. Volanakis JE. Human c-reactive protein: expression, structure, and function. *Mol Immunol* (2001) 38(2-3):189–97. doi: 10.1016/S0161-5890(01)00042-6
17. Agrawal A, Cha-Molstad H, Samols D, Kushner I. Overexpressed nuclear factor-kappaB can participate in endogenous c-reactive protein induction, and enhances the effects of C/EBPbeta and signal transducer and activator of transcription-3. *Immunology* (2003) 108(4):539–47. doi: 10.1046/j.1365-2567.2003.01608.x
18. Ganapathi MK, Rzewnicki D, Samols D, Jiang SL, Kushner I. Effect of combinations of cytokines and hormones on synthesis of serum amyloid A and c-reactive protein in hep 3B cells. *J Immunol* (1991) 147(4):1261–5. doi: 10.4049/jimmunol.147.4.1261
19. Ramadori G, Sipe JD, Dinarello CA, Mizel SB, Colten HR. Pretranslational modulation of acute phase hepatic protein synthesis by murine recombinant interleukin 1 (IL-1) and purified human IL-1. *J Exp Med* (1985) 162(3):930–42. doi: 10.1084/jem.162.3.930
20. Banait T, Wanjari A, Danade V, Banait S, Jain J. Role of high-sensitivity c-reactive protein (Hs-CRP) in non-communicable diseases: a review. *Cureus* (2022) 14 (10):e30225. doi: 10.7759/cureus.30225
21. Suffredini AF, Fantuzzi G, Badolato R, Oppenheim JJ, O'Grady NP. New insights into the biology of the acute phase response. *J Clin Immunol* (1999) 19 (4):203–14. doi: 10.1023/A:1020563913045
22. Du Clos TW. Function of c-reactive protein. *Ann Med* (2009) 32:274–8. doi: 10.3109/07853890009011772
23. Marnell L, Mold C, Du Clos TW. C-reactive protein: ligands, receptors and role in inflammation. *Clin Immunol* (2005) 117(2):104–11. doi: 10.1016/j.clim.2005.08.004
24. Szalai AJ, van Ginkel FW, Wang Y, McGhee JR, Volanakis JE. Complement-dependent acute-phase expression of c-reactive protein and serum amyloid p-component. *J Immunol* (2000) 165(2):1030–5. doi: 10.4049/jimmunol.165.2.1030
25. Babcock MC, DuBose LE, Witten TL, Stauffer BL, Hildreth KL, Schwartz RS, et al. Oxidative stress and inflammation are associated with age-related endothelial dysfunction in men with low testosterone. *J Clin Endocrinol Metab* (2022) 107(2):e500–e14. doi: 10.1210/clinem/dgab715
26. Eklund CM. Proinflammatory cytokines in CRP baseline regulation. *Adv Clin Chem* (2009) 48:111–36. doi: 10.1016/S0065-2423(09)48005-3
27. Bautmans I, Salimans L, Njemini R, Beyer I, Lieten S, Liberman K. The effects of exercise interventions on the inflammatory profile of older adults: a systematic review of the recent literature. *Exp Gerontol*. (2021) 146:111236. doi: 10.1016/j.exger.2021.111236
28. Song IU, Chung SW, Kim JS, Lee KS. Association between high-sensitivity c-reactive protein and risk of early idiopathic parkinson's disease. *Neurological Sci* (2011) 32:31–4. doi: 10.1007/s10072-010-0335-0

## Funding

Author NL – Recipient of grant funding through K23NS123506.  
Author DC – Recipient of grant funding through U01NS113851.

## Conflict of interest

The authors declare that the research was conducted in the absence of any commercial or financial relationships that could be construed as a potential conflict of interest.

## Publisher's note

All claims expressed in this article are solely those of the authors and do not necessarily represent those of their affiliated organizations, or those of the publisher, the editors and the reviewers. Any product that may be evaluated in this article, or claim that may be made by its manufacturer, is not guaranteed or endorsed by the publisher.

29. Sawada H, Oeda T, Umemura A, Tomita S, Kohsaka M, Park K, et al. Baseline c-reactive protein levels and life prognosis in Parkinson disease. *PloS One* (2015) 10(7): e0134118. doi: 10.1371/journal.pone.0134118
30. Luan YY, Yao YM. The clinical significance and potential role of c-reactive protein in chronic inflammatory and neurodegenerative diseases. *Front Immunol* (2018) 9:1302. doi: 10.3389/fimmu.2018.01302
31. Andican G, Konukoglu D, Bozluolcay M, Bayulkem K, Firtiina S, Burcak G. Plasma oxidative and inflammatory markers in patients with idiopathic parkinson's disease. *Acta Neurol Belg.* (2012) 112(2):155–9. doi: 10.1007/s13760-012-0015-3
32. Moghaddam HS, Valitabar Z, Ashraf-Ganjouei A, Zadeh MM, Sherbaf FG, Aarabi MH. Cerebrospinal fluid c-reactive protein in parkinson's disease: associations with motor and non-motor symptoms. *NeuroMolecular Med* (2018) 20:376–85. doi: 10.1007/s12017-018-8499-5
33. Lindqvist D, Hall S, Surova Y, Nielsen HM, Janelidze S, Brundin L, et al. Cerebrospinal fluid inflammatory markers in parkinson's disease—associations with depression, fatigue, and cognitive impairment. *Brain Behav Immun* (2013) 33:183–9. doi: 10.1016/j.bbi.2013.07.007
34. Michigan A, Johnson TV, Master VA. Review of the relationship between c-reactive protein and exercise. *Mol Diagn Ther* (2011) 15(5):265–75. doi: 10.1007/BF03256418
35. Nalls MA, Pankratz N, Lill CM, Do CB, Hernandez DG, Saad M, et al. Large-Scale meta-analysis of genome-wide association data identifies six new risk loci for parkinson's disease. *Nat Genet* (2014) 46(9):989–93. doi: 10.1038/ng.3043
36. Kohut ML, McCann DA, Russell DW, Konopka DN, Cunnick JE, Franke WD, et al. Aerobic exercise, but not flexibility/resistance exercise, reduces serum IL-18, CRP, and IL-6 independent of beta-blockers, BMI, and psychosocial factors in older adults. *Brain Behav Immun* (2006) 20(3):201–9. doi: 10.1016/j.bbi.2005.12.002
37. Rose GL, Skinner TL, Mielke GI, Schaumborg MA. The effect of exercise intensity on chronic inflammation: a systematic review and meta-analysis. *J Sci Med Sport.* (2021) 24(4):345–51. doi: 10.1016/j.jsams.2020.10.004
38. Khalafi M, Malandish A, Rosenkranz SK. The impact of exercise training on inflammatory markers in postmenopausal women: a systemic review and meta-analysis. *Exp Gerontology.* (2021) 150. doi: 10.1016/j.exger.2021.111398
39. Collier TJ, Kanaan NM, Kordower JH. Aging and parkinson's disease: different sides of the same coin? *Mov Disord* (2017) 32(7):983–90. doi: 10.1002/mds.27037
40. Bennett DA, Beckett LA, Murray AM, Shannon KM, Goetz CG, Pilgrim DM, et al. Prevalence of parkinsonian signs and associated mortality in a community population of older people. *N Engl J Med* (1996) 334(2):71–6. doi: 10.1056/NEJM199601113340202
41. Tysnes OB, Storstein A. Epidemiology of parkinson's disease. *J Neural Transm (Vienna).* (2017) 124(8):901–5. doi: 10.1007/s00702-017-1686-y
42. Patterson CG, Joslin E, Gil AB, Spigle W, Nemet T, Chahine L, et al. Study in parkinson's disease of exercise phase 3 (SPARX3): study protocol for a randomized controlled trial. *Trials* (2022) 23(1):855.



## OPEN ACCESS

## EDITED BY

Yi Wu,  
Xi'an Jiaotong University, China

## REVIEWED BY

Ivan Melnikov,  
Ministry of Health of the Russian  
Federation, Russia  
Matteo Stravalaci,  
Humanitas University, Italy

## \*CORRESPONDENCE

Mariana Pavel-Tanasa  
✉ mariana.pavel-tanasa@umfiasi.ro

RECEIVED 27 April 2023

ACCEPTED 30 May 2023

PUBLISHED 14 June 2023

## CITATION

Paranga TG, Pavel-Tanasa M,  
Constantinescu D, Plesca CE, Petrovici C,  
Miftode I-L, Moscalu M, Cianga P  
and Miftode EG (2023) Comparison of  
C-reactive protein with distinct  
hyperinflammatory biomarkers in  
association with COVID-19 severity,  
mortality and SARS-CoV-2 variants.  
*Front. Immunol.* 14:1213246.  
doi: 10.3389/fimmu.2023.1213246

## COPYRIGHT

© 2023 Paranga, Pavel-Tanasa,  
Constantinescu, Plesca, Petrovici, Miftode,  
Moscalu, Cianga and Miftode. This is an  
open-access article distributed under the  
terms of the [Creative Commons Attribution  
License \(CC BY\)](https://creativecommons.org/licenses/by/4.0/). The use, distribution or  
reproduction in other forums is permitted,  
provided the original author(s) and the  
copyright owner(s) are credited and that  
the original publication in this journal is  
cited, in accordance with accepted  
academic practice. No use, distribution or  
reproduction is permitted which does not  
comply with these terms.

# Comparison of C-reactive protein with distinct hyperinflammatory biomarkers in association with COVID-19 severity, mortality and SARS-CoV-2 variants

Tudorita Gabriela Paranga<sup>1,2</sup>, Mariana Pavel-Tanasa<sup>3,4\*</sup>,  
Daniela Constantinescu<sup>3,4</sup>, Claudia Elena Plesca<sup>1,2</sup>,  
Cristina Petrovici<sup>1,2</sup>, Ionela-Larisa Miftode<sup>1,2</sup>, Mihaela Moscalu<sup>5</sup>,  
Petru Cianga<sup>3,4</sup> and Egidia Gabriela Miftode<sup>1,2</sup>

<sup>1</sup>Department of Infectious Diseases (Internal Medicine II), Faculty of Medicine, Grigore T. Popa University of Medicine and Pharmacy, Iasi, Romania, <sup>2</sup>St. Parascheva Clinical Hospital for Infectious Diseases, Iasi, Romania, <sup>3</sup>Department of Immunology, Faculty of Medicine, Grigore T. Popa University of Medicine and Pharmacy, Iasi, Romania, <sup>4</sup>Laboratory of Immunology, St. Spiridon County Clinical Emergency Hospital, Iasi, Romania, <sup>5</sup>Department of Preventive Medicine and Interdisciplinarity, Faculty of Medicine, Grigore T. Popa University of Medicine and Pharmacy, Iasi, Romania

C-reactive protein (CRP) has been one of the most investigated inflammatory-biomarkers during the ongoing COVID-19 pandemics caused by severe acute respiratory syndrome coronavirus-2 (SARS-CoV-2). The severe outcome among patients with SARS-CoV-2 infection is closely related to the cytokine storm and the hyperinflammation responsible for the acute respiratory distress syndrome and multiple organ failure. It still remains a challenge to determine which of the hyperinflammatory biomarkers and cytokines are the best predictors for disease severity and mortality in COVID-19 patients. Therefore, we evaluated and compared the outcome prediction efficiencies between CRP, the recently reported inflammatory modulators (suPAR, sTREM-1, HGF), and the classical biomarkers (MCP-1, IL-1 $\beta$ , IL-6, NLR, PLR, ESR, ferritin, fibrinogen, and LDH) in patients confirmed with SARS-CoV-2 infection at hospital admission. Notably, patients with severe disease had higher serum levels of CRP, suPAR, sTREM-1, HGF and classical biomarkers compared to the mild and moderate cases. Our data also identified CRP, among all investigated analytes, to best discriminate between severe and non-severe forms of disease, while LDH, sTREM-1 and HGF proved to be excellent mortality predictors in COVID-19 patients. Importantly, suPAR emerged as a key molecule in characterizing the Delta variant infections.

## KEYWORDS

COVID-19, CRP, suPAR, s-TREM-1, HGF, biomarkers, disease severity, mortality

# 1 Introduction

The end of 2019 marked the beginning of a difficult period for humanity, the COVID-19 Pandemic, which put pressure on the health system all around the world. A new coronavirus, SARS-CoV-2 (severe acute respiratory syndrome coronavirus-2), first reported in Wuhan, Hubei, China, has widely spread, so that on January 30, 2020, the WHO declared a public health emergency of international interest, and a few weeks later (March 11, 2020) a global pandemic (1, 2).

In order to cope with the large numbers of COVID-19 patients during the peak periods of the pandemic waves, optimizing the hospital resources, by early discharging the patients at no risk of developing a severe form of disease, became a general necessity (1, 2). Since the pandemics' beginning, it has been widely accepted that the acute respiratory distress syndrome (ARDS) was associated with the severe/critical forms of disease and represented the main cause of death. However, the general clinical features of SARS-CoV-2 infection were heterogeneous and non-specific, covering a large spectrum of respiratory, digestive, cardiovascular, renal, neurological or psychiatric clinical manifestations, and showing unpredictable evolution towards critical illness (respiratory failure, septic shock, and/or multiple organ dysfunction) even in some patients with initial mild or moderate symptoms (3, 4). In this context, only considering the clinical evaluation as a decisive criterion for the early but safe discharge of patients was not possible, and hence, the need and the general effort for establishing laboratory-derived biomarkers that would facilitate the identification of patients at risk for disease progression or fatal outcome (4, 5).

For the confirmed cases of SARS-CoV-2 infection, a series of routinely-investigated biomarkers, including C-reactive protein (CRP), leukocyte count, lactate dehydrogenase (LDH) and alanine transaminase (ALT), was associated with severe disease and mortality (5, 6). Importantly, the high serum levels of CRP, which are normally lacking in viral infections, but observed in the severe cases since the beginning of COVID-19 pandemic, may be explained by the high production of IL-6 accompanying the Macrophage Activation Syndrome (5–8). Consequently, COVID-19 patients developing ARDS have increased plasma levels of pro-inflammatory cytokines, such as interleukins-1 beta and -6 (IL-1 $\beta$ , IL-6), tumor necrosis factor alpha (TNF- $\alpha$ ), chemokines—CXCL10 (IP-10), CCL2 (monocyte chemoattractant protein-1, MCP-1), and CCL3 (macrophage inflammatory protein-1 alpha, MIP-1 $\alpha$ ) (9, 10). These cytokines cause distinct positive feedback loops on other immune cells, contributing to recruiting them, generating an exponential growth of inflammation which ultimately leads to multiple organ damage (9–12). For instance, CCL2, despite being an important player in the antiviral defense, due to its overwhelming secretion caused by the SARS-CoV-2 infection, becomes one of the key contributors in generating ARDS and even death in patients with severe COVID-19 (13). Additionally, Sarif J. et al. identified the soluble urokinase plasminogen activator receptor (suPAR) as a key pathogenic circulating molecule linking the systemic hyperinflammation to a hypercoagulable status in

severe and critical COVID-19 patients, and thus, suggested using suPAR as a predictor for disease severity and mortality (14). To counteract the hyperinflammation, the immune system starts then releasing pleiotropic molecules with anti-inflammatory properties, such as the hepatocyte growth factor (HGF) and the soluble form of the triggering receptor expressed on myeloid cells (sTREM-1), such as neutrophils, monocytes and macrophages. These molecules, being produced in high amounts, intensify the coagulation abnormalities and the multiple organ failure, and are associated with disease severity and poor clinical outcome in COVID-19 (15–17). Recent systematic evaluation and meta-analysis studies conducted for identifying valuable biomarkers of disease prognosis and treatment responses in COVID-19 patients, also reported the potential usefulness of fibrinogen, D-dimers or neutrophil-lymphocyte ratio (NLR) (6, 18, 19).

Despite having a generous diversity of inflammatory mediators involved in poor outcomes, it still remains a challenge to determine which of these above-mentioned cytokines or chemokines are the best predictors of disease progression and mortality in COVID-19 patients with various forms of disease, ranging from mild, moderate to severe or critical illness (3).

Being well aware of the important contribution that these biomarkers would have on the management of the SARS-CoV-2 infected patient, we set out to evaluate and compare the prediction efficiency of CRP, the best described biomarker during the COVID-19 pandemic, with the more recent reported modulators with pro-inflammatory (such as suPAR, MCP-1, IL-1 $\beta$ , IL-6, NLR, platelet-lymphocyte ratio (PLR), ESR, ferritin, fibrinogen, and LDH) and anti-inflammatory (sTREM-1 and HGF) properties in a group of patients confirmed with SARS-CoV-2 infection and stratified as mild, moderate and severe cases. Importantly, the cases were investigated between October 2021 and May 2022, time frame which comprised the transition period from Delta to Omicron variants (the end of 2021), and this allowed us to additionally report our biomarkers' observations to distinct SARS-CoV-2 variant infections. Here we identified that CRP was the best predictor of disease severity among our investigated biomarkers, with suPAR levels being correlated with Delta infection, while LDH, sTREM-1 and HGF proved to best discriminate between survivors and non-survivors.

## 2 Materials and methods

### 2.1 Study participants and serum collection

Blood samples were collected at *St. Parascheva* Clinical Hospital for Infectious Diseases (Iasi, Romania) between October 2021 and May 2022 from SARS-CoV-2 infected individuals at hospital admission. Patients' inclusion criteria were: (1) adult patients of either sex; (2) SARS-CoV-2 infection confirmed by qRT-PCR tests through nasopharyngeal and oropharyngeal swab samples; (3) need for hospitalization; (4) either status of vaccination anti-SARS-CoV-2: yes or no; (5) given consent for the recruitment into the study. Exclusion criteria were as follows: (1) age < 18 years; (2)



administration of anti-inflammatory medication prior hospital admission; (3) immunocompromised patients (e.g. HIV/AIDS, transplant, cancer), (4) pregnancy; (5) no inclusion in other clinical studies.

The patients were next stratified according to disease severity in mild, moderate and severe cases, based on the signs and symptoms at hospital admission, and according to the international clinical spectrum guidelines of SARS-CoV-2 infection. More precisely, the mild group comprised the cases with few symptoms (low fever, cough, myalgias, fatigue, anorexia) without evidence of viral pneumonia or hypoxia. The moderate group comprised the cases with clinical signs of pneumonia (fever, cough, dyspnea, fast breathing), but no signs of severe pneumonia, including  $\text{SpO}_2 \geq 90\%$  on room air. In the severe group, we categorized the patients with clinical signs of pneumonia (fever, cough, dyspnea) plus one of the following: respiratory rate  $> 30$  breaths/min; severe respiratory distress; or  $\text{SpO}_2 < 90\%$  on room air. The patients who were discharged from the hospital were designated as survivors, while those who died during hospitalization were named non-survivors or deceased. Since the first two cases of Omicron infection were officially reported in Romania on the 4<sup>th</sup> of December 2021 by the Romanian National Institute of Public Health (RNIPH), all the cases before 1<sup>st</sup> of December 2021 were categorized as Delta SARS-CoV-2 infections, and the cases hospitalized in December were excluded from our study. As from the 1<sup>st</sup> week of 2022, the Omicron variant of concern represented more than 60% of the nasopharyngeal/oropharyngeal swab samples sequenced by RNIPH (20, 21), the cases after 1<sup>st</sup> of January 2022 were categorized as predominantly Omicron infections.

Inclusion in the study did not influence the patients' management and the therapeutic decision was left at the discretion of the attending physicians. This study has been reviewed and approved by the institutional ethics committees (St. Parascheva Clinical Hospital for Infectious Diseases, Iasi), and an informed consent was obtained from all the participants in this study. More precisely, 153 participants agreed for CRP and other pro-inflammatory biomarkers' testing (fibrinogen, ferritin, LDH, NLR – neutrophil-lymphocyte ratio, PLR – platelet-lymphocyte ratio), of which 140 subjects also agreed for inflammatory cytokine profile (suPAR, sTREM-1, MCP-1, HGF, IL-1 $\beta$ , IL-6). The information related to age and gender was included in a database together with a unique identifier, in order to keep the sample's identity unknown to the researcher. Overall patients' characteristics are detailed in [Supplementary Table 1](#).

## 2.2 Sample processing

Blood samples were collected in vacutainers with no anticoagulant and processed within 6 hours of receipt. More precisely, blood was spun at 2000 G for 5 min, and the serum was separated, while aliquots of 500  $\mu\text{L}$  were kept for storage at  $-80^\circ\text{C}$  until further analysis of the cytokines' profile.

• **for assessing CRP, classical inflammatory biomarkers and hematological parameters**

The analysis of CRP, ferritin, complete blood count, coagulation profile (fibrinogen, D-Dimers, prothrombin index), multiple organ failure biomarkers (aspartate transaminase (AST), ALT, total bilirubin, urea, creatinine, potassium, sodium, ionized calcium, chloride) was performed immediately after serum separation at St. Parascheva Hospital Laboratory using designated *in vitro* diagnosis kits for the automated platforms Rx Imola and Cobas. CRP levels were detected using the automated immunoturbidimetric Randox Full-Range Assay on the RxImola platform with a wide measuring range of 1.8–1650 mg/L.

### • for assessing the cytokine profile

The cytokine profiles were assessed at the Immunology Laboratory of St Spiridon County Emergency Hospital, Iasi. After thawing, the samples were centrifuged at 2,000 G for 5 min. The analysis of serum concentrations of various inflammatory cytokines/chemokines (sTREM-1, MCP-1/CCL-2, HGF, IL-1 $\beta$ , IL-6) was performed using a human pre-mixed multi-analyte kit (LXSAHM-05) from R&D systems and performed on a Luminex 100/200 analyzer. A 2-fold dilution was performed for all samples using the calibrator diluent RD6-52 before processing according to the manufacturer's instructions. Briefly, 50  $\mu\text{L}$  of standards and samples were mixed with 50  $\mu\text{L}$  magnetic microparticle cocktail and left for a 2 hours incubation at room temperature on a horizontal orbital microplate shaker set at 800 rpm. Following a washing procedure comprising 3 washes and the use of a magnetic device designated to accommodate the microplate, 50  $\mu\text{L}$  of diluted biotin-antibody cocktail were added to each well and the plate was incubated for 1 hour at room temperature on the shaker at 800 rpm. After another washing step, 50  $\mu\text{L}$  of the diluted streptavidin-PE solution was added for 30 min at room temperature on the shaker. After a final wash, the microparticles were resuspended in 100  $\mu\text{L}$  of wash buffer, incubated for 2 minutes and then the plate was read within 60 minutes. For suPAR analysis, the suPARnostic AUTO Flex ELISA kit from ViroGates (E001) was used. The samples were used undiluted. Briefly, 15  $\mu\text{L}$  of standards, controls or samples were pre-mixed with 135  $\mu\text{L}$  of conjugation working solution, mix from which 100  $\mu\text{L}$  was further transferred to the ELISA plate and left for 1 hour incubation at room temperature in the dark. The plate was then washed 3 times with 250  $\mu\text{L}$  of wash buffer using the TECAN hydroflex platform. Then, 100  $\mu\text{L}$  of TMB (tetramethylbenzidine) solution was added to each well and the enzymatic reaction was stopped after 20 minutes. The plate absorbance was read at 450 nm with the reference filter of 650 nm using the TECAN reader infinite 200 pro.

## 2.3 Statistical analysis

Statistical analysis was performed using Graph Pad Prism, v5 (Graph Pad Software, San Diego, CA, USA) and SPSS, v25 (IBM SPSS Software, Chicago, IL, USA). Data are presented as scatter dots, bars with information about the mean and SEM, or box and whiskers plots. Each figure legend contains the relevant statistical information: the  $n$ , total number of participants, the significance  $p$ -value and the corresponding statistical tests performed. All data

were checked for both normality and variance using the Shapiro-Wilk test. The parametric data were analyzed using the unpaired t-test and one-way ANOVA with *Post-hoc* Tukey's Multiple Comparison test. The majority of the data were non-parametric and the statistical tests applied were: Mann-Whitney test (the non-parametric counterpart to unpaired t-test), and Kruskal-Wallis with Dunn's Multiple Comparison test (the non-parametric counterpart to one-way ANOVA). Spearman's correlation coefficients (R) were used to assess positive or negative associations between measured variables. R values between 0.2-0.39 were treated as weak, between 0.4-0.59 as moderate, and between 0.6-0.79 as very strong correlation factors. Each linear regression graph was performed using Graph Pad Prism v5 and shows the best-fit line with the 95% confidence band. The coefficient of determination R-squared (R<sup>2</sup>) was used as a goodness-of-fit measure and the F-test to determine the level of significance for each linear regression. The receiver operating characteristic (ROC) curves were generated in SPSS, v25 in order to compare the sensitivity (sn) vs. specificity (sp) across a range of possible cut-off values, and the area under those curves (AUC) was used as a measure of test performance. The optimal cut-off values were determined as previously described in (22). The Kaplan-Meier survival curves, together with the univariate and multivariate analysis, were also generated using SPSS, v25. The *p* values less than 0.05 was considered statistically significant.

### 3 Results

#### 3.1 Serum CRP, suPAR, sTREM-1 and HGF levels increased in severe COVID-19 patients

Blood samples were collected from 153 SARS-CoV-2 infected patients in the first day of hospitalization, between October 2021 and May 2022. The patients were categorized based on disease severity (patients' characteristics are displayed in [Supplementary Table 1](#)) in mild (14 cases [9.15%]), moderate (71 cases [46.41%]), and severe (68 cases [44.44%]) cases. All mild cases survived and were hospitalized for a median of 6 days (IQR 5-9), while the moderate severe patients registered a 2.82% death rate for a median of 10 days of hospitalization (IQR 10-12), which significantly increased among severe COVID-19 individuals, reaching 26.5% mortality rate and a hospitalization period of 13 days (IQR 8-18) ([Figure 1A](#) and [Supplementary Table 1](#)). The median age was 55 years (IQR 45.5-66) for mild cases, which increased to 67 (IQR 57-73) and 70 (IQR 57.5-79.5) for moderate and severe patients. Each group was further stratified by gender and the female to male ratios were 1.8, 0.78 and 0.79 for mild, moderate and severe COVID-19 patients, suggesting an increased risk for moderate and/or severe SARS-CoV-2 infection among male individuals (Odd Ratio of 2.3). In the mild group, 11 cases (78.6%) had increased serum CRP levels over the normal range of 0-5 mg/L, while 61 (85.9%) and 65 (95.6%) cases had abnormally increased CRP levels in the moderate and severe groups. More precisely, the serum CRP levels ranged from 12.59 mg/L [95% CI 2.52-22.66] in mild cases to 67.25 mg/L [95% CI 2.52-22.66] and 107.7 mg/L [95% CI 90.61-124.9] for moderate and severe patients, respectively ([Figure 1B](#) and [Supplementary Table 2](#)).

The differences in CRP levels among the three groups of COVID-19 severity were significant for both female ( $p < 0.0001$ ) and male ( $p = 0.0012$ ) subgroups. These changes were sustained by similar changes in the serum levels of newly characterized biomarkers of systemic inflammation (suPAR, sTREM-1, HGF) and classical biomarkers (cytokines - IL-1 $\beta$ , IL-6, chemokines - MCP-1/CCL2, and hematological/biochemical markers - NLR, PLR, ESR, fibrinogen, ferritin and LDH) ([Table 1](#)).

For instance, the serum suPAR levels showed 2.51- and 3.45-fold increases in moderate and severe cases, respectively, when compared to the mild SARS-CoV-2 infected patients (1.47 ng/mL [95% CI 1.17-1.77],  $p < 0.0001$ ) with no significant differences among the female and male subgroups ([Figure 1C](#)). Interestingly, also the serum levels of soluble molecules with anti-inflammatory function, such as the soluble form of triggering receptor expressed on myeloid cells 1 (sTREM-1) and hepatocyte growth factor (HGF), showed similar significant increasing trends ( $p < 0.0001$ , and  $p = 0.0173$ , respectively). While sTREM-1 serum levels showed 1.97- and 2.42- fold increases in moderate and severe cases irrespective of gender ([Figure 1D](#)), the HGF levels largely depended on gender with 2.8- and 4.6-fold increases in moderate and severe female cases and only 1.7- and 2.3- fold increases in moderate and severe male patients when compared to the mild subjects' values (238.6 pg/mL [95% CI 29.81-447.4] for females, and larger values of 534.9 pg/mL [95% CI 190.8-879.1] for males; [Figure 1E](#) and [Table 1](#)). The MCP-1/CCL2 values also described an increasing trend from mild to severe cases, but with no significant differences between the three groups ( $p = 0.1820$ , [Figure 1F](#)). On the other hand, IL-1 $\beta$  showed a similar 2.6-fold change irrespective of gender in the moderate and severe cases ( $p = 0.006$ ) when compared to the mild group characterized by a mean value of 1.29 pg/mL [95% CI 0.67-1.91] ([Figure 1G](#)). IL-6 values, similar to HGF, showed significant increases among the three severity groups only for females ( $p < 0.0001$ ), but with more prominent differences as the total levels varied from 2.64 pg/mL [95% CI 0.68-4.61] in mild cases to 18.78 pg/mL [95% CI 7.37-30.19] in moderate, and 46.26 pg/mL [95% CI 26.52-65.99] in severe COVID-19 patients ([Figure 1H](#)).

Among the classical hematological and biochemical inflammatory biomarkers, neutrophil-lymphocyte ratio (NLR), platelet-lymphocyte ratio (PLR), erythrocyte sedimentation rate (ESR), fibrinogen, ferritin, and lactate dehydrogenase (LDH) showed a general similar significant rising trend as the CRP levels from mild to moderate and then, to severe subjects ([Figure 2](#)). However, the described differences for NLR ( $p = 0.0001$ ), PLR ( $p = 0.0346$ ) and ferritin serum levels ( $p = 0.0003$ ) were significant only for the subgroup of female patients ([Table 1](#)). The pro-inflammatory landscape noticed in the severe form of COVID-19 was hence associated with hematological changes, including the described increase of NLR and PLR values. The WBC had a general tendency to increase from mild to severe, and most importantly, both the total number and percentage of neutrophils and eosinophils increased at the expense of lymphocytes which significantly decreased from  $1.29 \times 10^3/\mu\text{L}$  (95% CI 0.94-1.64) in mild cases to  $0.79 \times 10^3/\mu\text{L}$  (95% CI 0.58-0.96) in severe patients. The platelet counts did not significantly differ among the three groups of subjects. The present data clearly show that CRP and the

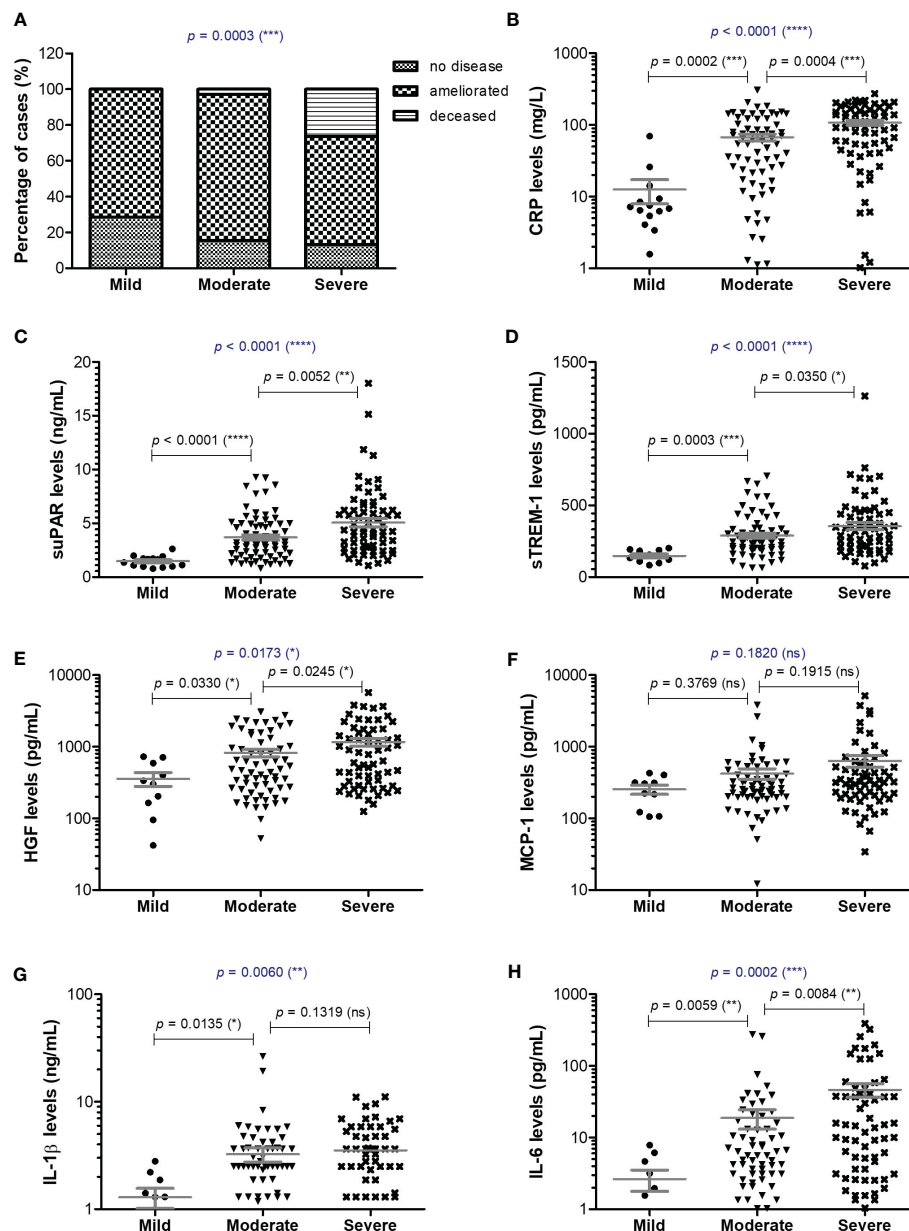


FIGURE 1

Serum profile of CRP and pro-inflammatory cytokines in mild, moderate and severe COVID-19 disease. (A) Patients' discharge status (no disease, ameliorated symptoms or deceased) for each category of COVID-19 disease: mild, moderate, severe (\*\* $p < 0.001$ ; chi-squared test). Serum levels of (B) CRP, (C) suPAR, (D) sTREM-1, (E) HGF, (F) MCP-1, (G) IL-1 $\beta$ , (H) IL-6 for each category of COVID-19 disease: mild, moderate or severe. The gray lines represent the mean  $\pm$  SEM (\*\*\*\* $p < 0.0001$ , \*\*\* $p < 0.001$ , \*\* $p < 0.01$ , \* $p < 0.05$ , ns – not significant; (A) chi-squared test; (B–H) Kruskal-Wallis with Dunn's Multiple Comparison test).

other investigated pro-inflammatory biomarkers gradually increase from mild to moderate and/or severe COVID-19 cases and this is supported by an expansion of neutrophils and eosinophils together with a reduction in the lymphocyte count.

### 3.2 CRP levels are not influenced by age in COVID-19 patients

Next, we wondered whether the serum levels of CRP and of the other investigated inflammatory biomarkers vary according

to age (Figure 3A). First, CRP and suPAR levels did not seem to be influenced by age in our study group (Figures 3B, C). Interestingly, significant correlations (total correlation  $R = 0.35$ ,  $p < 0.0001$ ) with patients' age were noticed for sTREM-1 values for all three categories of mild ( $R = 0.68$ ), moderate ( $R = 0.45$ ) and severe ( $R = 0.21$ ) cases. Indeed, when stratified by age, the subgroup of subjects older than 60 years constantly showed higher values of sTREM-1 (an average of 1.4-fold increase) in each subgroup: mild, moderate or severe (Figure 3D). Significant general correlations were also observed for NLR ( $p = 0.0016$ ) and PLR ( $p = 0.0036$ ) with a moderate value of 0.45 within the group of

TABLE 1 The values of inflammatory biomarkers for each category of COVID-19 patients: mild, moderate and severe.

Analyte	Mild		Moderate		Severe		p-value
	Median [IQR]	Mean [95% CI]	Median [IQR]	Mean [95% CI]	Median [IQR]	Mean [95% CI]	
<b>CRP (mg/L)</b>	7.01 [5.05-10.57]	12.59 [2.516-22.66]	54.14 [16.45-102.9]	67.25 [52.69-81.81]	99.18 [45.64-166]	107.7 [90.61-124.9]	<b>&lt; 0.0001</b>
<b>F</b>	6.45 [4.72-17.69]	15.33 [-1.162-31.83]	29.56 [9.34-85.91]	52.47 [31.75-73.19]	94.95 [40.67-146]	98.2 [74.88-121.5]	<b>&lt; 0.0001</b>
<b>M</b>	7.2 [4.19-11.32]	7.644 [2.051-13.24]	72.35 [29.42-122.1]	78.71 [58.4-99.01]	113.2 [55.07-184.2]	115.3 [90.07-140.5]	<b>0.0012</b>
<b>suPAR (ng/mL)</b>	1.51 [0.99-1.78]	1.47 [1.17-1.77]	3.14 [2.05-4.92]	3.68 [3.19-4.18]	4.31 [2.71-6.23]	5.06 [4.29-5.82]	<b>&lt; 0.0001</b>
<b>F</b>	1.12 [0.98-1.83]	1.36 [1.009-1.713]	2.99 [1.82-4.92]	3.6 [2.79-4.41]	4.3 [2.64-7.08]	5.39 [3.96-6.81]	<b>&lt; 0.0001</b>
<b>M</b>	1.68 [1.13-2.18]	1.66 [0.87-2.45]	3.31 [2.34-4.97]	3.75 [3.11-4.39]	4.54 [2.73-6.22]	4.8 [3.96-5.64]	<b>0.0030</b>
<b>sTREM-1 (pg/mL)</b>	144.5 [106.4-189.9]	146.8 [115.7-178]	249.9 [194.8-341.9]	288.8 [252.5-325]	318.3 [211.3-453.7]	354.8 [304.3-405.3]	<b>&lt; 0.0001</b>
<b>F</b>	139 [94.46-188.1]	140.7 [90.88-190.5]	240.9 [155.8-303.9]	250.1 [197.4-302.7]	317.4 [189.7-448.9]	353.5 [259.5-447.5]	<b>0.0051</b>
<b>M</b>	160.7 [115-192.4]	156 [89.65-222.4]	275 [198-428.8]	315.6 [266.1-365]	319.2 [212.5-466]	355.7 [297.2-414.2]	<b>0.0188</b>
<b>HGF (pg/mL)</b>	318.7 [147.6-619.3]	357.1 [180.4-533.8]	478.6 [262.7-1184]	818.5 [628.7-1008]	705.4 [295.8-1691]	1157 [872.3-1441]	<b>0.0173</b>
<b>F</b>	184.5 [82.13-399.1]	238.6 [29.81-447.4]	366.5 [205.3-1021]	662.7 [410.2-915.2]	891.6 [322.5-1733]	1086 [733.4-1439]	<b>0.0042</b>
<b>M</b>	555.5 [326.2-723]	534.9 [190.8-879.1]	598.9 [265.9-1587]	926.3 [652.9-1200]	569.1 [272.3-1629]	1208 [774.8-1642]	0.3299
<b>MCP-1 (pg/mL)</b>	265.1 [118.1-337.8]	254.2 [169.6-338.7]	265.1 [199.6-429.1]	421.2 [283.9-558.5]	323.5 [210.3-551]	634.6 [404.2-865]	0.1820
<b>F</b>	220.5 [118.1-337.8]	231.5 [112.2-350.9]	248.7 [179-328.9]	266 [213.9-318]	341.6 [232.3-607.7]	805.2 [340.3-1270]	<b>0.0136</b>
<b>M</b>	309.8 [156.1-398.2]	288.1 [75.83-500.3]	285.1 [203.7-596.2]	528.7 [301.1-756.2]	301.4 [179.3-544]	510.1 [285.5-734.7]	0.8543
<b>IL-1<math>\beta</math> (pg/mL)</b>	1.301 [0.743-1.958]	1.291 [0.6735-1.909]	2.493 [1.301-3.656]	3.238 [2.268-4.208]	3.251 [1.301-4.754]	3.533 [2.891-4.174]	<b>0.0060</b>
<b>F</b>	1.126 [0.0915-2.356]	1.229 [0.05828-2.4]	2.493 [0.954-3.638]	3.068 [1.133-5.004]	2.493 [1.874-4.754]	3.226 [2.395-4.056]	<b>0.0312</b>
<b>M</b>	1.356 [1.041-1.758]	1.385 [0.7805-1.989]	2.493 [1.301-3.709]	3.356 [2.32-4.391]	3.638 [1.301-5.578]	3.757 [2.8-4.713]	0.2042
<b>IL-6 (pg/mL)</b>	1.75 [0.4-5.02]	2.64 [0.6754-4.605]	5.65 [2.59-13.85]	18.78 [7.371-30.19]	12.77 [3.235-40.95]	46.26 [26.52-65.99]	<b>0.0002</b>
<b>F</b>	0.5 [0.0775-1.95]	0.9683 [-0.292-2.228]	4.23 [2.33-10.57]	8.161 [4.032-12.29]	15.85 [4.64-49.07]	61.47 [21.3-101.6]	<b>&lt; 0.0001</b>
<b>M</b>	5.4 [2.623-7.42]	5.148 [1.169-9.126]	5.65 [2.59-24.4]	26.13 [7.025-45.24]	9.69 [2.565-39.32]	35.15 [16.36-53.95]	0.4600
<b>NLR</b>	2.675 [1.33-4.795]	3.73 [1.922-5.538]	5.076 [3.226-7.288]	6.239 [5.059-7.419]	9.254 [3.421-13.72]	10.31 [8.442-12.17]	<b>&lt; 0.0001</b>
<b>F</b>	3.864 [2.013-8.795]	5.096 [0.6332-9.559]	5.281 [3.06-8.084]	6.975 [5.001-8.948]	8.612 [3.317-12.85]	9.412 [7.248-11.58]	<b>0.0001</b>
<b>M</b>	2.469 [1.124-3.247]	2.972 [0.8438-5.099]	4.933 [3.383-6.814]	5.29 [4.335-6.245]	9.87 [4.745-15.64]	11.44 [8.111-14.77]	0.1033
<b>PLR</b>	150.8 [116.8-208.8]	199.7 [112.6-286.9]	221.3 [145.9-336.4]	277.8 [232.5-323.1]	263.9 [178.8-415.9]	327.7 [270.3-385.1]	<b>0.0177</b>
<b>F</b>	144.1 [121.4-192.1]	205.1 [67.48-342.8]	233.3 [184.6-304.3]	283.2 [221.8-344.5]	256.9 [176.3-422.5]	354.2 [241.4-467]	<b>0.0346</b>

(Continued)

TABLE 1 Continued

Analyte	Mild		Moderate		Severe		p-value
	Median [IQR]	Mean [95% CI]	Median [IQR]	Mean [95% CI]	Median [IQR]	Mean [95% CI]	
<b>M</b>	189.1 [99.83-280.6]	190 [67.33-312.7]	213 [127.1-336.8]	273.6 [206.3-340.9]	275 [178.8-421]	306.8 [250.6-363]	0.1966
<b>ESR (mm/h)</b>	29.5 [16.5-53.75]	38.5 [20.6-56.4]	60.5 [40-80]	64.31 [55.97-72.66]	70 [42.5-102]	71.86 [62.53-81.2]	<b>0.0055</b>
<b>F</b>	39 [20-75]	45.11 [19.62-70.6]	60 [30-75]	62.22 [47.95-76.49]	60 [43.75-107]	71.63 [57.54-85.72]	0.1041
<b>M</b>	15 [6.5-52.5]	26.6 [-5.064-58.26]	61 [46-85]	65.84 [55.26-76.42]	75 [36-100]	72.06 [58.95-85.17]	<b>0.0254</b>
<b>Fibrinogen (g/L)</b>	3.475 [3.215-4.08]	3.592 [3.248-3.936]	4.78 [3.74-5.37]	4.681 [4.404-4.958]	5.37 [4.29-5.82]	5.269 [4.907-5.63]	<b>&lt; 0.0001</b>
<b>F</b>	3.61 [3.19-4.42]	3.721 [3.197-4.245]	4.61 [3.61-5.37]	4.611 [4.158-5.065]	4.875 [3.785-5.618]	4.821 [4.403-5.24]	<b>0.0202</b>
<b>M</b>	3.44 [3.055-3.625]	3.36 [2.934-3.786]	4.875 [4.14-5.498]	4.736 [4.375-5.097]	5.82 [4.545-7.11]	5.632 [5.082-6.181]	<b>0.0007</b>
<b>Ferritin (µg/L)</b>	213.6 [100.8-490.1]	408.4 [25.4-791.3]	498.2 [209.9-1261]	1034 [515.6-1553]	862.5 [353.3-1794]	1568 [779.1-2357]	<b>0.0029</b>
<b>F</b>	102.2 [76.43-253.8]	152.5 [-23.47-328.5]	280.7 [103.7-468.8]	378.2 [200-556.3]	658.1 [298.5-1674]	1133 [711.9-1553]	<b>0.0003</b>
<b>M</b>	454.5 [213.6-1220]	664.2 [-179-1507]	916.2 [457.3-1633]	1510 [645.1-2374]	920.6 [362.7-2000]	1891 [530.6-3252]	0.3693
<b>LDH (U/L)</b>	168.5 [133.3-196.8]	166 [143.1-188.9]	280 [202.3-386]	294.3 [264.1-324.5]	338 [240-481]	396.4 [339.9-452.8]	<b>&lt; 0.0001</b>
<b>F</b>	162 [132-211]	161.3 [121.5-201]	225.5 [184-298.8]	250.7 [218.6-282.7]	382 [308-531.5]	420.9 [350.6-491.2]	<b>&lt; 0.0001</b>
<b>M</b>	177 [148.5-194.5]	172.6 [139.4-205.8]	304.5 [248.3-413.8]	325.8 [280.7-370.8]	311 [211.3-472.5]	377.6 [291.5-463.8]	<b>0.0210</b>

CRP, C-reactive protein; suPAR, soluble urokinase plasminogen activator receptor; sTREM-1, soluble triggering receptor expressed on myeloid cells-1; HGF, hepatocyte growth factor; MCP-1, monocyte chemoattractant protein-1; IL-1 $\beta$ , interleukin-1 beta; IL-6, interleukin-6; NLR, neutrophil-lymphocyte ratio; PLR, platelet-lymphocyte ratio; ESR, erythrocyte sedimentation rate; LDH, lactate dehydrogenase; F, females; M, males; IQR, interquartile range; CI, confidence interval; p, statistical significance coefficient. The bold values are the statistically significant p-values.

mild subjects (Figure 3A). A moderate variation with age was also observed in the mild group for HGF ( $R = 0.51$ , Figure 3E). Based on these observations, we can conclude that CRP and the majority of inflammatory biomarkers (except sTREM-1, NLR and PLR) had a weak variation by age in COVID-19 patients.

### 3.3 sTREM-1, HGF, ESR, fibrinogen and LDH best correlated with CRP in severe COVID-19 patients

To better picture the general landscape of CRP and of the other 12 biomarkers serum levels in moderate and severe COVID-19 patients, we further investigated the correlation coefficients between any combination of bio-signatures (Figure 4A). First, we noticed higher associations among CRP, suPAR, sTREM-1, HGF, MCP-1, IL-1 $\beta$ , IL-6 and NLR in the severe group when compared to moderate subjects. Next, CRP showed significant moderate correlation with sTREM-1 and HGF in both moderate and severe patients, while suPAR showed good correlations with sTREM-1, HGF and MCP-1 only in the severe group (Figures 4A–D). Interestingly, sTREM-1 showed moderate association with HGF,

MCP-1 and IL-6 in the moderate group, but good and very good correlations with all the above-mentioned biomarkers in severe cases (Figure 4E). When investigating the correlations with classical hematological and biochemical inflammatory signatures, we observed a clear association of ESR, fibrinogen, LDH with CRP in both moderate and severe patients (Figure 5). These results suggest that the severe form of COVID-19 is characterized by a strong pro-inflammatory phenotype, and most importantly, by a clear association between CRP and sTREM-1, a recently described biomarker of COVID-19 severity and mortality.

### 3.4 SARS-CoV-2-infection with Delta variants, compared to Omicron, induced higher inflammatory responses

As the Delta SARS-CoV-2 infection was associated with a higher death rate worldwide when compared to the other variants (23), we next aimed to investigate the differences, if any, in our selected inflammatory biomarkers. Indeed, in our group of investigated patients, the death rate was 15% among the Delta-infected individuals, and lowered to 9% for the Omicron-infection



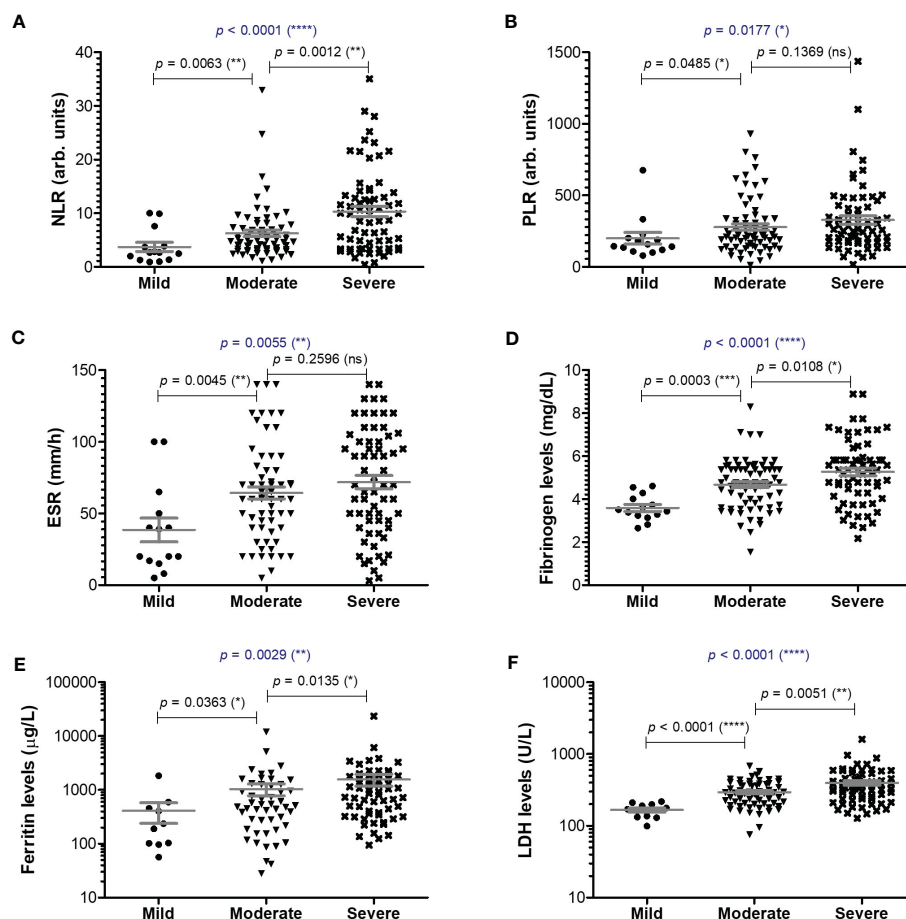


FIGURE 2

Serum profile of common pro-inflammatory biomarkers in mild, moderate and severe COVID-19 disease. Serum levels of (A) NLR (neutrophil-lymphocyte ratio), (B) PLR (platelet-lymphocyte ratio), (C) ESR (erythrocyte sedimentation rate), (D) fibrinogen, (E) ferritin, (F) LDH for each category of COVID-19 disease: mild, moderate or severe. The gray lines represent the mean  $\pm$  SEM (\*\*\*\* $p$  < 0.0001, \*\*\* $p$  < 0.001, \*\* $p$  < 0.01, \* $p$  < 0.05, ns – not significant; Kruskal-Wallis with Dunn's Multiple Comparison test).

(Supplementary Figure 1). Interestingly, the most prominent difference was noticed for the serum suPAR levels, where significantly higher levels were observed for the Delta variant infections in both moderate and severe cases (moderate cases: 4.61 ng/mL for Delta vs. 1.9 ng/mL for Omicron; severe cases: 5.74 ng/mL for Delta vs. 2.37 ng/mL for Omicron), Figure 6A and Table 2. Importantly, CRP and most of the other biomarkers showed overall higher values for the Delta infection compared to the other variants (Figures 6B–G). Among those, HGF, IL-1 $\beta$  and fibrinogen showed significant differences in the group of moderate COVID-19 cases. For instance, HGF levels reached 580.8 pg/mL [95% CI 327.5–1610] in the Delta moderate infection compared to 299.2 pg/mL [95% CI 195.7–625.1] in the Omicron infection. For fibrinogen, increased levels were noticed in 87% of the Delta infected individuals compared to only 48% for the Omicron infections. A similar trend was also observed for ESR and LDH (Supplementary Figure 2). Most of these described differences were significant in the case of moderate disease severity. Interestingly, these differences were attenuated in the severe COVID-19 cases. In accordance with an overall higher pro-inflammatory response induced by the Delta variant, the percentage of severe cases was

also increased (50% of severe cases within the Delta infection group vs. 34.5% of severe cases within the Omicron group;  $p$  = 0.0015; Figure 6H).

### 3.5 CRP and pro-inflammatory cytokines' levels at hospital admission were higher in the severe COVID-19 patients who did not survive

Since most of the deceased patients were from the severe category of COVID-19 patients (26.5% mortality rate), we next wondered which were the discrepancies, if any, between the severe subjects that survived and those who died. For CRP, the mean values were higher with 45% in the deceased group compared to the survivors' group (Figure 7). Similarly, suPAR, sTREM-1, and IL-1 $\beta$  initial levels were higher by 45–50% in the deceased group, while HGF, MCP-1, and IL-6 initial serum levels were even higher, showing an increase of 75–80% compared to the survivors' group (Figure 7 and Supplementary Table 3). Importantly, among the hematological and biochemical inflammatory biomarkers, only

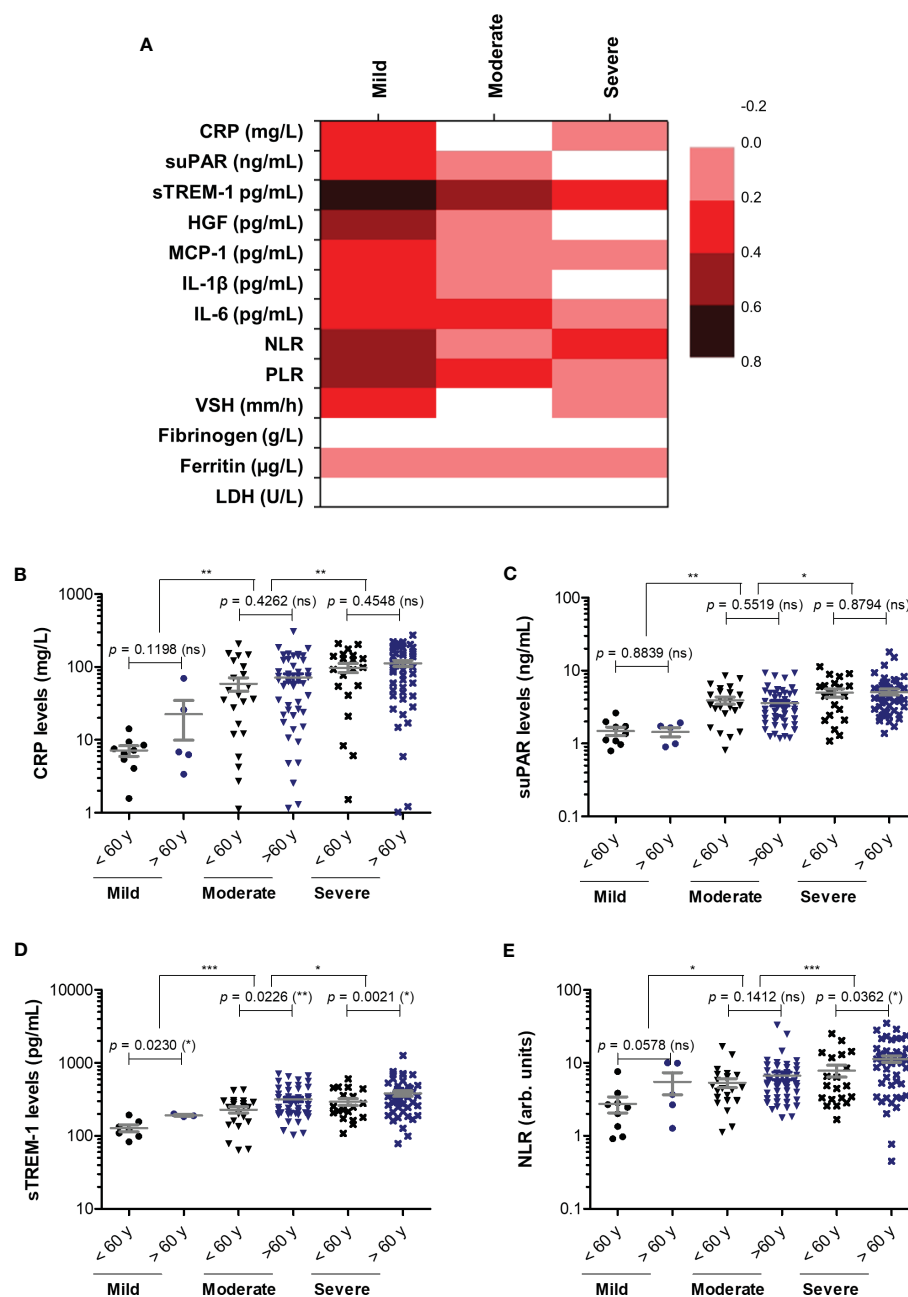


FIGURE 3

Correlation of pro-inflammatory biomarkers with age in mild, moderate and severe SARS-CoV-2 infections. **(A)** Heat map of correlation coefficients (R) for each category of COVID-19 disease: mild, moderate, severe (0.2–0.39: weak; 0.4–0.59: moderate; 0.6–0.8 strong). **(B)** CRP levels, **(C)** suPAR levels, **(D)** sTREM-1 levels, and **(E)** NLR values in mild, moderate and severe COVID-19 patients stratified by age (younger or older than 60 years). The gray lines represent the mean  $\pm$  SEM (\*\* $p < 0.001$ , \*\* $p < 0.01$ , \* $p < 0.05$ , ns – not significant; Kruskal-Wallis with Dunn's Multiple Comparison test).

LDH showed a significant increase in the deceased group, but only of 29% (Supplementary Table 3). These data reveal that the initial high levels of CRP and cytokines correlated with an increased mortality risk.

As vaccination could have influenced the outcome of patients, we also evaluated the vaccination status among the subjects included in this study. For the mild group, 9 out of 14 cases were vaccinated (64.3%), while the rate of vaccination was significantly

lower among moderate and severe cases (22.5% and 17.6%, respectively, Supplementary Figure 3A). Among severe cases, no differences in the vaccination rates were observed between survivors and non-survivors (Supplementary Figure 3B). Consistently, no positive association between the vaccination status and mortality emerged (Supplementary Figure 4), probably also due to the relatively low percentage of general vaccination rate of only 24% in our study group. No consistent significant laboratory

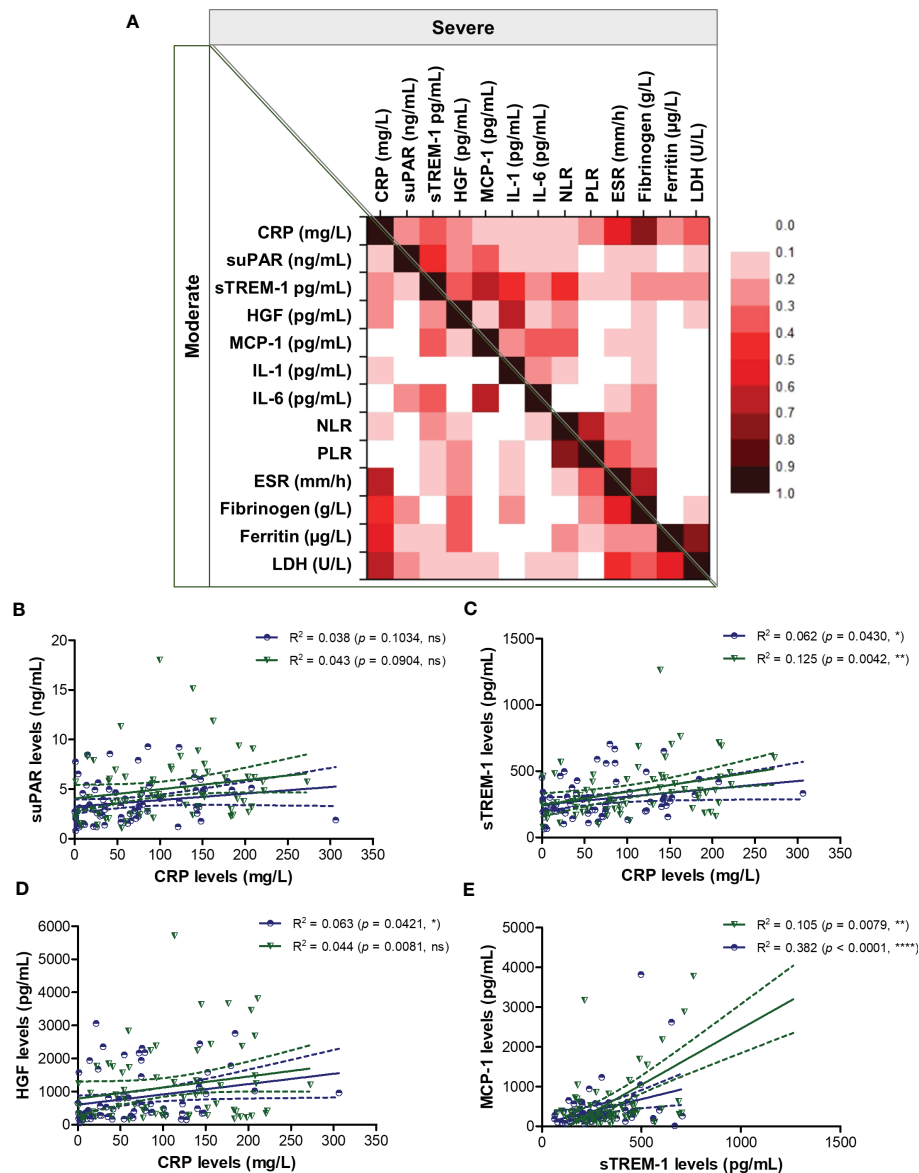


FIGURE 4

Regression statistics describing the association between CRP and other pro-inflammatory biomarkers in moderate and severe cases of SARS-CoV-2 infection. (A) Heat map of correlation coefficients (R) for each category of COVID-19 disease: moderate (left-bottom corner) and severe (right-upper corner). Linear regression analysis for (B) CRP and suPAR levels, (C) CRP and sTREM-1 levels, (D) CRP and HGF levels, and (E) sTREM-1 and MCP-1 levels in moderate and severe COVID-19 patients (\*\*\*\* $p < 0.0001$ , \*\* $p < 0.01$ , \* $p < 0.05$ , ns – not significant; Spearman test). The blue lines and dots correspond to moderate cases, while the green lines and dots state for severe cases.

differences were noticed between previously vaccinated and non-vaccinated subjects for each category of disease severity (Supplementary Table 4).

### 3.6 CRP associated with severe COVID-19, suPAR with Delta variant, while sTREM-1, HGF and LDH with mortality prediction

We next aimed to investigate which of the inflammatory biomarkers were associated with disease severity, SARS-CoV-2 Delta variant and mortality prediction. Among all the markers, the best correlation with the severe form of COVID-19 was observed

for the serum CRP levels ( $R = 0.415$ ,  $p < 0.001$ , Figure 8A), results confirmed also by the ROC analysis (AUC = 0.720, 95% CI 0.625–0.816,  $p < 0.0001$ ). A cut-off value of 76.07 mg/L for CRP yielded a sensitivity of 0.66 and a specificity of 0.71 (Table 3). For predicting the severe form of COVID-19, higher AUC values were achieved when CRP was analyzed together with the other inflammatory markers which also showed significant independent associations (Model1\_1). The association of CRP with cytokines (suPAR, sTREM-1, HGF, IL-6 – Model 1\_2) gave a similar AUC value as the association of CRP with the classical inflammatory biomarkers (NLR, PLR, ESR, fibrinogen, ferritin, LDH – Model 1\_3): 0.766 (95% CI 0.678–0.855,  $p < 0.0001$ ) vs. 0.769 (95% CI 0.680–0.857,  $p < 0.0001$ ) – see Figure 8B and Supplementary Table 5.

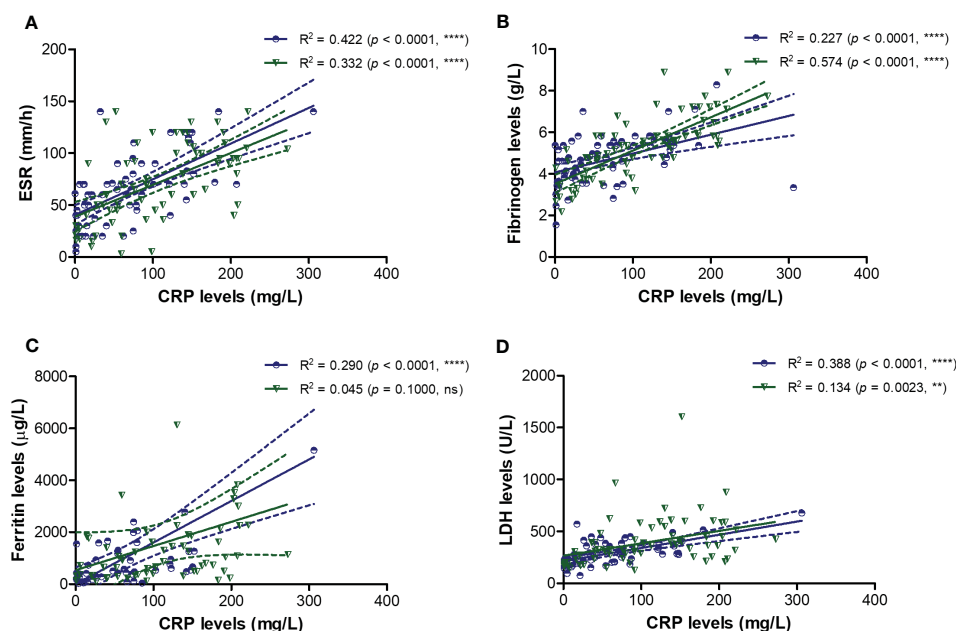


FIGURE 5

Regression statistics describing the association between CRP and classical pro-inflammatory biomarkers in moderate and severe cases of SARS-CoV-2 infection. Linear regression analysis for CRP and (A) ESR, (B) fibrinogen, (C) ferritin, and (D) LDH in moderate and severe COVID-19 patients (\*\*\*\* $p < 0.0001$ , \*\*\* $p < 0.001$ , \*\* $p < 0.01$ , ns – not significant; Spearman test). The blue lines and dots correspond to moderate cases, while the green lines and dots state for severe cases.

Importantly, CRP analyzed together with any of the following markers, suPAR, sTREM-1 or HGF reached significantly higher AUC values (0.744, 0.738, and 0.731, respectively) than CRP alone. To validate these observations, we also performed univariate and multivariate analysis for the above established cut-off values in relation to age (older than 60 years), gender and vaccination status. As shown in [Supplementary Table 6](#), only CRP and NLR could serve as independent predictors for disease severity.

When examining the inflammation caused by the Delta variant, suPAR levels showed the highest correlation ( $R = 0.548$ ,  $p < 0.0001$ ) and an outstanding AUC value of 0.912 (95% CI 0.860–0.963,  $p < 0.0001$ ). For suPAR, the cut-off value of 3.24 ng/mL yielded a sensitivity of 0.77 and a specificity of 0.91 ([Table 4](#)). All the other markers showed moderate or low differentiation capacity between Delta and Omicron infections ([Figure 8C](#) and [Supplementary Table 7](#)). As shown in [Supplementary Table 8](#), the multivariate analysis also confirmed that suPAR could indeed serve as an independent discriminator between the two variant infections (Delta vs. Omicron).

The best predictors for mortality were represented by the initial values of LDH, HGF, sTREM-1, followed by suPAR and IL-1 $\beta$  serum levels. This observation resulted from computing both the correlations and AUC values for those biomarkers, and the identified cut-off values were: 380 U/L for LDH, 5.2 ng/mL for suPAR, 803 pg/mL for HGF, 334 pg/mL for sTREM-1, and 3.44 pg/mL for IL-1 $\beta$  ([Table 5](#)). Importantly, the association of LDH with the other biomarkers yielded an improved AUC value of 0.851 (95% CI 0.769–0.933,  $p < 0.0001$ ) when compared to LDH alone (AUC 0.809, 95% CI 0.710–0.907,  $p < 0.0001$ ), see [Figure 8D](#) and [Supplementary Table 9](#). The Kaplan-Meier survival curves confirmed these observations, as the severe COVID-19 patients

([Figure 8E](#)) and those with values higher than the indicated cut-off scores had a poorer prognosis than those with mild/moderate disease or lower values ([Supplementary Figures 5, 6](#)). Furthermore, we performed univariate and multivariate Cox regression analysis, and identified that LDH could serve as a promising independent prognostic factor for patients with COVID-19, as shown in [Table 6](#).

At this point we were able to conclude that the initial values of distinct inflammatory biomarkers are good or excellent predictors for disease severity (e.g., CRP), Delta variant infection (e.g., suPAR) and mortality (e.g., LDH, sTREM-1, HGF, suPAR).

### 3.7 Disease severity and mortality associated a higher rate of comorbidities: thrombocytopenia, diseases of the circulatory system and liver

As the panel of our inflammatory biomarkers did not yield outstanding associations with disease severity and mortality, we hypothesized that additional criteria might have influenced the COVID-19 disease evolution. Thus, we next investigated the comorbidities' rate among severe and non-severe patients or between those that survived or died. As expected, more comorbidities were present in severe subjects, and among those, the endocrine and metabolic disorders, together with liver diseases showed an increasing trend, while the diseases of circulatory system yielded a significant rise from 65% in non-severe cases to 80% among severe subjects ([Figure 9A](#) and [Supplementary Figure 7A, B](#)). When comparing the survivors' group with the deceased one, we

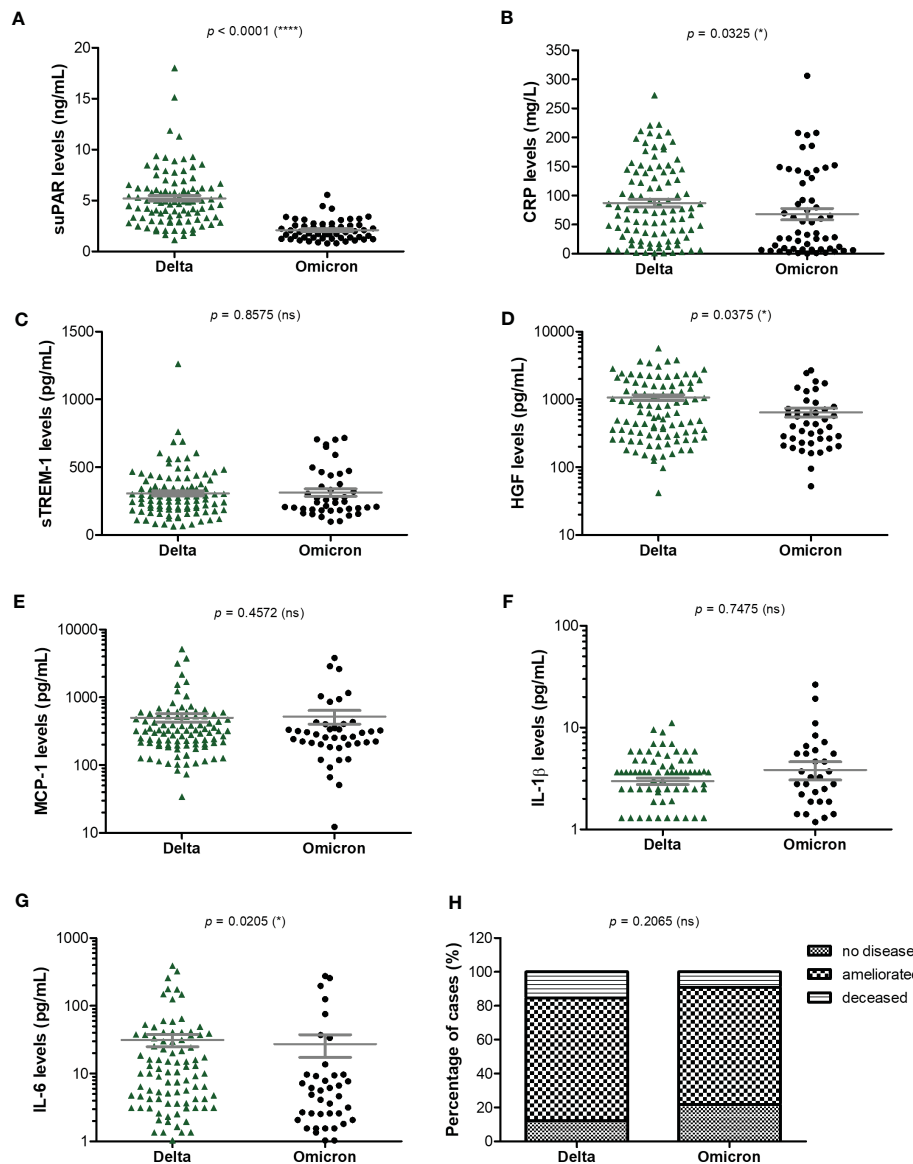


**FIGURE 6**  
Serum profile of CRP and pro-inflammatory cytokines in Delta and Omicron SARS-CoV-2 infections. Serum levels of (A) suPAR, (B) CRP, (C) sTREM-1, (D) HGF, (E) MCP-1, (F) IL-1 $\beta$ , (G) IL-6 for each category of SARS-CoV-2 infection: Delta or Omicron. The gray lines represent the mean  $\pm$  SEM (\*\*\*\* $p < 0.0001$ , \* $p < 0.05$ , ns – not significant; two-tailed Mann-Whitney test). (H) Patients' discharge status (no disease, ameliorated symptoms or deceased) for each category of SARS-CoV-2 infection: Delta or Omicron (ns – not significant; chi-squared test).

noticed significant changes among the rate of thrombocytopenia and other blood diseases (from 21% in the survivors' group to 45% in the deceased group) and liver diseases (showing an increase from 5% to 21% in deceased subjects, who showed either cirrhosis, fatty liver or hepatic failure – **Figures 9B, C** and **Supplementary Figures 7C, D**). Next, we investigated the mortality prediction given by CRP and inflammatory cytokines (those biomarkers that yielded significant differences among survivors and deceased individuals in the severe group). Among those, suPAR and IL-6 generated the highest AUC values of 0.748 and 0.763, respectively. A combined model of all inflammatory biomarkers reached a similar AUC of 0.757 (Model 4\_1), while when combined with the presence of comorbidities (Model 4\_2) the prediction model reached an excellent AUC of 0.824 (**Supplementary Table 10**). These data are

valuable as they point out the importance of comorbidities in influencing the COVID-19 evolution in severe patients.

As the fatal outcome could also be influenced by the therapeutic management, we next investigated the effect exerted by the anti-inflammatory therapy on the survival rate among COVID-19 severe cases. Thus, we categorized the severe cases based on the therapeutic strategies applied by physicians: 18 patients received Tocilizumab, an anti-IL-6 monoclonal antibody, in the first hours-days of hospital admission (median 0 days [IQR 0-1]), 30 patients received Anakinra, an IL-1R antagonist, at a median of 2 days after hospital admission, and the rest 20 severe cases were not administered any of the above anti-interleukin therapies (thus, being designated as the non-AIT group) – **Supplementary Tables 11, 12**. The anti-interleukin therapy did not prove



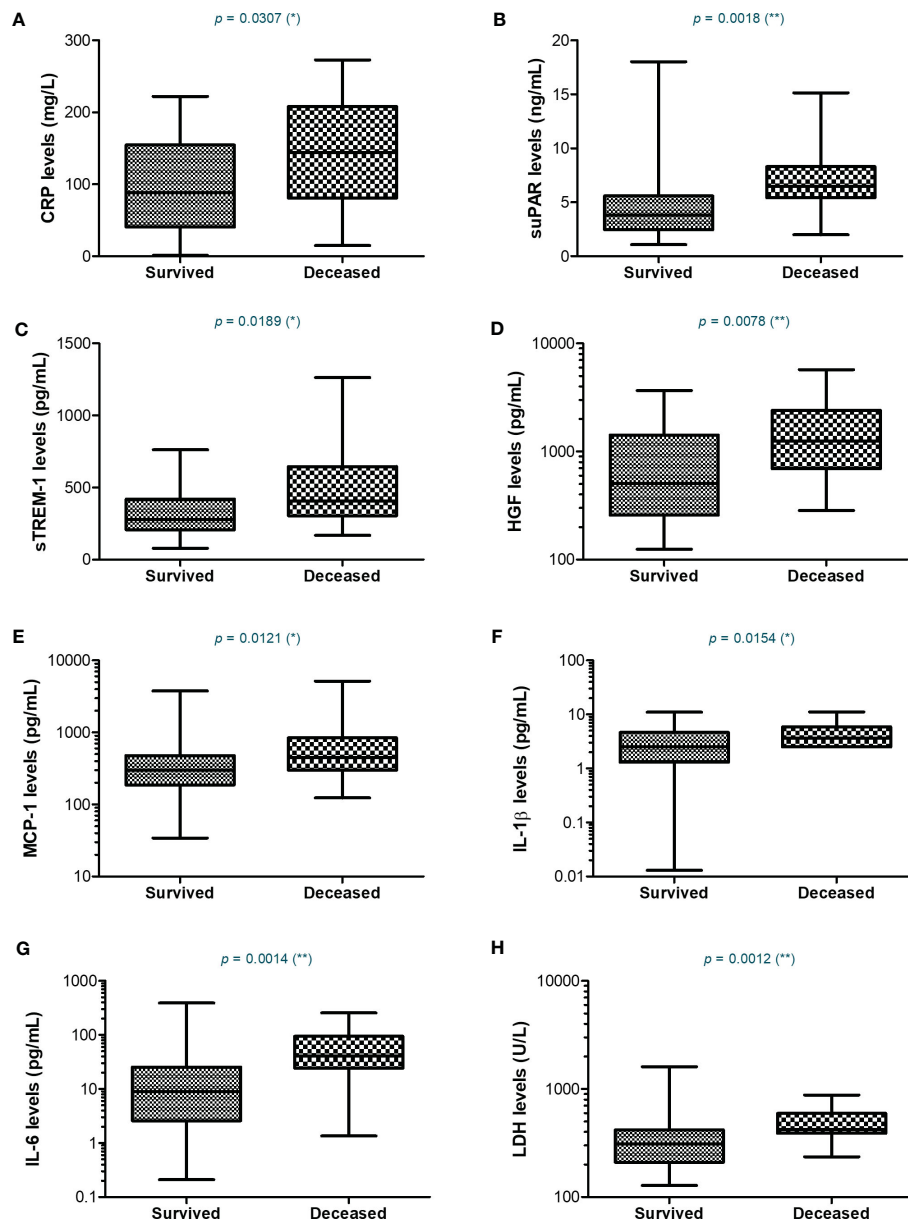


FIGURE 7

Serum profile of CRP and pro-inflammatory cytokines in severe COVID-19 patients stratified based on survival. Box and whiskers representation of (A) CRP, (B) suPAR, (C) sTREM-1, (D) HGF, (E) MCP-1, (F) IL-1 $\beta$ , (G) IL-6, and (H) LDH serum levels for each category of SARS-CoV-2 severe infection: survived or deceased (\*\* $p < 0.01$ , \* $p < 0.05$ , ns – not significant; two-tailed Mann-Whitney test).

significant beneficial effects on the overall survival rate, with Anakinra treatment apparently associating a higher death rate of 43% (Supplementary Figure 8A and Supplementary Table 11). Interestingly, the group of severe cases receiving Tocilizumab had higher levels of ferritin and LDH at hospital admission than the non-AIT group, and comprised 4 non-survivors out of 18 subjects. On the contrary, the group of cases receiving Anakinra had higher levels of multiple inflammatory biomarkers compared to the non-AIT group, including CRP (median value of 144.9 mg/L), suPAR (median value of 5.98 ng/mL), sTREM-1 (median value of 380.7 pg/mL), fibrinogen, ferritin and LDH (Supplementary Figures 8, 9 and Supplementary Table 12). Importantly, no

statistical differences in co-administered medications or co-morbidities were observed among the three analyzed groups of severe cases (Supplementary Table 12).

### 3.8 Discussions

Multiple studies reporting the immunological, hematological, biochemical and coagulation perturbations caused by COVID-19 have emerged during the past 2 years, delineating the hyperinflammatory state that culminates with the cytokine storm and the multiple organ system failure, which are associated with a

TABLE 2 The values of inflammatory biomarkers for each category of COVID-19 patients (mild, moderate and severe) based on SARS-CoV-2 variant infection, Delta or Omicron.

Analyte	Mild		Moderate			Severe		
	Delta	Omicron	Delta	Omicron	p-value	Delta	Omicron	p-value
CRP (mg/L)	5.38 [1.57-6.45]	7.54 [6.24-14.18]	56.91 [20.45-107.8]	35.18 [8.32-103.3]	0.3762	99.77 [50.22-164.8]	92.28 [28.25-183.2]	0.7533
suPAR (ng/mL)	1.99 [1.12-2.63]	1.36 [0.97-1.72]	4.605 [2.985-5.525]	1.9 [1.295-2.665]	<b>&lt; 0.0001</b>	5.74 [3.83-7.11]	2.37 [1.71-3.2]	<b>&lt; 0.0001</b>
sTREM-1 (pg/mL)	109.1 [82.89-121.7]	183.7 [132.7-193.6]	260.3 [191.3-336.8]	243.2 [199.1-486.6]	0.1125	317.4 [212.4-452.1]	319.2 [207.2-464.4]	0.8121
HGF (pg/mL)	204.1 [42.15-301.5]	400.6 [165-710.4]	580.8 [327.5-1610]	299.2 [195.7-625.1]	<b>0.0322</b>	827 [303.7-1762]	569.1 [286.9-1489]	0.3542
MCP-1 (pg/mL)	106.6 [105.9-315.7]	306.8 [217.5-404]	307.1 [201.8-528.2]	253.5 [184.2-330.9]	0.2062	322.4 [207.7-544]	335.3 [209.7-857.4]	0.8211
IL-1 $\beta$ (pg/mL)	1.301 [0-1.301]	1.41 [0.95-2.21]	2.493 [1.301-3.638]	2.104 [0.954-5.541]	<b>0.0405</b>	3.638 [1.301-4.754]	3.251 [1.301-5.541]	0.7272
IL-6 (pg/mL)	0.1 [0.01-1.95]	3.15 [0.5-6.16]	6.025 [3.11-18.01]	4.5 [2.07-8.813]	0.3049	15.11 [4.89-44.78]	6.16 [1.81-37.04]	0.147
NLR	2.469 [0.9167-3.864]	2.678 [1.349-7.59]	5.195 [3.313-7.912]	4.933 [2.742-6.888]	0.4234	8.505 [3.392-13.74]	10.63 [3.566-13.85]	0.6818
PLR	144.1 [135-189.1]	157.6 [107.8-227.9]	231.8 [187.5-336.6]	164.7 [109.6-325.8]	0.0955	249 [178.3-404.5]	302.6 [182.5-429.4]	0.5476
ESR (mm/h)	20 [5-100]	39 [17-50]	67.5 [47.75-80]	60 [26.25-81]	0.3479	75 [45-105]	55 [32-96.25]	0.4037
Fibrinogen (g/L)	4.29 [2.82-4.61]	3.44 [3.24-3.74]	5.065 [4.253-5.58]	3.82 [3.365-5.075]	<b>0.0088</b>	5.37 [4.545-5.82]	5.05 [3.473-6.08]	0.3042
Ferritin ( $\mu$ g/L)	236.6 [236.6-236.6]	190.5 [99.31-525.6]	525.2 [189-1301]	444.5 [261.6-1019]	0.6605	837 [366.5-1624]	988.8 [316.6-2830]	0.7174
LDH (U/L)	137 [130-211]	170 [147-194.5]	295 [214.3-387.8]	225.5 [187.5-317.5]	0.1088	362 [272-525]	331.5 [176-422.3]	0.1471

CRP, C-reactive protein; suPAR, soluble urokinase plasminogen activator receptor; sTREM-1, soluble triggering receptor expressed on myeloid cells-1; HGF, hepatocyte growth factor; MCP-1, monocyte chemoattractant protein-1; IL-1 $\beta$ , interleukin-1 beta; IL-6, interleukin-6; NLR, neutrophil-lymphocyte ratio; PLR, platelet-lymphocyte ratio; ESR, erythrocyte sedimentation rate; LDH, lactate dehydrogenase; p, statistical significance coefficient. The bold values are the statistically significant p-values. The different coloring was performed in order to make it easier to discriminate between the three different groups: mild (gray color), moderate (blue color) and severe (peach color).

high risk of mortality [systematically reviewed by Qin et al. (6)]. Interestingly, many of these studies have centered their investigations on certain parameters and tackled their potential associations with disease severity, mortality or comorbidities (24, 25). For instance, separate studies, collected in a recently published systematic review and meta-analysis, have identified a general pro-inflammatory hypercytokinemia profile (IL-1 $\beta$ , IL-6, IL-8, IL-10, IL-18, TNF- $\alpha$ , IFN- $\gamma$ , MCP-1), augmented by high serum levels of CRP and ferritin, hematological abnormalities (dominated by lymphocytopenia and neutrophilia), coagulation dysfunction (indicated by increased D-dimer, fibrinogen and abnormal APTT and PT) and multiple organ injury (revealed by increased LDH, creatinine, urea, AST, ALT, total bilirubin), to be associated with COVID-19 severity and/or mortality (6). Additional studies, have focused on disparate biomarkers, investigating either the role of suPAR in relation to vascular inflammation, thromboembolism and progression to respiratory failure and disease severity (26–30), the role of sTREM-1 as a sepsis biomarker and mortality predictor (15, 16, 31, 32), or how upregulation of HGF, an anti-inflammatory cytokine, predicted ICU admission and death probability (17, 33,

34). It is worth mentioning that many of these investigations compared severe and non-severe, and hardly discriminated between mild and moderate COVID-19.

Importantly, the present study analyzes CRP, one of the first-identified and best-investigated biomarkers during the COVID-19 pandemics, together with the other above-mentioned biomarkers at hospital admission, and compares their efficiencies in predicting disease severity and mortality. Moreover, we also delineated the biomarkers' profiles in two distinct groups of COVID-19 patients: Delta or predominantly-Omicron infections. First of all, CRP is normally lacking in viral infections; however, the macrophage activation syndrome which characterizes COVID-19 causes the pro-inflammatory hypercytokinemia profile which results in increasing the CRP synthesis by hepatocytes (11, 35). Elevated CRP levels lead to activation of endothelial cells and macrophages, stimulation of complement system *via* the classical route and inhibition of apoptosis of neutrophils, pathophysiological changes that exacerbate the vascular inflammation and thrombotic complication events which culminate with the cytokine storm (7, 11, 35). Indeed, recent studies have reported that elevated CRP

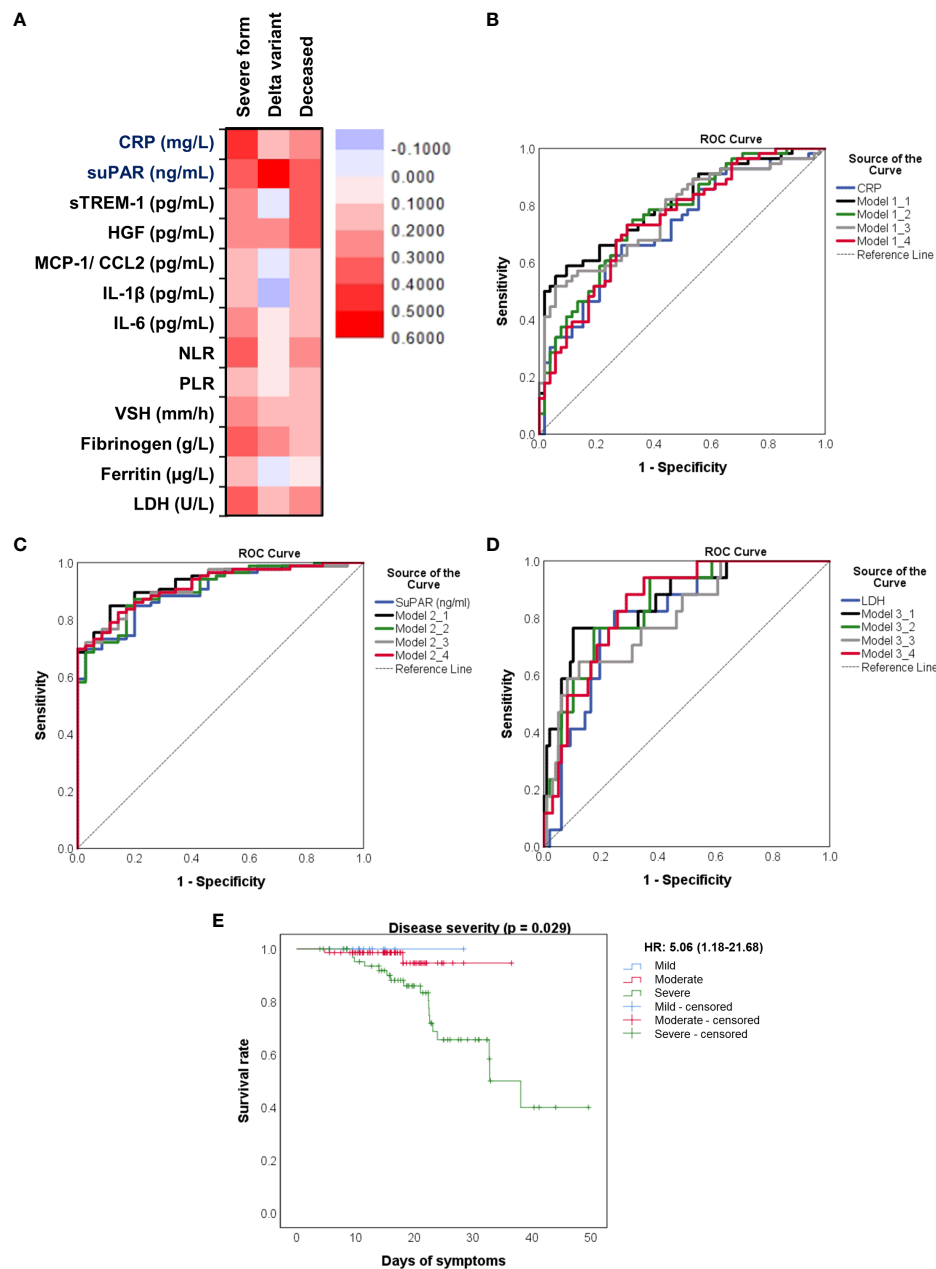


FIGURE 8

Distinct pro-inflammatory biomarkers associate with disease severity, Delta variant infection or increased death rate. **(A)** Heat map of correlation coefficients of pro-inflammatory biomarkers with disease severity, Delta variant infection or deceased status. ROC curves generated for the **(B)** association of CRP and other pro-inflammatory biomarkers with severe COVID-19, **(C)** association of suPAR and other pro-inflammatory biomarkers with Delta variant infection, **(D)** association of LDH and other inflammatory biomarkers with mortality. The mathematical models from **(B–D)** are detailed in [Supplementary Tables 3–5](#), respectively. **(E)** Kaplan-Meier survival curves for each category of COVID-19 patients: mild, moderate and severe.

together with higher D-Dimers and fibrinogen serum levels characterize the hyperinflammation and hypercoagulable states seen in severe and/or deceased COVID-19 patients (7, 36). Additional observational studies have reported higher CRP, NLR and LDH values in non-survivors, and their association with an increased risk of developing acute respiratory distress syndrome, cytokine release syndrome and sepsis (reviewed in (35)). Importantly, several studies have found that high CRP levels (> 100 mg/L) were associated with higher odds for ventilator

requirements (OR 2.5) and upgrade to ICU (OR 3.2), or even increased mortality rate (77.4% compared to 22.6% characterizing the group of cases with CRP < 100 mg/L) (8, 37). Interestingly, in a cohort study conducted on 2782 COVID-19 subjects, the serum CRP levels above 108 mg/L were associated with a 32.2% mortality rate (compared to only 17.8%, as seen for those with lower CRP values) and a 1.8-fold higher risk for disease severity (7). Importantly, high CRP levels associated with increased LDH and creatinine values as predictors for disease severity and death in

TABLE 3 Statistical evaluation of pro-inflammatory biomarkers in association with severe COVID-19.

Analyte	AUC	S.E.	<i>p</i> -value	95% Confidence Interval	Cut-off value	Sensitivity	Specificity
CRP (mg/L)	0.720	0.049	<b>0.000</b>	0.625-0.816	76.07	0.661	0.712
suPAR (ng/mL)	0.698	0.050	<b>0.000</b>	0.599-0.797	3.76	0.643	0.673
sTREM-1 (pg/mL)	0.674	0.052	<b>0.002</b>	0.572-0.777	247.27	0.696	0.635
HGF (pg/mL)	0.613	0.054	<b>0.042</b>	0.507-0.719	777.52	0.500	0.731
MCP-1 (pg/mL)	0.590	0.055	0.108	0.483-0.697	267.75	0.625	0.558
IL-1 $\beta$ (pg/mL)	0.582	0.055	0.141	0.474-0.690	3.16	0.464	0.692
IL-6 (pg/mL)	0.680	0.051	<b>0.001</b>	0.580-0.781	7.31	0.643	0.692
NLR	0.692	0.052	<b>0.001</b>	0.590-0.793	8.21	0.571	0.827
PLR	0.634	0.054	<b>0.016</b>	0.527-0.741	242.99	0.625	0.712
ESR (mm/h)	0.633	0.054	<b>0.017</b>	0.527-0.738	73.50	0.518	0.731
Fibrinogen (g/L)	0.703	0.050	<b>0.000</b>	0.606-0.801	4.64	0.732	0.558
Ferritin ( $\mu$ g/L)	0.658	0.053	<b>0.005</b>	0.555-0.761	620.80	0.643	0.635

CRP, C-reactive protein; suPAR, soluble urokinase plasminogen activator receptor; sTREM-1, soluble triggering receptor expressed on myeloid cells-1; HGF, hepatocyte growth factor; MCP-1, monocyte chemoattractant protein-1; IL-1 $\beta$ , interleukin-1 beta; IL-6, interleukin-6; NLR, neutrophil-lymphocyte ratio; PLR, platelet-lymphocyte ratio; ESR, erythrocyte sedimentation rate; LDH, lactate dehydrogenase; AUC, area under curve; *p*, statistical significance coefficient. The bold values are the statistically significant *p*-values.

TABLE 4 Statistical evaluation of pro-inflammatory biomarkers in association with Delta variant infection.

Analyte	AUC	S.E.	<i>p</i> -value	95% Confidence Interval	Cut-off value	Sensitivity	Specificity
CRP (mg/L)	0.577	0.062	0.199	0.455-0.698	65.36	0.616	0.571
suPAR (ng/mL)	0.912	0.026	<b>0.000</b>	0.860-0.963	3.24	0.767	0.914
sTREM-1 (pg/mL)	0.560	0.060	0.312	0.442-0.679	246.06	0.616	0.571
HGF (pg/mL)	0.659	0.055	<b>0.007</b>	0.553-0.766	434.61	0.630	0.600
MCP-1 (pg/mL)	0.580	0.059	0.177	0.465-0.695	316.67	0.493	0.686
IL-1 $\beta$ (pg/mL)	0.534	0.063	0.564	0.411-0.658	2.27	0.603	0.543
IL-6 (pg/mL)	0.670	0.057	<b>0.004</b>	0.559-0.781	9.87	0.534	0.829
NLR	0.570	0.061	0.239	0.451-0.689	6.34	0.548	0.600
PLR	0.584	0.064	0.161	0.458-0.710	202.78	0.671	0.486
ESR (mm/h)	0.627	0.058	<b>0.033</b>	0.513-0.742	67.50	0.548	0.657
Fibrinogen (g/L)	0.635	0.063	<b>0.023</b>	0.512-0.759	3.90	0.849	0.543
Ferritin ( $\mu$ g/L)	0.521	0.062	0.725	0.399-0.643	466.15	0.644	0.457
LDH (U/L)	0.655	0.060	<b>0.009</b>	0.538-0.773	254.00	0.753	0.600

CRP, C-reactive protein; suPAR, soluble urokinase plasminogen activator receptor; sTREM-1, soluble triggering receptor expressed on myeloid cells-1; HGF, hepatocyte growth factor; MCP-1, monocyte chemoattractant protein-1; IL-1 $\beta$ , interleukin-1 beta; IL-6, interleukin-6; NLR, neutrophil-lymphocyte ratio; PLR, platelet-lymphocyte ratio; ESR, erythrocyte sedimentation rate; LDH, lactate dehydrogenase; AUC, area under curve; *p*, statistical significance coefficient. The bold values are the statistically significant *p*-values.

other coronavirus infections, SARS in 2003 and MERS in 2012 (38–40). In influenza pneumonia (H1N1, H7N9), a high CRP value also correlated with disease severity, proving to be an independent predictor of mortality in the H7N9 infection, while leading to the cytokine storm characterized by elevated IL-6, MCP-1, and IP-10 levels (41, 42).

In our study we have shown that the mean serum CRP levels evolved from 12.59 mg/L in mild cases to 67.25 mg/L and 107.7 mg/L in moderate and severe patients, respectively. Among moderate cases, 25.4% had CRP values above 100 mg/L at hospital admission

and survived, while the 2 deceased subjects had the CRP levels less than 100 mg/L. Among the severe cases, 39.4% of the COVID-19 subjects with high CRP (> 100 mg/L) died, while the mortality rate was only 14.3% among the cases with CRP less than 100 mg/L. In our study group (153 COVID-19 patients), the general mortality rate varied from 6.9% for CRP < 100 mg/L to 25.5% for cases with CRP > 100 mg/L. Importantly, the CRP values varied significantly between survivors (96.19 mg/L [95% CI 77.13–115.3]) and non-survivors (139.8 mg/L [95% CI 103.6–176], *p* = 0.0307), and a cut-off value of 79.12 mg/L yielded a sensitivity of 0.765 and specificity of

TABLE 5 Statistical evaluation of pro-inflammatory biomarkers in association with mortality.

Analyte	AUC	S.E.	<i>p</i> -value	95% Confidence Interval	Cut-off value	Sensitivity	Specificity
CRP (mg/dL)	0.698	0.069	<b>0.010</b>	0.562-0.834	79.12	0.765	0.604
suPAR (ng/mL)	0.771	0.060	<b>0.000</b>	0.653-0.889	5.20	0.765	0.780
sTREM-1 (pg/mL)	0.767	0.066	<b>0.001</b>	0.637-0.896	334.06	0.765	0.747
HGF (pg/mL)	0.797	0.054	<b>0.000</b>	0.692-0.902	802.76	0.824	0.703
MCP-1 (pg/mL)	0.701	0.067	<b>0.009</b>	0.570-0.832	389.32	0.588	0.758
IL-1 $\beta$ (pg/mL)	0.785	0.048	<b>0.000</b>	0.691-0.879	3.44	0.706	0.692
IL-6 (pg/mL)	0.752	0.062	<b>0.001</b>	0.631-0.873	14.86	0.765	0.736
NLR	0.685	0.069	<b>0.016</b>	0.550-0.820	8.39	0.588	0.670
PLR	0.524	0.074	0.758	0.378-0.669	242.99	0.529	0.549
ESR (mm/h)	0.562	0.067	0.418	0.431-0.693	73.50	0.529	0.626
Fibrinogen (g/L)	0.594	0.066	0.220	0.464-0.724	5.07	0.588	0.560
Ferritin ( $\mu$ g/L)	0.703	0.058	<b>0.008</b>	0.590-0.816	1017.50	0.706	0.681
LDH (U/L)	0.809	0.050	<b>0.000</b>	0.710-0.907	379.50	0.824	0.758

CRP, C-reactive protein; suPAR, soluble urokinase plasminogen activator receptor; sTREM-1, soluble triggering receptor expressed on myeloid cells-1; HGF, hepatocyte growth factor; MCP-1, monocyte chemoattractant protein-1; IL-1 $\beta$ , interleukin-1 beta; IL-6, interleukin-6; NLR, neutrophil-lymphocyte ratio; PLR, platelet-lymphocyte ratio; ESR, erythrocyte sedimentation rate; LDH, lactate dehydrogenase; AUC, area under curve; *p*, statistical significance coefficient. The bold values are the statistically significant *p*-values.

TABLE 6 Univariate and multivariate Cox regression analysis of paraclinical and clinical variables in COVID-19 patients.

Variable	Univariate analysis			Multivariate analysis		
	HR	95% CI	<i>p</i> -value	HR	95% CI	<i>p</i> -value
CRP (mg/L)	2.364	0.844-6.623	0.102			
suPAR (mg/mL)	7.747	2.807-21.384	<b>&lt; 0.0001</b>	6.688	1.692-26.435	<b>0.007</b>
sTREM-1 (pg/mL)	5.109	1.798-14.522	<b>0.002</b>	1.901	0.513-7.044	0.336
HGF (pg/mL)	4.121	1.570-10.819	<b>0.004</b>	1.334	0.309-5.762	0.699
MCP-1 (pg/mL)	2.917	1.143-7.444	<b>0.025</b>	0.323	0.084-1.239	0.099
IL-1 (pg/mL)	3.251	1.289-8.203	<b>0.013</b>	0.814	0.225-2.940	0.753
IL-6 (pg/mL)	5.276	1.903-14.628	<b>0.001</b>	10.358	2.238-47.943	<b>0.003</b>
NLR	2.120	0.746-6.026	0.159			
Ferritin ( $\mu$ g/L)	4.257	1.693-10.707	<b>0.002</b>	0.809	0.262-2.495	0.713
LDH (U/L)	5.740	1.897-17.373	<b>0.002</b>	6.794	1.945-23.733	<b>0.003</b>
Severe (yes)	5.367	1.206-23.892	<b>0.027</b>	1.408	0.273-7.259	0.683
Age (> 60 years)	1.141	0.378-3.442	0.815			
Gender (M)	1.359	0.537-3.436	0.518			
Vaccination (no)	1.830	0.641-5.223	0.259			

CRP, C-reactive protein; suPAR, soluble urokinase plasminogen activator receptor; sTREM-1, soluble triggering receptor expressed on myeloid cells-1; HGF, hepatocyte growth factor; MCP-1, monocyte chemoattractant protein-1; IL-1 $\beta$ , interleukin-1 beta; IL-6, interleukin-6; NLR, neutrophil-lymphocyte ratio; LDH, lactate dehydrogenase; HR, hazard ratio; CI, confidence interval; *p*, statistical significance coefficient. The bold values are the statistically significant *p*-values.

0.604 for mortality prediction. The CRP values further significantly correlated with immunological changes (marked increase of the pro-inflammatory biomarkers IL-1 $\beta$ , IL-6, MCP-1, with more pronounced changes in females than in male subjects) hematological abnormalities (increased WBC, neutrophilia, lymphopenia and eosinopenia with elevated NLR, PLR),

hypercoagulation (increased D-Dimers, fibrinogen, and suPAR), and end-organ damage (high LDH, urea, AST).

Referring to hypercoagulation with venous thromboembolic events (VTE), recent studies have pointed out that the traditional markers such as D-Dimers and fibrinogen are less reliable than suPAR in predicting VTE in COVID-19 (30). The uPAR is a



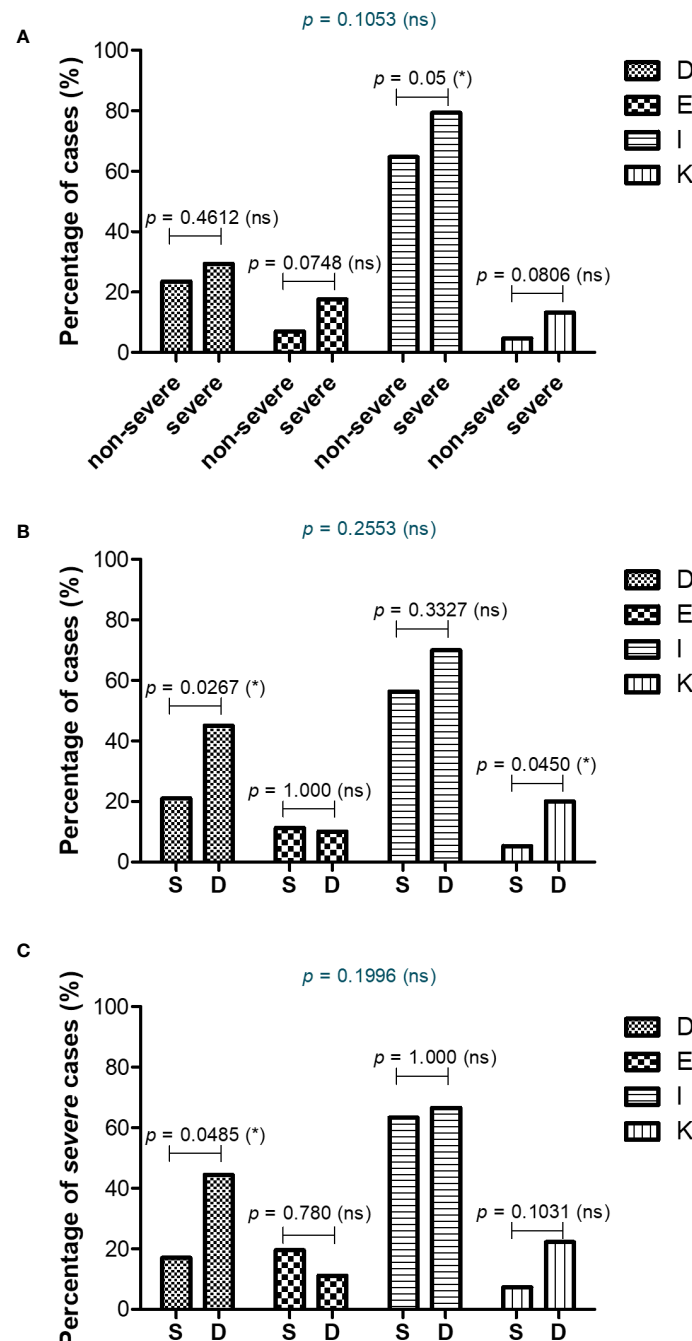


FIGURE 9

Comorbidities associated with COVID-19 severity and mortality. Differences in comorbidity rates (A) between non-severe and severe COVID-19 patients, (B) between survived and deceased COVID-19 patients, and (C) between survived and deceased severe COVID-19 cases (\* $p < 0.05$ , ns – not significant; chi-squared test). D = Diseases of the blood involving the immune mechanism (anemia, purpura and other hemorrhagic conditions), E = Endocrine and metabolic disorders, I = Diseases of the circulatory system, K = Diseases of liver and gallbladder.

glycosylphosphatidylinositol-anchored membrane protein bound to immune cells (monocytes, macrophages and activated T cells), fibroblasts and endothelial cells. During inflammation, uPAR is cleaved and the soluble form, named suPAR, is released into circulation, and acting as a “damage-associated molecular pattern” (DAMP), it exerts local vascular inflammation or distal immune effects (26, 43). Elevated suPAR concentrations have been reported in other viral infections caused by hepatitis C and B

viruses, HIV or Hantavirus, where it showed correlation with disease severity and mortality (44–47). SuPAR was also shown to be a discriminator of COVID-19 severity and a predictor of hospitalization time, findings which we have confirmed in our study (27–29). Additionally, we identified the mean serum values in mild, moderate and severe COVID-19 cases that followed a gradual increasing trend: 1.47 ng/mL, 3.68 ng/mL, and 5.06 ng/mL. Of interest, the suPAR levels showed the highest difference between

Delta and Omicron cases: mean values of 5.21 ng/mL vs 2.09 ng/mL. Additionally, we have identified suPAR as a good independent discriminator between non-survivors and survivors, with a cut-off value of 5.2 ng/mL yielding a sensitivity of 0.765 and a specificity of 0.780. As the suPAR levels corroborate with cardiovascular diseases (CVD) (48), it is important to mention that no significant differences were noticed in the CVD comorbidities among severe and non-severe COVID-19 subjects or survivors and non-survivors.

As an indirect readout of hyperinflammation, we further considered investigating the serum levels of anti-inflammatory molecules, such as sTREM-1 and HGF. Interestingly, the high CRP levels were also associated with the up-regulation of both these two biomarkers that play central roles in modulating inflammation. For instance, TREM-1 is a recently characterized pathogen recognition receptor (PRR) constitutively expressed on the surface of peripheral neutrophils and monocytes, but also by macrophages, epithelial and endothelial cells (31, 49, 50). Upon TLR signaling, its expression is up-regulated to further amplify the pro-inflammatory innate immune responses, by activating its downstream effectors such as PLC $\gamma$ , MAPK and PI3K which promote the synthesis and release of inflammatory cytokines/chemokines (51, 52). During sepsis and hyperinflammation, TREM-1 activity is enhanced, leading to overactivation of macrophages that start to release metalloproteinases that are believed to proteolytically cleave the membrane TREM-1 and generate its soluble form, sTREM-1 (15, 53). During these pathological processes, sTREM-1 is believed to be additionally produced by macrophages and neutrophils as a splicing variant (54). Of interest, sTREM-1 act as a decoy for unknown TREM-1 ligands, thus counteracting the inflammatory cytokine release. Similarly, the synthesis of HGF, a pleiotropic cytokine, is up-regulated in macrophages and mesenchymal cells by pro-inflammatory cytokines such as IL-1 $\beta$ , TNF- $\alpha$  and IFN- $\gamma$  (55–57). Importantly, HGF acts by promoting lung tissue repair through inhibiting the apoptosis of endothelial and epithelial cells, and plays a predominantly anti-inflammatory role by reducing IL-6 secretion at the expense of IL-10 production by macrophages (57–59). HGF has been previously shown to be also increased in severe cases of H1N1-induced pneumonia (60). Both sTREM-1 and HGF have been identified as predictors for disease severity and poor outcome in patients with COVID-19 (15–17, 31–34).

In our study we highlighted a gradual increase from mild to severe cases for both these two biomarkers, sTREM-1 and HGF. For instance, sTREM-1 mean values ranged from 147 pg/mL in mild cases to 289 pg/mL and 355 pg/mL in moderate and severe subjects, respectively. For HGF, the mean values from mild, to moderate, and severe were: 357 pg/mL, 819 pg/mL, and 1157 pg/mL. Importantly, sTREM-1 showed a very strong correlation with MCP-1 levels, while serum HGF strongly correlated with IL-1 $\beta$  in severe cases. They also showed significantly higher values in non-survivors compared to survivors (50% and 80% increase for sTREM-1 and HGF, respectively). While the sTREM-1 values were the same between the Delta and the predominantly-Omicron infected groups, the HGF values were significantly higher in the Delta group.

When comparing these inflammatory biomarkers for predicting the disease severity, the serum CRP levels at hospital admission best

discriminated between severe and non-severe cases, followed by the LDH levels. For discriminating between Delta and Omicron infections, the suPAR levels showed the most prominent differences between these two variant infections with 64.3% of Delta cases with values over 4 ng/mL (the upper limit of the normal range) compared to only 5% of Omicron cases, observation which reassures the previous studies reporting lower rate of thromboembolic events in Omicron-infected individuals. Interestingly, when investigating the prediction capacity for poor outcome, LDH proved an excellent discrimination capacity, followed by HGF, sTREM-1 and suPAR in our study group.

As age might influence the serum levels of our investigated biomarkers (6), we further stratified the COVID-19 patients in two categories, younger or older than 60 years. Of all biomarkers, only sTREM-1 serum levels showed consistently higher values in the older groups of mild, moderate and severe subjects. We also noticed discrepancies between females and males: the females subjects showed more prominent significant changes with disease severity than male individuals. We could speculate that this is happening as males are known to exhibit higher basal inflammation and a weaker response against a stimulus, while displaying less efficient antioxidant mechanisms. These physiological differences might also contribute to the increased risk for males of developing severe forms of COVID-19 and a worse overall outcome, when compared with females. Nevertheless, the higher frequency of comorbidities observed in the severe group of subjects, including metabolic disorders and diseases of the circulatory system, might have contributed to the initial higher serum values of the here-in investigated inflammatory biomarkers.

Our study has also some limitations, including the sample size limited to 153 COVID-19 patients. However, the patient cohort was well-characterized due to the prospective design of the study, with proper review for all medical records and comorbidities, and assessment of clinical/paraclinical variables. Additionally, we should mention that not all the cases included in the Omicron group were confirmed by sequencing. Still, the predominantly-Omicron group comprised the cases admitted to the hospital in a time-frame when a general reduction in the Delta variant infections was nationally confirmed by the Romanian National Institute of Public Health (20, 21). Of note, larger cohort studies are needed to further confirm our described observations.

Overall, our data clearly state an important hyperinflammatory phenotype associated with disease severity characterized by enhanced serum levels of CRP, MCP-1, IL-1 and IL-6. When comparing this disease profile with the effect obtained upon vaccination, several differences were detected. For instance, in our previous study (22), while comparing the humoral responses following dual BNT162b2 vaccination in naïve or previously-infected SARS-CoV-2 individuals, a previous natural infectious status was associated with increased anti-SARS-CoV-2 antibody titers accompanied by increased IL-1 and IL-6, but lower levels of CRP and MCP-1. This serum profile reflects rather an effective polarization of the immune response towards Th2 with augmented specific-antibody generation, while minimizing the effects of the Th1 arm on cellular immunity, indirectly mirrored by reduced inflammation with lower CRP and MCP-1 levels following

vaccination in primed subjects. Importantly, the severe cases of COVID-19 investigated in the present study associated a major increase in the CRP and MCP-1 serum levels assisted by enhanced suPAR, sTREM-1 and HGF values. The levels of these mentioned inflammation modulators were extremely higher in non-survivors and this molecular profile might also explain the coagulation abnormalities and the higher rate of hematological comorbidities (thrombocytopenia and anemia) characterizing these subjects at hospital admission. Starting from these observations, several questions emerge for potential studies to be tackled in future research. For instance, is it a stronger Th2 response, with humoral immunity assisted by a lower Th1-induced pro-inflammatory phenotype, beneficial for minimizing disease severity and mortality in SARS-CoV-2-infected patients? Preliminary reported data have indeed suggested that early treatment of COVID-19 with drugs targeting IL-1 (using an IL-1 receptor antagonist) or IL-6 (using humanized anti-IL-6 receptor monoclonal antibodies) proved to be beneficial, by reducing the mortality rate among severe cases of COVID-19 (11, 29, 30, 61). The retrospective analysis of our cohort of severe patients did not reveal significant improvement in the survival rate of those exposed to therapies targeting IL-6 (Tocilizumab) or IL-1 (Anakinra). However, the initial laboratory tests indicated a higher pro-inflammatory response in those patients compared to the subjects not exposed to such therapies, thus causing difficulties in achieving solid conclusions. It is most likely that the reported death rate among severe patients to be underestimated considering the expected beneficial effects of the applied anti-interleukin therapies. Importantly, no significant differences in the basal laboratory tests were observed among non-vaccinated or previously vaccinated subjects (which encountered only for 24%), in the context of a national vaccination rate of 40%.

To conclude, our data are of importance, as this is the first study to our knowledge that analyzes and compares CRP with the other 12 key predictors of disease severity and mortality, previously reported for COVID-19 (including suPAR, sTREM-1, HGF, MCP-1, LDH), while including mild, moderate and severe cases. Thus, we were able to identify that the CRP serum levels, among all investigated biomarkers, best discriminate between severe and non-severe subjects, while suPAR showed significant higher values in Delta-infections, and LDH proved to be an excellent predictor for mortality in COVID-19.

## Data availability statement

The original contributions presented in the study are included in the article/Supplementary Material. Further inquiries can be directed to the corresponding author.

## Ethics statement

The studies involving human participants were reviewed and approved by Institutional Ethics Committee - St Parascheva Clinical Hospital for Infectious Diseases, Iasi, Romania. The patients/

participants provided their written informed consent to participate in this study.

## Author contributions

TP, MP-T and EGM conceptualized the study. TP, CEP, CGP, I-LM collected the samples and the relevant clinical information for each patient. MP-T and DC processed the samples. MP-T performed the initial statistical analysis with additional contribution from MM. TP, MP-T, PC and EGM analyzed the data. TP and MP-T prepared the initial draft which was reviewed and commented by all authors. All authors contributed to the article and approved the submitted version.

## Funding

The research was funded from the budget of a doctoral grant from *Grigore T. Popa* University of Medicine and Pharmacy of Iasi no. 158/2022 and POC/448/1/1/127606 CENEMED project no. 367/390043/2021.

## Acknowledgments

The authors would like to thank all co-workers from the Laboratory of *St Parascheva* Clinical Hospital for Infectious Diseases and from the Laboratory of Immunology at *St. Spiridon* County Clinical Emergency Hospital of Iasi for their support during the research time and to express their deepest gratitude to all participants in this study.

## Conflict of interest

The authors declare that the research was conducted in the absence of any commercial or financial relationships that could be construed as a potential conflict of interest.

## Publisher's note

All claims expressed in this article are solely those of the authors and do not necessarily represent those of their affiliated organizations, or those of the publisher, the editors and the reviewers. Any product that may be evaluated in this article, or claim that may be made by its manufacturer, is not guaranteed or endorsed by the publisher.

## Supplementary material

The Supplementary Material for this article can be found online at: <https://www.frontiersin.org/articles/10.3389/fimmu.2023.1213246/full#supplementary-material>

## References

- Bollyky TJ, Castro E, Aravkin AY, Bhangdia K, Dalos J, Hulland EN, et al. Assessing COVID-19 pandemic policies and behaviours and their economic and educational trade-offs across US states from Jan 1, 2020, to July 31, 2022: an observational analysis. *Lancet* (2023) 401(10385):1341–60. doi: 10.1016/S0140-6736(23)00461-0
- Antonelli M, Pujol JC, Spector TD, Ourselin S, Steves CJ. Risk of long COVID associated with delta versus omicron variants of SARS-CoV-2. *Lancet* (2022) 399(10343):2263–4. doi: 10.1016/S0140-6736(22)00941-2
- Mehta OP, Bhandari P, Raut A, Kacimi SEO, Huy NT. Coronavirus disease (COVID-19): comprehensive review of clinical presentation. *Front Public Health* (2020) 8:582932. doi: 10.3389/fpubh.2020.582932
- Mardian Y, Kosasih H, Karyana M, Neal A, Lau CY. Review of current COVID-19 diagnostics and opportunities for further development. *Front Med (Lausanne)* (2021) 8:615099. doi: 10.3389/fmed.2021.615099
- Malik P, Patel U, Mehta D, Patel N, Kelkar R, Akrmah M, et al. Biomarkers and outcomes of COVID-19 hospitalisations: systematic review and meta-analysis. *BMJ Evid Based Med* (2021) 26(3):107–8. doi: 10.1136/bmjebm-2020-111536
- Qin R, He L, Yang Z, Jia N, Chen R, Xie J, et al. Identification of parameters representative of immune dysfunction in patients with severe and fatal COVID-19 infection: a systematic review and meta-analysis. *Clin Rev Allergy Immunol* (2023) 64(1):33–65. doi: 10.1007/s12016-021-08908-8
- Smilowitz NR, Kunichoff D, Garshick M, Shah B, Pillinger M, Hochman JS, et al. C-reactive protein and clinical outcomes in patients with COVID-19. *Eur Heart J* (2021) 42(23):2270–9. doi: 10.1093/eurheartj/ehaa1103
- Bouayed MZ, Laaribi I, Chatar CEM, Benaini I, Bouazzaoui MA, Oujidi Y, et al. C-reactive protein (CRP): a poor prognostic biomarker in COVID-19. *Front Immunol* (2022) 13:1040024. doi: 10.3389/fimmu.2022.1040024
- Li Q, Wang Y, Sun Q, Knopf J, Herrmann M, Lin L, et al. Immune response in COVID-19: what is next? *Cell Death Differ* (2022) 29(6):1107–22. doi: 10.1038/s41418-022-01015-x
- Pan Y, Jiang X, Yang L, Chen L, Zeng X, Liu G, et al. SARS-CoV-2-specific immune response in COVID-19 convalescent individuals. *Signal Transduct Target Ther* (2021) 6(1):256. doi: 10.1038/s41392-021-00686-1
- Chen CH, Lin SW, Shen CF, Hsieh KS, Cheng CM. Biomarkers during COVID-19: mechanisms of change and implications for patient outcomes. *Diagnostics (Basel)* (2022) 12(2):509. doi: 10.3390/diagnostics12020509
- Song P, Li W, Xie J, Hou Y, You C. Cytokine storm induced by SARS-CoV-2. *Clin Chim Acta* (2020) 509:280–7. doi: 10.1016/j.cca.2020.06.017
- Ranjbar M, Rahimi A, Baghernejadan Z, Ghorbani A, Khorramdelazad H. Role of CCL2/CCR2 axis in the pathogenesis of COVID-19 and possible treatments: all options on the table. *Int Immunopharmacol* (2022) 113(Pt A):109325. doi: 10.1016/j.intimp.2022.109325
- Sarif J, Raychaudhuri D, D'Rozario R, Bandopadhyay P, Singh P, Mehta P, et al. Plasma gradient of soluble urokinase-type plasminogen activator receptor is linked to pathogenic plasma proteome and immune transcriptome and stratifies outcomes in severe COVID-19. *Front Immunol* (2021) 12:738093. doi: 10.3389/fimmu.2021.738093
- da Silva-Neto PV, de Carvalho JCS, Pimentel VE, Perez MM, Toro DM, Fraga-Silva TFC, et al. sTREM-1 predicts disease severity and mortality in COVID-19 patients: involvement of peripheral blood leukocytes and MMP-8 activity. *Viruses* (2021) 13(12):2521. doi: 10.3390/v13122521
- de Noijer AH, Grondman I, Lambden S, Kooistra EJ, Janssen NAF, Kox M, et al. Increased sTREM-1 plasma concentrations are associated with poor clinical outcomes in patients with COVID-19. *Biosci Rep* (2021) 41(7):BSR20210940. doi: 10.1042/BSR20210940
- Perreau M, Suffiotti M, Marques-Vidal P, Wiedemann A, Levy Y, Laouenan C, et al. The cytokines HGF and CXCL13 predict the severity and the mortality in COVID-19 patients. *Nat Commun* (2021) 12(1):4888. doi: 10.1038/s41467-021-25191-5
- Bivona G, Agnello L, Ciccio M. Biomarkers for prognosis and treatment response in COVID-19 patients. *Ann Lab Med* (2021) 41(6):540–8. doi: 10.3343/alm.2021.41.6.540
- Trofin F, Nastase EV, Vata A, Iancu LS, Lunca C, Buzila ER, et al. The immune, inflammatory and hematological response in COVID-19 patients, according to the severity of the disease. *Microorganisms* (2023) 11(2):319. doi: 10.3390/microorganisms11020319
- Briciu V, Topan A, Calin M, Dobrota R, Leucuta DC, Lupse M. Comparison of COVID-19 severity in vaccinated and unvaccinated patients during the delta and omicron wave of the pandemic in a Romanian tertiary infectious diseases hospital. *Healthcare (Basel)* (2023) 11(3):373. doi: 10.3390/healthcare11030373
- The Romanian National Institute of Public Health. Available at: <https://www.cnsrbt.ro/index.php/analiza-cazuri-confirmate-covid19/2929-s-01-informare-cazuri-cu-variante-care-determina-ingrijorare-voc/file> (Accessed 21 November 2022).
- Pavel-Tanasa M, Constantinescu D, Cianga CM, Anisie E, Mereuta AI, Tuchilus CG, et al. Associate with antibody immune responses following dual BNT162b2 vaccination within individuals younger than 60 years. *Front Immunol* (2022) 13:1000006. doi: 10.3389/fimmu.2022.1000006
- Wang C, Liu B, Zhang S, Huang N, Zhao T, Lu QB, et al. Differences in incidence and fatality of COVID-19 by SARS-CoV-2 omicron variant versus delta variant in relation to vaccine coverage: a world-wide review. *J Med Virol* (2023) 95(1):e28118. doi: 10.1002/jmv.28118
- Miftode E, Miftode L, Coman I, Prepeliuc C, Obreja M, Stamateanu O, et al. Diabetes mellitus-a risk factor for unfavourable outcome in COVID-19 patients-the experience of an infectious diseases regional hospital. *Healthcare (Basel)* (2021) 9(7):788. doi: 10.3390/healthcare9070788
- Miftode E, Lunca C, Manciu C, Vata A, Hunea I, Miftode L, et al. COVID-19: a course through stormy waters. *Medical-Surgical J* (2020) 124(3):351–63.
- Rasmussen LJH, Petersen JEV, Eugen-Olsen J. Soluble urokinase plasminogen activator receptor (suPAR) as a biomarker of systemic chronic inflammation. *Front Immunol* (2021) 12:780641. doi: 10.3389/fimmu.2021.780641
- Enocsson H, Idoff C, Gustafsson A, Govender M, Hopkins F, Larsson M, et al. Soluble urokinase plasminogen activator receptor (suPAR) independently predicts severity and length of hospitalisation in patients with COVID-19. *Front Med (Lausanne)* (2021) 8:791716. doi: 10.3389/fmed.2021.791716
- Rovina N, Akinosoglou K, Eugen-Olsen J, Hayek S, Reiser J, Giamarellos-Bourboulis EJ. Soluble urokinase plasminogen activator receptor (suPAR) as an early predictor of severe respiratory failure in patients with COVID-19 pneumonia. *Crit Care* (2020) 24(1):187. doi: 10.1186/s13054-020-02897-4
- Altintas I, Eugen-Olsen J, Seppala S, Tingleff J, Stauning MA, El Caidi NO, et al. suPAR cut-offs for risk stratification in patients with symptoms of COVID-19. *biomark Insights* (2021) 16:11772719211034685. doi: 10.1177/11772719211034685
- Luo S, Vasbinder A, Du-Fay-de-Lavallaz JM, Gomez JMD, Suboc T, Anderson E, et al. Soluble urokinase plasminogen activator receptor and venous thromboembolism in COVID-19. *J Am Heart Assoc* (2022) 11(18):e025198. doi: 10.1161/JAHA.122.025198
- Siskind S, Brenner M, Wang P. TREM-1 modulation strategies for sepsis. *Front Immunol* (2022) 13:907387. doi: 10.3389/fimmu.2022.907387
- Van Singer M, Brahier T, Ngai M, Wright J, Weckman AM, Erice C, et al. COVID-19 risk stratification algorithms based on sTREM-1 and IL-6 in emergency department. *J Allergy Clin Immunol* (2021) 147(1):99–106 e4. doi: 10.1016/j.jaci.2020.10.001
- Meizlish ML, Pine AB, Bishai JD, Goshua G, Nadelmann ER, Simonov M, et al. A neutrophil activation signature predicts critical illness and mortality in COVID-19. *Blood Adv* (2021) 5(5):1164–77. doi: 10.1182/bloodadvances.2020003568
- Haljasmagi L, Salumets A, Rumm AP, Jurgenson M, Krassohhina E, Remm A, et al. Longitudinal proteomic profiling reveals increased early inflammation and sustained apoptosis proteins in severe COVID-19. *Sci Rep* (2020) 10(1):20533. doi: 10.1038/s41598-020-77525-w
- Luan YY, Yin CH, Yao YM. Update advances on c-reactive protein in COVID-19 and other viral infections. *Front Immunol* (2021) 12:720363. doi: 10.3389/fimmu.2021.720363
- McAlpine LS, Zubair AS, Maran I, Chojecka P, Lleba P, Jasne AS, et al. Ischemic stroke, inflammation, and endotheliopathy in COVID-19 patients. *Stroke* (2021) 52(6):e233–8. doi: 10.1161/STROKEAHA.120.031971
- Ullah W, Thalambedu N, Haq S, Saeed R, Khanal S, Tariq S, et al. Predictability of CRP and d-dimer levels for in-hospital outcomes and mortality of COVID-19. *J Community Hosp Intern Med Perspect* (2020) 10(5):402–8. doi: 10.1080/20009666.2020.1798141
- Gao H, Yao H, Yang S, Li L. From SARS to MERS: evidence and speculation. *Front Med* (2016) 10(4):377–82. doi: 10.1007/s11684-016-0466-7
- Stadler K, Masignani V, Eickmann M, Becker S, Abbrignani S, Klenk HD, et al. SARS—beginning to understand a new virus. *Nat Rev Microbiol* (2003) 1(3):209–18. doi: 10.1038/nrmicro775
- Vijayanand P, Wilkins E, Woodhead M. Severe acute respiratory syndrome (SARS): a review. *Clin Med (Lond)* (2004) 4(2):152–60. doi: 10.7861/clinmedicine.4-2-152
- Vasileva D, Badawi A. C-reactive protein as a biomarker of severe H1N1 influenza. *Inflammation Res* (2019) 68(1):39–46. doi: 10.1007/s00011-018-1188-x
- Wu W, Shi D, Fang D, Guo F, Guo J, Huang F, et al. A new perspective on c-reactive protein in H7N9 infections. *Int J Infect Dis* (2016) 44:31–6. doi: 10.1016/j.ijid.2016.01.009

43. Backes Y, van der Sluijs KF, Mackie DP, Tacke F, Koch A, Tenhunen JJ, et al. Usefulness of suPAR as a biological marker in patients with systemic inflammation or infection: a systematic review. *Intensive Care Med* (2012) 38(9):1418–28. doi: 10.1007/s00134-012-2613-1
44. Huang Z, Wang N, Huang S, Chen Y, Yang S, Gan Q, et al. Increased serum soluble urokinase plasminogen activator receptor predicts short-term outcome in patients with hepatitis b-related acute-on-Chronic liver failure. *Gastroenterol Res Pract* (2019) 2019:3467690. doi: 10.1155/2019/3467690
45. Berres ML, Schlosser B, Berg T, Trautwein C, Wasmuth HE. Soluble urokinase plasminogen activator receptor is associated with progressive liver fibrosis in hepatitis c infection. *J Clin Gastroenterol* (2012) 46(4):334–8. doi: 10.1097/MCG.0b013e31822da19d
46. Outinen TK, Tervo L, Makela S, Huttunen R, Maenpaa N, Huhtala H, et al. Plasma levels of soluble urokinase-type plasminogen activator receptor associate with the clinical severity of acute puumala hantavirus infection. *PLoS One* (2013) 8(8):e71335. doi: 10.1371/journal.pone.0071335
47. Sidenius N, Sier CF, Ullum H, Pedersen BK, Lepri AC, Blasi F, et al. Serum level of soluble urokinase-type plasminogen activator receptor is a strong and independent predictor of survival in human immunodeficiency virus infection. *Blood* (2000) 96(13):4091–5. doi: 10.1182/blood.V96.13.4091
48. Hodges GW, Bang CN, Wachtell K, Eugen-Olsen J, Jeppesen JL. suPAR: a new biomarker for cardiovascular disease? *Can J Cardiol* (2015) 31(10):1293–302. doi: 10.1016/j.cjca.2015.03.023
49. Bouchon A, Facchetti F, Weigand MA, Colonna M. TREM-1 amplifies inflammation and is a crucial mediator of septic shock. *Nature* (2001) 410(6832):1103–7. doi: 10.1038/35074114
50. Roe K, Gibot S, Verma S. Triggering receptor expressed on myeloid cells-1 (TREM-1): a new player in antiviral immunity? *Front Microbiol* (2014) 5:627. doi: 10.3389/fmicb.2014.00627
51. Tammaro A, Derive M, Gibot S, Leemans JC, Florquin S, Dessing MC. TREM-1 and its potential ligands in non-infectious diseases: from biology to clinical perspectives. *Pharmacol Ther* (2017) 177:81–95. doi: 10.1016/j.pharmthera.2017.02.043
52. Dantas P, Matos AO, da Silva Filho E, Silva-Sales M, Sales-Campos H. Triggering receptor expressed on myeloid cells-1 (TREM-1) as a therapeutic target in infectious and noninfectious disease: a critical review. *Int Rev Immunol* (2020) 39(4):188–202. doi: 10.1080/08830185.2020.1762597
53. Gomez-Pina V, Soares-Schanoski A, Rodriguez-Rojas A, Del Fresno C, Garcia F, Vallejo-Cremades MT, et al. Metalloproteinases shed TREM-1 ectodomain from lipopolysaccharide-stimulated human monocytes. *J Immunol* (2007) 179(6):4065–73. doi: 10.4049/jimmunol.179.6.4065
54. Baruah S, Keck K, Vrenios M, Pope MR, Pearl M, Doerschug K, et al. Identification of a novel splice variant isoform of TREM-1 in human neutrophil granules. *J Immunol* (2015) 195(12):5725–31. doi: 10.4049/jimmunol.1402713
55. Matsumoto K, Okazaki H, Nakamura T. Up-regulation of hepatocyte growth factor gene expression by interleukin-1 in human skin fibroblasts. *Biochem Biophys Res Commun* (1992) 188(1):235–43. doi: 10.1016/0006-291x(92)92375-8
56. Skibinski G, Skibinska A, James K. The role of hepatocyte growth factor and its receptor c-met in interactions between lymphocytes and stromal cells in secondary human lymphoid organs. *Immunology* (2001) 102(4):506–14. doi: 10.1046/j.1365-2567.2001.01186.x
57. Nishikoba N, Kumagai K, Kanmura S, Nakamura Y, Ono M, Eguchi H, et al. HGF-MET signaling shifts M1 macrophages toward an M2-like phenotype through PI3K-mediated induction of arginase-1 expression. *Front Immunol* (2020) 11:2135. doi: 10.3389/fimmu.2020.02135
58. Yanagita K, Matsumoto K, Sekiguchi K, Ishibashi H, Niho Y, Nakamura T. Hepatocyte growth factor may act as a pulmotrophic factor on lung regeneration after acute lung injury. *J Biol Chem* (1993) 268(28):21212–7. doi: 10.1016/S0021-9258(19)36912-1
59. Panganiban RA, Day RM. Hepatocyte growth factor in lung repair and pulmonary fibrosis. *Acta Pharmacol Sin* (2011) 32(1):12–20. doi: 10.1038/aps.2010.90
60. Bradley-Stewart A, Jolly L, Adamson W, Gunson R, Frew-Gillespie C, Templeton K, et al. Cytokine responses in patients with mild or severe influenza A (H1N1)pdm09. *J Clin Virol* (2013) 58(1):100–7. doi: 10.1016/j.jcv.2013.05.011
61. Kyriazopoulou E, Poulakou G, Milionis H, Metallidis S, Adamis G, Tsiakos K, et al. Early treatment of COVID-19 with anakinra guided by soluble urokinase plasminogen receptor plasma levels: a double-blind, randomized controlled phase 3 trial. *Nat Med* (2021) 27(10):1752–60. doi: 10.1038/s41591-021-01499-z





## OPEN ACCESS

## EDITED BY

Yi Wu,  
Xi'an Jiaotong University, China

## REVIEWED BY

Shang-Rong Ji,  
Lanzhou University, China  
Karlheinz Peter,  
Baker Heart and Diabetes Institute,  
Australia

## \*CORRESPONDENCE

János G. Filep  
✉ janos.g.filep@umontreal.ca

RECEIVED 09 June 2023

ACCEPTED 07 July 2023

PUBLISHED 26 July 2023

## CITATION

Rizo-Téllez SA, Sekheri M and Filep JG  
(2023) C-reactive protein: a target for  
therapy to reduce inflammation.  
*Front. Immunol.* 14:1237729.  
doi: 10.3389/fimmu.2023.1237729

## COPYRIGHT

© 2023 Rizo-Téllez, Sekheri and Filep. This is  
an open-access article distributed under the  
terms of the [Creative Commons Attribution  
License \(CC BY\)](#). The use, distribution or  
reproduction in other forums is permitted,  
provided the original author(s) and the  
copyright owner(s) are credited and that  
the original publication in this journal is  
cited, in accordance with accepted  
academic practice. No use, distribution or  
reproduction is permitted which does not  
comply with these terms.

# C-reactive protein: a target for therapy to reduce inflammation

Salma A. Rizo-Téllez <sup>1,2</sup>, Meriem Sekheri <sup>1,2</sup>  
and János G. Filep <sup>1,2\*</sup>

<sup>1</sup>Department of Pathology and Cell Biology, University of Montreal, Montreal, QC, Canada, <sup>2</sup>Research Center, Maisonneuve-Rosemont Hospital, Montreal, QC, Canada

C-reactive protein (CRP) is well-recognized as a sensitive biomarker of inflammation. Association of elevations in plasma/serum CRP level with disease state has received considerable attention, even though CRP is not a specific indicator of a single disease state. Circulating CRP levels have been monitored with a varying degree of success to gauge disease severity or to predict disease progression and outcome. Elevations in CRP level have been implicated as a useful marker to identify patients at risk for cardiovascular disease and certain cancers, and to guide therapy in a context-dependent manner. Since even strong associations do not establish causality, the pathogenic role of CRP has often been over-interpreted. CRP functions as an important modulator of host defense against bacterial infection, tissue injury and autoimmunity. CRP exists in conformationally distinct forms, which exhibit distinct functional properties and help explaining the diverse, often contradictory effects attributed to CRP. In particular, dissociation of native pentameric CRP into its subunits, monomeric CRP, unmasks “hidden” pro-inflammatory activities in pentameric CRP. Here, we review recent advances in CRP targeting strategies, therapeutic lowering of circulating CRP level and development of CRP antagonists, and a conformation change inhibitor in particular. We will also discuss their therapeutic potential in mitigating the deleterious actions attributed to CRP under various pathologies, including cardiovascular, pulmonary and autoimmune diseases and cancer.

## KEYWORDS

C-reactive protein, monomeric CRP, CRP antagonists, CRP lowering therapies, inflammation, cardiovascular disease, autoimmunity, cancer

## Introduction

The prototypic acute-phase reactant C-reactive protein (CRP), discovered as a protein that precipitates C-polysaccharide of *Streptococcus pneumoniae*, has long been recognized as a sensitive biomarker of inflammation (1). Elevations in baseline serum CRP level have been detected in numerous pathologies, and have been suggested to being useful to monitor disease progression. CRP has received considerable attention as a diagnostic and prognostic

marker in autoimmune diseases (2, 3), cardiovascular diseases (4–6), chronic kidney disease (7), cancer (8) and COVID-19 (9, 10) as well as for guiding therapy (8, 11). Although there is a continuing debate over whether CRP is primarily a passive indicator of inflammation or is a “culprit” mediating disease (12–18), CRP plays important roles in host defense against invading pathogens, autoimmunity and inflammation. CRP exhibits many, often conflicting pro- and anti-inflammatory activities (14, 19–21), which makes delineating its pathogenetic roles even more challenging. Results from structure-function studies challenge the long-held and rather simplistic view of CRP as a stable pentameric protein and identified conformationally distinct forms, including native pentameric CRP (pCRP) and modified/monomeric CRP (mCRP), which exhibit distinct functional properties and may explain many of the opposing biological activities attributed to CRP (21, 22). CRP synthesis, structure and biological activities have been reviewed in detail elsewhere (19, 21, 23–25). In this review, we aimed to critically assess the competing views on the role of CRP isomers in disease pathogenesis and therapy, focusing on recent advances that may provide a rationale basis for guiding therapy and/or therapeutic targeting of CRP isomers to limit inflammation underlying various diseases.

## CRP expression, structural properties

Native CRP is member of the pentraxin family, an evolutionarily highly conserved class of pattern recognition molecules. The human CRP gene, located on chromosome 1, q23-q24 encodes for a CRP subunit of a single polypeptide chain of 206 amino acids (23). CRP is composed of five identical non-covalently bound subunits forming a planar ring with a central pore (23). The two opposite faces of the pentamer, and thus each protomer, have distinct binding properties. The A-face binds and activates complement C1q, whereas the B-face contains the  $\text{Ca}^{2+}$ -dependent binding pocket for phosphocholine, expressed by bacterial, fungal and eukaryotic cells (24, 26). CRP also binds to nuclear antigens, the oxidized LDL receptor, apoptotic cell membrane, glycan components of microorganisms, and many other ligands (24, 27, 28), though some of these interactions have been disputed.

Native CRP is predominantly synthesized in hepatocytes under transcriptional control by cytokines (IL-6 and to a lesser extent IL-1 $\beta$  and TNF- $\alpha$ ), the transcription factors hepatic nuclear factor (HNF) 1 $\alpha$  and HNF3 as part of the “reorchestration” of hepatic gene expression in response to infection or tissue injury (19), promoter methylation and a distal enhancer (29). Hepatic secretion of pCRP accounts for rapid increases in serum pCRP levels during the acute-phase reaction. The serum half-life of pCRP is about 19 h under both physiological and pathological conditions (30), thus directly reflecting the rate of its hepatic synthesis. Ethnicity, sex and polymorphism in the apolipoprotein E and CRP genes are known to influence baseline serum pCRP levels in humans (31, 32). CRP gene polymorphism influences gene expression and may predispose to systemic lupus erythematosus (31), but do not appear to be associated with increased risk for

cardiovascular diseases (33, 34). Additionally, the kidney has been reported as a second site of pCRP formation in humans (35). Expression of CRP mRNA and pCRP synthesis has also been detected in the diseased vessel wall, coronary artery bypass grafts and neurons (35–37). The contribution of these sites to circulating pCRP remains to be investigated.

Under physiological conditions, pCRP appears to exist in a NaCl concentration-dependent pentamer-decamer equilibrium (38). Another form of CRP, characterized by multiple-size lettuce-like structures of about 300–500kDa, were detected in the serum of obese patients (39). The origin and pathological significance of these CRP forms are not known.

## Elevated plasma CRP levels

Although not specific for a single disease process, CRP is commonly used as a static measurement and CRP levels have been correlated with disease activity and to some degree, severity and prognosis in several diseases. CRP has been promoted as an independent predictor of cardiovascular events and metabolic syndrome (40–42), though the association is considerably weaker than previously thought (43, 44). The data from Mendelian randomization studies (33, 34) coupled with animal studies with injection of human pCRP and transgenic mice over-expressing human CRP may support an association between CRP and cardiovascular disease, but provide no direct evidence for a causative role for pCRP. In the Dallas Heart study hs-CRP was not independently associated with atherosclerotic burden in the coronary artery and abdominal aorta (45), whereas the REVERSAL trial reported that lower hs-CRP levels were independently and significantly correlated with atherosclerosis progression (46). Other studies have concluded that hs-CRP likely serves as a biomarker of vascular inflammation underlying atherosclerosis (14, 44). Thus, whereas the potential of therapeutic targeting of pCRP in cardiovascular disease remains unresolved, hs-CRP has clinical usefulness in guiding therapy as discussed below.

Other clinical studies reported positive correlation between elevated plasma CRP levels and myocardial infarct size (47), reduced lung function in chronic obstructive pulmonary disease (48) or the severity of COVID-19-evoked respiratory distress (49, 50). Higher plasma CRP levels were found to predict flares in systemic lupus erythematosus (2) and to portend poor prognosis in melanoma (51). Patients with non-small cell lung cancer who received the immune checkpoint PD-1 inhibitor nivolumab, early increases in hs-CRP and IL-6 were predictive for the efficacy of treatment (52). Nivolumab evoked a CRP flare-response (defined as a rapid, more than twofold increase in CRP levels followed by decrease below baseline values within 3 months) in about 25% of patients with metastatic renal cell carcinoma and this was associated with significant tumor shrinkage and improved 1-year survival rate (53).

The association of CRP with prognosis should, however, be interpreted with caution as an indication of direct causal contribution of CRP to disease pathogenesis. A definitive way to test this is the use of compounds that specifically block binding of

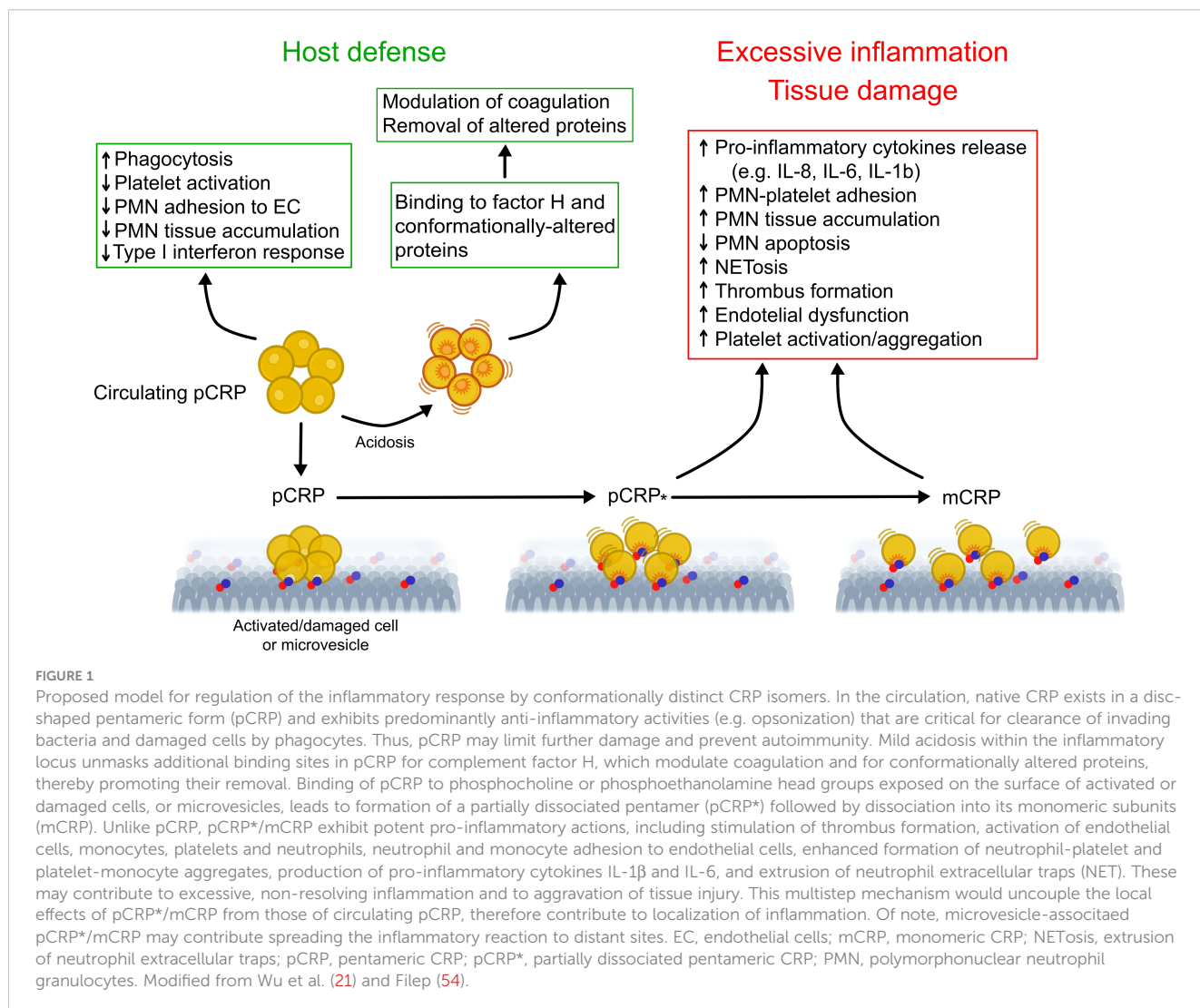
CRP to its ligands and/or receptors to assess its pro-inflammatory effects *in vivo*.

## Modulation of the inflammatory response by CRP isomers

While pCRP has been postulated to be stable under physiological conditions (24), compelling evidence indicates that CRP exists in conformationally distinct forms and conformational changes in pCRP results in expression of potent pro-inflammatory activities (Figure 1) (21). The mild acidic environment within inflamed tissues confers pCRP binding specificities for factor H (55) and conformationally altered proteins, such as oxidized LDL and complement C3b (56) that do not bind to pCRP at physiological pH. Binding of circulating pCRP to phosphocholine or phosphoethanolamine head groups of membrane lipids expressed on the surface of activated platelets or apoptotic cells induces the formation of a partially dissociated pentamer (pCRP\*), which then dissociates into the monomeric subunits, mCRP (57–59). pCRP\* and mCRP exhibit potent pro-inflammatory activities,

including stimulation of IL-8 secretion from neutrophils and human coronary artery endothelial cells (60, 61), promote neutrophil adhesion to platelets and endothelial cells (62, 63), delay neutrophil apoptosis (64) and trigger extrusion of neutrophil extracellular traps (65), characteristic features of the inflammatory response. pCRP\* binds and activate complement C1q (66), which, in turn, can amplify pre-existing inflammation and tissue damage (21, 57, 67). Accumulation of pro-inflammatory CRP isoforms within inflamed/injured but not in healthy tissues, and local expression of mCRP, for example within arteriosclerotic plaques (68) and in circulating microparticles (69, 70) would ensure localization of inflammation (57) and precipitate tissue injury (21).

While purified human pCRP itself does not evoke inflammation when injected into healthy individuals (71), it can amplify tissue injury in animal models, induce the expression of adhesion molecules and production of IL-6 and IL-8 (24, 72–75). Caution should be exercised in interpreting these observations because many of these effects can be attributed to contaminants (endotoxin or the preservative sodium azide) in commercial CRP preparations not to pCRP itself (13, 21). By contrast, other studies documented pCRP



protection against the assembly of the terminal complement attack complex (27) and bacterial sepsis (76), reversal of proteinuria in autoimmune mice (77), and prevention of autoimmunity (78). Recently, pCRP was found to reduce immune complex-triggered type I interferon response, consistent with a protective action in systemic lupus erythematosus (79). This action was lost in mCRP, further highlighting the complexity of regulation of immune response by CRP isomers in autoimmune diseases.

CRP isomers bind to distinct receptors. Thus, pCRP binds primarily to the low affinity Ig receptor FcγRIIa (CD32) and to some extent to the high affinity IgG receptor FcγRI (CD64) on phagocytes and endothelial cells (21, 80), and α<sub>I</sub>β<sub>3</sub> integrin on platelets (81), whereas mCRP binds to FcγRIIIb (CD64) on phagocytes and lipid rafts on human endothelial cells (82).

The concept of activation-induced conformational changes could explain why pCRP itself is not pro-inflammatory in the absence of infection or tissue injury. Conformational changes in pCRP, and generation of pCRP\* and mCRP, would unmask “hidden” pro-inflammatory activities that may collectively amplify the initial inflammatory signal evoked by infection or tissue injury, leading to exacerbation of tissue damage and more severe disease (21, 73). However, further studies are needed to explore the clinical importance of mCRP or other CRP conformers.

## CRP as a target for therapy

### Therapeutic lowering of serum CRP

The association of persisting modest elevations in plasma CRP level (detected by high sensitivity assays) with chronic diseases has attracted considerable clinical interest and often contradictory interpretations. CRP is generally recognized as a biomarker of ongoing inflammation and to a varying degree as a predictor of clinical outcome. Although conclusive evidence for a causal role for pCRP (and/or CRP isomers) is still lacking, lowering pCRP levels is widely anticipated to reduce the adverse effects attributed to CRP. Indeed, several approaches have been developed and tested for lowering plasma pCRP level or countering CRP's actions (Table 1).

Observational studies reported a relationship between life style changes, encouraging cessation of smoking, weight loss, more physical activity and Mediterranean diet, with concurrent reduction in hs-CRP levels and the risk for future cardiovascular events (83–86). Studies with angiotensin converting enzyme inhibitors, angiotensin II (type I) receptor blockers, vitamins E and C, and the anti-platelet agents clopidogrel and aspirin, yielded conflicting results in regard with their efficiency to lowering hs-CRP levels (94, 107). Unlike insulin, the anti-diabetic drugs rosiglitazone and pioglitazone have been found to significantly decrease serum CRP, though the molecular mechanisms and the potential clinical benefits remain largely unknown (94).

Evidence derived mainly from trials with statins support the potential value of hs-CRP for primary and secondary prevention of cardiovascular disease, though this notion still remains controversial. The landmark JUPITER trial demonstrated the benefits of rosuvastatin therapy in primary prevention as well as

the utility of hs-CRP for identifying a population at risk for cardiovascular disease (88–90). A new meta-analysis from the PROMINENT, REDUCE-IT and STRENGTH trials (which were originally designed to test triglyceride-lowering) showed that inflammation, and thus hs-CRP is more tightly linked than LDL cholesterol to future adverse effects in patients already on statins (91). Limitations of this analysis include the effects of confounding bias (e.g. high intensity statin use and diabetes) and lack of attention to primary versus secondary prevention (108). These concerns notwithstanding, the meta-analysis would argue for routine hs-CRP testing to assess residual inflammatory risk (109) and a combined approach to aggressive lipid-lowering and inflammation-inhibiting therapy with colchicine, IL-1 or IL-6 inhibitors or bempedoic acid (91, 93).

## Antisense oligonucleotides

Another approach to reduce CRP production is the use of antisense oligonucleotides (ASO) to specifically inhibit mRNA translation in particular in the liver, the predominant site of pCRP synthesis (23) where ASOs have a propensity to accumulate (110). Lowering plasma CRP level with rat-specific ASO ISIS 197178 was associated with reduction of infarct size and improved cardiac function in a rat model of myocardial infarction (111). Human-specific ASO ISIS 353512 reduced neointima formation in human CRP transgenic mice subjected to carotid artery ligation (98). In healthy subjects, ASO ISIS 329993 (ISIS-CRP<sub>Rx</sub>) reduced by about 70% of the peak plasma CRP response to endotoxin challenge without affecting cytokine production and coagulation (100). Treatment with ISIS-CRP<sub>Rx</sub> of patients with rheumatoid arthritis also decreased plasma CRP level, but did not reduce disease activity (99). Unexpectedly, another ASO, ISIS 353512 increased IL-6 and CRP levels in healthy volunteers (112), illustrating the challenges with CRP-ASO therapy.

## Selective CRP apheresis

Another strategy to investigate pathogenetic roles for pCRP (and arguably other CRP isomers) is reducing plasma pCRP level by selective apheresis, which appears to be a relatively simple, efficient and clinically safe approach (49, 113). In this protocol, patients are subjected to a 4–6 h extracorporeal circuit and blood plasma is applied to phosphocholine-linked resin. A case report and studies on small cohorts of patients with ST elevation myocardial infarction (STEMI) demonstrated efficient lowering of plasma CRP levels (47, 102, 114, 115). However, results from the multi-center pilot CAMI-1 (CRP Apheresis in Acute Myocardial Infarction-1) study were inconclusive in regard with correlation of reduced CRP levels with myocardial infarct size (47) because the study was not randomized. The ongoing trials on the effects of CRP apheresis on the course of STEMI (NCT04939805) and ischemic stroke (CASTRO-B, NCT03884153) are anticipated to address this issue. There are several case reports with mixed results on reducing lung injury with CRP apheresis in patients with COVID-19-evoked respiratory distress syndrome (49, 103–105).

TABLE 1 CRP targeting strategies.

Agent	Species	Disease/Model	Effect	Reference
CRP lowering approaches				
Lifestyle changes				
<ul style="list-style-type: none"><li>- Exercise</li><li>- Diet</li><li>- Weight loss</li><li>- Vitamin supplementation</li><li>- Smoking cessation</li></ul>	Human	Healthy Cardiovascular disease Metabolic syndrome	↓ CRP levels ↓ cardiovascular events ↓ body weight	(83–87)
Medication-associated decreases in CRP level				
Statins	Human	Cardiovascular disease	↓ CRP levels (15-60%) ↓ Cholesterol ↓ cardiovascular events	(88–92)
Bempedoic acid	Human	Cardiovascular disease	↓ CRP levels by 27% ↓ Total cholesterol by 15%	(93)
Rosiglitazone Pioglitazone Dipeptidyl peptidase 4 inhibitors	Human	Diabetes	↓ CRP levels	(94, 95)
Angiotensin-converting enzyme inhibitors	Human	Cardiovascular disease Metabolic syndrome	↓ CRP levels ↓ IL-6 levels	(94, 96)
Antisense oligonucleotides				
CRP-mRNA antisense oligonucleotides	Human	Primary hepatocytes	↓ CRP mRNA	(97)
	Mouse	CRP transgenic mice with collagen-induced arthritis	↓ human CRP levels ↑ arthritis clinical score	
	Rat	Acute myocardial infarction	↓ CRP levels by >60% ↑ heart function	(98)
	Human	Healthy Rheumatoid arthritis	↓ CRP levels No effect on arthritis clinical score	(99)
		Healthy Endotoxin challenge	↓ CRP level	(100)
		Atrial fibrillation	↓ CRP levels by 64% No effect on atrial fibrillation burden	(101)
CPR selective apheresis				
PentraSorb®	Human	ST-segment Elevation Myocardial Infarction	↓ CRP levels by 50% ↓ infarct size ↑ wound healing	(47, 49, 102)
		Severe COVID-19	↓ CRP levels by 50-90% ↓ mortality	(49, 103–105)
Small-molecule CRP inhibitors				
(1,6-bis (phosphocholine) -hexane)	Rat	Acute myocardial infarction	↓ mortality ↓ infarct size ↓ cardiac dysfunction	(72)
		LPS-inflamed cremasteric tissue	↓ CRP deposition ↓ leukocyte adhesion	(59, 67)
		Acute myocardial infarction	↓ CRP deposition ↓ leukocyte infiltration ↓ caspase 3 expression ↓ TNF-α and IL-6 expression	
		Renal ischemia- reperfusion	↓ lesions ↑ excretory function ↓ monocyte infiltration	(75)
	Human	THP-1 or Jurkat cell-derived microvesicles	↓ calcium-dependent binding	(59)

(Continued)



TABLE 1 Continued

Agent	Species	Disease/Model	Effect	Reference
	Mouse	Lethal influenza virus infection	↓ mortality ↓ viral titers ↓ lung lesions ↓ inflammatory cells infiltration	(106)
Phosphonate compound C10M	Human	ADP-activated platelets	↓ CRP binding to platelets	(65)
		Monocytes	↓ platelet-monocyte aggregates ↓ monocyte adhesion	
		Endothelial cells	↓ ICAM-1 and VCAM-1 expression	
		Neutrophils	↓ CD11b expression ↓ ROS production ↓ NET formation No effect on phagocytosis	
	Rat	Renal ischemia- reperfusion	↓ CRP deposition ↑ excretory function ↓ monocyte infiltration	
		Acute hindlimb allograft rejection	↓ graft loss ↓ monocyte infiltration ↓ CRP deposition	

NET, neutrophil extracellular traps; ROS, reactive oxygen species.

↓ (arrow down) decreased.

↑ (arrow up) increased.

The subsequently planned trial on pulmonary, myocardial and/or renal injury in COVID-19 (NCT04898062) has been withdrawn [<https://www.clinicaltrials.gov>, as of June 4, 2023].

Similar to other CRP lowering strategies, the fundamental question whether the beneficial effects can be attributed to lowering pCRP level directly or to reduction of formation of conformationally altered CRP secondary to reduced availability of the parent molecule pCRP remains unanswered. While short-term reductions of plasma CRP levels may be beneficial under certain circumstances, markedly lower CRP levels over prolonged periods of time may impair antimicrobial defense, and thus augmenting the risk of bacterial or viral infection. Whether this would limit the clinical utility of CRP apheresis and what plasma CRP levels after CRP apheresis will be still sufficient to support innate defense functions remain to be investigated.

## Small molecule CRP inhibitors

Two distinct CRP targeting strategies have been developed. In 2006, the Pepys group has designed and synthesized the first small-molecule inhibitor of CRP (72). The bivalent compound, 1,6-bis (phosphocholine)-hexane (bis-PC) bridges the phosphocholine-binding pockets on the B-face of two separate CRP pentamers, bringing the phosphocholine-binding surfaces together in a parallel fashion (72). The resulting decamer structure stabilizes conformation of pCRP and prevents binding of other ligands to the B-face. Bis-PC has also been reported to inhibit dissociation of pCRP to mCRP on the surface of circulating microparticles isolated from the blood of patients with myocardial infarction (69). Pretreatment with bis-PC abolished the increase in infarct size and cardiac dysfunction produced by injection of human pCRP in a

rat model of myocardial infarction (72). A controversy exists whether rat CRP can activate rat complement and whether rat factor H, the native complement-control protein, could interact with human CRP (116, 117). Hence, the translational implication of these observations remains to be clarified. Binding of CRP decamers to Fcγ receptors or possible deposition of large CRP complexes might trigger immune reactions, thereby limiting the therapeutic use of bis-PC. This compound is apparently no longer being considered for clinical development [<http://pentrxin.wordpress.com/rd-programs/>].

Considering the role of native CRP in host defense, therapies aimed at reducing serum pCRP level would likely impair defense mechanisms and predispose to infection. Thus, an attractive alternative approach is to selectively block expression of pro-inflammatory properties “hidden” in pCRP without interfering with its protective functions. As a proof of this concept, Zeller et al. (65) developed a low molecular weight monovalent compound C10M [3-(dibutyl amino)propyl] phosphonic acid]. C10M binds to the phosphocholine binding pocket of pCRP and prevents pCRP binding to phosphocholine residues exposed on the surface of activated or damaged cells or microvesicles, and subsequently the formation of pCRP\*/mCRP (65). Apart from the occupied phosphocholine binding pocket, the B-face remains accessible to other ligands, including misfolded or aggregated proteins or proteins whose secondary structure is predominantly β-sheet (56) as well as neutrophils. Consistently, C10M inhibited pCRP\*/mCRP-stimulated activation of monocytes and neutrophils, extrusion of neutrophil extracellular traps (NETs), monocyte adhesion to activated endothelial cells, and formation of platelet-monocyte aggregates (65). C10M reduction of pCRP\*/mCRP-triggered, presumably ROS-dependent NET release (i.e. *via* the suicidal pathway) could contribute to preventing NET-mediated tissue

damage under pathological conditions (54, 118). Importantly, C10M did not impair antibacterial host defense as evidenced by unaltered pCRP opsonization-mediated phagocytosis of bacteria by monocytes and neutrophils (65). Furthermore, C10M efficiently suppressed tissue deposition of human pCRP\*/mCRP and monocyte accumulation within the affected organs in murine models of renal ischemia-reperfusion and allograft rejection of hindlimb transplants (65). Consistently, C10M significantly improved renal function following ischemia-reperfusion, and prevented premature loss of allograft transplants driven by human pCRP. While these findings would indicate the functional importance of mCRP, further studies are needed to distinguish the effects of CRP antagonists on endogenous CRP and injected human CRP in these and other experimental models.

## Concluding remarks

CRP is a well-established biomarker of inflammation and much written about its association with disease state. Circulating hs-CRP may identify patients at risk, predict disease progression and outcome, and guide therapy in a context-dependent manner. Nevertheless, since even strong associations do not establish causality, further studies are clearly warranted to elucidate its potential pathogenic roles. Activation-induced conformational changes in pCRP would unmask “hidden” pro-inflammatory properties as opposed to the largely protective role of pCRP. CRP lowering strategies yielded promising, but often inconclusive data on altering disease progression. Development of CRP antagonists, and in particular recent development of a phosphocholine mimetic that binds to pCRP and inhibits conformation change-mediated expression of pro-inflammatory activities without impairing pCRP’s defense function, should facilitate future investigations into the full spectrum of the roles of CRP isomers in

inflammatory pathologies. This approach has the potential of opening a novel therapeutic avenue for preventing or limiting the deleterious actions attributed to CRP.

## Author contributions

All authors contributed to the article and approved the submitted work.

## Acknowledgments

The authors apologize to those experts whose articles have not been cited due to space limitations. This work was supported by a grant from the Canadian Institutes of Health Research (PJT-169075 to JF).

## Conflict of interest

The authors declare that the research was conducted in the absence of any commercial or financial relationships that could be construed as a potential conflict of interest.

## Publisher’s note

All claims expressed in this article are solely those of the authors and do not necessarily represent those of their affiliated organizations, or those of the publisher, the editors and the reviewers. Any product that may be evaluated in this article, or claim that may be made by its manufacturer, is not guaranteed or endorsed by the publisher.

## References

- Gabay C, Kushner I. Acute-phase proteins and other systemic responses to inflammation. *N Engl J Med* (1999) 340(6):448–54. doi: 10.1056/NEJM199902113400607.1999
- Gaitonde S, Samols D, Kushner I. C-reactive protein and systemic lupus erythematosus. *Arth Rheum* (2008) 59(12):1814–20. doi: 10.1002/art.24316
- Pope JE, Choy EH. C-reactive protein and implications in rheumatoid arthritis and associated comorbidities. *Semin Arthritis Rheum* (2021) 51(1):219–29. doi: 10.1016/j.semarthrit.2020.11.005
- Tsimikas S, Willerson JT, Ridker PM. C-reactive protein and other emerging blood biomarkers to optimize risk stratification of vulnerable patients. *J Am Coll Cardiol* (2006) 47(8 Suppl):C19–31. doi: 10.1016/j.jacc.2005.10.066
- Casas JP, Shah T, Hingorani AD, Danesh J, Pepys MB. C-reactive protein and coronary heart disease: a critical review. *J Intern Med* (2008) 264(4):295–314. doi: 10.1111/j.1365-2796.2008.02015.x
- Kushner I, Elyan M. Why does C-reactive protein predict coronary events? *Am J Med* (2008) 121(7):e11. doi: 10.1016/j.amjmed.2008.03.004
- Menon V, Greene T, Wang X, Pereira AA, Marcovina SM, Beck GJ, et al. C-reactive protein and albumin as predictors of all-cause and cardiovascular mortality in chronic kidney disease. *Kidney Int* (2005) 68(2):766–72. doi: 10.1111/j.1523-1755.2005.00455.x
- Allin KH, Nordestgaard BG. Elevated C-reactive protein in the diagnosis, prognosis, and cause of cancer. *Crit Rev Clin Lab Sci* (2011) 48(4):155–70. doi: 10.3109/10408363.2011.599831
- Luo X, Zhou W, Yan X, Guo T, Wang B, Xia H, et al. Prognostic value of C-reactive protein in patients with COVID-19. *Clin Infect Dis* (2020) 71(16):2174–9. doi: 10.1093/cid/ciaa641
- Smilowitz NR, Kunichoff D, Garshick M, Shah B, Pillinger M, Hochman JS, et al. C-reactive protein and clinical outcomes in patients with COVID-19. *Eur J Heart* (2021) 42:2270–9. doi: 10.1093/eurheartj/ehaa1103
- Koenig W. High-sensitivity C-reactive protein and atherosclerotic disease: from improved risk prediction to risk-guided therapy. *Int J Cardiol* (2013) 168(5):5126–134. doi: 10.1016/j.ijcard.2013.07.113
- Bisoendial RJ, Kastelein JJ, Levels JH, Zwaginga JJ, van den Bogaard B, Reitsma PH, et al. Activation of inflammation and coagulation after infusion of C-reactive protein in humans. *Circ Res* (2005) 96(7):714–6. doi: 10.1161/01.RES.0000163015.67711.AB
- Lowe GDO, Pepys MB. C-reactive protein and cardiovascular disease: weighing the evidence. *Curr Atheroscler Rep* (2006) 8(5):421–8. doi: 10.1007/s11883-006-0040-x
- Scirica BM, Morrow DA. Is C-reactive protein an innocent bystander or proatherogenic culprit? *Circulation* (2006) 113(17):2128–34. doi: 10.1161/CIRCULATIONAHA.105.611350
- Verma S, Devaraj S, Jialal I. Is C-reactive protein an innocent bystander or proatherogenic culprit? C-reactive protein promotes atherothrombosis. *Circulation* (2006) 113(17):2135–50. doi: 10.1161/CIRCULATIONAHA.105.611350
- McGrath EE, Memon SS, Anderson PB. C-reactive protein – marker of inflammation or future therapeutic target? *Am J Respir Crit Care Med* (2007) 176(6):624. doi: 10.1164/ajrccm.176.6.624

17. Yousuf O, Mohanty BD, Martin SS, Joshi PH, Blaha MJ, Nasir K, et al. High-sensitivity C-reactive protein and cardiovascular disease. A resolute belief or an elusive link? *J Am Coll Cardiol* (2013) 62(5):397–408. doi: 10.1016/j.jacc.2013.05.016
18. Zimmerman MA, Selzman CH, Cothre C, Sorensen AC, Raeburn CD, Harken AH. Diagnostic implications of C-reactive protein. *Arch Surg* (2003) 138:220–4. doi: 10.1001/archsurg.138.2.220
19. Black S, Kushner I, Samols D. C-reactive protein. *J Biol Chem* (2004) 279(47):48487–90. doi: 10.1074/jbc.R400025200
20. Kushner I, Agrawal A. CRP can play both pro-inflammatory and anti-inflammatory roles. *Mol Immunol* (2007) 44(4):670–1. doi: 10.1016/j.molimm.2006.02.001
21. Wu Y, Potempa LA, El Kebir D, Filep JG. C-reactive protein and inflammation: conformational changes affect function. *Biol Chem* (2015) 396(11):1181–97. doi: 10.1515/hsz-2015-0149
22. Ullah N, Wu Y. Regulation of conformational changes in C-reactive protein alters its bioactivity. *Cell Biochem Biophys* (2022) 80(4):595–608. doi: 10.1007/s12013-022-01089-x
23. Volanakis JE. Human C-reactive protein: expression, structure, and function. *Mol Immunol* (2001) 38(2-3):189–97. doi: 10.1016/S0161-5890(01)00042-6
24. Pepys MB, Hirschfield GM. C-reactive protein: A critical update. *J Clin Invest* (2003) 111(12):1805–12. doi: 10.1172/JCI18921
25. Kushner I. C-reactive protein - My perspective on its first half century, 1930-1982. *Front Immunol* (2023) 14:1150103. doi: 10.3389/fimmu.2023.1150103
26. Agrawal A, Shrive AK, Greenhough TJ, Volanakis JE. Topology and structure of the C1q-binding site on C-reactive protein. *J Immunol* (2001) 166(6):3998–4004. doi: 10.4049/jimmunol.166.6.3998
27. Gershov D, Kim SJ, Brot N, Elkon KB. C-reactive protein binds to apoptotic cells, protects the cells from the assembly of the terminal complement components, and sustains an antiinflammatory innate immune response. *J Exp Med* (2000) 192(9):1353–64. doi: 10.1084/jem.192.9.1353
28. Singh SK, Suresh MV, Prayter DC, Moorman JP, Rusinol AE, Agrawal A. Exposing of hidden functional site of C-reactive protein by site-directed mutagenesis. *J Biol Chem* (2012) 287(5):3550–8. doi: 10.1074/jbc.M111.310011
29. Wielscher M, Mandaviya PR, Kuehnle B, Joehanes R, Mustafa R, Robinson O, et al. DNA methylation signature of chronic low-grade inflammation and its role in cardio-respiratory diseases. *Nat Commun* (2022) 13(1):2408. doi: 10.1038/s41467-022-29792-6
30. Aziz N, Fahey JL, Detels R, Butch AW. Analytical performance of a highly sensitive C-reactive protein-based immunoassay and the effects of laboratory variables on levels of protein in blood. *Clin Diagn Lab Immunol* (2003) 10(4):652–7. doi: 10.1128/cdli.10.4.652-657.2003
31. Russell AI, Cunningham Graham DS, Shepherd C, Robertson CA, Whittaker J, Meeks J, et al. Polymorphism in the C-reactive protein locus influences gene expression and predisposes to systemic lupus erythematosus. *Hum Mol Genet* (2004) 13(1):137–47. doi: 10.1093/hmg/ddh021
32. März W, Scharnagl H, Hoffmann MM, Boehm BO, Winkelmann BR. The apolipoprotein E polymorphism is associated with circulating C-reactive protein (the Ludwigshafen risk and cardiovascular health study). *Eur Heart J* (2004) 25(23):2109–19. doi: 10.1016/j.ehj.2004.08.024
33. Crawford DC, Sanders CL, Qin X, Smith JD, Shephard C, Wong M, et al. Genetic variation is associated with C-reactive protein levels in the third national health and nutrition examination survey. *Circulation* (2006) 114(23):2458–65. doi: 10.1161/CIRCULATIONAHA.106.615740
34. Kardys I, de Maat MP, Uitterlinden AG, Hofman A, Witteman JC. C-reactive protein gene haplotypes and risk of coronary heart disease: the Rotterdam Study. *Eur Heart J* (2006) 27(11):1331–7. doi: 10.1093/eurheartj/ehl018
35. Jabs WJ, Logering BA, Gerke P, Kreft B, Wolber EM, Klinger MH, et al. The kidney as a second site of human C-reactive protein formation *in vivo*. *Eur J Immunol* (2003) 33(1):152–61. doi: 10.1002/immu.200390018
36. Sun H, Koike T, Ichikawa T, Hatakeyama K, Shiomi M, Zhang B, et al. C-reactive protein in atherosclerotic lesions: its origin and pathophysiological significance. *Am J Pathol* (2005) 167:1139–48. doi: 10.1016/S0002-9440(05)61202-3
37. Slevin M, Matou-Nasri S, Turu M, Luque A, Rovira N, Badimon L, et al. Modified C-reactive protein is expressed by stroke neovessels and is a potent activator of angiogenesis *in vitro*. *Brain Pathol* (2010) 20(1):151–65. doi: 10.1111/j.1750-3639.2008.00256.x
38. Okemefuna AI, Stach L, Rana S, Bueta AJ, Gor J, Perkins SJ. C-reactive protein exists in an NaCl concentration-dependent pentamer-decamer equilibrium in physiological buffer. *J Biol Chem* (2010) 285(2):1041–52. doi: 10.1074/jbc.M109.044495
39. Asztalos BF, Horan MS, Horvath KV, McDermott AY, Chalasani NP, Schaefer EJ. Obesity associated molecular forms of C-reactive protein in human. *PLoS One* (2014) 9(10):e109238. doi: 10.1371/journal.pone.0109238
40. Oh J, Teoh H, Leiter LA. Should C-reactive protein be a target of therapy? *Diabetes Care* (2011) 34(Suppl.2):S155–60. doi: 10.2337/dc11-s211
41. Burger PM, Pradhan AD, Dorresteyn JAN, Koudstaal S, Teraa M, de Borst GJ, et al. Utrecht Cardiovascular Cohort-Second Manifestations of ARterial disease study group. C-reactive protein and risk of cardiovascular events and mortality in patients with various cardiovascular disease locations. *Am J Cardiol* (2023) 197:13–23. doi: 10.1016/j.amjcard.2023.03.025
42. Dietrich M, Jialal I. The effect of weight loss on a stable biomarker of inflammation, C-reactive protein. *Nutr Rev* (2005) 63:22–8. doi: 10.1111/j.1753-4887.2005.tb00107.x
43. Levinson SS, Miller JJ, Elin RJ. Poor predictive value of high-sensitivity C-reactive protein indicates need for reassessment. *Clin Chem* (2004) 50:1733–5. doi: 10.1373/clinchem.2004.037895
44. Genest J. C-reactive protein: Risk factor, biomarker and/or therapeutic target? *Can J Cardiol* (2010) 26(Suppl A):41A–4A. doi: 10.1016/s0828-282x(10)71061-8
45. Khera A, De Lemos JA, Peshock RM, Lo HS, Stanek HG, Murphy SA, et al. Relationship between C-reactive protein and subclinical atherosclerosis: the Dallas Heart Study. *Circulation* (2006) 113(1):38–43. doi: 10.1161/CIRCULATIONAHA.105.575241
46. Nissen SE, Tuzcu EM, Schoenhagen P, Brown BG, Ganz P, Vogel RA, et al. Effect of intensive compared with moderate lipid-lowering therapy on progression of coronary atherosclerosis: a randomized controlled trial. *JAMA* (2004) 291(9):1071–80. doi: 10.1001/jama.291.9.1071
47. Ries W, Torzewski J, Heigl F, Pfluecke C, Kelle S, Darius H, et al. C-reactive protein apheresis as anti-inflammatory therapy in acute myocardial infarction: Results of the CAMI-1 Study. *Front Cardiovasc Med* (2021) 8:591714. doi: 10.3389/fcvm.2021.591714
48. Donaldson GC. C-reactive protein: does it prevent mortality? *Am J Respir Crit Care Med* (2007) 175(3):209–10. doi: 10.1164/rccm.200610-1565ED
49. Torzewski J, Brunner P, Ries W, Garlich CD, Kayser S, Heigl F, et al. Targeting C-reactive protein by selective apheresis in humans: Pros and Cons. *J Clin Med* (2022) 11:1771. doi: 10.3390/jcm11071771
50. Pepys MB. C-reactive protein predicts outcome in COVID-19: is it also a therapeutic target? *Eur Heart J* (2021) 42:2280–3. doi: 10.1093/eurheartj/ehab169
51. Fang S, Wang Y, Sui D, Liu H, Ross MI, Gershenwald JE, et al. C-reactive protein as a marker of melanoma progression. *J Clin Oncol* (2015) 33(12):1389–96. doi: 10.1200/JCO.2014.58.0209
52. Ozawa Y, Amano Y, Kanata K, Hasegawa H, Matsui T, Kakutani T, et al. Impact of early inflammatory cytokine elevation after commencement of PD-1 inhibitors to predict efficacy in patients with non-small cell lung cancer. *Med Oncol* (2019) 36(4):33. doi: 10.1007/s12032-019-1255-3
53. Fukuda S, Saito K, Yasuda Y, Kijima T, Yoshida S, Yokoyama M, et al. Impact of C-reactive protein flare-response on oncological outcomes in patients with metastatic renal cell carcinoma treated with nivolumab. *J Immuno Ther Cancer* (2021) 9:e001564. doi: 10.1136/jitc-2020-001564
54. Filep JG. Targeting conformational changes in C-reactive protein to inhibit pro-inflammatory actions. *EMBO Mol Med* (2023) 15(1):e17003. doi: 10.15252/emmm.202217003
55. Perkins SJ, Okemefuna AI, Nan R. Unravelling protein-protein interactions between complement factor H and C-reactive protein using a multidisciplinary strategy. *Biochem Soc Trans* (2010) 38(4):894–900. doi: 10.1042/BST0380894
56. Hammond DJR, Singh SK, Thompson JA, Beeler BW, Rusinol AE, Pangburn MK, et al. Identification of acidic pH-dependent ligands of pentameric C-reactive protein. *J Biol Chem* (2010) 285(46):36235–44. doi: 10.1074/jbc.M110.142026
57. Eisenhardt SU, Habersberger J, Murphy A, Chen Y-C, Woollard KJ, Bassler N, et al. Dissociation of pentameric to monomeric C-reactive protein on activated platelets localizes inflammation to atherosclerotic plaques. *Circ Res* (2009) 105(2):128–37. doi: 10.1161/CIRCRESAHA.108.190611
58. Molins B, Pena E, de la Torre R, Badimon L. Monomeric C-reactive protein is prothrombotic and dissociates from circulating pentameric C-reactive protein on adhered activated platelets under flow. *Cardiovasc Res* (2011) 92(2):328–37. doi: 10.1093/cvr/cvr226
59. Braig D, Nero TL, Koch HG, Kaiser B, Wang X, Thiele JR, et al. Transitional changes in the CRP structure lead to the exposure of proinflammatory binding sites. *Nat Commun* (2017) 8:14188. doi: 10.1038/ncomms14188
60. Kheiss T, József L, Potempa LA, Filep JG. Conformational rearrangement in C-reactive protein is required for proinflammatory actions on human endothelial cells. *Circulation* (2004) 109(16):2016–22. doi: 10.1161/01.CIR.0000125527.41598.68
61. Kheiss T, József L, Potempa LA, Filep JG. Loss of pentameric symmetry in C-reactive protein induces interleukin-8 secretion through peroxynitrite signaling in human neutrophils. *Circ Res* (2005) 97(7):690–7. doi: 10.1161/01.RES.0000183881.11739.CB
62. Kheiss T, József L, Potempa LA, Filep JG. Opposing effects of C-reactive protein isoforms on shear-induced neutrophil-platelet adhesion and neutrophil aggregation in whole blood. *Circulation* (2004) 110(17):2713–20. doi: 10.1161/01.CIR.0000146846.00816.DD
63. Zouki C, Haas B, Chan JSD, Potempa LA, Filep JG. Loss of pentameric symmetry of C-reactive protein is associated with promotion of neutrophil-endothelial cell adhesion. *J Immunol* (2001) 167(9):5355–61. doi: 10.4049/jimmunol.167.9.5355
64. Kheiss T, József L, Hossain S, Chan JS, Potempa LA, Filep JG. Loss of pentameric symmetry of C-reactive protein is associated with delayed apoptosis of



human neutrophils. *J Biol Chem* (2002) 277(43):40775–81. doi: 10.1074/jbc.M205378200

65. Zeller J, Cheung Tung Shing KS, Nero TL, McFadyen JD, Krippner G, Bogner B, et al. A novel phosphocholine-mimetic inhibits a pro-inflammatory conformational change of C-reactive protein. *EMBO Mol Med* (2023) 15(1):e16236. doi: 10.15252/emmm.202216236

66. Braig D, Kaiser B, Thiele JR, Bannasch H, Peter K, Stark GB, et al. A conformational change of C-reactive protein in burn wounds unmasks its proinflammatory properties. *Int Immunol* (2014) 26(8):467–78. doi: 10.1093/intimm/idx056

67. Thiele JR, Habersberger J, Braig D, Schmidt Y, Goerendt K, Maurer V, et al. Dissociation of pentameric to monomeric C-reactive protein localizes and aggravates inflammation: in vivo proof of a powerful proinflammatory mechanism and new anti-inflammatory strategy. *Circulation* (2014) 130(1):35–50. doi: 10.1161/CIRCULATIONAHA.113.007124

68. Wang MY, Ji S-R, Bai C-J, El Kebir D, Li H-Y, Shi J-M, et al. A redox switch in C-reactive protein modulates activation of endothelial cells. *FASEB J* (2011) 25(9):3186–96. doi: 10.1096/fj.11-182741

69. Habersberger J, Strang F, Scheichl A, Htun N, Bassler N, Merivirta RM, et al. Circulating microparticles generate and transport monomeric C-reactive protein in patients with myocardial infarction. *Cardiovasc Res* (2012) 96(1):64–72. doi: 10.1093/cvr/cvs237

70. Crawford JR, Trial J, Nambi V, Hoogeveen RC, Taffet GE, Entman ML. Plasma levels of endothelial microparticles bearing monomeric C-reactive protein are increased in peripheral artery disease. *J Cardiovasc Transl Res* (2016) 9(3):184–93. doi: 10.1007/s12265-016-9678-0

71. Lane T, Wassef N, Poole S, Mistry Y, Lachmann HJ, Gillmore JD, et al. Infusion of pharmaceutical-grade natural human C-reactive protein is not proinflammatory in healthy adult human volunteers. *Circ Res* (2014) 114(4):672–6. doi: 10.1161/CIRCRESAHA.114.302770

72. Pepys MB, Hirschfield GM, Tennent GA, Gallimore JR, Kahan MC, Bellotti V, et al. Targeting C-reactive protein for the treatment of cardiovascular disease. *Nature* (2006) 440(7088):1217–21. doi: 10.1038/nature04672

73. McFadyen JD, Kiefer J, Braig D, Loeffel-Silver J, Potempa LA, Eisenhardt SU, et al. Dissociation of C-reactive protein localizes and amplifies inflammation: Evidence for a direct biological role of C-reactive protein and its conformational changes. *Front Immunol* (2018) 9:1351. doi: 10.3389/fimmu.2018.01351

74. Gill R, Kemp JA, Sabin C, Pepys MB. Human C-reactive protein increases cerebral infarct size after middle cerebral artery occlusion in adult rats. *J Cereb Blood Flow Metab* (2004) 24(11):1214–8. doi: 10.1097/01.WCB.0000136517.61642.99

75. Thiele JR, Zeller J, Kiefer J, Braig D, Kreuzaler S, Lenz Y, et al. A conformational change in C-reactive protein enhances leukocyte recruitment and reactive oxygen species generation in Ischemia/Reperfusion injury. *Front Immunol* (2018) 9:675. doi: 10.3389/fimmu.2018.00675

76. Xia D, Samols D. Transgenic mice expressing rabbit C-reactive protein are resistant to endotoxemia. *Proc Natl Acad Sci USA* (1997) 94(6):2575–80. doi: 10.1073/pnas.94.6.2575

77. Rodriguez W, Mold C, Kataranovski M, Hutt JA, Marnell LL, Verbeek JS, et al. C-reactive protein mediated suppression of nephrotoxic nephritis: role of macrophages, complement, and Fcγ receptors. *J Immunol* (2007) 178(1):530–8. doi: 10.4049/jimmunol.178.1.530

78. Du Clos TW, Mold C. C-reactive protein: an activator of innate immunity and a modulator of adaptive immunity. *Immunol Res* (2004) 30(3):261–77. doi: 10.1385/IR.30.3.261

79. Svanberg C, Enocsson H, Govender M, Martinsson K, Potempa LA, Rajab IM, et al. Conformational state of C-reactive protein is critical for reducing immune complex-triggered type I interferon response: Implications for pathogenic mechanisms in autoimmune diseases imprinted by type I interferon gene dysregulation. *J Autoimmun* (2023) 135:102998. doi: 10.1016/j.jaut.2023.102998

80. Lu J, Marnell LL, Marjon KD, Mold C, Du Clos TW, Sun PD. Structural recognition and functional activation of FcγR2b by innate pentraxins. *Nature* (2008) 456(7224):989–92. doi: 10.1038/nature07468

81. Brennan MP, Moriarty RD, Grennan S, Chubb AJ, Cox D. C-reactive protein binds to αIIbβ3. *J Thromb Haemost* (2008) 6(7):1239–41. doi: 10.1111/j.1538-7836.2008.02993.x

82. Ji SR, Ma L, Bai CJ, Shi JM, Li HY, Potempa LA, et al. Monomeric C-reactive protein activates endothelial cells via interaction with lipid raft microdomains. *FASEB J* (2009) 23(6):1806–16. doi: 10.1096/fj.08-116962

83. Fedewa MV, Hathaway ED, Ward-Ritacco C, Ward-Ritacco CL. Effect of exercise training on C reactive protein: a systematic review and meta-analysis of randomised and non-randomised controlled trials. *Br J Sports Med* (2017) 1(8):670–76. doi: 10.1136/bjsports-2016-095999

84. Selvin E, Paynter NP, Erlinger TP. The effect of weight loss on C-Reactive protein: A systematic review. *Arch Intern Med* (2007) 167:31–9. doi: 10.1001/ARCHINTE.167.1.31

85. Scheurig AC, Thorand B, Fischer B, Heier M, Koenig W. Association between the intake of vitamins and trace elements from supplements and C-reactive protein: results of the MONICA/KORA Augsburg study. *Eur J Clin Nutr* (2008) 62:127–37. doi: 10.1038/sj.ejcn.1602687

86. Smidowicz A, Regula J. Effect of nutritional status and dietary patterns on human serum C-reactive protein and interleukin-6 concentrations. *Adv Nutr* (2015) 6:738–47. doi: 10.3945/AN.115.009415

87. Gallus S, Lugo A, Suatoni P, Taverna F, Bertocchi E, Boffi R, et al. Effect of tobacco smoking cessation on C-Reactive protein levels in A cohort of low-dose computed tomography screening participants. *Sci Rep* (2018) 8:12908. doi: 10.1038/s41598-018-29867-9

88. Ridker PM, Danielson E, Fonseca FA, Genest J, Gotto AM Jr, Kastelein JJP, et al. Rosuvastatin to prevent vascular events in men and women with elevated C-reactive protein. *N Engl J Med* (2008) 359(21):2195–207. doi: 10.1056/NEJMoa0807646

89. Ridker PM, Danielson E, Fonseca FA, Genest J, Gotto AM Jr, Kastelein JJP, et al. Reduction in C-reactive protein and LDL cholesterol and cardiovascular event rates after initiation of rosuvastatin: a prospective study of the JUPITER trial. *Lancet* (2009) 373(9670):1175–82. doi: 10.1016/S0140-6736(09)60447-5

90. Zhang J, Wang X, Tian W, Wang T, Jia J, Lai R, et al. The effect of various types and doses of statins on C-reactive protein levels in patients with dyslipidemia or coronary heart disease: A systematic review and network meta-analysis. *Front Cardiovasc Med* (2022) 9:936817. doi: 10.3389/fcvm.2022.936817

91. Ridker PM, Bhatt DL, Pradhan AD, Glynn RJ, McFadyen JG, Nissen SE, et al. Inflammation and cholesterol as predictors of cardiovascular events among patients receiving statin therapy: a collaborative analysis of three randomised trials. *Lancet* (2023) 401(10384):1293–1301. doi: 10.1016/S0140-6736(23)00215-5

92. Kandelouei T, Abbasifard M, Imani D, Aslani S, Razi B, Fasihi M, et al. Effect of Statins on Serum level of hs-CRP and CRP in Patients with Cardiovascular Diseases: A Systematic Review and Meta-Analysis of Randomized Controlled Trials. *Mediators Inflammation* (2022) 2022:8732360. doi: 10.1155/2022/8732360

93. Cicero AFG, Fogacci F, Hernandez AV, Banach M, Alnouri F, Amar F, et al. Efficacy and safety of bempedoic acid for the treatment of hypercholesterolemia: A systematic review and meta-analysis. *PLoS Med* (2020) 17:e1003121. doi: 10.1371/JOURNAL.PMED.1003121

94. Prasad K. C-reactive protein (CRP)-lowering agents. *Cardiovasc Drug Rev* (2006) 24(1):33–50. doi: 10.1111/j.1527-3466.2006.00033.x

95. Liu D, Jin B, Chen W, Yun P. Dipeptidyl peptidase 4 (DPP-4) inhibitors and cardiovascular outcomes in patients with type 2 diabetes mellitus (T2DM): a systematic review and meta-analysis. *BMC Pharmacol Toxicol* (2019) 20(1):18. doi: 10.1186/S40360-019-0293-Y

96. Awad K, Zaki MM, Mohammed M, Lewek J, Lavie CJ, Banach M. Effect of the renin-angiotensin system inhibitors on inflammatory markers: A systematic review and meta-analysis of randomized controlled trials. *Mayo Clin Proc* (2022) 97:1808–23. doi: 10.1016/j.MAYOCP.2022.06.036

97. Jones NR, Pegues MA, McCrory MA, Singleton W, Bethune C, Baker BF, et al. A selective inhibitor of human C-reactive protein translation is efficacious in vitro and in C-reactive protein transgenic mice and humans. *Mol Ther Nucleic Acids* (2012) 1:e52. doi: 10.1038/MTNA.2012.44

98. Szalai AJ, McCrory MA, Xing D, Hage FG, Miller A, Oparil S, et al. Inhibiting C-reactive protein for the treatment of cardiovascular disease: promising evidence from rodent models. *Med Inflammation* (2014) 2014:353614. doi: 10.1155/2014/353614

99. Warren MS, Hughes SG, Singleton W, Yamashita M, Genovese MC. Results of a proof of concept, double-blind, randomized trial of a second-generation antisense oligonucleotide targeting high-sensitivity C-reactive protein (hs-CRP) in rheumatoid arthritis. *Arthritis Res Ther* (2015) 17(1):80. doi: 10.1186/s13075-015-0578-5

100. Noveck R, Stroes ESG, Flaim JD, Baker BF, Hughes S, Graham MJ, et al. Effects of an antisense oligonucleotide inhibitor of C-reactive protein synthesis on the endotoxin challenge response in healthy human male volunteers. *J Am Heart Assoc* (2014) 3(4):e001084. doi: 10.1161/JAHA.114.001084

101. Sugihara C, Freemantle N, Hughes SG, Furniss S, Sulke N. The effect of C-reactive protein reduction with a highly specific antisense oligonucleotide on atrial fibrillation assessed using beat-to-beat pacemaker Holter follow-up. *J Interv Card Electrophysiol* (2015) 43:91–8. doi: 10.1007/S10840-015-9986-3/METRICS

102. Skarabis H, Torzewski J, Ries W, Heigl F, Garlachs CD, Kunze R, et al. Sustainability of C-Reactive protein apheresis in acute myocardial infarction—Results from a supplementary data analysis of the exploratory C-Reactive protein in acute myocardial infarction-1 study. *J Clin Med* (2022) 11:6446. doi: 10.3390/JCM11216446

103. Ringel J, Ramlow A, Bock C, Sheriff A. Case report: C-Reactive protein apheresis in a patient with COVID-19 and fulminant CRP increase. *Front Immunol* (2021) 12:708101. doi: 10.3389/fimmu.2021.708101

104. Schumann C, Heigl F, Rohrbach JJ, Sheriff A, Wagner L, Wagner F, et al. A report on the first 7 sequential patients treated within the C-Reactive protein apheresis in COVID (CACOV) registry. *Am J Case Rep* (2021) 23:e935263. doi: 10.12659/AJCR.935263

105. Eposito F, Matthes H, Schad F. Seven COVID-19 patients treated with C-Reactive protein (CRP) apheresis. *J Clin Med* (2022) 11:1956. doi: 10.3390/JCM11071956/S1

106. Gao R, Wang L, Bai T, Zhang Y, Bo H, Shu Y. C-Reactive protein mediating immunopathological lesions: A potential treatment option for severe influenza A diseases. *EBioMedicine* (2017) 22:133. doi: 10.1016/j.EBIO.2017.07.010

107. Block G, Jansen CD, Dalvi TB, Norkus EP, Hudes M, Crawford PB, et al. Vitamin C treatment reduces elevated C-reactive protein. *Free Radic Biol Med* (2009) 46(1):70–7. doi: 10.1016/j.freeradbiomed.2008.09.030
108. Tardif J-C, Samuel M. Inflammation contributes to cardiovascular risk in patients receiving statin therapy. *Lancet* (2023) 401(10384):1245–7. doi: 10.1016/S0140-6736(23)00454-3
109. Aday AW, Ridker PM. Targeting residual inflammatory risk: A shifting paradigm for atherosclerotic disease. *Front Cardiovasc Med* (2019) 6:16. doi: 10.3389/fcvm.2019.00016
110. Dhuri K, Bechtold C, Quijano E, Pham H, Gupta A, Vikram A, et al. Antisense oligonucleotides: An emerging area in drug discovery and development. *J Clin Med* (2020) 9(6):2004. doi: 10.3390/jcm9062004
111. Xing D, Hage FG, Chen Y-F, McCrory MA, Feng W, Skibinski GA, et al. Exaggerated neointima formation in human C-reactive protein transgenic mice is IgG Fc receptor type I (FcγRI)-dependent. *Am J Pathol* (2008) 172:22–30. doi: 10.2353/ajpath.2008.070154
112. Burel SA, Macherer T, Baker BF, Kwok TJ, Paz S, Younis H, et al. Early-stage identification and avoidance of antisense oligonucleotides causing species-specific inflammatory responses in human volunteer peripheral blood mononuclear cells. *Nucleic Acid Ther* (2022) 32(6):457–72. doi: 10.1089/NAT.2022.0033
113. Sheriff A, Schindler R, Vogt B, Abdel-Aty H, Unger JK, Bock C, et al. Selective apheresis of C-reactive protein: A new therapeutic option in myocardial infarction? *J Clin Apher* (2014) 30:15–21. doi: 10.1002/jca.21344
114. Ries W, Sheriff A, Heigl F, Zimmermann O, Garlich CD, Torzewski J. “First in man”: case report of selective C-Reactive protein apheresis in a patient with acute ST segment elevation myocardial infarction. *Case Rep Cardiol* (2018) 2018:4767105. doi: 10.1155/2018/4767105
115. Ries W, Heigl F, Garlich C, Sheriff A, Torzewski J. Selective C-reactive protein-apheresis in patients. *Ther Apher Dial* (2019) 23(6):570–4. doi: 10.1111/1744-9987.12804
116. Kraus VB, Jordan JM. Serum C-reactive protein (CRP), Target for therapy or trouble? *biomark Insights* (2006) 1:77–80. doi: 10.1177/117727190600100020
117. Diaz Padilla N, Bleeker WK, Lubbers Y, Rigter GMM, Van Mierlo GJ, Daha MR, et al. Rat C-reactive protein activates the autologous complement system. *Immunology* (2003) 109(4):564–71. doi: 10.1046/J.1365-2567.2003.01681.X
118. Yipp BG, Kubes P. NETosis: how vital is it? *Blood* (2013) 122(14):2784–94. doi: 10.1182/blood-2013-04-457671





## OPEN ACCESS

## EDITED BY

Alok Agrawal,  
East Tennessee State University,  
United States

## REVIEWED BY

Thomas Vorup-Jensen,  
Aarhus University, Denmark  
Utpal Sengupta,  
The Leprosy Mission Trust India, India

## \*CORRESPONDENCE

John G. Raynes  
✉ john.raynes@lshtm.ac.uk

RECEIVED 10 July 2023

ACCEPTED 14 August 2023

PUBLISHED 31 August 2023

## CITATION

Seow ES, Doran EC, Schroeder JH,  
Rogers ME and Raynes JG (2023)  
C-reactive protein binds to short  
phosphoglycan repeats of *Leishmania*  
secreted proteophosphoglycans and  
activates complement.  
*Front. Immunol.* 14:1256205.  
doi: 10.3389/fimmu.2023.1256205

## COPYRIGHT

© 2023 Seow, Doran, Schroeder, Rogers and  
Raynes. This is an open-access article  
distributed under the terms of the [Creative  
Commons Attribution License \(CC BY\)](#). The  
use, distribution or reproduction in other  
forums is permitted, provided the original  
author(s) and the copyright owner(s) are  
credited and that the original publication in  
this journal is cited, in accordance with  
accepted academic practice. No use,  
distribution or reproduction is permitted  
which does not comply with these terms.

# C-reactive protein binds to short phosphoglycan repeats of *Leishmania* secreted proteophosphoglycans and activates complement

Eu Shen Seow, Eve C. Doran, Jan-Hendrik Schroeder,  
Matthew E. Rogers and John G. Raynes\*

Department of Infection Biology, Faculty of Infectious and Tropical Diseases, London School of Hygiene and Tropical Medicine, London, United Kingdom

Human C-reactive protein (CRP) binds to lipophosphoglycan (LPG), a virulence factor of *Leishmania* spp., through the repeating phosphodisaccharide region. We report here that both major components of promastigote secretory gel (PSG), the filamentous proteophosphoglycan (fPPG) and the secreted acid phosphatase (ScAP), are also ligands. CRP binding was mainly associated with the flagellar pocket when LPG deficient *Leishmania mexicana* parasites were examined by fluorescent microscopy, consistent with binding to secreted material. ScAP is a major ligand in purified fPPG from parasite culture as demonstrated by much reduced binding to a ScAP deficient mutant fPPG in plate binding assays and ligand blotting. Nevertheless, in sandfly derived PSG fPPG is a major component and the major CRP binding component. Previously we showed high avidity of CRP for LPG ligand required multiple disaccharide repeats. ScAP and fPPG only have short repeats but they retain high avidity for CRP revealed by surface plasmon resonance because they are found in multiple copies on the phosphoglycan. The fPPG from many species such as *L. donovani* and *L. mexicana* bound CRP strongly but *L. tropica* and *L. amazonensis* had low amounts of binding. The extent of side chain substitution of [-PO<sub>4</sub>-6Galβ1-4Manα1-] disaccharides correlates inversely with binding of CRP. The ligand for the CRP on different species all had similar binding avidity as the half maximal binding concentration was similar. Since the PSG is injected with the parasites into host blood pools and phosphoglycans (PG) are known to deplete complement, we showed that CRP makes a significant contribution to the activation of complement by PSG using serum from naive donors.

## KEYWORDS

C-reactive protein, proteophosphoglycan, *Leishmania*, complement, promastigote secretory gel, secreted acid phosphatase

# 1 Introduction

Leishmaniasis is a zoonotic disease caused by the *Leishmania* genus of protozoan parasites and a major neglected tropical disease, with 500,000 to 900,000 estimated new cases and 18,700 fatalities per year (1). It affects diverse mammalian species and is transmitted by female Phlebotominae sand flies during bloodmeal feeding attempts.

During the insect stage and during the infection of mammalian hosts the parasites produce a variety of phosphoglycan structures that aid in their survival and virulence (2). These include the relatively well studied membrane-associated lipophosphoglycan (LPG) ligand. However, parasites also produce proteophosphoglycans (PPG) including filamentous proteophosphoglycan (fPPG) and secreted acid phosphatase (ScAP) in the infected sand fly. The secreted PPGs are introduced into the feeding site as part of the promastigote secretory gel (PSG) alongside mammalian-infectious metacyclic promastigotes and sand fly saliva. Studies using knock out of LPG1 or LPG2 (3) have shown a complicated virulence phenotype differing in different parasites, for instance, LPG deficiency in *Leishmania major* (4) and *Leishmania infantum* (5) suggests virulence in mammalian infection studies but *Leishmania mexicana* did not (3, 6).

Proteophosphoglycans share similar glycan moieties to LPG, as shown by the cross-reactivity of many antibodies between LPG and the PSG components fPPG and ScAP (7). ScAP and fPPG have high carbohydrate contents, which form more than 70% of their molecular weight. While their exact function is currently unknown, PSG injected with or without saliva promotes cutaneous leishmaniasis infection in murine studies, suggesting that PSG may be a virulence factor (8, 9). The main component of PSG and PPG is fPPG, a mucin-like molecule. The types and structures of the phosphoglycans show some similarities but also significant differences between species in terms of when expressed, glycan content and whether secreted or membrane bound. ScAP, while not the primary constituent of PPG, is associated with fPPG and the subunits are hard to dissociate from the polymer structure (10). The potential role of PSG in establishing human infection remains an underreported field of study, particularly in light of the likely importance of the early immune response to the determination of Leishmaniasis outcome.

Among possible innate recognition molecules, CRP has been shown to bind to *Leishmania* surface LPG (11). Classically CRP is known to bind in a calcium dependent way to phosphorylcholine (PCh) which is a common component in a variety of fungal, bacterial and parasitic products. In this manner, CRP acts as an important innate immune activator of the classical complement pathway via CRP (12, 13). In the case of *Leishmania*, CRP binds with high affinity in a calcium dependent manner to the phosphorylated galactose mannose disaccharide repeat found in *Leishmania* LPG (11). High affinity interactions required between 3 and 10 repeats of [-PO4-6Gal $\beta$ 1-4Man $\alpha$ 1-] when provided as chemically synthesised soluble form (14). This interaction with LPG has biological relevance for a number of reasons. It can lead to increased uptake into macrophages under physiological conditions,

although this may not lead to increased killing but rather aid the parasite in establishing infection (15). In addition, the binding of the CRP to the surface of the parasite has also been shown to help the parasite initiate transformation in *L. mexicana* (16) and *L. donovani* (17). CRP interaction with LPG thus has importance in infection of the mammalian host from the sand fly.

This report now investigates the potential interaction of CRP with the PSG phosphoglycans. Whilst the longer LPG from metacyclic parasites shows greatly increased binding to CRP compared to 'non-infectious log phase promastigotes' both these have much greater length than that reported for the phosphoglycans of ScAP and proteophosphoglycans that have typically an average of 2-3 repeats (10). Individual soluble synthetic structures were shown to have only weak ability to interact with CRP (14). However, we demonstrate here that the interaction of CRP with proteophosphoglycan is high avidity when these short repeats of [-PO4-6Gal $\beta$ 1-4Man $\alpha$ 1-] are presented in multiple sites on the extended structure.

One way in which the interaction of CRP might alter infection rates and/or survival of the parasite is through the complement pathway. Importantly CRP binding of a ligand does not inevitably lead to complement activation as seen recently for a phosphorylcholine substituted glycoprotein ES-62 (18). The LPG is a known activator of complement particularly to extended LPG in metacyclic forms causing deposition of C3b but without damaging the parasite (19). This is in contrast to logarithmic phase parasites which are all rapidly killed by complement. It is already known that a potentially important role of secreted PPGs in PSG such as fPPG and ScAP is the activation and depletion of complement. PPG injected into a mouse could dramatically deplete complement by 90% within 30 minutes (20). The potential mechanisms of this could be classical or lectin pathway mediated as the activation was calcium dependent but a role for CRP was not assessed. Here we show that using naive donor sera CRP makes a significant contribution to the total complement activation by the proteophosphoglycan thereby implicating a role in complement depletion.

## 2 Methods

### 2.1 Purification of proteophosphoglycan

Parasites of *Leishmania mexicana* (MNYC/BZ/62/M379); *Leishmania major* (LV39; (MRHO/SU/59/P); *Leishmania donovani* (MHOM/ET/67/HU3); *Leishmania panamenensis* (MHOM/PA/67/BOYNTON); *Leishmania infantum* (MHOM/BR/76/M4192); *Leishmania amazonensis* (LV79: MPRO/BR/72/M1841); *Leishmania aethiopica* (MHOM/ET/84/KH); *Leishmania tropica* (MHOM/AF/2015/HTD7) were cultured as described (21). Lipophosphoglycan (LPG) and phosphoglycan deficient *L. mexicana* were a kind gift from Dr Thomas Ilg. The LPG-deficient mutant (*lpg1*-/-) lacks the LPG1 gene, which encodes a galactofuranosyltransferase required for synthesis of the LPG glycan core, rendering them deficient in LPG alone whilst *L. mexicana*

*lpg2*<sup>-/-</sup> lacks all repeating phosphodisaccharide. Selection antibiotics hygromycin (20 µg/ml) and phleomycin (2.5 µg/ml) were added to the culture medium (3, 6) for deficient *L. mexicana* mutants *lpg1*<sup>-/-</sup> and *lpg2*<sup>-/-</sup>. *L. mexicana* ( $\Delta$ lmscAP1/2) and an add back of ScAP2 were a kind gift of Dr Wiese (22) which employed a similar selection antibiotic pressure but including G418 (10 µg/ml) in the add back.

Culture supernatants were clarified by centrifugation at low speed (800g) and passed through an anion exchange column (DE52) equilibrated in 20 mM Tris-HCl, 100 mM NaCl, pH 7.5 at a rate of 2 ml/min and eluted in 20 mM Tris-HCl, pH 7.5 containing 500 mM NaCl (23). Following anion exchange, material was pelleted by ultracentrifugation at 100,000 g, 4°C for 4 hours in a Ti90 rotor and the pellet washed and resuspended in PBS.

A further step to remove more hydrophobic fractions such as LPG used hydrophobic interaction chromatography. Pelleted PPG was adjusted to 1 M ammonium sulphate via dilution with concentrated ammonium sulphate solution (10 M NH<sub>2</sub>SO<sub>4</sub>, 1:9 v/v ratio relative to material and added to a 5 ml column of octyl-Sepharose equilibrated in 20 mM Tris-HCl, 1 M NH<sub>2</sub>SO<sub>4</sub>, 5 mM EDTA, pH 7.5. This was followed by low ionic strength Tris-buffered saline (10 ml, 20 mM Tris-HCl, 100 mM NaCl, pH 7.5), Tris-buffered saline (20 ml, 20 mM Tris-HCl, pH 7.5) and then propan-1-ol (20%, 70% v/v) which eluted more hydrophobic glycans such as LPG. Quantification was based on A280 (Nanodrop) which correlated with the carbohydrate assay using the phenol-sulphuric acid method (24). PPG material was dialysed and stored at -80°C in 20 µl aliquots. The purified PPG was confirmed to be high molecular weight (above 100kD) and heterogeneous by SDS PAGE and detection by Stains-all and confirmed as phosphoglycan using Western blotting with CA7AE (22).

The biotinylation of PPG was performed using a method using NHS-LC-biotin in pH 9.6 carbonate buffer described previously (23). Labelled material was repurified by anion exchange on DE-52 as used for purification with extensive washing to remove unreacted biotin. Plate assays showed biotin-PPG and PPG had similar CRP binding dose response (data not shown).

## 2.2 CRP and biotinylated CRP

Human CRP and recombinant CRP were purified as described previously (18). Rat CRP was purified using phosphorylcholine (PCh) Sepharose by the same protocol. CRP was biotinylated at a neutral pH as described for the reagent NHS-LC-biotin (ThermoFisher) to prevent CRP denaturation. The CRP biotin was repurified on PCh-Sepharose to remove non-binding protein with extensive washing to remove unreacted biotin.

## 2.3 PPG-pentraxin plate binding assays

Purified PPG (0–3 µg/ml) in PBS pH 7.4 was coated onto 96 well microtiter plates (Immulon<sup>TM</sup> 2 HB 96-Well Microtiter EIA Plate, ImmunoChemistry Technologies, LLC). Biotinylated and affinity purified CRP (0–3 µg/ml) in HBSC-BSA was added and the plates

were incubated at room temperature for 1 hour. For inhibition assays, PCh chloride (Sigma-Aldrich) or EDTA (10 mM) or MgCl<sub>2</sub> (0.5 mM) and 10 mM EGTA or CRP depleted serum (5% v/v) was added at the CRP incubation stage. After washing with HBSC, the bound CRP was detected with streptavidin HRP (Biosource diluted 1 in 15,000) and 3,3',5,5'-Tetramethylbenzidine (TMB, 0.1 mg/ml) in phosphate-citrate buffer (0.05 M, pH 5.0) with hydrogen peroxide (0.006% v/v) added following an HRP-conjugated antibody incubation stage. The subsequent colour change reaction was stopped with H<sub>2</sub>SO<sub>4</sub> (2 M, 15 µl). The plate was read at wavelength 450 nm with subtraction of the reference wavelength at 405 nm (Titertek Multiskan MCC/340). Alternatively native pure CRP was used and detected with primary antibody rabbit anti-CRP (Dako: 1:800) followed by HRP-conjugated Goat anti-rabbit IgG (Bio-Rad, 1:3000) in HBSC-BSA. Mouse CRP binding was examined using the same buffer system and plates but using mouse CRP and affinity purified goat anti-mouse CRP (both R and D).

## 2.4 Western/ligand blot and protein gel staining

SDS-PAGE was performed using an extended 4% stacking gel layer in combination with a 6% or 10% resolving gel layer with reducing conditions. The molecular weight standards used were prestained, broad range (10–250 kDa, New England Biolabs).

Gels were then transferred by semi-dry blotting to PVDF membranes. Membranes were blocked with PBST containing 2% (w/v) BSA at 4°C o/n. Membranes were incubated with CRP biotin (1 µg/ml) or CRP (as shown in Figures) in TBST containing 0.5 mM CaCl<sub>2</sub> and 1% (w/v) BSA for 1 hour at room temperature and after 3 washes in the same buffer, bands where CRP bound were visualised with streptavidin alkaline phosphatase (AP) (1 in 500; SA5100 Vector labs) or anti-CRP-AP and colorimetric detection with substrate BCIP/NBT as described (18). Detection of phosphoglycan repeated disaccharide was performed using 1:1000 CA7AE (GeneTex) then followed by 1:30,000 anti-mouse IgM-AP (Sigma).

## 2.5 Surface plasmon resonance

Polycarboxylate chips with high charge density (Xantec, C30M) were washed and activated with EDC and NHS for 7 minutes. 0.5 mM aminodesthiobiotin in 10 mM sodium maleate buffer pH 6.8 was added at a flow rate of 2 µl/min for 40 minutes to give 150 RU attached. Reactive groups on both test and control surfaces were blocked with 1 M ethanolamine pH 8.0. Neutravidin (10 µg/ml) in calcium-containing HEPES buffer (HBSPC) was then immobilised on the desthiobiotin surface of both test and control surface to give a further 150 RU. Biotin labelled purified fPPG was then added at 20 µg/ml till 220 RU was attached to the test well only. CRP was flowed over at 30 µl/min for 3 minutes at various concentrations in HBSPC buffer containing 0.5 mM CaCl<sub>2</sub> and dissociation assessed for 5 minutes before CRP was dissociated with HBS containing 10 mM EDTA. In other experiments, inhibitors were added with the CRP

or other proteins. Between each addition, the chip was washed with HBS containing 10 mM EDTA.

Analysis was performed using BiaEval 4.1.1. Control flow cells were subtracted and traces overlain. Kinetic data was obtained using simultaneous  $k_a/k_d$  1:1 Langmuir analysis which achieved a good fit at low ligand immobilization.

## 2.6 Serum CRP depletion

Carboxylated Magnetic beads (Mobictec-beads, 100 $\mu$ l) were washed into PBS buffer. N-(3-Dimethylaminopropyl)-N'-ethylcarbodiimide (10  $\mu$ l, 10 mg/ml) was added to the beads and left to incubate at room temperature on a rocker for 5 minutes. Chicken anti-CRP IgG antibody (1 mg/ml, 25  $\mu$ l, Norwegian Antibodies) was added and left to incubate and cross-link overnight at room temperature. Blocking of remaining active cross-linking sites was achieved by incubation in 0.1 M glycine buffer (pH 8.3) for 1 hour at room temperature. Beads were washed into phosphate-buffered saline pH 7.4 with BSA (1% w/v) then washed into HEPES-buffered saline (20 mM HEPES, 150 mM NaCl, pH 7.4) with 0.5 mM  $\text{CaCl}_2$  (HBSC) and stored at 4°C. Whole serum from normal, healthy donors collected under ethical approval (100  $\mu$ l) was mixed with the anti-CRP beads and allowed to incubate on a rocker at 2°C for an hour immediately prior to experiments. Typical reduction in CRP concentrations were 50-95% determined using a sandwich ELISA for CRP (25).

## 2.7 Complement assays

### 2.7.1 C1q capture assay

An immune complex capture assay (18) was used to measure complex formation between CRP and different CRP ligands, including PPG or control PCh-BSA. Purified C1q (Calbiochem, 10  $\mu$ g/ml) was coated onto 96 well microtiter plates (Immulon 4 HBX, Thermo Fisher Scientific) at 4°C overnight. Plates were incubated with BSA (3% w/v) and Tween 20 (0.05% v/v) in PBS for non-specific site blocking at room temperature for 2 hours. Serum was obtained from healthy donors under informed consent at London School of Hygiene and Tropical Medicine (ethical approval 10672/RR/3680). Serum was diluted (1:20 v/v) with CRP (1  $\mu$ g/ml) and BSA (1% w/v) in veronal-buffered saline (VBS) with 0.15 mM  $\text{CaCl}_2$  and 0.5 mM  $\text{MgCl}_2$ , with or without EDTA (10 mM). CRP ligand (fPPG, PCBSA) was added at a range of concentrations (0-3  $\mu$ g/ml), and the plate was incubated at room temperature for 1 hour. Detection step was performed with a sheep anti-CRP conjugated with horseradish peroxidase (1:2000).

### 2.7.2 3d deposition assay

To assess C3 convertase formation, an existing protocol to detect the C3 convertase downstream product C3d was adapted (18). *L. infantum* or *L. mexicana* fPPG (4  $\mu$ g/ml) or PCh-BSA (0.4  $\mu$ g/ml) was diluted in PBS and immobilised on 96 well microtiter plates (Immulon™ 2 HB 96-Well Microtiter EIA Plate, ImmunoChemistry Technologies, LLC). Ligand concentration was

chosen to allow equivalent CRP binding as determined by previous CRP-ligand ELISA.

All additions were done with the reagents, serum and microtiter plate on ice. Donor serum was added to the wells (1:100 dilution) in GVBSCaMg (VBS with 0.2% v/v gelatin, 0.15 mM  $\text{CaCl}_2$  and 0.5 mM  $\text{MgCl}_2$ ), or GVBSEDTA (VBS with 10mM EDTA) or GVBSEGTAMg (VBS with 10mM EGTA plus 0.5 mM  $\text{MgCl}_2$ ) with or without additional purified CRP (0.4  $\mu$ g/ml). Plates were brought up to a uniform temperature in a water bath (37°C) and incubated for 20 minutes. For C3d detection, plates were incubated with primary biotinylated anti-C3d antibody (1:1000) followed by HRP conjugated streptavidin (1:15000) in HBSC-BSA.

### 2.7.3 iC3b deposition assay

Assay was performed as for C3d assay but plates were washed and iC3b detected with 1  $\mu$ g/ml biotinylated antibody to neoepitope of iC3b (Quidel) followed by streptavidin-HRP (Invitrogen).

## 2.8 Immunofluorescent (confocal) microscopy

$10^6$  *lpg1*<sup>-/-</sup> and WT parasites were washed with PBS and incubated in M199 medium containing 10  $\mu$ g/ml CRP, control media only or media with CRP and 15 mM EDTA for 1 hour at room temperature. Parasites were centrifuged and fixed in 4% (w/v) PFA, washed and  $2.5 \times 10^5$  parasites, air dried onto slides. Slides were rehydrated and stained with rabbit anti human CRP (Calbiochem) followed by anti-rabbit IgG FITC (Dako) both for 1 hour with washing between stages. The slides were dried and counterstained with vectashield + DAPI and coverslips attached. Slides were visualised using the Zeiss LSM880 confocal microscope.

## 3 Results

### 3.1 *L. mexicana* PPG binds to CRP

Purified fPPG was heterogeneous and high molecular weight as previously described (23). This material was adsorbed onto a microtitre plate and CRP showed strong binding with a half maximal binding seen at 30 ng/ml (Figure 1A) with significant binding detected at less than 1 ng/ml CRP. This binding was not inhibited by the presence of 5% (v/v) CRP-depleted serum indicating a lack of competition by other serum proteins at any CRP concentration (Figure 1B). Although most LPG is removed at the hydrophobic interactions stage of purification, to confirm that CRP binding was not due to contamination by small quantities of LPG we also showed binding to PPG from a mutant lacking LPG (*lpg1*<sup>-/-</sup>) (Figure 1C). In contrast, the same preparations from the LPG2 mutant that lacks all addition of phosphoglycan to any protein or lipid showed no binding of CRP (Figure 1C). As expected for an interaction with the major ligand binding site on CRP, the relatively lower affinity ligand soluble monomer phosphorylcholine (PCh) significantly inhibits CRP-binding in a competitive manner (Figure 1D). The binding was inhibitable completely with either



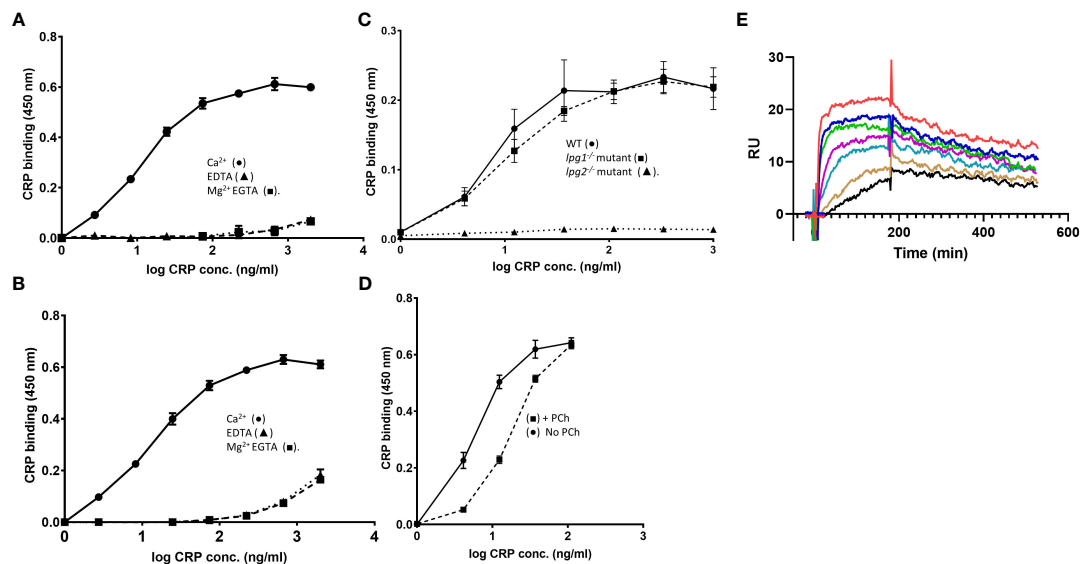


FIGURE 1

(A–E) CRP binds to *L. mexicana* fPPG. (A) CRP binds to fPPG in a calcium but not magnesium dependent manner. (A) *L. mexicana* wild-type fPPG (1  $\mu$ g/ml) was immobilised on microtitre plates and biotin-conjugated CRP (0–2.0  $\mu$ g/ml) was added in the presence of Ca<sup>2+</sup> (0.5 mM) (●); EDTA (10 mM) (▲) or Mg<sup>2+</sup> EGTA (10 mM) (■). CRP binding was detected using HRP conjugated Streptavidin (1:15000) and TMB substrate (OD 450 nm). (B) Serum components do not compete with CRP binding. As in (A) but 5% (v/v) CRP depleted serum was added. (C) CRP binding to fPPG is independent of LPG. Biotinylated CRP (0–1.0  $\mu$ g/ml) binds to immobilised *L. mexicana* fPPG coated at 0.3  $\mu$ g/ml from WT (●) and *lpg1*<sup>-/-</sup> mutant (■) but not *lpg2*<sup>-/-</sup> mutant (▲). (D) PCh competition inhibits CRP binding to fPPG. As in (A) but in the presence (■) or absence (●) of added PCh (10 mM). n=3. Error bars represent standard deviation. (E) Biosensor analysis of CRP binding to *L. mexicana* fPPG biotin immobilised onto neutravidin surface. 185 RU of neutravidin captured 340 RU of biotinylated fPPG. CRP (0.6–40  $\mu$ g/ml) was added for 3 minutes followed by 5 minutes dissociation. Traces show dose response of binding at two-fold dilutions after control flow cell subtraction.

EDTA or EGTA Mg (Figures 1A, B) consistent with the calcium dependent binding site seen previous for binding of CRP to LPG (11, 14).

### 3.2 Kinetics of CRP PSG interaction by SPR

Binding of CRP to immobilised *L. mexicana* fPPG (Figure 1E) was examined over a range of CRP concentrations utilising the calcium dependency to allow complete elution of CRP between associations. As previously reported for other ligands, CRP shows complex interaction kinetics as expected for a pentamer binding to a ligand that is also potentially multimeric (18). The analysis used a low density of fPPG on the surface to reduce interaction of surface bound molecules. This low ligand density allowed analysis using simple 1:1 binding model with good fit (Figure S1A). The off-rate ( $k_d$ ) was  $1.57 \times 10^{-3} \pm 3 \times 10^{-5} \text{ s}^{-1}$  and on rate  $4.3 \times 10^5 \pm 5 \times 10^3 \text{ M}^{-1} \text{ s}^{-1}$ . Overall avidity was estimated at  $3.6 \times 10^{-9} \text{ M}$  consistent with the nanomolar CRP concentrations at which CRP binds in plate assays. fPPG from *L. mexicana* LPG deficient (*lpg1*<sup>-/-</sup>) mutant with PPG but no LPG also bound in SPR experiments (data not shown).

### 3.3 The major CRP binding component of the purified fPPG is the ScAP component

CRP was also shown to bind to the fPPG when separated by electrophoresis and transferred to membrane and the membrane

was probed with CRP. Binding in the resolving gel was consistent with the molecular weight of ScAP. Binding to the material in the stacking gel could be to the filamentous proteophosphoglycan or to the acid phosphatase as this is strongly associated with the fPPG (10).

Therefore we used a mutant of *L. mexicana* that lacks both secreted acid phosphatases ( $\Delta$ ImScAP1/2) and an add back of ScAP2 (22). The filamentous phosphoglycan is also a ligand as the mutant still retained binding in the stacking gel by blotting which could only be the fPPG (Figure 2A). Quantitation of relative binding by microtitre plate binding assay confirmed the reduced CRP binding to the ScAP deficient PPG (Figure 2B). Binding of CRP was partially restored in the add back as seen in both assays (Figures 2A, B). In the add back, the amount of restored CRP binding was low, consistent with the plate binding assays but clearly associated with the ScAP2 that generated a band in the region of 200 kDa (Figure 2A). This suggested that the ScAP was a major ligand for CRP binding in the fPPG.

### 3.4 CRP binding to PPG from different *Leishmania* species shows similar high avidity but different ligand density

We examined the binding to fPPG derived from different *Leishmania* species. The species included were 5 from the Old World and 3 from the New World and are shown in these groups in



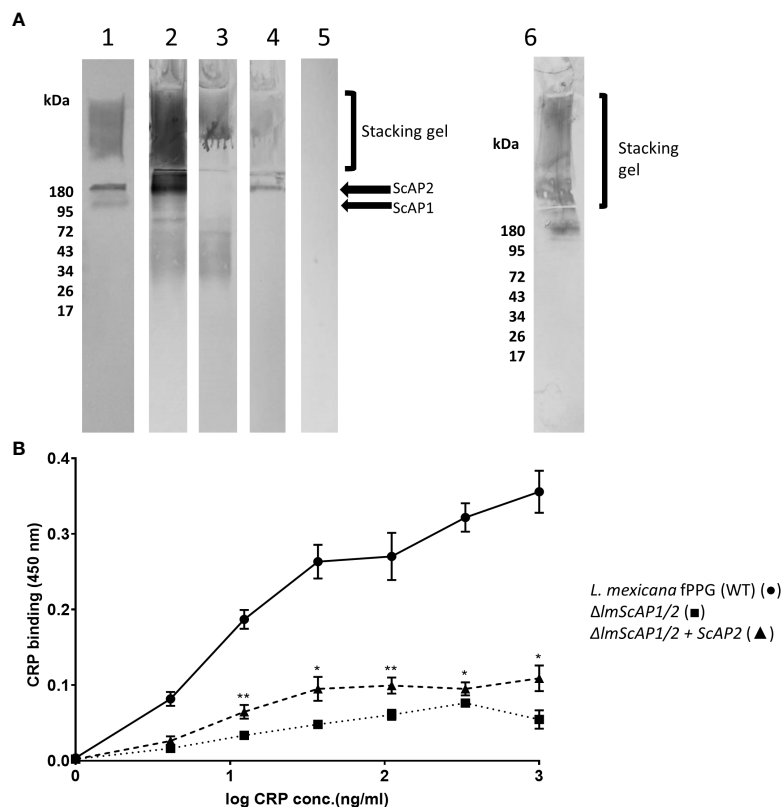


FIGURE 2

CRP binds to ScAP and fPPG from *L. infantum* and *L. mexicana* (A) Binding of CRP to *L. mexicana* Wt, ScAP<sup>-/-</sup>; and ScAP<sup>-/-</sup>-ScAP2 fPPG separated by SDS gels and transferred to membrane. fPPG (3  $\mu$ g) was separated on 10% gels with stacking gel and transferred to PVDF membranes. Lane 1 membranes were probed with CA7AE and anti-mouse IgM to detect repeating disaccharide. Lanes 2 - 6 were probed with CRP and anti-CRP except Lane 5 which was a no CRP control. *L. mexicana* WT (Lanes 1, 2 and 5),  $\Delta$ ImScAP1/2 (Lane 3),  $\Delta$ ImScAP1/2 + ScAP2 (Lane 4), *L. infantum* WT probed with CRP (Lane 6). (B) ScAP provides the majority of CRP binding capacity in purified phosphoglycan. Dose-Response of binding of purified CRP (0 - 1.0  $\mu$ g/ml) to immobilised *L. mexicana* fPPG (WT) (●),  $\Delta$ ImScAP1/2 (■),  $\Delta$ ImScAP1/2 + ScAP2 (▲). In both (A, B), CRP binding was detected using rabbit anti-CRP antibody, HRP-conjugated goat anti rabbit antibody and TMB substrate (OD 450nm). n=4. Error bars represent standard deviation. Statistical comparison was performed for ScAP deficient versus add-back ( $\Delta$ ImScAP1/2 vs  $\Delta$ ImScAP1/2 + ScAP2). \*p<0.01 \*\* p<0.001.

Figures 3A where binding was performed with a dose response of CRP to a constant PPG on the plate. In contrast, the panels in Figure 3B show the binding of a constant CRP to a range of ligand coating. The dose response of CRP binding to all parasites (Figure 3A) suggests that the ligand is of a similar high avidity for most parasites since the half maximal binding concentration (1-20 ng/ml) was similar for most species. High amounts of CRP binding represented a greater density of sites and binding to different species varied considerably at constant CRP (Figure 3B), for example, *L. donovani* had approximately 2 orders of magnitude more bound CRP than *L. major*. There was no link between Old and New World species, nor did CRP binding appear different between species that cause different clinical presentation (visceral, cutaneous, or mucocutaneous). Previous studies by Thomas Ilg had characterised the proteophosphoglycan structures of different *Leishmania* species and correlated this with reactivity to monoclonal antibodies. A major factor in differences between species was side chain substitution, with strongest binding seen to those species that had little side chain substitution (discussed later).

The binding of CRP in plate assays was confirmed by the ligand blotting assays which showed a large amount of binding to material in the separating gel consistent with binding to ScAP (Figure S2). *L. donovani* and *L. panamenensis* PPG had particularly high binding capacity. *L. tropica* as in the plate assays displayed very little CRP binding activity.

### 3.5 CRP of other mammalian species also binds to repeating disaccharide

To determine if CRP interaction with phosphoglycan was restricted to human CRP or a feature of wider mammalian CRP we tested binding and showed that rat CRP bound strongly to the fPPG in a calcium dependent way (Figure S3). This analysis used a higher surface density of fPPG and a different immobilization chemistry on the chip surface. The rat CRP binding was calcium

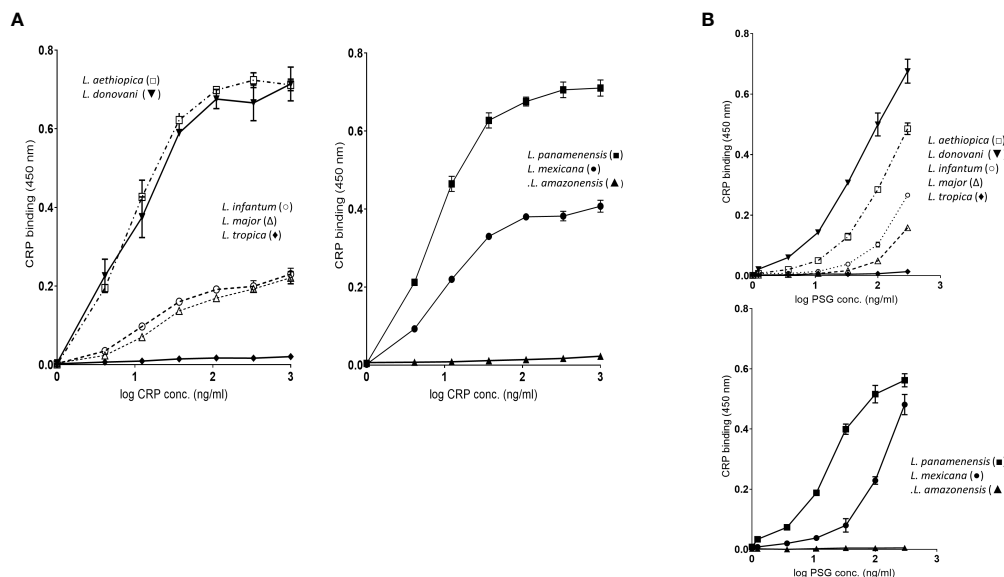


FIGURE 3

(A) fPPG from different *Leishmania* species exhibit widely varying CRP binding capacities. Dose response of binding of purified CRP (0 - 1.0  $\mu$ g/ml) to fPPG (0.3  $\mu$ g/ml) from different *Leishmania* species immobilised on microtitre plates. Bound CRP was detected using anti-CRP HRP. Left hand panels Old World species: Right hand panels New World Species. (B) CRP binding to varied fPPG coating concentrations with a constant CRP concentration (0.3  $\mu$ g/ml). Highly substituted phosphoglycans (C3-galactose) *L. tropica*; *L. amazonensis*, Low or absent side chain substitution *L. panamenensis*, *L. donovani*, *L. infantum*, *L. mexicana*. *L. aethiopica* has substitution on C-2 of mannose. Error bars represent standard deviation  $n=3$ .

dependent but showed a lower number of available sites than human CRP but a slower off-rate. We saw little interaction with human SAP which was previously shown not to bind to LPG nor to hamster female protein an SAP homologue. A further control confirmed that these proteins purified on PCh were not binding to PCh as a monoclonal antibody to PCh (TEPC15) did not bind to fPPG (data not shown). Although CRP in mice is relatively low in concentration and sex dependent, the low concentrations required for binding are within physiological concentrations and we tested recombinant mouse CRP binding to PSG from different species. The order of binding was in broad agreement with that seen for human CRP (Figure S4).

### 3.6 CRP binding to PPG in *lpg1*<sup>-/-</sup> parasites is located to the flagellar pocket

In order to locate the CRP ligand in the LPG deficient and wild type parasites we performed immunofluorescent detection of ligand on live mutant and wild type parasites. The wild type showed strong and even binding across the surface of the parasite (Figure 4B) consistent with previous data for *L. donovani* (11). In contrast the *lpg1*<sup>-/-</sup> strain showed staining that was localised close to the flagellar pocket (Figure 4A). In order to observe this, the methodology was altered to reduce washing post CRP addition. If the parasites were centrifuged and resuspended in wash buffer then we observed numerous punctate staining particles separate from the parasites consistent with detached secreted PPG CRP complex (data not shown).

### 3.7 CRP binding to native sand fly derived proteophosphoglycan (PSG) is mainly to fPPG

Although CRP binds to the purified cultured parasite fPPG, it was important to determine the binding to the physiological native promastigote secretory gel (PSG) found in infected sand flies. Previously it was shown that in *L. mexicana* the sand fly PSG was mainly composed of fPPG and there was little ScAP (26). PSG is associated with the parasites in the sand fly but also introduced at sand fly bites, therefore PSG was generated by microdissection and tested for binding to the CRP. Consistent with the limited ScAP presence we saw little binding to 200 kDa but very strong binding to the stacking gel and fPPG (Figure 5). This suggests that the main ligand in sand fly PSG was fPPG in contrast to the purified PSG from cultured parasites. Since the PSG from infected sand flies also contains *Leishmania* parasites the presence of LPG is detected as a broad band at around 50 kDa.

### 3.8 CRP binding to PSG activates complement

It was previously shown that *L. infantum* fPPG when injected with parasites caused an increased local survival of parasites (9) and *L. infantum* phosphoglycan is implicated in parasite virulence (5). fPPG and ScAP from *L. infantum* and *L. mexicana* bound CRP in a similar way (Figures 2, 3). A proteophosphoglycan from *L. mexicana* amastigotes with similar carbohydrate structure to fPPG including repeating disaccharide was previously shown to deplete complement

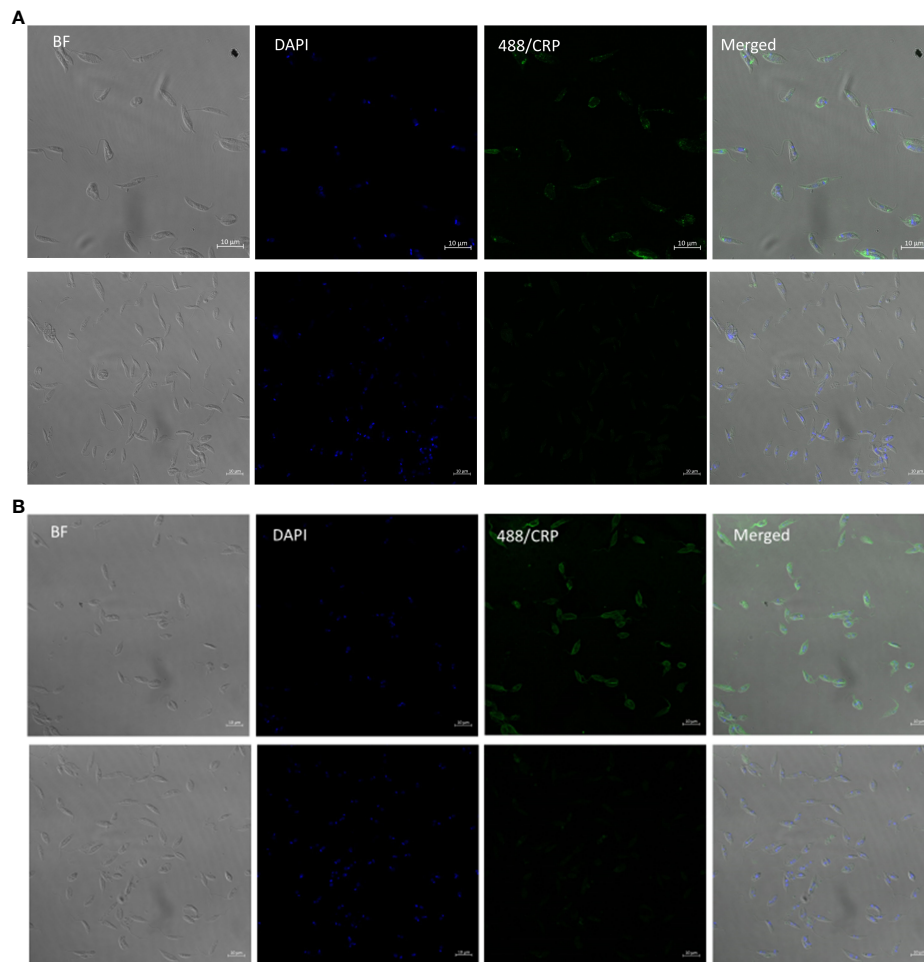


FIGURE 4

*L. mexicana* WT binds CRP all over surface in contrast to *lpg1*<sup>-/-</sup> mutant binding at flagellar pocket. (A) *L. mexicana lpg1*<sup>-/-</sup> and (B) *L. mexicana* WT parasites were incubated with CRP and gently washed before fixing and CRP detected rabbit anti human CRP followed by anti-rabbit IgG FITC. DAPI was used as a counterstain. Images from left to right; phase contrast, DAPI, CRP immunofluorescence; merged Upper panels with CRP, lower panels without CRP.

(20). Therefore, we chose fPPG from both these parasites to explore the ability of bound CRP to activate complement.

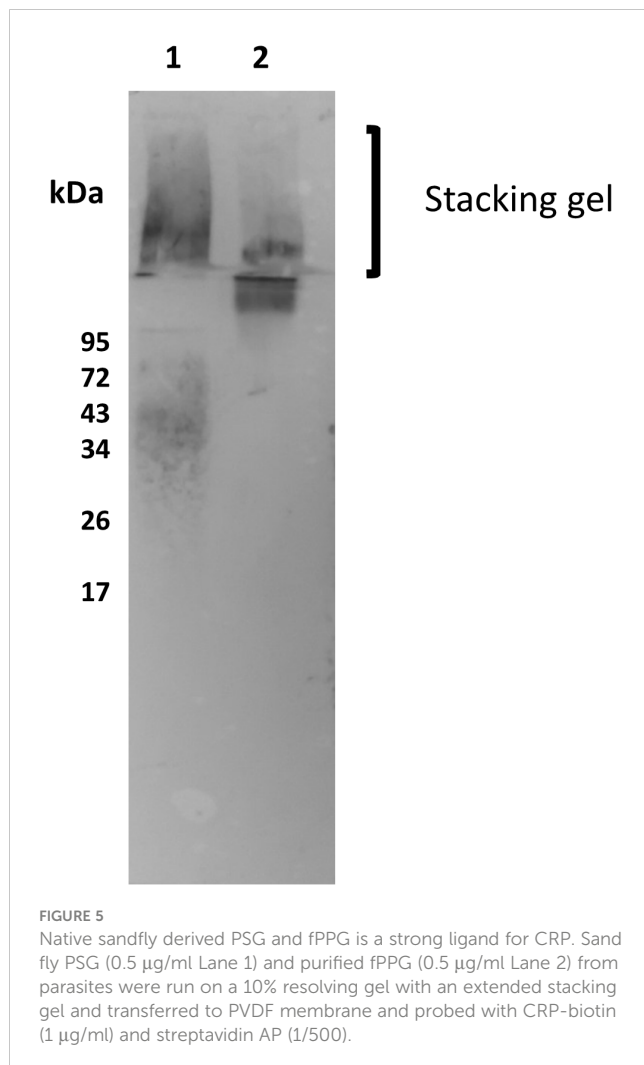
Using a capture assay with C1q attached to the plate and addition of serum containing CRP there was no observed binding of CRP to the C1q until fPPG addition which then generated a complex with the C1q. This showed a dose response as expected (Figure 6A). *L. tropica* did not lead to CRP binding to C1q consistent with the fPPG from this species failing to interact with CRP previously (Figures 3A, B). This interaction would be expected to lead to complement activation. This was confirmed when *L. mexicana* fPPG was used as a ligand in activation product assays that showed deposition of C3bi or C3d was by the classical pathway (Figure 6B). Classical pathway activation was increased by addition of CRP and reduced when CRP was partially depleted (Figure 6C). The depletion of CRP we achieved was only partial (50-95%) and the strong binding of CRP to its ligand suggests that the CRP would still have some contribution to the overall complement activation in depleted sera. Nevertheless, it was possible to demonstrate that a significant proportion of the activation of complement in serum

was mediated by CRP. The lack of phosphoglycan and CRP ligand in *L. mexicana lpg2*<sup>-/-</sup> mutant resulted in a lack of CRP dependent complement activation (Figure S5). When CRP was added to individual sera and C3d activation was assayed there was a clear and consistent increase in activation apparent across different individual sera (Figure 6D). Activation was similar or greater than that for a PCh-BSA positive control, a known strong ligand for CRP mediated complement activation. The background activation by fPPG was however also variable suggesting that potentially a cross-reacting antibody was present in some sera.

## 4 Discussion

### 4.1 CRP binding to ScAP and proteophosphoglycan

Previously we demonstrated CRP binding to the extended repeating disaccharide of LPG. Here we have demonstrated the



CRP can also bind with high avidity to multiple short disaccharides expressed on a backbone of a high molecular weight glycoprotein. Although previously we observed weak binding of CRP to soluble short repeats of the disaccharide in solution (14), the binding to multiple such structures on fPPG or ScAP was able to generate affinities similar to those seen previously to LPG. Although serum did not inhibit binding to the repeating disaccharide suggesting that CRP is the only major serum protein interacting with this epitope, CRP is not the only serum protein that binds to fPPG and the glycan structures present which include sidechain and cap structures. These include antibody and mannose-binding lectin (MBL) which have been detected by us using methods such as immunoprecipitation and others such as MBL which bound to amastigote PPG (aPPG) containing similar phosphoglycans to fPPG (20). The relative contribution of innate activators may vary considerably between *Leishmania* since we have shown that fPPG from *L. mexicana* and *L. infantum* bind much lower amounts of MBL than some other species such as *L. donovani*. The binding was consistent with the known binding properties of CRP in terms of calcium dependency and phosphorylcholine inhibition, in addition the kinetics showed that the avidity of binding was largely related to a slow off-rate (Figure 1E).

The observation that rat and mouse CRP binds *L. mexicana* fPPG is interesting, showing the phenomena is not restricted to human CRP although this observation needs extending to further species. Rat CRP has interesting binding features in that it binds to PCh but does not require the amino regions of the choline. In contrast, the HFP which is a homologue of SAP but also binds to phosphocholine in addition to phosphoethanolamine (27) did not bind.

For purified fPPG we observed that most of the binding was to the ScAP component despite being a minor component in terms of amount produced (22). fPPG having less binding for CRP is possible due to differences in the glycosylation of the PPG which has shorter Gal-Man repeats compared with ScAP and more frequent end capping that could mask the availability of the short repeat structure (28). However, the purification involved column separations and it is quite plausible that this process has enriched the lower molecular species at the expense of fPPG rich complexes trapped due to size by affinity media. The major ligand in PSG from sand flies was fPPG as very little binding was seen in resolving gels corresponding to ScAP. This does not rule out some binding in the stacker gel being due to ScAP but since fPPG is the major component this indicates that the major ligand in the gel is fPPG. The *fppg1* gene is present in most *Leishmania* and fPPG has been shown in *L. mexicana*, *L. major*, *L. amazonensis*, *Leishmania braziliensis*, *L. tropica* and *L. aethiopica* (29). The gel of PSG from infected sand flies also contains LPG as expected, revealed by CRP and CA7AE binding. CRP binds to the glycan of many PPGs but these may not always form filament networks as reported for *L. donovani* (30). Differences in size of fPPG and developmental changes have been shown for *L. major*, *L. mexicana* and *L. donovani* (31). There was no evidence for binding to other phosphoglycans such as aPPG or pPPG2 (32), since we did not examine amastigotes nor is aPPG a likely ligand since repeating disaccharide monoclonal LT6 does not bind (28).

## 4.2 Secretion of proteophosphoglycan

The secreted polymer fPPG has previously been shown to be located and polymer proposed to assemble in the flagellar pocket (30) so that we expected that fPPG would be localised here and this was demonstrated in LPG deficient parasites and shown to be quite different to the pattern for wild type LPG containing parasites where the LPG ligand is located over the whole parasite surface. Our data showed localisation of the secreted fPPG to the flagellar pocket in contrast to a previous study when *L. donovani* was analysed (33). In this study using an antibody generated to a protein part of fPPG the whole surface was also found to be labelled but there is little evidence elsewhere for the presence of fPPG bound to the surface. However, alternative carbohydrate substituted variants may be possible and there was heterogeneity in fPPG observed in our studies and elsewhere. Membrane PPGs (mPPG2) have been reported but do not appear to be a major feature in *L. mexicana* in terms of CRP binding as seen in the lack of CRP binding to the membrane in fluorescent micrographs of *lpg1<sup>-/-</sup>* parasites and consistent with structure discussed earlier.

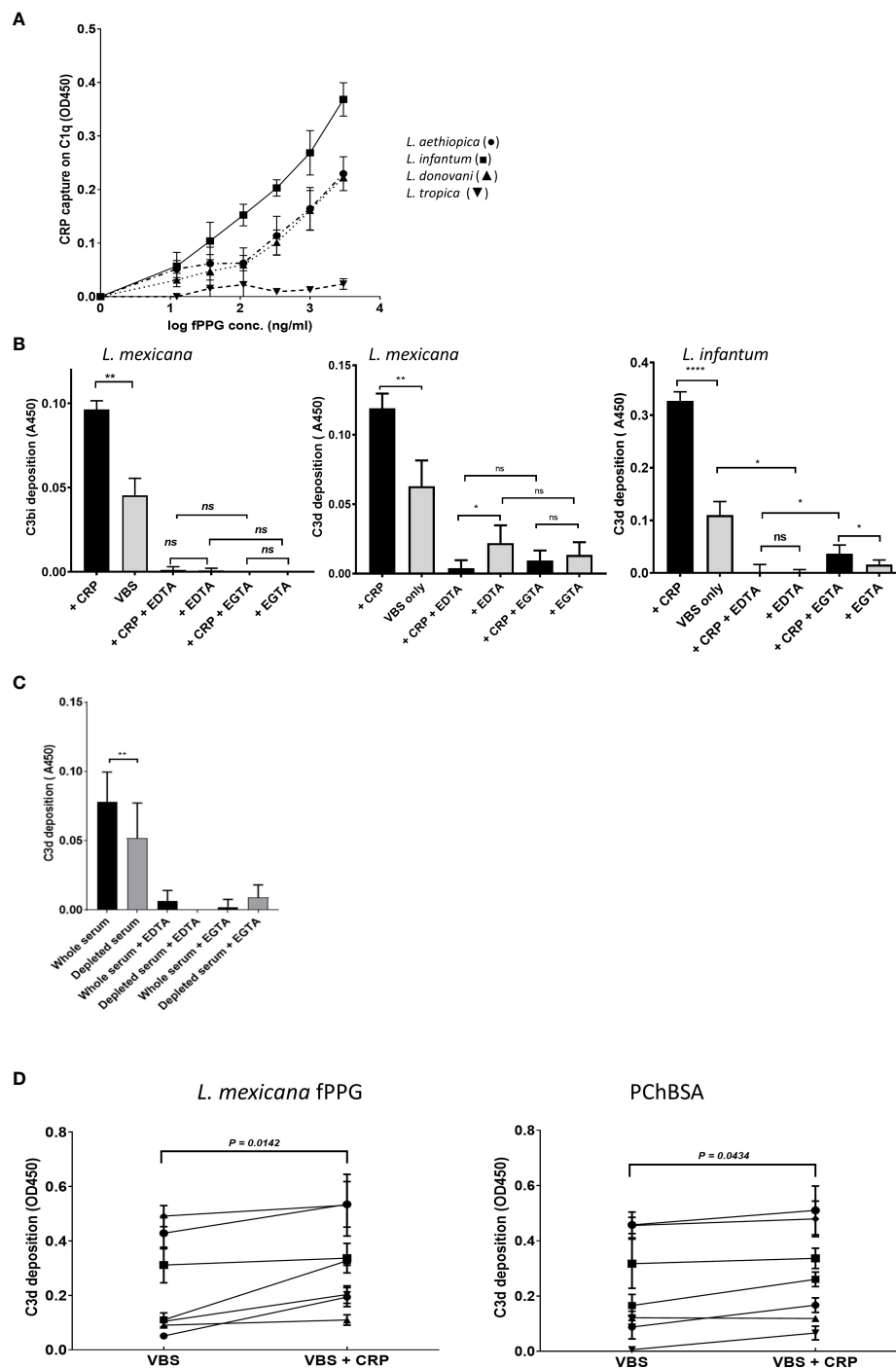


FIGURE 6

CRP contributes to fPPG mediated complement activation. (A) CRP that has bound to fPPG in fluid phase can be captured on C1q coated plates. Plates were coated with C1q. CRP (1  $\mu\text{g/ml}$ ) was added with different amounts of fPPG (0–3  $\mu\text{g/ml}$ ) and complex binding to the surface was detected with anti-CRP. Error bars represent standard deviation ( $n = 3$ ) *L. aethiopica* (●) *L. infantum* (■) *L. donovani* (▲) *L. tropica* (▼). (B) fPPG from *L. mexicana* or *L. infantum* activates complement through the classical pathway and CRP. Microtitre plate assays of complement activation by fPPG from *L. mexicana* or *L. infantum* coated at (2  $\mu\text{g/ml}$ ). Wells with immobilised fPPG were incubated with serum (1:100 dilution) for 20 mins at 37°C in the presence (filled bars) or absence (shaded bars) of additional purified CRP (0.4  $\mu\text{g/ml}$ ) in VBS Mg Ca buffer, or EDTA (5mM) or and Mg EGTA. Deposited C3bi or C3d was detected with biotinylated antibody followed by streptavidin HRP. C3bi mean and s.d,  $n = 6$ . C3d Mean and s.d,  $n = 4$ . \* $p < 0.05$ ; \*\* $p < 0.01$ ; \*\*\*\* $p < 0.0001$ ; ns not significant. (C) Depletion of CRP in serum decreases the classical complement activation in response to *L. mexicana* fPPG. Methods as in (B), but with whole serum and partially CRP depleted serum compared at the same dilution. (D) Variation in CRP mediated fPPG classical complement pathway activation in multiple donors. Added CRP (0.4  $\mu\text{g/ml}$ ) increases complement activation measured through C3d deposition as in (A) in response to fPPG coated at 0.4  $\mu\text{g/ml}$  and PChBSA (0.1  $\mu\text{g/ml}$ ) and PChBSA in the presence and absence of additional purified CRP. Paired t test on 7 donors.



### 4.3 Inverse correlation of binding and side chain substitution

Previous analysis of CRP binding to different *Leishmania* species showed strong binding to *L. donovani* LPG and others whilst some others only showed very weak or lack of binding to LPG. The binding was correlated inversely with the presence of LPG side chain substitution on the repeating disaccharide regions which hindered access to the disaccharide (34). Monoclonals generated against phosphoglycan structures show strong similarity in their ability to bind proteophosphoglycan and LPG from the same parasite (6, 35). In addition, comparison of the LPG and PPG side chains characterised by anion exchange HPLC show essentially the same pattern of structure for LPG and PPG but for *L. mexicana* the PPG contained much less side chain (23). Therefore, we hypothesized that CRP binding to PPG from different *Leishmania* would show the same pattern of binding as seen for LPG. *L. donovani* LPG is classified as type I with no side chain substitution and therefore we predicted that *L. donovani* PPG would be a strong binder as was found. Also in the *Viannia* subgenus, *L. braziliensis* and *L. panamenensis* have little side chain substitution (36) and *L. panamenensis* was found to be a good binder of CRP. In other reports *L. braziliensis* procyclic forms have side chain substitution but the metacyclic forms do not (37). The binding to *L. donovani* was also interesting because it had much longer repeat units (up to 32) on the ScAP analogous to that seen in LPG (38). *L. infantum* is devoid of side chain in the procyclic LPG form but has some in the metacyclic stage (39) and most strains of *L. infantum* are type I but variability is seen in certain strains (40).

*L. tropica* LPG (classified as type 2) has been shown to be highly substituted with almost all repeating units substituted at the C-3 position of the galactose with structures that are longer and often terminated with arabinopyranose (41). *L. amazonensis* has a high proportion of C-3 Gal positions substituted with chains of 2-3 sugars (42) and notably does not have significant binding to the CA7AE antibody that binds to repeating disaccharide repeats. Both these would suggest that CRP would have poor binding as indeed was demonstrated. Another LPG type 2 is *L. major* but this parasite shows considerable variation between strains for side chain substitution (41). It was observed that the side chain substitution of the *L. major* fPPG was less than that observed for the LPG from the same parasite, perhaps leading to significant CRP binding in these studies compared to *L. tropica* which did not bind.

*L. aethiopica* is known to be a type 3 LPG with substitution of a single mannose on the C-2 of mannose of the LPG repeats (41). It was previously suggested that this substitution site would have considerable effects on the conformation of LPG and its backbone which was supported by the failure of monoclonals to the repeating disaccharide to bind to this parasite LPG (43). CRP bound strongly to this fPPG, suggesting the different conformation of the repeating disaccharide allows CRP binding.

Phosphoglycans including the repeating disaccharide appear to be a feature across the *Leishmania* spectrum and most recently were confirmed in *Leishmania (Mundinia) enriettii* (44). However, there is no information about *Leishmania (Sauroleishmania) tarentolae*.

The good correlation between low side chain substitution of *Leishmania* PPGs and strong CRP binding is consistent with the presence of the genes responsible for phosphoglycan synthesis, particularly those responsible for repeating disaccharide and side chain substitution (SCGs and SCGR families) in different species (45).

### 4.4 Complement activation by PSG

Given the role of PPG in depleting complement and that it aids parasite survival it was important to know if CRP activated complement at and beyond the C3 stage when binding to a phosphoglycan. Previously we showed that binding of CRP to another glycan structure terminating in a phosphorylcholine substituted onto an N glycan of filaria parasites effectively bound C1q and was able to generate C4b. However, this did not efficiently activate C2 and thus did not lead to an active C3 convertase but did functionally deplete complement (18). This property was related to the mobility of the glycan. For filaria, the lack of complement activation was important since any inflammatory response is damaging to survival, however infectious *Leishmania* is largely resistant to complement attack. It is not surprising therefore that the parasite generates material capable of strong activation of complement. PPG injected into a mouse could dramatically deplete complement by 90% within 30 minutes (20) and lasted for 24 hours. Whilst the mouse is unusual in that CRP is present at low levels even during inflammation the levels are sufficient to bind to the fPPG. Whilst there is little evidence for CRP or other innate proteins such as MBL or innate antibody having a role in killing metacyclic infectious promastigotes, these experimental systems may be too simplistic and do not rule out other roles for such activation in terms of altering survival *in vivo*.

It was previously shown that infection with *L. amazonensis* promastigotes caused a reduction in complement in mice. Complement-depleted mice showed a reduced inflammatory response and cell infiltrate and phagocytosis along with an increased parasite burden (46). A recent paper reported that *L. infantum* promastigotes activated both the classical and alternative pathways to different extents in different sera (dog, cat, and human) but each caused functional depletion of both pathways (47). Sandfly infection would be a better evaluation rather than footpad inoculation to evaluate fPPG and parasites and fPPG has been reported to be involved in several cell responses in the infected host (48), thus CRP may also have influence on responses other than complement or other responses indirectly through the complement effect. CRP makes a significant contribution to the activation of complement seen to the fPPG in human serum. Although significant data was generated with addition and depletion, our methodology for CRP depletion and addition was only partially effective with residual CRP in depleted sera and normal non supplemented sera still able to provide some activation. Thus, the relative contribution of CRP may be underestimated. Whilst normal CRP concentrations (less than 10 µg/ml) are sufficient to cause strong binding to PPG, concentrations are usually high in *Leishmania* patients (49).

These data demonstrate CRP-PPG interactions can have a role in parasite infection in sand flies when CRP is ingested as part of the blood meal. Effects of the blood meal are complex and have significant effects on infectivity and parasite differentiation and infectivity (49). This may be further complicated because insects have complement-inactivation mechanisms to protect their own epithelium which will affect the parasite susceptibility to blood meal derived complement (50). CRP may alter the physiological state of the phosphoglycan and/or the interaction with the parasite.

In conclusion, we found CRP is able to bind both ScAP and fPPG that make up PSG. CRP binding to PPGs from different *Leishmania* species is inversely correlated with side chain substitution, similar to previously seen for CRP binding to LPG. The CRP-PPG interaction is able to activate and deplete complement. Though the current study focuses on the role of CRP within the human host, these interactions may also be applicable to the sand fly vector.

## Data availability statement

The original contributions presented in the study are included in the article/**Supplementary Material**. Further inquiries can be directed to the corresponding author.

## Ethics statement

The studies involving human participants were reviewed and approved by the ethical committee of London School of Hygiene and Tropical Medicine. Written informed consent to participate in this study was provided by the participants.

## Author contributions

JR: Conceptualization, Funding acquisition, Investigation, Methodology, Resources, Supervision, Writing – original draft, Writing – review & editing. ES: Investigation, Writing – original draft. ED: Investigation, Writing – original draft, Writing – review & editing. JHS: Investigation, Writing – review & editing. MR:

Conceptualization, Funding acquisition, Investigation, Project administration, Resources, Supervision, Writing – review & editing.

## Funding

MR and JHS were supported by the BBSRC (David Phillips Fellowship awarded to MR, BB/H022406/1). ED was funded by Medical Research Council grant MR/N013638/1.

## Acknowledgments

The authors acknowledge the facilities, and the scientific and technical assistance of the LSHTM Wolfson Cell Biology Facility, with specific thanks to Dr Liz McCarthy. *Leishmania* were provided by Dr Vanessa Yardley and Dr Katrien Van Bocxlaer (LSHTM).

## Conflict of interest

The authors declare that the research was conducted in the absence of any commercial or financial relationships that could be construed as a potential conflict of interest.

## Publisher's note

All claims expressed in this article are solely those of the authors and do not necessarily represent those of their affiliated organizations, or those of the publisher, the editors and the reviewers. Any product that may be evaluated in this article, or claim that may be made by its manufacturer, is not guaranteed or endorsed by the publisher.

## Supplementary material

The Supplementary Material for this article can be found online at: <https://www.frontiersin.org/articles/10.3389/fimmu.2023.1256205/full#supplementary-material>

## References

1. Abbafati C, MaChado DB, Cislighi B, Salman OM, Karanikolos M, McKee M, et al. Global burden of 369 diseases and injuries in 204 countries and territories, 1990–2019: a systematic analysis for the Global Burden of Disease Study 2019. *Lancet*. (2020) 396:1204–22. doi: 10.1016/S0140-6736(20)30925-9
2. Rogers ME. The role of *Leishmania* proteophosphoglycans in sand fly transmission and infection of the mammalian host. *Front Microbiol* (2012) 3:223. doi: 10.3389/fmicb.2012.00223
3. Ilg T. Lipophosphoglycan is not required for infection of macrophages or mice by *Leishmania mexicana*. *EMBO J* (2000) 19(9):1953–62. doi: 10.1093/emboj/19.9.1953
4. Spath GF, Epstein L, Leader B, Singer SM, Avila HA, Turco SJ, et al. Lipophosphoglycan is a virulence factor distinct from related glycoconjugates in the protozoan parasite *Leishmania major*. *Proc Natl Acad Sci USA* (2000) 97(16):9258–63. doi: 10.1073/pnas.160257897
5. Jesus-Santos FH, Lobo-Silva J, Ramos PIP, Descoteaux A, Lima JB, Borges VM and Farias LP. LPG2 gene duplication in *Leishmania infantum*: a case for CRISPR-Cas9 gene editing. *Front Cell Infect Microbiol* (2020) 10:408. doi: 10.3389/fcimb.2020.00408
6. Ilg T, Demar M, Harbecke D. Phosphoglycan repeat-deficient *Leishmania mexicana* parasites remain infectious to macrophages and mice. *J Biol Chem* (2001) 276(7):4988–97. doi: 10.1074/jbc.M008030200
7. Ilg T, Harbecke D, Wiese MA, Overath P. Monoclonal antibodies directed against *Leishmania* secreted acid phosphatase and lipophosphoglycan. *Eur J Biochem* (1993) 217:603–15. doi: 10.1111/j.1432-1033.1993.tb18283.x
8. Rogers ME, Ilg T, Nikolaev AV, Ferguson MA, Bates PA. Transmission of cutaneous leishmaniasis by sand flies is enhanced by regurgitation of fPPG. *Nature*. (2004) 430:463–7. doi: 10.1038/nature02675

9. Rogers ME, Corware K, Müller I, Bates PA. *Leishmania infantum* proteophosphoglycans regurgitated by the bite of its natural sand fly vector, *Lutzomyia longipalpis*, promote parasite establishment in mouse skin and skin-distant tissues. *Microbes Infect* (2010) 12(11):875–9. doi: 10.1016/j.micinf.2010.05.014
10. Ilg T, Overath P, Ferguson MA, Rutherford T, Campbell DG, McConville MJ. O- and N-glycosylation of the *Leishmania mexicana*-secreted acid phosphatase. Characterization of a new class of phosphoserine-linked glycans. *J Biol Chem* (1994) 269(39):24073–81.
11. Culley FJ, Harris RA, Kaye PM, McAdam KPWJ, Raynes JG. C-reactive protein binds to a novel ligand on *Leishmania donovani* and increases uptake into human macrophages. *J Immunol* (1996) 156:4691–6. doi: 10.4049/jimmunol.156.12.4691
12. Kaplan MH, Volanakis JE. Interaction of C-reactive protein complexes with the complement system. I. Consumption of human complement associated with the reaction of C-reactive protein with pneumococcal C-polysaccharide and with the choline phosphatides, lecithin and sphingomyelin. *J Immunol* (1974) 112:2135–47. doi: 10.4049/jimmunol.112.6.2135
13. Haapasalo K, Meri S. Regulation of the complement system by pentraxins. *Front Immunol* (2019) 10:1750. doi: 10.3389/fimmu.2019.01750
14. Culley FJ, Bodman-Smith KB, Ferguson MAJ, Nikolaev AV, Shantilal N, Raynes JG. C-reactive protein binds to phosphorylated carbohydrates. *Glycobiology*. (2000) 10:59–65. doi: 10.1093/glycob/10.1.59
15. Bodman-Smith KB, Mbuchi M, Culley FJ, Bates PA, Raynes JG. C-reactive protein mediated phagocytosis of *Leishmania donovani* promastigotes does not alter parasite survival or macrophage responses. *Parasite Immunol* (2002) 24:447–54. doi: 10.1046/j.1365-3024.2002.00486.x
16. Bee A, Culley FJ, Alkhalife IS, Bodman Smith K, Pratdesaba RA, Raynes JG, et al. *Leishmania mexicana*; differentiation and signal transduction in metacyclic promastigotes mediated by C-reactive protein. *Parasitology*. (2001) 122:521–9. doi: 10.1017/S0031182001007612
17. Mbuchi M, Bates PA, Ilg T, Coe JE, Raynes JG. C-reactive protein initiates transformation of *Leishmania donovani* and *L. mexicana* through binding to lipophosphoglycan. *Mol Biochem Parasitol* (2006) 146(2):259–64.
18. Ahmed UK, Maller NC, Iqbal AJ, Al-Riyami L, Harnett W, Raynes JG. The carbohydrate-linked phosphorylcholine of the Parasitic Nematode product ES-62 modulates complement activation. *J Biol Chem* (2016) 291(22):11939–53. doi: 10.1074/jbc.M115.702746
19. Sacks DL. The structure and function of the surface lipophosphoglycan on different developmental stages of *Leishmania* promastigotes. *Infect Agents Dis* (1992) 1(4):200–6.
20. Peters C, Kawakami M, Kaul M, Ilg T, Overath P, Aebischer T. Secreted proteophosphoglycan of *Leishmania mexicana* amastigotes activates complement by triggering the mannan binding lectin pathway. *Eur J Immunol* (1997) 27(10):2666–72. doi: 10.1002/eji.1830271028
21. Rogers M, Kropf P, Choi BS, Dillon R, Podinovskaia M, Bates P, et al. Proteophosphoglycans regurgitated by *Leishmania*-infected sand flies target the L-arginine metabolism of host macrophages to promote parasite survival. *PLoS Pathog* (2009) 5(8):e1000555. doi: 10.1371/journal.ppat.1000555
22. Wiese M. A mitogen-activated protein (MAP) kinase homologue of *Leishmania mexicana* is essential for parasite survival in the infected host. *EMBO J* (1998) 17(9):2619–28. doi: 10.1093/emboj/17.9.2619
23. Ilg T, Stierhof YD, Craik D, Simpson R, Handman E, Bacic AJ. Purification and structural characterization of a filamentous, mucin-like proteophosphoglycan secreted by *Leishmania* parasites. *J Biol Chem* (1996) 271(35):21583–96. doi: 10.1074/jbc.271.35.21583
24. Masuko T, Minami A, Iwasaki N, Majima T, Nishimura S-I, Lee YC. Carbohydrate analysis by a phenol-sulfuric acid method in microplate format. *Anal Biochem* (2005) 339(1):69–72. doi: 10.1016/j.ab.2004.12.001
25. de Jong SE, Selman MHJ, Adegnikaa AA, Amoah AS, van Riet E, Kruize YCM, et al. IgG1 Fc N-glycan galactosylation as a biomarker for immune activation. *Sci Rep* (2016) 6:28207. doi: 10.1038/srep28207
26. Stierhof YD, Bates PA, Jacobson RL, Rogers ME, Schleim Y, Handman E, et al. Filamentous proteophosphoglycan secreted by *Leishmania* promastigotes forms gel-like three-dimensional networks that obstruct the digestive tract of infected sandfly vectors. *Eur J Cell Biol* (1999) 78(10):675–89. doi: 10.1016/S0171-9335(99)80036-3
27. Coe JE, Margossian SS, Slayter HS, Sogn JA. Hamster female protein. A new Pentraxin structurally and functionally similar to C-reactive protein and amyloid P component. *J Exp Med* (1981) 153(4):977–91. doi: 10.1084/jem.153.4.977
28. Klein C, Gopfert U, Goehring N, Stierhof Y-D, Ilg Y. Proteophosphoglycans of *Leishmania mexicana* biochem. J. (1999) 344:775–86.
29. Ilg T, Stierhof YD, Etges R, Adrian M, Harbecke D, Overath P. Secreted acid phosphatase of *Leishmania mexicana*: a filamentous phosphoglycoprotein polymer. *PNAS* (1991) 88(19) 8774–87. doi: 10.1073/pnas.88.19.8774
30. Stierhof YD, Ilg T, Russel DG, Hohenberg H, Overath P. Characterization of polymer release from the flagellar pocket of *Leishmania mexicana* promastigotes. *J Cell Biol* (1994) 125(2):321–31. doi: 10.1083/jcb.125.2.321
31. Montgomery J, Curtis J, Handman E. Genetic and structural heterogeneity of proteophosphoglycans in *Leishmania*. *Mol Biochem Parasitol* (2002) 121(1):75–85. doi: 10.1016/S0166-6851(02)00024-5
32. Göpfert U, Goehring N, Klein C, Ilg T. Proteophosphoglycans of *Leishmania mexicana*. Molecular cloning and characterization of the *Leishmania mexicana* ppg2 gene encoding the proteophosphoglycans aPPG and pPPG2 that are secreted by amastigotes and promastigotes. *Biochem J* (1999) 344(Pt 3):787–95.
33. Samant M, Sahasrabudhe AA, Singh N, Gupta SK, Sundar S, Dube A. Proteophosphoglycan is differentially expressed in sodium stibogluconate-sensitive and resistant Indian clinical isolates of *Leishmania donovani*. *Parasitology* (2007) 134:1175–784. doi: 10.1017/S0031182007002569
34. Raynes JG, Curry A, Harris RA. Binding of C-reactive protein to *Leishmania*. *Biochem Soc Trans* (1994) 22(1):3S. doi: 10.1042/bst022003s
35. Muskus C, Segura I, Oddone R, Turco SJ, Leiby DA, Toro L, et al. Carbohydrate and LPG expression in *Leishmania viannia* subgenus. *J Parasitol* (1997) 83(4):671–8. doi: 10.2307/3284245
36. Soares RP, Cardoso TL, Barron T, Araujo MS, Pimenta PF, Turco SJ. *Leishmania Braziliensis*: a novel mechanism in the lipophosphoglycan regulation during metacyclogenesis. *Int J Parasitol* (2005) 35(3):245–53. doi: 10.1016/j.ijpara.2004.12.008
37. Lippert DN, Dwyer DW, Li F, Olafson RW. Phosphoglycosylation of a secreted acid phosphatase from *Leishmania donovani*. *Glycobiology* (1999) 9(6):627–36. doi: 10.1093/glycob/9.6.627
38. Soares RRP, Macedo ME, Ropert C, Gontijo NF, Almeida IC, Gazzinelli RT, et al. *Leishmania chagasi*: lipophosphoglycan characterization and binding to the midgut of the sand fly vector *Lutzomyia longipalpis*. *Mol Biochem Parasitol* (2002) 121(2):213–24. doi: 10.1016/S0166-6851(02)00033-6
39. Coelho-Finamore JM, Freitas VC, Assis RR, Melo MN, Novozhilova N, Secundino NF, et al. *Leishmania infantum*: lipophosphoglycan intraspecific variation and interaction with vertebrate and invertebrate hosts. *Int J Parasitol* (2011) 41(3–4):333–42. doi: 10.1016/j.ijpara.2010.10.004
40. McConville MJ, Schnur LF, Jaffe C, Schneider P. Structure of *Leishmania* lipophosphoglycan: inter- and intra-specific polymorphism in Old World species. *Biochem J* (1995) 310(Pt 3):807–18. doi: 10.1042/bj3100807
41. Nogueira PM, Guimarães AC, Assis RR, Sadlova J, Myskova J, Pruzinova K, et al. Lipophosphoglycan polymorphisms do not affect *Leishmania amazonensis* development in the permissive vectors *Lutzomyia migonei* and *Lutzomyia longipalpis*. *Parasites Vectors* (2017) 10(1):608. doi: 10.1186/s13071-017-2568-8
42. Schnur LF, Zuckerman A, Greenblatt CL. *Leishmania* serotypes as distinguished by the gel diffusion of factors excreted *in vitro* and *in vivo*. *Isr J Med Sci* (1972) 8(7):932–42.
43. Paranaíba LF, de Assis RR, Nogueira PM, Torrecilhas AC, Campos JH, Silveira AC, et al. *Leishmania enriettii*: biochemical characterisations of lipophosphoglycans (LPGs) and glycoinositolphospholipids (GIPLs) and infectivity to *Cavia porcellus*. *Parasites Vectors* (2015) 8(31). doi: 10.1186/s13071-015-0633-8
44. Azevedo LG, de Queiroz ATL, Barral A, Santos LA, Ramos PIP. Proteins involved in the biosynthesis of lipophosphoglycan in *Leishmania*: a comparative genomic and evolutionary. *Parasit Vectors*. (2020) 13:44. doi: 10.1186/s13071-020-3914-9
45. Laurenti MD, Orn A, Sinhorini IL, Corbett CEP. The role of complement in the early phase of *Leishmania (Leishmania) amazonensis* infection in BALB/c mice. *Braz J Med Biol Res* (2004) 37(3):427–34. doi: 10.1590/s0100-879x2004000300021
46. Tirado TC, Bavia L, Ambrosio AR, Campos MP, de Almeida Santiago M, Messias-Reason IJ, et al. A comparative approach on the activation of the three complement system pathways in different hosts of visceral Leishmaniasis after stimulation with *Leishmania infantum*. *Dev Comp Immunol* (2021) 120:104061. doi: 10.1016/j.dci.2021.104061
47. Wasunna KM, Raynes JG, Were JBO, Muigai R, Sherwood J, Gachihi G, et al. Acute phase protein concentrations predict clearance rate during therapy for visceral leishmaniasis. *Trans R Soc Trop Med Hyg* (1995) 89(6):678–81. doi: 10.1016/0035-9203(95)90442-5
48. Serafim TD, Coutinho-Abreu IV, Oliveira F, Meneses C, Kamhawi S, Valenzuela JG. Sequential blood meals promote *Leishmania* replication and reverse metacyclogenesis augmenting vector infectivity. *Nat Microbiol* (2018) 3(5):548–55. doi: 10.1038/s41564-018-0125-7
49. Mendes-Sousa AF, Nascimento AAS, Queiroz DC, Vale VF, Fujiwara RT, Araújo RN, et al. Different host complement systems and their interactions with saliva from *Lutzomyia longipalpis* (Diptera, Psychodidae) and *Leishmania infantum* promastigotes. *PLoS One* (2013) 8(11):e79787. doi: 10.1371/journal.pone.0079787
50. Bates PA, Hermes I, Dwyer DM. Golgi-mediated post-translational processing of secretory acid phosphatase by *Leishmania donovani* promastigotes. *Mol Biochem Parasitol* (1990) 39(2):247–55. doi: 10.1016/0166-6851(90)90063-r



## OPEN ACCESS

## EDITED BY

Yi Wu,  
Xi'an Jiaotong University, China

## REVIEWED BY

Ivan Melnikov,  
Ministry of Health of the Russian  
Federation, Russia  
Li Haiyun,  
Xi'an Jiaotong University, China

## \*CORRESPONDENCE

Francis R. Hopkins  
✉ francis.hopkins@liu.se

<sup>†</sup>These authors share last authorship

RECEIVED 14 July 2023

ACCEPTED 11 August 2023

PUBLISHED 01 September 2023

## CITATION

Hopkins FR, Nordgren J,  
Fernandez-Botran R, Enocsson H,  
Govender M, Svanberg C, Svensson L,  
Hagbom M, Nilsdotter-Augustinsson Å,  
Nyström S, Sjöwall C, Sjöwall J and  
Larsson M (2023) Pentameric C-reactive  
protein is a better prognostic biomarker  
and remains elevated for longer than  
monomeric CRP in hospitalized patients  
with COVID-19.  
*Front. Immunol.* 14:1259005.  
doi: 10.3389/fimmu.2023.1259005

## COPYRIGHT

© 2023 Hopkins, Nordgren,  
Fernandez-Botran, Enocsson, Govender,  
Svanberg, Svensson, Hagbom,  
Nilsdotter-Augustinsson, Nyström, Sjöwall,  
Sjöwall and Larsson. This is an open-access  
article distributed under the terms of the  
[Creative Commons Attribution License  
\(CC BY\)](#). The use, distribution or  
reproduction in other forums is permitted,  
provided the original author(s) and the  
copyright owner(s) are credited and that  
the original publication in this journal is  
cited, in accordance with accepted  
academic practice. No use, distribution or  
reproduction is permitted which does not  
comply with these terms.

# Pentameric C-reactive protein is a better prognostic biomarker and remains elevated for longer than monomeric CRP in hospitalized patients with COVID-19

Francis R. Hopkins<sup>1\*</sup>, Johan Nordgren<sup>1</sup>,  
Rafael Fernandez-Botran<sup>2</sup>, Helena Enocsson<sup>3</sup>,  
Melissa Govender<sup>1</sup>, Cecilia Svanberg<sup>1</sup>, Lennart Svensson<sup>1,4</sup>,  
Marie Hagbom<sup>1</sup>, Åsa Nilsdotter-Augustinsson<sup>3,5</sup>,  
Sofia Nyström<sup>1,6</sup>, Christopher Sjöwall<sup>3†</sup>,  
Johanna Sjöwall<sup>3,5†</sup> and Marie Larsson<sup>1†</sup>

<sup>1</sup>Division of Molecular Medicine and Virology, Department of Biomedical and Clinical Sciences, Linköping University, Linköping, Sweden, <sup>2</sup>Department of Pathology & Laboratory Medicine, University of Louisville, Louisville, KY, United States, <sup>3</sup>Division of Inflammation and Infection, Department of Biomedical and Clinical Sciences, Linköping University, Linköping, Sweden, <sup>4</sup>Division of Infectious Diseases, Department of Medicine, Karolinska Institute, Stockholm, Sweden, <sup>5</sup>Department of Infectious Diseases, Vrinnevi Hospital, Norrköping, Sweden, <sup>6</sup>Clinical Immunology and Transfusion Medicine, Department of Biomedical and Clinical Sciences, Linköping University, Linköping, Sweden

The differing roles of the pentameric (p) and monomeric (m) C-reactive protein (CRP) isoforms in viral diseases are not fully understood, which was apparent during the COVID-19 pandemic regarding the clinical course of severe acute respiratory syndrome coronavirus 2 (SARS-CoV-2) infection. Herein, we investigated the predictive value of the pCRP and mCRP isoforms for COVID-19 severity in hospitalized patients and evaluated how the levels of the protein isoforms changed over time during and after acute illness. This study utilized samples from a well-characterized cohort of Swedish patients with SARS-CoV-2 infection, the majority of whom had known risk factors for severe COVID-19 and required hospitalization. The levels of pCRP were significantly raised in patients with severe COVID-19 and in contrast to mCRP the levels were significantly associated with disease severity. Additionally, the pCRP levels remained elevated for at least six weeks post inclusion, which was longer compared to the two weeks for mCRP. Our data indicates a low level of inflammation lasting for at least six weeks following COVID-19, which might indicate that the disease has an adverse effect on the immune system even after the viral infection is resolved. It is also clear that the current standard method of testing pCRP levels upon hospitalization is a useful marker for predicting disease severity and mCRP testing would not add any clinical relevance for patients with COVID-19.

## KEYWORDS

CRP, COVID-19, SARS-CoV-2, isoforms, prognostic marker



## Introduction

Severe acute respiratory syndrome coronavirus 2 (SARS-CoV-2) is the agent of the COVID-19 pandemic and gives rise to mild or moderate symptoms in most infected individuals. However, 10–15% progress to severe disease with pneumonia, acute respiratory distress syndrome (ARDS), and multiple organ failure. SARS-CoV-2 infection activates innate and adaptive immune responses, which can lead to uncontrolled inflammation, a so called “cytokine storm”, which is advocated as a key pathogenetic factor in severe COVID-19 (1). Among the factors induced by the infection is the C-reactive protein (CRP), an acute-phase protein mainly produced in the liver by hepatocytes (2). While CRP levels are typically low in healthy individuals, the level of this protein can increase significantly in the presence of inflammation, making it a widely used and valuable diagnostic biomarker for e.g., inflammatory diseases such as rheumatoid arthritis (RA), and bacterial infections (3, 4).

CRP is initially produced and released into the bloodstream in its pentameric isoform (pCRP), which can irreversibly dissociate to a monomeric isoform (mCRP) at sites of inflammation. In an inflammatory setting the pCRP isoform binds phosphatidylcholine on the surface of microorganisms and damaged host cells and this leads to its degradation to mCRP (5). The two different isoforms of CRP exhibit distinct characteristics and can have both pro-inflammatory and anti-inflammatory functions depending on the specific disease context and cell types involved (6–9). The mCRP induces higher levels of inflammatory factors including nitric oxide, C-X-C motif chemokine ligand 8 (CXCL8), and monocyte chemoattractant protein 1 (MCP-1) in immune cells such as neutrophils compared to pCRP and support the recruitment of immune cells to areas of inflammation (10–12). The CRP isoforms can bind a variety of ligands, including complement component 1q (C1q), Fc $\gamma$ -receptors (Fc $\gamma$ -R), as well as nuclear antigens (13, 14). pCRP has been found to bind to both Fc $\gamma$ -RI and Fc $\gamma$ -RIIa, while mCRP has been suggested to bind with higher affinity to Fc $\gamma$ -RIII (5). The different binding affinities of mCRP and pCRP to Fc $\gamma$ -Rs may contribute to their differential functions and deposition on different immune cells. There are indications that pCRP is more potent at activating the complement system and promoting clearance of microorganisms by immune cells compared to mCRP (15). In addition, the ratio of pCRP to mCRP may be altered in certain disease states, such as sepsis and systemic lupus erythematosus, where an increase in mCRP levels has been observed (4, 7).

In patients with severe COVID-19 a significant increase in pCRP levels has been observed compared to patients with mild disease (16–19), and pCRP levels have been linked to increased mortality in COVID-19 (20). Indeed, elevated pCRP levels reflect the hyperinflammatory response, which is a major clinical manifestation of severe COVID-19 that might lead to severe lung damage and death (21). In addition, several of the elevated inflammatory markers in patients with COVID-19, e.g., interleukin-6 (IL-6), tumor necrosis factor (TNF), and ferritin have been found to correlate positively with pCRP levels (22). In a recent study mCRP levels were shown to independently associate with COVID-19 severity (23).

The aims of the current study were to determine if pCRP and mCRP levels are associated with COVID-19 disease severity to establish if they can be used as biomarkers, and to assess the levels of

pCRP and mCRP over time in hospitalized patients with COVID-19. We found that while pCRP levels were higher in patients with severe/critical COVID-19, the mCRP levels were similar between patients with mild/moderate and severe/critical disease. Additionally, both pCRP and mCRP were increased at the two-week follow-up, with pCRP levels remaining elevated for at least six weeks, suggesting that the inflammation still is ongoing, likely due to the damage caused by the initial high level of inflammation triggered by the SARS-CoV-2 infection.

## Materials and methods

### Demographics and clinical characteristics of patients

Hospitalized COVID-19 patients (N=62) were included in the study from August 2020 to May 2021 as soon as possible following admission to the Department of Infectious Diseases at the Vrinnevi Hospital, Norrköping, Sweden. Healthy, SARS-CoV-2 RNA negative controls (N=31) were recruited among health care workers at the Vrinnevi Hospital, Norrköping, Sweden. The study protocol was approved by the Swedish Ethical Review Authority (Decision number 2020–02580). Oral and written informed consent was obtained from all participants.

At inclusion in the study, a panel of clinical markers, including CRP, lactate dehydrogenase (LDH), and numbers of neutrophils, monocytes, and lymphocytes, was assessed (Table 1). In addition, data concerning smoking habits, medication, body mass index (BMI), and co-morbidities such as diabetes, cardiovascular disease, renal failure, and chronic pulmonary disease was collected. The patients were divided into two groups based on disease severity and according to the NIH COVID-19 patient treatment criteria, including symptoms, oxygen saturation in room air, clinical findings, and chest imaging, and also taking into account the highest level of care (pandemic department, intermediate or intensive care unit). The first group included cases with mild/moderate disease (mild, without oxygen supplementation at pandemic department, and moderate with oxygen supplementation  $\leq 5$  L/min at pandemic department). The second group included cases with severe/critical disease (severe, with oxygen supplementation  $> 5$  L/min supplemented by high-flow nasal oxygen (HFNO) or continuous positive airway pressure (CPAP) at pandemic department or intermediate care unit, and critical with treatment in intensive care unit with or without mechanical ventilator) (24).

Additional clinically relevant data regarding the levels of soluble urokinase plasminogen activator receptor (suPAR) and viral load in nasopharynx samples were drawn from previously performed studies and used as clinical parameters (6, 25).

### pCRP and mCRP measurements

Serum samples from the hospitalized patients taken at inclusion 2-week, and 6-week visits, and from healthy controls, were assessed for pCRP and mCRP. Levels of pCRP were measured using a



TABLE 1 Clinical characteristics and analytical variables of hospitalized patients with COVID-19.

Variable	Total N=62	Mild/Moderate disease N=31	Severe/Critical disease N=31	P-value*
Age, years median (range)	57.5 (32-91)	59 (32-91)	57 (32-78)	0.526
Male sex, N (%)	41 (66)	20 (65)	21 (68)	0.788
Symptom duration, days median (range)	10 (2-30)	10 (2-24)	10 (5-30)	0.576
Length of hospital stay, days median (range)	7 (2-54)	6 (2-23)	10 (3-54)	<0.001*
Intensive care, N (%)	8 (13)	0	8 (26)	0.005*
Stay at intensive care unit, days median (range)	9 (1-24)	N/A	9 (1-24)	N/A
Remdesivir, N (%)	22 (35)	8 (26)	14 (45)	0.184
Corticosteroid therapy, N (%)	40 (65)	14 (45)	26 (84)	0.003*
Mechanical ventilation, N (%)	4 (6.5)	0	4 (13)	0.113
Deceased, N (%)	3 (4.8)	0	3 (9.7)	0.238
<b>Pre-existing comorbidities</b>				
Diabetes, N (%)	15 (24)	6 (19)	9 (29)	0.554
Cardiovascular disease, N (%)	35 (56)	14 (45)	21 (68)	0.124
Chronic pulmonary disease, N (%)	15 (24)	8 (26)	7 (23)	1
Current or ex-smoker, N (%)	34 (55)	17 (55)	17 (55)	1
Acute renal failure, N (%)	10 (16)	6 (19)	4 (13)	0.731
Chronic renal failure, N (%)	7 (11)	3 (9.7)	4 (13)	1
Renal replacement therapy, N (%)	3 (4.8)	0	3 (9.7)	0.238
Body mass index (kg/m <sup>2</sup> ), median (range)	30 (22-45)	27.5 (22-43)	31 (24-45)	0.024*
Immunocompromised <sup>‡</sup> at inclusion, N (%)	8 (13)	5 (16)	3 (9.7)	0.449
<b>Analytical variables</b>				
Haemoglobin g/L	140 (90-171)	130 (90-149)	126 (97-171)	0.451
White blood cell count (x10 <sup>9</sup> /L)	6.7 (0.4-49)	6.2 (0.4-17)	7.2 (1.4-49)	0.149
Platelet count (x10 <sup>9</sup> /L)	239 (20-668)	234 (20-543)	239 (134-668)	0.475
Neutrophil count (x10 <sup>9</sup> /L)	4.95 (0-17.5)	4.2 (0-15.6)	6.1 (0.9-17.5)	0.012*
Lymphocyte count (x10 <sup>9</sup> /L)	1 (0.1-2.8)	1.2 (0.3-2.2)	0.9 (0.1-2.8)	0.089
Plasma creatinine (μmol/L)	69 (36-1224)	70 (40-390)	66 (36-1224)	0.46
eGFR MDRD (mL/min/1.73m <sup>2</sup> )	95 (4-95)	95 (10-95)	95 (4-95)	0.652
Lactate dehydrogenase (μkat/L)	6.45 (3.2-16)	5.6 (3.2-16)	7.2 (4-16)	0.002*
suPAR (ng/mL) median (range)	5.9 (2.9-29)	5.0 (2.9-11.1)	6.6 (4.2-29) <sup>‡</sup>	0.002*
Neutrophil-lymphocyte ratio median (range)	4.9 (0.2-87.5)	3.7 (0.2-8.9)	6.1 (0.4-87.5)	0.002*
SARS-CoV-2 viral load (ct-value) <sup>†</sup>	35.9 (17.8-39.0)	39.0 (21.8-39.0)	32.2 (17.8-39.0)	0.015*
pCRP (μg/mL)	63 (6-477)	40 (6-376)	90 (10-477)	0.043*
mCRP (ng/mL)	33.02 (12.6-57.7)	32.72 (12.6-57.7)	33.3 (21.7-50.4)	0.736

N/A, Not applicable.

ct-value, cycle threshold-value.

\*P ≤ 0.05 = significant. NR, not relevant, <sup>‡</sup>values missing for two patients, <sup>†</sup>values missing for two patients, <sup>‡</sup>values missing for one patient, <sup>†28</sup>.

turbidimetry high sensitivity technique at the routine clinical chemistry department, at Linköping University Hospital.

Levels of mCRP were measured using an in-house sandwich enzyme-linked immunosorbent assay (ELISA) as previously described (7). Briefly, 96-well plates were coated overnight with a goat anti-human mCRP polyclonal antibody diluted in PBS and thereafter blocked overnight at 4°C with PBS containing 1% bovine serum albumin (PBS-BSA). Patient samples and standards of different concentrations of recombinant mCRP were added to the plate and incubated for 2h at room temperature. A mouse anti-human mCRP monoclonal antibody (8C10) diluted 1:200 in PBS-BSA was then added and incubated for 90min at room temperature, followed by incubation with a goat anti-mouse IgG antibody conjugated with horseradish peroxidase (Abcam (ab6789), Waltham, MA, USA). After an hour incubation at room temperature, substrate solution (3,3',5,5' tetramethylbenzidine) was added. The reaction was stopped using 1M H<sub>2</sub>SO<sub>4</sub> and optical density measured at 450nm. Reagents for the mCRP ELISA (goat anti-human mCRP and the monoclonal 8C10 anti-mCRP antibody (26) were kindly provided by Drs. Lawrence Potempa and Ibrahim Rahab (Roosevelt University, Schaumburg, IL, USA).

## Statistical analyses

Statistical differences between pCRP and mCRP levels in the two severity groups were calculated in GraphPad Prism 9.4.0 using Mann-Whitney test. ANOVA with Dunn's multiple comparisons test was performed using GraphPad Prism version 8.0 for Windows, GraphPad Software, San Diego, California USA, [www.graphpad.com](http://www.graphpad.com).

Univariate analysis was done either by Fisher's exact test for binary variables or Mann-Whitney U test for continuous variables using SPSS version 27. Multivariate logistic regression was performed with the variables: BMI, suPAR, neutrophil to lymphocyte ratio, LDH, and viral load at inclusion, which were included in the model after being associated with disease severity at  $p < 0.1$  level after univariate analysis (6).

## Results

### Clinical characteristics of COVID-19 patients

A total of 62 hospitalized patients with COVID-19 were included in this study. They comprised 41 males and 21 females, with a median age of 57.5 years. The two severity groups (mild/moderate and severe/critical) were of equal size (N=31). Length of hospital stay, corticosteroid therapy, body mass index, neutrophil count, NLR, suPAR, viral load, and LDH levels differed significantly between the groups (Table 1). The median age in the control group was 45 years old. The cohort is well characterized (6, 25, 27, 28) and reflects characteristics and co-morbidities commonly seen in hospitalized patients with COVID-19.

### Hospitalized patients with severe/critical COVID-19 had significantly higher levels of pCRP at inclusion compared to mild/moderate disease

The levels of pCRP and mCRP were measured in blood samples taken from hospitalized patients with COVID-19 at inclusion (Figure 1). pCRP exhibited a significant difference between mild/moderate and severe/critical disease (Figure 1A), whereas there was no difference in mCRP levels between the severity groups (Figure 1B). Next, we performed a multivariate analysis using variables that associated in a univariate analysis; BMI (aOR 1.23,  $p=0.011$ ), suPAR (aOR 1.47,  $p=0.046$ ), neutrophil to lymphocyte ratio (aOR 1.074,  $p=0.29$ ), LDH (aOR 1.2,  $p=0.23$ ), and viral load; (aOR 7.04,  $p=0.054$  for Ct value  $<30$ ). pCRP did not associate with disease severity (adjusted odds ratio (aOR) 1.003,  $p=0.53$ ) in this multivariate model. Nonetheless, comparing pCRP levels against only COVID-19 severity showed pCRP levels in COVID-19 patients to be a predictor for disease severity, supporting the use of pCRP as a biomarker.

### Persistence of elevated pCRP levels for at least 6 weeks in hospitalized patients with COVID-19

Levels of pCRP and mCRP in serum samples collected from COVID-19 patients at inclusion, and at the 2-week, and 6-week follow-up were measured by turbidimetry high sensitivity assay and ELISA, respectively. pCRP levels in patients with COVID-19 were significantly increased at inclusion compared to healthy controls (Figure 2A). The pCRP levels decreased significantly between the inclusion and 2-week timepoint, and also between the 2-week and 6-week timepoints. Of note, pCRP levels were still significantly higher at the 6-week timepoint compared to the controls (Figure 2A). There were also significantly higher mCRP levels at inclusion and the 2-week time points compared to the healthy controls despite a significant drop between these two timepoints (Figure 2B). The mCRP levels had reached the level of healthy controls at the 6-week timepoint (Figure 2B). Although mCRP levels were significantly elevated as seen for pCRP, they returned more quickly to normal levels in circulation.

## Discussion

During the COVID-19 pandemic numerous biomarkers were evaluated for their ability to predict the severity of the SARS-CoV-2 infection. Here we investigated the pCRP and mCRP levels within a cohort of hospitalized COVID-19 patients throughout 2020 and 2021 in Sweden, to determine if both isoforms of CRP could be useful prognostic indicators for serious disease. We found pCRP but not mCRP levels were associated with COVID-19 disease severity, and the pCRP data is in line with multiple previous studies (16–19). Our mCRP data is not in line with a recently published study (23),

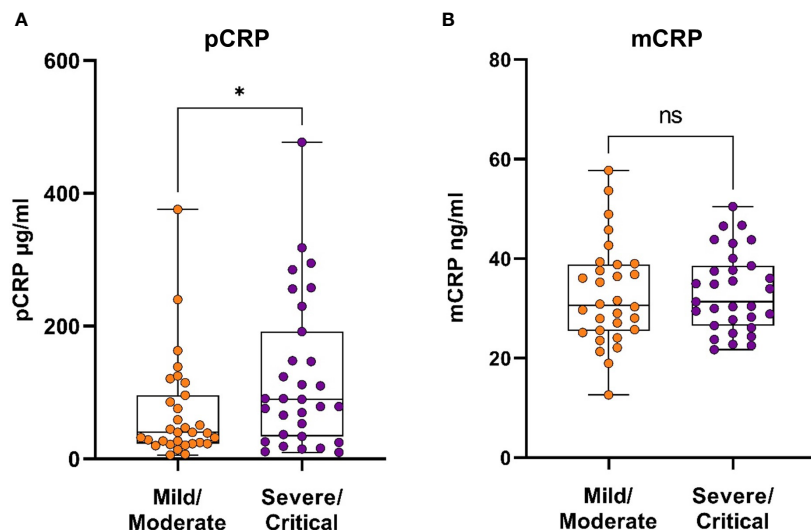


FIGURE 1

CRP isoforms in patients with COVID-19, stratified based on disease severity. Serum samples were taken from COVID-19 patients (N=62) upon hospitalization and assayed to determine the levels of circulating pCRP (A) and mCRP (B). Mann-Whitney U test was used for statistical comparison. \* $P \leq 0.05$ , ns, non-significant.

in which mCRP was shown to have a better prognostic value for COVID-19 severity than pCRP.

Although pCRP is mostly considered to be a marker of inflammation, bacterial infection or sepsis, it was established early on that pCRP levels increase during SARS-CoV-2 infection (17, 18,

20, 23). Persistent elevated plasma levels of pCRP are found in chronic inflammatory diseases such as rheumatoid arthritis (3), type 2 diabetes mellitus, and Parkinson's disease (29), and in chronic obstructive pulmonary disease (30). Whether mCRP levels are elevated in these diseases is not known, but mCRP has

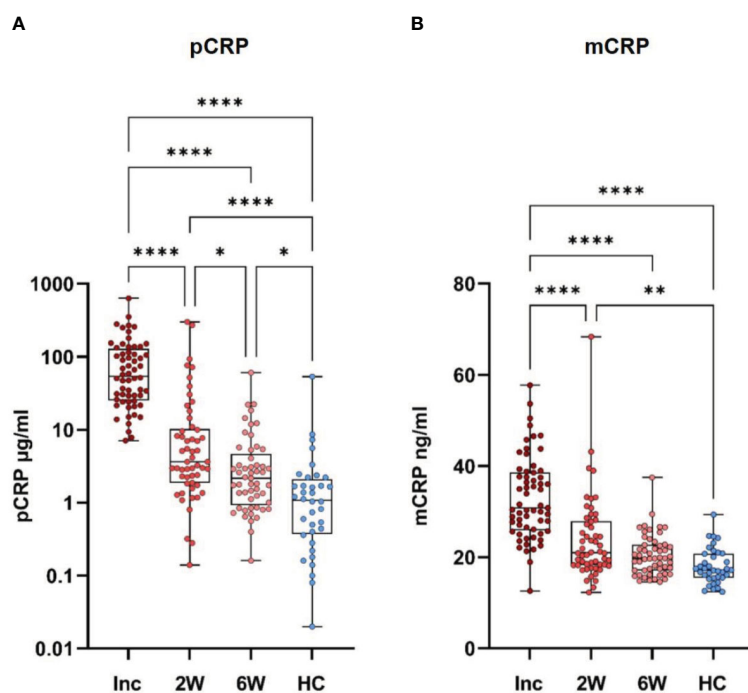


FIGURE 2

CRP isoforms are sustained for different length of time following hospitalization for COVID-19. Serum samples were taken from healthy controls (N=31) and COVID-19 patients at hospitalization (N=62). Follow up samples were taken at 2 and 6 weeks. All samples were assayed for pCRP (A) and mCRP (B). Statistical testing was done by one way ANOVA with Dunn's multiple comparisons test. \* $P \leq 0.05$ , \*\* $P \leq 0.01$ , \*\*\*\* $P \leq 0.0001$ . Inc, inclusion; 2W, 2 weeks; 6W, 6 weeks; HC, healthy controls.

been implicated to play a pathogenic role in cardiovascular disease where it is detected in atherosclerotic plaques, and to cause neuroinflammation where it is found in the affected neuronal tissue (31–33). Consequently, mCRP is likely deposited in the inflamed lung tissue in patients with severe COVID-19. Therefore, in circulation, pCRP with its dynamic range is a better biomarker for COVID-19, whereas mCRP could be of more relevance to measure in the inflamed airway.

Of note, the elevation of pCRP following SARS-CoV-2 infection was sustained for a longer time compared to mCRP. Elevated pCRP levels are observed after acute COVID-19 infection, in people suffering from so-called ‘Long COVID’ (34), and our data here suggests that they are elevated even in convalescent people who do not have that specific syndrome. We also found a long-term elevation of circulating pCRP following the resolution of the infection and healing of the airways. We have previously shown that immune cells such as T cells, dendritic cells and monocyte subsets are affected up to 6 months after COVID-19, with an ongoing low level of inflammation, probably due to tissue damage and repair of the airways (27, 28). The elevated levels of pCRP may be a part in this ongoing inflammation, and further research should elucidate more of the mechanisms behind this. Work is also needed to clarify if mCRP plays any role in the ongoing inflammation, as one would expect from a modulator of inflammatory responses. It is of interest that the elevation of pCRP is more prolonged than that of mCRP, suggesting that the post-COVID immune environment is supportive for the production of pCRP but there is less dissociation into its monomeric form.

We used the National Institute of Health (NIH), USA COVID-19 patient treatment criteria (24) to stratify our patients according to disease severity, which could be one reason for the lack of association between mCRP levels and severity of COVID-19 in our study compared to the findings by Molins et al, which classified severe disease as intensive care admission and/or in-hospital mortality (23). Seeing that there were few mild and critical ill cases among our hospitalized COVID-19 patients, including patients might have improved the predictive power of mCRP, as similar studies used a cohort with a greater proportion of patients with mild and fatal disease (23). Additionally, it would have been of interest to investigate a wider range of inflammatory markers including cytokines. The cytokine storm is a well-described aspect of a severe SARS-CoV-2 infection and cytokines such as IL-6 and TNF have been shown to correlate to COVID-19 severity (22, 35). To date, there are no commercially available mCRP tests that can be employed efficiently in the clinical routine blood testing. Considering this, and the lack of correlation between mCRP and disease severity in our study, it appears unlikely that mCRP will make a better diagnostic test or be more useful as biomarker than pCRP in the clinical setting. In conclusion, in a cohort of hospitalized patients with COVID-19 we found that the inflammation, as shown by elevated pCRP levels, lasted for more than 6 weeks after SARS-CoV-2 infection. This indicates that COVID-19 gives rise to adverse effects on the immune system that last even after the viral infection has resolved. It is also clear that the clinical pCRP testing of COVID-19 patients upon hospitalization is a useful biomarker for predicting COVID-19

severity, as has been demonstrated here and by several studies (16–19) and would not be improved by additional analysis of mCRP levels.

## Data availability statement

The raw data supporting the conclusions of this article will be made available by the authors, without undue reservation.

## Ethics statement

The studies involving humans were approved by Swedish Ethical Review Authority Decision number 2020–0258. The studies were conducted in accordance with the local legislation and institutional requirements. The participants provided their written informed consent to participate in this study.

## Author contributions

FH: Data curation, Formal Analysis, Investigation, Visualization, Writing – original draft. JN: Data curation, Formal Analysis, Visualization, Writing – review & editing. RF-B: Investigation, Resources, Writing – review & editing. HE: Methodology, Writing – review & editing. MG: Writing – review & editing. CeS: Writing – review & editing. LS: Funding acquisition, Writing – review & editing. MH: Writing – review & editing. ÅN-A: Writing – review & editing. SN: Writing – review & editing. ChS: Conceptualization, Data curation, Funding acquisition, Methodology, Resources, Writing – review & editing. JS: Conceptualization, Data curation, Funding acquisition, Methodology, Resources, Writing – review & editing. ML: Conceptualization, Data curation, Funding acquisition, Methodology, Project administration, Supervision, Writing – original draft, Writing – review & editing.

## Funding

The author(s) declare financial support was received for the research, authorship, and/or publication of this article. This work has been supported by grants through: ML SciLifeLab/KAW COVID-19 Research Program, Swedish Research Council project grant 201701091, COVID-19 ALF (Linköping University Hospital Research Fund), Region Östergötland ALF Grant, RÖ935411 (JS); Regional ALF Grant 2021 (ÅN-A and JS), Vrinnevi Hospital in Norrköping).

## Acknowledgments

We thank all the study participants, as well as those who contributed to the study, especially the health care staff at the Clinic of Infectious Diseases and at the Intensive Care Unit at the Vrinnevi Hospital, Norrköping, Sweden. We would also like to

thank Annette Gustafsson for study coordination and collecting samples from the donors. We are indebted to Drs. Lawrence Potempa and Ibraheem Rahab (Roosevelt University, Schaumburg, IL, USA) for their generous supply of reagents for the mCRP ELISA.

## Conflict of interest

The authors declare that the research was conducted in the absence of any commercial or financial relationships that could be construed as a potential conflict of interest.

## References

- Mangalmurti N, Hunter CA. Cytokine storms: understanding COVID-19. *Immunity* (2020) 53:19–25. doi: 10.1016/j.immuni.2020.06.017
- Du Clos TW. Pentraxins: structure, function, and role in inflammation. *ISRN Inflammation* (2013) 2013:379040. doi: 10.1155/2013/379040
- Kay J, Upchurch KS. ACR/EULAR 2010 rheumatoid arthritis classification criteria. *Rheumatol (Oxford)* (2012) 51 Suppl 6:vi5–9. doi: 10.1093/rheumatology/kes279
- Povoa P. C-reactive protein: a valuable marker of sepsis. *Intensive Care Med* (2002) 28:235–43. doi: 10.1007/s00134-002-1209-6
- Heuertz RM, Schneider GP, Potempa LA, Webster RO. Native and modified C-reactive protein bind different receptors on human neutrophils. *Int J Biochem Cell Biol* (2005) 37:320–35. doi: 10.1016/j.biocel.2004.07.002
- Hopkins FR, Govender M, Svanberg C, Nordgren J, Waller H, Nilsson-Augustinsson A, et al. Major alterations to monocyte and dendritic cell subsets lasting more than 6 months after hospitalization for COVID-19. *Front Immunol* (2022) 13:1082912. doi: 10.3389/fimmu.2022.1082912
- Karlsson J, Wettero J, Weiner M, Ronnelid J, Fernandez-Botran R, Sjowall C. Associations of C-reactive protein isoforms with systemic lupus erythematosus phenotypes and disease activity. *Arthritis Res Ther* (2022) 24:139. doi: 10.1186/s13075-022-02831-9
- McFadyen JD, Kiefer J, Braig D, Loeffler-Silver J, Potempa LA, Eisenhardt SU, et al. Dissociation of C-reactive protein localizes and amplifies inflammation: evidence for a direct biological role of C-reactive protein and its conformational changes. *Front Immunol* (2018) 9:1351. doi: 10.3389/fimmu.2018.01351
- Sproston NR, Ashworth JJ. Role of C-reactive protein at sites of inflammation and infection. *Front Immunol* (2018) 9:754. doi: 10.3389/fimmu.2018.00754
- Khreiss T, Jozsef L, Potempa LA, Filep JG. Opposing effects of C-reactive protein isoforms on shear-induced neutrophil-platelet adhesion and neutrophil aggregation in whole blood. *Circulation* (2004) 110:2713–20. doi: 10.1161/01.CIR.0000146846.00816.DD
- Khreiss T, Jozsef L, Potempa LA, Filep JG. Loss of pentameric symmetry in C-reactive protein induces interleukin-8 secretion through peroxynitrite signaling in human neutrophils. *Circ Res* (2005) 97:690–7. doi: 10.1161/01.RES.0000183881.11739.CB
- Thiele JR, Habersberger J, Braig D, Schmidt Y, Goerendt K, Maurer V, et al. Dissociation of pentameric to monomeric C-reactive protein localizes and aggravates inflammation: in vivo proof of a powerful proinflammatory mechanism and a new anti-inflammatory strategy. *Circulation* (2014) 130:35–50. doi: 10.1161/CIRCULATIONAHA.113.007124
- Gershov D, Kim S, Brot N, Elkon KB. C-Reactive protein binds to apoptotic cells, protects the cells from assembly of the terminal complement components, and sustains an antiinflammatory innate immune response: implications for systemic autoimmunity. *J Exp Med* (2000) 192:1353–64. doi: 10.1084/jem.192.9.1353
- Mold C, Baca R, Du Clos TW. Serum amyloid P component and C-reactive protein opsonize apoptotic cells for phagocytosis through Fcγ receptors. *J Autoimmun* (2002) 19:147–54. doi: 10.1006/jaut.2002.0615
- Ruiz-Fernandez C, Gonzalez-Rodriguez M, Francisco V, Rajab IM, Gomez R, Conde J, et al. Monomeric C reactive protein (mCRP) regulates inflammatory responses in human and mouse chondrocytes. *Lab Invest* (2021) 101:1550–60. doi: 10.1038/s41374-021-00584-8
- Yitbarek GY, Walle Ayehu G, Asnakew S, Ayele FY, Bariso Gare M, Mulu AT, et al. The role of C-reactive protein in predicting the severity of COVID-19 disease: A systematic review. *SAGE Open Med* (2021) 9:20503121211050755. doi: 10.1177/20503121211050755
- Ahnach M, Zbiri S, Nejari S, Ousti F, Elkettani C. C-reactive protein as an early predictor of COVID-19 severity. *J Med Biochem* (2020) 39:500–7. doi: 10.5937/jomb0-27554
- Luo X, Zhou W, Yan X, Guo T, Wang B, Xia H, et al. Prognostic value of C-reactive protein in patients with coronavirus 2019. *Clin Infect Dis* (2020) 71:2174–9. doi: 10.1093/cid/ciaa641
- Stringer D, Braude P, Myint PK, Evans L, Collins JT, Verduri A, et al. The role of C-reactive protein as a prognostic marker in COVID-19. *Int J Epidemiol* (2021) 50:420–9. doi: 10.1093/ije/dyab012
- Lentner J, Adams T, Knutson V, Zeien S, Abbas H, Moosavi R, et al. C-reactive protein levels associated with COVID-19 outcomes in the United States. *J Osteopath Med* (2021) 121:869–73. doi: 10.1515/jom-2021-0103
- SayedAlinaghi S, Karimi A, Mirzapour P, Afroughi F, Noroozi A, Arjmand G, et al. The relationship between C-reactive protein and levels of various cytokines in patients with COVID-19: A systematic review and correlation analysis. *Health Sci Rep* (2022) 5:e868. doi: 10.1002/hsr2.868
- Zeng F, Huang Y, Guo Y, Yin M, Chen X, Xiao L, et al. Association of inflammatory markers with the severity of COVID-19: A meta-analysis. *Int J Infect Dis* (2020) 96:467–74. doi: 10.1016/j.ijid.2020.05.055
- Molins B, Figueras-Roca M, Valero O, Llorenç V, Romero-Vazquez S, Sibila O, et al. C-reactive protein isoforms as prognostic markers of COVID-19 severity. *Front Immunol* (2022) 13:1105343. doi: 10.3389/fimmu.2022.1105343
- NIH. COVID-19 treatment guidelines panel. coronavirus disease 2019. (COVID-19) treatment guidelines (2020). Available at: <https://www.covid19treatmentguidelines.nih.gov/>
- Enocsson H, Idoff C, Gustafsson A, Govender M, Hopkins F, Larsson M, et al. Soluble urokinase plasminogen activator receptor (suPAR) independently predicts severity and length of hospitalisation in patients with COVID-19. *Front Med (Lausanne)* (2021) 8:791716. doi: 10.3389/fmed.2021.791716
- Diehl EE, Haines GK, Radosevich JA, Potempa LA. Immunohistochemical localization of modified C-reactive protein antigen in normal vascular tissue. *Am J Med Sci* (2000) 319:79–83. doi: 10.1016/S0002-9629(15)40692-5
- Govender M, Hopkins FR, Goransson R, Svanberg C, Shankar EM, Hjorth M, et al. T cell perturbations persist for at least 6 months following hospitalization for COVID-19. *Front Immunol* (2022) 13:931039. doi: 10.3389/fimmu.2022.931039
- Waller H, Carmona-Vicente N, James A, Govender M, Hopkins FR, Larsson M, et al. Viral load at hospitalization is an independent predictor of severe COVID-19. *Eur J Clin Invest* (2023) 53:e13882. doi: 10.1111/eci.13882
- Luan YY, Yao YM. The clinical significance and potential role of C-reactive protein in chronic inflammatory and neurodegenerative diseases. *Front Immunol* (2018) 9:1302. doi: 10.3389/fimmu.2018.01302
- Hassan A, Jabbar N. C-reactive protein as a predictor of severity in chronic obstructive pulmonary disease: an experience from a tertiary care hospital. *Cureus* (2022) 14:e28229. doi: 10.7759/cureus.28229
- Melnikov I, Kozlov S, Saburova O, Avtaeva Y, Guria K, Gabbasov Z. Monomeric C-reactive protein in atherosclerotic cardiovascular disease: advances and perspectives. *Int J Mol Sci* (2023) 24:2079. doi: 10.3390/ijms24032079
- Slevin M, Heidari N, Azamfiroi L. Monomeric C-reactive protein: current perspectives for utilization and inclusion as a prognostic indicator and therapeutic target. *Front Immunol* (2022) 13:866379. doi: 10.3389/fimmu.2022.866379
- Al-Baradie RS, Pu S, Liu D, Zeinolabediny Y, Ferris G, Sanfeli C, et al. Monomeric C-reactive protein localized in the cerebral tissue of damaged vascular brain regions is associated with neuro-inflammation and neurodegeneration-an immunohistochemical study. *Front Immunol* (2021) 12:644213. doi: 10.3389/fimmu.2021.644213
- Pasini E, Corsetti G, Romano C, Scarabelli TM, Chen-Scarabelli C, Saravolatz L, et al. Serum metabolic profile in patients with long-covid (PASC) syndrome: clinical implications. *Front Med (Lausanne)* (2021) 8:714426. doi: 10.3389/fmed.2021.714426
- Del Valle DM, Kim-Schulze S, Huang HH, Beckmann ND, Nirenberg S, Wang B, et al. An inflammatory cytokine signature predicts COVID-19 severity and survival. *Nat Med* (2020) 26:1636–43. doi: 10.1038/s41591-020-1051-9

The authors declared that they were an editorial board member of Frontiers, at the time of submission. This had no impact on the peer review process and the final decision

## Publisher's note

All claims expressed in this article are solely those of the authors and do not necessarily represent those of their affiliated organizations, or those of the publisher, the editors and the reviewers. Any product that may be evaluated in this article, or claim that may be made by its manufacturer, is not guaranteed or endorsed by the publisher.





## OPEN ACCESS

## EDITED BY

Alok Agrawal,  
East Tennessee State University,  
United States

## REVIEWED BY

Karlheinz Peter,  
Baker Heart and Diabetes Institute,  
Australia  
Shang-Rong Ji,  
Lanzhou University, China

## \*CORRESPONDENCE

Sihai Zhao

✉ sihaizhao@xjtu.edu.cn

Enqi Liu

✉ liuenqi@xjtu.edu.cn

<sup>†</sup>These authors share first authorship

RECEIVED 02 June 2023

ACCEPTED 25 August 2023

PUBLISHED 11 September 2023

## CITATION

Fu Y, Liu H, Li K, Wei P, Alam N, Deng J, Li M, Wu H, He X, Hou H, Xia C, Wang R, Wang W, Bai L, Xu B, Li Y, Wu Y, Liu E and Zhao S (2023) C-reactive protein deficiency ameliorates experimental abdominal aortic aneurysms. *Front. Immunol.* 14:1233807. doi: 10.3389/fimmu.2023.1233807

## COPYRIGHT

© 2023 Fu, Liu, Li, Wei, Alam, Deng, Li, Wu, He, Hou, Xia, Wang, Wang, Bai, Xu, Li, Wu, Liu and Zhao. This is an open-access article distributed under the terms of the [Creative Commons Attribution License \(CC BY\)](#). The use, distribution or reproduction in other forums is permitted, provided the original author(s) and the copyright owner(s) are credited and that the original publication in this journal is cited, in accordance with accepted academic practice. No use, distribution or reproduction is permitted which does not comply with these terms.

# C-reactive protein deficiency ameliorates experimental abdominal aortic aneurysms

Yu Fu<sup>1†</sup>, Haole Liu<sup>1†</sup>, Kexin Li<sup>1</sup>, Panpan Wei<sup>1</sup>, Naqash Alam<sup>1</sup>, Jie Deng<sup>2</sup>, Meng Li<sup>3</sup>, Haibin Wu<sup>1</sup>, Xue He<sup>1</sup>, Haiwen Hou<sup>1</sup>, Congcong Xia<sup>1</sup>, Rong Wang<sup>1</sup>, Weirong Wang<sup>1</sup>, Liang Bai<sup>1</sup>, Baohui Xu<sup>4</sup>, Yankui Li<sup>3</sup>, Yi Wu<sup>5</sup>, Enqi Liu<sup>1\*</sup> and Sihai Zhao<sup>1,2\*</sup>

<sup>1</sup>Institute of Cardiovascular Science, Translational Medicine Institute, Xi'an Jiaotong University Health Science Center, Xi'an, Shaanxi, China, <sup>2</sup>Department of Cardiology, The Second Affiliated Hospital of Xi'an Jiaotong University, Xi'an, Shaanxi, China, <sup>3</sup>Department of Vascular Surgery, The Second Hospital of Tianjin Medical University, Tianjin, China, <sup>4</sup>Department of Surgery, Stanford University School of Medicine, Stanford, CA, United States, <sup>5</sup>Key Laboratory of Environment and Genes Related to Diseases, Ministry of Education, Xi'an, Shaanxi, China

**Background:** C-reactive protein (CRP) levels are elevated in patients with abdominal aortic aneurysms (AAA). However, it has not been investigated whether CRP contributes to AAA pathogenesis.

**Methods:** CRP deficient and wild type (WT) male mice were subjected to AAA induction via transient intra-aortic infusion of porcine pancreatic elastase. AAAs were monitored by *in situ* measurements of maximal infrarenal aortic external diameters immediately prior to and 14 days following elastase infusion. Key AAA pathologies were assessed by histochemical and immunohistochemical staining procedures. The influence of CRP deficiency on macrophage activation was evaluated in peritoneal macrophages *in vitro*.

**Results:** CRP protein levels were higher in aneurysmal than that in non-aneurysmal aortas. Aneurysmal aortic dilation was markedly suppressed in CRP deficient (aortic diameter:  $1.08 \pm 0.11$  mm) as compared to WT ( $1.21 \pm 0.08$  mm) mice on day 14 after elastase infusion. More medial elastin was retained in CRP deficient than in WT elastase-infused mice. Macrophage accumulation was significantly less in aneurysmal aorta from CRP deficient than that from WT mice. Matrix metalloproteinase 2 expression was also attenuated in CRP deficient as compared to WT aneurysmal aortas. CRP deficiency had no recognizable influence on medial smooth muscle loss, lymphocyte accumulation, aneurysmal angiogenesis, and matrix metalloproteinase 9 expression. In *in vitro* assays, mRNA levels for tumor necrosis factor  $\alpha$  and cyclooxygenase 2 were reduced in lipopolysaccharide activated peritoneal macrophages from CRP deficient as compared to wild type mice.

**Conclusion:** CRP deficiency suppressed experimental AAAs by attenuating aneurysmal elastin destruction, macrophage accumulation and matrix metalloproteinase 2 expression.

## KEYWORDS

abdominal aortic aneurysms, C-reactive protein, macrophages, matrix metalloproteinase 2, inflammation

## Introduction

Abdominal aortic aneurysms (AAA) are local dilation of aortic segments particularly infrarenal aorta resulted from media destruction and diagnosed when the diameter exceeds 50% of adjacent aortic diameter (1). AAAs progress asymptotically but fatal upon premature rupture with an estimated annual death of 100,000 worldwide (1–3). While poorly defined, inflammation is crucial in AAA pathogenesis (1, 4).

C-reactive protein (CRP) is an acute inflammatory protein and increases dramatically in response to almost tissue injury, infection and inflammation, thus being used as an inflammatory marker in clinic (5–9). CRP binds phosphorylated choline of pneumococcal C-polysaccharides, activates classical complement pathway or interacts with the Fc gammaR1/2 (FcγR1/2) receptor, altogether promoting the clearance of pathogens and cellular debris (10). CRP also modulates the function of immune cells including macrophages and lymphocytes (11–15). Thus, CRP is important for both host defense and human disease pathogenesis by regulating innate and adaptive immunity.

In clinical AAAs, it has been reported that the CRP levels were positively associated with aneurysm diameter (16–20). CRP was also highly expressed in aneurysmal as compared to non-aneurysmal aortas (21). Additionally, serum CRP levels have been used for helping AAA diagnosis as well as predicting clinical outcomes following AAA repair (22, 23). However, it has not been investigated whether CRP mediates AAA pathogenesis. Therefore, this study assessed the influence of CRP deficiency on experimental AAA formation and progression in the intra-aortic elastase infusion-induced AAA model.

## Materials and methods

### Mice

CRP deficient mice were previously generated using CRISPR/Cas9 and homologous recombination technology to knock-in a STOP cassette at the ATG site of the CRP gene on C57BL/6 genetic background) at Shanghai Biomodel Organism Science &

Technology Development Co., Ltd (Shanghai, China) (24). CRP deficient and C57BL/6 wild type (WT) mice were used for all experiments. The use and care of animals in this study were approved by the Laboratory Animal Management Committee of Xi'an Jiaotong University, Xi'an, China (No. 2022-623).

### Identification of CRP deficient mice

Genomic DNA was extracted from tail tips of less than 3 weeks old mice. Genotyping was conducted using the polymerase chain reaction (PCR) assay and gene-specific primer set. PCR primers were sense primer P1, (GCAGTTGGCCAGGGAAAGTT) and antisense primer P2 (CATGATCAGAAGGCACCAGAGTAG) for WT allele (PCR product size: 552 base pairs) and sense primer P1 and antisense primer P3 (CCTCGCCGGACACGCTGAA) for targeted allele (PCR product size: 637 base pairs), respectively. Quantitative real-time reverse transcription- polymerase chain reaction (qRT-PCR) was assessed CRP mRNA levels in liver tissues using the primers (Table 1). Western blotting analysis was utilized to determine CRP protein expression. Antibodies for Western blotting were a goat anti-mouse CRP polyclonal antibody (1:4000, Cat#: BAF1829, R&D Systems, Inc, Minneapolis, MN, USA), a rabbit anti-mouse β-actin polyclonal antibody (1:10000, Cat#: bs-0061R, Bioss Technology, Beijing, China), and an horseradish peroxidase-conjugated donkey anti-goat polyclonal antibody (1:5000, Cat#: EK030, Zhuangzhi Biological Technology, Xi'an, China) or goat anti-rabbit polyclonal antibody (1:10000, Cat#: bs-40295G, Bioss Technology) (25).

### AAA creation in mice

Male CRP-deficient and WT control mice at 9 weeks of age were used for experiments. AAAs were induced in infrarenal aorta under sterile condition using porcine pancreatic elastase (PPE) infusion method as previously described (26–28). Briefly, mice were anesthetized by 2% isoflurane inhalation, and a laparotomy was created to expose the infrarenal aorta. Mice were infused with PPE

TABLE 1 Primer sequences used for qRT-PCR assay.

Gene	Forward (5'-3')	Reverse (5'-3')
C-reactive protein	GTC TGC TAC GGG GAT TGT AGA	CAC CGC CAT ACG AGT CCT G
Interleukin-1β	CGT GGA CCT TCC AGG ATG AG	CAT CTC GGA GCC TGT AGT GC
Interleukin-6	CGG CCT TCC CTA CTT CAC AA	TTC TGC AAG TGC ATC ATC GT
Cyclooxygenase 2	CTG ACC CCC AAG GCT CAA AT	TCC ATC CTT GAA AAG GCG CA
Tumor necrosis factor-α	TGA GCA CAG AAA GCA TGA TCC	GCC ATT TGG GAA CTT CTC ATC
Arginase 1	CTT GCG AGA CGT AGA CCC TG	CTT CCT TCC CAG CAG GTA GC
Resistin-like molecule α	CTG GGA TGA CTG CTA CTG GG	CAG TGG TCC AGT CAA CGA GTA
Chitinase 3-like 3	CCA GCA GAA GCT CTC CAG AAG	TCA GCT GGT AGG AAG ATC CCA
beta-actin	CAT CCG TAA AGA CCT CTA TGC CAA C	ATG GAG CCA CCG ATC CAC A

solution for 5 minutes (1.5 units/mL, Cat#: E-1250, Sigma-Aldrich, St Louis, MO, USA) through the aortotomy in temporarily controlled infrarenal aortic segment using a pressure pump (29). Thereafter, aortotomy and laparotomy were sequentially closed using 10-0 and 6-0 silk sutures, respectively. Mice were recovered, housed in individual cages, and monitored daily for morbidity and mortality.

## Measurements of aneurysmal aortic diameters

External infrarenal aortic diameters were measured *in situ* using a digital microscope. Briefly, infrarenal aortic segment was photographed immediately prior to (baseline) and 14 days following PPE. Maximal external infrarenal aortic diameters were determined using Motic Image Plus 3.0 ML software (Motic Electric Group Co., Ltd, Xiamen, China). An AAA was defined as a more than 50% increase in external diameter over the baseline level (29).

## Immunostaining of CRP in experimental aneurysmal aorta

Mice were euthanized by carbon dioxide inhalation 14 days following PPE infusion. Aortas were harvested, embedded in optical cutting temperature compound, sectioned (6  $\mu$ m) and fixed with cold acetone. Infrarenal aortas from naïve WT mice were processed identically and served as non-aneurysmal controls. Frozen sections were stained with hematoxylin and eosin (H&E) and a standard streptavidin peroxidase immunohistochemical method for the assessment of morphological alterations and CRP protein expression, respectively. Reagents for CRP tissue immunostaining were a rabbit anti-mouse CRP polyclonal antibody (1:200, Cat#: bs-0155R) and normal rabbit IgG (1:200, Cat#: bs-0295P) from Bioss Technology. Other reagents were biotinylated goat anti-rabbit IgG antibody (1:400, Cat#: BA-1000) and AEC substrate kit (Cat#: SK-4200, Vector Laboratories, Inc, Newark, CA, USA) and streptavidin-peroxidase conjugate (1:200, Cat#: 016-030-084, Jackson ImmunoResearch, West Grove, PA, USA).

## Histological analysis of medial elastin degradation and smooth muscle cell depletion in aneurysmal aortas

H&E and Elastic van Gieson (EVG) staining were performed frozen aortic sections to assess general morphological changes and elastin contents, respectively. To assess SMC retention, frozen aortic sections were sequentially stained with a goat anti-SMC  $\alpha$ -actin polyclonal antibody (1:200, Cat#: NB300-978, Novus Biologicals, Centennial, CO, USA), a biotinylated rabbit anti-goat IgG antibody (1:400, Cat#: BA-5000, Vector Laboratories, Inc) and streptavidin-peroxidase conjugate (1:200, Cat#: 016-030-084, Jackson ImmunoResearch), and staining was visualized using the AEC substrate kit (Vector Laboratories, Inc). Elastin fragmentation and

SMC loss were scored as the grade I (mild) to IV (severe) using a histological grading system as reported previously (26–31).

## Immunohistochemical staining for leukocytes, angiogenesis and matrix metalloproteinases in aneurysmal aortas

A standard biotin-streptavidin-peroxidase method was used for all immunohistochemical staining. Reagents used in this study were monoclonal antibodies against CD68 (macrophages, 1:200, clone #: FA-11, Cat#: 137002), CD4 (CD4<sup>+</sup> T cells, 1:200, clone #: GK1.5, Cat#: 100402), CD8 (CD8<sup>+</sup> T cells, 1:200, clone #: 53-6.7, Cat#: 100702), B220 (B cells, 1:200, clone #: RA3-6B2, Cat#: 103202) and CD31 (1:200, clone#: 390, Cat#: 102402) (all above mentioned primary antibodies from Biolegend Inc, San Diego, CA, USA), goat anti-mouse polyclonal antibodies against MMP2 (1:200, Cat#: AF1488, R&D Systems) and MMP9 (1:200, Cat#: AF909, R&D Systems), a biotinylated goat anti-rat secondary antibody (1:400, Cat#: BA-9400, Vector Laboratories, Inc) or rabbit anti-goat IgG secondary antibody (1:400, Cat#: BA-5000, Vector Laboratories, Inc), and streptavidin-peroxidase conjugate (1:200, Cat#: 016-030-084, Jackson ImmunoResearch) (27–32). Macrophage accumulation was scored as the grade I to IV, and the densities of CD4<sup>+</sup> T cells, CD8<sup>+</sup> T cells, B220<sup>+</sup> B cells and angiogenesis were quantified as the number of positively stained cells or neovessels per aortic cross section (ACS) (30). MMP expression levels were quantified as a positively stained area percentage of aortic wall using WinRood 6.5 image software, Mitani Co. Ltd., Tokyo, Japan.

## Measurements of macrophage activation *in vitro*

Primary macrophages were isolated from 8 weeks old WT and CRP deficient mice 3 days following intraperitoneal injection of 3% thioglycolate and suspended in RPMI-1640 medium containing 10% fetal bovine serum and 1% penicillin/streptomycin. Following 6 hours activation with lipopolysaccharide (LPS, 50 ng/mL, Cat#: L2630, Sigma-Aldrich) or incubation with vehicle at 37°C, 5% CO<sub>2</sub> for 6 h, cells were harvested. For interleukin-4 (IL-4) stimulated experiment, macrophages were treated with IL-4 (10 ng/mL; Cat#: 214-14, PeproTech, Inc. Cranbury, NJ, USA) or vehicle for 16 hours. Total RNA was extracted with RNAiso Plus (Cat#: 9109), and complementary DNA was synthesized PrimeScript RT kit (Cat#: RR036A) (all from Takara Bio Inc, Kusatsu, Shiga, Japan) and amplified using RealStar Green Power mix (Cat#: A311-10; GenStar, Beijing, China) and gene-specific primers (Table 1). mRNA levels were quantitated as fold changes in relative to vehicle-treated macrophages.

## Statistical analysis

All statistical analyses were performed using the GraphPad software Version 9.0 (Boston, MA, USA). Data on continuous

variables were presented as either mean  $\pm$  standard deviation if normally distributed, and statistical significance was tested using Student's t-test, or one, two-way ANOVA followed by two group comparison tests. Otherwise, data were given as median and interquartile range, and statistical significance was determined using nonparametric Mann-Whitney test. Statistical significance level was set at  $p < 0.05$ .

## Results

### CRP protein is increased in experimental aneurysmal aortas

To examine whether CRP protein expression is altered in aneurysmal aortas, we stained aortic frozen sections from aneurysmal (PPE-infused) and non-aneurysmal WT mice. As depicted in **Figure 1**, rare or no positive staining was not seen in non-aneurysmal aorta. In contrast, an intense and diffusion CRP staining was noted in aneurysmal aortas (**Figure 1**). In serial sections, CRP staining was coincident with inflammatory cell accumulation in aneurysmal aortas.

### CRP deficiency mitigates experimental aneurysmal aortic dilation

To clarify the effect of CRP in experimental AAAs, previously generated CRP-deficient (CRP<sup>-/-</sup>) mice were used in this study (24). The homozygotes of CRP-deficient mice were screened by PCR genotyping and Western blotting (**Figure 2A**). Luminal PPE infusion in infrarenal aorta was performed to induce AAAs in both WT and CRP<sup>-/-</sup> mice. Fourteen days following PPE infusion, aortic dilation, as measured by external aortic diameter, was seen in both WT and CRP<sup>-/-</sup> mice as compared to the baseline level. However, maximal external aortic diameter was significantly smaller in CRP<sup>-/-</sup> ( $1.08 \pm 0.11$  mm) than that in WT ( $1.21 \pm$

0.08 mm) mice on day 14 after PPE infusion (**Figures 2B, C**). When subtracting aortic dilation due to the pressed infusion (approximately 0.8 mm), CRP deficiency per se led to a 32% reduction in aneurysmal enlargement (**Figure 2C**). Even considering the influence of baseline aortic diameter, a remarkable reduction in external aortic diameter was observed in CRP<sup>-/-</sup> as compared to WT mice 14 days following PPE infusion (**Figure 2D**). Thus, CRP may in part mediate experimental aneurysmal expansion.

### CRP deficiency attenuates medial elastin degradation and SMC loss

In EVG staining for medial elastin, more medial elastin was maintained in CRP<sup>-/-</sup> [score as 3 (2–3) (median with interquartile range)] as compared to WT [score as 4 (3–4)] mice (**Figures 2E, F**,  $p = 0.019$ ). Similarly, substantial retention of SMCs was noted in CRP<sup>-/-</sup> [score as 3 (2–3)] as compared to WT [score as 4 (3–4)]. However, the difference in SMC grades did not reach statistical significant level (**Figures 2E, G**) probably due to insufficient sample size. Thus, experimental AAA suppression mediated by CRP deficiency is associated with marked preservation of medial elastin.

### CRP deficiency reduces macrophages accumulation in aneurysmal aorta

Leukocytes contribute to experimental AAA pathogenesis (29, 33). In non-aneurysmal aorta, few leukocytes, almost CD68<sup>+</sup> macrophages in aortic adventitia, were stained positively with subset-specific mAbs (**Figure 3A**). However, leukocytes infiltrated intensely throughout aortic wall in aneurysmal aortas (**Figure 3A**). CD68<sup>+</sup> macrophages accumulated significantly less in CRP<sup>-/-</sup> mice [score as 3 (2–4) (median with interquartile range)] than WT mice did [score as 4 (3–4)] ( $p = 0.025$ ) (**Figures 3A, B**). While CD4<sup>+</sup> T cells, CD8<sup>+</sup> T cells and B220<sup>+</sup> B cells also accumulated in CRP<sup>-/-</sup> and

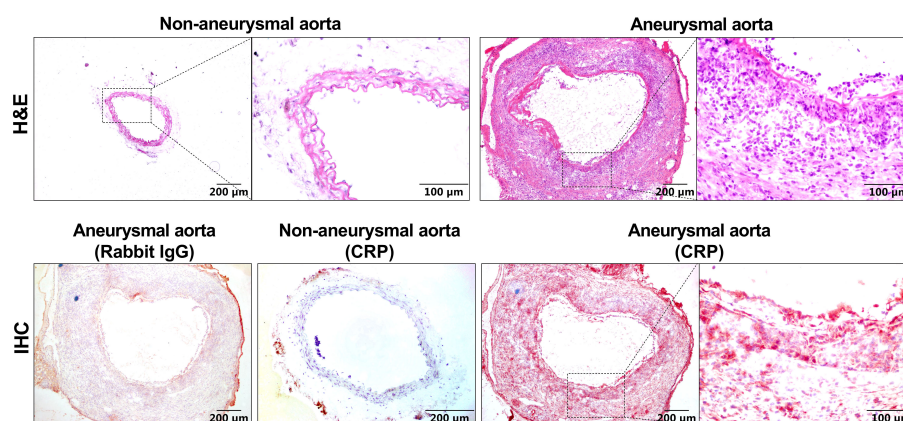


FIGURE 1

CRP expression is elevated in experimental aneurysmal aortas. H&E staining or CRP immunostaining using a rabbit anti-mouse CRP antibody or normal rabbit IgG as the negative control were performed on frozen sections from non-aneurysmal and aneurysmal aortas.



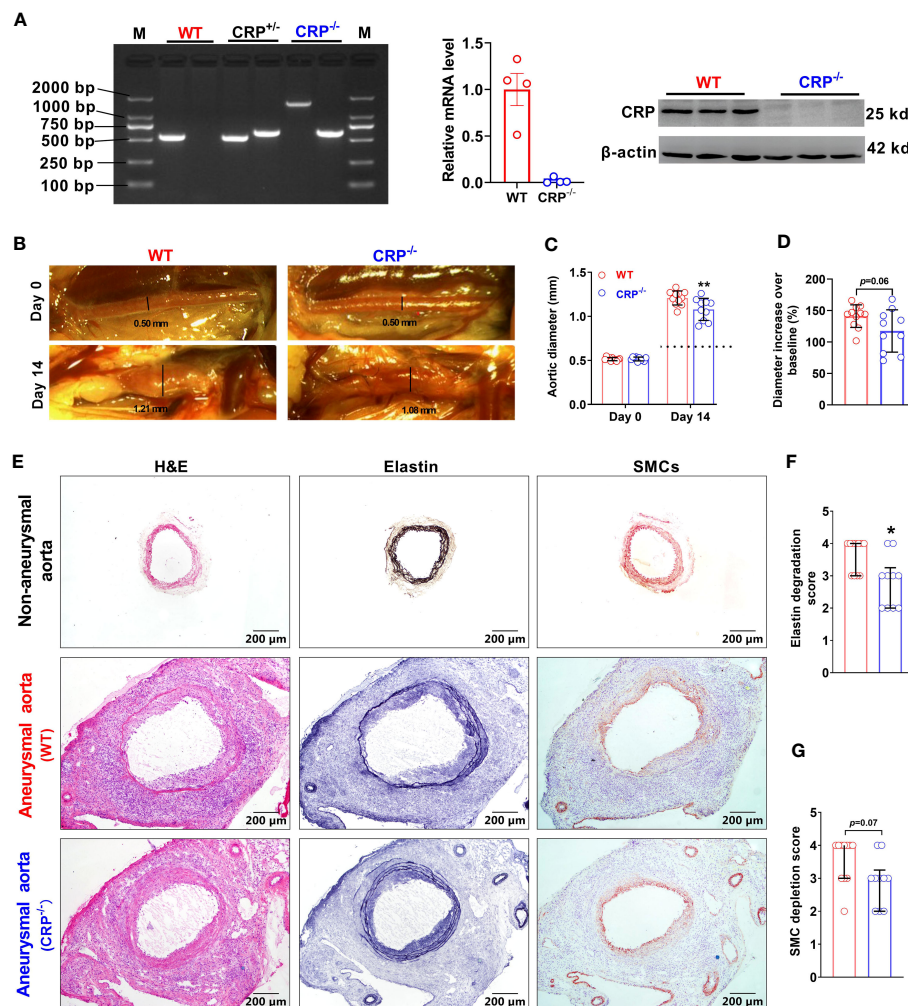


FIGURE 2

CRP deficiency suppresses experimental aneurysmal dilation. **(A)**: Phenotype identification of CRP deficient mice. Phenotyping for CRP homozygotes (CRP deficient mice: CRP<sup>-/-</sup>), CRP heterozygotes (CRP<sup>+/+</sup>) and wild type (WT) mice using PCR assay. CRP expression levels in the livers of CRP<sup>-/-</sup> and WT mice were determined via qRT-PCR and Western blotting analyses. **(B)**: Representative photographic images for infrarenal aortas of wild type and CRP<sup>-/-</sup> mice prior to and 14 days after the elastase infusion. AAAs were induced in male CRP<sup>-/-</sup> and its wild type control mice using intra-aortic infusion of PPE. Influence on AAAs were assessed *in situ* measurements of maximal infrarenal aortic diameters. Dotted line indicates aortic expansion even after PPE solvent (PBS) pressed infusion (about 0.8 mm in our lab) **(C, D)**: Maximal infrarenal aortic external diameters presented as absolute diameter on days 0 (baseline) and 14 after PPE infusion **(C)** or the percentage of diameters over baseline **(D)**. n=10–11 mice per group. Two-ANOVA followed by two group comparison, \*\*p<0.01 compared to wild type mice at same timepoint **(C)**. Student t-test, p=0.06 compared to wild type mice **(D)**. **(E)**: Representative aortic images for H&E (left panels), elastin via Elastic Van Gieson (middle panels), and SMCs via an anti-SMC α antibody immunostaining (right panels) from non-aneurysmal and aneurysmal (wild type and CRP<sup>-/-</sup>) mice. **(F, G)**: Quantification of medial elastin degradation **(F)** and SMC depletion **(G)** scores (media and interquartile) of wild type and CRP<sup>-/-</sup> aneurysmal aortas. Nonparametric Mann-Whitney test, \*p<0.05 compared to wild type mice.

WT mice, no significant difference in either subset was seen between two mouse strains (Figures 3A, C–E).

## CRP deficiency diminishes MMP2 expression in aneurysmal aorta

Both MMP2 and MMP9 are important mediators of AAA pathogenesis (34). In our immunohistochemical staining, MMP2 expression was reduced in PPE-infused CRP<sup>-/-</sup> [expressed as positive staining area ratio (%): 49.51 ± 13.77] as compared to WT (29.55 ± 9.98) mice (Figure 4A), with a 40% reduction in CRP<sup>-/-</sup>

mice (Figure 4B). However, there was no significant difference in MMP9 expression between PPE-infused CRP<sup>-/-</sup> and WT mice (Figures 4A, C).

## CRP deficiency has no recognizable impact on angiogenesis in aneurysmal aorta

Angiogenesis, an additional key AAA pathology, also contributes to the progression of AAAs (35, 36). Angiogenesis, as determined by the density of CD31<sup>+</sup> neovessels, was not differentiated between CRP<sup>-/-</sup> (50.82 ± 13.40/ACS) and WT (43.90 ± 12.23/ACS) mice (Figure 5).



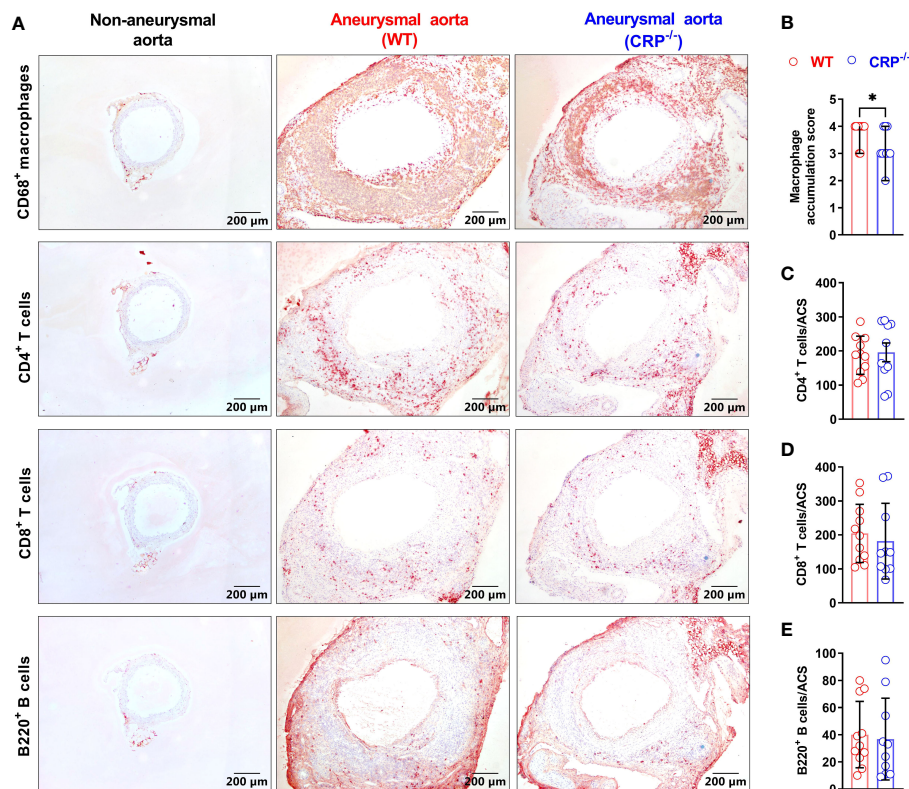


FIGURE 3

CRP deficiency alters aortic leukocyte accumulation. (A): Representative aortic immunostaining images for CD68<sup>+</sup> macrophages, CD4<sup>+</sup> T cells, CD8<sup>+</sup> T cells and B220<sup>+</sup> B cells from non-aneurysmal normal aorta (left panels) and aneurysmal (wild type: middle panels; CRP<sup>-/-</sup> mice: right panels). (B): Quantification of macrophage accumulation scores (media and interquartile) in WT and CRP<sup>-/-</sup> aneurysmal aorta. N=10–11 mice per group, Non-parametric Mann-Whitney, \*P<0.01 compared to WT mice. (C–E): Quantification of different lymphocyte subsets of aortic leukocytes [mean ± standard deviation for positive cells/aortic cross-section (ACS)] from the aneurysmal aortas of WT and CRP<sup>-/-</sup> mice. No statistical difference in all lymphocyte subsets between two mouse strains.

Thus, neoangiogenesis may have no or limited contribution to the suppression of experimental AAAs by CRP deficiency.

## CRP deficiency limits classic macrophage activation *in vitro*

Classic macrophage activation (conventionally known as proinflammatory M1 macrophage activation/polarization) promotes AAA formation and progression (33, 37). In classical activated macrophage by LPS, the expression levels of mRNA for TNF- $\alpha$  and COX-2, but not IL-1 $\beta$ , IL-6 (M1 marker genes) were significantly reduced in CRP deficient as compared to WT macrophages (Figure 6). However, no significant influences were found for the expression levels of all alternative activation macrophage markers (conventionally known as anti-inflammatory M2 macrophages) after activated by IL-4 (Supplementary Figure 1).

## Discussion

Although the detailed mechanism of AAA pathogenesis is still unclear, the involvement of inflammation in the formation and

progression of AAAs has become a consensus in this field (38). CRP, as one of the important inflammatory acute phase proteins, is involved in the development of many cardiovascular diseases (39–45). In this study, we found increased expression of CRP protein in experimental AAAs. CRP deficiency inhibited experimental AAA enlargement in the PPE infusion AAA model. Histologically, the suppression of experimental AAAs by CRP deficiency was associated with the attenuation of medial elastin destruction, aneurysmal wall macrophage accumulation and MMP2 expression. Additionally, CRP deficiency partially inhibited proinflammatory macrophage activation/polarization. Thus, our study indicated that CRP may in part mediate AAA pathogenesis.

In previous studies, CRP has been shown to regulate phenotypic differentiation and activity of macrophages (46–48). In patients with certain cardiovascular diseases, CRP expression levels was positively correlated with M1 macrophage activation (48). This was consistent with our findings that CRP deficiency downregulated the expression levels of M1 macrophages marker genes. Nuclear factor kappa B (NF- $\kappa$ B) regulates proinflammatory macrophages polarization as well as CRP activity, thus reduced M1 macrophage polarization due to CRP deficiency may potentially associate with altered NF- $\kappa$ B signaling activity (42, 47, 49, 50). Additionally, reduced M1 macrophage activation in CRP deficient

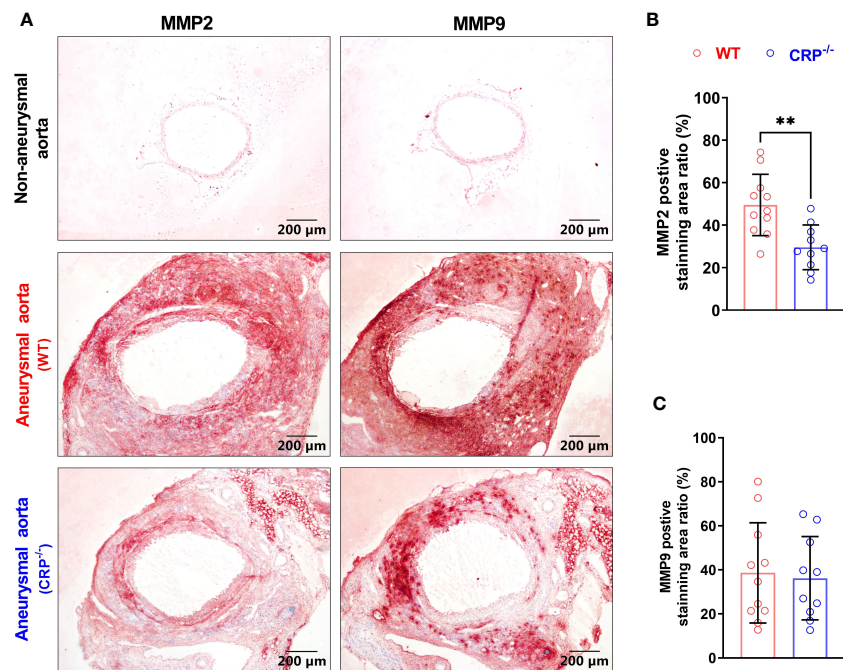


**FIGURE 4**  
CRP deficiency reduces aneurysmal aortic MMP2 expression. **(A)**: Representative immunostaining images for MMP2 and MMP9 in non-aneurysmal normal or aneurysmal (WT and CRP<sup>-/-</sup>) aortas. **(B, C)**: Quantification of MMP2 and MMP9 expression (mean ± standard for the percentage of positively stained area in total aortic cross section area) in wild type and CRP<sup>-/-</sup> aneurysmal aortas. Student's *t* tests, *n*=10-11 mice per group, \*\**p*<0.01 compared to wild type mice.

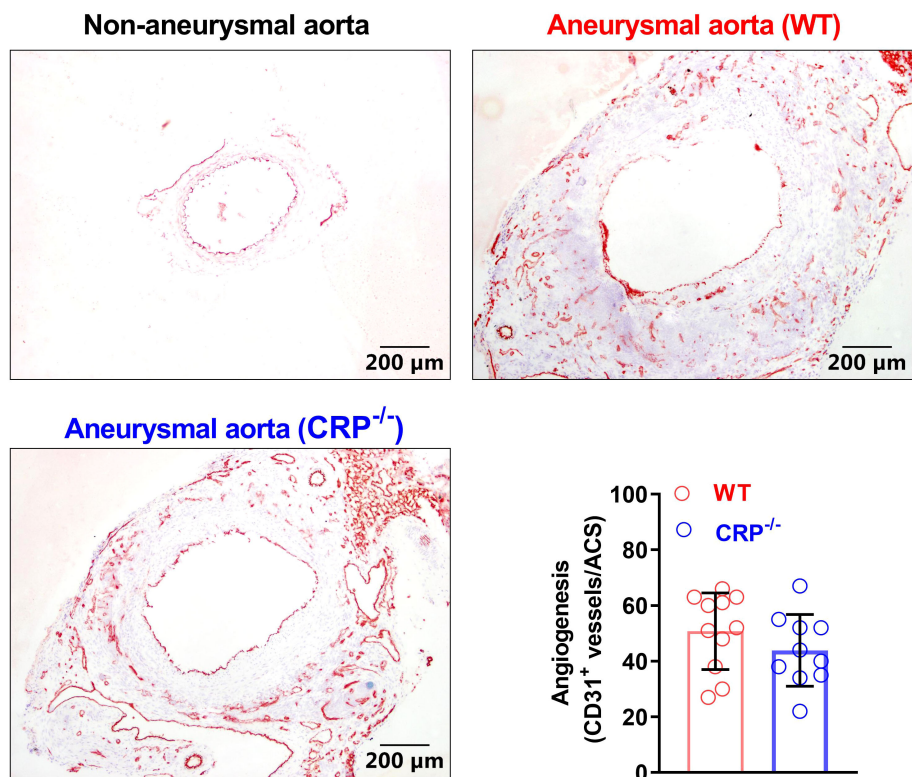


**FIGURE 5**  
CRP deficiency has no remarkable impact on angiogenesis in aneurysmal aortas. Frozen sections were prepared from the aortas of non-aneurysmal normal (upper left) and aneurysmal (wild type: upper right; CRP<sup>-/-</sup>: lower left) mice (*n*=10-11 mice per group) and stained with an anti-CD31 antibody to assess aneurysmal angiogenesis. Lower right panel: angiogenesis in wild and CRP<sup>-/-</sup> aneurysmal mouse aortas was quantitated as the number of CD31-positive neovessels per ACS. Data are mean ± standard deviation. Student's *t* tests, no significant difference between two groups.

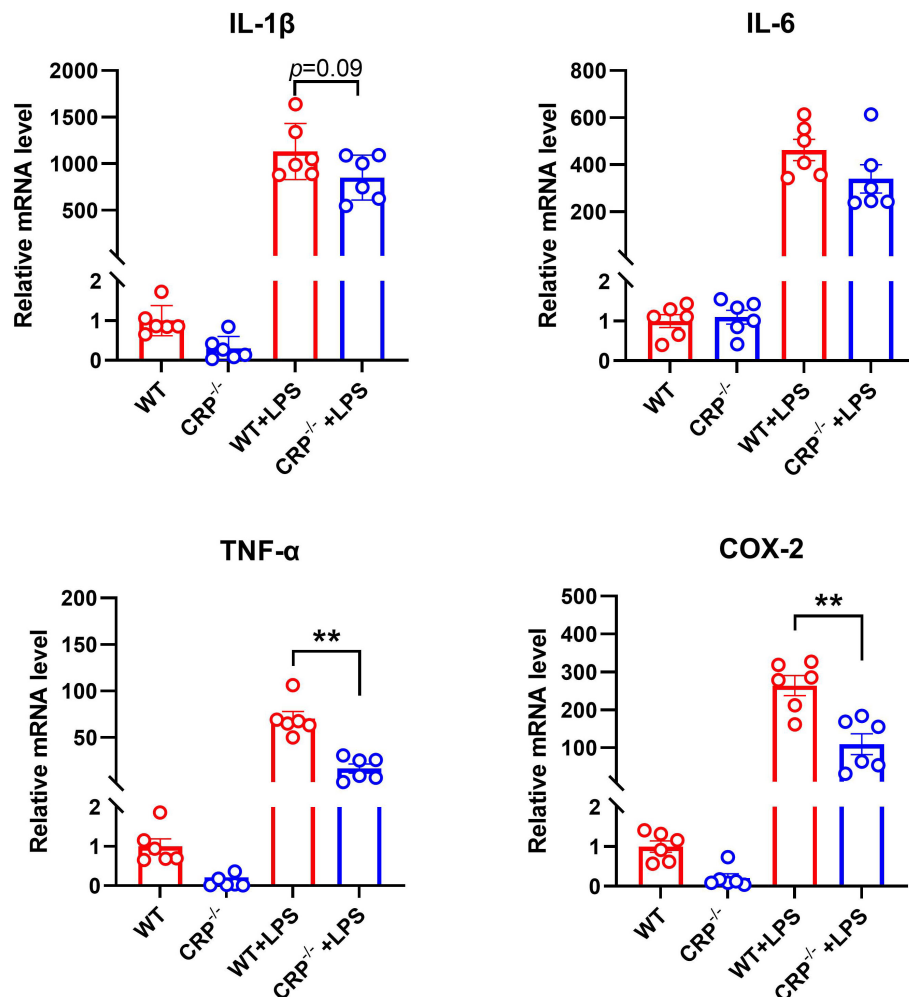


FIGURE 6

CRP deficiency impairs classic proinflammatory macrophage activation/polarization. Peritoneal macrophages from non-aneurysmal wild type (WT) and CRP<sup>-/-</sup> mice underwent the classic activation (conventionally known as M1 macrophages) in the presence of LPS (50 ng/ml) or vehicle alone for 6 hours. The mRNA expression levels of indicated classic activation macrophage marker genes were detected by using qRT-PCR. mRNA levels are presented as mean  $\pm$  standard deviation fold changes relative to vehicle-treated WT macrophages. Two-way ANOVA followed two group comparison, \*\* $p < 0.01$  between two groups,  $n = 6$  biological repeats for each group.

macrophages may attenuate the expression of proaneurysmal mediators including cytokines and MMPs consequently leading to experimental AAA inhibition.

We found that CRP expression was elevated in experimental AAA lesion. While we have no data showing the source for increased CRP, this may result from locally and/or systemically increased CRP as reported in other pathological condition (51, 52). Macrophages have been reported to be the main cellular source for non-liver derived CRP (53). CRP interacts with macrophage Fc $\gamma$ R1/2 or lectin-like oxidized LDL receptor 1 (LOX-1) and bind to Oxidized low-density lipoprotein (Ox-LDL), thus regulating macrophage functional activity through multiple pathways and mediating vascular inflammatory diseases (10, 54–57). Alternatively, the interaction of CRP with LOX-1 and Ox-LDL also enhances CRP expression in endothelial cells, which further promote vascular inflammation (58). Therefore, the potential modulation of macrophage activity by CRP may partially

contribute to experimental AAA pathogenesis in the PPE AAA model.

Although the loss of endogenous CRP reduced experimental AAAs, the inhibition was not strong as demonstrated for other agents including metformin (59–61). Therefore, we need more experimental evidence to validate whether CRP can be a therapeutic target for AAA disease. In summary, this study demonstrates a partial role of CRP in experimental AAA pathogenesis of AAAs using CRP deficient mice.

## Data availability statement

The data presented in the study are included in the article/Supplementary Material. Further inquiries can be directed to the corresponding author.



## Ethics statement

The animal study was approved by Laboratory Animal Management Committee of Xi'an Jiaotong University. The study was conducted in accordance with the local legislation and institutional requirements.

## Author contributions

SZ, YW, EL, and BX designed this study; YF, HL, KL, SZ, JD, PW, ML, HW, XH, HH, RW, LB, WW, and YL collected and analyzed data, as well as drafted the manuscript; YF, HL, KL, PW, ML, HW, XH, and HH performed experiments; YW, NA, BX, and SZ critically revised manuscript. All authors contributed to the article and approved the submitted version.

## Funding

This work was partly supported by the Natural Science Project of Shaanxi Province (2023-CX-PT-17 to SZ, 2022PT-41 to CX), Natural Science Project of Xi'an Jiaotong University (YXJLRH2022073 to SZ and JD) and Project of Key Laboratory of Medical Large Animal Models of Guangdong Province (Klmlam 202204 to SZ).

## References

1. Sakalihasan N, Michel JB, Katsargyris A, Kuivaniemi H, Defraigne JO, Nchimi A, et al. Abdominal aortic aneurysms. *Nat Rev Dis Primers* (2018) 4(1):34. doi: 10.1038/s41572-018-0030-7
2. Sampson UK, Norman PE, Fowkes FG, Aboyans V, Yanna S, Harrell FE Jr., et al. Global and regional burden of aortic dissection and aneurysms: Mortality trends in 21 world regions, 1990 to 2010. *Glob Heart* (2014) 9(1):171–80. doi: 10.1016/j.jheart.2013.12.010
3. Singh K, Bonaa KH, Jacobsen BK, Bjork L, Solberg S. Prevalence of and risk factors for abdominal aortic aneurysms in a population-based study: The tromso study. *Am J Epidemiol* (2001) 154(3):236–44. doi: 10.1093/aje/154.3.236
4. Jagadeesham VP, Scott DJ, Carding SR. Abdominal aortic aneurysms: An autoimmune disease? *Trends Mol Med* (2008) 14(12):522–9. doi: 10.1016/j.molmed.2008.09.008
5. Pepys MB, Hirschfield GM. C-reactive protein: A critical update. *J Clin Invest* (2003) 111(12):1805–12. doi: 10.1172/JCI18921
6. Shine B, de Beer FC, Pepys MB. Solid phase radioimmunoassays for human C-reactive protein. *Clin Chim Acta* (1981) 117(1):13–23. doi: 10.1016/0009-8981(81)90005-x
7. Bottazzi B, Doni A, Garlanda C, Mantovani A. An integrated view of humoral innate immunity: Pentraxins as a paradigm. *Annu Rev Immunol* (2010) 28:157–83. doi: 10.1146/annurev-immunol-030409-101305
8. Sproston NR, Ashworth JJ. Role of C-reactive protein at sites of inflammation and infection. *Front Immunol* (2018) 9:754. doi: 10.3389/fimmu.2018.00754
9. Thompson D, Pepys MB, Wood SP. The physiological structure of human C-reactive protein and its complex with phosphocholine. *Structure* (1999) 7(2):169–77. doi: 10.1016/S0969-2126(99)80023-9
10. Marnell LL, Mold C, Volzer MA, Burlingame RW, Du Clos TW. C-reactive protein binds to fc gamma ri in transfected cos cells. *J Immunol* (1995) 155(4):2185–93. doi: 10.4049/jimmunol.155.4.2185
11. Devaraj S, Yun JM, Duncan-Staley C, Jialal I. C-reactive protein induces M-CSF release and macrophage proliferation. *J Leukoc Biol* (2009) 85(2):262–7. doi: 10.1189/jlb.0808458
12. Cai SY, Nie L, Chen J. C-reactive protein/serum amyloid P promotes pro-inflammatory function and induces M1-type polarization of monocytes/macrophages in mudskipper, *Boleophthalmus pectinirostris*. *Fish Shellfish Immunol* (2019) 94:318–26. doi: 10.1016/j.fsi.2019.09.021
13. Zhang L, Liu SH, Wright TT, Shen ZY, Li HY, Zhu W, et al. C-reactive protein directly suppresses th1 cell differentiation and alleviates experimental autoimmune encephalomyelitis. *J Immunol* (2015) 194(11):5243–52. doi: 10.4049/jimmunol.1402909
14. Kim Y, Ryu J, Ryu MS, Lim S, Han KO, Lim IK, et al. C-reactive protein induces G2/M phase cell cycle arrest and apoptosis in monocytes through the upregulation of B-cell translocation gene 2 expression. *FEBS Lett* (2014) 588(4):625–31. doi: 10.1016/j.febslet.2014.01.008
15. Whisler RL, Newhouse YG, Mortensen RF. C-reactive protein- (Crp) mediated modulation of human B cell colony development. *J Immunol* (1983) 130(1):248–53. doi: 10.4049/jimmunol.130.1.248
16. Shangwei Z, Yingqi W, Jiang X, Zhongyin W, Juan J, Dafang C, et al. Serum high-sensitive C-reactive protein level and crp genetic polymorphisms are associated with abdominal aortic aneurysm. *Ann Vasc Surg* (2017) 45:186–92. doi: 10.1016/j.avsg.2017.05.024
17. Stather PW, Sidloff DA, Dattani N, Gokani VJ, Choke E, Sayers RD, et al. Meta-analysis and meta-regression analysis of biomarkers for abdominal aortic aneurysm. *Br J Surg* (2014) 101(11):1358–72. doi: 10.1002/bjs.9593
18. Cersit S, Ocal L, Keskin M, Gursay MO, Kalcik M, Bayam E, et al. Association of C-reactive protein-to-albumin ratio with the presence and progression of abdominal aortic aneurysm. *Angiology* (2021) 72(2):153–8. doi: 10.1177/0003319720954084
19. Qin Y, Yang Y, Liu R, Cao X, Liu O, Liu J, et al. Combined cathepsin S and hs-crp predicting inflammation of abdominal aortic aneurysm. *Clin Biochem* (2013) 46(12):1026–9. doi: 10.1016/j.clinbiochem.2013.05.065
20. Badger SA, Soong CV, O'Donnell ME, Mercer C, Young IS, Hughes AE. C-reactive protein (Crp) elevation in patients with abdominal aortic aneurysm is independent of the most important crp genetic polymorphism. *J Vasc Surg* (2009) 49(1):178–84. doi: 10.1016/j.jvs.2008.07.081

## Conflict of interest

The authors declare that the research was conducted in the absence of any commercial or financial relationships that could be construed as a potential conflict of interest.

## Publisher's note

All claims expressed in this article are solely those of the authors and do not necessarily represent those of their affiliated organizations, or those of the publisher, the editors and the reviewers. Any product that may be evaluated in this article, or claim that may be made by its manufacturer, is not guaranteed or endorsed by the publisher.

## Supplementary material

The Supplementary Material for this article can be found online at: <https://www.frontiersin.org/articles/10.3389/fimmu.2023.1233807/full#supplementary-material>

### SUPPLEMENTARY FIGURE 1

The effect of CRP deficiency in IL-4 induced M2 polarization in cultured macrophages. Peritoneal macrophages from non- WT and CRP<sup>-/-</sup> mice underwent the alternative activation (conventionally known as M2 polarization) in the presence of IL-4 (10 ng/ml) or vehicle alone. The mRNA expression levels of indicated M2 macrophage marker genes were measured by using qRT-PCR. Two-way ANOVA followed two group comparison, no significant influence of CRP deficiency on either M2 maker mRNA levels, n=3 biological repeats for each group.

21. Kim EN, Yu J, Lim JS, Jeong H, Kim CJ, Choi JS, et al. Crp immunodeposition and proteomic analysis in abdominal aortic aneurysm. *PLoS One* (2021) 16(8): e0245361. doi: 10.1371/journal.pone.0245361
22. De Haro J, Bleda S, Acin F. C-reactive protein predicts aortic aneurysmal disease progression after endovascular repair. *Int J Cardiol* (2016) 202:701–6. doi: 10.1016/j.ijcard.2015.09.122
23. Astrom Malm I, De Basso R, Blomstrand P, Wagsater D. Association of il-10 and crp with pulse wave velocity in patients with abdominal aortic aneurysm. *J Clin Med* (2022) 11(5):1182. doi: 10.3390/jcm11051182
24. Li HY, Tang ZM, Wang Z, Lv JM, Liu XL, Liang YL, et al. C-reactive protein protects against acetaminophen-induced liver injury by preventing complement overactivation. *Cell Mol Gastroenterol Hepatol* (2022) 13(1):289–307. doi: 10.1016/j.jcmgh.2021.09.003
25. Chen J, Luo H, Tao M, Liu Z, Wang G. Quantitation of nucleoprotein complexes by uv absorbance and bradford assay. *Biophys Rep* (2021) 7(6):429–36. doi: 10.52601/bpr.2021.210028
26. Liu H, Tian K, Xia C, Wei P, Xu B, Fu W, et al. Kunming mouse strain is less susceptible to elastase-induced abdominal aortic aneurysms. *Anim Model Exp Med* (2022) 5(1):72–80. doi: 10.1002/ame2.12197
27. Fu W, Liu H, Wei P, Xia C, Yu Q, Tian K, et al. Genetic deficiency of protein inhibitor of activated stat3 suppresses experimental abdominal aortic aneurysms. *Front Cardiovasc Med* (2023) 10:1092555. doi: 10.3389/fcvm.2023.1092555
28. Liu H, Wei P, Fu W, Xia C, Li Y, Tian K, et al. Dapagliflozin ameliorates the formation and progression of experimental abdominal aortic aneurysms by reducing aortic inflammation in mice. *Oxid Med Cell Longev* (2022) 2022:8502059. doi: 10.1155/2022/8502059
29. Tian K, Xia C, Liu H, Xu B, Wei P, Fu W, et al. Temporal and quantitative analysis of aortic immunopathologies in elastase-induced mouse abdominal aortic aneurysms. *J Immunol Res* (2021) 2021:6297332. doi: 10.1155/2021/6297332
30. Ikezoe T, Shoji T, Guo J, Shen F, Lu HS, Daugherty A, et al. No effect of hypercholesterolemia on elastase-induced experimental abdominal aortic aneurysm progression. *Biomolecules* (2021) 11(10):1434. doi: 10.3390/biom11101434
31. Xu B, Iida Y, Glover KJ, Ge Y, Wang Y, Xuan H, et al. Inhibition of vegf (Vascular endothelial growth factor)-a or its receptor activity suppresses experimental aneurysm progression in the aortic elastase infusion model. *Arterioscler Thromb Vasc Biol* (2019) 39(8):1652–66. doi: 10.1161/ATVBAHA.119.312497
32. Tanaka H, Xu B, Xuan H, Ge Y, Wang Y, Li Y, et al. Recombinant interleukin-19 suppresses the formation and progression of experimental abdominal aortic aneurysms. *J Am Heart Assoc* (2021) 10(17):e022207. doi: 10.1161/JAHA.121.022207
33. Raffort J, Lareyre F, Clement M, Hassen-Khodja R, Chinetti G, Mallat Z. Monocytes and macrophages in abdominal aortic aneurysm. *Nat Rev Cardiol* (2017) 14(8):457–71. doi: 10.1038/nrcardio.2017.52
34. Longo GM, Xiong W, Greiner TC, Zhao Y, Fiotti N, Baxter BT. Matrix metalloproteinases 2 and 9 work in concert to produce aortic aneurysms. *J Clin Invest* (2002) 110(5):625–32. doi: 10.1172/JCI15334
35. Lukasiewicz A, Reszec J, Kowalewski R, Chyczewski L, Lebkowska U. Assessment of inflammatory infiltration and angiogenesis in the thrombus and the wall of abdominal aortic aneurysms on the basis of histological parameters and computed tomography angiography study. *Folia Histochem Cytobiol* (2012) 50(4):547–53. doi: 10.5603/20323
36. Thompson MM, Jones L, Nasim A, Sayers RD, Bell PR. Angiogenesis in abdominal aortic aneurysms. *Eur J Vasc Endovasc Surg* (1996) 11(4):464–9. doi: 10.1016/s1078-5884(96)80183-3
37. Song H, Yang Y, Sun Y, Wei G, Zheng H, Chen Y, et al. Circular rna cdy1 promotes abdominal aortic aneurysm formation by inducing M1 macrophage polarization and M1-type inflammation. *Mol Ther* (2022) 30(2):915–31. doi: 10.1016/j.ymthe.2021.09.017
38. Shi J, Guo J, Li Z, Xu B, Miyata M. Importance of nlrp3 inflammasome in abdominal aortic aneurysms. *J Atheroscler Thromb* (2021) 28(5):454–66. doi: 10.5551/jat.RV17048
39. Fu Y, Wu Y, Liu E. C-reactive protein and cardiovascular disease: From animal studies to the clinic (Review). *Exp Ther Med* (2020) 20(2):1211–9. doi: 10.3892/etm.2020.8840
40. Ji SR, Zhang SH, Chang Y, Li HY, Wang MY, Lv JM, et al. C-reactive protein: The most familiar stranger. *J Immunol* (2023) 210(6):699–707. doi: 10.4049/jimmunol.2200831
41. Razavi E, Ramezani A, Kazemi A, Attar A. Effect of treatment with colchicine after acute coronary syndrome on major cardiovascular events: A systematic review and meta-analysis of clinical trials. *Cardiovasc Ther* (2022) 2022:8317011. doi: 10.1155/2022/8317011
42. Agrawal A, Cha-Molstad H, Samols D, Kushner I. Overexpressed nuclear factor-kappa b can participate in endogenous C-reactive protein induction, and enhances the effects of C/ebp beta and signal transducer and activator of transcription-3. *Immunology* (2003) 108(4):539–47. doi: 10.1046/j.1365-2567.2003.01608.x
43. Romero-Vazquez S, Adan A, Figueras-Roca M, Llorenç V, Slevin M, Vilahur G, et al. Activation of C-reactive protein proinflammatory phenotype in the blood retinal barrier *in vitro*: Implications for age-related macular degeneration. *Aging (Albany NY)* (2020) 12(14):13905–23. doi: 10.18632/aging.103655
44. Slevin M, Garcia-Lara E, Capitanescu B, Sanfeliu C, Zeinolabediny Y, AlBaradie R, et al. Monomeric C-reactive protein aggravates secondary degeneration after intracerebral haemorrhagic stroke and may function as a sensor for systemic inflammation. *J Clin Med* (2020) 9(9):3053. doi: 10.3390/jcm9093053
45. Ruiz-Fernandez C, Gonzalez-Rodriguez M, Francisco V, Rajab IM, Gomez R, Conde J, et al. Monomeric C reactive protein (Mcrp) regulates inflammatory responses in human and mouse chondrocytes. *Lab Invest* (2021) 101(12):1550–60. doi: 10.1038/s41374-021-00584-8
46. Kaplan M, Shur A, Tendler Y. M1 macrophages but not M2 macrophages are characterized by upregulation of crp expression via activation of nf-kappa b: A possible role for ox-ldl in macrophage polarization. *Inflammation* (2018) 41(4):1477–87. doi: 10.1007/s10753-018-0793-8
47. Devaraj S, Jialal I. C-reactive protein polarizes human macrophages to an M1 phenotype and inhibits transformation to the M2 phenotype. *Arterioscler Thromb Vasc Biol* (2011) 31(6):1397–402. doi: 10.1161/ATVBAHA.111.225508
48. Bonaventura A, Mach F, Roth A, Lenglet S, Burger F, Brandt KJ, et al. Intraplaque expression of C-reactive protein predicts cardiovascular events in patients with severe atherosclerotic carotid artery stenosis. *Mediators Inflammation* (2016) 2016:9153673. doi: 10.1155/2016/9153673
49. Yang X, Hu W, Zhang Q, Wang Y, Sun L. Puerarin inhibits C-reactive protein expression via suppression of nuclear factor kappa b activation in lipopolysaccharide-induced peripheral blood mononuclear cells of patients with stable angina pectoris. *Basic Clin Pharmacol Toxicol* (2010) 107(2):637–42. doi: 10.1111/j.1742-7843.2010.00548.x
50. Voleti B, Agrawal A. Regulation of basal and induced expression of C-reactive protein through an overlapping element for oct-1 and nf-kappa b on the proximal promoter. *J Immunol* (2005) 175(5):3386–90. doi: 10.4049/jimmunol.175.5.3386
51. Jabs WJ, Theissing E, Nitschke M, Bechtel JF, Duchrow M, Mohamed S, et al. Local generation of C-reactive protein in diseased coronary artery venous bypass grafts and normal vascular tissue. *Circulation* (2003) 108(12):1428–31. doi: 10.1161/01.CIR.0000092184.43176.91
52. Torzewski J, Torzewski M, Bowyer DE, Frohlich M, Koenig W, Waltenberger J, et al. C-reactive protein frequently colocalizes with the terminal complement complex in the intima of early atherosclerotic lesions of human coronary arteries. *Arterioscler Thromb Vasc Biol* (1998) 18(9):1386–92. doi: 10.1161/01.atv.18.9.1386
53. Ciubotaru I, Potempa LA, Wander RC. Production of modified C-reactive protein in U937-derived macrophages. *Exp Biol Med* (Maywood) (2005) 230(10):762–70. doi: 10.1177/153537020523001010
54. Meuwissen M, van der Wal AC, Niessen HW, Koch KT, de Winter RJ, van der Loos CM, et al. Colocalisation of intraplaque C reactive protein, complement, oxidised low density lipoprotein, and macrophages in stable and unstable angina and acute myocardial infarction. *J Clin Pathol* (2006) 59(2):196–201. doi: 10.1136/jcp.2005.027235
55. Bharadwaj D, Stein MP, Volzer M, Mold C, Du Clos TW. The major receptor for C-reactive protein on leukocytes is fc gamma receptor ii. *J Exp Med* (1999) 190(4):585–90. doi: 10.1084/jem.190.4.585
56. Fujita Y, Kakino A, Harada-Shiba M, Sato Y, Otsui K, Yoshimoto R, et al. C-reactive protein uptake by macrophage cell line via class-a scavenger receptor. *Clin Chem* (2010) 56(3):478–81. doi: 10.1373/clinchem.2009.140202
57. Bournazos S, Gupta A, Ravetch JV. The role of igg fc receptors in antibody-dependent enhancement. *Nat Rev Immunol* (2020) 20(10):633–43. doi: 10.1038/s41577-020-00410-0
58. Stancel N, Chen CC, Ke LY, Chu CS, Lu J, Sawamura T, et al. Interplay between crp, atherogenic ldl, and lox-1 and its potential role in the pathogenesis of atherosclerosis. *Clin Chem* (2016) 62(2):320–7. doi: 10.1373/clinchem.2015.243923
59. Itoga NK, Rothenberg KA, Suarez P, Ho TV, Mell MW, Xu B, et al. Metformin prescription status and abdominal aortic aneurysm disease progression in the U.S. Veteran population. *J Vasc Surg* (2019) 69(3):710–6 e3. doi: 10.1016/j.jvs.2018.06.194
60. Fujimura N, Xiong J, Kettler EB, Xuan H, Glover KJ, Mell MW, et al. Metformin treatment status and abdominal aortic aneurysm disease progression. *J Vasc Surg* (2016) 64(1):46–54 e8. doi: 10.1016/j.jvs.2016.02.020
61. Xu B, Li G, Li Y, Deng H, Cabot A, Guo J, et al. Mechanisms and efficacy of metformin-mediated suppression of established experimental abdominal aortic aneurysms. *JVS Vasc Sci* (2023) 4:100102. doi: 10.1016/j.jvssci.2023.100102





## OPEN ACCESS

## EDITED BY

Yi Wu,  
Xi'an Jiaotong University, China

## REVIEWED BY

Hong Lei,  
The Affiliated Children's Hospital of Xi'an  
Jiaotong University, China  
Naeem Ullah,  
Chulalongkorn University, Thailand

## \*CORRESPONDENCE

Maria Ballester  
✉ maria.ballester@irta.cat

RECEIVED 30 June 2023

ACCEPTED 28 August 2023

PUBLISHED 14 September 2023

## CITATION

Hernández-Banqué C,  
Jové-Juncà T, Crespo-Piazuelo D,  
González-Rodríguez O, Ramayo-Caldas Y,  
Esteve-Codina A, Mercat M-J, Bink MCAM,  
Quintanilla R and Ballester M (2023)  
Mutations on a conserved distal enhancer  
in the porcine C-reactive protein gene  
impair its expression in liver.  
*Front. Immunol.* 14:1250942.  
doi: 10.3389/fimmu.2023.1250942

## COPYRIGHT

© 2023 Hernández-Banqué, Jové-Juncà,  
Crespo-Piazuelo, González-Rodríguez,  
Ramayo-Caldas, Esteve-Codina, Mercat,  
Bink, Quintanilla and Ballester. This is an  
open-access article distributed under the  
terms of the [Creative Commons Attribution  
License \(CC BY\)](#). The use, distribution or  
reproduction in other forums is permitted,  
provided the original author(s) and the  
copyright owner(s) are credited and that  
the original publication in this journal is  
cited, in accordance with accepted  
academic practice. No use, distribution or  
reproduction is permitted which does not  
comply with these terms.

# Mutations on a conserved distal enhancer in the porcine C-reactive protein gene impair its expression in liver

Carles Hernández-Banqué<sup>1</sup>, Teodor Jové-Juncà<sup>1</sup>,  
Daniel Crespo-Piazuelo<sup>1</sup>, Olga González-Rodríguez<sup>1</sup>,  
Yuliaxis Ramayo-Caldas<sup>1</sup>, Anna Esteve-Codina<sup>2,3</sup>,  
Marie-José Mercat<sup>4</sup>, Marco C. A. M. Bink<sup>5</sup>, Raquel Quintanilla<sup>1</sup>  
and Maria Ballester<sup>1\*</sup>

<sup>1</sup>Animal Breeding and Genetics Program, Institute of Agrifood Research and Technology (IRTA), Caldes de Montbui, Spain, <sup>2</sup>CNAG-CRG, Centre for Genomic Regulation (CRG), Barcelona Institute of Science and Technology (BIST), Barcelona, Spain, <sup>3</sup>Universitat Pompeu Fabra (UPF), Barcelona, Spain, <sup>4</sup>IFIP-Institut Du Porc and Alliance R&D, Le Rheu, France, <sup>5</sup>Hendrix Genetics Research, Technology & Services B.V., Boxmeer, Netherlands

C-reactive protein (CRP) is an evolutionary highly conserved protein. Like humans, CRP acts as a major acute phase protein in pigs. While *CRP* regulatory mechanisms have been extensively studied in humans, little is known about the molecular mechanisms that control pig *CRP* gene expression. The main goal of the present work was to study the regulatory mechanisms and identify functional genetic variants regulating *CRP* gene expression and CRP blood levels in pigs. The characterization of the porcine *CRP* proximal promoter region revealed a high level of conservation with both cow and human promoters, sharing binding sites for transcription factors required for *CRP* expression. Through genome-wide association studies and fine mapping, the most associated variants with both mRNA and protein CRP levels were localized in a genomic region 39.3 kb upstream of *CRP*. Further study of the region revealed a highly conserved putative enhancer that contains binding sites for several transcriptional regulators such as STAT3, NF-κB or C/EBP-β. Luciferase reporter assays showed the necessity of this enhancer-promoter interaction for the acute phase induction of *CRP* expression in liver, where differences in the enhancer sequences significantly modified *CRP* activity. The associated polymorphisms disrupted the putative binding sites for HNF4α and FOXA2 transcription factors. The high correlation between *HNF4α* and *CRP* expression levels suggest the participation of HNF4α in the regulatory mechanism of porcine *CRP* expression through the modification of its binding site in liver. Our findings determine, for the first time, the relevance of a distal regulatory element essential for the acute phase induction of porcine *CRP* in liver and identify functional polymorphisms that can be included in pig breeding programs to improve immunocompetence.

## KEYWORDS

C-reactive protein, fine-mapping, luciferase assays, enhancer, pig, RNA-seq

## 1 Introduction

The C-reactive Protein (CRP) is an evolutionary well-conserved protein that plays a significant role in the acute phase response to inflammation. This protein belongs to the pentraxins family and has two conformations: native CRP (nCRP) and monomeric CRP (mCRP). Although this protein is mainly produced by hepatocytes, it is also synthesized, in marginal concentrations, in neurons, monocytes, lymphocytes and adipocytes (1).

Depending on the conformation present in any given stage of the inflammatory process, CRP serves as a pro-inflammatory molecule through the activation of the initial stages of the complement system and the modulation of nitric oxide release and cytokine synthesis. Moreover, CRP functions as an anti-inflammatory compound by controlling the progression and intensity of the late stages of inflammation and modulating apoptosis and phagocytosis processes (2–5). CRP protein levels are currently being used as a stable marker in humans for the prediction, prevention and prognosis of cardiovascular disease as well as several other chronic diseases (6–8).

There is sufficient evidence that CRP blood levels are a complex phenotype with several environmental and genetic determinants. External factors such as the weight or the overall stress levels of individuals may potentially modulate the levels of this protein (9, 10). At genetic level, several studies in humans have determined the impact of polymorphisms in *CRP* and in other inflammatory-related genes on CRP blood levels (11–13). In pigs, a genome wide association study (GWAS) in a commercial Duroc population identified the genomic region in which *CRP* is annotated as associated with the variation in its translated protein levels (14). Furthermore, according to several studies, a variety of transcription factors affect the expression of this gene, highlighting the need to further study the interaction and effects of *CRP* regulatory pathways (15–19). While HNF-1, HNF-3, and OCT-1 transcription factors are involved in the regulation of basal *CRP* expression levels (20–22), the induction of the acute phase expression of *CRP* is mediated by the effect of cytokines, particularly IL-6, IL-1 $\beta$  and TNF- $\alpha$ , through the activation of STAT3, NF- $\kappa$ B and C/EBP- $\beta$  transcription factors (16, 19, 23–25). In this regard, a recent study in human Hep3B cells identified an enhancer upstream of the *CRP* promoter enriched in binding sites for STAT3 and C/EBP- $\beta$  with a major impact on the acute phase induction of *CRP* expression (26).

Considering the high resemblance between pig and human immune responses, understanding the molecular mechanisms that control porcine *CRP* gene expression may further support the use of the pig as a biomedical animal model for the study of human diseases. In other vein, genetic selection for immunity traits in livestock has been proposed as a promising approach for improving animal robustness and disease resistance, thus contributing to healthier livestock while reducing the emergence of antibiotic resistances (27–30).

The present work aimed to study the regulatory mechanisms affecting the expression of porcine *CRP* and identify causal genetic variants that influence CRP levels in blood to better understand the genomic physiology of immunocompetence in pigs.

## 2 Methods

### 2.1 Ethics

All experimental protocols and procedures with pigs were approved by the Institut de Recerca i Tecnologia Agroalimentàries (IRTA) Ethical Committee in accordance with the Spanish Policy for Animal Protection RD53/2013, which meets the European Union Directive 2010/63/EU for the correct practices and protection of the animals used in experimentation.

### 2.2 Animal material and phenotypic parameters

The study was performed with a population of 432 healthy piglets (217 males and 215 females of around 60 days of age) belonging to a commercial Duroc pig line. The pigs came from six batches ( $72 \pm 1$  animals per batch) and were raised in the same farm with an *ad libitum* cereal-base commercial diet. At the moment of sampling, the animals did not present any sign of infection or pathology, and no antibiotics were supplied.

Blood was collected via the external jugular vein into vacutainer tubes with or without anticoagulants (Sangüesa S.A., Spain), which required the restraint of the animals but not their sedation. Serum samples, in duplicate, diluted 1:3000 were used to measure CRP levels by ELISA kit (Abcam Plc., Spain) following manufacturer's instructions. Absorbance was read at 450 nm using an ELISA plate reader (Bio-Rad) and analysed using the Microplate manager 5.2.1 software (Bio-Rad). Genomic DNA was extracted from blood samples using the NucleoSpin Blood (Macherey–Nagel, Germany). DNA concentration and purity were measured in a Nanodrop ND-1000 spectrophotometer.

### 2.3 SNP genotyping

The 432 animals of the Duroc population were genotyped with the GGP Porcine HD Array (Illumina, San Diego, CA) using the Infinium HD Assay Ultra protocol. The software PLINK/v1.90b3.42 (31) was used to remove those single-nucleotide polymorphisms (SNPs) with a minor allele frequency (MAF) lower than 5%, SNPs with more than 10% missing genotypes, and SNPs that did not map to the porcine reference genome (Sscrofa11.1). A subset of 42,641 SNPs remained for further analysis. Additionally, the rs327446000 SNP within the *CRP* gene was genotyped for the 432 animals by custom designed Taqman assays in a QuantStudio™ 12K Flex Real-Time PCR System (ThermoFisher Scientific).

### 2.4 Whole genome and RNA sequencing data

Whole-genome sequences from 300 pigs (n=100 Landrace, n=100 Large White, and n=100 Duroc) (32) were used to identify

and estimate the segregation of CRP polymorphisms. All DNA samples were sequenced (NovaSeq6000 platform) to a minimum read depth of 10X. DNA sequences were mapped against the reference genome (*Sscrofa11.1* assembly) with BWA-MEM/0.7.17 (33) and 44,127,400 polymorphisms (SNPs and indels) were extracted using the GATK/4.1.8.0 Haplotype Caller (34). After filtering genetic variants with PLINK/v1.90b3.42 software a total of 25,315,878 polymorphisms remained for downstream analysis. Furthermore, the expression levels of CRP isoforms in the liver were quantified in RNA-seq data from the same 300 pigs (32). RNA-seq reads were mapped against the reference genome (*Sscrofa11.1* assembly) with STAR/v2.5.3a (35) using ENCODE parameters. Annotated genes and isoforms in Ensembl Genes 101 database were quantified with RSEM/1.3.0 (36) using default parameters.

## 2.5 Identification of polymorphisms in the CRP gene and comparative promoter analysis

SNPs and indels within and in the vicinity of the CRP (between positions 90.7–90.8 Mb on SSC4) were extracted from whole genome sequencing (WGS) data. VEP software (37) was used to locate and predict the consequences of variants on the CRP protein sequence using the Ensembl Genes 106 annotation database and the *Sscrofa11.1* assembly. The promoter regions of the porcine CRP isoforms were aligned to the reference human and cow orthologue promoter sequences annotated in the Ensembl database with the Multalin software (38) in order to measure the level of conservation between them.

A computer-assisted identification of putative transcription factors binding sites in CRP regulatory regions (enhancer and proximal promoter) was performed with LASAGNA-Search 2.0 (39).

## 2.6 Polymorphism association analysis

The association between polymorphisms identified in both the regulatory and coding regions of CRP and CRP blood levels (n=100 Duroc individuals) was analyzed by using the *aov()* function in R. Normality of CRP data was checked through Shapiro-Wilk test in R, and logarithm transformation was applied to reach normal distribution of residuals ( $P$ -value > 0.05). Systematic non-genetic putative effects (sex and batch) were tested by using the *lm()* function in R. When significant, sex and/or batch effects were considered for subsequent analyses. Multiple testing corrections were performed with the false discovery rate (FDR) method using the *p.adjust* function in R (40). Significance threshold for the association was set at  $FDR \leq 0.05$ .

## 2.7 Genome wide association study

GWAS was performed using 42,641 SNPs, together with the rs327446000 CRP SNP, and the CRP levels in serum of 432 Duroc

animals using the GCTA 1.94.1 software (41) with the following model:

$$(1) \quad y_{ij} = b_j + u_i + s_{li}a_l + e_{ij}$$

Where  $y_{ij}$  corresponds to the phenotype (log transformed CRP levels in serum) of the  $i^{\text{th}}$  individual in the  $j^{\text{th}}$  batch;  $b_j$  corresponds to the  $j^{\text{th}}$  batch effect (6 levels);  $u_i$  is the infinitesimal genetic effect of individual  $i$ , with  $u \sim N(0, G^2_u)$ , where  $G$  is the genomic relationship matrix (GRM) calculated using the filtered autosomal SNPs based on the methodology of (42) and  $\sigma^2_u$  is the additive genetic variance;  $s_{li}$  is the genotype (coded as 0, 1, 2) for the  $l^{\text{th}}$  SNP, being  $a_l$  its allele substitution effect on the trait under study; and  $e_{ij}$  is the residual term.

The false discovery rate (FDR) method of multiple testing described by Benjamini and Hochberg (40) was used to measure the statistical significance for association studies at genome-wide level with the *p.adjust* function of R. The significant association threshold was set at  $FDR \leq 0.05$ . A Manhattan plot based on the resulting significance was generated using the R package qqman (43).

## 2.8 Chromosome 4 association and fine mapping

WGS data from 100 individuals of the same Duroc population was used to impute genotypes at the whole genome level of the 354 individuals (332 piglets and 22 boars) that had been previously genotyped with the GGP Porcine HD Array.

Imputation and haplotype reconstruction was performed with 19,610 SNPs ( $MAF \geq 5\%$ ), covering the SSC4:88,251,177–92,759,955 bp genomic region, using DualPHASE/v2.3 software (44). This haplotype-based approach exploits population (linkage disequilibrium; LD) and family information (Mendelian segregation and linkage analysis; LA) through a Hidden Markov model. Linkage was estimated based on the equivalence 1Mb~1cM.

GWAS for the CRP levels in serum and the 19,610 SNPs was performed using the fastGWA option of the GCTA 1.94.1 (41) software, following the previous model (1). QTL fine-mapping was performed with Qxpak/v5 (45) based on the reconstructed haplotypes to simultaneously exploiting LA and LD with the following mixed model:

$$(2) \quad Y = X\beta + Z_h h + Z_u u + e$$

Where  $\beta$  corresponds to the vector containing the batch fixed effect,  $h$  is the vector of random QTL effects corresponding to the  $K$  cluster defined by the Hidden State (HS),  $u$  is the vector of random individual polygenic effects and  $e$  is the vector containing the residuals.

Multiple test correction was performed using the Bonferroni method (46). The significant association threshold was set at  $p_{\text{adjust}} \leq 0.05$ .

## 2.9 Expression GWAS

Expression GWAS (eGWAS) were performed with a total of 25,315,878 genetic variants and the RNA-seq expression data of each CRP isoform in the 300 pigs (n=100 Landrace, n=100 Large

White and n=100 Duroc). The association was estimated by fitting the previously described model (1) using the GCTA software (41):

$$(3) \quad y_{ijk} = \text{sex}_j + \text{breed}_k + u_i + s_{il}a_l + e_{ijk}$$

Where  $y_{ijk}$  corresponds to the gene expression in the  $i^{\text{th}}$  individual of sex  $j$  and belonging to the  $k^{\text{th}}$  breed (3 levels);  $u_i$ ,  $s_{il}$ ,  $a_l$  and  $e_{ijk}$  are as defined in the previous GWAS model. After multiple testing adjustment, association threshold was established at  $\text{FDR} \leq 0.05$ . Manhattan plots were generated in R as previously mentioned.

## 2.10 Luciferase assay

Two individuals of the Duroc population with different haplotypes (Haplotype P1: G – T – C – G – C – T – G – A – C and Haplotype P2: A – A – C – A – T – C – A – G – T) for *CRP* proximal promoter polymorphisms were selected for the cloning process. Genomic DNA was used to amplify two fragments of ~600bp corresponding to *CRP* promoter regions of the selected animals, using the forward primer 5'-GAGGATATCAAGATCGATCAAGCACATGTTTCACTGC-3' and the reverse primer 5'-CCGGATTGCCAAGCTCCCCTTGGAGAAGATGCC-3', containing the *Hind*III and *Bgl*II restriction sites. Amplification of the fragments was performed by PCR with Hot-Star Taq Master Mix Kit (Qiagen, Spain) under the following conditions: 15 min at 94°C, 35 cycles of 1 min at 94°C, 1 min at 60°C and 1 min at 72°C and a final extension of 10 min at 72°C.

PCR products were cloned into pNL1.2[NlucP] vector (Promega, Spain) with the In-Fusion Snap Assembly cloning kit (Takara, Japan). Plasmids were purified using PureYield™ Plasmid Miniprep System kit (Promega, Spain). Enhancer region fragments of ~280bp for the same individuals (Haplotype E1: G – C – T – Ø – A – A – G – C – G and Haplotype E2: A – A – C – TTCTGTTGTGGGACCGGCCC – G – G – A – T – T) were amplified by PCR using the forward primer 5'-GCTCGCTAGCCTCGAGTGGAAGAGAGGGTGGGGTG-3' and the reverse primer 5'-TTGATCGATCTTGATATCGCAGCTACCTCAGAACACAGTC-3', containing the *Xho*I and *Eco*RV restriction sites, with Hot-Star Taq Master Mix Kit (Qiagen, Spain) and the previous conditions, and were inserted upstream of the promoter regions of the corresponding haplotypes. Nucleotide sequence of each DNA construct was confirmed by Sanger sequencing.

HepG2 cells (ATCC, USA) were seeded at a density of  $3 \times 10^4$  cells per well in a 96 wells plate in DMEM supplemented with 10% inactivated fetal bovine serum, 1% penicillin-streptomycin, 1% L-glutamine and 1% pyruvate. After 24h cells were cotransfected with 500ng of pNL1.2[NlucP] vector, 12.5ng of pGL4.54[luc2/TK] and 487.5ng of transfection carrier DNA (Promega, Spain) using ViaFect™ Transfection Reagent (3:1) (Promega, Spain) in serum-free medium for 16h. Cells were then treated with IL-6 (10ng/ml) and IL-1β (1ng/ml). Luciferase activity measurements were performed 24h after stimulation with Dual-Luciferase Reporter Assay System (Promega, Spain). Expression of nanoluc luciferase driven by inserted promoters and enhancers was normalized to the cotransfected firefly control vectors. Every luciferase assay was made by triplicate in different days with three replicates for each vector in each experiment to increase the robustness of the results.

## 3 Results

### 3.1 Comparative study of *CRP* proximal promoter region between human, pig and cow and identification of polymorphisms in the porcine *CRP* gene

Since human *CRP* gene has been proved to be regulated at the transcriptional level by the binding of transcription factors in its promoter region (18, 47), we characterized the pig *CRP* promoter region in order to assess the level of conservation between human and cow species. A highly conserved region in *Sus Scrofa* chromosome 4 (SSC4) at position 90,782,578-90,782,833 bp was identified when compared to the human (GRCh38 1:159,714,589-159,716,089) and cow (ARS-UCD1.2 3:9,982,001-9,983,501) *CRP* promoter regions (Supplementary Figure 1). In addition, we performed an *in-silico* characterization of transcription factor binding sites (TFBSs) in the pig *CRP* promoter region, identifying four TFBSs conserved between pig and cow, four more between pig and human and three binding motifs maintained in all three species (Supplementary Figure 1).

A total of 133 polymorphisms, most of them associated with plasma CRP levels, were identified in the *CRP* gene region in the WGS data from 100 Duroc pigs (Supplementary Table 1). The most significantly associated variant was rs327446000 (4:90,800,879 bp), located in the 3' untranslated region (UTR) of *CRP*. Furthermore, we identified five polymorphisms in the pig *CRP* promoter region affecting the binding sites for C/EBP, FOXA1 and p53 transcription factors (Figure 1).

### 3.2 GWAS for CRP levels in serum and fine mapping revealed associated polymorphisms in the 3'UTR and upstream the promoter region of *CRP*

The association between *CRP* polymorphisms and the variation of serum CRP levels was explored through GWAS with 42,641 SNPs plus the rs327446000 SNP from 432 Duroc pigs. A genomic region in SSC4 at 90.54-90.80 Mb was associated with serum CRP levels, with rs327446000 being the most significantly associated genetic variant (Table 1; Figure 2A).

Further exploration of the *CRP* QTL was performed by both GWAS and LDLA analyses using SSC4 genotypes from 19,610 SNPs comprising 4Mb (2Mb up and 2Mb down) of the previously declared associated genomic region. According to the GWAS results, a total of 1,482 SNPs located within a genomic region in SSC4 at 89.7-91.29 Mb were associated to the phenotype, being the top signal located at 90.80 Mb of SSC4 (rs327446000;  $P$ -value =  $1.49 \times 10^{-10}$ ) inside *CRP* (Figure 2B). In contrast, the LDLA study revealed a total of 483 significant signals which reduced the previous region to 90.53-90.80 Mb and positioned the maximum association at 90.53-90.62 Mb of SSC4 ( $P$ -value =  $1.88 \times 10^{-6}$ ) upstream of *CRP* (Figure 2C).



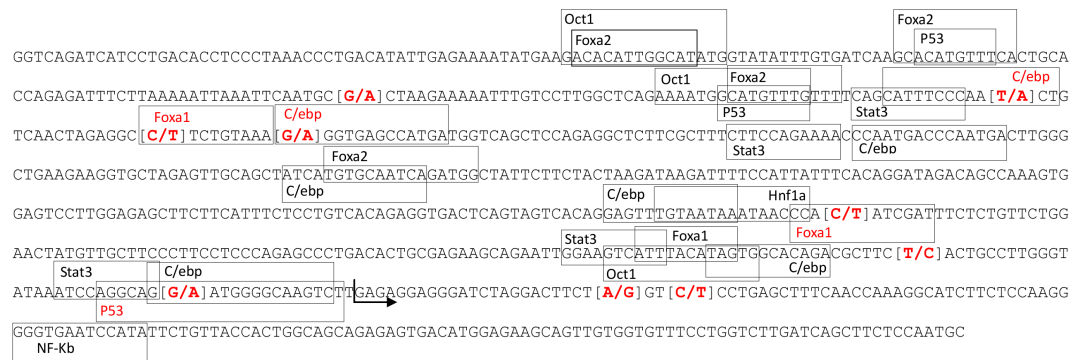


FIGURE 1

Position of the transcription factor binding sites located in the CRP promoter region. Marked in red are the SNPs found in the studied population and the transcription factors binding sites affected by the SNPs. The arrow marks the start of CRP-202 exon 1.

### 3.3 Expression GWAS for CRP isoforms also revealed an associated region upstream of the CRP gene

To identify potential functional variants affecting the expression of CRP, an eGWAS analysis was performed using 25,315,878 genetic variants and the expression of CRP isoforms in 300 pigs (n=100 Landrace, n=100 Large White, and n=100 Duroc).

A strongly associated region in SSC4 at 86-93 Mb for the expression of CRP isoform 202 (ENSSSCT00000054270.2) was identified (Figure 3), whereas not significantly associated regions in SSC4 were identified for the other CRP isoforms. A total of 8,250 polymorphisms were found associated ( $FDR \leq 0.05$ ) along SSC4. The top variants (adjusted  $P$ -value =  $3.40 \times 10^{-23}$ ) were rs793561911 and rs713631040, located in the positions 4:90,743,523 bp and 4:90,743,532 bp respectively, around 39.3 Kb upstream the CRP gene (Table 2; Supplementary Table 2).

### 3.4 Rs793561911 and rs713631040 polymorphisms are located in a conserved enhancer region for CRP

The polymorphisms most significantly associated with CRP-202 isoform expression were located in an intergenic region conserved between several pig breeds and other species such as cow, sheep and horse (Supplementary Figure 2). The alignment of this region in the porcine genome (SSC4:90,743,525-90,743,526) against the human

genome revealed the presence of a human conserved sequence corresponding to an enhancer element (ENSR00000931831). This distal enhancer region was also well conserved in the cow genome (ARS-UCD1.2 3:9,937,919:9,938,698). In the three species, this region was located at 39-44 Kb upstream of CRP. To better understand the regulatory role of this region on CRP-202 expression, an *in-silico* characterization of TFBSs was performed. Remarkably, a total of 26 TFBSs known to regulate CRP expression were found within this region. Eight of them were shared with the cow genome and another site was conserved in both cow and human genomes (Supplementary Figure 3).

In depth analysis of this region revealed that rs793561911 and rs713631040 variants were located within the binding site of the transcription factor HNF4 $\alpha$ . Furthermore, the insertion allele of the rs793561911 polymorphism (-/TTCTGTTTGTGGGACCGGCC) generated a binding site for the FOXA2 transcription factor. Seven other SNPs were found in this conserved region in the studied population (Figure 4). Moreover, a third polymorphism (rs338992142) in the position 4:90,743,570 bp was found to be in the potential binding site of both transcription factors HNF4 $\alpha$  and FOXA2. This SNP was also found to be associated with CRP expression in the eGWAS (Table 2). These three polymorphisms and a fourth significant SNP (rs330141279) located in the position 4:90,743,549 bp were in total linkage disequilibrium resulting the following haplotype combinations: Haplotype E1:  $\emptyset$  - A - A - G and Haplotype E2: TTCTGTTTGTGGGACCGGCC - G - G - A. Figure 4 shows the enhancer regions of animals with haplotypes E1 and E2.

TABLE 1 Significant polymorphisms associated to the CRP levels in serum: position, minimum allele frequency and allele substitution effect significance.

Name	Chr	Bp position	MAF	P-value	FDR
rs327446000	4	90800879	0.148	$1.33 \times 10^{-8}$	0.00056832
rs81233340	4	90535929	0.147	$1.62 \times 10^{-7}$	0.00172178
rs81382318	4	90598142	0.147	$1.62 \times 10^{-7}$	0.00172178
rs80958253	4	90804626	0.217	$1.16 \times 10^{-7}$	0.00172178
rs81285109	4	90736666	0.101	$1.99 \times 10^{-6}$	0.01699241



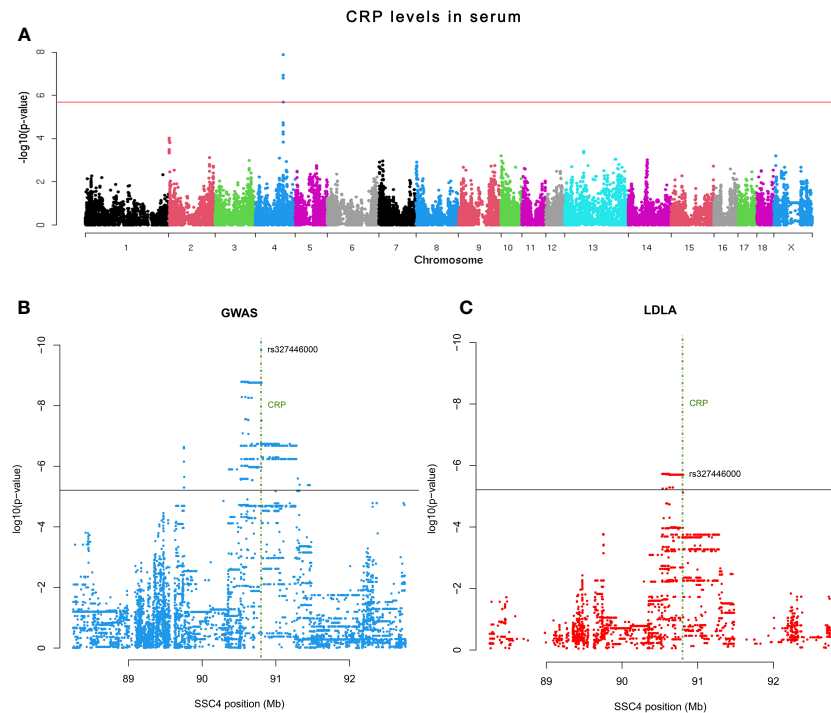


FIGURE 2

(A) Manhattan plot representing the association analysis between the CRP levels in serum and SNPs distributed along the pig chromosomes. (B) Scatter plot depicting P-value distribution of the CRP QTL at chromosome level. (C) Scatter plot depicting P-value distribution of the CRP QTL LDLA. Horizontal lines indicate the adjusted significance threshold ( $\leq 0.05$ ). Vertical green lines encompass the CRP gene location.

rs713631040, with higher correlation levels observed for the AA genotype when compared to GA and GG.

### 3.5 A distal enhancer upstream of the porcine *CRP* gene mediates the acute phase induction of *CRP* in HepG2 cells

To examine whether the pig proximal promoter is sufficient to mediate the induction of porcine *CRP* by IL-6 and IL-1 $\beta$  and whether the identified polymorphisms in its core promoter region may affect acute phase induction, luciferase reporter assays were carried out. Promoter activity was measured for two vectors containing different haplotypes (P1 and P2) of pig *CRP* promoter region in transfected HepG2 cells induced with IL6 and IL1- $\beta$ . No substantial increase in luciferase activity (Figure 6) was observed in transfected cells with both *CRP* promoter constructs, suggesting that the promoter alone is insufficient for the acute phase induction of porcine *CRP*.

To further understand the functional contribution of the putative enhancer region associated to the expression of *CRP*, two sequences with different haplotypes (E1 and E2) of the enhancer were inserted upstream of *CRP* proximal promoter constructs. The inclusion of the enhancer sequences in the transfected vectors increased the induction of luciferase activity in HepG2 cells (Figure 6), revealing the involvement of this distal regulatory element in the acute phase induction of pig *CRP* by IL-6 and IL-1 $\beta$ . Furthermore, the vector containing the haplotype E1 ( $\emptyset$  – A – A – G) generated higher levels of

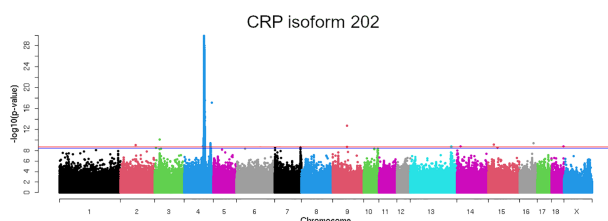


FIGURE 3

Manhattan plot representing the association analysis between the CRP mRNA expression of the isoform 202 and polymorphisms distributed along the pig chromosomes. Red line indicates the genome wide significance threshold (FDR  $\leq 0.05$ ).

When we studied the correlation between *CRP-202* mRNA expression and *HNF4 $\alpha$*  and *FOXA2* mRNA expression in 300 pigs, a higher correlation was observed between *HNF4 $\alpha$*  and *CRP* gene expression when compared to *FOXA2- CRP-202* correlation (Table 3). Remarkably, Duroc and Landrace animals presented higher correlations between *HNF4 $\alpha$*  and *CRP-202* mRNA levels than Large White animals ( $r_p = 0.515$  for Duroc,  $r_p = 0.47$  in Landrace and  $r_p = 0.297$  in Large White), in accordance with their higher frequency of the A allele in rs713631040, which creates a binding site for HNF4 $\alpha$  (Figure 5, Table 3). A similar correlation pattern between *HNF4 $\alpha$*  and *CRP-202* was observed when all animals were classified according to the genotypes of

TABLE 2 The 10 most significant polymorphisms associated to the CRP expression levels: position, alleles, minimum allele frequency and allele substitution effect significance.

Name	Chr	Bp Position	A1	A2	MAF	N°	P-value	FDR
rs793561911	4	90743523	TCTTCTGTTTGTGGGACCGGCC	T	0.2417	300	1.34 x10 <sup>-30</sup>	3.40 x10 <sup>-23</sup>
rs713631040	4	90743532	G	A	0.2417	300	1.34 x10 <sup>-30</sup>	3.40 x10 <sup>-23</sup>
rs330141279	4	90743549	G	A	0.24	299	2.24 x10 <sup>-30</sup>	5.67 x10 <sup>-23</sup>
rs334016742	4	90796210	G	C	0.245	300	2.53 x10 <sup>-30</sup>	6.39 x10 <sup>-23</sup>
rs325087855	4	90681003	C	T	0.2333	300	3.80 x10 <sup>-30</sup>	9.63 x10 <sup>-23</sup>
rs328995216	4	90744910	T	G	0.2467	300	4.14 x10 <sup>-30</sup>	1.05 x10 <sup>-22</sup>
rs338992142	4	90743570	A	G	0.2408	298	4.63 x10 <sup>-30</sup>	1.17 x10 <sup>-22</sup>
rs322057211	4	90673382	G	A	0.2391	299	6.66 x10 <sup>-30</sup>	1.69 x10 <sup>-22</sup>
rs693961338	4	90801224	C	T	0.238333	300	7.08 x10 <sup>-30</sup>	1.79 x10 <sup>-22</sup>
rs331519256	4	90679310	C	T	0.244147	299	7.12 x10 <sup>-30</sup>	1.80 x10 <sup>-22</sup>

luciferase activity than the rest (Figure 6), confirming the regulatory role of rs793561911 and rs713631040 on CRP gene expression.

## 4 Discussion

CRP is known to be highly conserved between different species (48). Multiples studies in humans have described the regulatory molecular mechanisms controlling CRP gene expression in liver, as well as identified mutations associated with CRP blood levels and cardiovascular disease risk (6, 49, 50). Since pig represents an ideal model for human diseases (51, 52), in the present work we have

delved into the genetic architecture and regulatory mechanisms involved in CRP gene expression in pigs. Furthermore, the identification of functional genetic variants associated to CRP blood levels could be valuable to improve the accuracy of genomic selection for immunocompetence in pigs.

Previous studies in humans and pigs have identified polymorphisms in the 3'UTR of CRP affecting serum levels of CRP (53–55). A GWAS study in our Duroc population also pointed out the polymorphism rs327446000 in the 3'UTR of CRP as the genetic variant most significantly associated with CRP serum levels. However, the haplotype-based approach maximized a region at 90.53-90.62 Mb in SSC4 as the most associated region with CRP

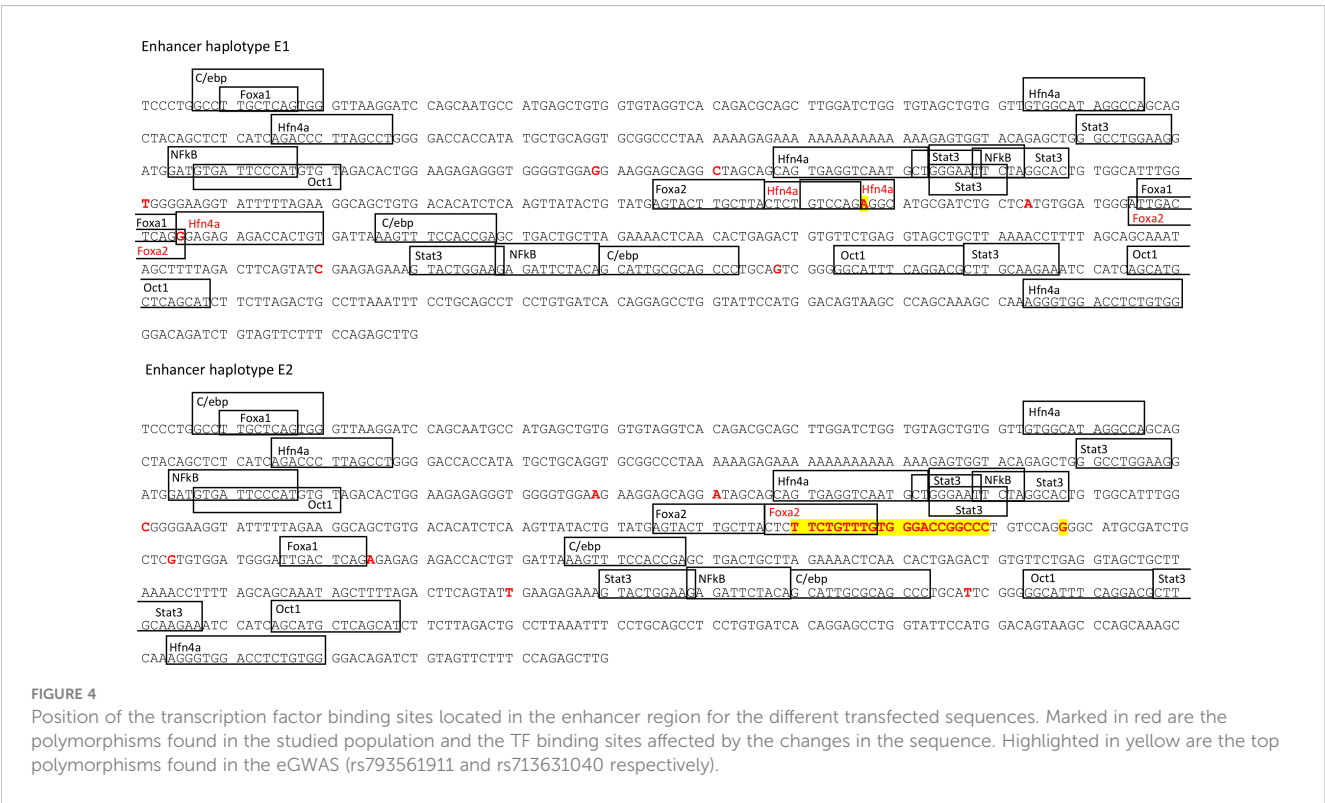


TABLE 3 Correlation coefficients of CRP-202 mRNA expression with HNF4A and FOXA2 mRNA expression in liver by breed and rs713631040 (SSC4:90,743,532 bp) genotype.

Liver mRNA CRP-202	HNF4α	FOXA2	Allele A frequency (rs713631040)
All	0.31	0.178	
Duroc	0.515	0.16	0.825
Landrace	0.47	0.076	0.87
Large White	0.297	0.069	0.58
rs713631040 A/A (n=178)	0.455	0.16	
rs713631040 G/A (n=99)	0.334	0.076	
rs713631040 G/G (n=23)	0.21	0.069	

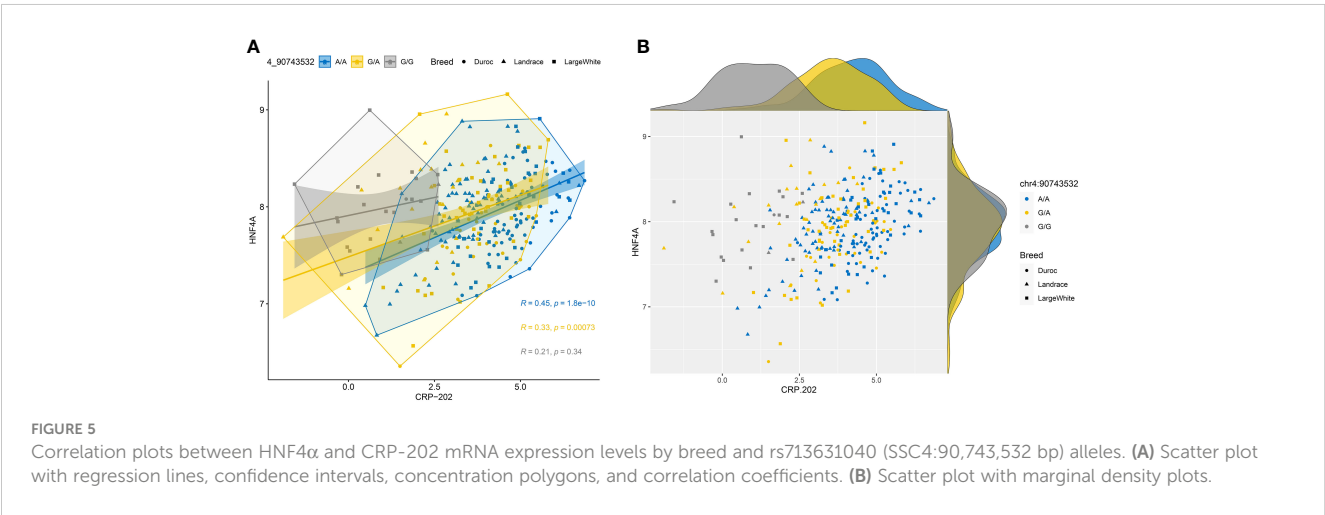


FIGURE 5 Correlation plots between HNF4α and CRP-202 mRNA expression levels by breed and rs713631040 (SSC4:90,743,532 bp) alleles. (A) Scatter plot with regression lines, confidence intervals, concentration polygons, and correlation coefficients. (B) Scatter plot with marginal density plots.

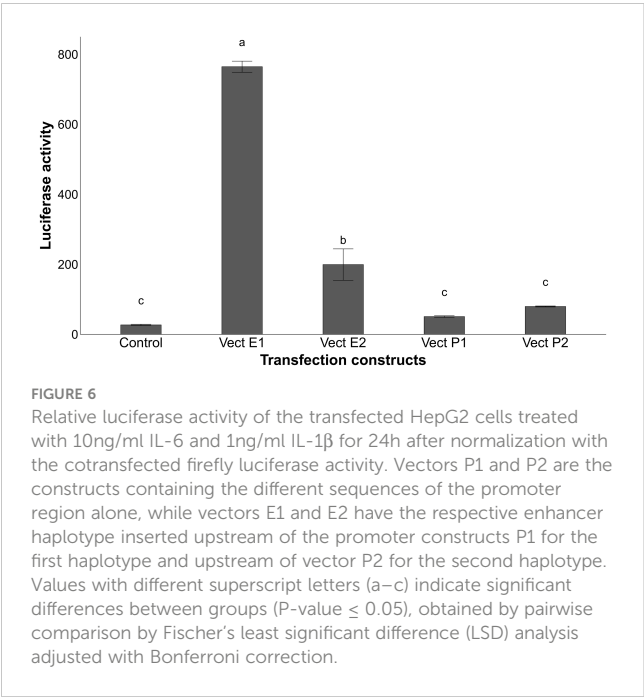


FIGURE 6 Relative luciferase activity of the transfected HepG2 cells treated with 10ng/ml IL-6 and 1ng/ml IL-1β for 24h after normalization with the cotransfected firefly luciferase activity. Vectors P1 and P2 are the constructs containing the different sequences of the promoter region alone, while vectors E1 and E2 have the respective enhancer haplotype inserted upstream of the promoter constructs P1 for the first haplotype and upstream of vector P2 for the second haplotype. Values with different superscript letters (a–c) indicate significant differences between groups (P-value ≤ 0.05), obtained by pairwise comparison by Fischer's least significant difference (LSD) analysis adjusted with Bonferroni correction.

serum levels. In addition, eGWAS analysis using 300 animals of different breeds identified a region at 86–93 Mb in SSC4 as the most associated with CRP mRNA expression levels in liver. Although we cannot discard the role of the 3'UTR region in the variation of CRP serum levels, our eGWAS and fine-mapping results pinpointed a genomic region located upstream of CRP gene associated with both mRNA expression and protein CRP levels.

A more detailed analysis of this region revealed the presence of a putative enhancer element conserved between human and cow species, and containing transcription factor binding sites for STAT3, C/EBP, NF-κB, HNF4α, OCT-1 FOXA1 and FOXA2. These transcription factors have been widely described as being required for the constitutive expression and/or acute phase induction of CRP (21, 22, 56–59). Remarkably, a recent study performed in humans identified an enhancer (E1) located 37.7 Kb upstream of the CRP promoter. Transcription factors STAT3, C/EBP-β, and USF1/2 appear to mediate the regulatory effects of E1 acting in conjunction with CRP proximal promoter for the acute phase induction by IL-6 and IL-1β of human CRP (16, 25, 26, 60). Furthermore, the constitutive expression of human CRP at the basal state seems to be mediated by promoter binding of transcription factors such as HNF-1, HNF-3 and OCT-1 (21, 56). Comparative analysis between human, cattle and porcine CRP promoter sequences also revealed a high level of sequence

conservation, with transcription factor binding sites for FOXA2, HNF-1 and STAT3 preserved in the three promoter regions. Furthermore, the porcine promoter sequence shared target sites with its bovine counterpart for C/EBP, c-Rel and p53 transcription factors, and, in different locations, with the human for C/EBP, p53, OCT-1 and FOXA1. It is worth noting that the identified OCT-1 binding site conserved in pigs and humans was previously found by Voleti et al. in 2012 (22) as a modulator of *CRP* expression in humans by positional competition with other binding sites in the region.

Similar to the results previously reported by Wang et al. (26), the interaction of the pig distal enhancer element with the *CRP* proximal promoter was required for the acute phase induction of porcine *CRP* by IL-6 and IL-1 $\beta$ , suggesting an evolutionary conservation of regulatory mechanisms involved in *CRP* expression between pigs and humans. These results are in agreement with the similar functions of this protein in humans and pigs compared to mouse *CRP* (48).

Several polymorphisms located in putative binding-regions of transcription factors and associated to *CRP* mRNA expression and protein levels were identified in the proximal promoter and distal enhancer of porcine *CRP*. In the proximal promoter region, five out of 17 described genetic variants were disrupting putative binding-sites for C/EBP, FOXA1 and p53. C/EBP has been described as an important transcription factor activated by IL-6 and necessary for the induction of *CRP* expression (60, 61). However, we did not observe differences in luciferase activity in transfected HepG2 cells with vectors containing different promoter haplotypes after cytokine stimulation, suggesting that the allelic variation in these putative C/EBP binding sites did not have a substantial effect in the expression of porcine *CRP*. By contrast, among the seven polymorphisms found in the porcine enhancer region, rs793561911, rs713631040 and rs338992142 were located within putative binding sites for HNF4 $\alpha$  and FOXA2, and potentially disrupting their regulatory effect. In fact, our luciferase assay showed a significant increase in luciferase activity in HEPG2 cells transfected with the enhancer haplotype that conserved the HNF4 $\alpha$  binding sites (E1), which is in accordance with the correlation observed between *CRP* and *HNF4 $\alpha$*  mRNA expression levels in liver.

Hepatocyte nuclear factor 4 alpha (HNF4 $\alpha$ ) encodes for a protein that controls the expression of several hepatic genes, HNF1 $\alpha$  among them, and plays a role in liver development (62, 63). Sucajtyś-Szulc et al. (19) revealed a coordinated upregulation of both hepatic nuclear factors, as well as IL-6 and *CRP* in livers of rats affected with either chronic renal failure or lipopolysaccharide-induced inflammation.

In the light of the above, our results describe for the first time the role of a distal enhancer in the acute phase expression of porcine *CRP*. Our analysis on *CRP* serum levels was limited to a closed commercial Duroc line, which is reflected in a high linkage disequilibrium. A larger sample size including other pig breeds and commercial lines would reduce the presence of large associated blocks and allow the identification of the causal implicated variants. Further functional analyses are warranted to better understand the regulatory mechanisms involved in *CRP* expression as well as to locate the causal mutation(s).

Finally, taking into account the strong similarities between porcine and human *CRP* regulation, this work improves the understanding of the complex mechanisms governing *CRP* expression in both species and reiterates the advantages of using the pig as a biomedical model for inflammation and cardiovascular diseases in humans. In addition, the

identified functional polymorphisms can be used in pig breeding programs to improve the immunocompetence profile of the herd.

## Data availability statement

The datasets presented in this study can be found in online repositories. The names of the repository/repositories and accession number(s) can be found below: <https://data.fang.org/>, PRJEB58030 and PRJEB58031.

## Ethics statement

The animal study was approved by Institut de Recerca i Tecnologia Agroalimentàries (IRTA) Ethical Committee. The study was conducted in accordance with the local legislation and institutional requirements.

## Author contributions

MB designed the study. MB, M-JM and MCAMB supervised the generation of the material animal. MB, OG-R, YR-C and RQ performed the sampling. MB, OG-R, TJ-J and CH-B carried out the laboratory analyses. TJ-J, CH-B, DC-P, AE-C, MB and RQ analysed the data. CH-B and MB interpreted the results and wrote the manuscript. All authors contributed to the article and approved the submitted version.

## Funding

The authors declare financial support was received for the research, authorship, and/or publication of this article. The study was funded by grants AGL2016-75432-R and PID2020-112677RB-C21 awarded by MCIN/AEI/10.13039/501100011033 and GENE-SWitCH project (<https://www.gene-switch.eu>), which is funded by the European Union's Horizon 2020 Research and Innovation Programme under the grant agreement n°817998. T. Jové-Juncà was funded with an IRTA fellowship (CPI1221) and C. Hernández-Banqué was supported by a FPI grant (PRE2021-097825) granted by the Spanish Ministry of Science and Innovation. YR-C was financially supported by a Ramon y Cajal contract (RYC2019-027244-I) from the Spanish Ministry of Science and Innovation. The authors are part to a Consolidated Research Group AGAUR, with the reference 2021-SGR-01552.

## Acknowledgments

We gratefully acknowledge the technical staff from IRTA and Selecció Batallé S.A. for their collaboration in the experimental protocols at farm and slaughterhouse.

## Conflict of interest

Author MCAMB was employed by the company Hendrix Genetics.

The remaining authors declare that the research was conducted in the absence of any commercial or financial relationships that could be construed as a potential conflict of interest.

## Publisher's note

All claims expressed in this article are solely those of the authors and do not necessarily represent those of their affiliated organizations, or those of the publisher, the editors and the

reviewers. Any product that may be evaluated in this article, or claim that may be made by its manufacturer, is not guaranteed or endorsed by the publisher.

## Supplementary material

The Supplementary Material for this article can be found online at: <https://www.frontiersin.org/articles/10.3389/fimmu.2023.1250942/full#supplementary-material>

## References

- Szalai AJ. The biological functions of C-reactive protein. *Vascul Pharmacol* (2002) 39(3):105–7. doi: 10.1016/S1537-1891(02)00294-X
- Sproston NR, Ashworth JJ. Role of C-reactive protein at sites of inflammation and infection. *Front Immunol* (2018) 9(APR):1–11. doi: 10.3389/fimmu.2018.00754
- Yao ZY, Zhang Y, Wu HB. Regulation of C-reactive protein conformation in inflammation. *Inflammation Res* (2019) 68(10):815–23. doi: 10.1007/s00011-019-01269-1
- Rajab IM, Hart PC, Potempa LA. How C-reactive protein structural isoforms with distinctive bioactivities affect disease progression. *Front Immunol* (2020) 11. doi: 10.3389/fimmu.2020.02126
- Ullah N, Wu Y. Regulation of conformational changes in C-reactive protein alters its bioactivity. *Cell Biochem Biophys* (2022) 80:595–608. doi: 10.1007/s12013-022-01089-x
- Boncler M, Wu Y, Watala C. The multiple faces of c-reactive protein-physiological and pathophysiological implications in cardiovascular disease. *Molecules* (2019) 24(11). doi: 10.3390/molecules24112062
- Pepys MB, Hirschfield GM, Tennent GA, Gallimore JR, Kahan MC, Bellotti V, et al. Targeting C-reactive protein for the treatment of cardiovascular disease. *Nature* (2006) 440(7088):1217–21. doi: 10.1038/nature04672
- Muthanna FM, Ibrahim HK, Al-Awkally NAM, Yousuf A. C-reactive protein in patients with COVID-19. *Int J Health Sci (Qassim)* (2022) 6:1610–20. doi: 10.53730/ijhs.v6n5.8920
- Möller K, Ostermann AI, Rund K, Thoms S, Blume C, Stahl F, et al. Influence of weight reduction on blood levels of C-reactive protein, tumor necrosis factor- $\alpha$ , interleukin-6, and oxylipins in obese subjects. *Prostaglandins Leukot Essent Fatty Acids* (2016) 106:39–49. doi: 10.1016/j.plefa.2015.12.001
- Gutiérrez AM, Montes A, Gutiérrez-Panizo C, Fuentes P, de la Cruz-Sánchez E. Gender influence on the salivary protein profile of finishing pigs. *J Proteomics* (2018) 178(December 2017):107–13. doi: 10.1016/j.jprot.2017.11.023
- Danik JS, Ridker PM. Genetic determinants of C-reactive protein. *Curr Atheroscler Rep* (2007) 9(3):195–203. doi: 10.1007/s11883-007-0019-2
- Reiner AP, Barber MJ, Guan Y, Ridker PM, Lange LA, Chasman DI, et al. Polymorphisms of the HNF1A gene encoding hepatocyte nuclear factor-1 $\alpha$  are associated with C-reactive protein. *Am J Hum Genet* (2008) 82(5):1193–201. doi: 10.1016/j.ajhg.2008.03.017
- Ley SH, Hegele RA, Connelly PW, Harris SB, Mamakeeick M, Cao H, et al. Assessing the association of the HNF1A G319S variant with C-reactive protein in Aboriginal Canadians: A population-based epidemiological study. *Cardiovasc Diabetol* (2010) 9:1–6. doi: 10.1186/1475-2840-9-39
- Ballester M, Ramayo-Caldas Y, González-Rodríguez O, Pascual M, Reixach J, Díaz M, et al. Genetic parameters and associated genomic regions for global immunocompetence and other health-related traits in pigs. *Sci Rep* (2020) 10(1). doi: 10.1038/s41598-020-75417-7
- Agrawal A, Samols D, Kushner I. Transcription factor c-Rel enhances C-reactive protein expression by facilitating the binding of C/EBP $\beta$  to the promoter. *Mol Immunol* (2003) 40(6):373–80. doi: 10.1016/S0161-5890(03)00148-2
- Nishikawa T, Hagihara K, Serada S, Isobe T, Matsumura A, Song J, et al. Transcriptional complex formation of c-fos, STAT3, and hepatocyte NF-1 $\alpha$  is essential for cytokine-driven C-reactive protein gene expression. *J Immunol* (2008) 180(5):3492–501. doi: 10.4049/jimmunol.180.5.3492
- Armendariz AD, Krauss RM. Hepatic nuclear factor 1- $\alpha$ : Inflammation, genetics, and atherosclerosis. *Curr Opin Lipidol* (2009) 20(2):106–11. doi: 10.1097/MOL.0b013e3283295ee9
- Thirumalai A. *Regulation of C-reactive protein gene expression and function*. Thirumalai, Avinash East Tennessee State University (2014).
- Sucajtys-Szulc E, Debska-Slizien A, Rutkowski B, Milczarek R, Pelikant-Malecka I, Sledzinski T, et al. Hepatocyte nuclear factors as possible C-reactive protein transcriptional inducer in the liver and white adipose tissue of rats with experimental chronic renal failure. *Mol Cell Biochem* (2018) 446(1–2):11–23. doi: 10.1007/s11010-018-3268-1
- Li SP, Goldman ND. Regulation of human C-reactive protein gene expression by two synergistic IL-6 responsive elements. *Biochemistry* (1996) 35(28):9060–8. doi: 10.1021/bi953033d
- Voleti B, Agrawal A. Regulation of basal and induced expression of C-reactive protein through an overlapping element for OCT-1 and NF- $\kappa$ B on the proximal promoter. *J Immunol* (2005) 175:3386–90. doi: 10.1021/bi953033d
- Voleti B, Hammond DJ, Thirumalai A, Agrawal A. Oct-1 acts as a transcriptional repressor on the C-reactive protein promoter. *Mol Immunol* (2012) 52(3–4):242–8. doi: 10.1016/j.molimm.2012.06.005
- Szalai AJ, van Ginkel FW, Wang Y, McGhee JR, Volanakis JE. Complement-dependent acute-phase expression of C-reactive protein and serum amyloid P-component. *J Immunol* (2000) 165(2):1030–5. doi: 10.4049/jimmunol.165.2.1030
- Kramer F, Torzewski J, Kamenz J, Veit K, Hombach V, Dedio J, et al. Interleukin-1 $\beta$  stimulates acute phase response and C-reactive protein synthesis by inducing an NF $\kappa$ B- and C/EBP $\beta$ -dependent autocrine interleukin-6 loop. *Mol Immunol* (2008) 45(9):2678–89. doi: 10.1016/j.molimm.2007.12.017
- Ngwa DN, Pathak A, Agrawal A. IL-6 regulates induction of C-reactive protein gene expression by activating STAT3 isoforms. *Mol Immunol* (2022) 146:50–6. doi: 10.1016/j.molimm.2022.04.003
- Wang MY, Zhang CM, Zhou HH, Ge ZB, Su CC, Lou ZH, et al. Identification of a distal enhancer that determines the expression pattern of acute phase marker C-reactive protein. *J Biol Chem* (2022) 298(8). doi: 10.1016/j.jbc.2022.102160
- Edfors-Lilja I, Watrang E, Marklund L, Moller M, Andersson-Eklund L, Andersson L, et al. Mapping quantitative trait loci for immune capacity in the pig. *J Immunol* (1998) 161(2):829–35. doi: 10.4049/jimmunol.161.2.829
- Millet S, Maertens L. The European ban on antibiotic growth promoters in animal feed: From challenges to opportunities. *Veterinary J Vet J* (2011) 187:143–4. doi: 10.1016/j.tvjl.2010.05.001
- Merks JWM, Mathur PK, Knol EF. New phenotypes for new breeding goals in pigs. *Animal* (2012) 6(4):535–43. doi: 10.1017/S1751731111002266
- Nowakiewicz A, Zięba P, Gnat S, Matuszewski Ł. Last call for replacement of antimicrobials in animal production: modern challenges, opportunities, and potential solutions. *Antibiotics (Basel)* (2020) 9(12):1–21. doi: 10.3390/antibiotics9120883
- Purcell S, Neale B, Todd-Brown K, Thomas L, Ferreira MAR, Bender D, et al. PLINK: A tool set for whole-genome association and population-based linkage analyses. *Am J Hum Genet* (2007) 81(3):559–75. doi: 10.1086/519795
- Crespo-Piazuelo D, Acloque H, González-Rodríguez O, Mongellaz M, Mercat MJ, Bink MCAM, et al. Identification of transcriptional regulatory variants in pig duodenum, liver, and muscle tissues. *Gigascience* (2023) 12:1–14. doi: 10.1093/gigascience/giad042
- Li H. Aligning sequence reads, clone sequences and assembly contigs with BWA-MEM. *arXiv* (2013). doi: 10.48550/arXiv.1303.3997
- McKenna A, Hanna M, Banks E, Sivachenko A, Cibulskis K, Kernysky A, et al. The genome analysis toolkit: A MapReduce framework for analyzing next-generation DNA sequencing data. *Genome Res* (2010) 20(9):1297–303. doi: 10.1101/gr.107524.110
- Dobin A, Davis CA, Schlesinger F, Drenkow J, Zaleski C, Jha S, et al. STAR: Ultrafast universal RNA-seq aligner. *Bioinformatics* (2013) 29(1):15–21. doi: 10.1093/bioinformatics/bts635
- Li B, Dewey CN. RSEM: Accurate transcript quantification from RNA-Seq data with or without a reference genome. *BMC Bioinf* (2011) 12. doi: 10.1186/1471-2105-12-323
- McLaren W, Gil L, Hunt SE, Riat HS, Ritchie GRS, Thormann A, et al. The ensemble effect predictor. *Journal Genome Biology* (2016) 17(1):. doi: 10.1186/s13059-016-0974-4



38. Corpet F. Multiple sequence alignment with hierarchical clustering. *Nucleic Acids Res* (1988) 16(22):10881–90. doi: 10.1093/nar/16.22.10881
39. Lee C, Huang CH. LASAGNA-search: An integrated web tool for transcription factor binding site search and visualization. *Biotechniques* (2013) 54(3):141–53. doi: 10.2144/000113999
40. Benjamini Y, Hochberg Y. Controlling the false discovery rate: A practical and powerful approach to multiple testing. *J R Stat Society: Ser B (Methodological)* (1995) 57(1):289–300. doi: 10.1111/j.2517-6161.1995.tb02031.x
41. Yang J, Lee SH, Goddard ME, Visscher PM. GCTA: A tool for genome-wide complex trait analysis. *Am J Hum Genet* (2011) 88(1):76–82. doi: 10.1016/j.ajhg.2010.11.011
42. Yang J, Benyamin B, McEvoy BP, Gordon S, Henders AK, Nyholt DR, et al. Common SNPs explain a large proportion of the heritability for human height. *Nat Genet* (2010) 42(7):565–9. doi: 10.1038/ng.608
43. Turner SD. qqman: an R package for visualizing GWAS results using Q-Q and manhattan plots. *J Open Source Softw* (2018) 3(25):731. doi: 10.21105/joss.00731
44. Druet T, Georges M. A hidden Markov model combining linkage and linkage disequilibrium information for haplotype reconstruction and quantitative trait locus fine mapping. *Genetics* (2010) 184(3):789–98. doi: 10.1534/genetics.109.108431
45. Pérez-Enciso M, Misztal I. Qxpak5: Old mixed model solutions for new genomics problems. *BMC Bioinf* (2011) 12. doi: 10.1186/1471-2105-12-202
46. Bonferroni C. Teoria statistica delle classi e calcolo delle probabilità. *Pubblicazioni del R Istituto Superiore di Sci Economiche e Commerciali di Firenze* (1936) 8:3–62.
47. Salazar J, Martínez MS, Chávez-Castillo M, Núñez V, Añez R, Torres Y, et al. C-reactive protein: an in-depth look into structure, function, and regulation. *Int Sch Res Notices* (2014) 2014:653045. doi: 10.1155/2014/653045
48. Pathak A, Agrawal A. Evolution of C-reactive protein. *Front Immunol* (2019) 10. doi: 10.3389/fimmu.2019.00943
49. Hage FG, Szalai AJ. C-reactive protein gene polymorphisms, C-reactive protein blood levels, and cardiovascular disease risk. *J Am Coll Cardiol* (2007) 50(12):1115–22. doi: 10.1016/j.jacc.2007.06.012
50. Carlson CS, Aldred SF, Lee PK, Tracy RP, Schwartz SM, Rieder M, et al. Polymorphisms within the C-reactive protein (CRP) promoter region are associated with plasma CRP levels. *Am J Hum Genet* (2008) 82(1):251. doi: 10.1016/j.ajhg.2007.12.007
51. Bassols A, Costa C, Eckersall PD, Osada J, Sabrià J, Tibau J. The pig as an animal model for human pathologies: A proteomics perspective. *Proteomics - Clin Applications. Wiley-VCH Verlag* (2014) 8:715–31. doi: 10.1002/prca.201300099
52. Pabst R. The pig as a model for immunology research. *Cell Tissue Res* (2020) 380:287–304. doi: 10.1007/s00441-020-03206-9
53. Brull DJ, Serrano N, Zito F, Jones L, Montgomery HE, Rumley A, et al. Human CRP gene polymorphism influences CRP levels: implications for the prediction and pathogenesis of coronary heart disease. *Arterioscler Thromb Vasc Biol* (2003) 23(11):2063–9. doi: 10.1161/01.ATV.0000084640.21712.9C
54. Łaszyn M, Sielawa H, Zyczko K. The relationship between crp gene polymorphism and the serum concentrations of C-reactive protein, total cholesterol and hdl cholesterol in suckling piglets. *Ann Anim Sci* (2013) 13(3):503–12. doi: 10.2478/aoas-2013-0033
55. Fransén K, Pettersson C, Hurtig-Wennlöf A. CRP levels are significantly associated with CRP genotype and estrogen use in The Lifestyle, Biomarker and Atherosclerosis (LBA) study. *BMC Cardiovasc Disord* (2022) 22(1). doi: 10.1186/s12872-022-02610-z
56. Toniatti C, Demartis A, Monaci P, Nicosia A, Ciliberto G. Synergistic trans-activation of the human C-reactive protein promoter by transcription factor HNF-1 binding at two distinct sites. *EMBO J* (1990) 9:4467–75. doi: 10.1002/j.1460-2075.1990.tb07897.x
57. Aghadi M, Elgendy R, Abdelalim EM. Loss of FOXA2 induces ER stress and hepatic steatosis and alters developmental gene expression in human iPSC-derived hepatocytes. *Cell Death Dis* (2022) 13(8). doi: 10.1038/s41419-022-05158-0
58. Heslop JA, Duncan SA. FoxA factors: the chromatin key and doorstep essential for liver development and function. *Genes Dev* (2020) 34:1003–4. doi: 10.1101/gad.340570.120
59. Bochkis IM, Shin S, Kaestner KH. Bile acid-induced inflammatory signaling in mice lacking Foxa2 in the liver leads to activation of mTOR and age-onset obesity. *Mol Metab* (2013) 2(4):447–56. doi: 10.1016/j.molmet.2013.08.005
60. Young DP, Kushner I, Samols D. Binding of C/EBP $\beta$  to the C-reactive protein (CRP) promoter in hep3B cells is associated with transcription of CRP mRNA. *J Immunol* (2008) 181(4):2420–7. doi: 10.4049/jimmunol.181.4.2420
61. Zhang SC, Wang MY, Feng JR, Chang Y, Ji SR, Wu Y. Reversible promoter methylation determines fluctuating expression of acute phase proteins. *Elife* (2020) 9:2420–7. doi: 10.7554/eLife.51317
62. Kyithar MP, Bonner C, Bacon S, Kilbride SM, Schmid J, Graf R, et al. Effects of hepatocyte nuclear factor-1A and -4A on pancreatic stone protein/regenerating protein and C-reactive protein gene expression: Implications for maturity-onset diabetes of the young. *J Transl Med* (2013) 11(1). doi: 10.1186/1479-5876-11-156
63. Thakur A, Wong JCH, Wang EY, Lotto J, Kim D, Cheng JC, et al. Hepatocyte nuclear factor 4-alpha is essential for the active epigenetic state at enhancers in mouse liver. *Hepatology* (2019) 70(4):1360–76. doi: 10.1002/hep.30631



## OPEN ACCESS

## EDITED BY

Alok Agrawal,  
East Tennessee State University,  
United States

## REVIEWED BY

Shang-Rong Ji,  
Lanzhou University, China  
Karlheinz Peter,  
Baker Heart and Diabetes Institute,  
Australia

## \*CORRESPONDENCE

Margaret E. Olson  
✉ mkurbanov01@roosevelt.edu

RECEIVED 20 July 2023

ACCEPTED 28 August 2023

PUBLISHED 15 September 2023

## CITATION

Olson ME, Hornick MG, Stefanski A,  
Albanna HR, Gjoni A, Hall GD, Hart PC,  
Rajab IM and Potempa LA (2023) A  
biofunctional review of C-reactive protein  
(CRP) as a mediator of inflammatory and  
immune responses: differentiating  
pentameric and modified CRP  
isoform effects.  
*Front. Immunol.* 14:1264383.  
doi: 10.3389/fimmu.2023.1264383

## COPYRIGHT

© 2023 Olson, Hornick, Stefanski, Albanna,  
Gjoni, Hall, Hart, Rajab and Potempa. This is  
an open-access article distributed under the  
terms of the [Creative Commons Attribution  
License \(CC BY\)](#). The use, distribution or  
reproduction in other forums is permitted,  
provided the original author(s) and the  
copyright owner(s) are credited and that  
the original publication in this journal is  
cited, in accordance with accepted  
academic practice. No use, distribution or  
reproduction is permitted which does not  
comply with these terms.

# A biofunctional review of C-reactive protein (CRP) as a mediator of inflammatory and immune responses: differentiating pentameric and modified CRP isoform effects

Margaret E. Olson\*, Mary G. Hornick, Ashley Stefanski,  
Haya R. Albanna, Alesia Gjoni, Griffin D. Hall, Peter C. Hart,  
Ibraheem M. Rajab and Lawrence A. Potempa

College of Science, Health and Pharmacy, Roosevelt University, Schaumburg, IL, United States

C-reactive protein (CRP) is an acute phase, predominantly hepatically synthesized protein, secreted in response to cytokine signaling at sites of tissue injury or infection with the physiological function of acute pro-inflammatory response. Historically, CRP has been classified as a mediator of the innate immune system, acting as a pattern recognition receptor for phosphocholine-containing ligands. For decades, CRP was envisioned as a single, non-glycosylated, multi-subunit protein arranged non-covalently in cyclic symmetry around a central void. Over the past few years, however, CRP has been shown to exist in at least three distinct isoforms: 1.) a pentamer of five identical globular subunits (pCRP), 2.) a modified monomer (mCRP) resulting from a conformational change when subunits are dissociated from the pentamer, and 3.) a transitional isoform where the pentamer remains intact but is partially changed to express mCRP structural characteristics (referred to as pCRP\* or mCRP<sub>m</sub>). The conversion of pCRP into mCRP can occur spontaneously and is observed under commonly used experimental conditions. In careful consideration of experimental design used in published reports of *in vitro* pro- and anti-inflammatory CRP bioactivities, we herein provide an interpretation of how distinctive CRP isoforms may have affected reported results. We argue that pro-inflammatory amplification mechanisms are consistent with the biofunction of mCRP, while weak anti-inflammatory mechanisms are consistent with pCRP. The interplay of each CRP isoform with specific immune cells (platelets, neutrophils, monocytes, endothelial cells, natural killer cells) and mechanisms of the innate immune system (complement), as well as differences in mCRP and pCRP ligand recognition and effector functions are discussed. This review will serve as a revised understanding of the structure-function relationship between CRP isoforms as related to inflammation and innate immunity mechanisms.

## KEYWORDS

CRP isoforms, mCRP, inflammation, C-reactive protein, innate immunity, complement

## Introduction

Despite long-standing recognition of C-reactive protein (CRP) as a non-specific, diagnostic biomarker for inflammation, only recently has the active role of CRP as an innate immune inflammatory mediator been revealed (1). CRP is primarily synthesized in the liver, though extrahepatic production in macrophages, vascular cells, endothelial cells, adipocytes, peripheral blood mononuclear cells (PBMCs), and the kidneys has been reported (2–11). The confounding functions of CRP relate to its dynamic, macromolecular structure in which CRP can exist in three isoforms: pCRP, pCRP\*, and mCRP. Originally, “CRP”, oft referred to as nCRP (native/natural), was characterized as a 115 kDa pentamer of homologous subunits that are 206 amino acids in length (23 kDa each) (Figure 1) (1). The pentameric subunits self-assemble into a discoid tertiary structure via non-covalent bonding around a central pore (12). Pentameric structural integrity is stabilized by two calcium ions that also dictate CRP’s ligand binding capacity to phosphocholine (PC)-containing polysaccharides, polycations, chromatin, histone, ribonucleoprotein, fibronectin, laminin, lipoproteins, and galactins (12). It is now known that CRP acts as an agglutinin, opsonin and neutralizing protein that scavenges for debris at sites of active inflammation; yet in early CRP literature, several contradictory reports were made regarding the biofunctional

properties of distinct CRP preparations. As early as the 1980’s, denatured CRP, via heat (H-CRP), metal chelation (F-CRP), acidic treatment (A-CRP), latex adsorption or freeze-thaw, yielded protein aggregates with antigenicity altered from native CRP (nCRP, primarily pCRP). The aforementioned conditions are now known to promote  $pCRP \rightarrow pCRP^* \rightarrow mCRP$  dissociation, exposing a neoepitope that is proinflammatory in nature (13–15). Subsequent studies demonstrated the *in vivo* relevance of this dissociation, which is prompted by acidic environments of inflammation in the body and PC/lipid ligand binding. Physiologically, CRP’s pro-inflammatory properties are evidenced by the presence of anti-(m)CRP antibodies in several autoimmune conditions, such as lupus nephritis, peripheral artery disease (PAD), and skin-related disorders (16–18). While a plethora of studies have now been performed to characterize the unique properties of the CRP isoforms, the field is absent of a single resource that reinterprets early CRP findings considering our current understanding. For example, initial investigation into CRP’s role as an inflammatory mediator were conducted with commercial CRP antisera, which is now known to contain recognition for both pCRP and mCRP, with up to 16% of the more potent mCRP neoepitope antigenicity present (19). The current review serves as the first comprehensive, detailed reevaluation of the historical CRP literature as related to immune system interactors with a current understanding of CRP conformational dynamics (Table 1). In the

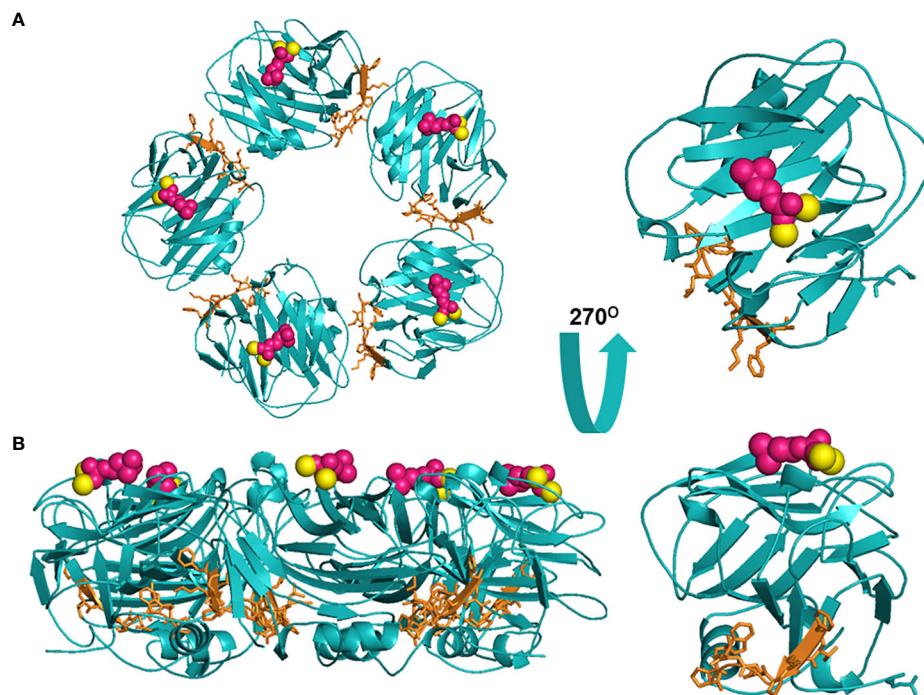
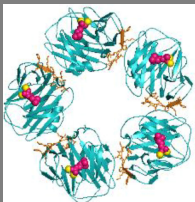
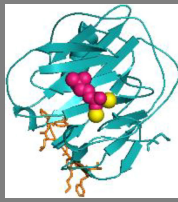


FIGURE 1

Structural rendering of pCRP and a pCRP monomer (PDB: 1B09). (A) provides a top-down view of pCRP and the pCRP monomer with the PC-binding face oriented upwards. (B) offers a side profile of pCRP and pCRP monomer. PC is depicted in pink, calcium ions in yellow, and the neoepitope (aa199–206) in orange. The x-ray crystal structure illustrates the  $Ca^{2+}$ -dependence of PC-pCRP binding, which can occur on each pCRP subunit. pCRP\* binding to C1q occurs on the effector face, opposite (facing down) to the PC-binding face. Both views highlight how the neoepitope (orange) is buried within pCRP at the monomeric interfaces. While the present depiction of the pCRP monomer does not accurately represent mCRP structure given the secondary and tertiary changes that occur upon dissociation, release of mCRP clearly exposes the pro-inflammatory neoepitope for interaction with immune effector cells. Graphic was generated using PyMOL.

TABLE 1 Historically reported bioactivities of CRP vs. current understanding of mCRP.

Effector Response	Bioactivities of "CRP" <sup>#</sup>	Bioactivities of mCRP
		
Platelets	<ul style="list-style-type: none"> <li>Maximizes responsiveness to ADP, epinephrine, thrombin, and collagen (38).</li> <li>Promotes aggregation and secretion of dense and alpha granules (41).</li> <li>Inhibition of PAF-induced platelet aggregation, activation, and platelet-neutrophil adherence (40).</li> <li>Inhibition of arachidonic acid synthesis by phospholipase A<sub>2</sub> (40).</li> </ul>	<ul style="list-style-type: none"> <li>Stimulates/augments aggregation and secretion reactions (42, 43).</li> <li>Upregulates P-selectin (44).</li> <li>Increases prothrombotic activities under sheer conditions (44).</li> <li>Captures and activates neutrophils (44).</li> </ul>
Neutrophils	<ul style="list-style-type: none"> <li>Stimulates phagocytosis (45, 48–51).</li> <li>Stimulates oxidative metabolism (41, 46, 55).</li> <li>Inhibition of neutrophil activation and chemotaxis (45, 46).</li> <li>Inhibition of ROS generation at higher concentrations (46, 52–54).</li> </ul>	<ul style="list-style-type: none"> <li>Induces neutrophil trafficking (46, 57).</li> <li>Reduces expression of L-selectin (65).</li> <li>Increases adhesion to ECs (32, 66–68).</li> <li>Stimulates IL-8 synthesis and release (24, 56).</li> <li>Stimulates iNOS-mediated NO synthesis (20, 64).</li> <li>Increases superoxide and peroxynitrite formation (ONOO<sup>-</sup>) (56).</li> <li>Increases NF-κB and AP-1 (56).</li> <li>Increases neutrophil-neutrophil and neutrophil-endothelial cell aggregation (44, 65, 66).</li> </ul>
Monocytes	<ul style="list-style-type: none"> <li>Activates monocytes for phagocytosis (58, 69–71).</li> <li>Stimulates oxidative responses (41).</li> <li>Induces TF synthesis (62).</li> <li>Promotes release of IL-1α, IL-1β, IL-6, IL-8, TNF-α, GRO-alpha and GRO-beta (60–62).</li> <li>Upregulates liver X receptor-alpha (63).</li> </ul>	<ul style="list-style-type: none"> <li>Potentiates respiratory burst response and increases ROS (41).</li> <li>Stimulates cytokine release (60–62).</li> <li>Increases monocyte adherence to ECs (32, 66–68).</li> <li>Increases production of NO by increasing iNOS levels (20, 64).</li> </ul>
Natural Killer Cells		<ul style="list-style-type: none"> <li>Enhances NK function (19, 72–75).</li> </ul>
Endothelial Cells	<ul style="list-style-type: none"> <li>Induces EC adhesion (32, 66–68).</li> <li>Inhibits eNOS (67).</li> </ul>	<ul style="list-style-type: none"> <li>Increases MCP-1, E-selectin, and IL-8 expression (25).</li> <li>Increases EC adhesion via ICAM-1 and VCAM-1 (44, 67, 76).</li> </ul>
Complement	<ul style="list-style-type: none"> <li>Regulates C activation (49, 69, 77–84).</li> <li>Binds C1q (85).</li> <li>Enhances opsonization for phagocytosis (50, 70, 71, 86).</li> </ul>	<ul style="list-style-type: none"> <li>Binds C1q when complexed with LDL. Does not activate C in fluid phase (85).</li> <li>Binds Factor H and C4bp (34, 87).</li> <li>Binds properdin (88).</li> </ul>

Bullet points colored in blue list anti-inflammatory CRP properties now known to be pCRP-specific.

<sup>#</sup>The designation "CRP" was historically understood to be pCRP, but likely reflects a mixture of pCRP and mCRP bioactivity.

following studies, where a specific CRP isoform was evaluated, the pCRP, pCRP\* and mCRP designators will be utilized. A study describing "CRP" should be assumed to refer to a biologically relevant mixture of CRP isoforms.

## Posited pCRP → mCRP conformational dynamics

In addition to their distinctive biofunctional features, CRP isoforms have unique pharmacokinetic properties, where pCRP is sera soluble. Conversely, mCRP is insoluble in sera unless protein-bound and is predominantly membrane-bound. pCRP, due to its detectability via blood testing, is the non-specific, diagnostic biomarker of inflammation, oft described in the literature, which rapidly rises up to 1000-fold in response to acute infection or injury (20). pCRP is also utilized as a prognostic marker for diseases of chronic inflammation, including autoimmune and cardiovascular diseases (1). Circulating pCRP localizes to sites of damaged tissue

(infection/injury) prior to undergoing a conformational change upon binding to damaged membranes, which exposes the pro-inflammatory CRP neoepitope of amino acids 199–206 (21, 22). Binding of pCRP to damaged membranes is posited to occur via lysophosphatidylcholine (LPC), a bioactive lipid found on the immune cell surface (23–25). Direct binding between the neoepitope of pCRP\*/mCRP and membrane receptors is suggested to occur via FcγRIIIa (CD16), but this binding event only partially explains mCRP's adhesive properties. Hydrophobic interactions with lipid rafts are predicted to compensate for non-receptor binding. Evidence for lipid-promoted conformational dynamics is exhibited by the association of mCRP with extracellular lipid vesicles (26). Activated leukocytes slough membrane-bound CRP, which enters circulation as extracellular vesicles upon cleavage. In an *in vitro* study, Trail et al. demonstrated lipid microparticle-promoted pCRP to mCRP dissociation on a timescale of twenty minutes (27). *In vivo*, mCRP-linked lipid microparticles are observed in PAD and after myocardial infarction with pro-inflammatory function (16, 28). Initially,



pCRP transitions to pCRP\*, a transient conformation that maintains a pentameric quaternary structure but displays the neoepitope of mCRP (21, 29, 30). pCRP\* further dissociates to proinflammatory mCRP (31). pCRP is completely converted to mCRP in 24–48 hrs (21). mCRP can also be generated *in vitro* in denaturing (heat, acid, chelation) or oxidative environments; conditions that were initially reported to generate an antigenic, serum-insoluble aggregate (13). mCRP exhibits the greatest proinflammatory activity once the intrachain disulfide bond, which staples together the two antiparallel  $\beta$ -sheets of the CRP monomer, is reduced (22). pCRP and mCRP isoforms can now be distinguished with conformation-specific antibodies (9C9, 3H12), though these antibodies are unable to parse pCRP\* from mCRP (32–37). Importantly, the pCRP  $\rightarrow$  pCRP\*  $\rightarrow$  mCRP transition is unidirectional, with mCRP incapable of regenerating pCRP.

## mCRP promotes platelet aggregation

Early studies investigating the effects of H-CRP, a thermally aggregated form, on platelet function demonstrated that H-CRP stimulated platelet aggregation under isolated, *in vitro* conditions, similar to heat-treated human IgG, and promoted the corresponding secretion of adenosine triphosphate (ATP) and  $\beta$ -thromboglobulin (38). While determined *not* to be a direct platelet agonist in the more complex environment of platelet-rich plasma (PRP), synergism between H-CRP and adenosine diphosphate (ADP) was observed resulting in irreversible platelet aggregation and ATP secretion. In an optimized combination, mCRP and ADP promoted the release of secretory granule components. H-CRP also synergized with epinephrine, collagen, and thrombin. Interestingly, H-CRP was produced by heat treatment at 63 °C, a temperature now known to promote pCRP to mCRP dissociation. The authors note that heat treatment forced aqueous insoluble protein aggregates accounting for 47–53% of the total CRP preparation. Upon removal of the initial H-CRP aggregate, an additional ~50% CRP could be precipitated with a second heat treatment. Both lots of H-CRP were effective in synergizing with known platelet activators in PRP. Given the heat dependence of CRP aggregation and their insoluble properties in aqueous buffer, it makes sense that the observed aggregates were enriched for mCRP, and the platelet activating properties are inherent to this isoform. Moreover, unmodified CRP, without heat treatment, failed to demonstrate platelet activating potential (39).

Conversely, several concurrent studies reported a protective role for CRP against platelet aggregation (40). Specifically, CRP, of unreported conformation, inhibited platelet-activating factor (PAF)-induced platelet aggregation in a dose dependent manner (1–20  $\mu$ g/ml) (40). This CRP preparation also inhibited the synthesis of arachidonic acid by phospholipase A<sub>2</sub>, limiting the production of proinflammatory cytokines. While no methodology is included to describe CRP's preparation in this study, it is reasonable to assume that the CRP was primarily unmodified. If so, these contradictory results to the former studies may be rationalized by the majority presence of pCRP.

In addition to heat aggregated CRP (H-CRP), other chemically-modified CRPs, including urea chelated (F), latex adsorbed, and

acid (A)-aggregated, have been found to activate platelet aggregation, promote dense and alpha-granule secretion and upregulate thromboxane A<sub>2</sub> synthesis (41). Treatment of CRP with hypochlorous acid (HOCl) prompted oxidative protein unfolding, exposing the hydrophobic interior of CRP in a tertiary structure analogous to mCRP (42). HOCl-CRP (50  $\mu$ g/ml) activated platelets in isolated preparations, inducing aggregation by ~80%, and was shown to interact with several platelet receptors (TLR-4, GPIIb/IIIa) and plasma proteins (C1q, IgG). Like with heat treatment, these observations suggest that acidic environments can promote pCRP to mCRP dissociation, which describes CRP's platelet activating properties. Importantly, a pH between 6–7 is commonly found at sites of inflammation. Further support for oxidative-mediated dissociation of pCRP to mCRP was observed when nCRP (pCRP) failed to activate platelets, though CRP treated with reactive oxygen species (ROS: Fe<sup>2+</sup> - Cu<sup>2+</sup> - ascorbate) irreversibly activated platelets in the presence of suboptimal levels of PAF, thrombin and ADP (43). Li et al. subsequently reported that Cu<sup>2+</sup>-induced oxidative and acidic environments induce the pCRP  $\rightarrow$  mCRP isoform transition (17). Taken together, when CRP is properly activated, i.e., in the mCRP conformation, platelet aggregation and activation is augmented. When later tested with recombinant proteins, mCRP activated and pCRP inhibited pro-thrombotic activities under sheer conditions (44).

## mCRP stimulates neutrophil migration, chemotaxis & phagocytosis; pCRP inhibits neutrophil activation and adhesion

Early studies of CRP effects on neutrophil function probed CRP uptake as a means of pathogenic ligand clearance and found that CRP enhanced neutrophil-mediated clearance of several bacterial species via binding interactions with the PC-containing bacterial membrane (45). In one study, CRP was found to mediate pneumococcal C-polysaccharide (CPS) uptake into neutrophils, promoting clearance, particularly in combination with activated complement (C). This CRP preparation was found to have no effect on neutrophil migration, leukotaxis, oxidative metabolism, or chemiluminescence. The uptake of CPS was CRP-dependent, as CPS alone was not phagocytosed by neutrophils. Though not as efficient, non-complexed CRP was internalized by neutrophils, while uptake was enhanced with the CRP-CPS complex. As CRP binding to PC-containing CPS promotes the pCRP to pCRP\* transition, a change that displays structural and antigenic characteristics of mCRP, the ultimate adhesive effects are characteristic of pro-inflammatory mCRP function. Interestingly, non-complexed CRP uptake was reduced in the presence of EDTA, which preferences the mCRP isoform. Interpreting these findings considering current CRP conformational dynamics, it is likely that pentameric forms of CRP must initiate ligand binding before CRP fully dissociates to mCRP.

Subsequent studies demonstrated the concentration dependence of CRP's effects on neutrophils. Low CRP



concentrations of 0.1–1  $\mu\text{g/mL}$  *do* promote neutrophil chemotaxis, but this effect is lost at higher concentrations (46). The abovementioned study interrogated neutrophil chemotaxis at significantly higher CRP concentrations of 60–120  $\mu\text{g/mL}$ , where no effect on leukotaxis was observed. In further studies, CRP concentrations of 25  $\mu\text{g/mL}$  demonstrated dose-dependent *inhibition* of neutrophil migration towards chemotactic stimuli with complete inhibition at 100  $\mu\text{g/mL}$ . CRP-specific leukotaxis could be explained by mCRP-specific receptors on the neutrophil surface and/or through mCRP-neutrophil hydrophobic interactions. Given the hydrophobic properties of mCRP, low CRP concentrations may preferentially represent the mCRP isoform due to rapid conversion of pCRP  $\rightarrow$  mCRP, exposing a hydrophobic binding surface for neutrophil adhesion. The role of hydrophobic binding interactions in chemotaxis has been described (47). Importantly, the binding interaction between CRP and neutrophils is saturable at CRP concentrations of  $<5 \mu\text{g/mL}$ , a range applicable to the observed activating effects of mCRP on neutrophils (46). Putatively, after mCRP binding sites are saturated, higher CRP concentrations, with increased pCRP representation, could promote inhibitory effects. This hypothesis parallels the acute inflammatory response where the majority of pCRP present at the earliest phases of host defense will be converted to mCRP (31).

A concentration dependent effect of CRP in combination with phorbol 12-myristate 13-acetate (PMA) on superoxide anion generation and secretion was also observed, where CRP  $<5 \mu\text{g/mL}$  demonstrated potentiation but CRP  $>10 \mu\text{g/mL}$  caused inhibition of this response (46). ROS generation results from the phagocytic respiratory burst of neutrophils and can be measured by light emission (chemiluminescence). At the acute phase CRP concentration of 1  $\mu\text{g/mL}$ , CRP enhanced neutrophil phagocytosis, even of non-PC liganded particles, extending the previous findings that CRP promoted neutrophil opsonization of PC-containing bacterial membranes/capsules (48–51). These findings are further supported by the observation that CRP inhibits PAF-mediated chemiluminescence at higher concentrations of 100  $\mu\text{g/mL}$  (52). The concentration dependence of these studies may allude to the conformational dynamics of pCRP  $\rightarrow$  mCRP transition, though this hypothesis is limited by the inability of mCRP to reassemble to pCRP. An alternative explanation is that high concentrations of CRP ( $>10 \mu\text{g/mL}$ ) increase intracellular cAMP levels; high cAMP concentrations are known to inhibit degranulation and PMA-activated neutrophil oxidative metabolism (53, 54). It is important to note that the cAMP-raising concentration of CRP at  $>10 \mu\text{g/mL}$  is greater than CRP concentrations with neutrophil inhibitory effects. Therefore, a relationship may exist where low CRP concentrations, inclusive of mCRP, exhibit proinflammatory function (increased adhesion/chemotaxis) to maximize damage to infective agents while simultaneously raising cAMP levels. At a certain threshold, both CRP and cAMP concentrations rise to a level with anti-inflammatory properties, putatively to minimize damage to the host.

In further studies with H-CRP, which is preferred for mCRP, chemiluminescence potentiation between H-CRP and heat aggregated-IgG (H-IgG) is observed (55). H-CRP was unable to stimulate hydrogen peroxide generation in neutrophils alone, but when dosed with H-IgG, hydrogen peroxide generation was

significantly enhanced. Importantly, this potentiation was selectively limited to intracellular  $\text{H}_2\text{O}_2$  generation, and failed to upregulate ROS release from neutrophils, putatively describing a pathogen-fighting mechanism within neutrophils at infected sites that limits ROS damage to surrounding tissues. Later studies demonstrated that F- and A-CRP similarly potentiate the chemiluminescent output of H-IgG treated neutrophils (41). nCRP (pCRP) exhibited no increase in H-IgG-induced chemiluminescence. In these studies, F-CRP, A-CRP, and H-CRP were dosed as mixtures of aggregated and soluble protein, with the potentiating activity associated solely with the protein aggregates. This observation tracks with insoluble mCRP exhibiting the proinflammatory phagocytotic characteristics, while soluble pCRP does not.

More recently, the distinct effects of pCRP and mCRP on neutrophils have been characterized. Recombinant mCRP increased superoxide and peroxynitrite ( $\text{ONOO}^-$ ) production, subsequently causing a rise in nuclear factor  $\kappa\text{B}$  (NF- $\kappa\text{B}$ ) and activator protein-1 (AP-1) (56). pCRP had no corresponding effect on ROS production within a similar timeframe. As both  $\text{ONOO}^-$  and NF- $\kappa\text{B}$  are known to increase IL-8, the impact of recombinant mCRP on IL-8 concentration was evaluated and increased levels were observed within 4 hours. pCRP also upregulated IL-8 expression, but on a timescale of 24-hr, which suggests pCRP dissociated to mCRP (24). mCRP-mediated effects were nullified with an anti-CD16 antibody; pCRP does not bind CD16 while mCRP does. In addition to ROS generation, mCRP has also been implicated in neutrophil-platelet and neutrophil-neutrophil adhesion, a proinflammatory marker of poor cardiovascular outcomes (44). Conversely, preincubation of whole blood samples with pCRP decreased shear-induced neutrophil-platelet adhesion and neutrophil aggregation in a dose-dependent relationship. Treatment with H-CRP (“mCRP”) resulted in complete loss of this protective activity. mCRP’s proinflammatory effects are platelet P-selectin mediated, as mCRP enhanced P-selectin expression and increased the rate of neutrophil-platelet and neutrophil-neutrophil adducts in a dose dependent manner (1–50  $\mu\text{g/mL}$ ). The cellular adhesion molecule CD18 was also implicated. In a study of pCRP with anti-P-selectin and anti-CD18, nearly complete blockade of adhesion events was observed. pCRP effects were attenuated by anti-CD32, while mCRP effects were attenuated by anti-CD16.

In a similar vein, mCRP was found to drive tissue damage in ischemia/reperfusion injury via proinflammatory mechanisms of leukocyte-endothelial cell aggregation, leukotaxis, and ROS generation (57). These proinflammatory effects were successfully abrogated with the small molecule pCRP  $\rightarrow$  mCRP dissociation inhibitor 1,6-bisPC.

## mCRP activates monocyte cytokine release

Monocytes regulate cellular homeostasis in times of inflammation by scavenging for invader cells and promoting the inflammatory response. Monocytes can differentiate into interstitial

dendritic cells, microglial cells, and macrophages, and migrate into lesions inflamed by the immune system. As with neutrophils and platelets, the association of elevated serum CRP levels during the inflammatory response suggests a role for CRP in monocyte-macrophage infiltration (58). Prior to our understanding of distinct CRP isoforms, “CRP” (10 µg/mL) was found to induce macrophages to a tumoricidal state, (59) and CRP (50 µg/mL) prompted monocytes to release interleukin 1 beta (IL-1β), interleukin 6 (IL-6) and tumor necrosis factor alpha (TNF-α), with 10-fold higher levels of each cytokine observed at 4 hours (60, 61). Additional studies found CRP also promoted a 75-fold increase in tissue factor (TF)-mediated procoagulant activity, and significantly higher levels of interleukin-1α (IL-1α), GRO-α, GRO-β and IL-8 (62). Interestingly, CRP also exhibited anti-inflammatory properties in the upregulation of liver X receptor (LXR)-α.(63)

Studies with H-CRP enabled the characterization of mCRP-specific activity; first for adhesion, 70% of monocytes and 8% of mononuclear leukocytes were found adhered to H-CRP (41). Moreover, a significant enhancement in chemiluminescence was observed in response to H-CRP/H-IgG treatment, resulting from the respiratory burst that occurs during monocyte activation. Thus, it is hypothesized that H-CRP synergizes with IgG to promote Fc receptor-mediated stimulation of monocyte oxidative metabolism. Recombinant mCRP was later demonstrated to increase nitric oxide (NO)/inducible nitric oxide synthase (iNOS) levels (64). Conversely, pCRP exhibited anti-inflammatory effects by decreasing NO/iNOS production in macrophages and iNOS activity in monocytes. As with neutrophils and platelets described previously, reevaluation of the historical literature presents an argument for CRP’s proinflammatory properties being inherent to the mCRP isoform, while pCRP exhibits the anti-inflammatory activity.

## mCRP upregulates endothelial cell adhesion

Proinflammatory effects associated with “CRP”, commercially available from Calbiochem, were also observed in early studies with umbilical vein and human coronary artery endothelial cells (HCAECs) (67, 76). Specifically, recombinant CRP upregulated intercellular adhesion molecules (ICAM-1) to levels nearly 10-fold baseline and increased vascular cell adhesion molecule (VCAM-1) and E-selectin. The induced expression mimicked the effects of IL-1β and is implicated in the recruitment of monocytes and leukocytes (89). CRP also exhibited an inhibitory effect on endothelial nitric oxide synthase (eNOS) at incubation times >24-hr, which has proinflammatory implications for atherogenesis (67). Reduced nitric oxide (NO) production leads to arterial vasoconstriction, platelet adhesion and aggregation, and monocyte-endothelium adhesion (32, 67, 68, 90). It was confirmed that in the presence of 24-hr “CRP” treatment, there was a significant increase in monocyte adhesion, VCAM-1, and ICAM-1 expression. Given the unknown storage conditions and age

of the commercially available CRP, and the long incubation time of these experiments (24-hr), the presence of mCRP as a CRP sub-population is probable. Importantly, the *in vivo* half-life of pCRP is 19-24 hrs (91).

Once the existence of the mCRP isoform was elucidated, targeted studies on mCRP’s ability to activate endothelial cells were performed. mCRP (0.1–200 µg/mL), but not pCRP, was found to markedly upregulate CD11b/CD18 expression on neutrophils and enhance the adhesion of neutrophils to HCAECs (66). Adhesion was negated in the presence of an anti-CD18 mAb, correlating with the previous finding that pCRP with anti-P-selectin and anti-CD18 promoted complete blockade of adhesion between neutrophils and monocytes (See Neutrophil Discussion) (65). mCRP (1–30 µg/mL), specifically, also increased monocyte chemoattractant protein-1 (MCP-1) and IL-8 secretion, key mediators of leukocyte recruitment, as well as neutrophil-endothelial cell adhesion via the expression of ICAM-1, VCAM-1 and E-selectin (25). To observe the similar effects with nCRP preparations, a 6x longer incubation was required, implicating that pentameric dissociation had occurred.

Multiple studies implicated mitogen-activated protein kinase (MAPK) involvement in mCRP’s activation of endothelial cells as increased phosphorylation of p21<sup>ras</sup> (RAS) and p38 MAPK, and downstream activation of Raf-1, MAPKK and ERK, was observed. As pCRP binds primarily to low-affinity IgG FcγRIIa (CD32) and somewhat to high affinity IgG FcγRI (CD64) while mCRP binds to low-affinity IgG immune complex FcγRIIIb (CD16) (92–94), the effect of anti-CD16 and anti-CD32 were interrogated. Anti-CD16, but not anti-CD32, reduced MCP-1 and IL-8 secretion, ICAM-1, VCAM-1 and E-selectin expression, and corresponding neutrophil-endothelial cell adhesion 14-32-fold. Moreover, these effects were blunted when mCRP was tested in the presence of p38 MAPK inhibitor SB 203580. The incomplete attenuation of anti-CD16 on mCRP’s proinflammatory effects was later explained by membrane insertion. mCRP also binds to cholesterol microdomains (lipid rafts) in membranes via aa35–47 (consensus cholesterol binding sequence) and aa199–206 (95). When mCRP’s ability to bind lipid rafts was inhibited by methyl-β-cyclodextrin or nystatin, MCP-1 and IL-8 secretion was also downregulated. Accordingly, adhesion between endothelial cells and neutrophils was also reduced.

## mCRP promotes natural killer cell activity

With physiologically relevant effects on effector cells of the innate immune response, the consequence of CRP on NK cell-mediated killing was explored starting in the early 1980’s. Specifically, the first experiments gauged whether NK cells bind CRP and whether such binding events affect NK function by treating human lymphocytes with anti-CRP and C (72). It was found that under such conditions, the ability of NK cells to kill cellular targets (K562, MOLT-4 cells) was significantly diminished. Using biotin-avidin amplification with biotinylated anti-CRP and fluorescent avidin, membrane-bound CRP specifically, and not

plasma solubilized CRP, was determined to bind a subset of NK cells (~4%) and this binding event served as a promoter of NK activity (19). Like with previously discussed proinflammatory mechanisms, it is now understood that membrane (lipid raft)-bound CRP is enriched for the pCRP\*/mCRP isoform and fluid-phase CRP is absent of the neoepitope (pCRP). Accordingly, the NK activating properties of CRP are associated with pentameric dissociation. Further refinement of this understanding comes from flow cytometry studies using  $\alpha$ -neo-CRP antisera. In these studies, NK cells, displaying the surface markers CD16, CD11b, Leu-7 and Leu-19, reacted with the pCRP\*/mCRP-recognizing antisera as did cells expressing B-cell markers (74).  $\alpha$ -Native CRP failed to react with NK cells (73). Hamoudi and Baum further probed the mechanism of CRP-mediated NK activation by determining how anti-CRP inhibits NK cell lysis. As with previous studies, it was found that anti-CRP had no effect on the number of effector cell : target cell conjugates formed (75). Yet, the number of target cells killed by NK cells was largely diminished. This observation was negated when anti-CRP's effect on NK cells was investigated in the absence of  $\text{Ca}^{2+}$ . In the absence of  $\text{Ca}^{2+}$ , pCRP dissociates to mCRP.

## CRP both activates and inhibits complement cascades

When CPS was added to serum containing nCRP, the components of the classical complement (C) pathway were consumed, suggesting that CRP-CPS complexation is essential to trigger CRP-mediated innate immune responses (77, 84). C activation was subsequently observed when CRP complexed with polycations, *i.e.*, protamine, (78–80) positively charged liposomes, (69) and nuclear DNA (83, 96). C activation resulting from CRP lipid binding requires either PC or sphingomyelin in a  $\text{Ca}^{2+}$ -dependent manner (45, 77, 97–99). Lipid acyl chain length, degree of unsaturation, cholesterol concentration, and positively-charged lipid content (e.g. stearylamine, cetyltrimethylammonium, galactosyl ceramide) also impacted the degree of CRP binding (100). It is now known that ligand binding initiates conformational changes that expose the mCRP neoepitope facilitating binding to complement component 1q (C1q) and additional mediators of host defense. Ji et al. provided further evidence for this hypothesis by demonstrating that recombinant mCRP bound C1q in the C1q's collagen-like region (85). Regarding bioactivity, mCRP bound to oxidized low-density lipoprotein (LDL) activated the classical C pathway upon C1q binding. Conversely, mCRP alone bound and inhibited C1q from engaging other complement intermediates.

CRP activates the classical C cascade by directly binding C1q at the membranes of damaged cells, leading to near complete consumption of C1, C4 and C2 and partial consumption of C3 with minimal activation of C5–C9 and no cell lysis (84, 86, 101). This favors opsonization without a strong, global inflammatory response. Activation of the C cascade by CRP stimulates monocyte and macrophage phagocytosis both *in vitro* and *in vivo* and enhances opsonization of microbes by phagocytic cells (50, 70, 71).

To limit inflammatory responses to the damaged area, CRP also influences alternative complement pathway (AP) activity, downregulating deposition of C3b on AP-activating surfaces, decreasing C3 and C5 convertase activity and inhibiting C amplification feedback (20). In particular, on stearylamine-containing liposomes and on Types 6 and R36a Streptococcal pneumonia surfaces, CRP decreased serum C3-activation implicating CRP as a regulatory protein that can limit the extent of inflammatory damage initiated by C activation (69, 102). Taken together, CRP binding to damaged membrane or bacterial surfaces can preference the immune response towards classical pathway activation and away from the AP (102). AP inhibitory activity was found to be Factor H dependent, with direct binding of Factor H to CRP implicated through ELISA experimentation. Factor H – CRP binding was not inhibited in the presence of EDTA or PC, highlighting the presence of pCRP in this inflammatory dampening response (71). Moreover, complement factor H-related protein, which is structurally similar to C Factor H, was demonstrated to bind both pCRP and mCRP, with the former binding event requiring  $\text{Ca}^{2+}$  (87). As CFHR4 localizes to necrotic tumor tissues and binds necrotic cells, CRP-CFHR4 binding is implicated in the opsonization of necrotic cells. CRP-mediated inhibition of AP activation can also be facilitated by C4b-binding protein (C4bp), which like Factor H, inhibits C cascade at the level of C3 (34). Interestingly, while evidence suggests that both mCRP and pCRP bind Factor H, C4bp binding is unique to mCRP to enhance degradation of C4b and C3b. Finally, mCRP was demonstrated to bind properdin, an initiator of the AP cascade that binds necrotic and ECs (88). pCRP failed to exhibit similar properdin binding. mCRP-bound properdin was unable to bind endothelial cells, thus inhibiting AP activation via C3 and C5b-9 deposition of ECs. In total, CRP acts as a regulator of C activation, recruiting both C1q, the activator, C4bp, the inhibitor of the classical pathway, and properdin, an inhibitor of the AP. As mCRP preferably binds both C4bp and properdin, the monomeric isoform likely elicits greater control over the C cascade. This design enables an acute, localized proinflammatory response that is subsequently inhibited to prevent further-reaching inflammatory damage.

## Conclusion

Reevaluating the historical CRP literature with a current understanding of distinct CRP isoforms clearly intimates both pro- and anti-inflammatory function as part of the acute immune response. Moreover, these isoform-defined activities help to explain the considerable differences in CRP expression, but similar phenotypes, across species (103, 104). While human CRP levels can rise to 1000-fold over baseline, mouse and rat CRP levels only rise 2–3-fold, respectively (105, 106). The disconnect between CRP expression levels and activity highlights the functional importance of the active mCRP isoform, in addition to the species' mCRP generating capacity. Notably, rat CRP, which exists at baseline in the highest concentrations, exhibits the lowest mCRP generating capacity,

while the inverse describes mice (low baseline levels, high mCRP generating capacity). (103, 104) Taken together, mCRP levels are responsible for the pro-inflammatory activities regardless of species.

To highlight mechanisms of the CRP-mediated inflammatory response (Figure 2), we posit that circulating, sera-soluble pCRP begins to dissociate upon binding to multivalent ligands (PC, polycations, chromatin, etc.) in damaged membranes or in the presence of acidic inflammatory environments. The dissociation process, promoted by the proximity of hydrophobic membrane lipids, overcomes the  $\text{Ca}^{2+}$  stabilizing effect on pCRP and produces a transient intermediate form, pCRP\*, which maintains the pentameric quaternary structure but displays the neoepitope of mCRP and the C1q binding site. C1q binding to pCRP\* activates the classical C cascade, enhancing opsonization and phagocytosis in a localized proinflammatory response. Concurrently, to modulate global inflammatory damage, pCRP and/or mCRP binding to Factor H/CFHR4/C4bp/properdin inhibits the AP. As the pCRP  $\rightarrow$  mCRP transition is irreversible, pCRP\*  $\rightarrow$  mCRP goes to completion upon dissociation from the membrane and initiates localized proinflammatory effects. mCRP promotes platelet aggregation, dense and alpha-granule secretion from platelets, and thromboxane A<sub>2</sub> synthesis. mCRP also stimulates neutrophil migration, chemotaxis, and phagocytosis. mCRP activates cytokine release, particularly IL-1 $\alpha$ , IL-1 $\beta$ , IL-6, IL-8, TNF- $\alpha$ , E-selectin, MCP-1, GRO- $\alpha$  and GRO- $\beta$ , and promotes monocyte and EC adhesion. Finally, mCRP upregulates NK cell activity. Conversely, pCRP inhibits PAF-induced platelet aggregation and neutrophil activation and adhesion. The unique binding properties of pCRP and mCRP can be explained, in part, by differing preferences for IgG receptors, with mCRP favorably binding Fc $\gamma$ RIIIa/b (CD16) and pCRP preferentially binding Fc $\gamma$ RIIa (CD32).

Globally, the relationship of CRP isoforms and their contradictory bioactivities describe a mechanism of immune modulator response. Upon tissue damage or infection, while CRP levels are rising, pCRP  $\rightarrow$  mCRP conversion is rapid with overall CRP function exhibiting mCRP's proinflammatory characteristics (31). This short, localized, and potent response amplifies the acute phase of inflammation. Yet, mCRP's pro-inflammatory properties require control to limit widespread tissue damage implying that the pCRP  $\rightarrow$  mCRP conversion slows. At this point, elevated levels of pCRP are detectable in patient sera. Multiple studies predict that the lag between compromised tissue homeostasis and increased pCRP levels is 6-12-hrs, which corresponds to the mCRP pro-inflammatory activities discussed in this text (107–109).

The next chapter of CRP studies requires continued efforts into the characterization of pCRP and mCRP effects in localized immune responses to hone the diagnostic value of CRP for various pathologies. Moreover, given the distinct bioactivities of the CRP isoforms, an opportunity exists for small molecule and biologic tool and therapeutic development to elicit specific structure-function control. Currently, efforts in small molecule and biologic development have accomplished modulators of mCRP that either (1) inhibit pCRP to mCRP dissociation or (2) block mCRP binding to effector cells, respectively. Treatment with mCRP-specific antibodies (3C, 8C10) have been shown to relieve leukocyte infiltration in mouse models of rheumatoid arthritis and lupus nephritis and abrogate mCRP-induced memory loss in a mouse model of dementia (110–112). From a pharmacologic perspective, the first small molecule pCRP dissociation inhibitor, which is based on a bisphosphocholine scaffold, exhibited reduced myocardial infarction volume, cardiac dysfunction, inflammation, and mCRP deposition in rats (30, 113). On-going efforts in structural biology have mapped the pCRP – phosphocholine binding site, implicating key amino acids and a hydrophobic

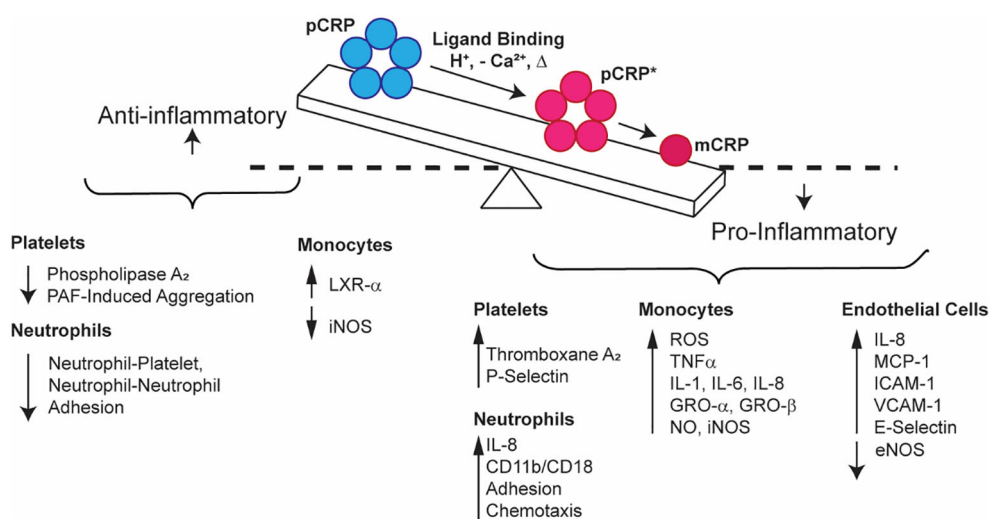


FIGURE 2

Schematic representation of the relationship between pro- (blue) and anti-inflammatory (red) CRP properties. pCRP exhibits anti-inflammatory outcomes, while mCRP exhibits proinflammatory activation of platelets, neutrophils, monocytes, endothelial cells, and natural killer cells. pCRP is the substrate for mCRP, which forms when pCRP undergoes a conformational change that first produces pCRP\*, an immunogenic, pentameric form, before fully dissociating to mCRP.



pocket that can drive further inhibitor development (112). While targeting mCRP offers a tantalizing opportunity for the next generation of anti-inflammatory drug development, a cautious approach towards understanding the implications of abrogating this conserved immune mechanism should be pursued. Regardless, the development of mCRP modulatory tools will be invaluable to further refine our understanding of CRP structure-function relationships.

## Author contributions

MO: Conceptualization, Formal Analysis, Investigation, Writing – original draft, Data curation, Writing – review & editing. MH: Formal Analysis, Writing – review & editing, Data curation, Investigation, Writing – original draft. AS: Data curation, Formal Analysis, Investigation, Writing – review & editing, Writing – original draft. HA: Writing – review & editing. AG: Writing – review & editing. GH: Writing – review & editing. PH: Formal Analysis, Writing – review & editing, Supervision. IR: Writing – review & editing. LP: Conceptualization, Data curation, Formal Analysis, Funding acquisition, Investigation, Project administration, Resources, Supervision, Writing – review & editing.

## References

1. Yao Z, Zhang Y, Wu H. Regulation of C-reactive protein conformation in inflammation. *Inflammation Res* (2019) 68:815–23. doi: 10.1007/s00011-019-01269-1
2. Dong Q, Wright JR. Expression of C-reactive protein by alveolar macrophages. *J Immunol* (1996) 156:4815–20. doi: 10.4049/jimmunol.156.12.4815
3. Yasojima K, Schwab C, McGeer EG, McGeer PL. Generation of C-reactive protein and complement components in atherosclerotic plaques. *Am J Pathol* (2001) 158:1039–51. doi: 10.1016/S0002-9440(10)64051-5
4. Calabró P, Willerson JT, Yeh ET. Inflammatory cytokines stimulated C-reactive protein production by human coronary artery smooth muscle cells. *Circulation* (2003) 108:1930–2. doi: 10.1161/01.CIR.0000096055.62724.C5
5. Jabs WJ, Lögering BA, Gerke P, Kreft B, Wolber EM, Klinger MH, et al. The kidney as a second site of human C-reactive protein formation in vivo. *Eur J Immunol* (2003) 33:152–61. doi: 10.1002/immu.200390018
6. Calabró P, Chang DW, Willerson JT, Yeh ET. Release of C-reactive protein in response to inflammatory cytokines by human adipocytes: linking obesity to vascular inflammation. *J Am Coll Cardiol* (2005) 46:1112–3. doi: 10.1016/j.jacc.2005.06.017
7. Kang DH, Park SK, Lee IK, Johnson RJ. Uric acid-induced C-reactive protein expression: implication on cell proliferation and nitric oxide production of human vascular cells. *J Am Soc Nephrol* (2005) 16:3553–62. doi: 10.1681/ASN.2005050572
8. Venugopal SK, Devaraj S, Jialal I. Macrophage conditioned medium induces the expression of C-reactive protein in human aortic endothelial cells: potential for paracrine/autocrine effects. *Am J Pathol* (2005) 166:1265–71. doi: 10.1016/S0002-9440(10)62345-0
9. Haider DG, Leuchten N, Schaller G, Gouya G, Kolodjaschna J, Schmetterer L, et al. C-reactive protein is expressed and secreted by peripheral blood mononuclear cells. *Clin Exp Immunol* (2006) 146:533–9. doi: 10.1111/j.1365-2249.2006.03224.x
10. Krupinski J, Turu MM, Martinez-Gonzalez J, Carvajal A, Juan-Babot JO, Iborra E, et al. Endogenous expression of C-reactive protein is increased in active (ulcerated noncomplicated) human carotid artery plaques. *Stroke* (2006) 37:1200–4. doi: 10.1161/01.STR.0000217386.37107.be
11. Vilahur G, Hernández-Vera R, Molins B, Casaní L, Duran X, Padró T, et al. Short-term myocardial ischemia induces cardiac modified C-reactive protein expression and proinflammatory gene (cyclo-oxygenase-2, monocyte chemoattractant protein-1, and tissue factor) upregulation in peripheral blood mononuclear cells. *J Thromb Haemost* (2009) 7:485–93. doi: 10.1111/j.1538-7836.2008.03244.x
12. Shrive AK, Gheetham GMT, Holden D, Myles DAA, Turnell WG, Volanakis JE, et al. Three dimensional structure of human C-reactive protein. *Nat Struct Biol* (1996) 3:346–54. doi: 10.1038/nsb0496-346
13. Potempa LA, Maldonado BA, Laurent P, Zemel ES, Gewurz H. Antigenic, electrophoretic and binding alterations of human C-reactive protein modified selectively in the absence of calcium. *Mol Immunol* (1983) 20:1165–75. doi: 10.1016/0161-5890(83)90140-2
14. Kresl JJ, Potempa LA, Anderson BE. Conversion of native oligomeric to a modified monomeric form of human C-reactive protein. *Int J Biochem Cell Biol* (1998) 30:1415–26. doi: 10.1016/S1357-2725(98)00078-8
15. Potempa LA, Yao ZY, Ji SR, Filep JG, Wu Y. Solubilization and purification of recombinant modified C-reactive protein from inclusion bodies using reversible anhydride modification. *Biophys Rep* (2015) 1:18–33. doi: 10.1007/s41048-015-0003-2
16. Crawford JR, Trial J, Nambi V, Hoogeveen RC, Taffet GE, Entman ML. Plasma levels of endothelial microparticles bearing monomeric C-reactive protein are increased in peripheral artery disease. *J Cardiovasc Transl Res* (2016) 9:184–93. doi: 10.1007/s12265-016-9678-0
17. Li QY, Li HY, Fu G, Yu F, Wu Y, Zhao MH. Autoantibodies against C-reactive protein influence complement activation and clinical course in lupus nephritis. *J Am Soc Nephrol* (2017) 28:3044–54. doi: 10.1681/ASN.2016070735
18. Zhang L, Li HY, Li W, Shen ZY, Wang YD, Ji SR, et al. An ELISA assay for quantifying monomeric C-reactive protein in plasma. *Front Immunol* (2018) 9:511. doi: 10.3389/fimmu.2018.00511
19. Samberg NL, Bray RA, Gewurz H, Landay AL, Potempa LA. Preferential expression of neo-CRP epitopes on the surface of human peripheral blood lymphocytes. *Cell Immunol* (1988) 116:86–98. doi: 10.1016/0008-8749(88)90212-2
20. Sproston NR, Ashworth JJ. Role of C-reactive protein at sites of inflammation and infection. *Front Immunol* (2018) 9:754. doi: 10.3389/fimmu.2018.00754
21. Ji S-R, Wu Y, Zhu L, Potempa LA, Sheng F-L, Lu W, et al. Cell membranes and liposomes dissociate C-reactive protein (CRP) to form a new, biologically active structural intermediate: mCRPm. *FASEB J* (2007) 21:284–94. doi: 10.1096/fj.06-6722com
22. Ullah N, Wu Y. Regulation of conformational changes in C-reactive protein alters its bioactivity. *Cell Biochem Biophys* (2022) 80:595–608. doi: 10.1007/s12013-022-01089-x
23. Haimovich B, Ji P, Ginalis E, Kramer R, Greco R. Phospholipase A2 enzymes regulate alpha IIb beta3-mediated, but not Fc gammaRII receptor-mediated,

## Funding

This work was funded by the National Institutes of Health (RF1 AG075832). The authors thank the Roosevelt University, College of Science, Health & Pharmacy for paying the publication fees.

## Conflict of interest

The authors declare that the research was conducted in the absence of any commercial or financial relationships that could be construed as a potential conflict of interest.

The author(s) declared that they were an editorial board member of Frontiers, at the time of submission. This had no impact on the peer review process and the final decision.

## Publisher's note

All claims expressed in this article are solely those of the authors and do not necessarily represent those of their affiliated organizations, or those of the publisher, the editors and the reviewers. Any product that may be evaluated in this article, or claim that may be made by its manufacturer, is not guaranteed or endorsed by the publisher.



- pp125FAK phosphorylation in platelets. *Thromb Haemost* (1999) 81:618–24. doi: 10.1055/s-0037-1614535
24. Wang HW, Sui SF. Dissociation and subunit rearrangement of membrane-bound human C-reactive proteins. *Biochem Biophys Res Commun* (2001) 288:75–9. doi: 10.1006/bbrc.2001.5733
25. Khreiss T, József L, Potempa LA, Filep JG. Conformational rearrangement in C-reactive protein is required for proinflammatory actions on human endothelial cells. *Circulation* (2004) 109:2016–22. doi: 10.1161/01.CIR.0000125527.41598.68
26. Potempa LA, Qiu WQ, Stefanski A, Rajab IM. Relevance of lipoproteins, membranes, and extracellular vesicles in understanding C-reactive protein biochemical structure and biological activities. *Front Cardiovasc Med* (2022) 9. doi: 10.3389/fcvm.2022.979461
27. Trial J, Potempa LA, Entman ML. The role of C-reactive protein in innate and acquired inflammation: new perspectives. *Inflammation Cell Signal* (2016) 3:e1409. doi: 10.14800/ics.1409
28. Habersberger J, Strang F, Scheichl A, Htun N, Bassler N, Merivirta RM, et al. Circulating microparticles generate and transport monomeric C-reactive protein in patients with myocardial infarction. *Cardiovasc Res* (2012) 96:64–72. doi: 10.1093/cvr/cvs237
29. Chang M-K, Binder CJ, Torzewski M, Witztum JL. C-reactive protein binds to both oxidized LDL and apoptotic cells through recognition of a common ligand: Phosphorylcholine of oxidized phospholipids. *Proc Natl Acad Sci USA* (2002) 99:13043–8. doi: 10.1073/pnas.192399699
30. Thiele JR, Habersberger J, Braig D, Schmidt Y, Goerendt K, Maurer V, et al. Dissociation of pentameric to monomeric C-reactive protein localizes and aggravates inflammation: in vivo proof of a powerful proinflammatory mechanism and a new anti-inflammatory strategy. *Circulation* (2014) 130:35–50. doi: 10.1161/CIRCULATIONAHA.113.007124
31. Rajab IM, Hart PC, Potempa LA. How C-reactive protein structural isoforms with distinctive bioactivities affect disease progression. *Front Immunol* (2020) 11:2126. doi: 10.3389/fimmu.2020.02126
32. Eisenhardt SU, Habersberger J, Murphy A, Chen YC, Woollard KJ, Bassler N, et al. Dissociation of pentameric to monomeric C-reactive protein on activated platelets localizes inflammation to atherosclerotic plaques. *Circ Res* (2009) 105:128–37. doi: 10.1161/CIRCRESAHA.108.190611
33. Slevin M, Matou-Nasri S, Turu M, Luque A, Rovira N, Badimon L, et al. Modified C-reactive protein is expressed by stroke neovessels and is a potent activator of angiogenesis in vitro. *Brain Pathol* (2010) 20:151–65. doi: 10.1111/j.1750-3639.2008.00256.x
34. Mhlan M, Blom AM, Kupreishvili K, Lauer N, Stelzner K, Bergström F, et al. Monomeric C-reactive protein modulates classic complement activation on necrotic cells. *FASEB J* (2011) 25:4198–210. doi: 10.1096/fj.11-186460
35. Strang F, Scheichl A, Chen YC, Wang X, Htun NM, Bassler N, et al. Amyloid plaques dissociate pentameric to monomeric C-reactive protein: a novel pathomechanism driving cortical inflammation in Alzheimer's disease? *Brain Pathol* (2012) 22:337–46. doi: 10.1111/j.1750-3639.2011.00539.x
36. Yang XW, Tan Y, Yu F, Zhao MH. Interference of antimodified C-reactive protein autoantibodies from lupus nephritis in the biofunctions of modified C-reactive protein. *Hum Immunol* (2012) 73:156–63. doi: 10.1016/j.humimm.2011.12.007
37. Braig D, Kaiser B, Thiele JR, Bannasch H, Peter K, Stark GB, et al. A conformational change of C-reactive protein in burn wounds unmasks its proinflammatory properties. *Int Immunol* (2014) 26:467–78. doi: 10.1093/intimm/dxu056
38. Fiedel BA. Platelet agonist synergism by the acute phase reactant C-reactive protein. *Blood* (1985) 65:264–9. doi: 10.1182/blood.V65.2.264.264
39. Fiedel BA, Simpson RM, Gewurz H. Activation of platelets by modified C-reactive protein. *Immunology* (1982) 45:439–47.
40. Vigo C. Effect of C-reactive protein on platelet-activating factor-induced platelet aggregation and membrane stabilization. *J Biol Chem* (1985) 260:3418–22. doi: 10.1016/S0021-9258(19)83638-4
41. Potempa LA, Zeller JM, Fiedel BA, Kinoshita CM, Gewurz H. Stimulation of human neutrophils, monocytes, and platelets by modified C-reactive protein (CRP) expressing a neoantigenic specificity. *Inflammation* (1988) 12:391–405. doi: 10.1007/BF00915774
42. Boncler M, Kehrel B, Szewczyk R, Stec-Martyna E, Bednarek R, Brodde M, et al. Oxidation of C-reactive protein by hypochlorous acid leads to the formation of potent platelet activator. *Int J Biol Macromol* (2018) 107:2701–14. doi: 10.1016/j.jbiomac.2017.10.159
43. Miyazawa K, Kiyono S, Inoue K. Modulation of stimulus-dependent human platelet activation by C-reactive protein modified with active oxygen species. *J Immunol* (1988) 141:570–4. doi: 10.4049/jimmunol.141.2.570
44. Khreiss T, Jozsef L, Potempa LA, Filep JG. Opposing effects of C-reactive protein isoforms on shear-induced neutrophil-platelet adhesion and neutrophil aggregation in whole blood. *Circulation* (2004) 110:2713–20. doi: 10.1161/01.CIR.0000146846.00816.DD
45. Shephard EG, Anderson R, Strachan AF, Kuhn SH, De Beer FC. CRP and neutrophils: functional effects and complex uptake. *Clin Exp Immunol* (1986) 63:718–27.
46. Buchta R, Fridkin M, Pontet M, Contessi E, Scaggiante B, Romeo D. Modulation of human neutrophil function by C-reactive protein. *Eur J Biochem* (1987) 163:141–6. doi: 10.1111/j.1432-1033.1987.tb10747.x
47. Wilkinson PC, Russell RJ, Allan RB. Leucocytes and Chemotaxis. *Agents Actions Suppl* (1977) 61–70. doi: 10.1007/978-3-0348-7290-4\_6
48. Kindmark CO. Stimulating effect of C-reactive protein on phagocytosis of various species of pathogenic bacteria. *Clin Exp Immunol* (1971) 8:941–8.
49. Mold C, Nakayama S, Holzer TJ, Gewurz H, Du Clos TW. C-reactive protein is protective against Streptococcus pneumoniae infection in mice. *J Exp Med* (1981) 154:1703–8. doi: 10.1084/jem.154.5.1703
50. Mold C, Edwards KM, Gewurz H. Effect of C-reactive protein on the complement-mediated stimulated of human neutrophils by Streptococcus pneumoniae serotypes 3 and 6. *Infect Immun* (1982) 37:987–92. doi: 10.1128/iai.37.3.987-992.1982
51. Holzer TJ, Edwards KM, Gewurz H, Mold C. Binding of C-reactive protein to the pneumococcal capsule or cell wall results in differential localization of C3 and stimulation of phagocytosis. *J Immunol* (1984) 133:1424–30. doi: 10.4049/jimmunol.133.3.1424
52. Tatsumi N, Hashimoto K, Okuda K, Kyougoku T. Neutrophil chemiluminescence induced by platelet activating factor and suppressed by C-reactive protein. *Clin Chim Acta* (1988) 172:85–92. doi: 10.1016/0009-8981(88)90123-4
53. Zurier RB, Weissmann G, Hoffstein S, Kammerman S, Tai HH. Mechanisms of lysosomal enzyme release from human leukocytes. II. Effects of cAMP and cGMP, autonomic agonists, and agents which affect microtubule function. *J Clin Invest* (1974) 53:297–309. doi: 10.1172/JCI107550
54. Spirer Z, Zakuth V, Diamant S, Stabinsky Y, Fridkin M. Studies on the activity of phorbol myristate acetate on the human polymorphonuclear leukocytes. *Experientia* (1979) 35:830–1. doi: 10.1007/BF01968279
55. Zeller JM, Sullivan BL. C-reactive protein selectively enhances the intracellular generation of reactive oxygen products by IgG-stimulated monocytes and neutrophils. *J Leukoc Biol* (1992) 52:449–55. doi: 10.1002/jlb.52.4.449
56. Khreiss T, Jozsef L, Potempa LA, Filep JG. Loss of pentameric symmetry in C-reactive protein induces interleukin-8 secretion through peroxynitrite signaling in human neutrophils. *Circ Res* (2005) 97:690–7. doi: 10.1161/01.RES.0000183881.11739.CB
57. Thiele JR, Zeller J, Kiefer J, Braig D, Kreuzaler S, Lenz Y, et al. A conformational change in C-reactive protein enhances leukocyte recruitment and reactive oxygen species generation in ischemia/reperfusion injury. *Front Immunol* (2018) 9:675. doi: 10.3389/fimmu.2018.00675
58. Whisler RL, Proctor VK, Downs EC, Mortensen RF. Modulation of human monocyte chemotaxis and procoagulant activity by human C-reactive protein (CRP). *Lymphokine Res* (1986) 5:223–8.
59. Zahedi K, Mortensen RF. Macrophage tumoricidal activity induced by human C-reactive protein. *Cancer Res* (1986) 46:5077–83.
60. Ballou SP, Lozanski G. Induction of inflammatory cytokine release from cultured human monocytes by C-reactive protein. *Cytokine* (1992) 4:361–8. doi: 10.1016/1043-4666(92)90079-7
61. Han KH, Hong KH, Park JH, Ko J, Kang DH, Choi KJ, et al. C-reactive protein promotes monocyte chemoattractant protein-1-mediated chemotaxis through upregulating CC chemokine receptor 2 expression in human monocytes. *Circulation* (2004) 109:2566–71. doi: 10.1161/01.CIR.0000131160.94926.6E
62. Cermak J, Key NS, Bach RR, Balla J, Jacob HS, Vercellotti GM. C-reactive protein induces human peripheral blood monocytes to synthesize tissue factor. *Blood* (1993) 82:513–20. doi: 10.1182/blood.V82.2.513.513
63. Hanriot D, Bello G, Ropars A, Seguin-Devaux C, Poitevin G, Grosjean S, et al. C-reactive protein induces pro- and anti-inflammatory effects, including activation of the liver X receptor alpha, on human monocytes. *Thromb Haemost* (2008) 99:558–69. doi: 10.1160/TH07-06-0410
64. Sproston NR, El Mohtadi M, Slevin M, Gilmore W, Ashworth JJ. The effect of C-reactive protein isoforms on nitric oxide production by U937 monocytes/macrophages. *Front Immunol* (2018) 9:1500. doi: 10.3389/fimmu.2018.01500
65. Zouki C, Beauchamp M, Baron C, Filep JG. Prevention of *In vitro* neutrophil adhesion to endothelial cells through shedding of L-selectin by C-reactive protein and peptides derived from C-reactive protein. *J Clin Invest* (1997) 100:522–9. doi: 10.1172/JCI119561
66. Zouki C, Haas B, Chan JS, Potempa LA, Filep JG. Loss of pentameric symmetry of C-reactive protein is associated with promotion of neutrophil-endothelial cell adhesion. *J Immunol* (2001) 167:5355–61. doi: 10.4049/jimmunol.167.9.5355
67. Venugopal SK, Devaraj S, Yuhanna I, Shaul P, Jialal I. Demonstration that C-reactive protein decreases eNOS expression and bioactivity in human aortic endothelial cells. *Circulation* (2002) 106:1439–41. doi: 10.1161/01.CIR.0000033116.22237.F9
68. Singh U, Devaraj S, Vasquez-Vivar J, Jialal I. C-reactive protein decreases endothelial nitric oxide synthase activity via uncoupling. *J Mol Cell Cardiol* (2007) 43:780–91. doi: 10.1016/j.jmcc.2007.08.015
69. Mold C, Gewurz H. Inhibitory effect of C-reactive protein on alternative C pathway activation by liposomes and Streptococcus pneumoniae. *J Immunol* (1981) 127:2089–92. doi: 10.4049/jimmunol.127.5.2089

70. Mold C, Du Clos TW, Nakayama S, Edwards KM, Gewurz H. C-reactive protein reactivity with complement and effects on phagocytosis. *Ann N Y Acad Sci* (1982) 389:251–62. doi: 10.1111/j.1749-6632.1982.tb22141.x
71. Mold C, Gewurz H, Du Clos TW. Regulation of complement activation by C-reactive protein. *Immunopharmacology* (1999) 42:23–30. doi: 10.1016/S0162-3109(99)00007-7
72. Baum LL, James KK, Glaviano RR, Gewurz H. Possible role for C-reactive protein in the human natural killer cell response. *J Exp Med* (1983) 157:301–11. doi: 10.1084/jem.157.1.301
73. James K, Baum L, Adamowski C, Gewurz H. C-reactive protein antigenicity on the surface of human lymphocytes. *J Immunol* (1983) 131:2930–4. doi: 10.4049/jimmunol.131.6.2930
74. Bray RA, Samberg NL, Gewurz H, Potempa LA, Landay AL. C-reactive protein antigenicity on the surface of human peripheral blood lymphocytes. Characterization of lymphocytes reactive with anti-neo-CRP. *J Immunol* (1988) 140:4271–8. doi: 10.4049/jimmunol.140.12.4271
75. Hamoudi WH, Baum LL. Anti-C-reactive protein inhibits the calcium-dependent stage of natural killer cell activation. *J Immunol* (1991) 146:2873–8. doi: 10.4049/jimmunol.146.8.2873
76. Pasceri V, Willerson JT, Yeh ET. Direct proinflammatory effect of C-reactive protein on human endothelial cells. *Circulation* (2000) 102:2165–8. doi: 10.1161/01.CIR.102.18.2165
77. Kaplan MH, Volanakis JE. Interaction of C-reactive protein complexes with the complement system. I. Consumption of human complement associated with the reaction of C-reactive protein with pneumococcal C-polysaccharide and with the choline phosphatides, lecithin and sphingomyelin. *J Immunol* (1974) 112:2135–47. doi: 10.4049/jimmunol.112.6.2135
78. Siegel J, Rent R, Gewurz H. Interactions of C-reactive protein with the complement system. I. Protamine-induced consumption of complement in acute phase sera. *J Exp Med* (1974) 140:631–47. doi: 10.1084/jem.140.3.631
79. Siegel J, Osmand AP, Wilson MF, Gewurz H. Interactions of C-reactive protein with the complement system. II. C-reactive protein-mediated consumption of complement by poly-L-lysine polymers and other polycations. *J Exp Med* (1975) 142:709–21. doi: 10.1084/jem.142.3.709
80. Mold C, Rodgers CP, Richards RL, Alving CR, Gewurz H. Interaction of C-reactive protein with liposomes. III. Membrane requirements for binding. *J Immunol* (1981) 126:856–60. doi: 10.4049/jimmunol.126.3.856
81. Volanakis JE. Complement activation by C-reactive protein complexes. *Ann N Y Acad Sci* (1982) 389:235–50. doi: 10.1111/j.1749-6632.1982.tb22140.x
82. Volanakis JE, Narkates AJ. Binding of human C4 to C-reactive protein-pneumococcal C-polysaccharide complexes during activation of the classical complement pathway. *Mol Immunol* (1983) 20:1201–7. doi: 10.1016/0161-5890(83)90143-8
83. Robey FA, Jones KD, Steinberg AD. C-reactive protein mediates the solubilization of nuclear DNA by complement *in vitro*. *J Exp Med* (1985) 161:1344–56. doi: 10.1084/jem.161.6.1344
84. Du Clos TW. Pentraxins: structure, function, and role in inflammation. *ISRN Inflammation* (2013) 2013:379040. doi: 10.1155/2013/379040
85. Ji SR, Wu Y, Potempa LA, Liang YH, Zhao J. Effect of modified C-reactive protein on complement activation: a possible complement regulatory role of modified or monomeric C-reactive protein in atherosclerotic lesions. *Arterioscler Thromb Vasc Biol* (2006) 26:935–41. doi: 10.1161/01.ATV.0000206211.21895.73
86. Edwards KM, Gewurz H, Lint TF, Mold C. A role for C-reactive protein in the complement-mediated stimulation of human neutrophils by type 27 *Streptococcus pneumoniae*. *J Immunol* (1982) 128:2493–6. doi: 10.4049/jimmunol.128.6.2493
87. Mhlan M, Hebecker M, Dahse HM, Hälbig S, Huber-Lang M, Dahse R, et al. Human complement factor H-related protein 4 binds and recruits native pentameric C-reactive protein to necrotic cells. *Mol Immunol* (2009) 46:335–44. doi: 10.1016/j.molimm.2008.10.029
88. O'Flynn J, van der Pol P, Dixon KO, Prohászka Z, Daha MR, van Kooten C. Monomeric C-reactive protein inhibits renal cell-directed complement activation mediated by properdin. *Am J Physiol Renal Physiol* (2016) 310:F1308–1316. doi: 10.1152/ajprenal.00645.2014
89. Patel SS, Thiagarajan R, Willerson JT, Yeh ET. Inhibition of alpha4 integrin and ICAM-1 markedly attenuate macrophage homing to atherosclerotic plaques in ApoE-deficient mice. *Circulation* (1998) 97:75–81. doi: 10.1161/01.CIR.97.1.75
90. Verma S, Wang CH, Li SH, Dumont AS, Fedak PW, Badiwala MV, et al. A self-fulfilling prophecy: C-reactive protein attenuates nitric oxide production and inhibits angiogenesis. *Circulation* (2002) 106:913–9. doi: 10.1161/01.CIR.0000029802.88087.5E
91. Hutchinson WL, Noble GE, Hawkins PN, Pepys MB. The pentraxins, C-reactive protein and serum amyloid P component, are cleared and catabolized by hepatocytes *in vivo*. *J Clin Invest* (1994) 94:1390–6. doi: 10.1172/JCI117474
92. Marnell LL, Mold C, Volzer MA, Burlingame RW, Du Clos TW. C-reactive protein binds to Fc gamma RI in transfected COS cells. *J Immunol* (1995) 155:2185–93. doi: 10.4049/jimmunol.155.4.2185
93. Stein MP, Edberg JC, Kimberly RP, Mangan EK, Bharadwaj D, Mold C, et al. C-reactive protein binding to Fc gamma RIa on human monocytes and neutrophils is allele-specific. *J Clin Invest* (2000) 105:369–76. doi: 10.1172/JCI7817
94. Heuertz RM, Schneider GP, Potempa LA, Webster RO. Native and modified C-reactive protein bind different receptors on human neutrophils. *Int J Biochem Cell Biol* (2005) 37:320–35. doi: 10.1016/j.biocel.2004.07.002
95. Ji SR, Ma L, Bai CJ, Shi JM, Li HY, Potempa LA, et al. Monomeric C-reactive protein activates endothelial cells via interaction with lipid raft microdomains. *FASEB J* (2009) 23:1806–16. doi: 10.1096/fj.08-116962
96. Shephard EG, van Helden PD, Strauss M, Böhm L, De Beer FC. Functional effects of CRP binding to nuclei. *Immunology* (1986) 58:489–94.
97. Parish WE. *Features of Human Spontaneous Vasculitis Reproduced Experimentally in Animals. Effects of Antiglobulins, C-Reactive Protein and Fibrin. Paper presented at: Experimental Models of Chronic Inflammatory Diseases*. Berlin, Heidelberg: Springer Berlin Heidelberg (1977).
98. Thompson D, Pepys MB, Wood SP. The physiological structure of human C-reactive protein and its complex with phosphocholine. *Structure* (1999) 7:169–77. doi: 10.1016/S0969-2126(99)80023-9
99. Wu Y, Potempa LA, El Kebir D, Filep JG. C-reactive protein and inflammation: conformational changes affect function. *Biol Chem* (2015) 396:1181–97. doi: 10.1515/hsz-2015-0149
100. Narkates AJ, Volanakis JE. C-reactive protein binding specificities: artificial and natural phospholipid bilayers. *Ann N Y Acad Sci* (1982) 389:172–82. doi: 10.1111/j.1749-6632.1982.tb22135.x
101. Haapasalo K, Meri S. Regulation of the complement system by pentraxins. *Front Immunol* (2019) 10:1750. doi: 10.3389/fimmu.2019.01750
102. Mold C, Kingzette M, Gewurz H. C-reactive protein inhibits pneumococcal activation of the alternative pathway by increasing the interaction between factor H and C3b. *J Immunol* (1984) 133:882–5. doi: 10.4049/jimmunol.133.2.882
103. Cheng B, Lv J-M, Liang Y-L, Zhu L, Huang X-P, Li H-Y, et al. Secretory quality control constrains functional selection-associated protein structure innovation. *Commun Biol* (2022) 5:268. doi: 10.1038/s42003-022-03220-3
104. Ji S-R, Zhang S-H, Chang Y, Li H-Y, Wang M-Y, Lv J-M, et al. C-reactive protein: the most familiar stranger. *J Immunol* (2023) 210:699–707. doi: 10.4049/jimmunol.2200831
105. Pepys MB, Hirschfield GM. C-reactive protein: a critical update. *J Clin Invest* (2003) 111:1805–12. doi: 10.1172/JCI200318921
106. Pathak A, Agrawal A. Evolution of C-reactive protein. *Front Immunol* (2019) 10:943. doi: 10.3389/fimmu.2019.00943
107. Kushner I, Feldmann G. Control of the acute phase response. Demonstration of C-reactive protein synthesis and secretion by hepatocytes during acute inflammation in the rabbit. *J Exp Med* (1978) 148:466–77. doi: 10.1084/jem.148.2.466
108. Colley CM, Fleck A, Goode AW, Muller BR, Myers MA. Early time course of the acute phase protein response in man. *J Clin Pathol* (1983) 36:203–7. doi: 10.1136/jcp.36.2.203
109. Nordgreen J, Munsterhjelm C, Aae F, Popova A, Boysen P, Ranheim B, et al. The effect of lipopolysaccharide (LPS) on inflammatory markers in blood and brain and on behavior in individually housed pigs. *Physiol Behav* (2018) 195:98–111. doi: 10.1016/j.physbeh.2018.07.013
110. Fujita C, Sakurai Y, Yasuda Y, Takada Y, Huang CL, Fujita M. Anti-monomeric C-reactive protein antibody ameliorates arthritis and nephritis in mice. *J Immunol* (2021) 207:1755–62. doi: 10.4049/jimmunol.2100349
111. García-Lara E, Aguirre S, Clotet N, Sawkulycz X, Bartra C, Almenara-Fuentes L, et al. Antibody protection against long-term memory loss induced by monomeric C-reactive protein in a mouse model of dementia. *Biomedicine* (2021) 9:828. doi: 10.3390/biomedicine9070828
112. Slevin M, Heidari N, Azamfirei L. Monomeric C-reactive protein: current perspectives for utilization and inclusion as a prognostic indicator and therapeutic target. *Front Immunol* (2022) 13:866379. doi: 10.3389/fimmu.2022.866379
113. Pepys MB, Hirschfield GM, Tennent GA, Gallimore JR, Kahan MC, Bellotti V, et al. Targeting C-reactive protein for the treatment of cardiovascular disease. *Nature* (2006) 440:1217–21. doi: 10.1038/nature04672



## OPEN ACCESS

## EDITED BY

Alok Agrawal,  
East Tennessee State University,  
United States

## REVIEWED BY

Shang-Rong Ji,  
Lanzhou University, China  
Partha Roy,  
Indian Institute of Technology Roorkee,  
India

## \*CORRESPONDENCE

Chayan Munshi  
✉ chayanbio@gmail.com

<sup>†</sup>These authors have contributed equally to this work

RECEIVED 11 June 2023

ACCEPTED 05 September 2023

PUBLISHED 04 October 2023

## CITATION

Bhattacharya S and Munshi C (2023)  
Biological significance of C-reactive  
protein, the ancient acute  
phase functionary.  
*Front. Immunol.* 14:1238411.  
doi: 10.3389/fimmu.2023.1238411

## COPYRIGHT

© 2023 Bhattacharya and Munshi. This is an open-access article distributed under the terms of the [Creative Commons Attribution License \(CC BY\)](#). The use, distribution or reproduction in other forums is permitted, provided the original author(s) and the copyright owner(s) are credited and that the original publication in this journal is cited, in accordance with accepted academic practice. No use, distribution or reproduction is permitted which does not comply with these terms.

# Biological significance of C-reactive protein, the ancient acute phase functionary

Shelley Bhattacharya<sup>1†</sup> and Chayan Munshi<sup>2\*†</sup>

<sup>1</sup>Department of Zoology, Visva-Bharati University, Santiniketan, India, <sup>2</sup>Ethophilia (An Autonomous Research Group), Santiniketan, India

C-reactive protein (CRP) is one of the major members of the family of acute phase proteins (APP). Interest in this CRP was the result of a seminal discovery of its pattern of response to pneumococcal infection in humans. CRP has the unique property of reacting with phosphocholine-containing substances, such as pneumococcal C-polysaccharide, in the presence of  $\text{Ca}^{2+}$ . The attention regarding the origin of CRP and its multifunctionality has gripped researchers for several decades. The reason can be traced to the integrated evolution of CRP in the animal kingdom. CRP has been unequivocally listed as a key indicator of infectious and inflammatory diseases including autoimmune diseases. The first occurrence of CRP in the evolutionary ladder appeared in arthropods followed by molluscs and much later in the chordates. The biological significance of CRP has been established in the animal kingdom starting from invertebrates. Interestingly, the site of synthesis of CRP is mainly the liver in vertebrates, while in invertebrates it is located in diverse tissues. CRP is a multifunctional player in the scenario of innate immunity. CRP acts as an opsonin in the area of complement activation and phagocytosis. Interestingly, CRP upregulates and downregulates both cytokine production and chemotaxis. Considering various studies of CRP in humans and non-human animals, it has been logically proposed that CRP plays a common role in animals. CRP also interacts with Fcγ receptors and triggers the inflammatory response of macrophages. CRP in other animals such as primates, fish, echinoderms, arthropods, and molluscs has also been studied in some detail which establishes the evolutionary significance of CRP. In mammals, the increase in CRP levels is an induced response to inflammation or trauma; interestingly, in arthropods and molluscs, CRP is constitutively expressed and represents a major component of their hemolymph. Investigations into the primary structure of CRP from various species revealed the overall relatedness between vertebrate and invertebrate CRP. Invertebrates lack an acquired immune response; they are therefore dependent on the multifunctional role of CRP leading to the evolutionary success of the invertebrate phyla.

## KEYWORDS

C-reactive protein, acute phase response, acute phase protein, innate immunity, inflammatory

**Abbreviations:** CRP, C-reactive protein; APP, acute phase protein; APR, acute phase response, ACRP, achitina CRP; SAP, serum amyloid P component.



## Phylogenetic history of CRP

Because of its special ability to react with the C-polysaccharide found in the pneumococcal cell wall, the protein is known as C-reactive protein (CRP) (1). Significant studies on CRP from *Limulus polyphemus* in the last century have conclusively proven the substance's antiquity (2, 3). CRP synthesis is activated in mammals (e.g., humans and rabbits), but it is constitutively expressed in the arthropod *Limulus* and makes up a significant portion of the hemolymph of horseshoe crabs at a concentration of 1–2 mg/mL (3). Additionally, the ophiurid (echinodermata) *Ophiocomina nigra* was found to have the CRP gene (4). A great deal of interest has been generated in investigating the relationships between the CRP gene and thromboxane A<sub>2</sub>, another chemical expressed in ophiurids, due to the properties of the transcriptome CRP that were determined to be particularly significant in this species (5, 6).

CRP has also been identified in the large African snail *Achatina fulica* (ACRP) as a typical hemolymph component (7). The newly hatched male has a concentration of 1 mg/mL, the most active hermaphrodite has a concentration of 3–5 mg/mL, and the sedentary female has a concentration of 1.5–2.8 mg/mL, demonstrating a direct association between the protein and the active phase of the animal (8). Like other vertebrate CRP, ACRP also acts as a scavenger of chromatin fragments as evidenced by its binding to the polycation poly-L-arginine. It is interesting that ACRP was found to enhance rat platelet aggregation *in vitro* in the presence of ADP and Ca<sup>2+</sup>, suggesting a probable role of ACRP in the aggregation of amoebocytes during the formation of plugs in injured tissue.

The estimated molecular weight of ACRP is 400 kDa, with a high absorbance in the 200–230 nm range, and it was discovered to be made up of four subunits with respective molecular weights of 110, 90, 62, and 60 kDa (8). The metal binding protein metallothionein, whose level in the hemolymph of *Achatina* increases from the male to the hermaphrodite to the female, showing a pattern that is very different from that of the ACRP titer, has been observed in vertebrates. ACRP has a high molar ratio (five) of metal binding, demonstrating its ability to sequester heavy metals. It was determined that the high level of metallothionein compensates functionally for the low titer of ACRP since both metallothionein and ACRP can sequester inorganic mercury in the sedentary female (8).

CRP has been observed in animals other than humans, including the freshwater fish *Channa punctatus* (9) and the Nile tilapia *Oreochromis niloticus* (10). Based on amino acid sequence analysis and the number of subunits, the main structure of human and rabbit CRP has been identified. CRP has been categorized into the pentraxin family of proteins (11, 12). As a result, gene sequence analyses provide information about the structure–function relationship of *Limulus* CRP as well as strong evidence of the two species' overall sequence similarity.

CRP is a cyclic oligomer found in different species that consists of nearly similar subunits with molecular weights of 20–30 kDa.

Phosphocholine is bound by CRP in a Ca<sup>2+</sup>-dependent way. It has also been shown that CRP from different species exhibit immunological cross-reactivity (13). It has been demonstrated that CRP exhibits ligand-binding specificities dependent on structure. Further research on invertebrate CRP is necessary to understand the factors that led to this evolution of CRP, as it has been suggested (13) that changes in intra- and inter-chain disulfide bonds and the glycosylation status of CRP caused the different structure–function relationships in various species.

The physiological role of CRP has not been well studied, despite a large number of findings on its biological effects in model systems and *in vitro*. Mice with endogenous CRP levels that are low even after an inflammatory stimulus were reported to be protected against infections with *Bacillus subtilis* and *Salmonella typhimurium* by *Achatina* CRP (ACRP). In addition, it was noted that the bacteria's growth curves demonstrated that ACRP has opposing effects on the two different types of bacteria, acting at a concentration of 50 µg/mL to be bacteriostatic against gram-negative salmonellae and bactericidal against gram-positive bacilli (14).

It has been established that the mechanism of action of ACRP was mediated by a loss of energy in the bacterial cells where ACRP inhibits the important carbohydrate metabolizing enzymes, disturbs the cellular redox potential homeostasis, reduces glutathione status, and is associated with a significantly increased rate of lipid peroxidation (14). By activating poly (ADP-ribose) polymerase-1 and caspase-3, ACRP may also cause the bacterial cells to die in a manner similar to apoptosis. Therefore, the production of reactive oxygen species (ROS) and metabolic impairment that resulted in apoptosis were the causes of the bacterial cells' demise (14). ACRP also works to reduce the load of environmental contaminants like lead (15). In this case, CRP was used to treat lead-treated mice and rats and reverse the hepatotoxicity (15).

*Achatina fulica* has attained widespread distribution and is currently regarded as one of the most successful evolutionary creatures. Researchers have been working to understand their intricate immune system over the past few decades in order to collect useful chemicals to treat human diseases. It has been shown that *Achatina* has crucial immunological components such the coagulation system, innate immune molecules, bioactive proteins, and CRP (16). The evolutionary importance of *Achatina* having strong innate immune defences and infection-fighting abilities has also been noted (17).

## Functional multiplicity of CRP

CRP is a versatile protein that has been known about since 1982 (18). It has long been known that vertebrates produce CRP as an acute phase protein (APP). CRP is a constitutively active protein in the hemolymph of the invertebrate phyla Arthropoda, Echinodermata, and Mollusca, whereas in the serum of vertebrates the concentration of CRP increases significantly following bacterial infections or other triggers such environmental toxins (19).

## Fish CRP

Five genes encoding similar molecules to CRP/serum amyloid-P component (SAP) were found when the entire genome of the Atlantic salmon (*Salmo salar*) was analyzed (20). It is interesting to note that these genes were divided into Group I (CRP/SAP-1a, CRP/SAP-1b, CRP/SAP-1c, and CRP/SAP-2) and Group II (CRP/SAP-3). The first group, known as the universal group, is found in all vertebrates, whereas the second group is unique to fish and amphibians. CRP/SAP-1a were found to be elevated by the cytokines interleukin (IL)- and interferon (IFN) in head kidney cells; however, the other four CRP/SAP were resistant, according to gene expression analyses (20). Serum amyloid-A5 (SAA-5) was the main APP in salmon, whose expression was solely induced by *Aeromonas salmonicida* in Atlantic salmon. This finding illustrates the potential functional distinction between salmon CRP/SAP and its mammalian homologues.

Nile tilapia's CRP gene has also been discovered (10). The data clearly demonstrate that CRP in Nile tilapia is a robust and active participant in the anti-bacterial immune response beginning with the agglutination of bacteria as well as the regulation of phagocytosis and inflammation. Tilapia CRP also plays a function during bacterial infection. Future research in this area will shed light on the defences the fish CRP employs against bacterial invasion.

## CRP in mammals

Under metal stress, the rabbit experiences a number of alterations, including the occurrence of CRP in the blood and a notable decrease in the serum titers of albumin and acetylcholinesterase (19). Marine mammals have also been linked to APP (21). The serum of manatees was used in immunological cross-reactivity experiments using SAA, haptoglobin, 1-acid glycoprotein, and CRP, and it was discovered that CRP was not a significant APP in this species (21). According to reports, SAA has this species' best diagnostic sensitivity for inflammatory illness (21). In stressed and injured manatees, SAA has been discovered to be an important prognostic marker (22). Additionally, specific CRP assays have been developed for use with serum samples from harbor seals suffering from inflammation-related illnesses such as pneumonia (23).

Several species of filarial worms are responsible for canine filariasis (24). The filaria lifecycle is primarily responsible for the pathophysiological response to infection. Many animal diseases, including filariasis in dogs afflicted with *Dirofilaria immitis*, *Brugia pahangi*, or both parasites, are diagnosed using serum protein profiles and CRP levels. Dogs with *D. immitis* or *B. pahangi* infections had average CRP levels of 69.9 mg/L and 12.9 mg/L, respectively. In contrast to *B. pahangi*-infected dogs, those with *D. immitis* infections had abnormally high CRP concentrations (24).

## Human CRP

Abdominal aortic aneurysm (AAA) and the CRP polymorphism rs3091244 are related. According to reports, AAA

involves an inflammatory process whose modulation is under the control of CRP (25). In a case-control study with two distinct populations of AAA patients, it was found that the rare T and A alleles were significantly associated with AAA presence in both populations and correlated with higher CRP levels and AAA diameter. This conclusion was drawn from the frequency of the functional triallelic (C, T, and A alleles) rs3091244 polymorphism.

The existing global data allow for the conclusion that atherosclerosis is the primary pathophysiologic contributor to cardiovascular disease, which is the major cause of morbidity and mortality in the adult population (26). The involvement of CRP in atherosclerosis is highlighted (26) because it is a fundamental aspect of chronic inflammation, is highly resistant to proteolysis, and is primarily synthesized in the liver in response to proinflammatory cytokines like IL-6, IL-1 $\beta$ , and tumor necrosis factor (TNF). In addition to causing apoptosis, vascular cell activation, monocyte recruitment, lipid buildup, and thrombosis, CRP also directly stimulates the complement system (26). It is interesting to note that in peripheral tissue and atheromatous plaques, where each form exhibits distinct affinities for ligands and receptors and exerts different effects in the progression of atherosclerosis, CRP dissociates from its native pentameric form into a monomeric form, and it was determined that CRP is a reliable criterion for the assessment of cardiovascular risk (26).

In one investigation, New Zealand white rabbits were used to assess how immunization affects APP (27). Plasma CRP levels changed after receiving several experimental vaccinations (27). When rabbits were treated with vaccines containing novel adjuvants that activate Toll-like receptors, it was observed that the incidence and intensity of responses associated with the acute phase response (APR), both positive and negative APP, increased. The notable changes in the plasma levels of CRP served as a foundation for the proposal of a classification scheme of high, medium, low, and none. According to the study's findings, the alterations in plasma proteins show that systemic inflammation is becoming more severe and is associated with significant clinical adverse effects in addition to reflecting an activation of the APR (27).

Erythrocyte sedimentation rate and CRP were measured in patients with hepato-splenomegaly, high blood pressure, diabetic mellitus with polyneuropathy, oral cavity infection, and other conditions of unknown etiology (28). The erythrocyte sedimentation rate was shown to be less sensitive and accurate in reflecting the APR than the CRP (28). With detection limits of less than 0.3 mg/L and a stronger risk prediction than LDL cholesterol, CRP levels were very high in arthritis and were thought to be positively associated with the risk of future coronary events like coronary artery, cerebrovascular, and peripheral arterial diseases (28). Nevertheless, in such cases, the use of CRP assay is advised.

In patients with hyperleptinemia, the interaction of CRP with the leptin receptor has also been documented (29). Ironically, leptin insufficiency is the root cause of morbid obesity, and people with this condition have elevated leptin levels. CRP is crucial in this medical condition for binding to leptin. The study of blood levels of CRP, leptin, and soluble leptin receptor following a solid phase binding test and the co-immunoprecipitation of CRP and soluble leptin receptor from human plasma with elevated levels of CRP were used to validate the interaction of CRP (29).



CRP is known to be largely produced by hepatocytes and can increase by a factor of 1,000 at infection sites. The native form of CRP is a homopentameric protein that permanently splits into five monomeric forms of CRP. However, smooth muscle cells, macrophages, endothelial cells, lymphocytes, and adipocytes are also capable of producing CRP. The CRP levels may also be impacted by estrogen used in hormone replacement therapy (30).

CRP can be found in two different states—native pentameric and monomeric—and these two forms can attach to various receptors or lipid rafts to take on various functional characteristics. While some studies have shown that CRP is also linked to chronic inflammation, it is recognized as a biomarker of acute inflammation. This indicates the clinical importance of CRP in chronic inflammatory and neurodegenerative diseases, including the role of CRP and its forms specifically in the pathogenesis of these diseases, including cardiovascular disease, type 2 diabetes mellitus, age-related macular degeneration, hemorrhagic stroke, Alzheimer's disease, and Parkinson's disease. These developments need to be translated into reliable methods for the diagnosis and treatment of inflammatory diseases (31).

It is commonly acknowledged that CRP has both pro- and anti-inflammatory characteristics. By binding to phosphocholine, phospholipids, histone, chromatin, and fibronectin, CRP plays a significant role in the identification and removal of pathogens as well as injured cells. It has been found to speed up the elimination of cellular debris, injured or apoptotic cells, and foreign pathogens by activating the traditional complement system and the phagocytic cells via Fc receptors (32). As seen in idiopathic thrombocytopenic purpura (32), this turns pathogenic if activated by autoantibodies with the phosphocholine arm that cause auto-immune processes. The indirect test of ESR for inflammation, on the other hand, has revealed that CRP cannot distinguish between bacterial and non-bacterial illnesses, and that CRP levels rise quickly at the start of an inflammatory stimulus and fall when it is removed (33–35). Elevated CRP levels are persistent in conditions like chronic inflammation or rheumatoid arthritis. Such elevated CRP levels have been observed in both acute and chronic diseases, with either infectious or non-infectious etiologies. However, noticeably increased levels of CRP are frequently connected to pathogen- or infection-related molecular pattern recognition (36). CRP levels increase with trauma (an alarm reaction), but these elevations have also been linked to a variety of conditions, from sleep disorders to periodontal disease. It can be challenging to draw any conclusions regarding the importance of a high CRP level as a prognostic marker for cardiovascular disease because chronic diseases such as inflammatory arthritis or SLE can result in chronically elevated CRP (32). As a result, it was suggested that CRP levels above 50 mg/dL are typically caused by a high rate of bacterial infection and have been used as a prognostic indicator for both acute and chronic cases of hepatitis C, dengue fever, and malaria (37–39).

## Concluding remarks

Animals have two different types of response proteins: heat shock proteins and APP. The end result of a long-ago stress reaction

to many sorts of stress-inducing environmental stressors are heat shock proteins. It has been noted that biodiversity stress responses are brought on by changing conditions and are significantly associated to the local biotic and abiotic components (40). Furthermore, it is an inducible response at a level probably determined during their development in a temperature-labile environment (41). The tolerance range of environmental temperature, on the other hand, reveals the resistance to climate change (42). Contrarily, a general systemic response is elicited in response to acute circumstances of inflammation brought on by primarily bacterial exposure, and specific proteins are categorized under acute phase proteins, where they are distinguished as CRP brought on by tissue damage (43). Since air-breathing animals, both invertebrates and vertebrates, have retained the imprint of heat shock response proteins during their history, it may be inferred that the evolution of CRP is controlled by epigenetic responses acquired during that time.

In general, all animals respond to all types of wounds and stress to keep the body's homeostasis system in place. This equilibrium is either achieved by specific or by non-specific mechanisms, such as leukocytosis as well as cytological and cytokine reactions. These reactions—the APR—lead to an alteration in the serum concentration of acute phase proteins. It has recently been proven that such assessments of the serum concentration of these acute phase proteins aid in determining the health condition of animals and disease prognosis. Since the APR is a dynamic process, when the triggering element is absent, the serum concentration of the APRs recovers to the basal level. Additionally, the APRs cause metabolic changes and send out early, non-specific signals of defence against an insult before specific immunity is developed. Therefore, there is great potential for CRP to be used in contemporary veterinary practise for illness diagnosis and health status evaluation in animals (44).

Recent research has shown that major depressive disorder in humans negatively affects the mental health of 264 million people worldwide (45). Although the risk has not been tied to polygenic CRP, blood CRP level has been found to be strongly associated with a history of mental disorders (46). Studies have also shown that polymorphisms in the CRP gene might have directly altered production of CRP in the liver in these patients (47). There is evidence that people with major depressive disorder have higher levels of CRP and other proinflammatory biomarkers.

Researchers have discovered a novel function for CRP, eloquently demonstrating the evolutionary significance of this old molecule. CRP initially manifested in invertebrates as constitutively produced proteins without pro- or anti-inflammatory characteristics. The intricate roles of CRP have gradually come into focus in higher evolutionary lineages, culminating in humans.

CRP is structurally a pentameric molecule composed of identical monomers. There are three types of CRP: monomeric CRP (mCRP), non-native pentameric CRP, and native pentameric CRP (native CRP). For host defence, both native and non-native CRP perform ligand-recognition tasks. Any pentameric CRP will dissociate into ligand-bound mCRP after binding to a ligand. If ligand-bound mCRP possesses the same proinflammatory properties as free mCRP, which have been demonstrated *in vitro*,

then both mCRP and the associated ligand must be eliminated from the site of inflammation. Pentameric CRP decreases the production of foam cells and the proinflammatory effects of atherogenic low-density lipoprotein (LDL) once it has been linked to atherogenic LDL. In a mouse model of atherosclerosis, it has been discovered that a CRP mutant, also known as non-native CRP, is atheroprotective. A medication that can only decrease cholesterol levels and not CRP levels, unlike statins, should thus be created. It is plausible that non-native CRP might be protective against all inflammatory conditions in which host proteins turn pathogenic because non-native CRP has been demonstrated to bind to all types of defective proteins in general. It would be preferable to use a small-molecule drug to target CRP with the aim of changing the conformation of endogenous native CRP rather than recombinant non-native CRP as a biologic to treat diseases brought on by pathogenic proteins like oxidized LDL if research using transgenic mice demonstrates that non-native CRP is advantageous for the host (48).

CRP is generated by the liver when there is inflammation, and atherosclerosis is an inflammatory cardiovascular disease. A putative function for CRP in atherosclerosis is suggested by the co-localization of CRP and low-density lipoproteins (LDL) at atherosclerotic lesions. If the phosphocholine groups in LDL are not accessible, CRP does not interact with LDL; it only interacts with molecules containing phosphocholine. However, if CRP's natural conformation is changed, it can attach to LDL without exposing phosphocholine groups. Site-directed mutagenesis produced the CRP mutant F66A/T76Y/E81A, which does not bind to phosphocholine. It was shown that this mutant CRP could attach to atherogenic LDL without undergoing any further conformational changes. A CRP mutant can bind to atherogenic LDL, is reported to have atheroprotective role in a murine model of atherosclerosis. Mice given mutant CRP treatment for 9 weeks had atherosclerotic lesions in their aortas that were 40% smaller in size than lesions in untreated mice's aortas. Thus, mutant CRP gave protection against atherosclerosis, demonstrating that a structural change brought on by local inflammation in wild-type CRP is necessary for CRP to limit the growth of atherosclerosis (49).

In the acute phase of the reaction, CRP levels in the serum significantly rise. Maximum CRP expression is seen in cells treated with both IL-6 and IL-1 in human hepatoma Hep3B cells. A synergistic interaction between IL-1 and IL-6 causes transcription of the CRP gene to be induced. Four consensus signal transducer and activator of transcription (STAT3)-binding sites located at positions 72, 108, 134, and 164 on the CRP promoter regulates the function of IL-6-activated transcription factor STAT3. Prior research has demonstrated that STAT3 binds to the location at 108 and activates CRP expression. Additionally, STAT3 bound to the other three sites, and several STAT3-containing complexes developed at each site, indicating the inclusion of other transcription factors and STAT3 isoforms in the complexes. Although the synergy between IL-6 and IL-1 was unaffected by the mutations, CRP expression was lowered in response to IL-6 and IL-1 treatment when the STAT3 sites

at positions 108, 134, or 164 were altered. Mutagenesis was unable to be used to study the STAT3 location at position 72. In Hep3B cells, IL-6 activated two STAT3 isoforms. The isoforms of STAT3 are STAT3 $\alpha$  and STAT3 $\beta$ , where the former has both DNA-binding domain and a transactivation domain whereas the latter contains only the DNA-binding domain (50).

In hepatocytes, the promoter of human CRP lies 37.7 kb upstream of a constitutively active enhancer (E1). We demonstrate that E1 is enriched in STAT3- and C/EBP-binding sites and is required for the entire induction of human CRP during the acute phase utilizing chromatin immunoprecipitation, luciferase reporter assay, *in situ* genetic modification, CRISPRi, and CRISPRa. Furthermore, by examining the activities of E1-promoter hybrids and the related epigenetic alterations, we show that E1 coordinates with the promoter of CRP to control its variable expression across tissues and species. These findings thus point to an intriguing form of molecular evolution in which expression-changing mutations in distal regulatory elements start a process of functional selection that involves interaction between distal/proximal regulatory alterations and activity-changing coding mutations (51).

CRP is a pentraxin with characteristics like those of a pattern recognition receptor. The *in vivo* activities of CRP and its involvement in health and illness, although being widely utilized as a clinical measure of inflammation, remain largely unestablished. This is partially explained by the fact that the expression patterns of CRP in mice and rats are radically different from one another. This raises questions regarding whether these activities of CRP are crucial and preserved across species, as well as how these model animals should be treated to investigate the *in vivo* effects of human CRP. The enhanced model architecture will help define the pathophysiological functions of CRP and aid in the creation of fresh CRP-targeting tactics (52).

In conclusion, almost all phylogenetic representatives have shown over the past several decades that CRP has a variety of functions, and it continues to be an intriguing and perplexing protein for animal survival. Further research will shed light on CRP's vital allies in the fight for survival of animals lacking an acquired immune response and will emphasize the protein's flexibility in influencing several survival pathways.

## Author contributions

SB and CM both contributed to writing the manuscript. All authors contributed to the article and approved the submitted version.

## Conflict of interest

The authors declare that the research was conducted in the absence of any commercial or financial relationships that could be construed as a potential conflict of interest.

## Publisher's note

All claims expressed in this article are solely those of the authors and do not necessarily represent those of their affiliated

organizations, or those of the publisher, the editors and the reviewers. Any product that may be evaluated in this article, or claim that may be made by its manufacturer, is not guaranteed or endorsed by the publisher.

## References

- Tillett WS, Francis T. Serological reactions in pneumonia with a nonprotein somatic fraction of pneumococcus. *J Exp Med* (1930) 52:561–71. doi: 10.1084/jem.52.4.561
- Nguyen NY, Suzuki A, Boykins RA, Liu TY. The amino acid sequence of *Limulus* C-reactive protein. Evidence of polymorphism. *J Biol Chem* (1986) 261:10456–9. doi: 10.1016/S0021-9258(18)67546-5
- Nguyen NY, Suzuki A, Cheng SM, Zon G, Liu TY. Isolation and characterization of *Limulus* C-reactive protein genes. *J Biol Chem* (1986) 261:10450–55. doi: 10.1016/S0021-9258(18)67545-3
- Leclerc M. New cytokine genes in an invertebrate: Thromboxane ones in Echinodermata. *J R Sci* (2019) 1:1–2.
- Carter AB, Monick MM, Hunninghake GW. Both Erk and p38 kinases are necessary for cytokine gene transcription. *Am J Respir Cell Mol Biol* (1999) 20:751–8. doi: 10.1165/ajrcmb.20.4.3420
- Leclerc M. CRP gene in an invertebrate: *Ophiocoma nigrum* (Echinodermata). *Genet Mol Med* (2019) 1:2–3. doi: 10.33425/2689-1077.1002
- Agrawal A, Mitra S, Ghosh N, Bhattacharya S. C-reactive protein (CRP) in hemolymph of a mollusc, *Achatina fulica* Bowdich. *Indian J Exp Biol* (1990) 28:788–9.
- Bose R, Bhattacharya S. C-reactive protein in the hemolymph of *Achatina fulica*: Interrelationship with sex steroids and metallothionein. *Comp Biochem Physiol - A Mol Integr Physiol* (2000) 125:485–95. doi: 10.1016/S1095-6433(00)00176-8
- Mitra S, Bhattacharya S. Purification of C-reactive protein from *Channa punctatus* (Bloch). *Indian J Biochem Biophys* (1992) 29:508–11.
- Li Q, Jiang B, Zhang Z, Huang Y, Xu Z, Chen X, et al. CRP involved in Nile Tilapia (*Oreochromis niloticus*) against bacterial infection. *Biol (Basel)* (2022) 11:1–7. doi: 10.3390/biology11081149
- Oliveira EB, Gotschlich EC, Liu TY. Primary structure of human C-reactive protein. *J Biol Chem* (1979) 254:489–502. doi: 10.1016/S0021-9258(17)37943-7
- Wang CM, Nguyen NY, Yonaha K, Robey F, Liu TY. Primary structure of rabbit C-reactive protein. *J Biol Chem* (1982) 257:13610–5. doi: 10.1016/S0021-9258(18)33491-4
- Pathak A, Agrawal A. Evolution of C-reactive protein. *Front Immunol* (2019) 10:943. doi: 10.3389/fimmu.2019.00943
- Mukherjee S, Barman S, Sarkar S, Mandal NC, Bhattacharya S. Anti-bacterial activity of *Achatina* CRP and its mechanism of action. *Indian J Exp Biol* (2014) 52:692–704.
- Mukherjee S, Chatterjee S, Sarkar S, Agarwal S, Kundu R, Maitra S, et al. Mollusc C-reactive protein crosses species barrier and reverses hepatotoxicity of lead in rodent models. *Indian J Exp Biol* (2013) 51:623–34.
- Mukherjee S, Sarkar S, Munshi C, Bhattacharya S. The uniqueness of *Achatina fulica* in its evolutionary success. *Intech Open* (2016) 11:13. doi: 10.5772/68134
- Lima MG, Augusto R de C, Pinheiro J, Thiengo SC. Physiology and immunity of the invasive giant African snail, *Achatina* (Lissachatina) *fulica*, intermediate host of *Angiostrongylus cantonensis*. *Dev Comp Immunol* (2020) 105:1–22. doi: 10.1016/j.dci.2019.103579
- Gewurz H, Mold C, Siegel J, Fiedel B. C-reactive protein and the acute phase response. *Adv Intern Med* (1982) 27:345–72. doi: 10.1080/21548331.1982.11702332
- Ghosh N, Bhattacharya S. Acute phase response of rabbit to HgCl<sub>2</sub> and CdCl<sub>2</sub>. *BioMed Environ Sci* (1993) 6:1–7.
- Lee PT, Bird S, Zou J, Martin SAM. Phylogeny and expression analysis of C-reactive protein (CRP) and serum amyloid-P (SAP) like genes reveal two distinct groups in fish. *Fish Shellfish Immunol* (2017) 65:42–51. doi: 10.1016/j.fsi.2017.03.037
- Harr K, Harvey J, Bonde R, Murphy D, Lowe M, Menchaca M, et al. Comparison of methods used to diagnose generalized inflammatory disease in manatees (*Trichechus manatus latirostris*). *J Zoo Wildl Med* (2006) 37:151–9. doi: 10.1638/05-023.1
- Cray C, Zaia S, Altman NH. Acute phase response in animals: A review. *Comp Med* (2009) 59:517–26.
- Cray C. *Acute phase proteins in animals*. (USA: American Association for Laboratory) (2012). pp. 113–50.
- Asawakarn S, Sirisawadi S, Kunnasut N, Kamkong P, Taweethavongsawat P. Serum protein profiles and C-reactive protein in natural canine filariasis. *Vet World* (2021) 14:860–4. doi: 10.14202/vetworld.2021.860-864
- Saratzis A, Bown M, Wild B, Sayers RD, Nightingale P, Smith J, et al. C-reactive protein polymorphism rs3091244 is associated with abdominal aortic aneurysm. *J Vasc Surg* (2014) 60:1332–9. doi: 10.1016/j.jvs.2013.07.105
- Salazar J, Martínez MS, Chávez-Castillo M, Núñez V, Afiez R, Torres Y, et al. C-reactive protein: An in-depth look into structure, function, and regulation. *Int Sch Res Not* (2014) 2014:1–11. doi: 10.1155/2014/653045
- Green MD. Acute phase responses to novel, investigational vaccines in toxicology studies: The relationship between C-reactive protein and other acute phase proteins. *Int J Toxicol* (2015) 34:379–83. doi: 10.1177/1091581815598750
- Ram M, Rao M, Gopal SD. Case study C-reactive protein -A critical review. *Int J Curr Microbiol App Sci* (2015) 4:55–61.
- Sudhakar M, Silambanan S, Chandran AS, Prabhakaran AA, Ramakrishnan R. C-reactive protein (CRP) and leptin receptor in obesity: Binding of monomeric CRP to leptin receptor. *Front Immunol* (2018) 9:1–13. doi: 10.3389/fimmu.2018.01167
- Sproston NR, Ashworth JJ. Role of C-reactive protein at sites of inflammation and infection. *Front Immunol* (2018) 9:1–11. doi: 10.3389/fimmu.2018.00754
- Luan YY, Yao YM. The clinical significance and potential role of C-reactive protein in chronic inflammatory and neurodegenerative diseases. *Front Immunol* (2018) 9:1–8. doi: 10.3389/fimmu.2018.01302
- Nehring SM, Goyal A, Patel BC. C reactive protein history. *StatPearls* (2019), 2–5.
- Cleland D, Eranki A. Procalcitonin. *StatPearls* (2023).
- Jungen MJ, Ter Meulen BC, Van Osch T, Weinstein HC, Ostelo RWJG. Inflammatory biomarkers in patients with sciatica: A systematic review. *BMC Musculoskelet Disord* (2019) 20:1–9. doi: 10.1186/s12891-019-2541-0
- Kramer NE, Cosgrove VE, Dunlap K, Subramaniapillai M, McIntyre RS, Suppes T. A clinical model for identifying an inflammatory phenotype in mood disorders. *J Psychiatr Res* (2019) 113:148–58. doi: 10.1016/j.jpsychires.2019.02.005
- Vanderschueren S, Deeren D, Knockaert DC, Bobbaers H, Bossuyt X, Peetermans W. Extremely elevated C-reactive protein. *Eur J Intern Med* (2006) 17:430–3. doi: 10.1016/j.ejim.2006.02.025
- de Souza Pires-Neto O, da Silva Graça Amorim E, Queiroz MAF, Demachki S, da Silva Conde SR, Ishak R, et al. Hepatic TLR4, MBL and CRP gene expression levels are associated with chronic hepatitis C. *Infect Genet Evol* (2020) 80:104200. doi: 10.1016/j.meegid.2020.104200
- Vuong NL, Le Duyen HT, Lam PK, Tam DTH, Van Vinh Chau N, Van Kinh N, et al. C-reactive protein as a potential biomarker for disease progression in dengue: A multi-country observational study. *BMC Med* (2020) 18:1–13. doi: 10.1186/s12916-020-1496-1
- Bhardwaj N, Ahmed M, Sharma S, Nayak A, Anvikar A, Pande V. C-reactive protein as a prognostic marker of Plasmodium falciparum malaria severity. *J Vector Borne Dis* (2019) 56:122–6. doi: 10.4103/0972-9062.263727
- Collins M, Peck LS, Clark MS. Large within, and between, species differences in marine cellular responses: Unpredictability in a changing environment. *Sci Total Environ* (2021) 794:148594. doi: 10.1016/j.scitotenv.2021.148594
- Clark MS, Fraser KPP, Peck LS. Antarctic marine molluscs do have an HSP70 heat shock response. *Cell Stress Chaperones* (2008) 13:39–49. doi: 10.1007/s12192-008-0014-8
- Morley SA, Chu JWF, Peck LS, Bates AE. Temperatures leading to heat escape responses in Antarctic marine ectotherms match acute thermal limits. *Front Physiol* (2022) 13:1–8. doi: 10.3389/fphys.2022.1077376
- Gabay C, Kushner I. Acute phase proteins and other systemic responses to inflammation. *N Engl J Med* (1999) 340:448–54. doi: 10.1056/NEJM199902113400607
- Yogeshpriya S, Selvaraj P. C-reactive protein in veterinary practice. *J Dairy Vet Sci* (2019) 13:1–3. doi: 10.19080/JDVS.2019.13.55858
- American Psychiatric Association. *Diagnostic and statistical manual of mental disorders*. 5th ed. Washington D.C: American Psychiatric Association (2013).
- Milton DC, Ward J, Ward E, Lyall DM, Strawbridge RJ, Smith DJ, et al. The association between C-reactive protein, mood disorder, and cognitive function in UK Biobank. *Eur Psychiatry* (2021) 64:1–10. doi: 10.1192/j.eurpsy.2021.6
- Halaris A, Prochaska D, Stefanski A, Maria Filip M. C-reactive protein in major depressive disorder: Promise and challenge. *J Affect Disord Rep* (2022) 10:100427. doi: 10.1016/j.jadr.2022.100427
- Singh SK, Agrawal A. Functionality of C-reactive protein for atheroprotection. *Front Immunol* (2019) 10:1655. doi: 10.3389/fimmu.2019.01655

49. Pathak A, Singh SK, Thewke DP, Agrawal A. Conformationally altered C-reactive protein capable of binding to atherogenic lipoproteins reduces atherosclerosis. *Front Immunol* (2020) 11:1780. doi: 10.3389/fimmu.2020.01780
50. Ngwa DN, Pathak A, Agrawal A. IL-6 regulates induction of C-reactive protein gene expression by activating STAT3 isoforms. *Mol Immunol* (2022) 146:50–6. doi: 10.1016/j.molimm.2022.04.003
51. Wang MY, Zhang CM, Zhou HH, Ge ZB, Su CC, Lou ZH, et al. Identification of a distal enhancer that determines the expression pattern of acute phase marker C-reactive protein. *J Biol Chem* (2022) 298(8):1–9. doi: 10.1016/j.jbc.2022.102160
52. Ji SR, Zhang SH, Chang Y, Li HY, Wang MY, Lv JM, et al. C-reactive protein: The most familiar stranger. *J Immunol* (2023) 210(6):699–707. doi: 10.4049/jimmunol.2200831



## OPEN ACCESS

## EDITED BY

Yi Wu,  
Xi'an Jiaotong University, China

## REVIEWED BY

Chiara Agostinis,  
Institute for Maternal and Child Health  
Burlo Garofolo (IRCCS), Italy  
József Dobó,  
Hungarian Academy of Sciences (MTA),  
Hungary

## \*CORRESPONDENCE

Antonio Inforzato

✉ antonio.inforzato@humanitasresearch.it

<sup>†</sup>These authors have contributed  
equally to this work and share  
first authorship

RECEIVED 08 August 2023

ACCEPTED 27 September 2023

PUBLISHED 09 October 2023

## CITATION

Massimino AM, Colella FE, Bottazzi B and  
Inforzato A (2023) Structural insights  
into the biological functions of the  
long pentraxin PTX3.  
*Front. Immunol.* 14:1274634.  
doi: 10.3389/fimmu.2023.1274634

## COPYRIGHT

© 2023 Massimino, Colella, Bottazzi and  
Inforzato. This is an open-access article  
distributed under the terms of the [Creative  
Commons Attribution License \(CC BY\)](#). The  
use, distribution or reproduction in other  
forums is permitted, provided the original  
author(s) and the copyright owner(s) are  
credited and that the original publication in  
this journal is cited, in accordance with  
accepted academic practice. No use,  
distribution or reproduction is permitted  
which does not comply with these terms.

# Structural insights into the biological functions of the long pentraxin PTX3

Anna Margherita Massimino<sup>1†</sup>, Filippo Emanuele Colella<sup>1†</sup>,  
Barbara Bottazzi<sup>2</sup> and Antonio Inforzato<sup>1,2\*</sup>

<sup>1</sup>Department of Biomedical Sciences, Humanitas University, Pieve Emanuele, Italy, <sup>2</sup>Laboratory of Cellular and Humoral Innate Immunity, IRCCS Humanitas Research Hospital, Rozzano, Italy

Soluble pattern recognition molecules (PRMs) are a heterogeneous group of proteins that recognize pathogen- and danger-associated molecular patterns (PAMPs and DAMPs, respectively), and cooperate with cell-borne receptors in the orchestration of innate and adaptive immune responses to pathogenic insults and tissue damage. Amongst soluble PRMs, pentraxins are a family of highly conserved proteins with distinctive structural features. Originally identified in the early 1990s as an early inflammatory gene, PTX3 is the prototype of long pentraxins. Unlike the short pentraxin C reactive protein (CRP), whose expression is mostly confined to the liver, PTX3 is made by several immune and non-immune cells at sites of infection and inflammation, where it intercepts fundamental aspects of infection immunity, inflammation, and tissue remodeling. Of note, PTX3 cross talks to components of the complement system to control cancer-related inflammation and disposal of pathogens. Also, it is an essential component of inflammatory extracellular matrices (ECMs) through crosslinking of hyaluronic acid and turn-over of provisional fibrin networks that assemble at sites of tissue injury. This functional diversity is mediated by unique structural characteristics whose fine details have been unveiled only recently. Here, we revisit the structure/function relationships of this long pentraxin in light of the most recent advances in its structural biology, with a focus on the interplay with complement and the emerging roles as a component of the ECM. Differences to and similarities with the short pentraxins are highlighted and discussed.

## KEYWORDS

pattern recognition molecules (PRM), pentraxins, PTX3, structure, complement, extracellular matrix

## 1 Introduction

The innate immune system is traditionally regarded as the first line of defense against invading pathogens (1). Cellular and molecular effector mechanisms of innate immunity are typically induced upon recognition of PAMPs (pathogen-associated molecular patterns, i.e. motifs shared by evolutionarily close microbial families that are often localized on the



cell surface and are essential for fitness) by PRMs (cell-borne or soluble pattern recognition molecules that are expressed both by immune and non-immune cells and act as transducers of activation and modulation signals) (2). Fluid-phase PRMs are regarded as evolutionary ancestors of antibodies in that they exert immunoprotective and immunomodulatory effects by means of opsonic and neutralizing properties, promotion of phagocytosis and complement activation. In addition to their roles in pathogen recognition and disposal, PRMs are increasingly acknowledged as key players in tissue remodeling, whereby they recognize DAMPs (damage/danger-associated molecular patterns) and convey biochemical messages for removal of cellular debris and tissue regeneration (3).

Pentraxins are an evolutionarily conserved family of soluble PRMs that share a common sequence motif (i.e., the pentraxin signature His-x-Cys-x-Ser/Thr-Trp-x-Ser) and typical quaternary structures (4). This comprises short and long pentraxins, each with distinctive structural and functional characteristics. First identified in the '30s as an opsonin that recognizes the C-type polysaccharide of *S. pneumoniae* (5), C-reactive protein (CRP) is the prototypical short pentraxin with five identical protomer subunits assembled into symmetric disc-like pentamers stabilized by non-covalent interactions [Figure 1A and (15)]. A similar structural organization is found in serum amyloid P component (SAP) (16), another short pentraxin identified in the '70s that shares with CRP calcium-dependent recognition of several ligands (17). High levels of sequence and structural homology across short pentraxins from evolutionary distant species suggest that this PRMs play essential roles in innate immunity, even though their functions as opsonizing and complement-fixing molecules have probably become redundant, being overshadowed by other players of the immune system like immunoglobulins (18). Experimental evidence from gene-modified animals indicates that CRP exerts host protective functions in bacterial, especially pneumococcal, infections (19). Importantly, this protein is extensively used in the clinical practice as a non-specific systemic marker of inflammation (20). Serendipitously discovered in studies designed to evaluate the effects of CRP on lymphocytes (18), SAP has been recently acknowledged as an important player in the innate immune reaction to the opportunistic fungal pathogen *A. fumigatus* (21). Also, SAP is long-known as a an essential component of amyloid deposits (22). This property has been clinically exploited to develop SAP-based scintigraphy tracers for *in vivo* imaging of amyloid deposits (23, 24), and combination therapies to target these pathological fibrils in amyloidosis and Alzheimer's disease (25, 26).

Cloned in the early '90s, PTX3 is considered the paradigm of long pentraxins (27). Additional members of this subfamily are pentraxin 4 [PTX4; (28)], neuronal pentraxins 1 (NPTX1 or NP1 (29);) and 2 [NPTX2, also called Narp or NP2; (30)], and the transmembrane protein neuronal pentraxin receptor [NPTXR (31)]; (see Figure 1A for an overview of the phylogenetic relationships across human pentraxins). Like all other long pentraxins, the PTX3 protomer contains a compact C-terminal domain with sequence homology to the short pentraxins and an

elongated N-terminal region (32–34). Initial functional evidence on PTX3 dates to the early 2000s, when a non-redundant immunoprotective role against *A. fumigatus* was documented by Garlanda et al. (35). Since this original discovery, other functions have emerged for this long pentraxin, including a crucial role in female fertility (11) and extrinsic oncosuppressive effects (36). Here, we reconsider the functional landscape of PTX3 in relation to the protein's structure, a high-resolution model of which have been recently published. Within this frame, we will discuss emerging vistas on the interplay between PTX3, complement and ECM.

## 2 Structural biology of PTX3

PTX3 is made at sites of infection and inflammation by several immune and non-immune cell types upon stimulation with inflammatory cytokines (i.e., interleukin-1 $\beta$ , IL-1 $\beta$ , and tumor necrosis factor- $\alpha$ , TNF- $\alpha$ ), microbial moieties (i.e., lipopolysaccharide, LPS) and intact microorganisms (i.e., *A. fumigatus*) (27). This marks a profound difference to CRP, whose synthesis is mostly induced in the liver by interleukin 6 (IL-6) and acts as a systemic (rather than local) marker of inflammation (37). Cellular sources and gene regulation of PTX3 are extensively reviewed in (27, 38). In this chapter, we will focus on the protein's structure that, as anticipated by our own work, and refined in recent biophysical studies, marks an additional deviation from short pentraxins.

In 2022 Noone et al. reported the first high-resolution 3D model of PTX3 (first of this kind for a long pentraxin, actually) based on a hybrid cryoelectron microscopy (Cryo-EM)/AlphaFold strategy (9). In this study a Cryo-EM 2.5-Å map of the C-terminal pentraxin domains was generated where these regions folded into a rather unique (compared to the short pentraxins) D4 symmetrical octamer. More precisely, the C-domains were found to form a dimer of tetramers, with each tetramer arranged into a planar ring stabilized by noncovalent interactions, and the two tetramers held together by disulfide bonds (Figure 1B). Despite a low level of sequence identity between the C-domain of PTX3 and CRP or SAP (~28%), these proteins all share a high degree of structural similarity (9). Nonetheless, the short pentraxins fold into pentamers (rather than tetramers; see Figure 1A) owing to poor conservation of the inter-subunit interfaces. Also, the metal-binding site present in CRP, SAP (17) and the other long pentraxin NPTX1 (9) is replaced by a disulfide bridge (C317/C318) (33) and an N-glycosylation site (39), which perhaps explains why PTX3 recognizes most of its ligand in a Ca<sup>2+</sup>-independent fashion (27). In the Cryo-EM map two water molecules were found proximal to the His residue of the pentraxin motif, raising the possibility that this residue might establish H-bonds with bulk water and thus act as a sensor of the microenvironment's pH (9) (an intriguing mechanism, given that acidic pH values have a fundamental impact on the function of PTX3 in the ECM (40); see below).

The cryo-EM map revealed  $\alpha$ -helical motifs protruding out of the pentraxin core that were partially resolved. AlphaFold was then used

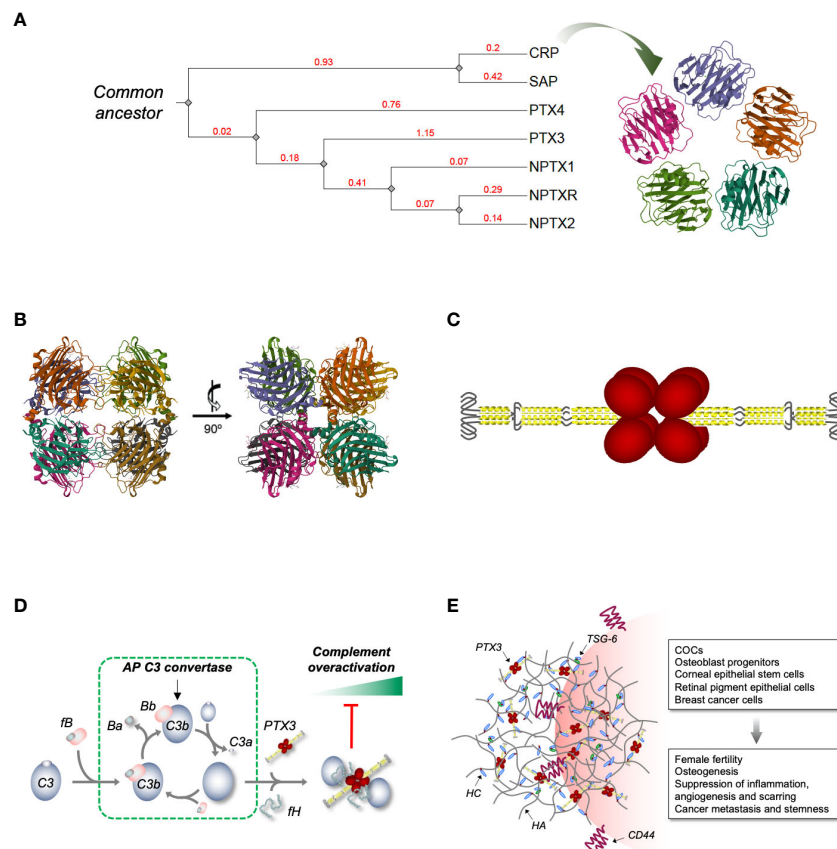


FIGURE 1

**Phylogenetic relationships across human pentraxins, 3D model of PTX3 and its interplay with complement and HA ECM.** (A) Phylogenetic tree of the human PTX family of proteins. The tree was constructed using the Phylogeny.fr web server (<http://www.phylogeny.fr/> and (6)), edited and annotated with the iTOL (Interactive Tree Of Life) online tool (<https://itol.embl.de/> and (7)). The extent of genetic variation across members of the family (i.e., the average number of amino acid substitutions per site) is indicated by the branch lengths. These are drawn to scale and expressed as arbitrary unit (in red) with tree nodes represented by grey diamonds. The accession numbers used for the analysis are NP\_000558.2 (CRP), NP\_001630.1 (SAP), NP\_002843.2 (PTX3), NP\_001013680.1 (PTX4), NP\_002513.2 (NPTX1), NP\_002514.1 (NPTX2) and NP\_055108.2 (NPTXR). Also, a 3D model of human CRP is shown [PDB-ID: 1GNH and (8)] that highlights the symmetric pentameric quaternary structure of this short pentraxin. (B) Orthogonal views of a high-resolution model of the C-terminal pentraxin domains of the human PTX3 based on Cryo-EM that show these domains to fold into octamers with D4 symmetry [PDB-ID: 7ZL1 and (9)]. (C) Schematic drawing of the PTX3 protein with the N-terminal regions (in yellow) forming two parallel tetrameric coiled coils at the opposite sides of the C-terminal core (in red) [based on (9)]. Hinge and intrinsically disordered regions (represented by black lines) bring flexibility to the structure. (D) We have reported that surface bound PTX3 forms a ternary complex with fH and C3b that acts as a “hot spot” for AP inhibition (10). Indeed, when bound to PTX3 and fH, C3b is no longer accessible to factor B (fB, which during AP activation is proteolytically processed to Ba and Bb, the latter being a component of the AP C3 convertase) and loses the ability to amplify the complement cascade (with further cleavage of C3 to C3a and C3b) and the associated inflammatory response (including production of the anaphylatoxin C3a). (E) PTX3 is an essential component of the HA-rich ECMs that transiently form in inflammatory and inflammatory-like conditions. Incorporation of PTX3 in these matrices requires synthesis of covalent adducts between HA and heavy chains (HCs) of the proteoglycan 1α1 (HC•HA), a reaction that is catalyzed by the hyaladherin TSG-6. PTX3 makes multiple, non-covalent interactions with the HC components of the HC•HA complex, and in this way cross-links HA. This mechanism has major implications in female fertility (11) and has been associated with the anti-inflammatory, -angiogenic and -scarring properties of the PTX3/HC•HA complex isolated from the human amniotic membrane (12). Also, through the HA receptor CD44, HA-embedded PTX3 has been recently reported to promote osteogenesis (13) and breast cancer growth, stemness and metastasis (14).

to generate *in silico* predictions of the remaining N-terminal regions and a 3D model was generated that showed the N-domains to form two long tetrameric coiled coils at opposite sides of the C-terminal complex (Figure 1C). Each tetramer contains two hinge regions (encompassing inter-chain disulfide bonds), which brings to the protein a high degree of flexibility (9). The two N-domains have a symmetric arrangement [as opposed to the asymmetric model we proposed based on mid-/low-resolution data (34)] and terminate with an intrinsically disordered region (initial 28–30 amino acids), which collectively provides an extended range of motion and possibly the ability to adapt to diverse interaction interfaces.

### 3 Structure/function relationships

The structural complexity of the PTX3 protein perhaps explains the rather vast spectrum of interactions and functions of this pentraxin, which ranges from infection immunity to regulation of inflammation, tissue remodeling and cancer (summarized in Table 1).

PTX3 acts as host protective soluble PRM towards a number of fungal, bacterial, and viral pathogens, including *A. fumigatus* (35, 46), *S. pneumoniae* (69), uropathogenic *E. coli* (49), influenza virus (44) and cytomegalovirus (45). Locally induced at sites of infection,

PTX3 opsonizes cognate microorganisms upon engagement of selected PAMPs [e.g., outer membrane protein A, OmpA, of *K. pneumoniae* (47), outer membrane vesicles, OMV, and meningococcal antigens of *N. meningitidis* (48), nucleocapsid protein of SARS\_COV\_2 (41)] and promotes viral neutralization as well as fungal and bacterial phagocytosis and killing (by professional phagocytes, mostly neutrophils). The latter processes imply a tight interaction with complement components (discussed below) and Fcγ-receptors [reviewed in (70)].

Several studies point to PTX3 as a modulator of inflammation in sterile (in addition to infectious) settings. In this regard, PTX3 is known to interact with P-selectin in a glycosylation-dependent manner and dampen, via a negative feedback mechanism, the P-selectin-mediated extravasation of neutrophils to sites of tissue damage (50). Also, PTX3 participates in the clearance of apoptotic cells and debris (including histones) by modulating their uptake by dendritic cells (71) and acting as an “eat me” tag for late apoptotic neutrophils (72), in addition to regulating complement activation on dying cells (73). Moreover, it tames complement-dependent, tumor-promoting inflammation (36).

PTX3 is acknowledged as an important player in tissue remodeling and cancer. As for this, it is known to sequester FGF2

and FGF8 through its N-terminal region and inhibit their angiogenic and inflammatory activities in models of neovascularization and FGF-dependent tumorigenesis (51–55). Also, an interaction has been suggested for PTX3 with DC-SIGN (dendritic cell-specific intercellular adhesion molecule-3-grabbing nonintegrin) that might be relevant to leukocyte activation and differentiation to fibrocyte (74), which however requires experimental validation. Other than FGFs, other ligands have been proposed for PTX3 that are relevant to cancer biology, including components of the complement system and CD44 (see below) with however conflicting outcomes (see (75) for further discussion). Finally, PTX3 is known to intercept major mechanisms of fibrin- and HA-remodeling which will be discussed in a separate paragraph.

### 3.1 Crosstalk with the complement system

As “ante-antibodies”, pentraxins functionally cooperate with complement, *de facto* extending and modulating both recognition and effector phases of this system (76). The first complement ligand of CRP and SAP to be identified was C1q, whose interaction with

TABLE 1 Major interactions of PTX3 and their functional outcomes.

	Ligand	Binding interface	Function	Refs.
Microorganisms	SARS-CoV-2	Nucleocapsid protein recognition by the PTX3 N-term	Prognostic indicator of short-term mortality in COVID-19	(41–43)
	Influenza virus	Viral hemagglutinin binding to sialic acid residues of the PTX3 C-term	Inhibition of hemagglutination, neutralization of virus infectivity, inhibition of viral neuraminidase	(44)
	Cytomegalovirus	Unknown	Inhibition of viral entry and infectivity <i>in vitro</i> , protection from murine CMV infection/reactivation and <i>A. fumigatus</i> superinfection <i>in vivo</i>	(45)
	<i>A. fumigatus</i>	Unknown cell wall ligand binding to the PTX3 N-term	Opsonization, promotion of phagocytosis and killing by neutrophils via complement and Fcγ receptors	(35, 46)
	<i>K. pneumoniae</i>	Ca <sup>2+</sup> -dependent recognition of KpOmpA (binding site on PTX3 unknown)	Amplification of the inflammatory response <i>in vivo</i>	(47)
	<i>N. meningitidis</i>	Ca <sup>2+</sup> -independent binding of meningococcal antigens GNA0667, GNA1030 and GNA2091 to the PTX3 N-term	Amplification of the antibody response and protection from infection <i>in vivo</i>	(48)
	<i>E. coli</i>	Unknown	Protection from urinary tract infection	(49)
Receptors	P-selectin	P-selectin binding to sialic acid residues of the PTX3 C-term	Inhibition of leukocyte extravasation	(50)
	FcγRIIa and III	Unknown	Promotion of phagocytosis	(46)
	CD44	209–217aa and 352–360aa regions of the PTX3 C-term	Osteogenesis and cancer growth/metastasis and	(13, 14)
Hemostasis	Fibrinogen/Fibrin	pH-dependent binding to the PTX3 N-term	Enhancement of plasmin-mediated fibrinolysis	(40)
	Plasminogen	pH-dependent binding of the KR3-KR5 domains to the PTX3 N-term		
Angiogenesis	FGF2	97–110aa sequence of the PTX3 N-term	Inhibition of angiogenesis, restenosis and cancer progression	(51–55)
	FGF8	Unknown		

(Continued)

TABLE 1 Continued

	Ligand	Binding interface	Function	Refs.
Complement	C1q	Sialic acid-dependent binding to the globular head of C1q (mainly through B chain Arg residues)	Control of the CP	(56, 57)
	C3b	Unknown	Inhibition of the AP	(10)
	fH proteins	Ca <sup>2+</sup> - and glycosylation-dependent recognition of CCP7 of fH and FHL-1 (by the PTX3 C-term) and CCP19-20 of fH and FHR1 (by the PTX3 N-term)	Inhibition of the AP	(10, 58–61)
	C4BP	Ca <sup>2+</sup> -dependent recognition of SCRs 1-3 of the C4BP $\alpha$ -chain (binding site on PTX3 unknown)	Inhibition of the CP/LP	(62)
	MBL	Unknown	Cross-activation of the LP	(63)
	Ficolins	Glycosylation-dependent interaction		(64)
ECM	I $\alpha$ I	Mg <sup>2+</sup> -dependent binding of the PTX3 N-term to HCs 1 and 2 of I $\alpha$ I	Assembly and stability of the HA ECM	(33, 65–67)
	TSG6	Link module recognition by the PTX3 N-term	Assembly and stability of the HA ECM and regulation of angiogenesis	(55, 67)
	TSP1	C-terminal globular domain (E123CaG-1) binding to the PTX3 N-term	Control of synaptogenesis	(68)
Others	Histones	N-term domain of histones (binding site on PTX3 unknown)	Protective functions against extracellular histone-mediated cytotoxicity	(32)

these short pentraxins results into activation of the classical pathway (CP) (77, 78). Follow-up studies revealed that components of the lectin pathway (LP) too, with major regard to ficolins, form complexes with CRP and SAP that favor complement-mediated disposal of apoptotic cells and microbial pathogens (75). Importantly, both CP and LP cooperate with pentraxins through additive and synergistic effects that broaden the repertoire of PAMPs/DAMPs recognition and effector functions of the humoral innate immunity [reviewed in (79)]. Despite fundamental immunoprotective functions, over-activation of the complement system can be pathogenic. In this regard, short pentraxins have been proposed to play a dual role. For example, in myocardial infarction and ischemic stroke CRP binds DAMPs on injured cells and exacerbates complement-dependent tissue damage (80). On the other hand, short pentraxins have been involved in suppressive pathways that limit this process by recruiting complement inhibitors, like C4b-binding protein [C4BP, major soluble inhibitor of the CP and LP that is recognized by SAP (81)] and factor H [fH, primary fluid phase inhibitor of the alternative pathway, AP, that is bound by CRP (82)].

Like the short pentraxins, PTX3 tightly cross talks to the three pathways of complement with varying and context-dependent outcomes (83). For example, recognition units of the LP (i.e., mannose-binding-lectin, MBL, and ficolins) form with PTX3 hetero-complexes with LP amplifying activity towards fungal pathogens, like *C. albicans* (63) and *A. fumigatus* (64). However, the interaction of PTX3 with C1q (56) results into either activation (on surfaces) or inhibition (in solution) of the CP (57). Also, this long pentraxin is known to interact with complement inhibitors and restrain overactivation of this system. In this regard, PTX3 recruits C4BP to sites of tissue remodeling, including ECM and apoptotic

cells, and inhibit activation of the CP/LP (62). More importantly, PTX3 is a ligand of members of the factor H family of proteins (i.e., fH, factor H-like protein 1, FHL-1, and factor H-related proteins 1 and 5, FHR-1 and -5) that collectively control the AP (58–61). This has implications in complement-driven cancer-related inflammation (36), opsonophagocytosis of *A. fumigatus* (46) and *P. aeruginosa* (84), atypical hemolytic uremic syndrome (aHUS) (60), and age-related macular degeneration (AMD) (85).

The retina is emerging as an important stage for the complement-modulating properties of PTX3. Indeed, this protein has been localized within and around the ECM of the outer blood-retinal barrier (oBRB), including the Bruch's membrane (BrM), retinal pigment epithelium (RPE), and choriocapillaris, major sites of complement dysregulation in AMD (86). We recently reported that PTX3 forms a ternary complex with C3b (component of the AP C3 convertase) and fH on acellular surfaces (that mimic the BrM) and acts as a “molecular trap” for AP activation (10) (Figure 1D). Also, we documented that PTX3 interacts with FHL-1 (a truncated form of fH that comprises complement control proteins, CCPs, 1-7 and retains the ability to inhibit the AP), and this interaction is affected by the Y402H polymorphism (a major AMD-associated allele that maps in CCP7 and is thus present both in fH and FHL-1) (61). Given that FHL-1 is a primary inhibitor of the AP in the oBRB and displays Y402H-dependent binding to the BrM (87), we postulate that PTX3 exerts BrM (i.e., ECM) anchoring properties towards FHL-1 (in addition to fH) and these might compensate the pathological effects of the 402H allele (88). It is therefore conceived that this long pentraxin participates in the mechanisms of complement homeostasis in the eye whereby its multimeric and flexible structure allows at a time incorporation in the oBRB ECM and retention of complement inhibition. In this regard, it is worth



reiterating here that ECM-embedded PTX3 exerts inhibitory (rather than activating) functions towards the CP/LP via a specific interaction with C4BP (62).

### 3.2 Roles in the ECM

In a pivotal study by Doni et al, primary components of hemostasis were identified as high affinity ligands of PTX3, i.e. fibrinogen/fibrin (FG) and plasminogen (PG) (40). These recognize non-overlapping sites in the PTX3 N-terminal domain in a calcium- and glycosylation-independent manner, which allows formation of a tripartite PTX3/FG/PG complex with fibrinolytic activity (in the presence of plasminogen activators). In an analogy with the AP components C3b and fH (10), PTX3 acted as a molecular scaffold to favor the interaction of PG with FG and ensure timely degradation of the fibrin clot (40). Consistent with this view, this long pentraxin had remodeling activity in several models of tissue injury, including skin wound, liver and lung damage, and arterial thrombosis. This activity is distinctive of PTX3 and its N-terminal domain (the short pentraxins lacks recognition of FG and PG) and, more importantly, is pH-dependent, whereby an acidic environment sets the PRM PTX3 in a tissue repair mode (40).

Back in 2002, Varani et al. reported that PTX3 deficiency is associated with severe subfertility in female mice (89). In a follow up study, Salustri et al. demonstrated that this is due to instability of the hyaluronic acid (HA) matrix that forms around the oocyte and the surrounding cumulus cells (a multicellular assembly known as cumulus oophorous complex, COC) prior to ovulation and is necessary for fertilization *in vivo* (11). More importantly, these preclinical findings were corroborated by epidemiological data, whereby PTX3 polymorphisms have been associated with frequency of offspring (90) and dizygotic twinning (91) in sub-Saharan females. The mechanisms underlying the role of PTX3 in fertility are paradigmatic examples of the structure/function complexity of this protein. In fact, in the preovulatory period the COC-associated HA undergoes physical and chemical remodeling due to the action of inter- $\alpha$ -trypsin inhibitor ( $\alpha_1$ I), a serum proteoglycan composed of two heavy chains (HCs) that enters the follicle due to permeabilization of the blood/follicle barrier (92), and the HA-binding protein TSG-6 (93), which is locally expressed by follicular cells and catalyzes the covalent transfer of HCs onto HA to form HC•HA complexes (94). These HC•HA adducts act as scaffolds for incorporation of the PTX3 protein that is secreted by cumulus cells upon stimulation with oocytic factors and second messengers (89). Owing to its multimeric structure, PTX3 has multiple  $Mg^{2+}$ -dependent binding sites (in the N-domain) for the HC components of HC•HA, and thus acts as a node in crosslinking HA, providing stability to the HA ECM (33, 65–67) (Figure 1E). Beside ovulation, these mechanisms might be relevant to pathology, including inflammatory and infectious diseases of the bone (95), joint (96) and lung (97), and are distinctive of PTX3, again due to lack of the N-terminal domain in CRP and SAP. Also, HA-embedded PTX3 has been recently proposed as a promoter of synaptogenesis in the developing central nervous system, where it

forms a rheostat with astrocyte-derived thrombospondin 1 (TSP1) (68).

Not only incorporation of PTX3 into HA-rich ECMs has scaffolding implications, but it also appears to convey intracellular signals. In this regard, PTX3 is present in the HA-dependent pericellular matrix of MC3T3-E1 osteoblasts, where it promotes a self-sustained osteogenic program in inflammatory conditions through a functional axis comprising HA, CD44 (major cellular receptor for HA) and the activated focal adhesion kinase (FAK)/protein kinase B (AKT) signaling cascade (13). On the same line, HA/HCs/PTX3 complexes isolated from the human amniotic membrane suppresses inflammation, angiogenesis and scarring in preclinical models of corneal and retinal pathology (12). Also, in a recent report by Hsiao et al, a direct interaction has been documented between CD44 and PTX3 that activates ERK1/2, AKT and NF- $\kappa$ B pathways and contributes to metastasis/invasion and stemness of a triple-negative breast cancer cell line (14) (see Figure 1D). It is not clear whether embedding into the HA pericellular matrix is required for PTX3 to recognize CD44, however, given that the CD44-binding interface is in the C-terminal domain (14), it is conceivable that, when incorporated into HA-ECMs [through its N-terminal region (66)], PTX3 retains binding to CD44 while modulating (e.g., via HA-crosslinking) its interaction with HA. This might have implications in leukocyte adhesion and activation (98), in addition to cancer metastasis and stemness (99).

## 4 Conclusion and perspectives

PTX3 has been implicated in various pathological conditions, including infections (100), cardiovascular diseases (101), bone disorders (95) and cancer (36, 102), where it has potential as a diagnostic and/or prognostic marker and therapeutic target. Importantly, the plasmatic levels of this pentraxin have been consistently associated with disease's severity and outcome in sepsis and septic shock, tuberculosis, dengue and meningitis [reviewed in (100)], and, more recently, COVID-19 (42, 43). Also, polymorphisms in the PTX3 gene have been associated with the protein's levels in the plasma and the risk of developing selected opportunistic fungal and bacterial infections [reviewed in (27)]. In this respect, the rs2305619, rs3816527 and rs1840680 single nucleotide polymorphisms (SNPs) form a common haplotypic block where the second SNP causes an amino acid substitution (Asp to Ala) at position 48 in the N-terminal domain. This polymorphism does not alter the protein structure substantially (56), neither does it affect the interaction of PTX3 with C1q (56) and *A. fumigatus* (103), however it is at present unknown whether it has any impact on the recognition of other ligands, with major regard to the complement proteins fH and C3b, and the incorporation of PTX3 in HA- and/or fibrin-rich ECMs.

CRP is widely used as a clinical biomarker to assess inflammation and predict the risk of cardiovascular diseases (104). Comparative analysis of the structure/function relationships of short and long pentraxins offers unprecedented opportunities to understand the roles of these PRMs in the immune response and their implications



in the pathogenesis of several diseases. Recent insights into the structure of PTX3 (the first long pentraxin to be unraveled in such detail) have shed light on its unique architecture and pinpointed the molecular determinants of its immune-modulatory functions (9). In this regard, multi-domain composition of the protomer subunits, glycosylation and quaternary organization collectively contribute to the diverse ligand recognition and interaction capabilities of this long pentraxin. Here we highlighted emerging aspects of the PTX3 biology that intercept fundamental processes of inflammation and tissue remodeling and have translational value in clinical settings that are characterized by dysregulation of complement activation and ECM turnover.

## Author contributions

AM: Data curation, Writing – original draft. FC: Data curation, Writing – original draft. BB: Writing – review & editing. AI: Conceptualization, Data curation, Funding acquisition, Project administration, Supervision, Validation, Visualization, Writing – original draft, Writing – review & editing.

## Funding

The authors declare financial support was received for the research, authorship, and/or publication of this article. The

article's publication fees are funded by Fondazione Beppe e Nuccy Angiolini.

## Acknowledgments

The authors gratefully acknowledge Fondazione Beppe e Nuccy Angiolini for funding a research project on the structure/function relationships of PTX3 in the bone ECM that inspired the writing of this manuscript.

## Conflict of interest

The authors declare that the research was conducted in the absence of any commercial or financial relationships that could be construed as a potential conflict of interest.

## Publisher's note

All claims expressed in this article are solely those of the authors and do not necessarily represent those of their affiliated organizations, or those of the publisher, the editors and the reviewers. Any product that may be evaluated in this article, or claim that may be made by its manufacturer, is not guaranteed or endorsed by the publisher.

## References

- Medzhitov R. Origin and physiological roles of inflammation. *Nature* (2008) 454 (7203):428–35. doi: 10.1038/nature07201
- Li D, Wu M. Pattern recognition receptors in health and diseases. *Signal Transduct Target Ther* (2021) 6(1):291. doi: 10.1038/s41392-021-00687-0
- Zindel J, Kubes P. DAMPs, PAMPs, and LAMPs in immunity and sterile inflammation. *Annu Rev Pathol* (2020) 15:493–518. doi: 10.1146/annurev-pathmechdis-012419-032847
- Bottazzi B, Doni A, Garlanda C, Mantovani A. An integrated view of humoral innate immunity: pentraxins as a paradigm. *Annu Rev Immunol* (2010) 28:157–83. doi: 10.1146/annurev-immunol-030409-101305
- Abernethy TJ, Avery OT. The occurrence during acute infections of a protein not normally present in the blood: I. Distribution of the reactive protein in patients' Sera and the effect of calcium on the flocculation reaction with C polysaccharide of pneumococcus. *J Exp Med* (1941) 73(2):173–82. doi: 10.1084/jem.73.2.173
- Dereeper A, Guignon V, Blanc G, Audic S, Buffet S, Chevenet F, et al. Phylogeny.fr: robust phylogenetic analysis for the non-specialist. *Nucleic Acids Res* (2008) 36(Web Server issue):W465–9. doi: 10.1093/nar/gkn180
- Letunic I, Bork P. Interactive Tree Of Life (iTOL) v5: an online tool for phylogenetic tree display and annotation. *Nucleic Acids Res* (2021) 49(W1):W293–6. doi: 10.1093/nar/gkab301
- Shrive AK, Cheetham GM, Holden D, Myles DA, Turnell WG, Volanakis JE, et al. Three dimensional structure of human C-reactive protein. *Nat Struct Biol* (1996) 3 (4):346–54. doi: 10.1038/nsb0496-346
- Noone DP, Dijkstra DJ, van der Klugt TT, van Veelen PA, de Ru AH, Hensbergen PJ, et al. PTX3 structure determination using a hybrid cryoelectron microscopy and AlphaFold approach offers insights into ligand binding and complement activation. *Proc Natl Acad Sci U.S.A.* (2022) 119(33):e2208144119. doi: 10.1073/pnas.2208144119
- Stravalaci M, Davi F, Parente R, Gobbi M, Bottazzi B, Mantovani A, et al. Control of complement activation by the long pentraxin PTX3: implications in age-related macular degeneration. *Front Pharmacol* (2020) 11:591908. doi: 10.3389/fphar.2020.591908
- Salustri A, Garlanda C, Hirsch E, De Acetis M, Maccagno A, Bottazzi B, et al. PTX3 plays a key role in the organization of the cumulus oophorus extracellular matrix and in in vivo fertilization. *Development* (2004) 131:1577–86. doi: 10.1242/dev.01056
- Tseng SCG. HC-HA/PTX3 purified from amniotic membrane as novel regenerative matrix: insight into relationship between inflammation and regeneration. *Invest Ophthalmol Visual Sci* (2016) 57(5):ORSFh1-8. doi: 10.1167/iovs.15-17637
- Dong W, Xu X, Luo Y, Yang C, He Y, Dong X, et al. PTX3 promotes osteogenic differentiation by triggering HA/CD44/FAK/AKT positive feedback loop in an inflammatory environment. *Bone* (2022) 154:116231. doi: 10.1016/j.bone.2021.116231
- Hsiao YW, Chi JY, Li CF, Chen LY, Chen YT, Liang HY, et al. Disruption of the pentraxin 3/CD44 interaction as an efficient therapy for triple-negative breast cancers. *Clin Trans Med* (2022) 12(1):e724. doi: 10.1002/ctm2.724
- Thompson D, Pepys MB, Wood SP. The physiological structure of human C-reactive protein and its complex with phosphocholine. *Structure* (1999) 7(2):169–77. doi: 10.1016/S0969-2126(99)80023-9
- Emsley J, White HE, O'Hara BP, Oliva G, Srinivasan N, Tickle IJ, et al. Structure of pentameric human serum amyloid P component. *Nature* (1994) 367(6461):338–45. doi: 10.1038/367338a0
- Kinoshita CM, Gewurz AT, Siegel JN, Ying SC, Hugli TE, Coe JE, et al. A protease-sensitive site in the proposed Ca(2+)-binding region of human serum amyloid P component and other pentraxins. *Protein Sci* (1992) 1(6):700–9. doi: 10.1002/pro.5560010602
- Pepys MB. The pentraxins 1975–2018: serendipity, diagnostics and drugs. *Front Immunol* (2018) 9:2382. doi: 10.3389/fimmu.2018.02382
- Simons JP, Loeffler JM, Al-Shawi R, Ellmerich S, Hutchinson WL, Tennent GA, et al. C-reactive protein is essential for innate resistance to pneumococcal infection. *Immunology* (2014) 142(3):414–20. doi: 10.1111/imm.12266
- Pepys MB. C-reactive protein and the acute phase response. *Nature* (1982) 296 (5852):12. doi: 10.1038/296012a0
- Doni A, Parente R, Laface I, Magrini E, Cunha C, Colombo FS, et al. Serum amyloid P component is an essential element of resistance against *Aspergillus fumigatus*. *Nat Commun* (2021) 12(1):3739. doi: 10.1038/s41467-021-24021-y

22. Cathcart ES, Skinner MS, Cohen AS, Lawless OJ, Benson MD. Antigenic determinants in amyloid deposits. *Nature* (1970) 228(5276):1090–1. doi: 10.1038/2281090b0
23. Hawkins PN, Myers MJ, Lavender JP, Pepys MB. Diagnostic radionuclide imaging of amyloid: biological targeting by circulating human serum amyloid P component. *Lancet* (1988) 1(8600):1413–8. doi: 10.1016/S0140-6736(88)92235-0
24. Hawkins PN, Lavender JP, Pepys MB. Evaluation of systemic amyloidosis by scintigraphy with 123I-labeled serum amyloid P component. *N Engl J Med* (1990) 323(8):508–13. doi: 10.1056/NEJM199008233230803
25. Richards DB, Cookson LM, Berges AC, Barton SV, Lane T, Ritter JM, et al. Therapeutic clearance of amyloid by antibodies to serum amyloid P component. *N Engl J Med* (2015) 373(12):1106–14. doi: 10.1056/NEJMoa1504942
26. Al-Shawi R, Tennent GA, Millar DJ, Richard-Londt A, Brandner S, Werring DJ, et al. Pharmacological removal of serum amyloid P component from intracerebral plaques and cerebrovascular Abeta amyloid deposits in vivo. *Open Biol* (2016) 6(2):150202. doi: 10.1098/rsob.150202
27. Garlanda C, Bottazzi B, Magrini E, Inforzato A, Mantovani A. Ptx3, a humoral pattern recognition molecule, in innate immunity, tissue repair, and cancer. *Physiol Rev* (2018) 98(2):623–39. doi: 10.1152/physrev.00016.2017
28. Martinez de la Torre Y, Fabbri M, Jaillon S, Bastone A, Nebuloni M, Vecchi A, et al. Evolution of the pentraxin family: the new entry PTX4. *J Immunol* (2010) 184(9):5055–64. doi: 10.4049/jimmunol.0901672
29. Omeis IA, Hsu YC, Perin MS. Mouse and human neuronal pentraxin 1 (NPTX1): conservation, genomic structure, and chromosomal localization. *Genomics* (1996) 36(3):543–5. doi: 10.1006/geno.1996.0503
30. Hsu YC, Perin MS. Human neuronal pentraxin II (NPTX2): conservation, genomic structure, and chromosomal localization. *Genomics* (1995) 28(2):220–7. doi: 10.1006/geno.1995.1134
31. Dodds DC, Omeis IA, Cushman SJ, Helms JA, Perin MS. Neuronal pentraxin receptor, a novel putative integral membrane pentraxin that interacts with neuronal pentraxin 1 and 2 and taipoxin-associated calcium-binding protein 49. *J Biol Chem* (1997) 272(34):21488–94. doi: 10.1074/jbc.272.34.21488
32. Bottazzi B, Vouret-Craviari V, Bastone A, De Gioia L, Matteucci C, Peri G, et al. Multimer formation and ligand recognition by the long pentraxin PTX3. Similarities and differences with the short pentraxins C-reactive protein and serum amyloid P component. *J Biol Chem* (1997) 272(52):32817–23. doi: 10.1074/jbc.272.52.32817
33. Inforzato A, Rivieccio V, Morreale AP, Bastone A, Salustri A, Scarchilli L, et al. Structural characterization of PTX3 disulfide bond network and its multimeric status in cumulus matrix organization. *J Biol Chem* (2008) 283(15):10147–61. doi: 10.1074/jbc.M708535200
34. Inforzato A, Baldock C, Jowitt TA, Holmes DF, Lindstedt R, Marcellini M, et al. The angiogenic inhibitor long pentraxin PTX3 forms an asymmetric octamer with two binding sites for FGF2. *J Biol Chem* (2010) 285(23):17681–92. doi: 10.1074/jbc.M109.085639
35. Garlanda C, Hirsch E, Bozza S, Salustri A, De Acetis M, Nota R, et al. Non-redundant role of the long pentraxin PTX3 in anti-fungal innate immune response. *Nature* (2002) 420(6912):182–6. doi: 10.1038/nature01195
36. Bonavita E, Gentile S, Rubino M, Maina V, Papait R, Kunderfranco P, et al. PTX3 is an extrinsic oncosuppressor regulating complement-dependent inflammation in cancer. *Cell* (2015) 160(4):700–14. doi: 10.1016/j.cell.2015.01.004
37. Bottazzi B, Inforzato A, Messa M, Barbagallo M, Magrini E, Garlanda C, et al. The pentraxins PTX3 and SAP in innate immunity, regulation of inflammation and tissue remodelling. *J Hepatol* (2016) 64(6):1416–27. doi: 10.1016/j.jhep.2016.02.029
38. Doni A, Stravalaci M, Inforzato A, Magrini E, Mantovani A, Garlanda C, et al. The long pentraxin PTX3 as a link between innate immunity, tissue remodeling, and cancer. *Front Immunol* (2019) 10:712. doi: 10.3389/fimmu.2019.00712
39. Inforzato A, Peri G, Doni A, Garlanda C, Mantovani A, Bastone A, et al. Structure and function of the long pentraxin PTX3 glycosidic moiety: fine-tuning of the interaction with C1q and complement activation. *Biochemistry* (2006) 45(38):11540–51. doi: 10.1021/bi0607453
40. Doni A, Musso T, Morone D, Bastone A, Zambelli V, Sironi M, et al. An acidic microenvironment sets the humoral pattern recognition molecule PTX3 in a tissue repair mode. *J Exp Med* (2015) 212(6):905–25. doi: 10.1084/jem.20141268
41. Stravalaci M, Pagani I, Paraboschi EM, Pedotti M, Doni A, Scavellio F, et al. Recognition and inhibition of SARS-CoV-2 by humoral innate immunity pattern recognition molecules. *Nat Immunol* (2022) 23(2):275–86. doi: 10.1038/s41590-021-01114-w
42. Capra AP, Ardizzone A, Panto G, Paterniti I, Campolo M, Crupi L, et al. The prognostic value of pentraxin-3 in COVID-19 patients: A systematic review and meta-analysis of mortality incidence. *Int J Mol Sci* (2023) 24(4):3537. doi: 10.3390/ijms24043537
43. Brunetta E, Folci M, Bottazzi B, De Santis M, Gritti G, Protti A, et al. Macrophage expression and prognostic significance of the long pentraxin PTX3 in COVID-19. *Nat Immunol* (2021) 22(1):19–24. doi: 10.1038/s41590-020-00832-x
44. Reading PC, Bozza S, Gilbertson B, Tate M, Moretti S, Job ER, et al. Antiviral activity of the long chain pentraxin PTX3 against influenza viruses. *J Immunol* (2008) 180(5):3391–8. doi: 10.4049/jimmunol.180.5.3391
45. Bozza S, Bistoni F, Gaziano R, Pitzurra L, Zelante T, Bonifazi P, et al. Pentraxin 3 protects from MCMV infection and reactivation through TLR sensing pathways leading to IRF3 activation. *Blood* (2006) 108(10):3387–96. doi: 10.1182/blood-2006-03-009266
46. Moalli F, Doni A, Deban L, Zelante T, Zagarella S, Bottazzi B, et al. Role of complement and Fc[gamma] receptors in the protective activity of the long pentraxin PTX3 against *Aspergillus fumigatus*. *Blood* (2010) 116(24):5170–80. doi: 10.1182/blood-2009-12-258376
47. Jeannin P, Bottazzi B, Sironi M, Doni A, Rusnati M, Presta M, et al. Complexity and complementarity of outer membrane protein A recognition by cellular and humoral innate immunity receptors. *Immunity* (2005) 22(5):551–60. doi: 10.1016/j.immuni.2005.03.008
48. Bottazzi B, Santini L, Savino S, Giuliani MM, Duenas Diez AI, Mancuso G, et al. Recognition of *Neisseria meningitidis* by the long pentraxin PTX3 and its role as an endogenous adjuvant. *PLoS One* (2015) 10(3):e0120807. doi: 10.1371/journal.pone.0120807
49. Jaillon S, Moalli F, Ragnarsdottir B, Bonavita E, Puthia M, Riva F, et al. The humoral pattern recognition molecule PTX3 is a key component of innate immunity against urinary tract infection. *Immunity* (2014) 40(4):621–32. doi: 10.1016/j.immuni.2014.02.015
50. Deban L, Castro Russo R, Sironi M, Moalli F, Scanziani M, Zambelli V, et al. Regulation of leukocyte recruitment by the long pentraxin PTX3. *Nat Immunol* (2010) 11(4):328–34. doi: 10.1038/ni.1854
51. Presta M, Camozzi M, Salvatori G, Rusnati M. Role of the soluble pattern recognition receptor PTX3 in vascular biology. *J Cell Mol Med* (2007) 11(4):723–38. doi: 10.1111/j.1582-4934.2007.00061.x
52. Ronca R, Alessi P, Coltrini D, Salle ED, Giacomini A, Leali D, et al. Long pentraxin-3 as an epithelial-stromal fibroblast growth factor-targeting inhibitor in prostate cancer. *J Pathol* (2013). 230(2):228–38. doi: 10.1002/path.4181
53. Rodrigues PF, Matarazzo S, Maccarinelli F, Foglio E, Giacomini A, Silva Nunes JP, et al. Long pentraxin 3-mediated fibroblast growth factor trapping impairs fibrosarcoma growth. *Front Oncol* (2018) 8:472. doi: 10.3389/fonc.2018.00472
54. Turati M, Giacomini A, Rezzola S, Maccarinelli F, Gazzaroli G, Valentino S, et al. The natural FGF-trap long pentraxin 3 inhibits lymphangiogenesis and lymphatic dissemination. *Exp Hematol Oncol* (2022) 11(1):84. doi: 10.1186/s40164-022-00330-w
55. Leali D, Inforzato A, Ronca R, Bianchi R, Belleri M, Coltrini D, et al. Long pentraxin 3/tumor necrosis factor-stimulated gene-6 interaction: a biological rheostat for fibroblast growth factor 2-mediated angiogenesis. *Arteriosclerosis Thrombosis Vasc Biol* (2012) 32(3):696–703. doi: 10.1161/ATVBAHA.111.243998
56. Bally I, Inforzato A, Dalonneau F, Stravalaci M, Bottazzi B, Gaboriaud C, et al. Interaction of C1q with pentraxin 3 and IgM revisited: mutational studies with recombinant C1q variants. *Front Immunol* (2019) 10:461. doi: 10.3389/fimmu.2019.00461
57. Nauta AJ, Bottazzi B, Mantovani A, Salvatori G, Kishore U, Schwaebler WJ, et al. Biochemical and functional characterization of the interaction between pentraxin 3 and C1q. *Eur J Immunol* (2003) 33(2):465–73. doi: 10.1002/immu.200310022
58. Deban L, Jarva H, Lehtinen MJ, Bottazzi B, Bastone A, Doni A, et al. Binding of the long pentraxin PTX3 to Factor H: Interacting domains and function in the regulation of complement activation. *J Immunol* (2008) 181(12):8433–40. doi: 10.4049/jimmunol.181.12.8433
59. Csicsi AI, Kopp A, Zoldi M, Banlaki Z, Uzonyi B, Hebecker M, et al. Factor H-related protein 5 interacts with pentraxin 3 and the extracellular matrix and modulates complement activation. *J Immunol* (2015) 194(10):4963–73. doi: 10.4049/jimmunol.1403121
60. Kopp A, Strobel S, Tortajada A, Rodriguez de Cordoba S, Sanchez-Corral P, Prohaszka Z, et al. Atypical hemolytic uremic syndrome-associated variants and autoantibodies impair binding of factor h and factor h-related protein 1 to pentraxin 3. *J Immunol* (2012) 189(4):1858–67. doi: 10.4049/jimmunol.1200357
61. Swinkels M, Zhang JH, Tilakaratna V, Black G, Perveen R, McHarg S, et al. C-reactive protein and pentraxin-3 binding of factor H-like protein 1 differs from complement factor H: implications for retinal inflammation. *Sci Rep* (2018) 8(1):1643. doi: 10.1038/s41598-017-18395-7
62. Braunschweig A, Jozsi M. Human pentraxin 3 binds to the complement regulator C4b-binding protein. *PLoS One* (2011) 6(8):e23991. doi: 10.1371/journal.pone.0023991
63. Ma YJ, Doni A, Skjoedt MO, Honore C, Arendrup M, Mantovani A, et al. Heterocomplexes of mannose-binding lectin and the pentraxins PTX3 or serum amyloid P component trigger cross-activation of the complement system. *J Biol Chem* (2011) 286(5):3405–17. doi: 10.1074/jbc.M110.190637
64. Ma YJ, Doni A, Hummelshoj T, Honore C, Bastone A, Mantovani A, et al. Synergy between ficolin-2 and pentraxin 3 boosts innate immune recognition and complement deposition. *J Biol Chem* (2009) 284(41):28263–75. doi: 10.1074/jbc.M109.009225
65. Scarchilli L, Camaioni A, Bottazzi B, Negri V, Doni A, Deban L, et al. PTX3 interacts with inter-alpha-trypsin inhibitor: implications for hyaluronan organization and cumulus oophorus expansion. *J Biol Chem* (2007) 282(41):30161–70. doi: 10.1074/jbc.M703738200
66. Ievoli E, Lindstedt R, Inforzato A, Camaioni A, Palone F, Day AJ, et al. Implication of the oligomeric state of the N-terminal PTX3 domain in cumulus matrix assembly. *Matrix Biol* (2011) 30(5-6):330–7. doi: 10.1016/j.matbio.2011.05.002

67. Baranova NS, Inforzato A, Briggs DC, Tilakaratna V, Enghild JJ, Thakar D, et al. Incorporation of pentraxin 3 into hyaluronan matrices is tightly regulated and promotes matrix cross-linking. *J Biol Chem* (2014) 289(44):30481–98. doi: 10.1074/jbc.M114.568154
68. Fossati G, Pozzi D, Canzi A, Mirabella F, Valentino S, Morini R, et al. Pentraxin 3 regulates synaptic function by inducing AMPA receptor clustering via ECM remodeling and beta1-integrin. *EMBO J* (2019) 38(1):e99529. doi: 10.15252/emboj.201899529
69. Porte R, Silva-Gomes R, Theroude C, Parente R, Asgari F, Sironi M, et al. Regulation of inflammation and protection against invasive pneumococcal infection by the long pentraxin PTX3. *Elife* (2023) 12:e78601. doi: 10.7554/eLife.78601
70. Parente R, Possetti V, Erreni M, D'Autilia F, Bottazzi B, Garlanda C, et al. Complementary roles of short and long pentraxins in the complement-mediated immune response to aspergillus fumigatus infections. *Front Immunol* (2021) 12:785883. doi: 10.3389/fimmu.2021.785883
71. Rovere P, Peri G, Fazzini F, Bottazzi B, Doni A, Bondanza A, et al. The long pentraxin PTX3 binds to apoptotic cells and regulates their clearance by antigen-presenting dendritic cells. *Blood* (2000) 96(13):4300–6. doi: 10.1182/blood.V96.13.4300
72. Jaillon S, Jeannin P, Hamon Y, Fremaux I, Doni A, Bottazzi B, et al. Endogenous PTX3 translocates at the membrane of late apoptotic human neutrophils and is involved in their engulfment by macrophages. *Cell Death Differ* (2009) 16(3):465–74. doi: 10.1038/cdd.2008.173
73. Baruah P, Dumitriu IE, Peri G, Russo V, Mantovani A, Manfredi AA, et al. The tissue pentraxin PTX3 limits C1q-mediated complement activation and phagocytosis of apoptotic cells by dendritic cells. *J Leukocyte Biol* (2006) 80(1):87–95. doi: 10.1189/jlb.0805445
74. Cox N, Pilling D, Gomer RH. DC-SIGN activation mediates the differential effects of SAP and CRP on the innate immune system and inhibits fibrosis in mice. *Proc Natl Acad Sci U.S.A.* (2015) 112(27):8385–90. doi: 10.1073/pnas.1500956112
75. Giacomini A, Ghedini GC, Presta M, Ronca R. Long pentraxin 3: A novel multifaceted player in cancer. *Biochim Biophys Acta Rev Cancer* (2018) 1869(1):53–63. doi: 10.1016/j.bbcan.2017.11.004
76. Haapasalo K, Meri S. Regulation of the complement system by pentraxins. *Front Immunol* (2019) 10:1750. doi: 10.3389/fimmu.2019.01750
77. Agrawal A, Shrive AK, Greenhough TJ, Volanakis JE. Topology and structure of the C1q-binding site on C-reactive protein. *J Immunol* (2001) 166(6):3998–4004. doi: 10.4049/jimmunol.166.6.3998
78. Sorensen IJ, Nielsen EH, Andersen O, Danielsen B, Svehaug SE. Binding of complement proteins C1q and C4bp to serum amyloid P component (SAP) in solid contra liquid phase. *Scand J Immunol* (1996) 44(4):401–7. doi: 10.1046/j.1365-3083.1996.d01-326.x
79. Ma YJ, Garred P. Pentraxins in complement activation and regulation. *Front Immunol* (2018) 9:3046. doi: 10.3389/fimmu.2018.03046
80. Gill R, Kemp JA, Sabin C, Pepys MB. Human C-reactive protein increases cerebral infarct size after middle cerebral artery occlusion in adult rats. *J Cereb Blood Flow Metab* (2004) 24(11):1214–8. doi: 10.1097/01.WCB.0000136517.61642.99
81. Garcia de Frutos P, Dahlback B. Interaction between serum amyloid P component and C4b-binding protein associated with inhibition of factor I-mediated C4b degradation. *J Immunol* (1994) 152(5):2430–7. doi: 10.4049/jimmunol.152.5.2430
82. Okemefuna AI, Nan R, Miller A, Gor J, Perkins SJ. Complement factor H binds at two independent sites to C-reactive protein in acute phase concentrations. *J Biol Chem* (2010) 285(2):1053–65. doi: 10.1074/jbc.M109.044529
83. Inforzato A, Doni A, Barajon I, Leone R, Garlanda C, Bottazzi B, et al. PTX3 as a paradigm for the interaction of pentraxins with the Complement system. *Semin Immunol* (2013) 25(1):79–85. doi: 10.1016/j.smim.2013.05.002
84. Moalli F, Paroni M, Veliz Rodriguez T, Riva F, Polentarutti N, Bottazzi B, et al. The therapeutic potential of the humoral pattern recognition molecule PTX3 in chronic lung infection caused by *Pseudomonas aeruginosa*. *J Immunol* (2011) 186(9):5425–34. doi: 10.4049/jimmunol.1002035
85. Stravalaci M, Ferrara M, Pathak V, Davi F, Bottazzi B, Mantovani A, et al. The long pentraxin PTX3 as a new biomarker and pharmacological target in age-related macular degeneration and diabetic retinopathy. *Front Pharmacol* (2022) 12. doi: 10.3389/fphar.2021.811344
86. Wong JHC, Ma JYW, Jobling AI, Brandli A, Greferath U, Fletcher EL, et al. Exploring the pathogenesis of age-related macular degeneration: A review of the interplay between retinal pigment epithelium dysfunction and the innate immune system. *Front Neurosci* (2022) 16:1009599. doi: 10.3389/fnins.2022.1009599
87. Clark SJ, Schmidt CQ, White AM, Hakobyan S, Morgan BP, Bishop PN. Identification of factor H-like protein 1 as the predominant complement regulator in bruch's membrane: implications for age-related macular degeneration. *J Immunol* (2014) 193(10):4962–70. doi: 10.4049/jimmunol.1401613
88. Landowski M, Kelly U, Klingeborn M, Groelle M, Ding JD, Grigsby D, et al. Human complement factor H Y402H polymorphism causes an age-related macular degeneration phenotype and lipoprotein dysregulation in mice. *Proc Natl Acad Sci United States America* (2019) 116(9):3703–11. doi: 10.1073/pnas.1814014116
89. Varani S, Elvin JA, Yan C, DeMayo J, DeMayo FJ, Horton HF, et al. Knockout of pentraxin 3, a downstream target of growth differentiation factor-9, causes female subfertility. *Mol Endocrinol* (2002) 16:1154–67. doi: 10.1210/mend.16.6.0859
90. May L, Kuningas M, van Bodegom D, Meij HJ, Frolich M, Slagboom PE, et al. Genetic variation in pentraxin (PTX) 3 gene associates with PTX3 production and fertility in women. *Biol Reprod* (2010) 82(2):299–304. doi: 10.1095/biolreprod.109.079111
91. Sirugo G, Edwards DR, Ryckman KK, Bissey C, White MJ, Kebbeh B, et al. PTX3 genetic variation and dizygotic twinning in the Gambia: could pleiotropy with innate immunity explain common dizygotic twinning in Africa? *Ann Hum Genet* (2012) 76(6):454–63. doi: 10.1111/j.1469-1809.2012.00723.x
92. Lord MS, Melrose J, Day AJ, Whitelock JM. The inter-alpha-trypsin inhibitor family: versatile molecules in biology and pathology. *J Histochem Cytochem* (2020) 68(12):907–27. doi: 10.1369/0022155420940067
93. Day AJ, Milner CM. TSG-6: A multifunctional protein with anti-inflammatory and tissue-protective properties. *Matrix Biol* (2019) 78–79:60–83. doi: 10.1016/j.matbio.2018.01.011
94. Baranova NS, Nileback E, Haller FM, Briggs DC, Svedhem S, Day AJ, et al. The inflammation-associated protein TSG-6 cross-links hyaluronan via hyaluronan-induced TSG-6 oligomers. *J Biol Chem* (2011) 286(29):25675–86. doi: 10.1074/jbc.M111.247395
95. Parente R, Sobacchi C, Bottazzi B, Mantovani A, Grcevic D, Inforzato A. The long pentraxin PTX3 in bone homeostasis and pathology. *Front Immunol* (2019) 10:2628. doi: 10.3389/fimmu.2019.02628
96. Boutet MA, Nerviani A, Lliso-Ribera G, Leone R, Sironi M, Hands R, et al. Circulating and synovial pentraxin-3 (PTX3) expression levels correlate with rheumatoid arthritis severity and tissue infiltration independently of conventional treatments response. *Front Immunol* (2021) 12:686795. doi: 10.3389/fimmu.2021.686795
97. Tighe RM, Garantziotis S. Hyaluronan interactions with innate immunity in lung biology. *Matrix Biol* (2019) 78–79:84–99. doi: 10.1016/j.matbio.2018.01.027
98. McDonald B, Kubes P. Interactions between CD44 and hyaluronan in leukocyte trafficking. *Front Immunol* (2015) 6. doi: 10.3389/fimmu.2015.00068
99. Senbanjo LT, Chellaiah MA. CD44: A multifunctional cell surface adhesion receptor is a regulator of progression and metastasis of cancer cells. *Front Cell Dev Biol* (2017) 5. doi: 10.3389/fcell.2017.00018
100. Porte R, Davoudian S, Asgari F, Parente R, Mantovani A, Garlanda C, et al. The long pentraxin PTX3 as a humoral innate immunity functional player and biomarker of infections and sepsis. *Front Immunol* (2019) 10:794. doi: 10.3389/fimmu.2019.00794
101. Ristagno G, Fumagalli F, Bottazzi B, Mantovani A, Olivari D, Novelli D, et al. Pentraxin 3 in cardiovascular disease. *Front Immunol* (2019) 10:823. doi: 10.3389/fimmu.2019.00823
102. Watt J, Siddique I, Dowe T, Crnogorac-Jurcevic T, Allavena P, Kocher H. Role of PTX3 in pancreatic cancer. *Lancet* (2014) 383:106–6. doi: 10.1016/S0140-6736(14)60369-X
103. Cunha C, Aversa F, Lacerda JF, Busca A, Kurzai O, Grube M, et al. Genetic PTX3 deficiency and aspergillosis in stem-cell transplantation. *New Engl J Med* (2014) 370(5):421–32. doi: 10.1056/NEJMoa1211161
104. Kushner I. C-reactive protein - My perspective on its first half century, 1930-1982. *Front Immunol* (2023) 14:1150103. doi: 10.3389/fimmu.2023.1150103

## Glossary

aHUS	atypical hemolytic uremic syndrome
AKT	protein kinase B
AMD	age-related macular degeneration
BrM	Bruch's membrane
C4BP	C4b-binding protein
CCPs	complement control protein
COC	cumulus oophorous complex
CRP	C reactive protein
Cryo-EM	cryogenic electron microscopy
DAMPs	danger-associated molecular patterns
DC-SIGN	dendritic cell-specific intercellular adhesion molecule-3-grabbing nonintegrin
ECM	extracellular matrix
ERK1/2	extracellular signal-regulated kinase 1/2
FAK	focal adhesion kinase
fB	factor B
FG	fibrinogen/fibrin
FGFs	fibroblast growth factors
fH	factor H
FHL-1	factor H-like protein 1
FHR-1 & -5	factor H-related protein 1 & 5
HA	hyaluronic acid
HCS	heavy chains
IL-1 $\beta$	interleukin-1 $\beta$
I $\alpha$ I	inter-alfa-trypsin inhibitor
LPS	lipopolysaccharide
MBL	mannose binding lectin
NF- $\kappa$ B	nuclear factor kappa-B
NPTX1 or NP1	neuronal pentraxins 1
NPTX2 or Narp or NP2	neuronal pentraxins 2
NPTXR	neuronal pentraxin receptor
oBRB	outer blood-retinal barrier
OmpA	outer membrane protein A
OMV	outer membrane vesicles
PAMPs	pathogen-associated molecular patterns
PG	plasminogen
PRMs	pattern recognition molecules
PTX3	pentraxin 3

(Continued)

## Continued

PTX4	pentraxin 4
RPE	retinal pigment epithelium
SAP	serum amyloid P component
SARS_COV_2	severe acute respiratory syndrome coronavirus 2
TNF- $\alpha$	tumor necrosis factor- $\alpha$
TSG-6	tumor necrosis factor-inducible gene 6 protein
TSP1	thrombospondin 1





## OPEN ACCESS

## EDITED BY

Alok Agrawal,  
East Tennessee State University,  
United States

## REVIEWED BY

Melissa Govender,  
University of Oxford, United Kingdom  
Prakhar Gupta,  
Queen Mary University of London,  
United Kingdom  
Vladimir M. Pisarev,  
Federal Research and Clinical Center  
of Intensive Care Medicine and  
Rehabilitation, Russia

## \*CORRESPONDENCE

Qiuyu Li

✉ liqiuyu00@bjmu.edu.cn

Ling Liang

✉ liangling@bjmu.edu.cn

RECEIVED 15 July 2023

ACCEPTED 30 October 2023

PUBLISHED 23 November 2023

## CITATION

Liu C, Zheng C, Shen X, Liang L and Li Q  
(2023) Serum CRP interacts with SPARC  
and regulate immune response in severe  
cases of COVID-19 infection.  
*Front. Immunol.* 14:1259381.  
doi: 10.3389/fimmu.2023.1259381

## COPYRIGHT

© 2023 Liu, Zheng, Shen, Liang and Li. This  
is an open-access article distributed under  
the terms of the [Creative Commons  
Attribution License \(CC BY\)](#). The use,  
distribution or reproduction in other  
forums is permitted, provided the original  
author(s) and the copyright owner(s) are  
credited and that the original publication in  
this journal is cited, in accordance with  
accepted academic practice. No use,  
distribution or reproduction is permitted  
which does not comply with these terms.

# Serum CRP interacts with SPARC and regulate immune response in severe cases of COVID-19 infection

Chengyang Liu<sup>1</sup>, Chenyang Zheng<sup>2</sup>, Xipeng Shen<sup>2</sup>,  
Ling Liang<sup>3\*</sup> and Qiuyu Li<sup>4\*</sup>

<sup>1</sup>Department of Pathology, Institute of Systems Biomedicine, School of Basic Medical Sciences, Peking-Tsinghua Center for Life Sciences, Beijing Key Laboratory of Tumor Systems Biology, Peking University Health Science Center, Beijing, China, <sup>2</sup>School of Biological Science and Medical Engineering, Beihang University, Beijing, China, <sup>3</sup>Department of Biophysics, School of Basic Medical Sciences, Peking University Health Science Center, Beijing, China, <sup>4</sup>Department of Respiratory and Critical Care Medicine, Peking University Third Hospital, Beijing, China

Serum C-reactive protein (CRP) has been found elevated during COVID-19 infection, and associated with systematic inflammation as well as a poor clinical outcome. However, how did CRP participated in the COVID-19 pathogenesis remains poorly understood. Here, we report that serum C-reactive protein (CRP) levels are correlated with megakaryocyte marker genes and could regulate immune response through interaction with megakaryocytes. Molecular dynamics simulation through ColabFold showed a reliable interaction between monomeric form of CRP (mCRP) and the secreted protein acidic and rich in cysteine (SPARC). The interaction does not affect the physiological activities of SPARC while would be disturbed by pentamerization of CRP. Interplay between SPARC and mCRP results in a more intense immune response which may led to poor prognosis. This study highlights the complex interplay between inflammatory markers, megakaryocytes, and immune regulation in COVID-19 and sheds light on potential therapeutic targets.

## KEYWORDS

C-reactive protein, COVID-19, secreted protein acidic and rich in cysteine, cytokine response storm, megakaryocyte

## Introduction

One crucial feature of COVID-19 infection is the upregulation of serum C-reactive protein (CRP) level, an acute-phase protein usually considered as a sensitive index of tissue injury. CRP is classically synthesized in the liver hepatocytes upon interleukin-6 (IL-6) induction, consisting of five non-covalently linked subunits forming a disc-shaped pentamer (pCRP) and released to plasma circulating in pentameric form (1). At the inflammation and infection sites, CRP interacts with the bioactive lipids on the cell membrane of activated platelet or target cells and dissociates into monomeric subunits



called mCRP. Retrospective studies show that both the native pCRP and mCRP have predictive value of clinical severity in COVID-19 disease (2, 3).

Mechanically speaking, CRP participates in innate immunity through interaction with C1q and consequent activation of the complement pathway or binding to Fc receptors with the resulting release of pro-inflammatory cytokines (4). Previous clinical evidence suggests that CRP is elevated in bacterial rather than viral infections and usually lacks adaptive immunity. The high serum CRP levels during COVID-19 infection are associated with cytokine response storm (hypercytokinemia) or macrophage activation syndrome (2). Nevertheless, the impact of C-reactive protein (CRP) on the progression of COVID-19-associated pneumonia remains to be elucidated. Here, using open-access databases and clinical retrospective studies, we proposed a model of how CRP regulates immune responses in COVID-19 infection.

## Methods

### Collection of CRP-associated genes in COVID 19 patients

We selected whole blood RNA-seq datasets of COVID-19 patients from the Gene Expression Omnibus (GEO) database (<https://www.ncbi.nlm.nih.gov/geo/>) for discovery and validation of CRP-associated transcripts. Dataset (GSE157103) were used for discovery research (5). By performing Pearson correlation analysis, we obtained five transcripts that was positively correlated with serum CRP level. Dataset GSE172114, GSE167930 were used for verification (6, 7). Dataset GSE158055 were used for single-cell level analysis, <http://covid19.cancer-pku.cn> (8). This study was reviewed by the Ethics Committee of Peking University Third Hospital (IRB00006761-M2020060).

### Protein–protein interaction analysis and network construction

We constructed a PPI network using common transcripts and employed STRING (9), setting a minimum required interaction score of 0.4, while keeping other parameters at their default values. Subsequently, we analyzed and visualized the PPI results using Cytoscape (version 3.10.0) (10). To identify key proteins within the network, we utilized cytoHubba, a Cytoscape plug-in, and applied the degree topological algorithm to obtain the five hub proteins with the highest degree values.

### Molecular dynamics (MD) simulation analysis

The three-dimensional protein complex structure of mCRP interacting with SPARC was predicted using AlphaFold2 (11) as implemented in ColabFold (12) running locally in the alphafold2\_multimer\_v3 model. The Amber-relaxed, top-ranked

AlphaFold2 structure was used for MD simulation. The CHARMM-GUI website is used to process the protein file, and 150 mM NaCl was added to mimic physiological conditions. Prepared systems were first minimized using 5000 steps of a steepest descent algorithm. Next, 125 ps was used to equilibrate the system at 310 K, and a 300 ns MD simulation was conducted at a constant temperature of 310 K using the Gromacs 2023 software package. VMD was used to process and analyze the protein structure. The interface was analyzed by PISA available at <https://www.ebi.ac.uk/pdbe/pisa/> and the results were displayed using Pymol (The PyMOL Molecular Graphics System, Version 2.0 Schrödinger, LLC).

### Gene ontology and pathway enrichment analyses

In order to gain insights into the functional characteristics of CRP-associated megakaryocyte marker genes, a set of enrichment analyses was performed using R package Enrichr (13). This approach aimed to provide detailed information on the biological mechanisms and signaling pathways associated with these genes. The enrichment analyses encompassed gene ontology (GO) terms, including biological process, molecular function, and cellular component categories. Additionally, to achieve a more comprehensive understanding of the relevant signaling pathways, other databases such as WikiPathways, Reactome, BioCarta, and the KEGG pathway were also employed in the analysis.

## Results

### Serum CRP level is highly correlated with megakaryocyte marker genes during COVID-19 infection

The serum C-reactive protein (CRP) level has been identified as a marker correlating with the severity of COVID-19 infection. Higher CRP levels often indicate a more pronounced inflammatory response, leading to widespread inflammation in the body, causing tissue damage, organ dysfunction, and poorer clinical outcomes (14). Clinical studies of COVID-19 patients were integrated, and the expression trend of serum CRP during the disease process was depicted (Figures 1A, B). Collectively, patients bearing COVID-19 infection exhibited significantly higher levels of serum CRP (>100mg/ml) compared to either the healthy ones or non-COVID patients with respiratory infection. Furthermore, patients with severe COVID-19 infection, often with critical pneumonia and systemic symptoms, showed high CRP levels, probably due to inflammatory factor storm. This gradual upward trend aroused our curiosity about whether CRP contributed to the disease progression and, if so, how CRP worked.

Open-access RNA-seq databases of COVID-19 patients were mined to illustrate the specific interactions and mechanisms by which CRP contributed to COVID-19 infection (5). Pearson correlation analysis identified a group of 6 transcripts that were

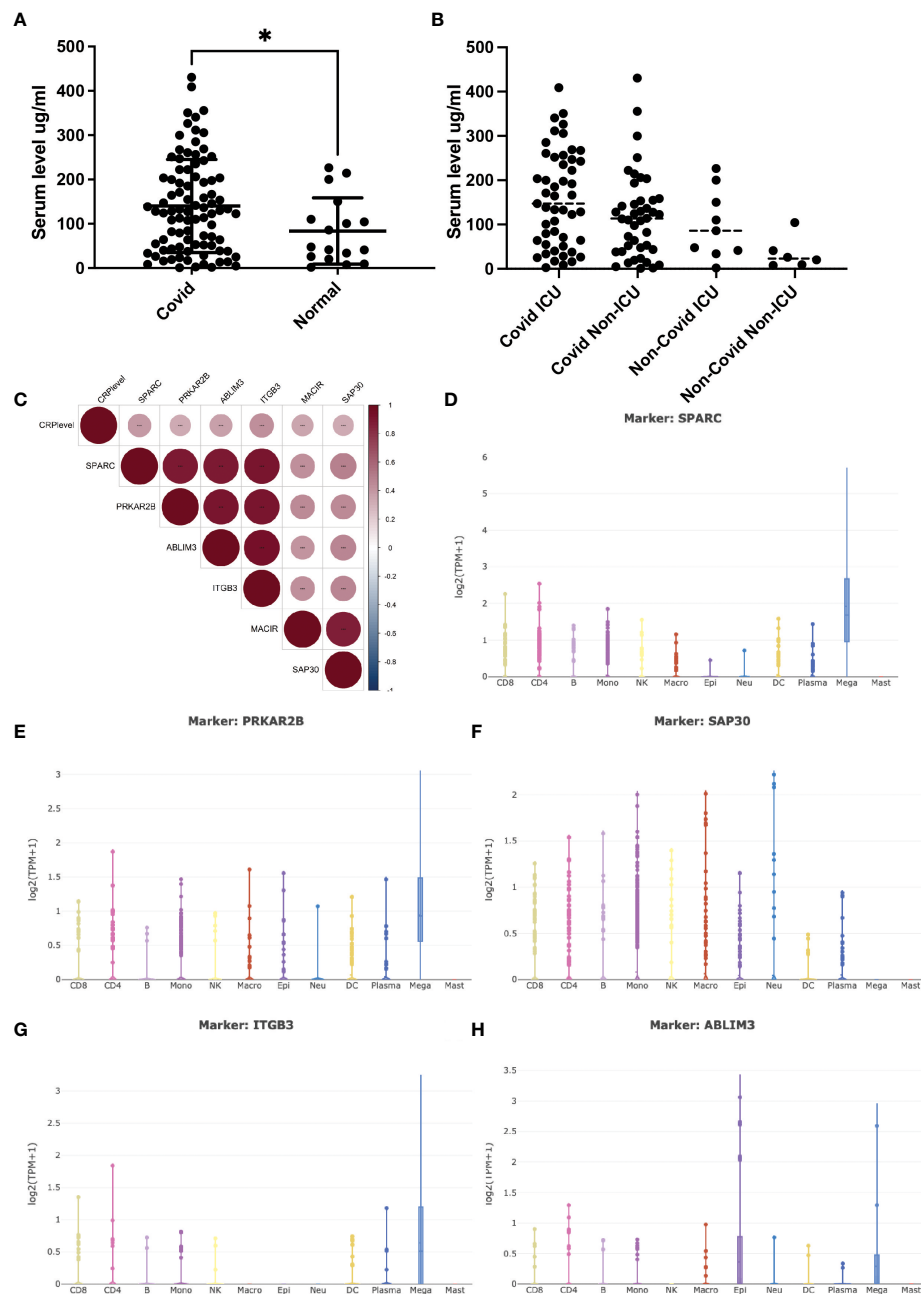


FIGURE 1

Serum CRP level and its related transcripts during Covid-19 infection. (A) Serum CRP level (ng/ml) in Covid-19 patients collected from Peking university third hospital. Two tailed unpaired t-test was performed,  $p=0.0362$ . \*:  $p<0.05$ . (B) Serum CRP level (ng/ml) in GSE157103 dataset; (C) Pearson correlation analysis of CRP-associated transcripts in GSE157103 dataset; (D–H) Single-cell analysis of CRP-associated transcripts in major blood celltypes.

significantly positively associated with serum CRP level (Figure 1C). Of these transcripts, ITGB3 was one of the vital predictive genes of COVID-19-related stroke as involved in integrin pathway signal transduction (15). PRKAR2B was a cAMP-MAPK kinase, which may bind to the NSP13 protein of SARS-COV-2 (16). SAP30 was a subunit of the histone deacetylase complex, which regulates gene acetylation modification levels and gene expression by binding to the HDAC complex (17). ABLIM3 was a microfilament-binding protein localized to microfilament stress fibers. MACIR was a macrophage immunometabolism regulator that only showed up in one RNA-seq

database. SPARC was a glycoprotein that regulated the extracellular matrix and had been reported to be a metabolic, immune checkpoint for inflammation and interferon responses, participating in the TGF-beta/TNF signaling pathway and converting anti-inflammatory macrophages into pro-inflammatory macrophages (18). The latter three had never appeared in COVID-19-related research.

To verify whether and how these six transcripts were involved in COVID-19 infection along with CPR, single-cell RNA-sequencing databases were used to depict their cell-type specific expression. As shown in Figures 1D–H, most of these transcripts

were mainly expressed by megakaryocytes (MK), while SAP30 was universally expressed in lymphoid and myeloid cells. As the precursors of platelets, MKs undergo a complex process of maturation and fragmentation to produce platelets. Megakaryocytes controlled the proliferation of hematopoietic cells, promoted the excretion of neutrophils from the bone marrow, and were not typically associated with acute inflammatory disease. In COVID-19 patients, abnormalities in blood parameters such as lymphopenia (reduced lymphocyte count) and thrombocytopenia (reduced platelet count) have been observed. Several lines of evidence suggested that MKs were significantly accumulated in progression/severe COVID-19 as a feature of the systemic inflammatory response, with SPARC being the marker gene (19, 20). However, whether and how CRP contributed to this process remains unclear, and it is essential to elucidate the direct correlation between CRP and MKs.

## SPARC interacts with mCRP through its Kazal-like domain

Whether serum CRP interacted with the megakaryocytes' signature genes was the first thing to be investigated. Since ABLIM3 and PRKAR2B were mainly expressed in the cytoplasm, we focused on the membrane protein ITGB3 and secreted protein SPARC. Furthermore, previous studies had suggested SPARC as a marker gene of MKs during cell type identification of scRNA-seq data (21, 22). Herein, ColabFold and molecular dynamics simulation were utilized to investigate SPARC-CRP interaction. Alphafold2 showed that mCRP exhibited a reliable interaction with

SPARC (Figure 2A). Three clusters of intermolecular interactions were formed, as shown in Figures 2B–E, including five hydrogen bonds and three salt bridges. The distance between interacting residues was around 2–3 Å. The entire model stabilizes during 300ns in molecular dynamics (Figure 2E).

As a secreted protein, SPARC has been reported to share interaction with multiple receptors and cell surface matrix-associated molecules, like CPS1 and COL1A1 (23, 24). However, previous studies could have illustrated the exact amino acids responsible for these interactions. SPARC has a unique structure composed of an N-terminal acidic domain, a follistatin-like domain, a Kazal-like domain, and a C-terminal extracellular calcium-binding (ECB) domain (25). Through molecular dynamics, we could predict residues involved in interaction with mCRP. As shown in Table 1, most centered around the Kazal-like domain of SPARC, and the other two residues were in the ECB domain. Residues responsible for calcium binding (e.g., D222, P225, E227, Y229) and for collagen binding (e.g., N156, R164, E246) were not affected by SPARC-mCRP linking, suggesting that physiological functions of SPARC were not affected by this interaction (26, 27).

The whole interface of SPARC-mCRP linking involved 54 residues collectively (Table 2). Residues of mCRP were mainly located on the beta-sheets (aa92–106, aa136–153), the structure of which remained stable and uniform in comparison with other peptides of mCRP. Aa35–47 and aa199–206 sequence of mCRP were reported to encompass potent ligand binding ability due to its soft, disordered conformation (28). However, none of these sequences form interaction with SPARC. Residues of mCRP on the interface were not fully investigated previously. Furthermore, in the pentameric form, the interface of mCRP was partially buried,

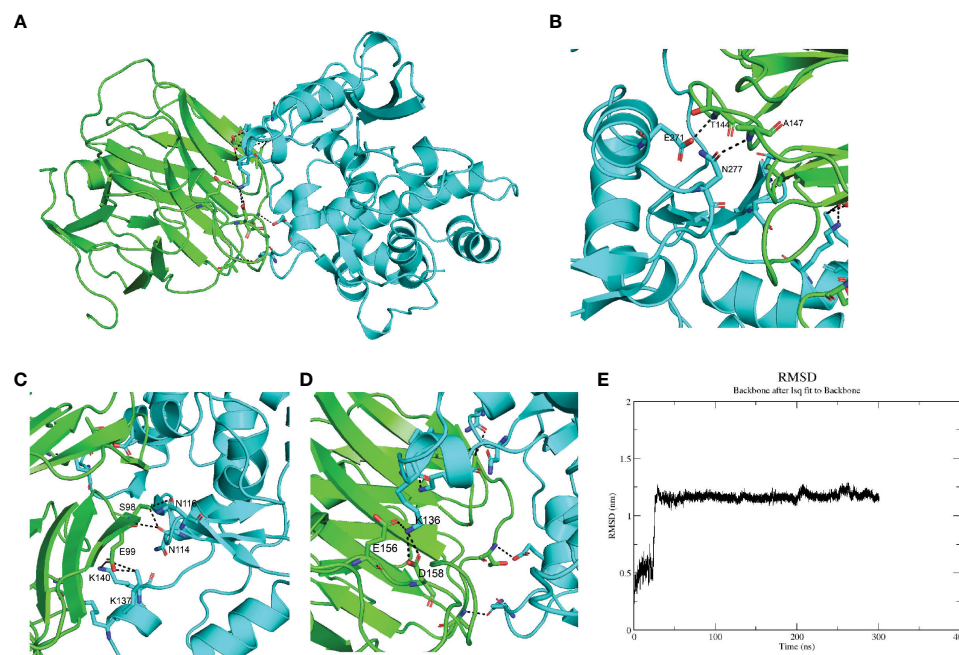


FIGURE 2

SPARC interacts with mCRP through its Kazal-like domain. (A) Molecular dynamics stimulation of mCRP-SPARC interaction models. green: mCRP; blue: SPARC. (B–D) Details of the interacting residues forming salt bridges and hydrogen bonds; (E) Root mean square deviation (RMSD) of mCRP-SPARC with respect to the initial structure during a 300 ns simulation.

TABLE 1 Intermolecular interactions between SPARC and CRP.

Hydrogen bonds				Salt bridges		
	SPARC	Dist.[Å]	CRP	SPARC	Dist.[Å]	CRP
1	ASN 114[O]	3.51	GLU 99[N]	LYS 136[NZ]	2.60	GLU 156[OE1]
2	ASN 114[O]	2.55	SER 98[OG]	LYS 136[NZ]	2.69	ASP 158[OD1]
3	ASN 116[OD1]	3.31	SER 98[OG]	LYS 136[NZ]	3.32	ASP 158[OD2]
4	GLU 271[OE2]	3.10	THR 144[N]	LYS 137[NZ]	3.86	GLU 99[OE1]
5	ASN 277[OD1]	2.83	ALA 147[N]	LYS 137[NZ]	2.66	GLU 99[OE2]
6				LYS 140[NZ]	2.64	GLU 99[OE1]

TABLE 2 Interface summary.

		SPARC		CRP	
Number of atoms	interface	92	3.80%	97	4.90%
	surface	1509	63.10%	988	49.90%
	total	2391	100.00%	1981	100.00%
Number of residues	interface	23	9.20%	31	15.00%
	surface	246	98.80%	183	88.40%
	total	249	100.00%	207	100.00%
Solvent-accessible area, Å	interface	867.3	5.10%	804	7.70%
	total	17116.8	100.00%	10483.2	100.00%
Solvation energy, kcal/mol	isolated structure	-222.2	100.00%	-207.5	100.00%
	gain on complex formation	0.9	-0.40%	0.8	-0.40%
	average gain	-1.2	0.60%	-2	1.00%
	P-value	0.793		0.862	

indicating that the pentamerization of CRP would affect its binding to SPARC. Since pCRP dissociates into mCRP to promote inflammation, we proposed that the SPARC-mCRP linking may further aggravate inflammation status in COVID-19 patients.

SPARC-mCRP linking affects inflammation status through megakaryocytes

Previous studies have revealed that CRP could potentiate the IL-1-rich-microparticle production in megakaryocytes and further promote systemic inflammation (29, 30). Using SPARC as the primary classifier, patients were clustered into two groups (Figure 3A). The volcano plot showed that four transcripts were downregulated in SPARC-high vs low comparison, while 112 transcripts were upregulated. Gene Set Enrichment Analysis (GSEA) of the differentially expressed genes showed a more intense immune response in the SPARC-high group, characterized by overactivation of phagocytosis, adaptive immune response, B-cell activation, and complement activation pathways (Figures 3B, C). Notably, although the primary source of SPARC

expression is megakaryocytes, no abnormalities in coagulation or platelet function were found.

Accumulation of megakaryocytes in severe progression cases and depression in convalescence patients was observed (Figures 3D, E; Table 3). Previous research identified an expansion of circulating megakaryocytes and increased erythropoiesis with features of hypoxic signaling in critical patients. However, most of these studies concluded that the expansion of MK led to hypercoagulability and thrombophilia in patients. Few articles mentioned the impact of MK cells on immune status. Our research proposed the possibility of megakaryocytes influencing inflammation response during COVID-19 through the SPARC-mCRP link. Further studies will be needed to illustrate the detailed mechanism of how CRP drove the expansion of megakaryocytes and the role of megakaryocytes in Covid-19 progression.

Discussion

Our study aimed to investigate how CRP regulates the immune responses during COVID-19 infection. Using open-access databases

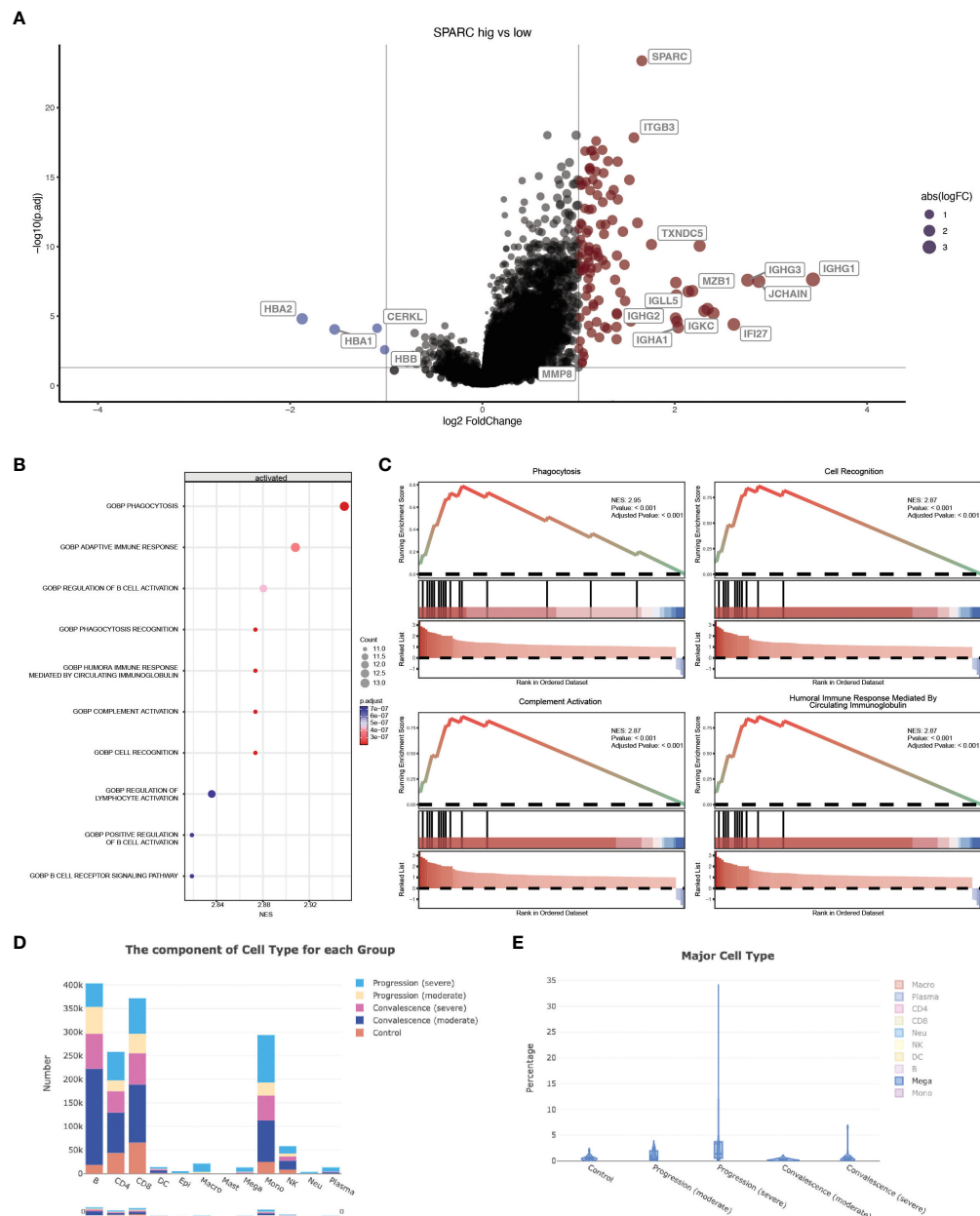


**FIGURE 3** SPARC-mCRP link influence immune response in COVID-19 patients. **(A)** Volcano plot showing differentially expressed transcripts (DET), patients were clustered into two groups according to SPARC expression level, DET were identified through limma regression; **(B)** GSEA enrichment of DETs between clusters; **(C)** GSEA plot showing the most influenced pathway in SPARC-high vs low comparison; **(D, E)** Change of megakaryocytes proportion during different infection stages.

and clinical retrospective studies, we noticed that serum CRP interacted with circulating megakaryocytes through SPARC and further regulated virus response and systematic inflammation in COVID-19 patients. We discovered a positive correlation between serum CRP levels and the proportion of circulating megakaryocytes.

The positive correlation between serum CRP levels and circulating megakaryocyte proportion suggests a potential link between inflammation and megakaryocyte biology. It is well-established that CRP is an acute-phase reactant produced by the liver in response to inflammation. Elevated CRP levels are commonly associated with increased inflammation in various

pathological conditions. In our study, the positive correlation suggests that as inflammation increases, the proportion of circulating megakaryocytes also increases.

Furthermore, our investigation revealed a potential mechanism by which CRP interacts with secreted protein acidic and rich in cysteine (SPARC) expressed by megakaryocytes to regulate virus response and immune regulation. SPARC is a multifunctional matricellular protein involved in various cellular processes, including immune modulation and tissue remodeling. The interaction between CRP and SPARC may affect the immune response and viral clearance in COVID-19.



TABLE 3 GSEA analysis of SPARC-high vs low comparison.

GOBP Pathway	Enrichment Score	NES	p.adjust
Activation of immune response	0.75	2.68	3.73E-06
Adaptive immune response	0.76	2.91	3.84E-07
Adaptive immune response based on somatic recombination of immune receptors built from immunoglobulin superfamily domains	0.75	2.68	3.73E-06
Antigen receptor mediated signaling pathway	0.75	2.68	3.73E-06
B cell activation	0.71	2.71	3.73E-06
B cell mediated immunity	0.82	2.81	8.74E-07
B cell receptor signaling pathway	0.82	2.82	7.36E-07
Biological process involved in interspecies interaction between organisms	0.52	2.33	0.0005447
Cell activation	0.51	2.26	0.00063476
Cell recognition	0.86	2.87	2.02E-07
Complement activation	0.86	2.87	2.02E-07
Defense response	0.52	2.32	0.00029081
Defense response to bacterium	0.66	2.61	3.73E-06
Defense response to other organism	0.57	2.49	9.85E-05
Endocytosis	0.69	2.67	7.21E-06
Humoral immune response	0.70	2.69	4.18E-06
Humoral immune response mediated by circulating immunoglobulin	0.86	2.87	2.02E-07
Immune effector process	0.73	2.73	2.71E-06
Immune response	0.56	2.52	5.30E-05
Immune response regulating cell surface receptor signaling pathway	0.75	2.68	3.73E-06
Immune response regulating signaling pathway	0.66	2.52	3.29E-05
Innate immune response	0.67	2.72	3.73E-06
Leukocyte mediated immunity	0.78	2.75	1.21E-06
Lymphocyte activation	0.63	2.52	2.01E-05
Lymphocyte mediated immunity	0.82	2.81	8.74E-07
Membrane invagination	0.78	2.76	1.04E-06
Membrane organization	0.72	2.64	4.38E-06
Phagocytosis	0.79	2.95	2.02E-07
Phagocytosis recognition	0.86	2.87	2.02E-07
Positive regulation of b cell activation	0.82	2.82	7.36E-07

(Continued)

TABLE 3 Continued

GOBP Pathway	Enrichment Score	NES	p.adjust
Positive regulation of cell activation	0.75	2.70	3.73E-06
Positive regulation of immune response	0.75	2.68	3.73E-06
Positive regulation of immune system process	0.66	2.61	3.73E-06
Regulation of b cell activation	0.80	2.88	4.40E-07
Regulation of cell activation	0.64	2.56	1.44E-05
Regulation of immune response	0.66	2.52	3.29E-05
Regulation of immune system process	0.56	2.39	0.00036199
Regulation of lymphocyte activation	0.77	2.84	7.28E-07
Response to bacterium	0.66	2.61	3.73E-06
Vesicle mediated transport	0.68	2.72	2.71E-06

The observed correlation between CRP and megakaryocytes, along with the potential interaction with SPARC, suggests that megakaryocytes could play a role in the immune response to COVID-19. Megakaryocytes are known to produce platelets, which have recently been implicated in immune regulation beyond their traditional role in hemostasis. The interaction between CRP and SPARC expressed by megakaryocytes may modulate the immune response and contribute to regulating viral clearance and inflammation in COVID-19 patients.

These findings highlight the complex interplay between inflammatory markers, megakaryocytes, and immune regulation in COVID-19. Understanding the mechanisms underlying the positive correlation between CRP and megakaryocytes, as well as the role of the CRP-SPARC interaction, could provide valuable insights into the pathogenesis of COVID-19 and potentially identify novel therapeutic targets.

It is essential to acknowledge the limitations of our study. Although we found a positive correlation between serum CRP levels and circulating megakaryocyte proportion, further investigations are needed to establish a causal relationship and elucidate the underlying mechanisms. Additionally, the generalizability of our findings may be influenced by factors such as patient population, disease severity, and comorbidities.

## Conclusion

Our study reveals a positive correlation between serum CRP levels and circulating megakaryocyte proportion, suggesting an interaction between CRP and megakaryocytes in COVID-19. Furthermore, the CRP-SPARC interaction may affect virus response and immune regulation. These findings contribute to understanding the intricate relationship between inflammation, megakaryocytes, and the immune

response in COVID-19, offering potential avenues for further research and therapeutic interventions.

## Data availability statement

The original contributions presented in the study are included in the article/supplementary material. Further inquiries can be directed to the corresponding author.

## Ethics statement

The studies involving humans were approved by This study was reviewed by the Ethics Committee of Peking University Third Hospital (IRB00006761-M2020060). The studies were conducted in accordance with the local legislation and institutional requirements. The human samples used in this study were acquired from primarily isolated as part of your previous study for which ethical approval was obtained. Written informed consent for participation was not required from the participants or the participants' legal guardians/next of kin in accordance with the national legislation and institutional requirements.

## Author contributions

CL: Conceptualization, Data curation, Formal Analysis, Writing – original draft, Writing – review & editing. CZ: Conceptualization, Data curation, Methodology, Writing – original draft. XS: Conceptualization, Data curation, Investigation, Methodology,

Writing – review & editing. LL: Methodology, Investigation, Visualization, Writing – review & editing. QL: Conceptualization, Funding acquisition, Investigation, Writing – review & editing.

## Funding

The author(s) declare financial support was received for the research, authorship, and/or publication of this article. This work was supported by the following grants to QL including National Natural Science Foundation of China (No. 81900641) and the Fundamental Research Funds for the Central University: the Research Funding of PKU (BMU2021MX020, BMU2022MX008).

## Conflict of interest

The authors declare that the research was conducted in the absence of any commercial or financial relationships that could be construed as a potential conflict of interest.

## Publisher's note

All claims expressed in this article are solely those of the authors and do not necessarily represent those of their affiliated organizations, or those of the publisher, the editors and the reviewers. Any product that may be evaluated in this article, or claim that may be made by its manufacturer, is not guaranteed or endorsed by the publisher.

## References

- Molins B, Figueras-Roca M, Valero O, Llorenç V, Romero-Vázquez S, Sibila O, et al. C-reactive protein isoforms as prognostic markers of COVID-19 severity. *Front Immunol* (2022) 13:1105343. doi: 10.3389/fimmu.2022.1105343
- Luan YY, Yin CH, Yao YM. Update advances on C-reactive protein in COVID-19 and other viral infections. *Front Immunol* (2021) 12:720363. doi: 10.3389/fimmu.2021.720363
- Li Q, Ding X, Xia G, Chen HG, Chen F, Geng Z, et al. Eosinopenia and elevated C-reactive protein facilitate triage of COVID-19 patients in fever clinic: A retrospective case-control study. *EClinicalMed* (2020) 23:100375. doi: 10.1016/j.eclinm.2020.100375
- Sproston NR, Ashworth JJ. Role of C-reactive protein at sites of inflammation and infection. *Front Immunol* (2018) 9:754. doi: 10.3389/fimmu.2018.00754
- Overmyer KA, Shishkova E, Miller IJ, Balnis J, Bernstein MN, Peters-Clarke TM, et al. Large-scale multi-omic analysis of COVID-19 severity. *Cell Syst* (2021) 12(1):23–40.e7. doi: 10.1016/j.cels.2020.10.003
- Carapito R, Li R, Helms J, Carapito C, Gujja S, Rolli V, et al. Identification of driver genes for critical forms of COVID-19 in a deeply phenotyped young patient cohort. *Sci Transl Med* (2022) 14(628):eabj7521. doi: 10.1126/scitranslmed.abj7521
- Zhou Z, Zhou X, Cheng L, Wen L, An T, Gao H, et al. Machine learning algorithms utilizing blood parameters enable early detection of immunothrombotic dysregulation in COVID-19. *Clin Transl Med* (2021) 11(9):e523. doi: 10.1002/ctm2.523
- Ren X, Wen W, Fan X, Hou W, Su B, Cai P, et al. COVID-19 immune features revealed by a large-scale single-cell transcriptome atlas. *Cell* (2021) 184(7):1895–1913.e19. doi: 10.1016/j.cell.2021.01.053
- Szklarczyk D, Gable AL, Lyon D, Junge A, Wyder S, Huerta-Cepas J, et al. STRING v11: protein-protein association networks with increased coverage, supporting functional discovery in genome-wide experimental datasets. *Nucleic Acids Res* (2019) 47(D1):D607–13. doi: 10.1093/nar/gky1131
- Shannon P, Markiel A, Ozier O, Baliga NS, Wang JT, Ramage, et al. Cytoscape: a software environment for integrated models of biomolecular interaction networks. *Genome Res* (2003) 13(11):2498–504. doi: 10.1101/gr.1239303
- Jumper J, Evans R, Pritzel A, Green T, Figurnov M, Ronneberger O, et al. Highly accurate protein structure prediction with AlphaFold. *Nature* (2021) 596(7873):583–9. doi: 10.1038/s41586-021-03819-2
- Mirdita M, Schütze K, Moriawaki Y, Heo L, Ovchinnikov S, Steinegger M. ColabFold: making protein folding accessible to all. *Nat Methods* (2022) 19(6):679–82. doi: 10.1038/s41592-022-01488-1
- Kuleshov MV, Jones MR, Rouillard AD, Fernandez NF, Duan Q, Wang Z, et al. Enrichr: a comprehensive gene set enrichment analysis web server 2016 update. *Nucleic Acids Res* (2016) 44(W1):W90–7. doi: 10.1093/nar/gkw377
- Li LQ, Huang T, Wang YQ, Wang ZP, Liang Y, Huang TB, et al. COVID-19 patients' clinical characteristics, discharge rate, and fatality rate of meta-analysis. *J Med Virol* (2020) 92(6):577–83. doi: 10.1002/jmv.25757
- Cen G, Liu L, Wang J, Wang X, Chen S, Song Y, et al. Weighted gene co-expression network analysis to identify potential biological processes and key genes in COVID-19-related stroke. *Oxid Med Cell Longev* (2022) 2022:4526022. doi: 10.1155/2022/4526022
- Wang T, Zhao M, Ye P, Wang Q, Zhao Y. Integrated bioinformatics analysis for the screening of associated pathways and therapeutic drugs in coronavirus disease 2019. *Arch Med Res* (2021) 52(3):304–10. doi: 10.1016/j.arcmed.2020.11.009
- Viiri KM, Jänis J, Siggers T, Heinonen TY, Valjakka J, Bulys ML, et al. DNA-binding and -bending activities of SAP30L and SAP30 are mediated by a zinc-dependent module and monophosphoinositides. *Mol Cell Biol* (2009) 29(2):342–56. doi: 10.1128/MCB.01213-08

18. Ryu S, Sidorov S, Ravussin E, Artyomov M, Iwasaki A, Wang A, et al. The matricellular protein SPARC induces inflammatory interferon-response in macrophages during aging. *Immunity* (2022) 55(9):1609–1626.e7. doi: 10.1016/j.immuni.2022.07.007
19. Bernardes JP, Mishra N, Tran F, Bahmer T, Best L, Blase JI, et al. Longitudinal multi-omics analyses identify responses of megakaryocytes, erythroid cells, and plasmablasts as hallmarks of severe COVID-19. *Immunity* (2020) 53(6):1296–1314.e9. doi: 10.1016/j.immuni.2020.11.017
20. Fortmann SD, Patton M, Frey BF, Tipper JL, Reddy SB, Vieira CP, et al. Circulating SARS-CoV-2+ Megakaryocytes associate with severe viral infection in COVID-19. *Blood Adv* (2023) 7(15):4200–14. doi: 10.1182/bloodadvances.2022009022
21. Li X, Garg M, Jia T, Liao Q, Yuan L, Li M, et al. Single-cell analysis reveals the immune characteristics of myeloid cells and memory T cells in recovered COVID-19 patients with different severities. *Front Immunol* (2022) 12:781432. doi: 10.3389/fimmu.2021.781432
22. Wang H, He J, Xu C, Chen X, Yang H, Shi S, et al. Decoding human megakaryocyte development. *Cell Stem Cell* (2021) 28(3):535–49.e8. doi: 10.1016/j.stem.2020.11.006
23. Faye C, Chautard E, Olsen BR, Ricard-Blum S. The first draft of the endostatin interaction network. *J Biol Chem* (2009) 284(33):22041–7. doi: 10.1074/jbc.M109.002964
24. Aseer KR, Kim SW, Choi MS, Yun JW. Opposite expression of SPARC between the liver and pancreas in streptozotocin-induced diabetic rats. *PLoS One* (2015) 10(6):e0131189. doi: 10.1371/journal.pone.0131189
25. Kos K, Wilding JPH. SPARC: a key player in the pathologies associated with obesity and diabetes. *Nat Rev Endocrinol* (2010) 6(4):225–35. doi: 10.1038/nrendo.2010.18
26. Hohenester E, Maurer P, Hohenadl C, Timpl R, Jansonius JN, Engel J. Structure of a novel extracellular Ca(2+)-binding module in BM-40. *Nat Struct Biol* (1996) 3(1):67–73. doi: 10.1038/nsb0196-67
27. Hohenester E, Sasaki T, Giudici C, Farndale RW, Bächinger HP. Structural basis of sequence-specific collagen recognition by SPARC. *Proc Natl Acad Sci* (2008) 105(47):18273–7. doi: 10.1073/pnas.0808452105
28. Li HY, Wang J, Meng F, Jia ZK, Su Y, Bai QF, et al. An intrinsically disordered motif mediates diverse actions of monomeric C-reactive protein. *J Biol Chem* (2016) 291(16):8795–804. doi: 10.1074/jbc.M115.695023
29. Cunin P, Nigrovic PA. Megakaryocytes as immune cells. *J Leukoc Biol* (2019) 105(6):1111–21. doi: 10.1002/JLB.MR0718-261RR
30. Machlus KR, Boilard E. The origin of the megakaryocyte. *Nat Cardiovasc Res* (2022) 1(7):593–4. doi: 10.1038/s44161-022-00099-5



## OPEN ACCESS

## EDITED BY

Kazuo Takahashi,  
Massachusetts General Hospital and Harvard  
Medical School, United States

## REVIEWED BY

Shang-Rong Ji,  
Lanzhou University, China  
Johannes Zeller,  
Freiburg University Medical Center, Germany

## \*CORRESPONDENCE

Alok Agrawal  
✉ agrawal@etsu.edu

RECEIVED 11 February 2024

ACCEPTED 25 March 2024

PUBLISHED 08 April 2024

## CITATION

Singh SK, Prislovsky A, Ngwa DN,  
Munkhsaikhan U, Abidi AH, Brand DD  
and Agrawal A (2024) C-reactive protein  
lowers the serum level of IL-17, but not  
TNF- $\alpha$ , and decreases the incidence of  
collagen-induced arthritis in mice.  
*Front. Immunol.* 15:1385085.  
doi: 10.3389/fimmu.2024.1385085

## COPYRIGHT

© 2024 Singh, Prislovsky, Ngwa, Munkhsaikhan,  
Abidi, Brand and Agrawal. This is an open-  
access article distributed under the terms of  
the [Creative Commons Attribution License](#)  
(CC BY). The use, distribution or reproduction  
in other forums is permitted, provided the  
original author(s) and the copyright owner(s)  
are credited and that the original publication  
in this journal is cited, in accordance with  
accepted academic practice. No use,  
distribution or reproduction is permitted  
which does not comply with these terms.

# C-reactive protein lowers the serum level of IL-17, but not TNF- $\alpha$ , and decreases the incidence of collagen-induced arthritis in mice

Sanjay K. Singh<sup>1</sup>, Amanda Prislovsky<sup>2</sup>, Donald N. Ngwa<sup>1</sup>,  
Undral Munkhsaikhan<sup>3</sup>, Ammaar H. Abidi<sup>3</sup>, David D. Brand<sup>2</sup>  
and Alok Agrawal<sup>1\*</sup>

<sup>1</sup>Department of Biomedical Sciences, James H. Quillen College of Medicine, East Tennessee State University, Johnson City, TN, United States, <sup>2</sup>The Lt. Col. Luke Weathers, Jr. VA Medical Center, Memphis, TN, United States, <sup>3</sup>College of Dental Medicine, Lincoln Memorial University, Knoxville, TN, United States

The biosynthesis of C-reactive protein (CRP) in the liver is increased in inflammatory diseases including rheumatoid arthritis. Previously published data suggest a protective function of CRP in arthritis; however, the mechanism of action of CRP remains undefined. The aim of this study was to evaluate the effects of human CRP on the development of collagen-induced arthritis (CIA) in mice which is an animal model of autoimmune inflammatory arthritis. Two CRP species were employed: wild-type CRP which binds to aggregated IgG at acidic pH and a CRP mutant which binds to aggregated IgG at physiological pH. Ten CRP injections were given on alternate days during the development of CIA. Both wild-type and mutant CRP reduced the incidence of CIA, that is, reduced the number of mice developing CIA; however, CRP did not affect the severity of the disease in arthritic mice. The serum levels of IL-17, IL-6, TNF- $\alpha$ , IL-10, IL-2 and IL-1 $\beta$  were measured: both wild-type and mutant CRP decreased the level of IL-17 and IL-6 but not of TNF- $\alpha$ , IL-10, IL-2 and IL-1 $\beta$ . These data suggest that CRP recognizes and binds to immune complexes, although it was not clear whether CRP functioned in its native pentameric or in its structurally altered pentameric form in the CIA model. Consequently, ligand-complexed CRP, through an as-yet undefined mechanism, directly or indirectly, inhibits the production of IL-17 and eventually protects against the initiation of the development of arthritis. The data also suggest that IL-17, not TNF- $\alpha$ , is critical for the development of autoimmune inflammatory arthritis.

## KEYWORDS

C-reactive protein, collagen-induced arthritis, IL-17, immune complex, TNF- $\alpha$

**Abbreviations:** A $\beta$ , amyloid- $\beta$ ; CIA, collagen-induced arthritis; CRP, C-reactive protein; IC, immune complex; mCRP, monomeric CRP; mono-IgG, monomeric IgG; agg-IgG, aggregated IgG; PCh, phosphocholine; RA, rheumatoid arthritis; WT, wild-type.

## Introduction

C-reactive protein (CRP) circulates in the blood and is deposited at sites of inflammation (1). CRP is composed of five identical subunits arranged in a cyclic pentameric symmetry and whose production and secretion by hepatocytes are increased in inflammatory states (2–4). CRP is a dual pattern recognition molecule; however, which pattern is recognized by CRP depends upon its pentameric structural conformation (5). In the plasma and elsewhere where CRP is present in its native conformation, CRP binds to phosphocholine (PCh)-containing substances and subsequently activates the classical pathway of complement (6–9). It has been suggested that the native pentameric conformation of CRP is subtly altered at sites of inflammation where an inflammatory milieu of acidic pH and redox condition is present (10–13). Such non-native pentameric CRP recognizes an additional pattern and that is amyloid-like structures exposed on immobilized proteins (5). Other mechanisms for the alteration of the native conformation of CRP have also been reported (14, 15). It has also been shown that the combination of the two recognition functions of CRP in two different pentameric conformations contributes to the protection against diseases caused by the deposition of otherwise fluid-phase proteins, such as pneumococcal infection (16, 17). Additionally, it has been hypothesized that the pathogen-defense functions of CRP are preserved even when the PCh-binding site of CRP is blocked by a PCh-mimicking compound (18). Non-native pentameric CRP may eventually lead to the generation of CRP monomers (mCRP) which shares the immobilized protein ligand-binding properties and antigenic epitopes of non-native pentameric CRP (1, 10, 19–22). The PCh-binding activity, however, is either retained, decreased or abolished in mCRP depending upon the method of generation of mCRP (23–25).

The changes in the structure of native pentameric CRP caused by acidic pH are reversible at physiological pH (10). Therefore, acidic pH-modified CRP cannot be administered into animal models of human diseases to explore the functions of non-native pentameric CRP *in vivo*. Accordingly, CRP mutants created by site-directed mutagenesis and which mimic the ligand-binding properties of acidic pH-modified native CRP have been employed in *in vivo* experiments (16, 17). One such CRP mutant is Y40F/E42Q CRP in which Tyr40 and Glu42 have been substituted with Phe and Gln, respectively (16, 26). Like acidic pH-treated native CRP, the Y40F/E42Q CRP mutant recognizes both PCh and amyloid-like structures exposed on immobilized proteins (5). The only difference in the functions of native CRP and mutant CRP is that, at physiological pH, native CRP recognizes PCh while mutant CRP recognizes both PCh and amyloid-like structures (5, 16, 26, and data not shown).

Rheumatoid arthritis (RA) is a joint disease characterized by the presence of immune complexes (ICs) in the joints (27, 28). The synovium of the RA joints has an inflammatory milieu characterized by acidic pH and redox conditions (29–32). CRP is also deposited in the synovium (33), raising the possibility that CRP is present in the synovium in both, native and non-native, pentameric conformations. It has also been shown that the serum

levels of IL-17, IL-6, TNF- $\alpha$ , IL-10, IL-2 and IL-1 $\beta$  are altered in RA patients (28, 34, 35). CRP is used as a nonspecific biomarker of inflammation during the development of RA (3, 36). Previously published reports suggest that pentameric CRP protects against the development of inflammatory arthritis in mice; however, the mechanism of action of CRP *in vivo* including the effects of CRP on the production of cytokines *in vivo* are not fully elucidated yet (37–39).

In this study, we administered wild-type (WT) CRP and the CRP mutant Y40F/E42Q in mice with collagen-induced arthritis (CIA) and monitored the development of the disease and measured the serum levels of IL-17, IL-6, TNF- $\alpha$ , IL-10, IL-2 and IL-1 $\beta$ . The CIA mouse model is a model of autoimmune inflammatory arthritis that shares many clinical features with human RA (40). We tested the hypothesis that CRP changes its structure in the synovium, binds to immobilized ICs, and subsequently protects against the development of arthritis. Accordingly, we also hypothesized that the CRP mutant might be more protective than WT CRP against the development of CIA.

## Materials and methods

### Preparation of aggregated IgG

Aggregated IgG (agg-IgG) was prepared according to a published method (41). In brief, human IgG (Sigma, I4506) at 10 mg/ml in normal saline was heated at 63°C for 20 min in a shaking water bath. After centrifugation at 10,000 rpm for 5 min, the precipitate was discarded. The concentration of IgG in the supernatant containing agg-IgG was determined by measuring the absorbance at 280 nm and adjusted to a final concentration of 1 mg/ml of agg-IgG. This preparation of agg-IgG was used as a model of ICs (42) to evaluate the binding of CRP to immobilized ICs.

### Detection of amyloid-like structures on immobilized IgG and agg-IgG

The presence of amyloid-like structures on immobilized IgG was detected as described previously (5). Microtiter wells (Corning, 9018) were coated with 10  $\mu$ g/ml of monomeric IgG (mono-IgG) or agg-IgG in TBS, pH 7.2, and incubated at 4°C overnight. The unreacted sites in the wells were blocked with TBS containing 0.5% gelatin at room temperature for 45 min. Both, polyclonal antibodies (Novus, NBP2-25093) and monoclonal antibodies (Novus, NBP2-13075) to amyloid- $\beta$  peptide 1-42 (A $\beta$ ) were used to detect the amyloid-like structures formed on the mono-IgG and agg-IgG following their immobilization. Normal rabbit IgG and normal mouse IgG were used as controls for the antibodies. The antibodies (10  $\mu$ g/ml) diluted in TBS containing 0.1% gelatin and 0.02% Tween 20 were added to the wells and incubated at 37°C for 1 h. After washing the wells, bound polyclonal anti-A $\beta$  antibodies were detected by using HRP-conjugated donkey anti-rabbit IgG (GE Healthcare) and bound monoclonal anti-A $\beta$  antibodies were detected by using HRP-conjugated goat anti-mouse IgG (Thermo



Fisher Scientific). Color was developed with ABTS reagent and the OD was read at 405 nm in a microtiter plate reader (Molecular Devices). Immobilized A $\beta$  peptide 1-42 (Bachem) was used as a control for immobilized IgG and for anti-A $\beta$  antibodies.

## Preparation of CRP

Native WT CRP was purified from discarded human pleural fluid as described previously (43). Recombinant mutant CRP Y40F/E42Q was expressed in CHO cells using the ExpiCHO Expression System (Thermo Fisher Scientific) and purified from the culture supernatant exactly as described for WT CRP (16). The construction of the Y40F/E42Q mutant CRP cDNA has been reported previously (26). In brief, WT and mutant CRP were purified by Ca<sup>2+</sup>-dependent affinity chromatography on a PCh-conjugated Sepharose column, followed by ion-exchange chromatography on a MonoQ column and gel filtration on a Superose12 column. Purified CRP was dialyzed against TBS, pH 7.2, containing 2 mM CaCl<sub>2</sub>, and was subsequently treated with Detoxi-Gel Endotoxin Removing Gel (Thermo Fisher Scientific) according to manufacturer's instructions. The concentration of endotoxin in CRP preparations was determined by using the Limulus Amebocyte Lysate kit QCL-1000 (Lonza). The concentration of endotoxin in WT and mutant CRP preparations were 0.52  $\pm$  0.06 EU/50  $\mu$ g and 0.60  $\pm$  0.07 EU/50  $\mu$ g, respectively. Purified CRP in TBS, pH 7.2, containing 2 mM CaCl<sub>2</sub>, was stored at 4°C, and was used within a week.

## CRP-IgG binding assay

The CRP-IgG binding assays were performed as described previously (12). In brief, microtiter wells (Corning, 9018) were coated with 10  $\mu$ g/ml of mono-IgG or agg-IgG diluted in TBS, pH 7.2, and incubated at 4°C overnight. The unreacted sites in the wells were blocked with TBS containing 0.5% gelatin. Mutant CRP was diluted in TBS, pH 7.2, containing 0.1% gelatin, 0.02% Tween 20, and 2 mM CaCl<sub>2</sub> (TBS-Ca) and added to the wells. WT CRP was diluted in TBS-Ca at pH 7.2 and also at pH 5.0 and added to the wells. The plate was then incubated at 37°C for 2 h. After washing the wells, HRP-conjugated goat anti-human CRP antibody (Alpha Diagnostic International, Cat # CRP-11-HRP) was used (5  $\mu$ g/ml, 37°C, 1 h) to detect bound WT and mutant CRP. Color was developed with ABTS reagent and the OD was read at 405 nm in a microtiter plate reader.

## CIA in mice

CIA was induced in DBA/1 mice as previously described (40). Eight-week-old female DBA/1J mice (Jackson Laboratories, stock# 000670) were used in experiments according to protocols approved by and conducted in accordance with the guidelines administered by the Institutional Animal Care and Use Committee of the Memphis VA Medical Center. Following acclimatization of mice

for one week, arthritis was induced by immunization of mice with bovine type II collagen extracted and purified in the investigator (DDB's) laboratory and emulsified 1:1 in complete Freund's adjuvant, which was also prepared freshly in DDB's laboratory.

Two different regimens were employed to evaluate the effects of passively administered WT and mutant CRP on the development of CIA in mice. In regimen 1, the administration of CRP began (day 26) about three weeks after immunization (day 7) and two weeks prior to the onset of the disease (day 40), and the injection of CRP continued till day 44. In regimen 2, the administration of CRP began (day 35) four weeks after immunization (day 7) and on the day of the onset of the disease (day 35), and the injection of CRP continued till day 53. In both regimens, a total of ten CRP injections (50  $\mu$ g/injection) were given intravenously on alternate days. The control group of mice was administered with TBS, the vehicle for CRP.

The development of arthritis in the fore and hind paws was monitored by visual inspection as described previously (40). Each paw could receive an arthritis score from 0 to 4, and the maximum score could reach 16 per mouse for four paws. Clinical scores were assessed every third day in a blinded manner for each paw, as follows: score 0, normal; score 1, one paw joint affected or minimal diffuse erythema and swelling; score 2, two paw joints affected or mild diffuse erythema and swelling; score 3, three paw joints affected or moderate diffuse erythema and swelling; score 4, all four-digit joints affected or severe diffuse erythema and severe swelling of the entire paw, unable to flex digits.

Four parameters were evaluated: 1. Incidence of arthritis which reflects the percentage of mice that were positive for arthritis. 2. Arthritic limbs/arthritis mouse which reflects the number of arthritic limbs in each arthritic mouse. 3. Clinical score of the severity of arthritis (1-4)/arthritic limb: Scores from all limbs in each arthritic mouse/number of arthritic limbs. 4. Clinical score of the severity of arthritis (1-16) (4 limbs and each 1-4) of all 4 limbs combined/arthritis mouse: Scores from all limbs in all arthritic mice/Number of arthritic mice. The statistical analyses of the data were performed by employing linear regression analysis of the slopes and nonparametric Mann-Whitney test using the GraphPad Prism 9 software and as described in detail in the figure legends.

## Measurement of cytokines

To measure the serum levels of cytokines (IL-17, IL-6, TNF- $\alpha$ , IL-10, IL-2, and IL-1 $\beta$ ), sera were collected from mice used in the experiment involving regimen 1. Mice used in the experiment involving regimen 2 were not analyzed for cytokines. On day 26, mice were divided into three groups, and the administration of either WT CRP, mutant CRP, or vehicle began. The injections continued till day 44; the disease onset was on day 40. Cytokines were measured in the sera collected on days 1, 19 and 47. The serum samples were thawed and brought to room temperature, then centrifuged before use. The cytokine levels were measured using Mesoscale Discovery (MSD) Mouse U-PLEX Custom Biomarker Multiplex Assays from Mesoscale Diagnostics, (Maryland, USA).

U-Plex assays use biotinylated capture antibodies that are specific for each analyte and MSD employs an electrochemiluminescence technique that allows for the multiplexing. Samples (10  $\mu$ l) were transferred onto a pre-coated MSD with 10  $\mu$ l diluent (2-fold dilution) per manufacturer's guidelines for cytokines IL-17, IL-6, TNF- $\alpha$ , IL-10, IL-2, and IL-1 $\beta$ . The samples were then incubated on a shaker for 2 h at room temperature, followed by washing and the addition of SULFO-TAG detection antibodies. The detection antibodies were incubated for another 2 h, and washed and removed from the plate. 150  $\mu$ l of 2x MSD read buffer was added and the U-Plex plate and the plate were immediately loaded onto the MSD instrument. Mesoscale SQ120 and SECTOR Imager SI 2400A were used to read the plates according to the manufacturer's instructions. The intensity of light emitted was then quantified, which was proportional to the sample analyte present. A five-parameter logistic regression method was used to calculate sample concentration and standard curves.

The scatter plots of the data and the median values of the concentrations of cytokines in each group were generated using the GraphPad Prism 9. To determine *p*-values for the differences in the level of each cytokine among various groups at each time point, scatter plots were compared using the software's Mann-Whitney test which included all the dots in the scatter plots and not just the median values for each time point.

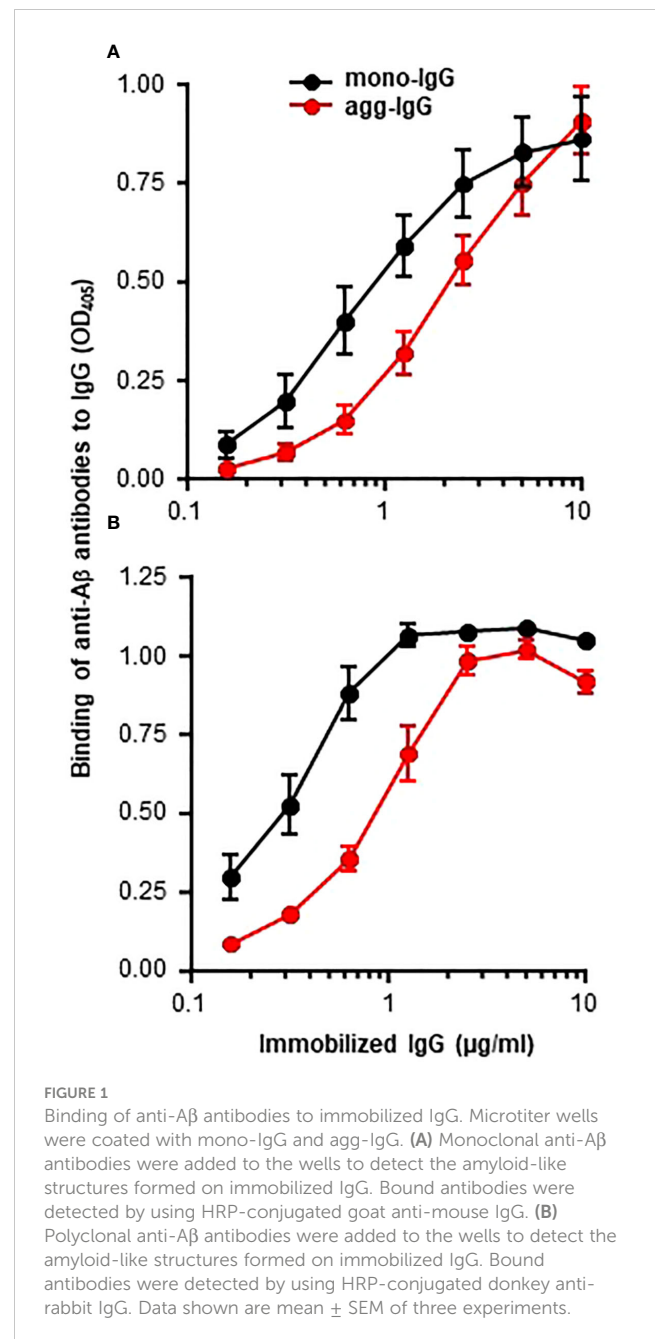
## Results

### Immobilized IgG expresses amyloid-like structures

It was reported recently that some proteins, when immobilized on microtiter plates, express amyloid-like structures that can be detected by using anti-A $\beta$  antibodies (5). In this study, we investigated whether immobilized IgG also expresses amyloid-like structures by employing normal human mono-IgG and agg-IgG coated on microtiter wells. Both mono-IgG and agg-IgG were immobilized; although, immobilization itself can cause aggregation of mono-IgG on the wells. Two different anti-A $\beta$  antibodies were used to identify the expression of amyloid-like structures on immobilized IgG. We have previously reported the authentication of these antibodies using purified A $\beta$  peptides (5). As shown in Figure 1, both immobilized mono-IgG and agg-IgG reacted with both monoclonal (Figure 1A) and polyclonal anti-A $\beta$  antibodies (Figure 1B). These data suggested that immobilized IgG expressed A $\beta$  epitopes, suggesting that immobilized ICs might also express A $\beta$  epitopes.

### CRP mutant Y40F/E42Q binds to immobilized IgG at physiological pH

Since A $\beta$  is a ligand of the CRP mutant Y40F/E42Q used in this study (5), and since immobilized IgG expresses A $\beta$  epitopes (Figure 1), we determined whether the CRP mutant can bind to immobilized IgG at physiological pH. WT CRP at pH 5.0 and pH 7.2 were included as positive and negative controls for the binding



of mutant CRP to immobilized IgG. As shown in Figure 2, and as has been reported previously (5), WT CRP did not bind to either mono-IgG or to agg-IgG at physiological pH, but, at acidic pH, WT CRP bound to immobilized IgG. The CRP mutant, however, bound to both mono-IgG and agg-IgG at physiological pH in a CRP concentration-dependent manner.

### CRP decreases the incidence of arthritis

Two different regimens were employed to evaluate the effects of CRP on the development of CIA (Figure 3A). In regimen 1, the administration of CRP (on day 26) began three weeks after immunization with CII (on day 7) and two weeks prior to the

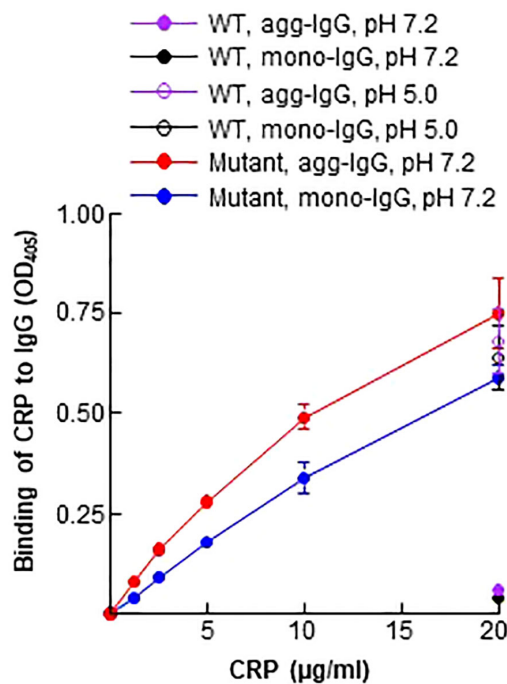


FIGURE 2

Binding of CRP to immobilized IgG. Microtiter wells were coated with mono-IgG and agg-IgG. WT CRP (a single concentration of 20 μg/ml), diluted in TBS-Ca, pH 7.2 and pH 5.0, was added to the wells. Mutant CRP (two-fold serial dilutions of 20 μg/ml) was diluted in TBS-Ca, pH 7.2, and was added to the wells. Bound CRP was detected by using HRP-conjugated goat anti-human CRP antibodies. Data shown are mean ± SEM of three experiments. Due to low SEM, the error bars are not visible for all the data points in the graph.

onset of the disease (on day 40), and the administration of CRP was continued until day 44. In regimen 2, the administration of CRP (on day 35) began four weeks after immunization (on day 7) and on the day of the onset of the disease (day 35), and the administration of CRP was continued until day 53. CRP was administered on alternate days between days 28–46 in regimen 1 and between days 35–53 in regimen 2.

The effects of CRP on the incidence of arthritis for both regimens are shown in Figure 3B. In regimen 1, the data were analyzed separately for days 40–61 and days 62–110 (Figure 3B, left), while in regimen 2 (Figure 3B, right), the data were analyzed separately for days 28–83 and days 84–153. In both regimens, and in both segments of the data, there were statistically significant differences between vehicle and WT CRP, between vehicle and mutant CRP, and between WT and mutant CRP.

In regimen 1, WT CRP was more protective than mutant CRP in reducing the incidence of CIA. The most dramatic difference in the incidence was around day 60 when the incidence was 72% in the vehicle group compared to 50% and 20% in mutant CRP-treated and WT CRP-treated groups, respectively. In regimen 2, during days 28–83, WT CRP was more protective than mutant CRP as in regimen 1; however, during days 84–153, mutant CRP was more protective than WT CRP. The most dramatic difference in the incidence was around day 80 when the incidence was 75% in the

vehicle group compared to 60% and 40% in mutant CRP-treated and WT CRP-treated groups, respectively.

Thus, both regimens gave similar results for incidence; it did not matter whether there was only one injection of CRP or whether there were six injections of CRP before the onset of the disease, that is, before the first mouse in the group developed CIA. Also, in addition to decreasing the incidence of CIA, CRP also delayed the progression of the disease by several days in both regimens.

## CRP does not reduce the severity of the disease

The effects of CRP treatment on the severity of CIA were assessed by measuring the following three parameters: arthritic limbs/arthritic mouse, clinical score/arthritic mouse and clinical score/arthritic limb. The number of arthritic limbs/arthritic mouse ranged from 1 to 2 in all three groups of mice (Figure 4A). The clinical score/arthritic mouse ranged from 4 to 8 in all three groups of mice (Figure 4B). The clinical score/arthritic limb ranged from 2.5 to 4 in all three groups of mice (Figure 4C). There were no statistically significant differences in the severity of CIA between any two groups, for all of the three parameters, and for both regimens.

## CRP decreases the level of IL-17 and IL-6 but not TNF-α

Six of the cytokines produced by either phagocytic cells or T cells and which have been implicated in RA were measured (28, 44) in the sera of mice from regimen 1 experiment (Figure 5). The serum levels of all six cytokines increased in response to immunization and subsequent development of the disease, although the timing of appearance of each cytokine was different.

The profiles of IL-17 and IL-6 were similar. The serum levels of both cytokines increased until day 47, as shown in the vehicle group. However, in the CRP-treated groups, the levels of IL-17 and IL-6 did not increase. On day 47, levels of IL-17 and IL-6 were the same as on day 19, which was a day before the onset of the disease and before CRP administration began. There was no difference between the cytokine-reducing effects of WT and mutant CRP.

Like the serum profiles of IL-17 and IL-6, the level of TNF-α also increased until day 47, as shown in the vehicle group. However, unlike the effects of CRP on IL-17 and IL-6, CRP treatment did not prevent the increase in serum level of TNF-α. On day 47, the level of TNF-α was same as on day 19. There was no difference between the effects of WT and mutant CRP.

The profiles of IL-10, IL-2 and IL-1β were similar to each other but different from that of IL-17, IL-6 and TNF-α. The serum levels IL-10, IL-2 and IL-1β increased as early as day 19 and then returned to almost normal level by day 47, as shown in the vehicle group. CRP-treatment was not required to prevent the rise in levels of IL-10, IL-2 and IL-1β. Combined data on the effects of CRP on the serum levels of cytokines suggest that CRP reduces the levels of IL-17 and IL-6 but not of TNF-α, IL-10, IL-2 and IL-1β.

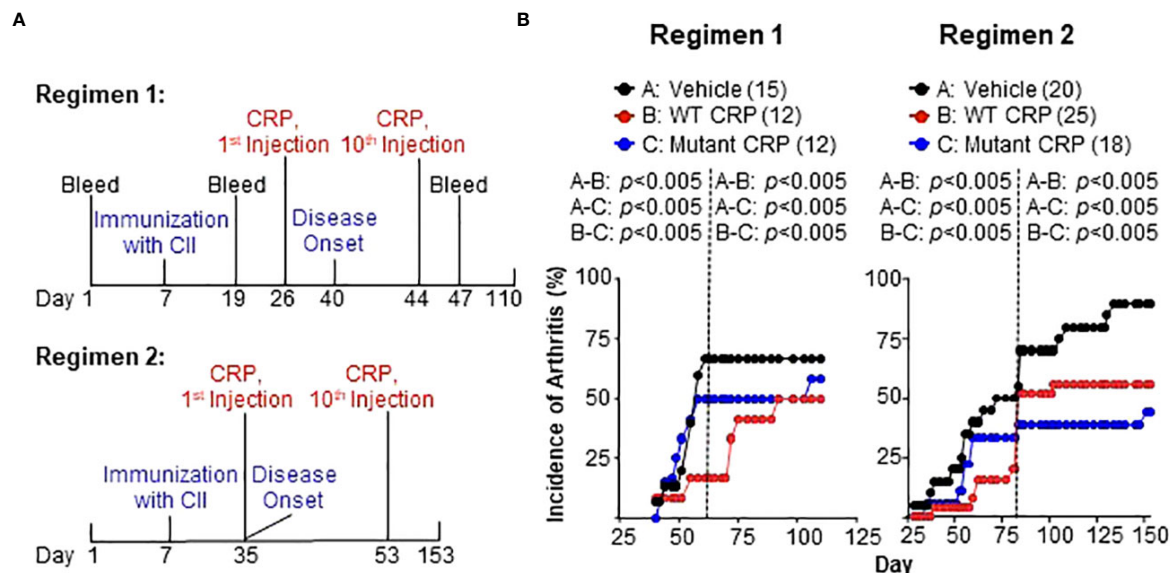


FIGURE 3

(A) Regimens for administering CRP. In regimen 1, CRP administration began two weeks prior to the onset of the disease, while in regimen 2, the CRP administration began on the same day as the onset of the disease. A total of ten CRP injections were given in both regimens. In regimen 1, the disease was monitored for 110 days while in regimen 2 the disease was monitored for 153 days. (B) Incidence of arthritis in mice from regimen 1 (left panel) and regimen 2 (right panel). The number of mice in each group is shown in the parentheses. For statistical analyses of the data, the curves in both panels were divided into two parts as shown by the dotted vertical lines. For regimen 1, the curves were divided into days 40–61 and 62–110. For regimen 2, the curves were divided into days 28–83 and 84–153. For the time period of 40–61 days in regimen 1 and 28–83 days in regimen 2,  $p$  values were determined by employing linear regression analysis of the slopes. For the time period of 62–110 days in regimen 1 and 84–153 days in regimen 2,  $p$  values were determined by employing Mann-Whitney test. The  $p$  values for the differences between groups A and B, groups A and C, and groups B and C are shown (all  $p < 0.005$ ).

## Discussion

In this study, we investigated the interaction between CRP and agg-IgG and the effects of CRP on the development of CIA in mice. Our major findings were: 1. Immobilized IgG, whether it was mono-IgG or agg-IgG, expressed amyloid-like structures which could be detected by the antibodies to A $\beta$ . 2. The Y40F/E42Q CRP mutant, which is in a non-native pentameric conformation, bound to immobilized IgG at physiological pH while WT CRP did so only at acidic pH. 3. CRP reduced the incidence of arthritis, that is, reduced the number of mice with developing arthritis. There was no difference in the protective capacities of WT and mutant CRP. 4. CRP did not affect the severity of disease in arthritic mice. 5. CRP decreased the serum level of IL-17, but not of TNF- $\alpha$ , in the CIA mouse model. There was no difference between WT and mutant CRP in preventing the rise in the serum level of IL-17.

Since ICs play a role in RA and in animal models of RA (45), interactions between CRP and ICs were evaluated, by employing agg-IgG. Agg-IgG is often used as a model of ICs (42). *In vitro* prepared ICs made up of any pair of antigen and antibody could not be used in the IgG-binding assays since WT CRP at acidic pH and mutant CRP at physiological pH were found to bind to both the antigen and the antibody when immobilized individually on microtiter plates (5, and data not shown).

Previous studies have also shown that WT CRP does not bind to either IgG or ICs, unless CRP was purchased commercially and used as it was (46, 47). However, CRP-IC complexes have been

found *in vivo* (48, 49) and circulating ICs isolated from sera from patients with inflammatory diseases contained IC-complexed CRP (46, 47, 50–53). Also, similar to the binding of WT CRP to IgG at acidic pH and the binding of CRP mutant to IgG at physiological pH, mCRP has been shown to bind to IgG (20–22, 54) and binding of mCRP to IgG was increased at acidic pH (20–22). These earlier reports combined with our findings on CRP-IgG interactions suggest that the native pentameric conformation of CRP must be altered *in vivo* in order to bind to ICs. In the CIA murine model reported here, it was not clear whether CRP functioned in its native pentameric form or in its structurally altered pentameric form. The possibility can't be ruled out that in the CIA mice WT CRP changed its structure *in vivo* after reaching the synovium and that's why no difference was seen between WT and mutant CRP on their effects on the development of CIA.

The molecular mechanism of CRP-IgG interactions remains unclear. Previously, it has been shown that the binding of mCRP to IgG was differential and selective for different types of IgG (20, 22). It was hypothesized that the reason behind the differential binding of mCRP to various IgG was due to differential glycosylation of different IgG (46, 53). More recently, it was shown that the binding of WT CRP to immobilized IgG and various other protein ligands at acidic pH was also differential for different protein ligands (10). Similarly, the binding of CRP mutants to various immobilized protein ligands at physiological pH was found to be different for different protein ligands (5). Since immobilization of IgG and various other immobilized proteins to which CRP binds (5)



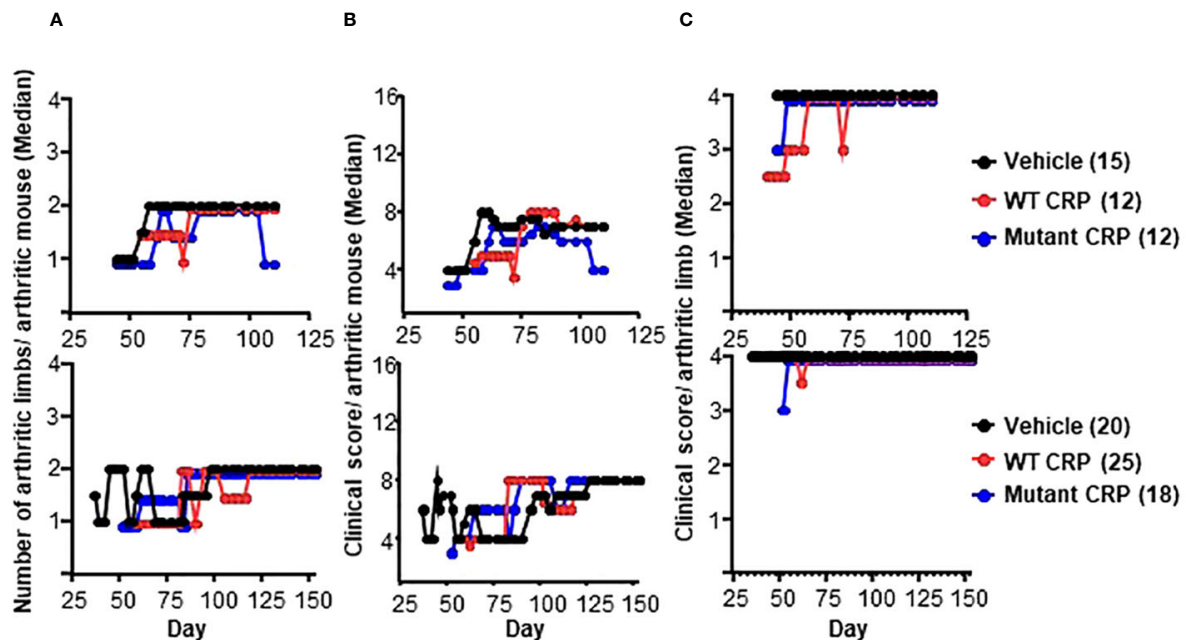


FIGURE 4

Severity of arthritis in mice from regimen 1 (top panels) and regimen 2 (bottom panels) experiments. (A) Median values for the number of arthritic limbs per arthritic mouse are shown. (B) Median values for the clinical score per arthritic mouse are shown. (C) Median values for the clinical score per arthritic limb are shown. The number of mice in each group is shown in the parentheses. To enhance the clarity of the graphs, in some panels, the numbers are not plotted as they were: For the vehicle groups, the numbers 1-4 are shown as 1-4. For WT CRP-treated groups, the numbers 1-4 are shown as 0.95, 1.95, 2.95 and 3.95. For mutant CRP-treated groups, the numbers 1-4 are shown as 0.9, 1.9, 2.9 and 3.9. There were no statistically significant differences between any two groups in all six panels (all  $p > 0.05$ ).

results in the generation of amyloid-like structures, our data suggest that the binding of CRP to IgG was not due to the interaction between CRP and IgG *per se*, but due to the interaction between CRP and amyloid-like structures present on immobilized IgG. The extent of amyloid-like structures is different for various immobilized proteins (5). Accordingly, we hypothesize that the selective binding of CRP to various protein ligands including IgG is due to differential glycosylation and hence differential exposure of amyloid-like structures on various proteins.

The incidences of CIA in our *in vivo* experiments were 70% maximum in one experiment and 90% maximum in another regimen experiment. This rate of incidence is consistent with previously published reports where maximum incidences were 70%-80% (55-57). Since mutant CRP binds to IgG at physiological pH while WT CRP requires acidic pH to do so, we hypothesized that mutant CRP would be more protective against CIA compared to WT CRP. However, no differences were observed between WT and mutant CRP in reducing the incidence of arthritis. Also, the protective effects of CRP against arthritis were seen irrespective of whether there was only one injection or six injections of CRP before the onset of the disease, that is, before the first mouse in the group developed arthritis. Although CRP reduced the incidence drastically, the disease in the remaining arthritic mice was not less severe, indicating that CRP had effects on the onset of the disease but not on its subsequent clinical course.

By employing CRP-deficient mice and mice expressing human CRP transgene in CIA experiments in mice, it was concluded from

the data that CRP exerts an early and beneficial effects on the development of arthritis (37, 38). However, the protection was due to the reduction in the severity of the disease. The reasons for the discrepancy in the results between these previously published studies (37, 38) and our study are not obvious. Not only in CIA, CRP has also been shown to alter immune responses in animal models of other autoimmune diseases including encephalomyelitis (58-63), antigen-induced arthritis (64) and nephritis (39, 65-67). In the case of encephalomyelitis, it has been shown that CRP was protective by suppressing both Th1 response directly and Th17 response indirectly (60). CRP has also been shown to have immunosuppressive functions in IC-induced immune cells (68).

IL-17 and TNF- $\alpha$  play crucial roles in the development of CIA (34, 57, 69). That serum levels of IL-17 and TNF- $\alpha$  increase in CIA mice has also been reported previously (57, 70-76). CRP did not significantly affect TNF- $\alpha$  levels in the CIA mice reported here, but *in vitro*, CRP has been found to inhibit the production of TNF- $\alpha$  in IC-induced monocytes (68). mCRP, however, increases the production of TNF from monocytes cultured *in vitro* (77). Our finding that CRP prevented rise in the serum level of IL-17 suggests that IL-17 is more critical than TNF- $\alpha$  for the initiation of the development of arthritis. This interpretation is supported by the findings that the deletion of the TNF- $\alpha$  gene does not confer complete protection from the occurrence of arthritis in CIA (78, 79) and that TNF- $\alpha$  and IL-17 act independently of each other under arthritic condition (80). In addition, when the effects of TNF- $\alpha$  inhibitors on IL-17 in patients with RA were evaluated, it was



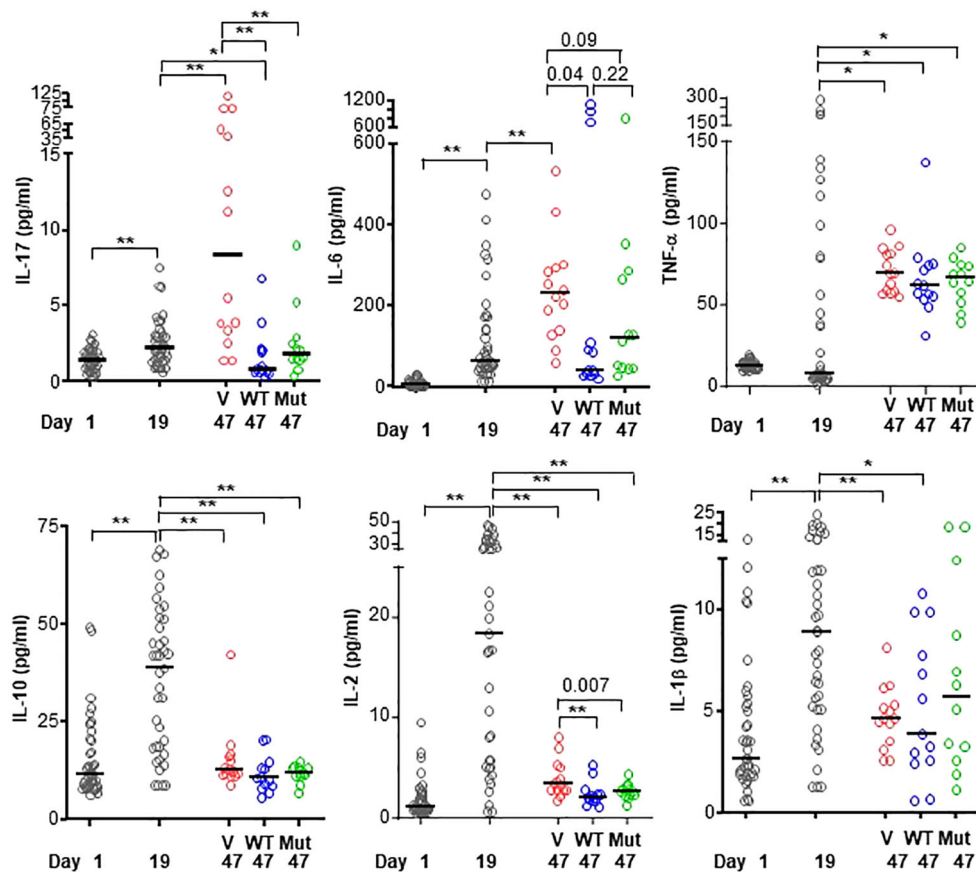


FIGURE 5

Levels of cytokines in the sera of mice from regimen 1 experiment. CIA was induced in 39 mice (black circles in all panels) on day 7. On day 26, mice were divided into three groups and treated with vehicle only (V; 15 mice; red circles in all panels), WT CRP (WT; 12 mice; blue circles in all panels) and mutant CRP (Mut; 12 mice; green circles in all panels). Sera were collected on day 1 (pre-immunization), day 19 (post-immunization and pre-CRP) and day 47 (post-CRP) for the measurement of cytokines. The median values of the concentrations of cytokines are shown. For clarity, *p* values are shown only for statistically significant differences (\**p* < 0.05, \*\**p* < 0.005); for some differences, the actual *p* values are shown.

found that the beneficial effects of anti-TNF-α therapy might involve a decrease in IL-17 in responders (35).

IL-6 is also required for the development of CIA (55). Our finding that the serum level of IL-6 increases in the CIA model is consistent with previously published studies on IL-6 in CIA (55, 56, 70, 72–74, 76, 81, 82). We found that, like IL-17, CRP also reduced the serum level of IL-6. It has been proposed previously that IL-6 is more relevant than TNF-α in the development of CIA (79). Thus, both cytokines, IL-17 and IL-6, which are critical than TNF-α in arthritis, are inhibited by CRP. The profiles of IL-1β, IL-2 and IL-10 reported here are also consistent with the previously published data (27, 68, 70, 72, 73, 83) and CRP had no effect on these three cytokines.

Taken together, we conclude that CRP is an anti-arthritis molecule in this model system. This function of CRP involves the binding of CRP to ICs. IC-complexed CRP, through an as yet undefined mechanism, directly or indirectly, inhibits the production of IL-17 and eventually protects against the initiation of the development of arthritis. The finding that there was no difference between WT and mutant CRP in preventing the rise in the serum level of IL-17 suggests that CRP executes its functions in

the synovium. Finally, the data suggest that IL-17, not TNF-α, is critical for the development of autoimmune inflammatory arthritis. It is also possible that CRP protects against autoimmunity in general, as has been hypothesized previously (84), by altering the levels of inflammatory cytokines *in vivo*.

## Data availability statement

The raw data supporting the conclusions of this article will be made available by the authors, without undue reservation.

## Ethics statement

Protocols approved by and conducted in accordance with the guidelines administered by the Institutional Animal Care and Use Committee of the Memphis VA Medical Center. The study was conducted in accordance with the local legislation and institutional requirements.

## Author contributions

SS: Data curation, Formal analysis, Investigation, Methodology, Writing – review & editing. AP: Data curation, Investigation, Writing – review & editing. DN: Data curation, Formal analysis, Investigation, Methodology, Writing – review & editing. UM: Data curation, Investigation, Writing – review & editing. AA: Data curation, Investigation, Writing – review & editing. DB: Data curation, Formal analysis, Investigation, Writing – review & editing. AA: Conceptualization, Formal analysis, Funding acquisition, Investigation, Supervision, Writing – original draft.

## Funding

The author(s) declare financial support was received for the research, authorship, and/or publication of this article. This work was supported by National Institutes of Health Grant AR068787.

## References

- Singh SK, Agrawal A. Functionality of C-reactive protein for atheroprotection. *Front Immunol.* (2019) 10:1655. doi: 10.3389/fimmu.2019.01655
- Shrive AK, Cheetham GMT, Holden D, Myles DAA, Turnell WG, Volanakis JE, et al. Three-dimensional structure of human C-reactive protein. *Nat Struct Biol.* (1996) 3:346–54. doi: 10.1038/nsb0496-346
- Kushner I. The phenomenon of the acute phase response. *Ann N Y Acad Sci.* (1982) 389:39–48. doi: 10.1111/j.1749-6632.1982.tb22124.x
- Ngwa DN, Pathak A, Agrawal A. IL-6 regulates induction of C-reactive protein gene expression by activating STAT3 isoforms. *Mol Immunol.* (2022) 146:50–6. doi: 10.1016/j.molimm.2022.04.003
- Ngwa DN, Agrawal A. Structurally altered, not wild-type, pentameric C-reactive protein inhibits formation of amyloid- $\beta$  fibrils. *J Immunol.* (2022) 209:1180–8. doi: 10.4049/jimmunol.2200148
- Volanakis JE, Kaplan MH. Specificity of C-reactive protein for choline phosphate residues of pneumococcal C-polysaccharide. *Proc Soc Exp Biol Med.* (1971) 136:612–4. doi: 10.3181/00379727-136-35323
- Thompson D, Pepys MB, Wood SP. The physiological structure of human C-reactive protein and its complex with phosphocholine. *Structure.* (1999) 7:169–77. doi: 10.1016/S0969-2126(99)80023-9
- Kaplan MH, Volanakis JE. Interaction of C-reactive protein complexes with the complement system. I. Consumption of human complement associated with the reaction of C-reactive protein with pneumococcal C-polysaccharide and with the choline phosphatides, lecithin, and sphingomyelin. *J Immunol.* (1974) 112:2135–47. doi: 10.4049/jimmunol.112.6.2135
- Singh SK, Ngwa DN, Agrawal A. Complement activation by C-reactive protein is critical for protection of mice against pneumococcal infection. *Front Immunol.* (2020) 11:1812. doi: 10.3389/fimmu.2020.01812
- Hammond DJ Jr, Singh SK, Thompson JA, Beeler BW, Rusiñol AE, Pangburn MK, et al. Identification of acidic pH-dependent ligands of pentameric C-reactive protein. *J Biol Chem.* (2010) 285:36235–44. doi: 10.1074/jbc.M110.142026
- Suresh MV, Singh SK, Agrawal A. Interaction of calcium-bound C-reactive protein with fibronectin is controlled by pH: *In vivo* implications. *J Biol Chem.* (2004) 279:52552–7. doi: 10.1074/jbc.M409054200
- Singh SK, Thirumalai A, Pathak A, Ngwa DN, Agrawal A. Functional transformation of C-reactive protein by hydrogen peroxide. *J Biol Chem.* (2017) 292:3129–36. doi: 10.1074/jbc.M116.773176
- Li S-L, Feng J-R, Zhou H-H, Zhang C-M, Lv G-B, Tan Y-B, et al. Acidic pH promotes oxidation-induced dissociation of C-reactive protein. *Mol Immunol.* (2018) 104:47–53. doi: 10.1016/j.molimm.2018.09.021
- Ji S-R, Wu Y, Zhu L, Potempa LA, Sheng F-L, Lu W, et al. Cell membranes and liposomes dissociate C-reactive protein (CRP) to form a new, biologically active structural intermediate: mCRPm. *FASEB J.* (2007) 21:284–94. doi: 10.1096/fj.06-6722com
- Lv J-M, Chen J-Y, Liu Z-P, Yao Z-Y, Wu Y-X, Tong C-S, et al. Cellular folding determinants and conformational plasticity of native C-reactive protein. *Front Immunol.* (2020) 11:583. doi: 10.3389/fimmu.2020.00583
- Ngwa DN, Singh SK, Gang TB, Agrawal A. Treatment of pneumococcal infection by using engineered human C-reactive protein in a mouse model. *Front Immunol.* (2020) 11:586669. doi: 10.3389/fimmu.2020.586669
- Pathak A, Singh SK, Thewke DP, Agrawal A. Conformationally altered C-reactive protein capable of binding to atherogenic lipoproteins reduces atherosclerosis. *Front Immunol.* (2020) 11:1780. doi: 10.3389/fimmu.2020.01780
- Zeller J, Cheung Tung Shing KS, Nero TL, McFadyen JD, Krippner G, Bogner B, et al. A novel phosphocholine-mimetic inhibits a pro-inflammatory conformational change in C-reactive protein. *EMBO Mol Med.* (2023) 15:16236. doi: 10.15252/emmm.202216236
- Li H-Y, Wang J, Meng F, Jia Z-K, Su Y, Bai Q-F, et al. An intrinsically disordered motif mediates diverse actions of monomeric C-reactive protein. *J Biol Chem.* (2016) 291:8795–804. doi: 10.1074/jbc.M115.695023
- Motie M, Brockmeier S, Potempa LA. Binding of model soluble immune complexes to modified C-reactive protein. *J Immunol.* (1996) 156:4435–41. doi: 10.4049/jimmunol.156.11.4435
- Boguslawski G, McGlynn PW, Potempa LA, Filep JG, Labarrere CA. Conduct unbecoming: C-reactive protein interactions with a broad range of protein molecules. *J Heart Lung Transplant.* (2007) 26:705–13. doi: 10.1016/j.healun.2007.04.006
- Boncler M, Dudzińska D, Nowak J, Watała C. Modified C-reactive protein selectively binds to immunoglobulins. *Scand J Immunol.* (2012) 76:1–10. doi: 10.1111/j.1365-3083.2012.02704.x
- Braig D, Nero TL, Koch H-G, Kaiser B, Wang X, Thiele JR, et al. Transitional changes in the CRP structure lead to the exposure of proinflammatory binding sites. *Nat Commun.* (2017) 8:14188. doi: 10.1038/ncomms14188
- Potempa LA, Maldonado BA, Laurent P, Zemel ES, Gewurz H. Antigenic, electrophoretic and binding alterations of human C-reactive protein modified selectively in the absence of calcium. *Mol Immunol.* (1983) 20:1165–75. doi: 10.1016/0161-5890(83)90140-2
- Williams RD, Moran JA, Fryer AA, Littlejohn JR, Williams HM, Greenhough TJ, et al. Monomeric C-reactive protein in serum with markedly elevated CRP levels shares common calcium-dependent ligand binding properties with an *in vitro* dissociated form of C-reactive protein. *Front Immunol.* (2020) 11:115. doi: 10.3389/fimmu.2020.00115
- Agrawal A, Xu Y, Ansardi D, Macon KJ, Volanakis JE. Probing the phosphocholine-binding site of human C-reactive protein by site-directed mutagenesis. *J Biol Chem.* (1992) 267:25352–8. doi: 10.1016/S0021-9258(19)74047-2
- Firestein GS. Evolving concepts of rheumatoid arthritis. *Nature.* (2003) 423:356–61. doi: 10.1038/nature01661
- Feldmann M, Brennan FM, Maini RN. Role of cytokines in rheumatoid arthritis. *Annu Rev Immunol.* (1996) 14:397–412. doi: 10.1146/annurev.immunol.14.1.397
- Treuhaff PS, McCarty DJ. Synovial fluid pH, lactate, oxygen and carbon dioxide partial pressure in various joint diseases. *Arthrit Rheum.* (1971) 14:475–84. doi: 10.1002/art.1780140407

## Conflict of interest

The authors declare that the research was conducted in the absence of any commercial or financial relationships that could be construed as a potential conflict of interest.

The author(s) declared that they were an editorial board member of Frontiers, at the time of submission. This had no impact on the peer review process and the final decision.

## Publisher's note

All claims expressed in this article are solely those of the authors and do not necessarily represent those of their affiliated organizations, or those of the publisher, the editors and the reviewers. Any product that may be evaluated in this article, or claim that may be made by its manufacturer, is not guaranteed or endorsed by the publisher.

30. Andersson SE, Lexmüller K, Johansson A, Ekström GM. Tissue and intracellular pH in normal periarticular soft tissue and during different phases of antigen-induced arthritis in the rat. *J Rheumatol*. (1999) 26:2018–24.
31. Biniecka M, Kennedy A, Fearon U, Ng CT, Veale DJ, O'Sullivan JN. Oxidative damage in synovial tissue is associated with *in vivo* hypoxic status in the arthritic joint. *Ann Rheum Dis*. (2010) 69:1172–8. doi: 10.1136/ard.2009.111211
32. Nagatomo F, Gu N, Fujino H, Okura T, Morimatsu F, Takeda I, et al. Effects of exposure to hyperbaric oxygen on oxidative stress in rats with type II collagen-induced arthritis. *Clin Exp Med*. (2010) 10:7–13. doi: 10.1007/s10238-009-0064-y
33. Gitlin JD, Gitlin JJ, Gitlin D. Localization of C-reactive protein in synovium of patients with rheumatoid arthritis. *Arthritis Rheum*. (1977) 20:1491–9. doi: 10.1002/art.1780200808
34. Gaffen SL. The role of interleukin-17 in the pathogenesis of rheumatoid arthritis. *Curr Rheumatol Rep*. (2009) 11:365–70. doi: 10.1007/s11926-009-0052-y
35. Chen D-Y, Chen Y-M, Chen H-H, Hsieh C-W, Lin C-C, Lan J-L. Increasing levels of circulating Th17 cells and interleukin-17 in rheumatoid arthritis patients with an inadequate response to anti-TNF- $\alpha$  therapy. *Arthritis Res Ther*. (2011) 13:126. doi: 10.1186/ar3431
36. Kushner I. C-reactive protein in rheumatology. *Arthritis Rheum*. (1991) 34:1065–8. doi: 10.1002/art.1780340819
37. Jones NR, Pegues MA, McCrory MA, Kerr SW, Jiang H, Sellati R, et al. Collagen-induced arthritis is exacerbated in C-reactive protein-deficient mice. *Arthritis Rheum*. (2011) 63:2641–50. doi: 10.1002/art.30444
38. Jones NR, Pegues MA, McCrory MA, Singleton W, Bethune C, Baker BF, et al. A selective inhibitor of human C-reactive protein translation is efficacious *in vitro* and in C-reactive protein transgenic mice and humans. *Mol Ther Nucleic Acids*. (2012) 1:52. doi: 10.1038/mtna.2012.44
39. Fujita C, Sakurai Y, Yasuda Y, Takada Y, Huang CL, Fujita M. Anti-monomeric C-reactive protein antibody ameliorates arthritis and nephritis in mice. *J Immunol*. (2021) 207:1755–62. doi: 10.4049/jimmunol.2100349
40. Brand DD, Latham KA, Rosloniec EF. Collagen-induced arthritis. *Nat Protoc*. (2007) 2:1269–75. doi: 10.1038/nprot.2007.173
41. Ostreiko KK, Tumanova IA, Sykulev YK. Production and characterization of heat-aggregated IgG complexes with pre-determined molecular masses: Light-scattering study. *Immunol Lett*. (1987) 15:311–6. doi: 10.1016/0165-2478(87)90134-9
42. Brown MR, Anderson BE. Receptor-ligand interactions between serum amyloid P component and model soluble immune complexes. *J Immunol*. (1993) 151:2087–95. doi: 10.4049/jimmunol.151.4.2087
43. Thirumalai A, Singh SK, Hammond DJ Jr, Gang TB, Ngwa DN, Pathak A, et al. Purification of recombinant C-reactive protein mutants. *J Immunol Methods*. (2017) 443:26–32. doi: 10.1016/j.jim.2017.01.011
44. Joosten LA, Helsen MM, van de Loo FA, van den Berg WB. Anti-cytokine treatment of established type II collagen-induced arthritis in DBA/1 mice: A comparative study using anti-TNF $\alpha$ , anti-IL-1 $\alpha/\beta$ , and IL-1Ra. *Arthritis Rheum*. (1996) 39:797–809. doi: 10.1002/art.1780390513
45. Wipke BT, Wang Z, Nagengast W, Reichert DE, Allen PM. Staging the initiation of autoantibody-induced arthritis: A critical role for immune complexes. *J Immunol*. (2004) 172:7694–702. doi: 10.4049/jimmunol.172.12.7694
46. Ballou SP, Macintyre SS. Absence of a binding reactivity of human C-reactive protein for immunoglobulin or immune complexes. *J Lab Clin Med*. (1990) 115:332–8.
47. Gupta RC, Badhwar AK, Bisno AL, Berrios X. Detection of C-reactive protein, streptolysin O, and anti-streptolysin O antibodies in immune complexes isolated from the sera of patients with acute rheumatic fever. *J Immunol*. (1986) 137:2173–9. doi: 10.4049/jimmunol.137.7.2173
48. Ramanathan VD, Parkash O, Ramu G, Parker D, Curtis J, Sengupta U, et al. Isolation and analysis of circulating immune complexes in leprosy. *Clin Immunol Immunopathol*. (1984) 32:261–8. doi: 10.1016/0090-1229(84)90270-8
49. Grutzmeier S, von Schenck H. C-reactive protein-immunoglobulin complexes in two patients with macroglobulinemia. *Scand J Clin Lab Invest*. (1987) 47:819–22. doi: 10.3109/00365518709168951
50. Maire MA, Barnet M, Carpentier N, Miescher PA, Lambert PH. Identification of components of IC purified from human sera. I. Immune complexes purified from sera of patients with SLE. *Clin Exp Immunol*. (1983) 51:215–24.
51. Croce MV, Segal-Eiras A. Identification of acute-phase proteins (APP) in circulating immune complexes (CIC) in esophageal cancer patients' sera. *Cancer Invest*. (1996) 14:421–6. doi: 10.3109/0737590609018899
52. Sjöwall C, Zapf J, von Lönnheysen S, Magorivska I, Biermann M, Janko C, et al. Altered glycosylation of circulating native IgG molecules is associated with disease activity of systemic lupus erythematosus. *Lupus*. (2015) 24:569–81. doi: 10.1177/0961203314558861
53. Stümer J, Biermann MHC, Knopf J, Magorivska I, Kastbom A, Svärd A, et al. Altered glycan accessibility on native immunoglobulin G complexes in early rheumatoid arthritis and its changes during therapy. *Clin Exp Immunol*. (2017) 189:372–82. doi: 10.1111/cei.12987
54. Köttgen E, Hell B, Kage A, Tauber R. Lectin specificity and binding characteristics of human C-reactive protein. *J Immunol*. (1992) 149:445–53. doi: 10.4049/jimmunol.149.2.445
55. Alonzi T, Fattori E, Lazzaro D, Costa P, Probert L, Kollias G, et al. Interleukin-6 is required for the development of collagen-induced arthritis. *J Exp Med*. (1998) 187:461–8. doi: 10.1084/jem.187.4.461
56. Wei X-Q, Leung BP, Arthur HML, McInnes IB, Liew FY. Reduced incidence and severity of collagen-induced arthritis in mice lacking IL-18. *J Immunol*. (2001) 166:517–21. doi: 10.4049/jimmunol.166.1.517
57. Nakae S, Nambu A, Sudo K, Iwakura Y. Suppression of immune induction of collagen-induced arthritis in IL-17-deficient mice. *J Immunol*. (2003) 171:6173–7. doi: 10.4049/jimmunol.171.11.6173
58. Szalai AJ, Nataf S, Hu XZ, Barnum SR. Experimental allergic encephalomyelitis is inhibited in transgenic mice expressing human C-reactive protein. *J Immunol*. (2002) 168:5792–7. doi: 10.4049/jimmunol.168.11.5792
59. Hu X-Z, Wright TT, Jones NR, Ramos TN, Skibinski GA, McCrory MA, et al. Inhibition of experimental autoimmune encephalomyelitis in human C-reactive protein transgenic mice is Fc $\gamma$ RIIB dependent. *Autoimmune Dis*. (2010) 2011:484936. doi: 10.4061/2011/484936
60. Shen Z-Y, Zheng Y, Pecsok MK, Wang K, Li W, Gong M-J, et al. C-reactive protein suppresses the Th17 response indirectly by attenuating the antigen presentation ability of monocyte derived dendritic cells in experimental autoimmune encephalomyelitis. *Front Immunol*. (2021) 12:589200. doi: 10.3389/fimmu.2021.589200
61. Szalai AJ, Weaver CT, McCrory MA, van Ginkel FW, Reiman RM, Kearney JF, et al. Delayed lupus onset in (NZB x NZW) F<sub>1</sub> mice expressing a human C-reactive protein transgene. *Arthritis Rheumat*. (2003) 48:1602–11. doi: 10.1002/art.11026
62. Du Clos TW, Zlock LT, Hicks PS, Mold C. Decreased autoantibody levels and enhanced survival of (NZB x NZW) F<sub>1</sub> mice treated with C-reactive protein. *Clin Immunol Immunopathol*. (1994) 70:22–7. doi: 10.1006/clin.1994.1005
63. Wright TT, Jimenez RV, Morgan TE, Bali N, Hou X, McCrory MA, et al. Hepatic but Not CNS-expressed human C-reactive protein inhibits experimental autoimmune encephalomyelitis in transgenic mice. *Autoimmune Dis*. (2015) 2015:640171. doi: 10.1155/2015/640171
64. Jiang S, Xia D, Samols D. Expression of rabbit C-reactive protein in transgenic mice inhibits development of antigen-induced arthritis. *Scand J Rheumatol*. (2006) 35:351–5. doi: 10.1080/03009740600575963
65. Ogden CA, Elkon KB. Single-dose therapy for lupus nephritis: C-reactive protein, nature's own dual scavenger and immunosuppressant. *Arthritis Rheum*. (2005) 52:378–81. doi: 10.1002/art.20847
66. Rodriguez W, Mold C, Marnell LL, Hutt J, Silverman GJ, Tran D, et al. Prevention and reversal of nephritis in MRL/lpr mice with a single injection of C-reactive protein. *Arthritis Rheum*. (2006) 54:325–35. doi: 10.1002/art.21556
67. Rodriguez W, Mold C, Kataranovski M, Hutt JA, Marnell LL, Verbeek JS, et al. C-reactive protein-mediated suppression of nephrotoxic nephritis: Role of macrophages, complement, and Fc $\gamma$  receptors. *J Immunol*. (2007) 178:530–8. doi: 10.4049/jimmunol.178.1.530
68. Svanberg C, Enocsson H, Govender M, Martinsson K, Potempa LA, Rajab IM, et al. Conformational state of C-reactive protein is critical for reducing immune complex-triggered type I interferon response: Implications for pathogenic mechanisms in autoimmune diseases imprinted by type I interferon gene dysregulation. *J Autoimmun*. (2023) 135:102998. doi: 10.1016/j.jaut.2023.102998
69. Williams RO, Feldmann M, Maini RN. Anti-tumor necrosis factor ameliorates joint disease in murine collagen-induced arthritis. *Proc Natl Acad Sci USA*. (1992) 89:9784–8. doi: 10.1073/pnas.89.20.9784
70. Rioja I, Bush KA, Buckton JB, Dickson MC, Life PF. Joint cytokine quantification in two rodent arthritis models: Kinetics of expression, correlation of mRNA and protein levels and response to prednisolone treatment. *Clin Exp Immunol*. (2004) 137:65–73. doi: 10.1111/j.1365-2249.2004.02499.x
71. Sarkar S, Cooney LA, White P, Dunlop DB, Endres J, Jorns JM, et al. Regulation of pathogenic IL-17 responses in collagen-induced arthritis: Roles of endogenous interferon- $\gamma$  and IL-4. *Arthritis Res Ther*. (2009) 11:158. doi: 10.1186/ar2838
72. Zhang Y, Ren G, Guo M, Ye X, Zhao J, Xu L, et al. Synergistic effects of interleukin-1 $\beta$  and interleukin-17A antibodies on collagen-induced arthritis mouse model. *Int Immunopharmacol*. (2013) 15:199–205. doi: 10.1016/j.intimp.2012.12.010
73. Hemmerle T, Doll F, Neri D. Antibody-based delivery of IL-4 to the neovascularature cures mice with arthritis. *Proc Natl Acad Sci U S A*. (2014) 111:12008–12. doi: 10.1073/pnas.1402783111
74. Wang Y, Lu S, Zhang G, Wu S, Yan Y, Dong Q, et al. Anti-inflammatory effects of HDL in mice with rheumatoid arthritis induced by collagen. *Front Immunol*. (2018) 19:1013. doi: 10.3389/fimmu.2018.01013
75. Skon-Hegg C, Zhang J, Wu X, Sagolla M, Ota N, Wuster A, et al. LACC1 regulates TNF and IL-17 in mouse models of arthritis and inflammation. *J Immunol*. (2019) 202:183–93. doi: 10.4049/jimmunol.1800636
76. Tang K-T, Lin C-C, Lin S-C, Wang J-H, Tsai S-W. Kurarinone attenuates collagen-induced arthritis in mice by inhibiting Th1/Th17 cell responses and oxidative stress. *Int J Mol Sci*. (2021) 22:4002. doi: 10.3390/ijms22084002
77. Kiefer J, Zeller J, Bogner B, Hörbrand IA, Lang F, Deiss E, et al. An unbiased flow cytometry-based approach to assess subset-specific circulating monocyte activation and cytokine profile in whole blood. *Front Immunol*. (2021) 12:641224. doi: 10.3389/fimmu.2021.641224

78. Campbell IK, O'Donnell K, Lawlor KE, Wicks IP. Severe inflammatory arthritis and lymphadenopathy in the absence of TNF. *J Clin Invest.* (2001) 107:1519–27. doi: 10.1172/JCI12724
79. Ferraccioli G, Bracci-Laudiero L, Alivernini S, Gremese E, Tolusso B, De Benedetti F. Interleukin-1 $\beta$  and interleukin-6 in arthritis animal models: Roles in the early phase of transition from acute to chronic inflammation and relevance for human rheumatoid arthritis. *Mol Med.* (2010) 16:552–7. doi: 10.2119/molmed.2010.00067
80. Koenders MI, Lubberts E, van de Loo FA, Oppers-Walgreen B, van den Bersselaar L, Helsen MM, et al. Interleukin-17 acts independently of TNF- $\alpha$  under arthritic conditions. *J Immunol.* (2006) 176:6262–9. doi: 10.4049/jimmunol.176.10.6262
81. Suzuki M, Tanaka K, Yoshida H, Yogo K, Matsumoto Y. Obesity does not diminish the efficacy of IL-6 signalling blockade in mice with collagen-induced arthritis. *Clin Exp Rheumatol.* (2017) 35:893–8.
82. Takagi N, Mihara M, Moriya Y, Nishimoto N, Yoshizaki K, Kishimoto T, et al. Blockage of interleukin-6 receptor ameliorates joint disease in murine collagen-induced arthritis. *Arthritis Rheum.* (1998) 41:2117–21. doi: 10.1002/(ISSN)1529-0131
83. Henningsson L, Eneljung T, Jirholt P, Tengvall S, Lidberg U, van den Berg WB, et al. Disease-dependent local IL-10 production ameliorates collagen-induced arthritis in mice. *PLoS One.* (2012) 7:49731. doi: 10.1371/journal.pone.0049731
84. Szalai AJ. C-reactive protein (CRP) and autoimmune disease: facts and conjectures. *Clin Dev Immunol.* (2004) 11:221–6. doi: 10.1080/17402520400001751

# Frontiers in Immunology

Explores novel approaches and diagnoses to treat immune disorders.

The official journal of the International Union of Immunological Societies (IUIS) and the most cited in its field, leading the way for research across basic, translational and clinical immunology.

## Discover the latest Research Topics

[See more →](#)

### Frontiers

Avenue du Tribunal-Fédéral 34  
1005 Lausanne, Switzerland  
[frontiersin.org](https://frontiersin.org)

### Contact us

+41 (0)21 510 17 00  
[frontiersin.org/about/contact](https://frontiersin.org/about/contact)

